

DOCTORAL THESIS

**“EFFECT OF POLY(ADP-RIBOSE)POLYMERASE (PARP) INHIBITION
ON GLIOBLASTOMA MULTIFORME”**

Jara Majuelos Melguizo

Instituto de Parasitología y Biomedicina “López Neyra”

Consejo Superior de Investigaciones Científicas (CSIC)

Departamento de Bioquímica y Biología Molecular III e
Inmunología

Universidad de Granada

Granada, 2015



Universidad de Granada

Editorial: Universidad de Granada. Tesis Doctorales

Autora: Jara Majuelos Melguizo

ISBN: 978-84-9125-262-7

URI: <http://hdl.handle.net/10481/40657>

El doctorando Jara Majuelos Melguizo y el director de la tesis Javier Oliver Pozo. Garantizamos, al firmar esta tesis doctoral, que el trabajo ha sido realizado por el doctorando bajo la dirección de los directores de la tesis y hasta donde nuestro conocimiento alcanza, en la realización del trabajo, se han respetado los derechos de otros autores a ser citados, cuando se han utilizado sus resultados o publicaciones.

En Granada,

Director de la Tesis

Doctorando

Fdo.: Javier Oliver Pozo

Fdo.: Jara Majuelos Melguizo

A mis padres.

“Descifrar lo que está delante de nuestros ojos requiere de un esfuerzo constante”.
George Orwell.

INDEX

| | |
|----------------------|----------|
| ABBREVIATIONS | 1 |
|----------------------|----------|

| | |
|----------------|----------|
| RESUMEN | 9 |
|----------------|----------|

| | |
|---------------------|-----------|
| INTRODUCTION | 13 |
|---------------------|-----------|

| | |
|----------------------------------|-----------|
| 1 GLIOBLASTOMA MULTIFORME | 15 |
|----------------------------------|-----------|

| | |
|------------------|----|
| 1.1 GENERAL VIEW | 15 |
|------------------|----|

| | |
|----------------------------|----|
| 1.2 GLIOBLASTOMA DETECTION | 16 |
|----------------------------|----|

| | |
|---|----|
| 1.3 MOLECULAR CHARACTERISTICS OF GLIOBLASTOMA | 17 |
|---|----|

| | |
|----------------------|----|
| 1.3.1 FIRST ATTEMPTS | 17 |
|----------------------|----|

| | |
|--------------------------------|----|
| 1.3.2 CURRENT CHARACTERIZATION | 17 |
|--------------------------------|----|

| | |
|--------------------------------|----|
| 1.4 CURRENT MOLECULAR SUBTYPES | 19 |
|--------------------------------|----|

| | |
|--|----|
| 1.5 PRIMARY AND SECONDARY GLIOBLASTOMA | 20 |
|--|----|

| | |
|-------------------------------|----|
| 1.6 TREATMENT OF GLIOBLASTOMA | 21 |
|-------------------------------|----|

| | |
|--------------------------------|----|
| 1.6.1 CURRENT STANDARD OF CARE | 21 |
|--------------------------------|----|

| | |
|-------------------------------------|----|
| 1.6.2 THERAPIES UNDER INVESTIGATION | 22 |
|-------------------------------------|----|

| | |
|--|----|
| 1.7 GLIOBLASTOMA ORIGIN: CANCER STEM CELLS | 23 |
|--|----|

| | |
|--|----|
| 1.7.1 NEURAL STEM CELLS (NSCs) IN THE ADULT CENTRAL NERVOUS SYSTEM (CNS) | 23 |
|--|----|

| | |
|-------------------------|----|
| 1.7.2 GLIOMA STEM CELLS | 24 |
|-------------------------|----|

| | |
|--|-----------|
| 2 POLY (ADP-RIBOSE) POLYMERASE 1 (PARP-1) | 28 |
|--|-----------|

| | |
|------------------|----|
| 2.1 GENERAL VIEW | 28 |
|------------------|----|

| | |
|---------------------|----|
| 2.2 PARP EXPRESSION | 28 |
|---------------------|----|

| | |
|---------------------|----|
| 2.3 PARP METABOLISM | 28 |
|---------------------|----|

| | |
|---------------------|----|
| 2.3.1 PAR SYNTHESIS | 28 |
|---------------------|----|

| | |
|-----------------------|----|
| 2.3.2 PAR DEGRADATION | 29 |
|-----------------------|----|

| | |
|----------------------|----|
| 2.4 PARP-1 STRUCTURE | 31 |
|----------------------|----|

| | |
|-----------------|----|
| 2.5 PARP FAMILY | 32 |
|-----------------|----|

| | |
|----------------------|----|
| 2.5.1 CLASSIFICATION | 32 |
|----------------------|----|

| | |
|--|----|
| 2.5.2 BRIEF DESCRIPTION OF PARP FAMILY MEMBERS | 34 |
|--|----|

| | |
|--------------------------------|----|
| 2.6 PARP ACTIVATION MECHANISMS | 34 |
|--------------------------------|----|

| | |
|--|----|
| 2.6.1 MOLECULAR EVENTS FOLLOWING PARP ACTIVATION | 35 |
|--|----|

| | |
|---------------------|----|
| 2.7 PARP FUNCTIONS: | 36 |
|---------------------|----|

| | |
|---------------------|----|
| 2.7.1 TRANSCRIPTION | 36 |
|---------------------|----|

| | |
|-------------------|----|
| 2.7.2 REPLICATION | 37 |
|-------------------|----|

| | |
|------------------|----|
| 2.7.3 DNA REPAIR | 38 |
|------------------|----|

| | |
|--|----|
| 2.7.4 GENOME ORGANIZATION: PARP AND GENOME INSTABILITY | 39 |
|--|----|

| | |
|-------------------------------------|----|
| 2.7.5 PROTEIN STABILITY/DEGRADATION | 41 |
|-------------------------------------|----|

| | |
|---------------------------|----|
| 2.7.6 PARP AND CELL CYCLE | 41 |
|---------------------------|----|

| | |
|--|----|
| 2.8 CELLULAR EFFECT OF PARP ACTIVATION | 42 |
|--|----|

| | | |
|----------|--|-----------|
| 2.8.1 | PROLIFERATION, CELL DEATH AND CELL SURVIVAL | 42 |
| 2.8.2 | DIFFERENTIATION | 45 |
| 2.8.3 | PARP AND DISEASE: | 45 |
| 2.9 | PARP INHIBITION | 48 |
| 3 | GENOME STABILITY: CELL CYCLE | 49 |
| 3.1 | GENERAL VIEW | 49 |
| 3.2 | REGULATION | 49 |
| 3.3 | MITOSIS | 50 |
| 3.3.1 | MITOSIS ENTRANCE | 50 |
| 3.3.2 | MITOSIS EXIT | 51 |
| 3.3.3 | PARP AND MITOSIS | 56 |
| 4 | DNA DAMAGE RESPONSE | 58 |
| 4.1 | DNA DAMAGE REPAIR | 58 |
| 4.1.1 | GENERAL VIEW | 58 |
| 4.1.2 | HOMOLOGOUS RECOMBINATION | 60 |
| 4.2 | CELL CYCLE CHECKPOINTS | 62 |
| 5 | CELL SURVIVAL: mTOR PATHWAY | 64 |
| 5.1 | GENERAL VIEW | 64 |
| 5.1.1 | mTOR BINDING PROTEINS | 64 |
| 5.2 | mTOR UPSTREAM SIGNALING PATHWAYS | 65 |
| 5.2.1 | UPSTREAM TSC: | 65 |
| 5.2.2 | FROM TSC TO mTOR | 66 |
| 5.2.3 | DOWNSTREAM mTOR | 67 |
| 5.3 | mTOR PATHWAY AND GBM | 68 |
| 6 | CELL SURVIVAL: PTEN | 69 |
| 6.1 | GENERAL VIEW | 69 |
| 6.2 | PTEN STRUCTURE | 69 |
| 6.3 | PTEN SUBCELLULAR LOCATION AND FUNCTIONS | 70 |
| 6.3.1 | CYTOSOL | 70 |
| 6.3.2 | NUCLEUS | 70 |
| 6.4 | PTEN AND PARP | 74 |
| 7 | CELL DEATH | 75 |
| 7.1 | APOPTOSIS OR TYPE I CELL DEATH | 77 |
| 7.1.1 | APOPTOSIS INITIATION: EXTRINSIC AND INTRINSIC BIOCHEMICAL PATHWAYS | 77 |
| 7.1.2 | APOPTOSIS EXECUTION: CASPASES | 80 |
| 7.1.3 | APOPTOSIS CONSEQUENCES: HALLMARKS OF APOPTOSIS | 81 |
| 7.2 | AUTOPHAGY OR TYPE II CELL DEATH | 82 |
| 7.2.1 | AUTOPHAGIC PROCESS IN MAMMALS | 83 |
| 7.2.2 | AUTOPHAGIC MOLECULAR PATHWAY | 84 |
| 7.2.3 | AUTOPHAGIC CELL DEATH | 86 |
| 7.2.4 | SIGNALING PATHWAYS REGULATING AUTOPHAGY | 87 |
| 7.2.5 | LIPOPHAGY | 88 |
| 7.3 | MITOTIC CATASTROPHE | 92 |
| 7.3.1 | GENERAL VIEW | 92 |
| 7.3.2 | MC INDUCERS: | 93 |

| | | |
|-------|---------------|----|
| 7.3.3 | MC PROGRAMMES | 93 |
| 7.3.4 | MC EXECUTORS | 95 |

OBJECTIVES _____ **97**

MATERIALS AND METHODS _____ **101**

| | | |
|----------|---|------------|
| 8 | MATERIALS | 103 |
| 8.1 | CELL CULTURE | 103 |
| 8.1.1 | CELL LINES | 103 |
| 8.1.2 | PATIENT-DERIVED GBM STEM-LIKE CELLS (GSCs) | 103 |
| 8.2 | REAGENTS | 104 |
| 8.2.1 | CULTURE MEDIUM | 104 |
| 8.2.2 | DRUGS AND INHIBITORS | 104 |
| 8.2.3 | ANTIBODIES | 105 |
| 8.2.4 | RNA INTERFERENCE | 106 |
| 8.2.5 | BUFFERS | 107 |
| 8.2.6 | PRIMERS | 108 |
| 8.2.7 | PLASMIDS FOR GENE RESTORATION | 108 |
| 9 | METHODS | 109 |
| 9.1 | WESTERN BLOT: | 109 |
| 9.1.1 | PROTEIN EXTRACTION | 109 |
| 9.1.2 | PROTEIN QUANTIFICATION | 109 |
| 9.1.3 | WESTERN BLOT: | 109 |
| 9.1.4 | DEVELOPMENT | 110 |
| 9.2 | IMMUNOFLUORESCENCE | 110 |
| 9.2.1 | SAMPLES PREPARATION | 110 |
| 9.2.2 | MICROSCOPY | 111 |
| 9.3 | SHORT TRANSIENT RNA INTERFERENCE | 111 |
| 9.4 | PLASMIDIC DNA TRANSIENT TRANSFECTION | 111 |
| 9.5 | CELL CYCLE ASSAY | 112 |
| 9.5.1 | CELLS PREPARATION | 112 |
| 9.5.2 | FLOW CITOMETRY AND DATA ANALYSIS | 112 |
| 9.6 | PROLIFERATION AND CELL VIABILITY ASSAYS | 112 |
| 9.6.1 | SHORT TERM VIABILITY ASSAY: MTT | 112 |
| 9.6.2 | NEUROSPHERES SELF-RENEWAL ASSAY | 113 |
| 9.7 | CELL DEATH ASSAYS | 113 |
| 9.7.1 | CELL DEATH QUANTIFICATION BY FLOW CITOMETRY | 113 |
| 9.8 | APOPTOSIS ASSAYS | 113 |
| 9.8.1 | SUBG1 ANALYSIS BY FLOW CITOMETRY | 113 |
| 9.8.2 | CASPASE 3/7 ACTIVATION | 114 |
| 9.8.3 | PIKNOTIC NUCLEI QUANTIFICATION | 114 |
| 9.9 | LIPID DROPLETS QUANTIFICATION | 114 |
| 9.9.1 | BODIPY ASSAY | 114 |

| | | |
|--------|---|-----|
| 9.9.2 | SUDAN RED STAINING | 115 |
| 9.10 | ELECTRON MICROSCOPY | 115 |
| 9.11 | HOMOLOGOUS RECOMBINATION ASSAY | 116 |
| 9.12 | GENOMIC INSTABILITY ANALYSIS: MICRONUCLEI DETECTION | 116 |
| 9.12.1 | SAMPLES PREPARATION | 116 |
| 9.12.2 | MICROSCOPY | 116 |
| 9.13 | PCR: | 117 |
| 9.13.1 | RNA EXTRACTION | 117 |
| 9.13.2 | RETROTRANSCRIPTION | 117 |
| 9.13.3 | PCR: | 117 |
| 9.14 | DNA REPAIR AND CELL CYCLE EXPRESSION MICROARRAY | 117 |
| 9.14.1 | RNA EXTRACTION | 117 |
| 9.14.2 | RETROTRANSCRIPTION | 117 |
| 9.14.3 | EXPRESSION MICROARRAY | 117 |
| 9.15 | CELLS IRRADIATION | 118 |
| 9.16 | PATIENT DATASETS AND DATA ANALYSIS | 118 |
| 9.17 | ETHICS STATEMENT | 118 |
| 9.18 | IN VIVO BIOLUMINESCENCE ASSAY | 118 |
| 9.19 | STATISTICAL ANALYSIS | 119 |

RESULTS **121**

| | | |
|----------|--|------------|
| 1 | PARP TARGETING COUNTERACTS GLIOMAGENESIS THROUGH INDUCTION OF MITOTIC CATASTROPHE AND AGGRAVATION OF DEFICIENCY IN HOMOLOGOUS RECOMBINATION IN PTEN-MUTANT GLIOMA | 123 |
| 1.1 | PARP INHIBITION IMPACTS DIFFERENTLY ON CELL VIABILITY IN PTEN WILD TYPE AND PTEN-MUTANT GLIOMA CELLS | 125 |
| 1.2 | PARP INHIBITION INDUCED DOWN-REGULATION OF THE SPINDLE ASSEMBLY CHECKPOINT (SAC) PROTEIN BUBR1, LEADING TO MITOTIC INSTABILITY IN PTEN DEFICIENT GLIOMA CELLS | 129 |
| 1.3 | IMPAIRED HOMOLOGOUS RECOMBINATION (HR) AFTER PARPi IN PTEN DEFICIENT GLIOMA CELLS | 132 |
| 1.4 | PARP BLOCKADE POTENTIATED IN VITRO AND IN VIVO EFFECT OF EGFR INHIBITION ON PTEN MUTANT GLIOMA CELLS | 135 |
| 2 | mTOR PATHWAY DOWN-REGULATION AND LIPOPHAGY IN ABSENCE OF PARP | 137 |
| 2.1 | mTOR PATHWAY DOWNREGULATION AND AUTOPHAGY ACTIVATION FOLLOWING PARP INHIBITION | 139 |
| 2.2 | LIPID DROPLETS FORMATION AFTER PARP INHIBITION | 141 |
| 2.3 | AUTOPHAGY INDUCED BY PARP INHIBITION REGULATES LIPID METABOLISM | 144 |
| 2.4 | GBM CELLS POTENTIATE THEIR OWN ADDICTION TO SURVIVAL PATHWAYS WHEN EXPOSED TO PARPi | 146 |
| 3 | PARP TARGETING COUNTERACTS GLIOMA STEM-LIKE CELLS PHENOTYPE THROUGH THE PROMOTION OF VIABILITY DECREASE, mTOR AXIS DOWN-REGULATION AND CELL DIFFERENTIATION. | 149 |
| 3.1 | PARPi PROMOTES GSCs VIABILITY DECREASE | 151 |

| | | |
|---------------------|---|------------|
| 3.2 | PARPi DOWNREGULATES mTOR AXIS AND PROMOTES AUTOPHAGY ACTIVATION IN GSCs. | 152 |
| 3.3 | PARPi ABROGATES GSCs PHENOTYPE, SUGGESTING THE INDUCTION OF CELL DIFFERENTIATION | 154 |
| DISCUSSION | | 157 |
| 1 | GENERAL DISCUSSION | 159 |
| 2 | PARP TARGETING COUNTERACTS GLIOMAGENESIS THROUGH INDUCTION OF MITOTIC CATASTROPHE AND AGGRAVATION OF DEFICIENCY IN HOMOLOGOUS RECOMBINATION IN PTEN-MUTANT GLIOMA | 160 |
| 3 | PARP REGULATES mTOR ACTIVATION AND LIPID DROPLETS TURNOVER IN GLIOBLASTOMA | 163 |
| 4 | PARP TARGETING COUNTERACTS GLIOMA STEM-LIKE CELLS PHENOTYPE THROUGH THE PROMOTION OF VIABILITY DECREASE, mTOR AXIS DOWN-REGULATION AND CELL DIFFERENTIATION. | 167 |
| 5 | REMARKABLE POINTS | 169 |
| CONCLUSIONES | | 171 |
| BIBLIOGRAPHY | | 175 |
| APPENDIX | | 217 |

ABBREVIATIONS

| | |
|---------------|--|
| ABC | ATP-Binding Cassette |
| ACC | Acetyl-CoA Carboxylase |
| ACD | Accidental Cell Death |
| ADP | Adenosine diphosphate |
| AGT | O ⁶ -alkylguanine-DNA alkyltransferases |
| AIF | Apoptosis Inducing Factor |
| ALA | 5-aminolevulinic acid |
| ALS | Amyotrophic Lateral Sclerosis |
| AMP | Adenosine monophosphate |
| AMPK | AMP-activated Protein Kinase |
| APC/C | Anaphase Promoting Complex/Cyclosome |
| ARH | ADP-Ribosyl Hydrolase |
| ATG | Autophagy-Related-Gene |
| ATM | Ataxia Telangiectasia Mutated |
| ATP | Adenosine triphosphate |
| ATR | Ataxia Telangiectasia and Rad3 related kinase |
| ATRIP | ATR Interacting Protein |
| BBB | Blood–Brain Barrier |
| BCRT | Breast Cancer-associated protein C-Terminal motif |
| BER | Base Excision Repair |
| BH | Bcl-2 Homology |
| BIR | Break-Induced Replication |
| BMP | Bone Morphogenetic Protein |
| BRRS | Bannayan-Riley-Ruvalcava Syndrome |
| BSA | Bovine Serum Albumine |
| BUB1 | Budding Uninhibited by Benomyl 1 |
| BUBR1 | BUB1-related 1 |
| CaMKK β | Ca ²⁺ /calmodulin-dependent kinase kinase β |
| CaMKK β | Ca ²⁺ /calmodulin-dependent kinase kinase β |
| CARD | CAspases Recruitment Domain |
| Caspase | Cysteine-dependent aspartate-directed protease |
| CD | Cowden Syndrome |
| CDK | Cyclin-Dependent-Kinases |
| CDKN2A | Cyclin-Dependent Kinase inhibitor 2A |
| CENP-A | Centromere Protein A |
| CENP-B | Centromere Protein B |
| CENP-C | Centromere Protein C |
| CENP-E | Centromere Protein E |
| CIN | Chromosome Instability |
| CKI | Cyclin Kinases Inhibitors |
| CM | Conditioned Medium |
| CNS | Central Nervous System |
| CPAP | Centrosomal P4.1-Associated Protein |

Abbreviations

| | |
|------------------|--|
| CPC | Chromosome Passenger Complex |
| cPLA2 | cytosolic Phospholipase A2 |
| CPT | Carnitine Palmitoyl Transferase |
| CSC | Cancer Stem Cell |
| CTLs | Cytotoxic T Lymphocytes |
| CSF | Cerebrospinal Fluid |
| DC | Dendritic Cell |
| DD | Death Domain |
| DDR | DNA Damage Response |
| DED | Death Effector Domain |
| DEPTOR | DEP domain-containing mTOR interacting protein |
| dHJ | Double Holliday Junction |
| DISC | Death-Inducing Signaling Complex |
| DNA | deoxyribonucleic acid |
| DNA pol α | DNA polymerase α |
| DR | Death Receptor |
| DRAM | Damage-Regulated Autophagy Modulator |
| DSBs | Double Strand Breaks |
| EGF | Epidermal Growth Factor |
| EGFR | Epidermal Growth Factor Receptor |
| EMT | Epithelial-Mesenchymal Transition |
| endoG | Endonuclease G |
| ESC | Embryonic Stem Cell |
| FA | Fatty Acid |
| FACS | Fatty Acid CoA Synthetase |
| FASL/CD95L | FAS/CD95 Ligand |
| FASN | Fatty Acid Synthase |
| FFA | Free Fatty Acid |
| FGF | Fibroblast Growth Factor |
| FOXO | Forkhead family of transcription factors |
| GBM | Glioblastoma |
| GFAP | Glial Fibrillar Acid Protein |
| GIN | Genome Instability |
| GIC | Glioma Initiating Cell |
| GSC | Glioma Stem Cell |
| GSK3 | Glycogen Synthase Kinase 3 |
| GWAS | Genome Wide Association |
| HER | Human Epidermal growth factor Receptor |
| HIF | Hypoxia-Inducible Factor |
| HR | Homologous Recombination |
| IAP | Inhibitors of Apoptosis Protein |
| IDH1 | Isocitrate Dehydrogenase 1 |
| IKD | Inter-Kinetochore Distance |

| | |
|---------|---|
| IMS | Intermembrane Space |
| INCENP | INner CEntromere Protein |
| IR | Ionizing Radiation |
| kDa | Kilodalton |
| KO | Knockout |
| KT | Kinetochores |
| LC3 | Microtubule-associated protein 1A/1B-Light Chain 3 |
| LD | Lipid Droplet |
| LOH | Loss of Heterocigosity |
| M phase | Mitosis phase |
| MAD | Mitotic Arrest Deficient |
| Mad2-C | Mad2-Close |
| Mad2-O | Mad2-Open |
| MAPK | RAS–Mitogen Activated Protein Kinase |
| MC | Mitotic Catastrophe |
| MCC | Mitotic Checkpoint Complex |
| MEFs | Murine Embryonic Fibroblasts |
| MGMT | O ₆ -methylguanine-DNA methyltransferase |
| miRNA | microRNA |
| MLST8 | Mammalian Lethal with Sec13 protein 8 |
| MMR | Mismatch Repair |
| MOMP | Mitochondrial Outer Membrane Permeabilization |
| MPS1 | Monopolar Spindle Protein 1 |
| MRE11 | Meiotic Recombination 11 |
| MRI | Magnetic Resonance Imaging |
| MSIN1 | Mammalian Stress-activated map kinase-Interacting protein 1 |
| mTOR | Mammalian Target Of Rapamycin |
| mTORC1 | Mammalian TOR complex 1 |
| mTORC2 | Mammalian TOR complex 2 |
| MVA | Mosaic Variegated Aneuploidy |
| MVP | Major Vault Protein |
| NAD | Nicotinamide-Adenine-Dinucleotide |
| NBS1 | Nijmegen breakage syndrome 1 |
| NCCD | Nomenclature Committee on Cell Death |
| NCCD | Nomenclature Committee on Cell Death |
| NER | Nucleotide Excision Repair |
| NHEJ | Non-Homologous End Joining |
| NLS | Nuclear Location Signal |
| NSC | Neural Stem Cell |
| NTR | N-terminal region |
| p70S6K1 | p70 S6 kinase 1 |
| PALB2 | Partner And Localizer of BRCA2 |
| PAR | Poly(ADP-ribose) |

Abbreviations

| | |
|----------|--|
| PARG | Poly(ADP-ribose) Glycohydrolase |
| PARP | Poly (ADP-ribose) polymerase |
| PARPi | PARP inhibition |
| PCD | Programmed Cell Death |
| PDGFR | Platelet-Derived Growth Factor Receptor |
| PKD1 | PI3K-Dependent Kinase 1 |
| PFA | Paraformaldehyde |
| PI3K | Phosphatidylinositol 3-Kinase |
| PI3KCI | Class I PI3K |
| PI3KCIII | Class III PI3K |
| PIP | Phosphatidylinositol 3-phosphate |
| PIPES | piperazine-N,N'-bis(2-ethanesulfonic acid) |
| PLK1 | Polo-like Kinase 1 |
| PRAs40 | 40 kDa Pro-rich Akt substrate |
| PROTOR | Protein Observed with RICTOR |
| PTEN | Phosphatase and TENsin homolog |
| RAPTOR | Regulatory-Associated Protein of mTOR |
| RCD | Regulated Cell Death |
| RICTOR | Rapamycin-Insensitive Companion of mTOR |
| RIP1 | Receptor Interacting Protein 1 |
| RNA | Ribonucleic acid |
| RNAi | RNA interference |
| RNApII | RNA polymerase II |
| RNS | Reactive Nitrogen Species |
| ROS | Reactive Oxygen Species |
| RPA | Replication Protein A |
| RPS6 | Ribosomal Protein S6 |
| RT | Radiotherapy |
| S phase | Synthesis phase |
| SAC | Spindle Assembly Checkpoint |
| SCF | SKP1-CUL1-Fbox protein |
| SDSA | Synthesis-Dependent-Strand-Annealing |
| SLE | Systemic Lupus Erythematosus |
| SNPs | Single Nucleotide Polymorphisms |
| SREBP1c | Sterol Regulatory Element Binding Protein 1c |
| SSBR | Single Strand Breaks Repair |
| SSBs | Simple Strand Breaks |
| TAK1 | Transforming growth factor beta-Activated Kinase 1 |
| TANK1 | Tankyrase 1 |
| TANK2 | Tankyrase 2 |
| TCA | Tri-Carboxylic-Acid |
| TCGA | The Cancer Genome Atlas |
| TG | Triglycerid |

| | |
|-------|---|
| TKR | Tyrosine Kinase Receptor |
| TMZ | Temozolomide |
| TNF | Tumor Necrosis Factor |
| TNFR | TNF Receptor |
| TOR | Target Of Rapamycin |
| TSC | Tuberous Sclerosis Complex |
| TUJ1 | β III Tubulin |
| VEGF | Vascular Endothelial Growth Factor |
| VEGFR | Vascular Endothelial Growth Factor Receptor |
| WHO | World Health Organization |
| Zn | Zinc |

RESUMEN

El glioblastoma multiforme (GBM) es un tumor de las células de la glía, en concreto de los astrocitos. Es uno de los tumores que peor pronóstico tiene en la actualidad, con una media de supervivencia de 14,6 meses. Su tratamiento se basa en la extirpación quirúrgica, en los casos en los que es posible, y el posterior tratamiento con radio y quimioterapia, siendo el quimioterapéutico de preferencia para este tumor la temozolomida.

Pese a los continuos esfuerzos, tanto de investigación básica (para comprender los mecanismos que subyacen al desarrollo de esta enfermedad) como clínicos (para mejorar la esperanza y la calidad de vida de los pacientes con este tumor), son escasos los avances registrados en los últimos años en su tratamiento. Por eso, se hace necesaria la investigación de posibles dianas que ayuden a la comprensión de la biología del glioblastoma y que puedan abrir nuevas oportunidades terapéuticas hacia su curación.

Las enzimas de la familia poli(ADP-ribosa)polimerasa (PARPs) desempeñan funciones celulares relacionadas con la reparación de ADN, transcripción génica, ciclo celular, muerte celular y estabilidad genómica, entre otros. PARP-1 es, de entre los 18 miembros descritos en la actualidad de la familia PARP, la responsable de la síntesis de la gran mayoría del polímero de ADP-ribosa que ocurre en la célula. Junto con PARP-2 y PARP-3, constituye el grupo de PARPs que se activan en respuesta a daño al ADN. En los últimos años, la familia PARP ha constituido una excelente diana antitumoral dado que su inhibición en monoterapia es capaz de revertir ciertos tumores en determinados contextos, y en combinación con quimio y radioterapia es capaz de potenciar el efecto de éstas últimas.

Así pues, el objetivo de esta tesis ha sido el estudio del efecto de la inhibición de PARP en glioblastoma multiforme, elucidando su impacto en la viabilidad del tumor y describiendo las rutas en las que PARP está implicada en el desarrollo de dicha enfermedad. De este modo, hemos observado un importante efecto de la inhibición de PARP en la supervivencia del tumor tanto *in vitro* con líneas celulares y células iniciadoras del tumor derivadas de pacientes, como *in vivo* en un modelo ortotópico de ratón. Además, hemos descrito que este efecto está mediado por un aumento en la inestabilidad mitótica y genómica que es dependiente de la presencia/ausencia del gen supresor de tumores PTEN. La inhibición de PARP conlleva, además, la disminución en la activación de rutas de supervivencia conduciendo a la célula a la activación de procesos autofágicos y la alteración del metabolismo lipídico. Por último, proponemos el uso de los inhibidores de PARP como potencial diana terapéutica frente a las células iniciadoras del glioblastoma, puesto que tanto su estado de dediferenciación como su viabilidad disminuye tras el tratamiento con inhibidores de PARP.

Contribuir al aumento del conocimiento existente sobre la biología de este tumor así como de la función que PARP desempeña en su desarrollo puede constituir un paso muy importante para la comprensión de los mecanismos implicados en el desarrollo del glioblastoma multiforme, constituyendo además una potencial diana terapéutica en su tratamiento.

INTRODUCTION

1 GLIOBLASTOMA MULTIFORME

1.1 GENERAL VIEW

Gliomas are tumors of the glial cells, or neuroglia, in the Central Nervous System (CNS), which make up approximately 30% of all central nervous system tumors and 80% of all malignant brain tumors.

In 1993 the World Health Organization (WHO) ratified a new comprehensive classification of neoplasms affecting the CNS. According to it, the classification of Gliomas is based on the premise that each type of tumor results from the abnormal growth of a specific cell type.

| GLIOMA SUBTYPE | TISSUE ORIGIN |
|------------------------|--|
| Astrocytoma | Astrocytes, the most abundant type of glia in the Central Nervous System (CNS). They anchor neurons to facilitate their blood supply. |
| Oligodendroglioma | Oligodendrocytes (cells that coat axons in the CNS with their cell membrane, forming a specialized membrane differentiation called myelin, producing the so-called myelin sheath. The myelin sheath provides insulation to the axon that allows electrical signals to propagate more efficiently). |
| Mixed Oligoastrocytoma | Astrocytes and oligodendrocytes. |
| Ependymoma | Ependymocytes, which are glial cells that line the spinal cord and the ventricular system of the brain. These cells are involved in the creation and secretion of cerebrospinal fluid (CSF). |

Table 1: different glioma subtypes according to their tissue origin. Adapted from Louis (Louis, Ohgaki et al. 2007).

Amongst gliomas, astrocytomas are the most common subtype. Interestingly, the WHO classification also provides a parallel grading scheme for each type of tumor in terms of invasion and growth rate. In this grading system most named tumors belong to a single defined grade. Thus, astrocytomas are classified by WHO as follows:

| TUMOR GRADE | TUMOUR NAME | DESCRIPTION |
|-------------|-------------------------|---|
| I | Pilocytic astrocytoma | Slow growing astrocytomas, benign, and associated with long-term survival. Complete surgical removal is possible in some cases. Even if the surgeon is not able to remove the entire tumor, it may remain inactive or be successfully treated with radiation. |
| II | Difuse astrocytoma | Relatively slow-growing astrocytomas, usually considered benign that sometimes evolve into higher grade tumors. Invasive gliomas, meaning that the tumor cells penetrate into the surrounding normal brain, making surgical cure more difficult. Due to the infiltrative nature of these tumors, recurrences are relatively common. |
| III | Anaplastic astrocytoma | Highly invasive glioma, with an invasion and growth rate higher than grade II glioma. |
| IV | Glioblastoma multiforme | The most aggressive glioma. It grows and spreads to other parts of the brain quickly. The extremely infiltrative nature of this tumor makes complete surgical removal impossible. |

Table 2: different astrocytoma subtypes according to their invasiveness and growth rate. (Burger 1995). Adapted.

As observed in the table above, Glioblastoma Multiforme (GBM) is the most common primary brain tumor in adults and one of the most aggressive cancers in humans. Despite technological advances in surgical resection, combined with radiotherapy and new generation chemotherapy, the median survival for this patients is 14,6 months (Krakstad and Chekenya 2010).

Due to the clinical relevance of this pathology, combined with the poor survival perspective of these patients, we decided to focus our project for the thesis on this type of brain tumor.

1.2 GLIOBLASTOMA DETECTION

Magnetic Resonance Imaging (MRI) is more sensitive than Computerized Tomography (CT) in the detection of GBM (Landy, Lee et al. 2000). GBM appears as a mass with partial contrast enhancement due to limited disruption of the blood-brain barrier (BBB). Therefore, irregular contours and a peripheral zone with strong contrast enhancement around a darker, hypodense, necrotic area is observed (Van Meir, Hadjipanayis et al. 2010).

Despite little variants, histological diagnosis is principally based on nuclear atypia and mitotic activity. Other defining histological traits of GBM are the presence of microvascular proliferation and central areas of tumor necrosis that are often, but not necessarily, associated with perinecrotic nuclei.

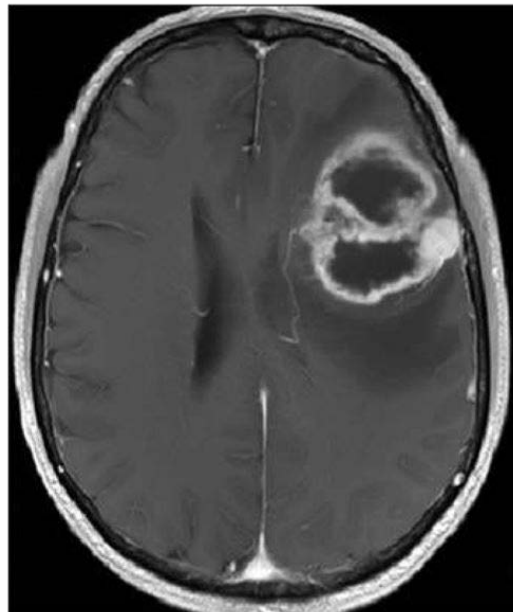


Figure 1: GBM detection. MRI showing 64-year-old man with GBM. (Essig, Nguyen et al. 2013)

1.3 MOLECULAR CHARACTERISTICS OF GLIOBLASTOMA

1.3.1 FIRST ATTEMPTS

In order to achieve a correct understanding of the origin of GBM, it is worth to focus not only on its histopathological characteristics, which define the growth and invasiveness rate established by WHO, but also on the molecular insights that generate this tumor (Goodenberger and Jenkins 2012).

For long it has been known that GBM bears different gene alterations.

- Epidermal Growth Factor Receptor (EGFR), strongly related with the activation of survival pathways, is largely known to be amplified in GBM. In 1985, Libermann et al (Libermann, Nusbaum et al. 1985) described *EGFR* gene amplification in 4 of 10 primary brain tumors analyzed. In 1987, Wong et al (Wong, Bigner et al. 1987) further advanced in this result, confirming Libermann study and concluding that increased expression of the *EGFR* gene is only found in tumors in which alterations of *EGFR* gene structure (i.e., amplification) can be detected.
- Phosphatase and tensin homolog (PTEN) is frequently downregulated in a broad range of tumors, including GBM, due to the loss of the region 23 of the long arm on chromosome 10. Thus, Loss of Heterocigosity (LOH) at chromosome 10q23 was early associated with GBM. In 1994, a molecular analysis of genomic abnormalities in human gliomas (Bello, de Campos et al. 1994) detected not only that the most frequent abnormality observed in the study was LOH for chromosome 10, but also associated this alteration with the amplification of *EGFR* gene. However, the identification of *PTEN* as the gene located in this region did not come up until 1997 (Li, Yen et al. 1997). Since then, PTEN has been described as a key tumor suppressor which alteration drives to the appearance of different tumoral processes.
- In addition to EGFR and PTEN, other genes have for long been largely associated with GBM. That is the case of the Platelet-Derived Growth Factor Receptor (*PDGFR*) (Nister, Libermann et al. 1988), *TP53* (encoding for the tumor suppressor protein p53) (Mercer, Shields et al. 1990, Chung, Whaley et al. 1991) or the Retinoblastoma gene *RB1* (Bello, de Campos et al. 1994, Hirvonen, Salonen et al. 1994).

Thus, two decades of molecular studies identified important genetic events in human GBM. Nevertheless, the understanding of this tumor has largely increased in the last years.

1.3.2 CURRENT CHARACTERIZATION

In the past few year new techniques have arisen, exponentially increasing our knowledge of the key human glioblastoma genes and core pathways and allowing the definition of different GBM subtypes according to their molecular characteristics.

The first attempt to define different GBM subtypes according to their molecular pattern was developed by Philips in 2006 (Phillips, Kharbanda et al. 2006). In 2008, GBM molecular knowledge further increased. Parsons et al (Parsons, Jones et al. 2008) firstly reported IDH1 mutation in 12% of GBM patients. In addition, The Cancer Genome Atlas (TCGA) contains a broad genomic characterization of glioma through microarray platforms (2008), identifying a wide range of mutated genes and three critical altered signaling pathways: (A) RTK/RAS/PI3K, (B) P53 and (C) RB signaling, as explained in the figure below.

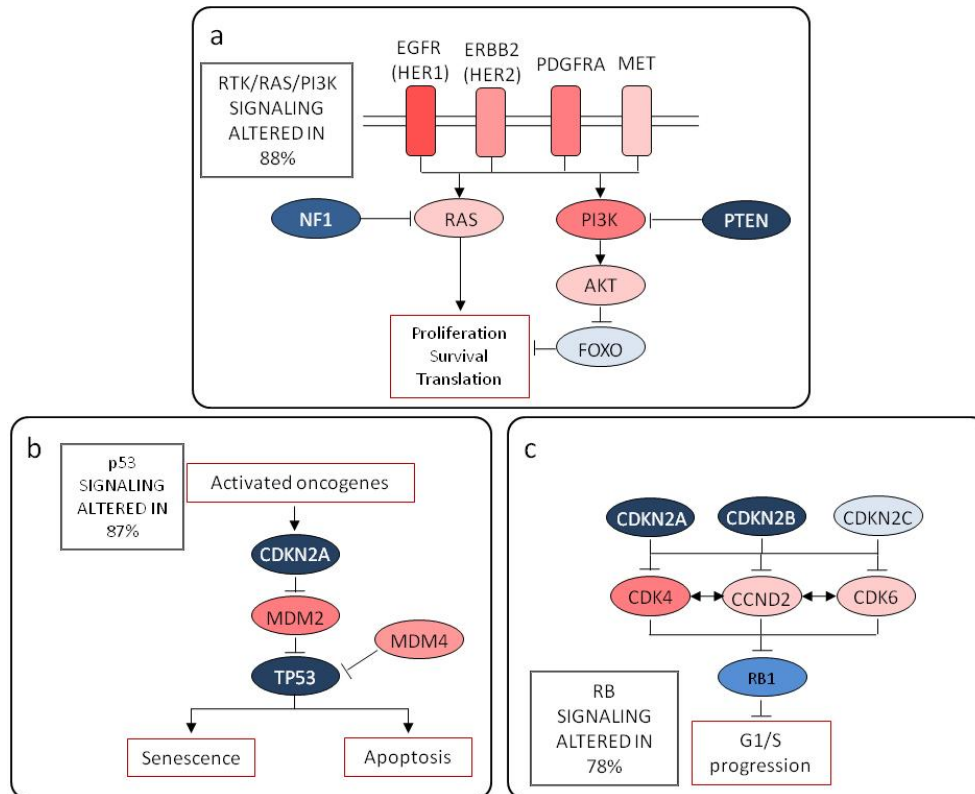


Figure 2: three major altered signaling pathways in GBM. Only altered genes in the pathway are shown. Red indicates activating genetic alterations, with frequent alterations showing deeper shades of red. Conversely, blue indicates inactivating alterations, with darker shades indicating higher percentage of alteration (Cancer Genome Atlas Research 2008).

Furthermore, Genome Wide Association (GWAs) has been used in order to determine Single Nucleotide Polymorphisms (SNPs) associated with the risk of glioma development. Thus, SNPs-containing regions within or near *TERT*, *CCDC26*, *CDKN2B*, *PHLDB1*, *RTEL1* (Shete, Hosking et al. 2009, Wensch, Jenkins et al. 2009) and *EGFR* (Sanso, Hosking et al. 2011) have been identified, further supporting the molecular characterization developed by TCGA.

1.4 CURRENT MOLECULAR SUBTYPES

The copy number data of the core samples described by TCGA has been the basis for the current molecular stratification of GBM subtypes (Verhaak, Hoadley et al. 2010):

- CLASSICAL: the classical subtype is defined by the paired events of chromosome 7 gain (involving *EGFR* amplification) and chromosome 10 loss (involving *PTEN* mutation) in 100% of cases. *vIII EGFR* mutation is also reported in this subtype. 9p21.3 homozygous deletion, targeting *CDKN2A*, is also frequent and almost mutually exclusive with aberrations of other RB pathway components, such as *RB1*, *CDK4* or *CCDN2*.
- MESENCHYMAL: this subtype is defined by the presence of mesenchymal markers such as *CHI3L1* and *MET*. 17q11.2 deletion (containing the gene *NF1*) is very frequent and can be accompanied by *PTEN* mutation. Genes in the Tumor Necrosis Factor (TNF) super family pathway and NF- κ B pathway are highly expressed.
- PRONEURAL: a younger age of onset and longer survival for patients with proneural glioblastoma has been reported. The primary genetic features of this subtype are point mutations in *IDH1* and *IDH2* and focal amplifications of the locus at 4q12, harboring *PDGFRA*. This amplification is seen in all subtypes, but at much higher rate in proneural samples. *TP53* mutations are more frequent in this subtype; however, the classic GBM event (chromosome 7 amplification paired with chromosome 10 loss) is less prevalent.
- NEURAL: this is the most controversial subtype, as the expression pattern is intermediate between the patterns of the mesenchymal and proneural subtypes. It is typified by the expression of neuron markers such as *NEFL*, *GABRA1*, *SYT1* and *SLC12A5*.

In addition, some alterations seem to be found in multiple subtypes. For example, homozygous 9p21.3 deletions, targeting *CDKN2A* and *CDKN2B*, are common in all GBM subtypes. Hypermethylation of the *MGMT* promoter has also been seen in all the subtypes. Finally, deletion of *NFKBIA*, a transcription factor activated by the *EGFR* pathway, is common in the three non-classical subtypes (Goodenberger and Jenkins 2012).

The gene expression-based molecular classification of GBM confers patterns of aberrant gene expression and copy alterations within the tumor, providing promising prognosis markers. This tool, together with the histopathological classification provided by WHO in terms of invasion and growth rate, may help to the establishment of new and personalized strategies in order to overcome the tumor.

1.5 PRIMARY AND SECONDARY GLIOBLASTOMA

GBM can be classified as primary or secondary. Primary GBM, which represents 90% of all the tumors, occurs *de novo* (Ohgaki and Kleihues 2013). In contrast, secondary GBM develops from an initially low grade astrocytoma (WHO grade II or III). Besides, patients with primary GBM tend to be older (mean age 55 years) than patients with secondary GBM (mean age 40 years).

Although primary and secondary GBM are indistinguishable based on histopathology, they evolve from different genetic precursors and harbor distinct genetic alterations. In 1996, Watanabe et al (Watanabe, Tachibana et al. 1996) reported that *EGFR* overexpression and *TP53* mutations are mutually exclusive in the evolution of primary and secondary GBM. Since then, several mutations have been differentially associated to each type of GBM.

The most typical genetic alterations for primary GBM are *EGFR* overexpression, *PTEN* mutations and loss of chromosome 10; whereas secondary GBM includes *TP53* mutations, *IDH1* mutations and *ATRX* mutations. The characterization of the *IDH1* mutation has allowed for reliable molecular differentiation of primary from secondary GBM, and accordingly associates proneural molecular subtype with secondary GBM. In addition, *ATRX* mutations define a subgroup of *IDH* mutant astrocytic tumours with better prognosis. Thus, an unequivocal separation of both types of GBM has been established (Parsons, Jones et al. 2008, Ohgaki and Kleihues 2013, Wiestler, Capper et al. 2013, Wilson, Karajannis et al. 2014).

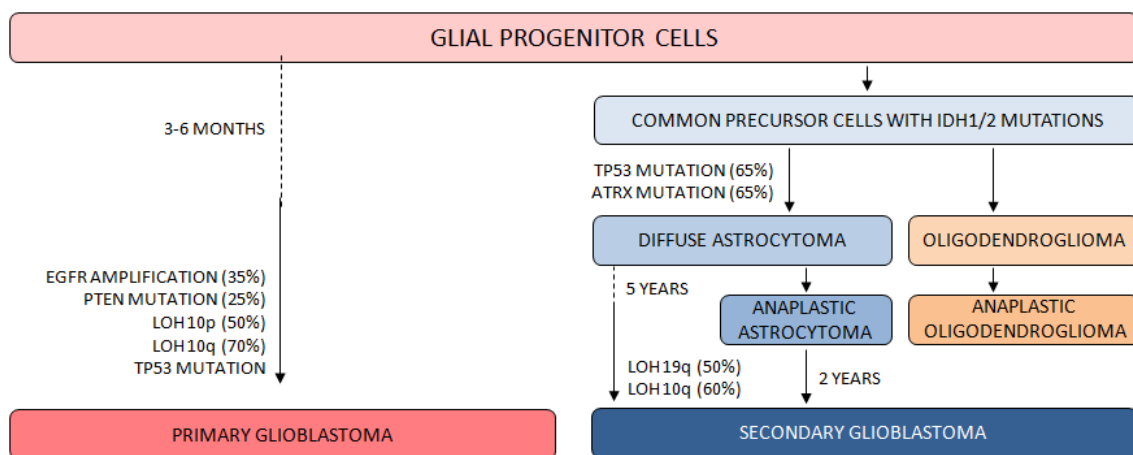


Figure 3: primary and secondary GBM origin. The origin of GBM involves the presence of different mutations, that are developed in the different stages through which the cell proceeds (Ohgaki and Kleihues 2011).

1.6 TREATMENT OF GLIOBLASTOMA

1.6.1 CURRENT STANDARD OF CARE

The current standard of care for patients with GBM includes maximal safe resection, followed by radiotherapy (RT) with concomitant and adjuvant administration of the alkylating chemotherapy Temozolomide (TMZ). Surgical resection alone results in a median survival of 6 months. Surgical resection combined with RT extends median survival to 12.1 months. Addition of TMZ further extends the median survival to 14.6 months (Stupp, Mason et al. 2005, Krakstad and Chekenya 2010, Wilson, Karajannis et al. 2014).

1.6.1.1 SURGICAL RESECTION

Surgery remains an important component in the treatment of GBM. Besides its therapeutic role by reducing intracranial pressure, it allows histological confirmation of the diagnosis (Wilson, Karajannis et al. 2014).

In the last years, advances in surgical imaging techniques have facilitated the delineation of tumor borders. Interestingly, fluorescence-guided surgery with 5-aminolevulinic acid (ALA) for resection of gliomas has been used as an effective therapeutic approach to discriminate malignant tissue from normal brain tissue. ALA-based photodynamic therapy is an effective adjuvant treatment modality for gliomas, and increases progression free at 6 months (Stummer, Pichlmeier et al. 2006, Chen, Wang et al. 2014).

However, in spite of the advances in surgical techniques, ultimately GBM does not have a “surgical answer”.

1.6.1.2 CHEMO AND RADIOTHERAPY

The combination of RT plus TMZ is the most efficacious adjuvant therapy to prolong survival after primary resection. Treatment following surgery usually consists of 6 weeks of RT to the surgical cavity and TMZ, followed by adjuvant TMZ.

For long, RT has been used in the treatment of GBM (Drake, Pfalzner et al. 1963). However, the current standard of care is focal and usually consists of 60 Gy of RT delivered in fractions of 2 Gy over 6 weeks (Leibel and Sheline 1987).

The addition of TMZ to the current standard care of GBM was proposed by Stupp and collaborators in 2001 establishing the so-called “Stupp regimen” standard of care for GBM treatment (Stupp and Newlands 2001). It consists of 75 mg/m²/day of TMZ for 6 weeks when given in combination with RT. For adjuvant therapy following completion of RT, patients receive 150 mg/m²/day for 5 days every 28 days for at least 6 cycles (Stupp, Mason et al. 2005).

TMZ is an alkylating agent that introduces a methyl group to O₆-guanine. This methyl group can be removed by O₆-Methylguanine Methyltransferase (MGMT), conferring resistance to chemotherapy. In some patients, MGMT expression has been decreased or silenced by

methylation of the promoter region, inducing sensitivity to the treatment. Thus, patients with unmethylated MGMT promoter are much less responsive to TMZ (Bobola, Tseng et al. 1996, Hegi, Liu et al. 2008).

1.6.2 THERAPIES UNDER INVESTIGATION

1.6.2.1 MOLECULARLY TARGETED THERAPIES

The knowledge of the molecular characteristics of GBM patients facilitates the establishment of personalized therapies according to the mutations harboured by the patient.

These findings have inspired the investigation of molecular therapies towards tumor-specific recurrent genetic alterations, addressing mainly (1) Tyrosine Kinase Receptors (TKR); (2) angiogenesis pathways, (3) survival pathways and (4) apoptosis. The genes and pathways targeted in personalized GBM therapy are summarized in Table 3.

However, despite these advances in molecular personalized therapy, GBM is broadly known to harbor different mutations not only intertumorally but also intratumorally. This scenario complicates the treatment and generally results in poor outcome following monotherapy; nonetheless, it can be ameliorated through the combination of different drugs, or the combination with surgery, chemo or radiotherapy.

| TARGET | | DRUG |
|---------------------|--------------------------|----------------------------------|
| TKR | EGFR | Tyrosine Kinase Inhibitors (TKI) |
| | | Antibodies |
| | PDGFR | TKI |
| Angiogenic pathways | VEGFR | Bevacizumab |
| RAF and MAPK | Farnesyl Transferase | Tipifarnib |
| | | Lonafarnib |
| mTOR | AKT | Perifosine |
| | mTOR | Rapamycin |
| | | Temsirolimus |
| | Sirolimus | |
| Apoptosis | Bcl2 | Gossypol |
| Multiple pathways | Raf kinase, VEGFR, PDGFR | Sorafenib |

Table 3: different pathways and proteins targeted by personalized molecular therapies.

1.6.2.2 IMMUNOTHERAPY

Immunotherapy attempts to harness the immune system to selectively destroy tumor cells. There exist passive and active strategies.

- Passive strategies utilize immune system components to target the tumor cells, without requiring the activation of the patient’s native immune response (Wilson, Karajannis et al. 2014).
- In contrast, active strategies attempt to stimulate the patient’s native immune response against the tumor, being similar in concept to vaccination. They include peptide-based and cell-based approaches .

1.6.2.3 GENE THERAPY

This method involves the delivery of genetic material into tumor cells for therapeutic purposes. Although some therapies have shown promising results in preclinical trials, clinical trials have been unable to show any significant therapeutic efficacy (Wilson, Karajannis et al. 2014).

1.7 GLIOBLASTOMA ORIGIN: CANCER STEM CELLS

For long, the oncogenes-tumor suppressor genes hypothesis, which deregulation derives in the accumulation of point mutations in few or even single founder cells, has been accepted in order to explain the origin of tumors. However, during the last 10-15 years, new tumor-origin related hypothesis have arisen.

The most accepted one is the “Cancer Stem-like Cells” (CSCs) hypothesis. CSCs firstly appeared in bibliography more than 30 years ago and the investigation was generally focused on the isolation and culture maintenance of the cells (Mattox and Von Hoff 1980, Hager and Heppner 1983). However, advances on this field exponentially increased in 2000s, when this population was proposed to be responsible of tumor initiation and recurrence after the treatment (Reya, Morrison et al. 2001, Dick 2003). In particular, this view was proposed due to (1) the similarities in the mechanisms that regulate self-renewal of normal stem cells and cancer cells; (2) the possibility that tumor cells might derive from normal stem cells; and (3) the possibility that tumor might contain CSCs.

Soon after that, Brain Cancer Stem-like Cells (Glioma Stem-like Cells of GSCs) evidences emerged. Thus, from 2002 to 2004 different groups independently identified, isolated and characterized GSCs (Ignatova, Kukekov et al. 2002, Hemmati, Nakano et al. 2003, Singh, Clarke et al. 2003, Galli, Binda et al. 2004).

Nowadays, the presence and involvement of GSCs in the initiation and propagation of brain tumors is broadly accepted, and the comprehension of their biology is a key factor in our attempt to overcome the disease.

1.7.1 NEURAL STEM CELLS (NSCs) IN THE ADULT CENTRAL NERVOUS SYSTEM (CNS)

Stem cells existence in CNS was a great discovery which challenged the “no new neuron” dogma that had persisted for decades. In 1960s, genesis of new and functional brain cells

(neurogenesis) was described (Altman and Das 1965, Altman 1966). Currently, it is well described that neurogenesis of mature cells persists throughout adult life within discrete brain regions, mainly the dentate gyrus of the hippocampus and the subventricular zone of the forebrain lateral ventricles. This process is probably crucial for the maintenance of brain integrity and optimal function, and involves the existence of a “stem-cell compartment” inside the brain (Ming and Song 2005). This compartment contains highly undifferentiated cells able to develop multipotency and self-renewal capacity by undergoing asymmetric divisions. Disruption of the regulatory mechanisms that control these processes is probably involved in the genesis of GSCs, which is supported by the fact that many GBMs develop next to the subventricular zone (Sanai, Alvarez-Buylla et al. 2005, Vescovi, Galli et al. 2006).

1.7.2 GLIOMA STEM CELLS

1.7.2.1 GENERAL VIEW AND SELECTION OF THE POPULATION

A valuable feature of adult NSCs, firstly demonstrated by Reynolds and Weiss in 1992 (Reynolds and Weiss 1992), is their ability to expand when placed in culture and stimulated with the appropriate growth factors, such as Epidermal Growth Factor (EGF) and Fibroblast Growth Factor (FGF). This “neurosphere approach” sets up that in a serum-free, selective culture system in which most differentiating or differentiated cells would die, neural stem cells respond to mitogens, divide and form neurospheres that can be dissociated and re-plated to generate secondary neurospheres. Thus, neurosphere assay is the preferred method for the *in vitro* isolation, expansion and identification of NSCs.

The finding of GSCs by the groups mentioned above allowed the establishment of functional and molecular characteristics of these cells: functionally, GSCs respond to the same mitogens that activate NSCs. Thus, they are also able to grow in a neurosphere assay; molecularly, GSCs own some molecular features, which are summarized in the table below:

| GENE/PROTEIN | FUNCTION | MARKER OF | EXPRESSION IN GSCs |
|----------------------------|--|-----------------|--------------------|
| GFAP | Astrocytic marker | Differentiation | Downregulated |
| β III Tubulin (TUJ1) | Neural marker | Differentiation | Downregulated |
| NESTIN | Neural progenitor marker | Stemness | Upregulated |
| SOX2 | Early transcription factor expressed in NSCs and the developing neural tube | Stemness | Upregulated |
| BMI-1 | Gene required for self-renewal and proliferation of normal and leukemic hematopoietic stem cells | Stemness | Upregulated |
| Mushashi (<i>MSI1</i>) | Neural RNA-binding protein expressed in NSCs | Stemness | Upregulated |
| CD133 | Cell surface protein expressed on all fetal human NSCs | Stemness | Upregulated |
| CD44 | Cell-surface glycoprotein involved in cell–cell interactions, cell adhesion and migration | Stemness | Upregulated |

Table 4: GSCs markers. Functions and expression.

In addition to functional and molecular markers, stem cell populations present high expression of ATP-binding cassette (ABC) drug transporters, which allow the efflux of cytotoxic agents protecting cells and contributing to resistance to drugs and toxins. In addition, ABC transporters can efflux the fluorescent dye Hoechst33342 which give ABC-high population an unique profile referred to as the side population when analyzed by flow cytometry (Dean, Fojo et al. 2005). Thus, this side population would be enriched in GSCs.

Nevertheless, the presence of these markers does not guarantee the stem properties of the tumor cell. Thus, not all neurosphere-forming cells express GSCs markers neither all cells expressing GSCs markers are able to form neurospheres. In the same way, the side population does not contain a pure stem-cell population. Thus, a combination of both functional and molecular GSCs selection is required in order to obtain a properly enriched GSCs culture.

1.7.2.2 ESSENTIAL FEATURES ON GLIOMA STEM CELLS

As seen above, the more techniques combined the more GSCs population obtained. However, the essential features that the population must present, independently of the methods used in order to obtain the GSCs are (Vescovi, Galli et al. 2006):

- Cancer-initiating ability upon orthotopic implantation (tumors should be a phenocopy of the tumor of origin).
- Extensive self-renewal ability, demonstrated either *ex vivo* (by showing both sequential-clonogenic and population-kinetic analyses) or *in vivo* (by serial, orthotopic transplantation).
- Differentiation capacity.
- Karyotypic of genetic alterations.
- Aberrant differentiation properties.
- Capacity to generate non-tumorigenic end cells.

Independently of the GSCs-isolation technique, if the population does not fit to these items it cannot be considered a GSC-enriched population.

1.7.2.3 TARGETING GSCs POPULATION

GSCs have been described as the responsible of tumor initiation in different models (Soltanian and Matin 2011) such as breast, brain, lung, prostate, testis, ovary, colon, skin, liver or acute myeloid leukaemia. In addition, due to their chemo and radioresistance, they are proposed to be involved in relapses following tumor treatment. Thus, different strategies have been designed in order to target this small population (they represent less than 1% of the tumor mass). Improvement in the comprehension of GSCs biology is a key factor in order to design efficient approaches to overcome this population and, extensively, the whole glioblastoma tumor mass.

Currently, different approaches have been designed in order to specifically target GSCs. They are summarized in the figure and briefly explained below (Cho, Lin et al. 2013):

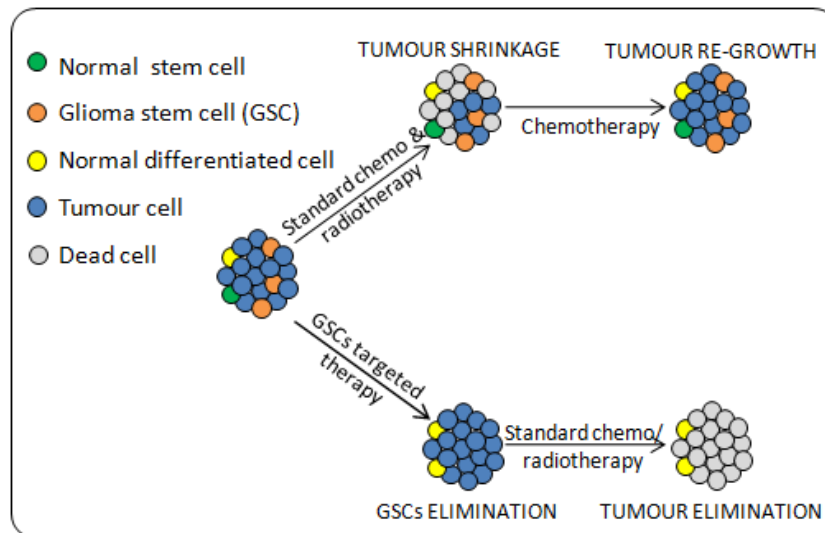


Figure 4: mechanism of action of GSCs-targeted therapies. The focus on GSCs elimination avoids tumour regrowth and promotes tumour elimination (Cho, Lin et al. 2013).

Targeting GSCs pathways is a strategy based on targeting key routes involved in GSCs expansion:

- NOTCH: this protein promotes proliferative signaling during neurogenesis. Thus, when its activity is inhibited, neural differentiation is promoted. Consistently, its blockade reduces neurosphere growth and clonogenicity in vitro (Hovinga, Shimizu et al. 2010).
- HEDGEHOG: cyclopamine-induced HEDGEHOG downregulation reduces stem-like cancer cells in glioblastoma (Bar, Chaudhry et al. 2007).
- VEGF: GSCs have been reported to develop in the vascular niche and to interact with their microenvironment (Borovski, Verhoeff et al. 2009). Thus, targeting the vascular niche through VEGF inhibitors has shown partial effect on reducing GSCs population (Calabrese, Poppleton et al. 2007).
- TGF- β : The TGF- β pathway acts as an oncogenic factor in advanced tumors, including high-grade gliomas (Massague 2008). Upon TGF- β binding, the receptor complex phosphorylates the transcription factors Smad2 and Smad3, which then bind to Smad4 and accumulate in the nucleus, where they regulate transcription. Thus, TGF- β can increase the self-renewal capacity of glioma-initiating cells (GICs) through the induction of LIF (Penuelas, Anido et al. 2009) or SOX2 (Ikushima, Todo et al. 2009). Treatment with the TGF- β receptor (TbRI) inhibitor repressed the expression of ID1 and CD44 in the tumor of the patient, confirming that the inhibition of the TGF- β pathway targets the GSCs population (Anido, Saez-Borderias et al. 2010).

- JAK-STAT pathway: targeting this route has also been demonstrated to exert an effect on reducing GSCs population. Stechishin et al showed slow tumor progression following STAT3 downregulation (Stechishin, Luchman et al. 2013). Besides, TGF- β pathway can also activate JAK-STAT route through induction of LIF (Penuelas, Anido et al. 2009), suggesting that anti-TGF- β therapy might target both pathways.

Besides targeting GSCs expansion pathways, other strategies have been tested regarding GSCs specific elimination:

- Targeting GSCs by radio sensitizers: this strategy is based on the use of different drugs combined with radiotherapy in order to sensitize GSCs to these agents. In this direction, ATM inhibition (Vecchio, Daga et al. 2014) radiosensitized GSCs.
- Targeting GSCs by promoting cell differentiation: chemo and radiotherapy are unable to target GSCs. Thus, one of the proposed strategies in order to overcome this population is based on their differentiation to chemo and radiosensitive brain tumor cells. Piccirillo and collaborators reported (Piccirillo, Reynolds et al. 2006) the role of Bone Morphogenetic Protein Family, particularly BMP4, in the differentiation of GSCs towards normal tumor cells by reducing the CD133-positive population *in vitro* and tumor growth *in vivo*.
- Targeting GSCs by immunotherapy: in the same way this technique is used to overcome GBM, immunotherapy strategies have arisen in order to eliminate GSCs. For instance, Ahmed and colleagues (Ahmed, Salsman et al. 2010) generated HER2-specific T cells capable to target not only HER2-positive GBMs, but also the CD133-positive stem cell compartment.
- Targeting GSCs by gene therapy: gene therapy has also been utilized in order to target GSCs. In this direction, Jiang et al (Jiang, Gomez-Manzano et al. 2007) reported adenovirus Delta-24-RGD, targeted to the abnormal retinoblastoma pathways, reduced the stem cell population in the tumor. Besides, Gangemi et al. (Gangemi, Griffiero et al. 2009) reported that silencing SOX2 expression by using retroviral vectors harboring a microRNA (miRNA) engineered to target SOX2 mRNA promoted loss of proliferation and tumorigenicity in GSCs. Finally, it is worth to mention lentiviral silencing of STAT3 avoided GSCs proliferation and self-renewal (Sherry, Reeves et al. 2009) .

In conclusion, the knowledge of GSCs biology has greatly increased in the recent years, providing new targets with potential therapy interest. Either way, to eliminate this population is an unavoidable step in order to overcome GBM.

2 POLY (ADP-RIBOSE) POLYMERASE 1 (PARP-1)

2.1 GENERAL VIEW

Poly (ADP-ribose) polymerases (PARPs), more recently named ADP-ribosyltransferases (ARTs) (Hottiger, Hassa et al. 2010) are a group of DNA-dependent nuclear enzymes which catalyze the synthesis and transfer of negatively charged ADP-ribose moieties from nicotinamide-adenine-dinucleotide (NAD⁺) to a number of target protein substrates (Peralta-Leal, Rodriguez-Vargas et al. 2009). The most representative member of this family is PARP-1 which was firstly described by Chambon et al. in 1963 (Chambon, Weill et al. 1963). Since then, many advances have been developed to decipher both structural, biological aspects and pathological consequences of misregulation of the PARP family.

2.2 PARP EXPRESSION

PARP-1 is the original constituent and also the most well studied PARP enzyme. Encoded by the region 1q41-q42 (Herzog, Zabel et al. 1989), it has a molecular weight of 114 kDa. It is constitutively expressed at high levels. In fact, PARP-1 promoter owns features typically found in housekeeping genes. Consistently, PARP-1 mRNA is present in all tissues, albeit at varying levels (Meyer-Ficca, Meyer et al. 2005).

Nevertheless, PARP-1 modulation is mainly developed not at the mRNA but at the protein level. Although PARP-1 is constitutively expressed, PARP-1 enzymatic activity is only switched-on under certain conditions and owns a fine-tuned metabolism regulation.

2.3 PARP METABOLISM

PARP-1 enzymatic activity consists on the synthesis of a polymer of poly(ADP-ribose) or PAR. In order to perform this activity, PARP-1 owes both poly(ADP-ribosyl) synthetase and transferase enzymatic activity. This process, also named parylation, possesses a life cycle that can be described as follows (Diefenbach and Burkle 2005, Hassa and Hottiger 2008).

2.3.1 PAR SYNTHESIS

– Initiation phase:

Firstly, poly(ADP-ribose) synthetase activity catalyzes the formation of ADP-ribose from the oxidized form of nicotinamide adenine dinucleotide (NAD⁺), by cleavage of the glycosidic bond between nicotinamide and ribose. As NAD⁺ is an essential coenzyme/transmitter for the generation of ATP, NAD⁺ depletion will also result in ATP depletion.

Subsequently, ADP-ribose is covalently attached to acceptor proteins, via formation of an ester bond between the protein (through glutamate, aspartate or lysine residues) and ADP-

ribose. (Ogata, Ueda et al. 1980, Ogata, Ueda et al. 1980, Diefenbach and Burkle 2005, Zhang, Wang et al. 2013).

– Elongation and branching reaction:

In addition, PARP-1-mediated poly(ADP-ribosyl) transferase activity is able to catalyze elongation and branching reactions using additional ADP-ribose units from NAD⁺. Polymer elongation involves the catalysis of a 2'-1' glycosidic bond, where the covalently bound mono-ADP-ribose serves as a starting unit. This generates novel ribosyl-ribosyl linkages and eventually results in the formation of polymers with chain lengths of approximately 200 ADP-ribose subunits. Branching points on the polymer occur on average after 20 ADP-ribose units.

2.3.2 PAR DEGRADATION

Poly(ADP-ribose) metabolism is very dynamic. PAR is rapidly synthesized at sites containing DNA strand breaks and is then rapidly degraded (half-life 0.5-5 min) (Boulikas 1992).

– PAR degradation:

Poly(ADP-ribose) glycohydrolase (PARG) (Miwa and Sugimura 1971) mediates PAR degradation. PARG is present in mammalian cells in three different isoforms: PARG99 and PARG102 (PARG isoforms of 99 kDa and 102 kDa, respectively), which localize in the cytoplasm; and PARG110 (PARG isoform of 111 kDa), which localizes predominantly to the nucleus (Meyer-Ficca, Meyer et al. 2004).

It possesses both endoglycosidase and exoglycosidase activity. First, both activities release free ADP-ribose monomers and shorter polymers from PARPs (Brochu, Duchaine et al. 1994). Second, PARG switches to a distributive exoglycosidic mechanism after polymers are reduced to a certain size by the endoglycosidic mode (Davidovic, Vodenicharov et al. 2001).

In addition to PARG, other PAR-degrading enzymes have been identified and characterized. It is worth to mention the ARH (ADP-ribosyl hydrolase) family. ARH3 is a PAR-degrading hydrolase that, similarly to PARG, can catalyze the removal of PAR but not mono(ADP-ribose). It has been implicated in the degradation of PAR that is associated with the mitochondrial matrix, but the function of ARH3 *in vivo* remains poorly understood (Oka, Kato et al. 2006).

– Ester bound breakage:

Once PAR has been degraded, ADP-ribosyl protein lyase removes the proximal mono(ADP-ribosyl) moiety bound to the acceptor protein (Oka, Ueda et al. 1984). However, during many years, lack of knowledge about these enzymes left this field unclear. Recently, a family of macrodomain enzymes present in viruses, yeast and animals that reverse cellular ADP-ribosylation by acting on mono-ADP-ribosylated substrates has been described (Jankevicius, Hassler et al. 2013, Sharifi, 2013 #437, Rosenthal, 2013 #439). Thus, Terminal ADP-Ribose protein Glycohydrolase (TARG1), MacroD1 and MacroD2 have reported as responsible for ester bound breakage.

– AMP and NAD obtaining:

The final products of PAR degradation are free poly(ADP-ribose) and ADP-ribose monomer, the latter being a potent protein-glycating sugar capable of causing protein damage. ADP-ribose pyrophosphatase (Bernet, Pinto et al. 1994) converts free ADP-ribose molecules into AMP and ribose 5-phosphate, thus producing compounds much less prone to induce glycation which can react in order to generate NAD⁺ (Diefenbach and Burkle 2005).

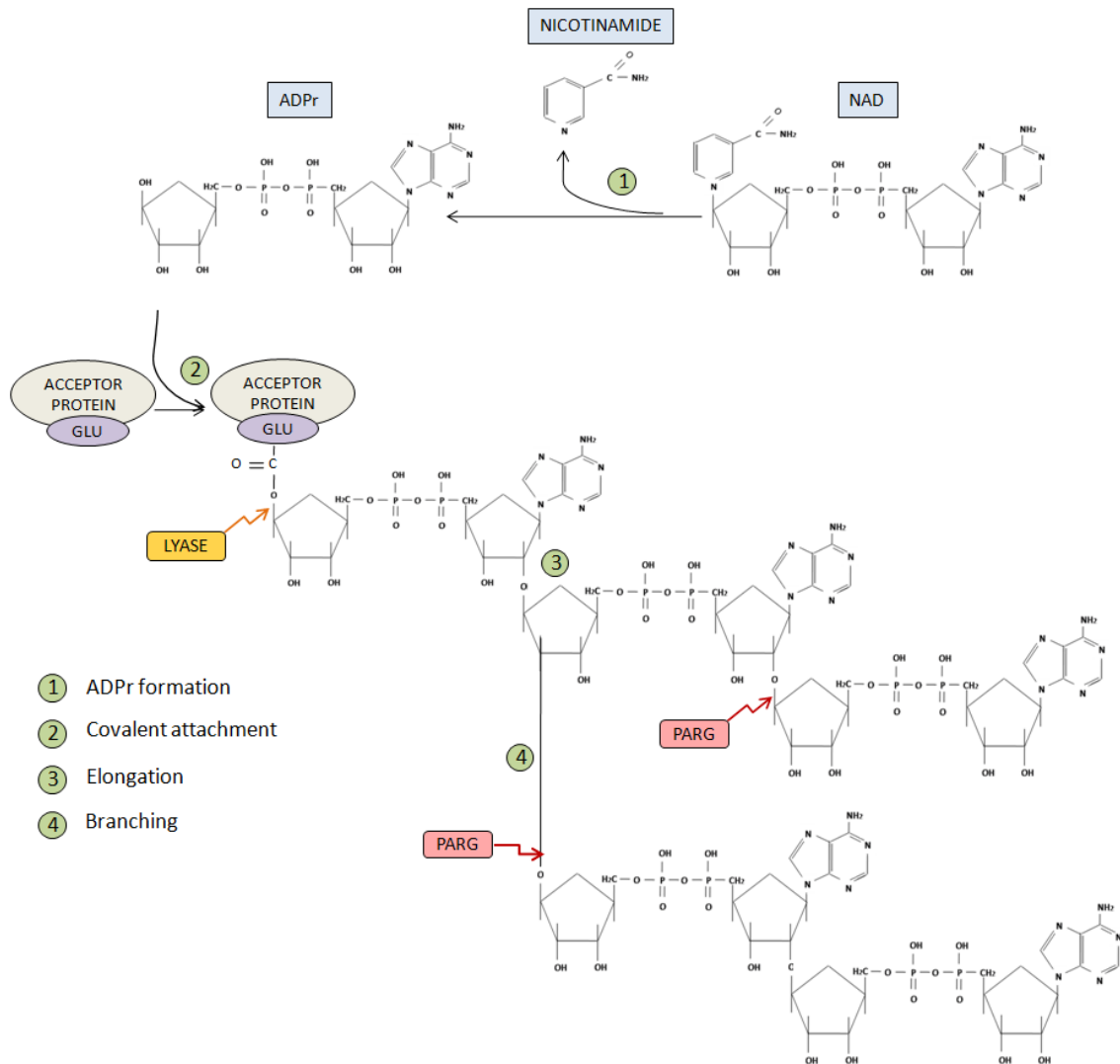


Figure 5: PARP metabolism. Different steps in polymer formation are shown in green. In contrast, the proteins involved in polymer degradation are shown in red and yellow (Kim, Zhang et al. 2005, Schreiber, Dantzer et al. 2006).

2.4 PARP-1 STRUCTURE

PARP-1 structure was firstly described in 1984 (Kameshita, Matsuda et al. 1984) and is composed by three domains:

- DNA-binding domain:
The 46 kDa DNA-binding domain contains three zinc-fingers (Zn1, Zn2, Zn3) which have different roles in DNA binding, interdomain cooperation, chromatin compaction and protein-protein interactions. Zn1 and Zn2 were firstly described in 1989 (Menissier-de Murcia, Molinete et al. 1989); however, Zn3 was recently described (Langelier, Servent et al. 2008). Furthermore, it has a Nuclear Localization Signal (NLS) (Schreiber, Molinete et al. 1992), which includes a DEVD motif specific for caspase cleavage (Kaufmann, Desnoyers et al. 1993).
- Automodification region:
This 22 kDa domain contains glutamate, aspartate and lysine residues that serve as putative acceptors for autoPARylation (Desmarais, Menard et al. 1991). In addition, it possesses a leucine zipper motif that mediates homo or heterodimerization (Uchida, Hanai et al. 1993). Finally, it includes a breast cancer-associated protein C-terminal motif (BRCT), which mediates protein-protein interactions (Bork, Hofmann et al. 1997).
- NAD-binding domain, which functions as the catalytic domain:
The 54 kDa catalytic domain contains the “PARP signature” sequence required for the catalysis of PAR synthesis (Ruf, Mennissier de Murcia et al. 1996). It also has a tryptophan-, glycine-, and arginine-rich WGR domain that is required for DNA-damage induced PAR synthesis (Langelier, Planck et al. 2012).

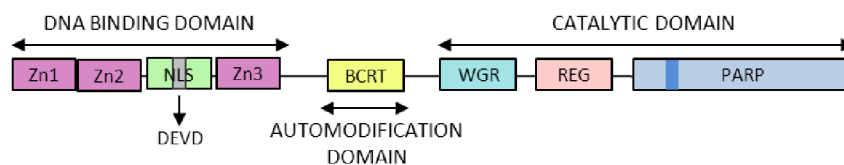


Figure 6: PARP-1 structure. The structure of the main member of PARP family is described above. Different domains are detailed in different colours (Rouleau, Patel et al. 2010).

2.5 PARP FAMILY

2.5.1 CLASSIFICATION

PARP proteins constitute a family of 17 members which share a highly conserved PARP signature motif (PARP signature) inside the catalytic domain (Peralta-Leal, Rodriguez-Vargas et al. 2009). However, this signature is not enough as to develop a functional classification. In contrast, the classification is developed according to their domain architectures and the type of enzymatic activity. Thus, PARP family was firstly divided in three subgroups (Hassa and Hottiger 2008, Rouleau, Patel et al. 2010) but currently, it is divided in four subfamilies as follows (Schreiber, Dantzer et al. 2006, Gibson and Kraus 2012):

- DNA-dependent PARPs which are activated by DNA lesions through their DNA-binding domain.
 - PARP-1 (ARTD1)
 - PARP-2 (ARTD2)
 - PARP-3 (ARTD3)

- Tankyrases, which contain large ankyrin domain repeats that facilitate protein-protein interactions. Sterile α motifs (SAM), also involved in protein-protein interactions, are specific of this subfamily too.
 - Tankyrase-1 (PARP-5A, ARTD5)
 - Tankyrase-2 (PARP-5B, ARTD6)

- CCCH PARPs, which contain CCCH motifs. They are zinc finger motifs of the $CX_{7-11}CX_{3-9}CX_3H$ type that is a putative RNA-binding module.
 - TIPARP (PARP-7, ARTD7)
 - PARP-12 (ARTD12)
 - PARP-13 (ARTD13)

- Macro-PARPs, which are characterized by the presence of macrodomain folds. These domains mediate the localization of the protein to positions of poly and perhaps also mono ADP-ribosylation.
 - BAL1 (PARP-9, ARTD9)
 - BAL2 (PARP-14, ARTD8)
 - BAL3 (PARP-15, ARTD7)

- Other PARP proteins do not accommodate into any of these four subgroups (Gibson and Kraus 2012).

| | |
|--|--|
| <ul style="list-style-type: none"> • PARP-4 (ARTD4) • PARP-6 (ARTD17) • PARP-8 (ARTD16) | <ul style="list-style-type: none"> • PARP-10 (ARTD10) • PARP-11 (ARTD11) • PARP-16 (ARTD15) |
|--|--|

In addition, there are some domains which are not specific of a PARP subfamily. For instance, WWE domain is putative protein–protein interaction motif that contains two conserved Trp residues and one Glu residue. The most common PARP proteins will be summarized below, apart from PARP-1 which will be further described in the next sections.

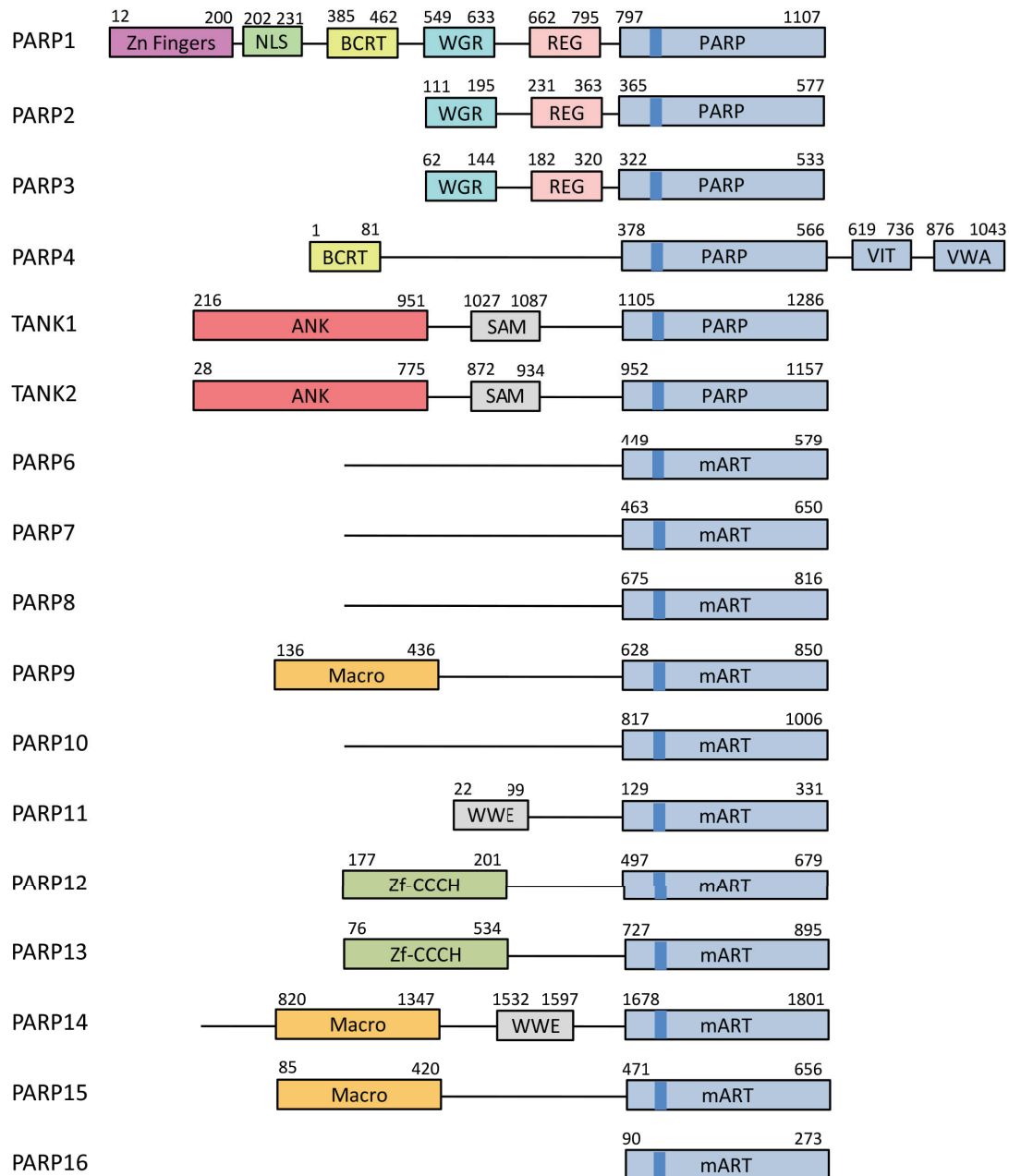


Figure 7: PARP family. The structure of the different members of PARP family is described. Different domains are detailed in different colours. Brighter blue shows PARP signature sequence, common throughout all the members of the family (Riffell, Lord et al. 2012). Adapted.

2.5.2 BRIEF DESCRIPTION OF PARP FAMILY MEMBERS

2.5.2.1 DNA-DEPENDENT PARPs

PARP-1, PARP-2 and PARP-3 have in common two C-terminal domains: WGR and the catalytic domain. In contrast, the N-terminal region (NTR) of PARP-1 is over 500 residues and includes four regulatory domains, whereas PARP-2 and PARP-3 have smaller NTRs (70 and 40 residues, respectively) of unknown structural composition and function. In addition, PARP-2 and PARP-3 are preferentially activated by DNA breaks harboring a 5-phosphate, suggesting selective activation in response to specific DNA repair intermediates, in particular structures that are suitable for DNA ligation (Langelier, Riccio et al. 2014).

2.5.2.2 TANKYRASES

Tankyrase-1 (TANK1) 142 kDa protein was firstly identified in 1998 (Smith, Giriat et al. 1998). Some years later, in 2001, Tankyrase-2 was described (Kaminker, Kim et al. 2001). Both proteins share Ankyrin-domain repeats, and although genetic knockout of either *Tnks* or *Tnks2* (the genes encoding TANK1 and TANK2, respectively) in mice generates no obvious phenotype, the inactivation of both genes is embryonically lethal, suggesting some level of functional redundancy between the two enzymes (Chiang, Nguyen et al. 2006, Chiang, Hsiao et al. 2008).

2.6 PARP ACTIVATION MECHANISMS

The “central dogma” of PARylation states that PARP-1 is activated by DNA damage. In fact, DNA strand breaks remarkably increase basal activity of PARP-1 (up to 500 times) (de Murcia, Schreiber et al. 1994). Consistently, reactive oxygen and nitrogen species (ROS and RNS, respectively) as well as DNA alkylating agents have been used to trigger PAR synthesis in various cellular models (Burkle and Virag 2013).

Several lines of evidence indicate that PARP-1 may also be activated in the absence of DNA breakage. Special non-B DNA structures such as bent, cruciform DNA or stably unpaired DNA regions have been described as stimulators of PARP activity (Lonskaya, Potaman et al. 2005). In addition, post-translational protein modifications may also trigger PARP-1 activation. PARP-1 interacts with various signaling pathways often involving a kinase phosphorylating PARP-1, which leads to its activation. Variations to this theme include (1) direct protein–protein interaction between PARP-1 and a pre-phosphorylated kinase. For instance, PARP-1 interaction with phosphorylated ERK2 derives in PARP-1 activation (Cohen-Armon 2007, Cohen-Armon, Visocek et al. 2007) and (2) kinase-mediated inhibition of PARP-1. (Suzuki, Tanaka et al. 1987, Bauer, Farkas et al. 1992, Hegedus, Lakatos et al. 2008). Furthermore, other posttranslational modifications such as acetylation (Hassa, Haenni et al. 2005) or ADP-ribosylation (Loseva, Jemth et al. 2010, Burkle and Virag 2013) are necessary for PARP to develop its function.

2.6.1 MOLECULAR EVENTS FOLLOWING PARP ACTIVATION

As explained in section 3, the best well-described effect of PARP activation is PARylation, or covalently protein modification by PAR. This process may affect PARP itself, or other proteins that become PARylated following PARP activation.

However, other mechanisms underlie PARP activation and PAR synthesis. They are summarized below:

- Non-covalent binding of selected proteins to free PAR (Sauermann and Wesierska-Gadek 1986, Panzeter, Realini et al. 1992). Consistently, some years later the first PAR-binding motif was identified (Pleschke, Kleczkowska et al. 2000), and in recent years, additional PAR-binding motifs have been discovered, such as WWE domain (Aravind 2001) a PAR-binding zinc finger motif (PBZ) (Ahel, Ahel et al. 2008), histone macrodomain (Timinszky, Till et al. 2009), or BCRT and FHA domains (Li, Lu et al. 2013).
- Free PAR can also serve as an important intracellular signaling molecule. This has been exemplified by the discovery of cell death induced by free PAR triggering the release of apoptosis-inducing factor from mitochondria (Yu, Wang et al. 2002, Andrabi, Kim et al. 2006, Yu, Andrabi et al. 2006, Wang, Kim et al. 2011).
- Under certain circumstances (mainly massive DNA damage) a cellular consequence of PARP activity is not only the formation of PAR, but also a significant consumption of its substrate, NAD⁺ as firstly reported by Berger et al (Berger, Sims et al. 1983). NAD⁺ depletion has important consequences on cell survival, which will be further explained in next sections.

These molecular events are responsible of the different functions and cellular effects that take place after PARP activation.

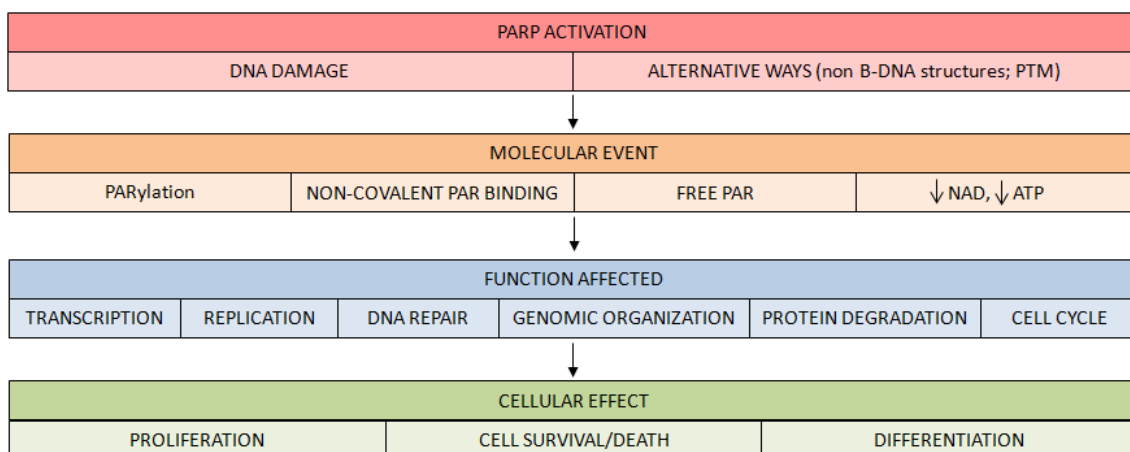


FIGURE 8: MOLECULAR EVENTS FOLLOWING PARP ACTIVATION. Once PARP is activated, downstream events of PARP signaling take place, involving either covalent PARylation of substrates, non-covalent binding of PAR polymer to proteins bearing a PAR-binding motif, liberation of free PAR to the cell or lowering of cellular NAD⁺/ATP levels. Via these pathways PARP/PARylation regulates functions such as transcription, replication, DNA repair, protein degradation and cell cycle, mediating various cellular phenomena such as proliferation, cell survival and cell death or differentiation.

2.7 PARP FUNCTIONS:

2.7.1 TRANSCRIPTION

PARP proteins participate in transcription processes through different molecular mechanisms that are described below (Kraus and Lis 2003).

2.7.1.1 PARP AND CHROMATIN MODULATION

in 1982, PARP was described to PARylate chromatin proteins (Poirier, de Murcia et al. 1982). Thus, the structure of chromatin changes from a condensed state to a less concentrated or “loose” state, which facilitates gene transcription. More recently PARP was described (Tulin and Spradling 2003) as a key factor in local chromatin loosening that may facilitate gene transcription and chromatin remodeling in *Drosophila* development. Furthermore, NAD⁺ status in the cell has a key role in PARP-mediated chromatin modulation (Kim, Mauro et al. 2004). Using NAD⁺ as a substrate, PARP-1 catalyzes its own automodification and as consequence, negatively charged polymer interacts with histones (H1, H2A, H2B), changing chromatin structure from the condensed to the “loose” state described above. In contrast, in absence of NAD⁺, PARP-1 binding to nucleosomes promotes chromatin compaction into higher structure orders. Finally, PARP-1 promotes RNApII activity through its interaction with RNApII promoters (Krishnakumar, Gamble et al. 2008). In presence of PARP-1, histone H1 is depleted at these promoters, which is associated with actively transcribed genes. Nevertheless, a high rate H1/PARP-1 promotes the opposite effect which is the repression of transcription.

Otherwise, an interaction between PARP-1 and chromatin-remodeling factors has been reported. The nucleosome remodeling ATPases ALC1 and ISWI have been described to interact with PARP. However, this interaction is developed through two different mechanisms, not fully understood: PARylated ISWI inhibits its ATPase activity, which decreases its binding affinity for nucleosomes, (Sala, La Rocca et al. 2008). Nevertheless, PARylated ALC1 stimulates its ATPase activity, promoting its recruitment to nucleosomes and the chromatin remodeling activity (Gottschalk, Timinszky et al. 2009).

2.7.1.2 PARP ROLE AT ENHANCER/PROMOTER REGULATORY COMPLEXES

For long, the ability of PARP-1 to recognize particular DNA sequences, allowing its role as a standard enhancer factor, has been described. More recently, PARP-1 direct binding to DNA has been well reported. Amire et collaborators (Amiri, Ha et al. 2006) reported that activated PARP-1 enhances CXCL1 expression owing to the loss of PARP-1 binding to the CXCL1 promoter. Besides, PARP-1 binding site in BCL6 locus and BCL6 transcription activation following PARP inhibition has been described (Ambrose, Papadopoulou et al. 2007). However, the exact mechanism by which PARP-1 develops its enhancer binding role remains unclear.

2.7.1.3 PARP AND SPLICING

There are two kinds of proteins that can be PARylated in order to decrease their ability to bind to RNA, consequently modulating splicing processes: Heterogeneous nuclear ribonucleoproteins or hnRNPs (which join to exonic and intronic splicing silencers) and Serine-Arginine-rich splicing factor SR (which join to exonic and intronic splicing enhancers) (Ji and Tulin 2010).

2.7.1.4 PARP-1 TRANSCRIPTIONAL CO-REGULATOR ROLE

PARP-1 function as a transcriptional co-regulator (either co-activator or co-repressor) has been well documented for different transcription factors such as NF κ B, HIF or NFAT. NF κ B is a transcription factor implicated in the regulation of the expression of genes associated to the inflammatory and stress response. PARP-1 can act both as inhibitor and activator of NF κ B-dependent transcription (Hassa and Hottiger 1999, Oliver, Menissier-de Murcia et al. 1999). Hypoxia Inducible Factors (HIFs) regulate an extensive transcription program that modulates the induction of genes involved in angiogenesis, metabolic adaptation to hypoxia, cell growth, metastasis, antiapoptosis and others, and are also modified by PARP-1 (Martin-Oliva, Aguilar-Quesada et al. 2006, Aguilar-Quesada, Munoz-Gamez et al. 2007, Aguilar-Quesada, Munoz-Gamez et al. 2007, Gonzalez-Flores, Aguilar-Quesada et al. 2013). NFAT, the master regulator of IL-2 gene transcription, binds to and is modified by PARP-1 (Olabisi, Soto-Nieves et al. 2008).

2.7.2 REPLICATION

Early studies have determined a link between PARP-1 and the DNA replication process. PARP-1 was shown to co-localize with replication foci throughout S phase, and it was also found to be enhanced in replicating cells suggesting that PARPs are an important component of the replication machinery (Dantzer and Santoro 2013).

PARP-1 has been described to interact with core proteins of a multiprotein replication complex, including DNA pol α , β , DNA primase, DNA helicase, DNA ligase and topoisomerases I and II (Simbulan-Rosenthal, Rosenthal et al. 1996). In addition, it has been proposed to function as part of the control of the replication fork progression when breaks are present in the template (Dantzer, Nasheuer et al. 1998). In support of these findings, PARP-1 interacts with the checkpoint protein p21 (Frouin, Maga et al. 2003) and the RecQ Helicase Werner Syndrome Protein (WRN) (Adelfalk, Kontou et al. 2003, von Kobbe, Harrigan et al. 2004). More recently, PARP-1 activity has been described to limit the restart of replication forks by RECQ1 following Topoisomerase I inhibition (Berti, Ray Chaudhuri et al. 2013).

Alltogether, these results suggest that PARP-1 may play a role at the intersection between DNA damage repair, DNA replication stalling and restart and checkpoint signaling (Petermann, Keil et al. 2005).

2.7.3 DNA REPAIR

For long, PARP-1 has been proposed to play a key role in DNA repair. Upon DNA damage, PARP plays different roles in order to allow the access of the DNA repair machinery at the damage site. On the one hand, opening of the chromatin structure occurs at DNA breaks by the removal of histones, by their poly(ADP-ribose)ylation by PARP-1 and through non-covalent association with poly(ADP-ribose)ated PARP-1 (Schreiber, Dantzer et al. 2006). On the other hand, PARP-1 DNA binding domain, through its zinc-finger motifs, binds specifically to DNA single and double strand breaks. This induces a conformational change of the PARP-1 protein, activates the catalytic domain and increases poly(ADP-ribose) synthesis (Meyer-Ficca, Meyer et al. 2005).

In addition, PARP-1 has been assigned different functions related with different DNA repair pathways:

2.7.3.1 PARP AND SINGLE STRAND BREAKS (SSB) REPAIR

PARP-1 exerts its role on SSB repair by its rapid binding to the SSB and subsequent activation. Specifically, PARP-1 is a critical player in Base Excision Repair (BER) pathway. In the short pathway of BER, ligation of DNA following DNA polymerase activity is carried out by Ligase III, which is recruited to the DNA damage region by the structural protein XRCC1. In order to develop its function, XRCC1 interacts with and is poly(ADP-ribose)ated by PARP-1. Thus, this interaction generates a PAR-dependent recruitment of XRCC1 to the DNA damage region (Masson, Niedergang et al. 1998, Okano, Lan et al. 2003, Okano, Lan et al. 2005).

2.7.3.2 PARP AND DOUBLE STRAND BREAKS (DSB) REPAIR

DSBs can be repaired by two different processes: the “error-prone” mechanism of Non-Homologous-End-Joining (NHEJ) and the “error-free” mechanism of Homologous Recombination (HR).

- **PARP and NHEJ pathway**

PARP-1 interacts with different proteins of the *classical* NHEJ pathway. For instance, poly(ADP-ribose)-binding sequence motif has been described in DNA-PK_{cs} and Ku70 proteins (Pleschke, Kleczkowska et al. 2000). In addition, PARP-1 operates in an alternative pathway that functions as backup to the *classical* pathway of NHEJ, Ku and DNA-PK dependent. Thus, in the *alternative* NHEJ pathway, PARP-1 binds DNA in order to signal DNA damage in absence of Ku (Wang, Wu et al. 2006). In addition, DNA ligation following polymerase activity is exerted by Ligase III, involving again PARP-1 to carry out its function (Audebert, Salles et al. 2004).

- **PARP and HR pathway**

For long there have been evidences about the role of PARP in HR. In 2006, Bryant and colleagues determined that PARP inhibition activated ATM (Ataxia Telangiectasia Mutated) protein, which is required for HR repair. They showed that PARP-1/ATM KO mouse was lethal, suggesting that ATM is important for cellular survival after the inhibition of PARP-1 and this

survival is caused by the involvement of ATM in PARP inhibition-induced HR repair. The inhibition of PARP generated an increase in unsolved SSBs at the DNA replication fork that turned into DSBs generating a stalled or even a collapsed replication fork. Since it has been reported that ATM is activated by DSBs (Khanna, Lavin et al. 2001), it was determined that the collapsed replication fork activates this protein.

Thus, the increased number of SSBs following PARP inhibition collapse into DSBs at the DNA replication forks. Such collapsed replication forks need HR for their repair, which is activated via ATM. Furthermore, an alternative pathway for the repair of the DSBs at the replication fork via NHEJ is also suggested after PARP inhibition through the ATM activation of Artemis protein (Riballo, Kuhne et al. 2004).

Aguilar-Quesada et al 2007 (Aguilar-Quesada, Munoz-Gamez et al. 2007) further advanced in the establishment of the relationship between PARP-1 and ATM, showing first, that ATM interacts with and is modified by PARP-1 and second, the dual effect of PARP inhibition on ATM activation. While poly(ADP-ribosylation) of ATM is probably needed for optimal ATM activation, long term exposure to PARP inhibitors result in the generation of DSBs and ATM activation.

Recent investigations have determined that PARP protein has an involvement in HR which is ATM-independent. It has been shown that PARP is activated at stalled replication forks to mediate Mre11-NBS1 dependent replication restart and HR (Haince, McDonald et al. 2008, Bryant, Petermann et al. 2009). Bryant and collaborators showed that HU treatment generates stalled replication forks with short regions of SSBs which are the stimulus for the recruitment of PARP to the stalled replication fork. PARP attracts Mre11 to the replication fork, generating the activation of RPA. Finally RPA will be replaced by RAD51, initiating HR. Otherwise, Haince and collaborators documented that the recruitment of Mre11 by PARP is due to their physical interaction and the recruitment of Mre11 by PARP can also be generated by DSBs induced by laser microirradiation.

In addition PARP has a role in RAD51 and BRCA modulation (Hegan, Lu et al. 2010). Mechanistically, PARP inhibition downregulates the expression of both proteins promoting increased occupancy of the BRCA1 and RAD51 promoters by repressive E2F4/p130 complexes.

In conclusion, PARP-1 has a dual role on the regulation of HR. On the one hand, PARP inhibition provokes genomic instability producing the accumulation of non-repaired SSBs at the replication fork that turn into DSBs activating ATM and HR. On the other hand, PARP-1 is necessary for HR pathway owing its interaction with ATM and, that is also modified by PARP; PARP recruitment to the damage site is necessary to form a complex with Mre11; PARP-1 is also necessary for RAD51 and BRCA1 transcription.

2.7.4 GENOME ORGANIZATION: PARP AND GENOME INSTABILITY

PARP-1 and PARylation are involved in the maintenance of chromosome stability, when DNA is damaged by exogenous agents as well as during cell division. In accordance with the above, inhibition of PAR synthesis gives rise to enhanced incidence of DNA strand lesions, leading to

gene amplification , recombination, micronuclei formation and sister chromatid exchanges (SCE), hallmarks of genomic instability.

2.7.4.1 GENOMIC INSTABILITY IN PARP-1 -/- KNOCKOUT

There is a large agreement that PARP-1 knockout mice develop genomic instability, in comparison with wild-type mice. De Murcia and colleagues (de Murcia, Niedergang et al. 1997) demonstrated that PARP-1 is a key survival factor for recovery from DNA damage, and this recovery is compromised in PARP-1-/- mice. Simbulan-Rosenthal and collaborators (Simbulan-Rosenthal, Haddad et al. 1999) further advanced in this result, showing an unbalanced chromosomal gains and losses affecting regions of chromosomes 4, 5 and 14 in cells from PARP-1 knockout mice, which taken together are all markers of genomic instability. However, the relationship between PARP-1-/- and telomere length is still discussed. Di Fagagna and colleagues (d'Adda di Fagagna, Hande et al. 1999) described that perturbation of PARP activity affects telomere length in mouse. In fact, MEFs PARP-1-/- showed shortened telomere length in comparison with wild-type MEFs. Other study (Espejel, Klatt et al. 2004) described that PARP deficiency did not affect telomere length or telomere capping, although they all observed higher levels of chromosomal instability following PARP ablation.

2.7.4.2 GENOMIC INSTABILITY IN PATIENTS

In addition to genomic stability defects observed in mice and cell lines following PARP ablation, Bieche and colleagues (Bieche, de Murcia et al. 1996) reported genetic instability in primary breast carcinomas carrying deregulated PARP expression. Thus, low levels of PARP gene expression were associated with loss of heterozygosity (LOH) amplification at a number of different chromosome loci.

2.7.4.3 PARP AND P53

p53, the “guardian of the genome”, becomes inactivated in many tumors and precancerous lesions, promoting the start of the carcinogenic process. Thus, p53 is associated with the maintenance of genome integrity, and its deficiency has been widely linked with the appearance of genome instability (Donehower, Godley et al. 1996). In addition, a connection between PARP-1 and p53 has been well described. In 1996, Wesierska and colleagues (Wesierska-Gadek, Schmid et al. 1996) reported PARylation of p53. Since then, subsequent publications showed an interaction of PARP-1 protein and p53 protein, in vitro and in vivo (Vaziri, West et al. 1997). Double knockout mice for p53 and PARP-1 displayed surprisingly increased life expectancy respect to single p53 null mice that was attributed to a diminished proinflammatory microenvironment in the absence of PARP-1 (Conde, Mark et al. 2001). More recently a key aspect of the interaction between PARP(s) and p53 has been uncovered assigning a role to PARylation of the nuclear export protein Crm1 to the p53 nuclear retention (Kanai, Hanashiro et al. 2007).

2.7.4.4 GENOMIC INSTABILITY CONSEQUENCES

Genome integrity is necessary for the maintenance of cell and organism homeostasis. As a consequence, PARP defects-associated genome instability will affect seriously the organism. Genome instability is for long well documented to be a marker of tumor development (d'Adda di Fagagna, Hande et al. 1999). Since PARP inhibition generates chromosomal instability, a hallmark of tumor development, it might seem contradictory with the current use of PARP inhibitors in cancer treatment (Peralta-Leal, Rodriguez-Vargas et al. 2009). However, this apparent contradiction is overcome if we take into account the following facts: first, it is possible to take advantage of genome instability in order to kill the tumor, which in our case genome instability may be generated by PARP inhibition. In fact, high rate of genome instability can drive to cell death through mechanisms including mitotic catastrophe (Chevanne, Zampieri et al. 2010). And second, there are other mechanisms apart from genome instability generated by PARP inhibition, that may be used to limit tumor development. Thus, hypoxia (Gonzalez-Flores, Aguilar-Quesada et al. 2014), angiogenesis or Epithelial-Mesenchymal-Transition (EMT) (Rodriguez, Peralta-Leal et al. 2013) are prevented by the use of PARP inhibitors, as is further reviewed in 2.8.3.1 section.

2.7.5 PROTEIN STABILITY/DEGRADATION

PARylation-dependent ubiquitylation is responsible for the proteolysis of different target proteins and can be taken over by several PARP proteins (Gibson and Kraus 2012). For instance, Tankyrase 2 parylates 3BP2, acting as a signal for RNF146-mediated ubiquitylation of the protein. Mutations affecting 3BP2 parylation sites prevent protein degradation, and activate signals that lead to cherubism disease (Levaot, Voytyuk et al. 2011).

2.7.6 PARP AND CELL CYCLE

PARP plays different roles in cell cycle through its involvement in different processes.

2.7.6.1 PARP-1 AND CELL CYCLE CHECKPOINTS

For long PARP-1 has been known to modulate cell cycle checkpoints due to its interaction with p53, which has been broadly explained above, as well as with p21 (Frouin, Maga et al. 2003). More recently, PARP-1 has been shown to interact with the key mitotic checkpoint protein BUBR1 (Fang, Liu et al. 2006), possibly suggesting a role of PARP-1 on mitotic checkpoint.

2.7.6.2 PARP AND SPINDLE POLE FORMATION

In 2000, Earle and colleagues (Earle, Saxena et al. 2000) described centromere localization of PARP. Two years later, Saxena and collaborators (Saxena, Saffery et al. 2002, Saxena, Wong et al. 2002) further advanced in this result, describing that centromere proteins Cenpa, Cenpb and Bub3 interact with and are PARylated by PARP-1 and PARP-2. In addition, PARP also has a role on centrosomes structure since PARP-3, as explained above, may have a centrosomal localization (Augustin, Spenlehauer et al. 2003). Finally, as also explained above, Tank1 and PARP-3 interact with NuMA (Chang, Dynek et al. 2005, Chang, Coughlin et al. 2009)

consequently contributing to mitotic spindle pole assembly. This function will be further analyzed in subsequent sections.

2.8 CELLULAR EFFECT OF PARP ACTIVATION

2.8.1 PROLIFERATION, CELL DEATH AND CELL SURVIVAL

DNA repair was one of the first functions assigned to PARP-1 and PARylation. Thus, it was early known that inhibition or absence of PARP may delay DNA repair resulting in cell death. However, in the early 80s Berger et al (Berger, Sims et al. 1983) reported a dual nature of PARylation, suggesting that severe PARylation following high DNA damage can also result on cell death.

Since then, PARP dual role in cell death and survival has been well reported. PARP can be assigned different roles in different cell death pathways (Virag, Robaszkiewicz et al. 2013). For some of them, low PAR levels are required. Nevertheless, high PAR amounts are needed in other pathways (Aredia and Scovassi 2014).

This section will be only focused on PARP-1 role in different cell death pathways. Further details about these pathways will be provided in next chapters.

2.8.1.1 LOW SYNTHESIS OF PAR: APOPTOSIS PATHWAY

Apoptosis (Programmed Cell Death type I) is an energy-dependent process characterized by caspases activation, phosphatidylserine externalization, dissipation of mitochondrial membrane potential, chromatin condensation, nuclear shrinkage, DNA fragmentation, protein cleavage, and apoptotic body formation.

DNA damage and cellular stress are largely known to activate PARP. As a consequence, ATP levels are reduced. Caspases activation, an event that requires ATP consumption, is the major event on the apoptotic pathway.

Cleavage of PARP-1 by caspases has been identified as one of the first biochemical markers of apoptosis. These proteases recognize a DEVD motif in the nuclear localization signal of PARP-1 (Lazebnik, Kaufmann et al. 1994) and cleavage at this site separates the DNA binding domain from the catalytic domain, resulting in the inactivation of the enzyme. Thus, DNA repair in a context where the cell is directed to death is downregulated, and second, competition between PARP-1 and caspases for ATP consumption is avoided following PARP-1 inactivation. Furthermore, blocking PARP-1 is vital for the proper function of the apoptotic machinery. Indeed, a caspase-3 insensitive PARP-1 was able to avoid apoptosis and promoted necrotic cell death (Oliver, de la Rubia et al. 1998).

2.8.1.2 PAR ACCUMULATION: A HALLMARK OF DIFFERENT PATHWAYS

- **PARthanatos**

Cells undergoing parthanatos and apoptosis display common features such as phosphatidylserine externalization, dissipation of mitochondrial membrane potential, chromatin condensation and nuclear shrinkage. However, parthanatos is accompanied by large scale DNA fragmentation, loss of cell membrane integrity and lack of dependence on energy or caspases activation (Cregan, Fortin et al. 2002, Wang, Dawson et al. 2009). Accordingly, the Nomenclature Committee on Cell Death (NCCD) classifies parthanatos as a programmed necrosis pathway (Galluzzi, Vitale et al. 2012).

PARP-1 plays a key role in parthanatos. When accumulated, PAR leaves the nuclei and enters in the mitochondria, functioning as a potent signal triggering AIF translocation from mitochondria to nucleus, where it is well-described to lead to cell death (Daugas, Nochy et al. 2000). AIF contains three PAR binding domains that play a crucial role on its interaction with PAR polymer. Interestingly, PAR binding is required for AIF to induce cell death. Prevention of AIF – PAR interaction avoided AIF translocation and consequently parthanatos activation (Wang, Kim et al. 2011).

- **Necroptosis**

For long, PARP-1 overactivation has been related to necrotic cell death (Berger 1985). With excessive activation of PARP, its substrate β -nicotinamide adenine dinucleotide (NAD^+) is depleted, and, in efforts to resynthesize NAD^+ , ATP is also exhausted leading to cell death by energy loss (Ha and Snyder 1999).

However, the cell death field has recently accepted the existence of regulated necrosis, since the prototypical death signal $\text{TNF}\alpha$ has been shown to activate a necrotic pathway mediated by Receptor Interacting Protein-1 (RIP1) kinase. RIP1 and TRAF2 are essential for necrosis induced by various stimuli such as not only $\text{TNF}\alpha$ but also H_2O_2 or arsenic, indicating a common role of RIP1 and TRAF2 in the regulation of necrosis (Baud and Karin 2001, Chen and Goeddel 2002). Consistent with this view, caspase-independent cell death induced by PARP-1 also requires the function of RIP1 and TRAF2. RIP1 and TRAF2 regulate PARP-1-induced-necrosis by influencing JNK activity, which appears to be a similar case in $\text{TNF}\alpha$ and H_2O_2 induced necrosis (Xu, Huang et al. 2006).

- **Autophagy**

Autophagy is a self-degradative process that ensures cell homeostasis by producing the turnover of cellular components. This process has a key role as energy sensor, that is mainly regulated by the action of mammalian Target Of Rapamycin (mTOR) and AMP-activated Protein Kinase (AMPK). Both enzymes are able to detect metabolic alterations and to regulate the autophagic response.

The consequence of NAD⁺ depletion in the context of PARP-1 overactivation, is a tremendous increase in the cellular AMP:ATP ratio, which can activate AMPK and induce an autophagic state through the inhibition of mTORC1-regulated cell growth (Zhou, Ng et al. 2013). Consistently, PARP inhibition has been shown to decrease AMPK activity and the autophagy rate (Munoz-Gamez, Rodriguez-Vargas et al. 2009, Rodriguez-Vargas, Ruiz-Magana et al. 2012), suggesting a regulatory function of autophagy by PARylation, possibly mediated by an effect on AMPK. However, a direct impact of PAR downstream mTOR pathway cannot be excluded since the mTOR companion Rictor has been described to possess a putative PAR binding motif (Gagne, Isabelle et al. 2008).

- **Cell fate: role of DNA damage and energy status**

There has been a long standing controversy over the role of PARP in DNA-damage signaling and, especially, in DNA damage-induced cell death. The two sides of the argument viewed PARP-1 either as an indispensable cellular survival factor or as an active mediator of cell death. In 2002, Virag and Szabo (Virag and Szabo 2002) proposed a unifying concept to integrate previous results. According to this theory, cells that are exposed to DNA-damaging agents can enter three pathways based on the intensity of the stimulus. In the first pathway, PARP1 activated by mild to moderate genotoxic stimuli facilitates DNA repair, at least partly by interacting with DNA-repair enzymes as explained above. As a result, DNA damage is repaired and cell survives.

In the second pathway, more severe DNA damage induces apoptotic cell death, promoting PARP-1 inactivation by caspases; this eliminates cells with severe DNA damage. The third pathway can be induced by extensive DNA breakage caused by oxidative or nitrosative stress. The overactivation of PARP depletes the cellular stores of its substrate NAD⁺ and, consequently, ATP. This severely compromised cellular energetic state prevents the apoptotic cell-death pathway from functioning, consequently inducing necrotic cell death.

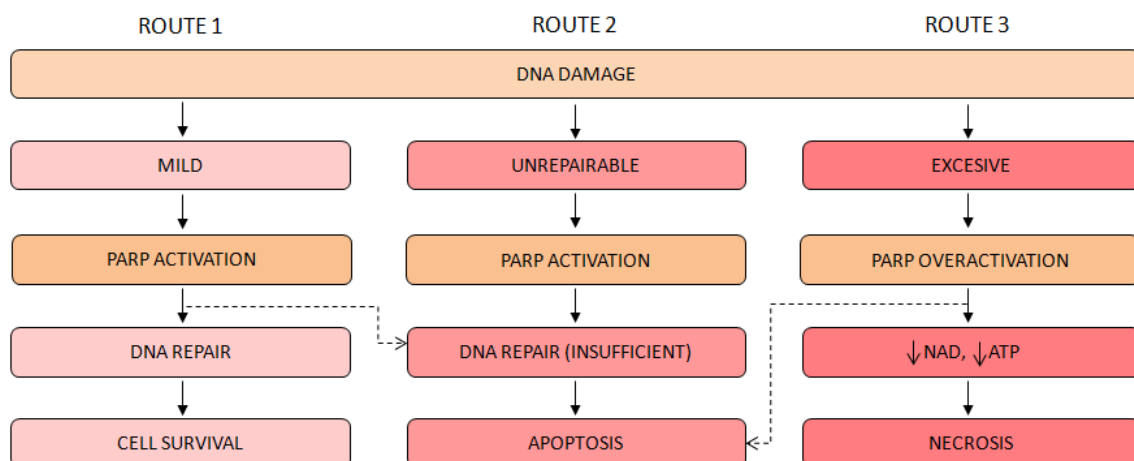


Figure 9: DNA damage levels determine cell fate. Depending on the intensity of the stimulus, PARP regulates three different pathways. Mild, unreparable or excessive DNA damage will respectively drive to cell survival, apoptosis or necrosis processes (Jagtap and Szabo 2005).

Thus, PARP and PARylation can drive the cell either to survival or death depending on the amount of the genotoxic damage, operating either as a prosurvival or death factor depending on the context.

2.8.2 DIFFERENTIATION

PARP-1 has been well documented to play a role in cell differentiation. However, according with the bibliography, PARP-1 plays opposite roles in this process depending on the context and cellular model.

On the one hand, PARP-1 is described to be involved in cell differentiation. In 1996, Simbulan-Rosenthal (Simbulan-Rosenthal, Rosenthal et al. 1996) described that 3T3-L1 cells expressing PARP-1 antisense RNA were unable to differentiate into adipocytes. The role of PARP in adipocyte differentiation was further confirmed in 2007 (Bai, Houten et al. 2007) when a role for PARP-2 in the process was described. In addition, PARP-1 and PARP-2 PARylate the Heterochromatin Protein HP1 α , which then recruits the Transcriptional Intermediary Factor TIF1 β to pericentric heterochromatin, promoting endoderm-specific gene transcription in endodermal differentiation (Quenet, Gasser et al. 2008). Finally, overexpression of PARP-1 activates the expression of the α -SMA gene (Acta2), which is a marker of myofibroblast differentiation in lung fibroblasts (Hu, Wu et al. 2013).

On the other hand, PARP-1 has also been described to avoid cell differentiation. In 2003, Hememberg M (Hemberger, Nozaki et al. 2003) determined that PARP -/- Embryonic Stem cell (ESCs) can differentiate to trophoblast derivatives, suggesting that PARP-1 can inhibit ESCs differentiation to trophoectodermal cells. Moreover PARylated PARP-1 interacts with SOX2, and this complex inhibits SOX2 binding to Oct-sox enhancers thus promoting cell pluripotency (Lai, Chang et al. 2012).

2.8.3 PARP AND DISEASE:

2.8.3.1 PARP AND TUMOR DEVELOPMENT

Over the last two decades, antitumoral effects of PARP inhibition have been well documented. However, it should be remembered that this effect can be explained at least through two different approaches.

The first approach is centered in PARP inhibition effect in combined therapy. It is based on the fact that PARP is involved in single and double strand DNA repair. Consequently, PARP inhibitors do potentiate the effect of chemo and radiotherapy, preventing the repair of DNA damage. Currently, different combined therapies are under clinical trial. Rucaparib, Olaparib, Veliparib or INO1001 have been tested in combination with different chemotherapies in breast cancer, lymphoma, melanoma and other solid tumors (Plummer, Jones et al. 2008, Bedikian, Papadopoulos et al. 2009, Khan, Gore et al. 2011, Kummar, Chen et al. 2011, Dent, Lindeman et al. 2013). Interestingly, phase I clinical trials in GBM combining TMZ with PARP inhibitors (<https://clinicaltrials.gov/ct2/results?term=%22glioma%22+AND+%22PARP%22&Search=Search>) Olaparib or veliparib, are currently under development.

The second approach is focused in the use of PARP inhibitors as monotherapy. In this case, two different mechanisms may explain the antitumoral effect.

On the one hand, PARP has been involved in different protumoral pathways. For example, tumor adaptation to hypoxic environment is modulated by PARP-1 as broadly demonstrated by our group (Martin-Oliva, Aguilar-Quesada et al. 2006, Gonzalez-Flores, Aguilar-Quesada et al. 2014). Since PARP-1 stabilizes Hypoxia-Inducible Factor (HIF), tumor growth under hypoxic conditions is compromised when PARP is inhibited. Besides, angiogenesis, which is a key process that has to take place in order to ensure tumor growth, is also modulated by PARP. Vimentin, an intermediary filament involved in angiogenesis and a hallmark of Endothelial-to-Mesenchymal transition downregulated following PARP inhibition (Rodriguez, Peralta-Leal et al. 2013). Additional invasion and metastasis markers such as Snail1 interact with and are modified by PARP-1 (Rodriguez, Gonzalez-Flores et al. 2011), promoting cell malignant transformation and Epithelial-Mesenchymal Transition (EMT). Interestingly, PARP inhibition decreases Snail1, favoring epithelial phenotype and avoiding metastasis.

On the other hand, the effect of PARP inhibitors in monotherapy can also be explained through “Synthetic Lethality” operating between two genes, which is defined as follows: loss of one cell function is compatible with cell life but the simultaneous loss of both functions drives to cell death. Although the exact molecular mechanism by which synthetic lethality takes place remains unclear, PARP’s role in DNA repair is a key event to explain this phenomenon, since it mainly operates in homologous recombination BRCA-deficient breast cancer (Bryant, Schultz et al. 2005). First attempt to explain synthetic lethality focused on PARP’s role in base excision repair (BER) given that single-strand breaks (SSBs) are usually repaired through the BER pathway (Bryant, Schultz et al. 2005). PARP inactivation would drive to the inhibition of this pathway, then increasing the number of unrepaired SSBs. Thus, SSBs would subsequently lead to double-strand breaks (DSBs) accumulation at replication forks. Since BRCA1/2 deficient cells have compromised DSBs repair, the accumulation of DSBs at the replication fork would drive to cell death. Nevertheless, other mechanisms have been proposed to explain synthetic lethality in BRCA-deficient tumors over the years (Strom, Johansson et al. 2011, Ying, Hamdy et al. 2012).

Either way, although further research is still required to elucidate the molecular mechanism behind synthetic lethality, PARP inhibition therapy has emerged as a promising strategy to efficiently target BRCA deficient tumors. In addition, new targets have emerged in the last years in order to achieve synthetic lethality when combined with PARP inhibition.

PTEN (phosphatase and tensin homolog) mutations have been related with a wide range of human tumors. Furthermore, this protein has recently been associated with Homologous Recombination Repair (Shen, Balajee et al. 2007) as described in next sections. It modulates Rad51 expression, making PTEN-null tumours compromised in Homologous Recombination Repair and consequently sensitive to PARP inhibition (Mendes-Pereira, Martin et al. 2009, McEllin, Camacho et al. 2010).

The Epidermal Growth Factor Receptor (EGFR) is overexpressed and associated with aggressive phenotype in triple negative breast cancer (Nakajima, Ishikawa et al. 2014). Moreover, its

inhibition has been related to altered DSBs repair (Li, Wang et al. 2008). Recent publications have shown contextual synthetic lethality between combined targeting of EGFR and PARP (Nowsheen, Bonner et al. 2011, Nowsheen, Cooper et al. 2012).

Finally, PARP inhibition is able to compromise Homologous Recombination Repair per se (Haince, McDonald et al. 2008, Bryant, Petermann et al. 2009, Hegan, Lu et al. 2010) as broadly explained in section 7.3. Due to the importance of this pathway on tumor development, new approaches in the use of PARP inhibitors will probably arise in the next few years, without the requirement of more aggressive therapies involving chemo and radiotherapy.

2.8.3.2 OTHER DISEASES

While the field of oncology has witnessed the clinical introduction of PARP inhibitors, the therapeutic use of these molecules have also progressed to target other diseases.

| DISEASE | HUMAN EVIDENCE FOR PARP ACTIVATION |
|--------------------------------|--|
| Stroke | PARP activation in brain sections from patients dying from stroke (Love, Barber et al. 1999). |
| Neurotrauma | PARP activation in brain sections from patients with brain trauma (Love, Barber et al. 2000). |
| Systemic inflammatory diseases | PARP activation in myocardial sections from patients with circulatory shock (Soriano, Nogueira et al. 2006). |
| Chronic heart failure | Increased poly(ADP-ribosyl)ation in human heart samples in heart failure (Pillai, Russell et al. 2005). |
| Neuroinflammatory diseases | PARP activation and AIF nuclear translocation in the CNS of human multiple sclerosis lesions (Veto, Acs et al. 2010) |
| Neurodegenerative diseases | Poly(ADP-ribosyl)ation in brain sections from patients with Alzheimer's disease (Love, Barber et al. 1999), Amyotrophic Lateral Sclerosis (ALS) and Parkinson's disease (Kim, Henkel et al. 2003, Soos, Engelhardt et al. 2004). |
| Local inflammatory diseases | Auto-antibodies against PARP in rheumatic arthritis and Systemic Lupus Erythematosus (SLE) (Okolie and Shall 1979, Negri, Scovassi et al. 1990). |
| Diabetes | High ROS production in islet beta-cells promoting PARP activation (Charron and Bonner-Weir 1999). |

Table 5: PARP activation in selected non-tumoral diseases.

Recent studies have shed new light on the molecular mechanisms of PARP-related cell death and PARP-associated inflammatory processes, which are relevant for various forms of neurological, inflammatory and cardiovascular diseases. In addition, PARP inhibitors have demonstrated therapeutic efficacy in many clinically relevant animal models of non-oncological settings, as shown in table above.

2.9 PARP INHIBITION

Most of the PARP inhibitors are competitive inhibitors for NAD⁺. They mimic the nicotinamide moiety of NAD⁺, blocking its binding to the enzyme therefore inhibiting PARP activity. The story of PARP inhibitors development started decades ago (Jagtap and Szabo 2005, Peralta-Leal, Rodriguez-Vargas et al. 2009).

First-generation inhibitors were developed 30 years ago: nicotinamides (IC_{50} = 210 μ M), benzamide (IC_{50} = 22 μ M) and substituted benzamide, in particular 3-aminobenzamide (3-AB), (IC_{50} = 33 μ M) were shown to be competitive inhibitors of PARP. Initial research demonstrated that benzamides are more potent inhibitors than nicotinamides (Purnell and Whish 1980). Nevertheless, they lacked specificity and potency, and had to be used at milimolar concentrations leading to sever and unspecific cytotoxic effects.

Second-generation inhibitors, developed in 1990s, were widely developed by Banasik and collaborators (Banasik, Komura et al. 1992). They are analogs of benzamide and are used in the micromolar range. A common feature of all very strong inhibitors is a carbonyl group, either attached to an aromatic ring or built into a polyaromatic skeleton. However, this group is not indispensable for the inhibitory action.

Third generation inhibitors are based on the optimization of Banasik's with increased potency, pharmacokinetics and water solubility at desired pH values. Many of these compounds are used in the nanomolar range and some of them have entered clinical trials, including ABT-888 (Veliparib), INO-1001, AG-014699 (Rucaparib) or AZD2281 (Olaparib).

The present work has been carried out using the following PARP inhibitors: Olaparib, with IC_{50} =5nM (PARP-1) and 1 nM (PARP-2); and PJ34 (N-(5,6-Dihydro-6-oxo-2-phenanthridinyl)-2-acetamide hydrochloride), with IC_{50} =20nM.

3 GENOME STABILITY: CELL CYCLE

3.1 GENERAL VIEW

Cell cycle on eukaryotic cells consists on the progression throughout different stages that finalizes with cell division (Norbury and Nurse 1992). DNA correct duplication and segregation in two cells daughters must be ensured in this process. Thus, DNA replication takes place in S (Synthesis) phase. After that, chromosomes segregation and cell division occurs in M (Mitosis) phase. Both phases are separated by “resting” phases: G1 phase between M and S, and G2 phase between S and M. Thus, cell cycle is composed by four sequential phases named G1, S, G2 and M. In addition, G1 and G2 play a key role ensuring cell conditions are optimal for DNA replication, chromatides segregation and cell division. If not, cells delay G1 progression or even enter in a quiescent state named G0. In adult mammals, most of the cells are in the quiescent state; out of the cell division program.

3.2 REGULATION

Cell cycle is tightly regulated, and depends on two main kinds of post-translational modifications that ensure the proper and unidirectional transition between phases:

- Phosphorylation: from yeast to human, cell cycle progression is controlled by Cyclin-Dependent-Kinases (CDKs), whose activity is modulated by activators (cyclins) and repressors or Cyclin Kinases Inhibitors (CKIs, among others). Only four CDKs are described to participate in cell cycle: CDK2, 4 and 6 are active in interphase while CDK1 is active in mitosis. Although CDK expression is constant through the cell cycle, cyclin activity suffers periodic degradations in every cell cycle (Reed 2003).

As a result of CDK/cyclin complex formation, specific substrates are phosphorylated. For instance, CDK2 phosphorylates DNA replication-related proteins. In contrast, CDK1 phosphorylates proteins involved in chromatin condensation, nuclear membrane rupture or Golgi fragmentation (Malumbres and Barbacid 2005).

- Ubiquitylation: protein degradation through ubiquitylation is another key event for proper cell cycle function. The complexes involved in this process are SKP1-CUL1-Fbox protein (SCF) which mainly acts in G1/S transition (Nakayama and Nakayama 2005), and Anaphase Promoting Complex/Cyclosome (APC/C); mainly involved in mitosis exit.
- In addition, cell cycle correct progression is controlled by checkpoints. These control mechanisms detect different failures (such as DNA damage or unaligned chromosomes in metaphase plate) and send out a signal that stops cell cycle until the failure is repaired. Specifically, checkpoints are not activated following the failure. In contrast, they are constitutively active but a response is generated only after detecting a failure. Finally, it is

important to remark that they guard key cell cycle transitions including start (the G1/S), entry into mitosis (G2/M), and exit from mitosis (metaphase/anaphase) (Rieder 2011).

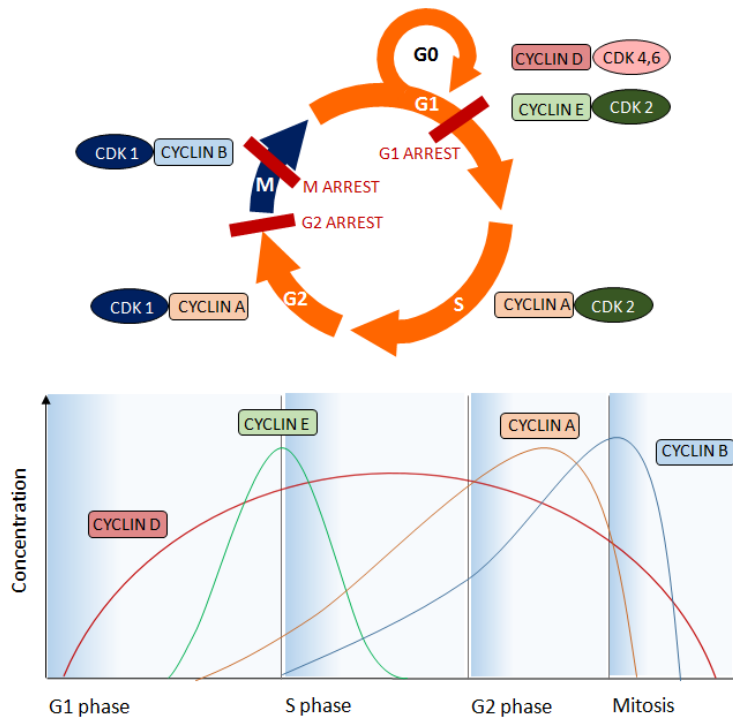


FIGURE 10: Cell cycle phases, checkpoints and Cyclin/CDK complex. Every phase of the cell cycle is related with an specific Cyclin/CDK complex (upper pannel). The amount of every cyclin differs between cycle phases (lower pannel).

3.3 MITOSIS

3.3.1 MITOSIS ENTRANCE

The term mitosis was described by Whalter Flemming in 1880. It refers to the step by which genetic material is distributed in two cells daughter.

The mechanism that modulates mitosis entrance in the cell is CDK1-CyclinB complex formation, which is modulated by different mechanisms. In G2 phase, CDK1 is inhibited through WEE1 and MYT1 kinase activities, which phosphorylate Tyr14 and Thr15 respectively (O'Farrell 2001). In Mitosis, Aurora A kinase activity through CDC25B phosphorylation (Dutertre, Cazales et al. 2004, Barr and Gergely 2007), and Polo-like Kinase (PLK1) through WEE1 inactivation (Watanabe, Arai et al. 2004), are required for CDK1 activity. Finally, once CDK1-cyclinB complex is formed, it stimulates its own activation. On the one hand, the own complex inactivates WEE1 and MYT1 activity; on the other hand, it activates CDC25C phosphatase which is essential for Tyr14 and Thr15 dephosphorylation and consequent CDK1 activation (Lindqvist, Rodriguez-Bravo et al. 2009).

3.3.2 MITOSIS EXIT

3.3.2.1 KINETOCHORE ROLE IN CHROMOSOMES-MICROTUBULES JUNCTIONS AND INITIATION OF ANAPHASE

Kinetochores, defined as a multiprotein structure assembled to centromeric DNA, play a key role in mitosis exit. They function as a platform for DNA assembly to microtubules in metaphase (Musacchio and Salmon 2007). When this assembly is properly established and sister chromatids kinetochores bind opposed poles (amphitelic junctions) anaphase is ready to start.

As explained above, one of the main processes that control cell cycle is ubiquitylation. APC/C is an E3 ubiquitin ligase whose activity is essential for anaphase initiation and mitosis exit. However, it is only active when binds one of its coactivators; either CDC20 or CDH1. The complex APC/C-CDC20 is essential for anaphase onset and mitosis exit by targeting through polyubiquitylation of securin (Yamamoto, Guacci et al. 1996) and cyclinB (King, Peters et al. 1995), promoting CDK1 inactivation and mitosis exit. This is followed by disassembly of the spindle, decondensation of chromosomes and re-assembly of the nuclear envelope.

However, if the junctions between kinetochore and spindle microtubules are improper, the mitotic checkpoint, also named Spindle Assembly Checkpoint (SAC), is activated thereby delaying chromosome segregation.

3.3.2.2 SAC

- **Components and location**

The SAC, which is conserved across eukaryotes, includes the Ser/Thr kinases Monopolar Spindle Protein 1 (MPS1) and Budding Uninhibited by Benomyl 1 (BUB1), as well as the non-kinase components Mitotic Arrest Deficient (MAD1), MAD2, BUB3 and the likely pseudo-kinases BUB1-related 1 (BUBR1; the human orthologue of yeast MAD3) (Hoyt, Totis et al. 1991, Li and Murray 1991).

These proteins delay premature chromosome segregation through the inactivation of CDC20 (Hwang, Lau et al. 1998).

In more detail, a Mitotic Checkpoint Complex (MCC) containing MAD2, BUBR1/MAD3 and BUB3, as well as CDC20 itself, has emerged as a possible SAC effectors (Sudakin, Chan et al. 2001). Besides MCC, other signals are required for proper SAC function. First, other “core” SAC proteins including MAD1, BUB1, MPS1 are required to amplify the SAC signal and the rate of MCC formation (Musacchio and Salmon 2007). And second, the Chromosome Passenger Complex (CPC), composed by Aurora B, INner CEntromere Protein (INCENP), Survivin and Borealin (Carmena, Wheelock et al. 2012) is also crucial for MCC activity.

The location of the SAC in the cell is constrained to kinetochores. This situation is essential, since it allows the complex to properly sense the status of kinetochore-microtubules junctions. Thus, kinetochore is not only a platform for the attachment between chromosomes and

microtubules, but it also allows the anchorage of checkpoint proteins, actively contributing to the detection of erroneous junctions that would lead to aberrant mitosis if not repaired (Santaguida and Musacchio 2009).

- **SAC mechanisms**

SAC activation is a complex mechanism that implicates multiple protein complexes. Whereas BUBR1 and BUB3 appear to bind constitutively throughout the cell cycle, the binding of MAD2 to CDC20 is catalyzed by unattached kinetochores during mitosis. Briefly, in prometaphase kinetochores are unbound; furthermore, CPC complex, specifically Aurora B, is located in kinetochores. Aurora B recruits MPS1, promoting MAD1 recruitment. In response to MAD1 recruitment, MAD2 changes its conformation from “open” or MAD2-O to “close” or MAD2-C, which binds MAD1. The heterodimer MAD1-MAD2-C acts as a signal, recruiting more MAD2-O molecules to kinetochores. In this case, MAD2-O changes its conformation to MAD2-C after binding CDC20. Then, presumably the subcomplex CDC20-MAD2-C may bind the subcomplex BUBR1-BUB3, forming the MCC complex (Musacchio and Salmon 2007).

Once metaphase is settled all kinetochores form amphitelic junctions with microtubules, SAC is compromised and anaphase is promoted. Although the exact mechanism underlying this process is not exactly determined, it seems that the tension generated might be regulating CDC20 liberation (Musacchio and Salmon 2007, Santaguida and Musacchio 2009).

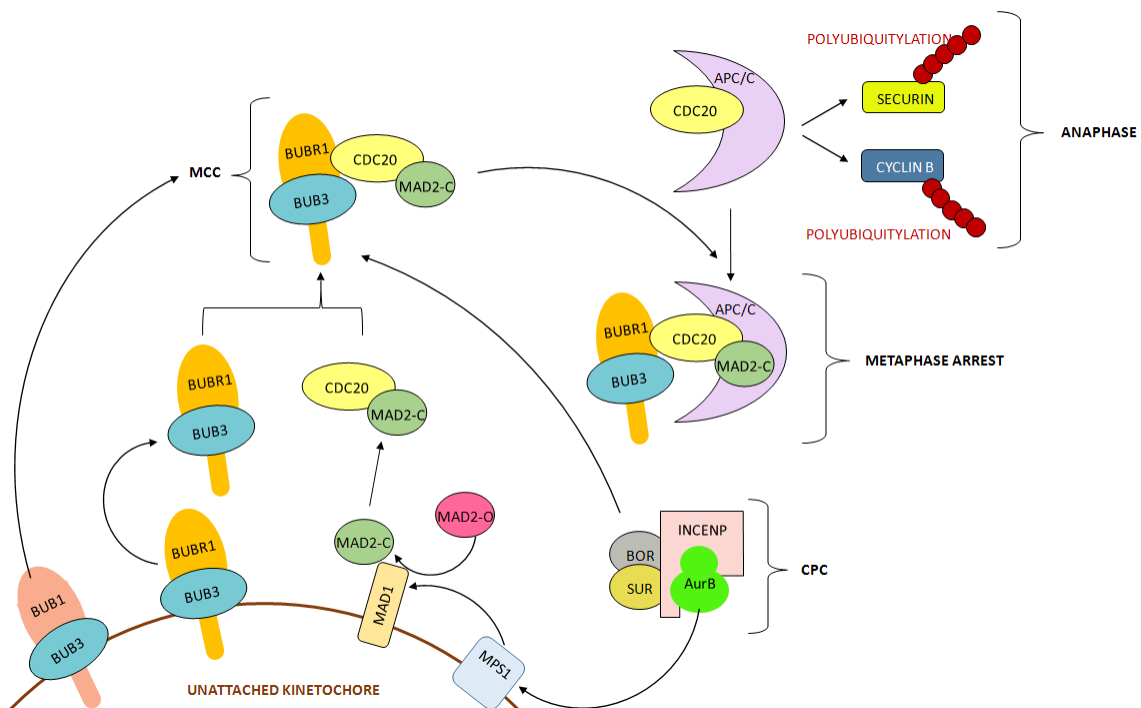


Figure 11: SAC mechanism. Inadequate microtubules attachment to kinetochore leads to BUBR1-BUB3 release from kinetochore; after that BUBR1-BUB3 interact with CDC20-MAD2-C to form the MCC. MCC then sequesters APC/C avoiding securin and cyclinB polyubiquitylation and subsequent anaphase onset. Other “core” SAC proteins including MAD1, BUB1 and MPS1; as well as the CPC are required to amplify the SAC signal and the rate of MCC formation (Musacchio and Salmon 2007, London and Biggins 2014). Adapted.

3.3.2.3 BUBR1

The multidomain protein kinase BUBR1 is expressed throughout the cell cycle. However, it only becomes phosphorylated in mitosis. It is a key protein in this project, thereby deserving its own section in this thesis. As reviewed above, it is a central component of the SAC. (Tang et al., 2001; Sudakin et al., 2001; Nilsson et al., 2008). However, its functions in the cell go beyond this aspect.

- **BUBR1 structure**

BUBR1 N-terminal domain is essential for an efficient SAC. It contains two KEN boxes (KEN1 and KEN2) related with CDC20 interaction and a GLEBS motif related with BUB3 interaction. In addition, BUBR1 owns a CDC20 interaction motif MAD2-independent named IC20BD. Finally, BUBR1 C-terminal domain is a Ser/Thr kinase domain.



Figure 12: BUBR1 structure. (Bolanos-Garcia and Blundell 2011).

- **BUBR1 functions**

Phosphorylation and dephosphorylation of SAC components involve a complex signaling cascade. BUBR1 is hyperphosphorylated in mitosis: on the one hand, it undergoes auto-phosphorylation when the SAC is unsatisfied; besides, it acts as the substrate of other kinases such as Aurora B (Ditchfield, Johnson et al. 2003), Polo-like kinase 1 (PLK1) (Elowe, Hummer et al. 2007), MPS1 (Huang, Hittle et al. 2008) and cyclin-dependent kinase 1 (CDK1) (Wong and Fang 2007). In one way or another, BUBR1 phosphorylation is essential for the development of its functions. However, kinase activity is not essential for all BUBR1 functions. In addition, BUBR1 N-terminal motifs such as KEN boxes and GLEBS, are also essential for the development of its functions.

Specifically, BUBR1 is involved in different functions, they all involved in the assurance of a proper mitosis process. They can be dividing according to its location, although they are intimately correlated:

- *BUBR1 kinetochore fraction*

Kinetochore provides a landing platform for SAC proteins. Consistently, BUBR1 is located in kinetochore, in association with BUB3 through its GLEBS motif as explained above.

Kinetochore-associated BUBR1 develops two distinct but interrelated functions:

First, BUBR1 is involved in the establishment of correct kinetochore-microtubules attachments. The mechanism by which BUBR1 exerts this function is based on the modulation of Aurora kinase B activity. BUBR1 activation is necessary for Aurora B interaction with phosphatase

PP2A (Suijkerbuijk, Vleugel et al. 2012). Thus, PP2A-mediated dephosphorylation can modulate Aurora B activity in kinetochores. However, BUBR1 depletion provokes PP2A downregulation thereby overactivating Aurora B kinase, which in turn phosphorylates Centromere Associated Protein A (CENP-A) (Lampson and Kapoor 2005). This cascade promotes severe chromosome misalignment phenotype, which can be restored, even in absence of BUBR1, through Aurora B kinase downregulation.

Second, kinetochore-associated BUBR1 serves as a signal for SAC activation. Specifically, the complex BUBR1-BUB3 is located nearby CENP-E. CENP-E (Centromere-Associated Protein E) is one of the proteins directly responsible for capture and stabilization of spindle microtubules by kinetochores (Lombillo, Nislow et al. 1995). In addition, it is described to associate with BUBR1 (Yao, Abrieu et al. 2000). This protein serves as a signal for anaphase onset. Thus, when CENP-E is not bound to microtubules, it stimulates BUBR1 kinase activity (Mao, Abrieu et al. 2003, Mao, Desai et al. 2005). However, this activity is repressed when CENP-E binds to microtubules, indicating that BUBR1 kinase activity is high before kinetochore-microtubule formation and inactivated following microtubule-kinetochore attachment. Hence, incorrect microtubule-kinetochore attachments would retain CENP-E dependent activation of BUBR1 promoting SAC activation and anaphase delay.

CENP-E has also been described to promote BUBR1 autophosphorylation (Guo, Kim et al. 2012). Hence, this mechanism might be involved in BUBR1 activation by CENP-E.

Finally, KEN boxes/MAD2 independent binding of BUBR1 to CDC20 has recently been described in the kinetochore. The interaction is established through BUBR1 internal CDC20 binding domain (referred to as IC20BD) that binds CDC20 in a MAD2-independent manner (Davenport, Harris et al. 2006). Although the exact function of the IC20BD has not been deeply analyzed, it seems that it would contribute to CDC20-MAD2-C subcomplex formation (Lischetti, Zhang et al. 2014).

- *BUBR1 soluble fraction*

Soluble BUBR1 is found as a part of MCC complex; thus its functions are related with Spindle Assembly checkpoint. Theoretically, once BUBR1 has been activated by CENP-E in the context of unattached kinetochores, this signal would promote BUBR1-BUB3 subcomplex release from kinetochore, which would become a soluble subcomplex with a key function in MCC formation.

APC/C is dependent of CDC20 to develop its activity, since CDC20 has the ability to recognize KEN motifs in the different APC/C substrates, thereby targeting them for APC/C ubiquitylation. BUBR1 also owes KEN boxes, as explained above, and consequently has the ability to bind CDC20, acting as a pseudosubstrate that competes with APC/C substrates for CDC20 binding (Burton and Solomon 2007). Thus, BUBR1 role in MCC is based on its ability to bind CDC20, impeding APC/C to develop its activity. A major role for this process has been assigned to KEN1 box; however, the role of KEN2 in CDC20 interaction is still poorly understood (Lara-Gonzalez, Scott et al. 2011). Interestingly, BUBR1 requires MAD2 for its stable association with CDC20 through the KEN boxes (Kulukian, Han et al. 2009).

- *BUBR1 and SAC silencing*

As a key modulator of mitosis checkpoint, BUBR1 is not only involved in SAC activation; in addition, once successful microtubule-kinetochore attachments are reached, an increasing role in SAC silencing has recently been reported for this protein.

First, KNL1 dephosphorylation by BUBR1-associated PP2A-B56, results in removal of the binding sites for BUB1, BUB3 and BUBR1 upon proper microtubule-kinetochore attachment. This leads to loss of BUB1 and BUBR1 from the kinetochore and initiation of SAC silencing.

In addition, once proper kinetochore–microtubule interactions are established, IC20BD motif of BUBR1 acts to destabilize the MCC for efficient mitotic exit, possibly by competing with the KEN box of BUBR1 for binding to CDC20 (Lischetti, Zhang et al. 2014).

Thus, BUBR1 regulates not only SAC activation but also SAC silencing. By acting in these two apparent opposite processes, globally BUBR1 ensures proper checkpoint function.

- *BUBR1 and genomic instability*

BUBR1 protein ensures accurate segregation of chromosomes through its role in the establishment of proper kinetochore-microtubule attachments and mitotic checkpoint function. Consistently, sustained high expression of BUBR1 preserves genomic integrity (Baker, Dawlaty et al. 2013), and low levels of BUBR1 promote chromosome instability and progressive aneuploidy (Hu, Liu et al. 2011) as well as aging-related phenotype (Baker, Jeganathan et al. 2004, Matsumoto, Baker et al. 2007). In fact, siRNA studies show mitosis acceleration and SAC abrogation following BUBR1 knockdown.

Notably, genetic mutations in BUBR1 are associated with the cancer-susceptible disorder Mosaic Variegated Aneuploidy (MVA). Cell lines derived from these patients show impaired mitotic checkpoint, chromosome alignment defects and low overall BUBR1 abundance (Suijkerbuijk, van Osch et al. 2010).

Altogether, these results show a major role for BUBR1 in the preservation of genome and chromosome integrity, and demonstrate that its downregulation is involved in aberrant chromosome segregation and genome instability, thereby deriving in tumor formation and age-related phenotype.

• **BUBR1 and PARP**

Interestingly, an interaction between PARP and BUBR1 has been described (Fang, Liu et al. 2006). In this work, physical interaction between PARP-1 and BUBR1 via co-immunoprecipitation was confirmed. This group also demonstrated that reduced levels of BUBR1 promoted PARP-1 downregulation. However, further investigation leading to elucidate the relationship between PARP-1 and BUBR1 needs to be done.

- **BUBR1 and GBM**

It has been recently described that glioblastoma tumors and genetically transformed cells have an added requirement for *BUB1B* to suppress lethal consequences of altered kinetochore (KT) function. Importantly, nontransformed cells do not require *BUB1B/BUBR1* for chromosome alignment. Thus, altered KT conformations, apparent in glioblastoma and genetically transformed cells, may predict cancer-specific sensitivity to *BUB1B* inhibition and perhaps other mitotic targets that affect kinetochore–microtubule stability (Ding, Hubert et al. 2013).

This group highlighted that BUBR1 activity is required to suppress lethal kinetochore instability. Consistently, glioma cells undergo abnormal anaphase following BUBR1 abrogation, thereby promoting cell death through mitotic catastrophe. Thus, targeting BUBR1 may provide a therapeutic window for GBM, without compromising nontransformed cells.

3.3.3 PARP AND MITOSIS

PARP role in mitosis extends beyond BUBR1. In fact, PARP has been described to act in different locations and to interact with different proteins involved in mitosis. Although it was previously explained in PARP section, it is worthy to deeply describe these interactions:

3.3.3.1 PARP IN SAC

PARP role in SAC is not restricted to BUBR1 interaction (Fang, Liu et al. 2006). In addition PARP-1 and PARP-2 interact with BUB3 (Saxena, Saffery et al. 2002, Saxena, Wong et al. 2002); thereby expanding the role of PARP in spindle assembly checkpoint.

3.3.3.2 PARP IN KINETOCHORES

In addition, a role for PARP in kinetochore, beyond SAC proteins interaction, has also been described. In 2000, Earle and colleagues (Earle, Saxena et al. 2000) described centromere localization of PARP. Two years later, Saxena and collaborators (Saxena, Saffery et al. 2002, Saxena, Wong et al. 2002) further advanced in this result. Centromeric Protein A (CENP-A) is proposed to be a component of a modified nucleosome or nucleosome-like structure in which it replaces one or both copies of conventional histone H3 in the (H3-H4)₂ tetrameric core of the nucleosome. In addition, its absence is lethal for the cell. In contrast, Centromeric Protein B (CENP-B) is part of the multiprotein complex that forms the inner kinetochore, and its absence is compatible with cell survival. Saxena group also described these two proteins interact with and are PARylated by PARP-1 and PARP-2.

In addition, CENP-C, with similar location and functions as CENP-B, interacts with PTEN (Shen, Balajee et al. 2007) and, as will be further explained in PTEN section, PTEN is PARylated by Tankyrases (Li, Zhang et al. 2015). Thus, a potential connection between CENP-C and PARylation can be hypothesized.

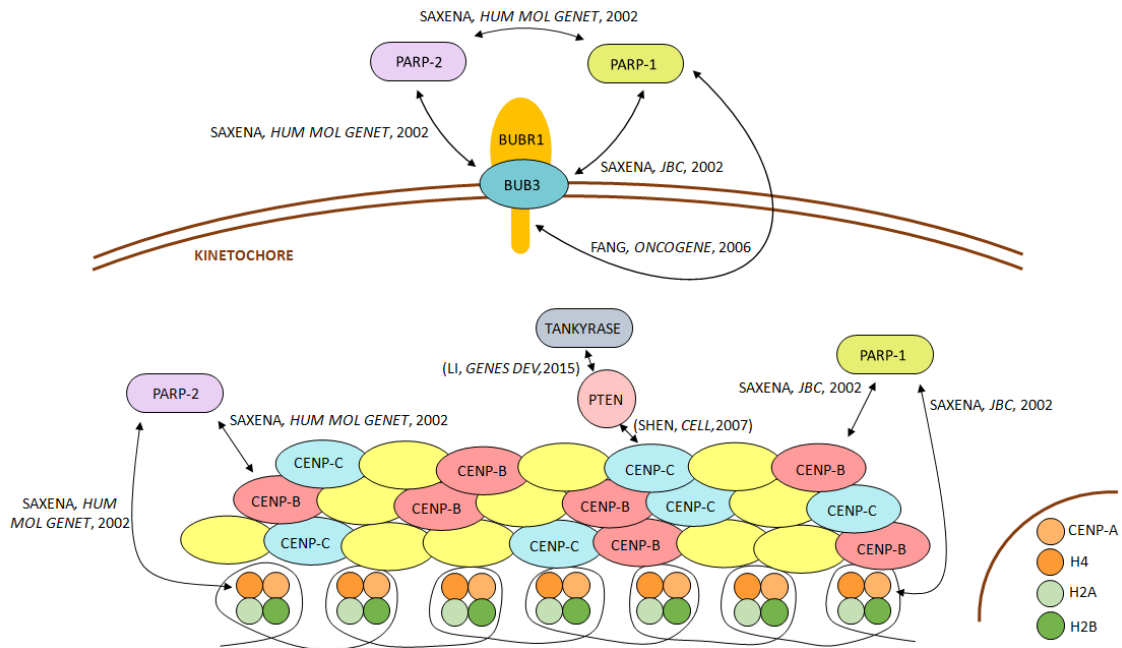


Figure 13: PARPs interactions in the kinetochore. PARP-1 and PARP-2 are described to interact between themselves as well as with BUB3, CENP-B and CENP-A. In addition, PARP-1 also interacts with BUBR1. Finally, Tankyrases are well-reported to PARylate PTEN, which is also part of the kinetochore due to its interaction with CENP-C. Thus, PARPs establish a complex net of connections in the kinetochore.

3.3.3.3 PARP AND CENTROSOMES

Besides, PARP also has a role on centrosomes structure since PARP-3, as explained above, may have a centrosomal localization (Augustin, Spenlehauer et al. 2003). As also explained above, TANK1 and PARP-3 interact with NuMA (Chang, Dynek et al. 2005, Chang, Coughlin et al. 2009, Boehler and Dantzer 2011, Boehler, Gauthier et al. 2011) consequently contributing to mitotic spindle pole assembly. Finally, TANK1 also PARylates the centrosome regulatory protein Centrosomal P4.1-Associated Protein (CPAP) (Kim, Dudognon et al. 2012), targeting it for proteasomal degradation. This mechanism avoids its overexpression and subsequent aberrant mitosis.

As a conclusion, according to all these data, PARP involvement in spindle pole formation and proper mitosis establishment can be affirmed. Thus, a role for PARPs and PARylation is well established in kinetochore and centrosome formation as well as Spindle Assembly Checkpoint function. However, the molecular mechanisms underlying these processes remain largely elusive.

4 DNA DAMAGE RESPONSE

In order to cope with DNA damage, cells have evolved to elaborate signaling cascades, collectively known as DNA Damage Response (DDR) pathways, that include DNA repair, cell cycle checkpoint activation and apoptosis activation (Su 2006, Shaltiel, Krenning et al. 2015).

The aim of this section is first, to elucidate the mechanisms involved in DDR. First, the specific routes that contribute to DNA repair are dissected. Due to the importance of Double Strand Breaks (DSBs) repair, specifically Homologous Recombination (HR) repair in this thesis, this section will go in depth in this pathway. Second, a brief explanation of cell cycle checkpoint is provided.

4.1 DNA DAMAGE REPAIR

4.1.1 GENERAL VIEW

4.1.1.1 DIRECT REPAIR

Nature has evolved several mechanisms in which the damage is directly reversed most often by a single repair protein without an incision on the DNA strand. Direct repair mechanisms may be carried out by three different groups of enzymes: (i) photolyases reverse UV light-induced photolesions; (ii) O⁶-alkylguanine-DNA alkyltransferases (AGTs) reverse a set of O-alkylated DNA damage; and (iii) the AlkB family dioxygenases reverse N-alkylated base adducts (Yi and He 2013).

4.1.1.2 SINGLE STRAND BREAKS REPAIR (SSBR)

DNA single-strand breaks (SSBs) are among the most frequent DNA lesions. Left unrepaired, SSBs are a major threat to genetic stability and cell survival. The different SSBR pathways in mammals are summarized below:

- Mismatch Repair (MMR) is a highly conserved DNA repair pathway that recognizes and repairs base-pairing errors that arise during DNA replication. Its role has been largely studied in the DDR to chemotherapeutic agents, although its role in Ionizing Radiation (IR) is poorly characterized. This pathway is initiated when the MutS α (MSH2/MSH6) heterodimer binds to the mismatched DNA. Then, heterodimers of MutL homologues as well as EXO1 or RPA and DNA polymerases are then recruited to this complex to complete the excision of the mismatches and the resynthesis of the DNA strand (Martin, Marples et al. 2010).
- Nucleotide Excision Repair (NER) pathway is initiated with the DNA damage recognition by XPC and XPA. Then, RPA complexes with XPC in order to stabilize the DNA “bubble” around the damage. Next, endonucleases XPG and XPF incise the damage containing DNA strand,

resulting in the removal of a 27-29 nucleotides DNA fragment. Finally, DNA polymerases and DNA ligases synthesize and seal the new oligonucleotide (Leibeling, Laspe et al. 2006).

- Base Excision Repair (BER) pathway has evolved to cope with the high level of spontaneous decay products that are formed in DNA, as well as those damages created upon reactions with natural endogenous chemicals, most notably ROS. BER pathway acts through the excision and replacing of incorrect or damaged bases derived from deamination, alkylation or oxidation. First, the incorrect base is removed by a DNA glycosylase to create an abasic intermediate site. Second, endonuclease creates an incision in the abasic site. Third, the remaining sugar fragment is removed by a lyase or phosphodiesterase and finally, the gap is filled by a DNA polymerase and sealed by a DNA ligase (Kim and Wilson 2012, Liu and Wilson 2012).

4.1.1.3 DOUBLE STRAND BREAKS REPAIR (DSBR)

DSBs are one of the most severe types of DNA damage. Unrepaired DSBs easily induce cell death and chromosome aberrations. To maintain genomic stability, cells have acquired DSBs repair mechanisms to respond to DNA damage, which can be classified in two different pathways.

- Non Homologous End Joining (NHEJ) pathway is based on the restoration of DNA integrity by simply joining two ends. Consistently, it is an error-prone mechanism, well-described to participate in V(D)J recombination, but with increasing significance in various cellular processes. The canonical NHEJ pathway is initiated by Ku proteins, which recognize DNA ends and facilitate the recruitment of DNA-PK, which promotes end-processing by the Artemis nuclease and subsequent rejoining of broken DNA ends by the ligase complex LigIV/XRCC4/XLF (Mladenov and Iliakis 2011).
- Homologous Recombination (HR) is broadly studied in this investigation. Thus, it will be deeply explained below.

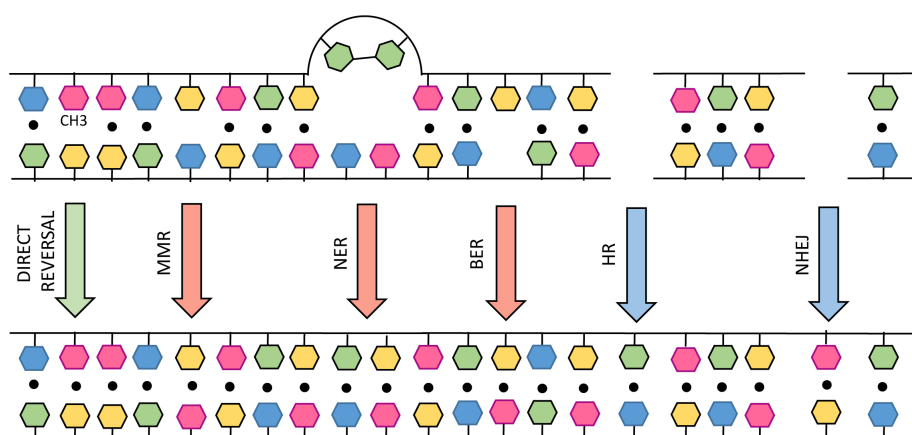


Figure 14: DNA repair pathways. Several repair pathways exist and deal with various types of DNA insults. These pathways include direct reversal pathway, MMR, NER, BER, HR and NHEJ pathway. (Hakem 2008).

4.1.2 HOMOLOGOUS RECOMBINATION

HR is the pathway that targets DSBs through an error-free mechanism. It is a key pathway to maintain genomic integrity between generations (meiosis) and during development in a single organism (DNA repair). Specifically, this pathway uses the sister chromatid as a mould for the repair of the damaged DNA strand. Besides, it is subject to a tight regulation; while a defect in HR may lead to genomic instability, an excess in HR may lead to undesired genome rearrangements (Heyer, Ehmsen et al. 2010).

4.1.2.1 HR MECHANISMS

- To start, HR pathway is activated when the components of the MRN complex, composed of the Meiotic Recombination 11 (MRE11), RAD50 and Nijmegen breakage syndrome 1 (NBS1) bind to DSBs (Stracker and Petrini 2011). Then, MRN complex promote different routes:
 - On the one hand, MRN complex recruits phosphorylated CtBP Interacting protein (CtIP), which activates the exonuclease activity of MRE11 (Sartori, Lukas et al. 2007). Thus, MRE11 associated with CtIP initiates DSB resection by removing the first 50-100 nucleotides from the DNA 5' termini. Then, 3' ssDNA overhangs will be extended to a length of several thousand basepairs by exonucleases EXO1 and DNA2 (Huertas 2010). The resulting ssDNA tail will be rapidly bound by the Replication Protein A (RPA), which is only capable to recognize long ssDNA.

Once the ssDNA is coated with RPA, it serves as a signal to recruit Ataxia Telangiectasia and Rad3 related kinase (ATR), and its binding partner ATR Interacting Protein (ATRIP), which then phosphorylates different substrates (H2AX and BRCA1 among others). ATR shows no changes in modification or activity after genotoxic stress. In contrast, relocalization of ATR to sites of damage via association with ssDNA-RPA complexes seems enough for ATR activation (Su 2006).
 - On the other hand, MRN activates the DNA damage-activated kinase Ataxia Telangiectasia-Mutated (ATM), resulting in ATM monomerization and autophosphorylation (Su 2006). Active ATM leads to phosphorylation and recruitment of H2AX, referred to as γH2AX. This phosphorylation directs the assembly of downstream components, including BRCA (Polo and Jackson 2011). Then, Partner And Localizer of BRCA2 (PALB2) binds the C-terminus of BRCA1 and the N-terminus of BRCA2, creating a bridge to recruit BRCA2 to the sites of DNA damage. Once in the damage region, BRCA2 binds phosphorylated Rad51, targeting active Rad51 to the ssDNA (De Lorenzo, Patel et al. 2013).
- Subsequently, RPA will be replaced by active RAD51 (Carreira, Hilario et al. 2009), promoting the creation of the so called RAD51 filament. The previous binding of RAD51 and BRCA2 will be an unavoidable requirement for this step.
- Then, RAD51 filaments induce DNA-strand invasion, and the generation of a displacement loop (D-loop) into homologous DNA sequences. Next, RAD51 dissociates from DNA to expose the 3' end required for DNA synthesis. Finally, the lesion-containing strand is

resynthesized by a DNA polymerase using the sister chromatid as a template (Liu and Huang 2014).

- In addition to RAD51, five RAD51-related proteins, also named RAD51 paralogs have been described, which are RAD51B, RAD51C, RAD51D, XRCC2, and XRCC3; and they are found to exist in vivo in two major complexes: RAD51B/RAD51C/RAD51D/XRCC2 and RAD51C/XRCC3 (Masson, Tarsounas et al. 2001). Although the functional significance of the two in vivo RAD51 paralog complexes in HR remains unclear, it is proposed that BRCA2 and the RAD51 paralogs work together, in the same pathway, during DNA break repair (Suwaki, Klare et al. 2011, Jensen, Ozes et al. 2013).

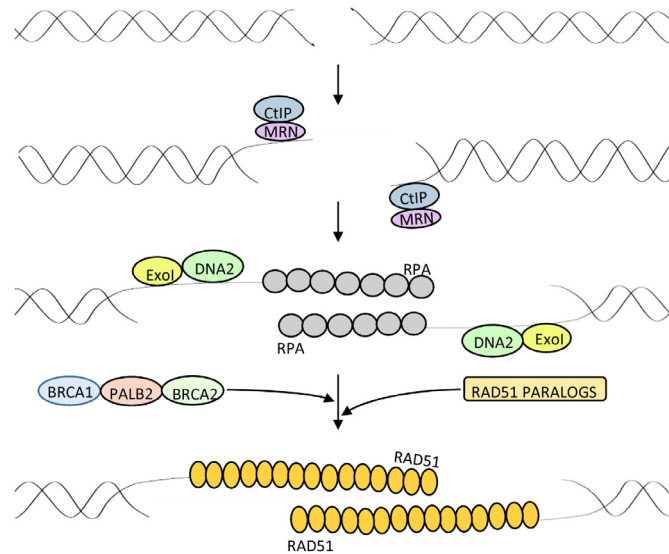


Figure 15: HR pathway. Upon induction of DSBs, the broken DNA is coated by MRN complex that processes DNA ends into short ssDNA tails which are then coated by RPA. In a subsequent step, ssDNA tails can be further resected into longer ssDNA tails by EXO1 and DNA2. Next, BRCA2 and RAD51 paralogs catalyze the replacement of RPA with RAD51, which promotes the invasion into homologous duplex DNA, leading to the formation of the D-loop. Adapted from (Heyer, Ehmsen et al. 2010, Liu and Huang 2014). Adapted.

4.1.2.2 CLASSIFICATION

Interestingly, HR may be classified in three different subpathways according to the mechanisms by which D-loop are resolved:

- In Double Holliday Junction (dHJ), the second DSB end is captured and a double Holliday Junction intermediate is established, which may be resolved to yield crossovers or non-crossovers recombination products. Although this is the purpose of meiotic recombination, recombinational DNA repair in somatic cells, which is the aim of this section, is rarely associated with crossovers. Thus, this pathway will not be further analyzed in this section.
- In Break-Induced Replication (BIR), occurring in DNA repair in somatic cells, in the absence of a second end the D-loop may become a full-fledged replication fork. Although this process restores the integrity of the chromosome, it may lead to loss-of-heterozygosity of all genetic information distal to the DSB.

- In Synthesis-Dependent-Strand-Annealing (SDSA), also occurring in DNA repair in somatic cells, the extended D-loop is dissolved by specialized DNA helicases, and the newly synthesized strand is annealed to with the ssDNA tail on the other break end (namely the second end), which is followed by gap-filling DNA synthesis and ligation. Thus, this subpathway of HR avoids crossovers and reduces the potential for genomic rearrangements. It is the main subpathway involved in DNA repair.

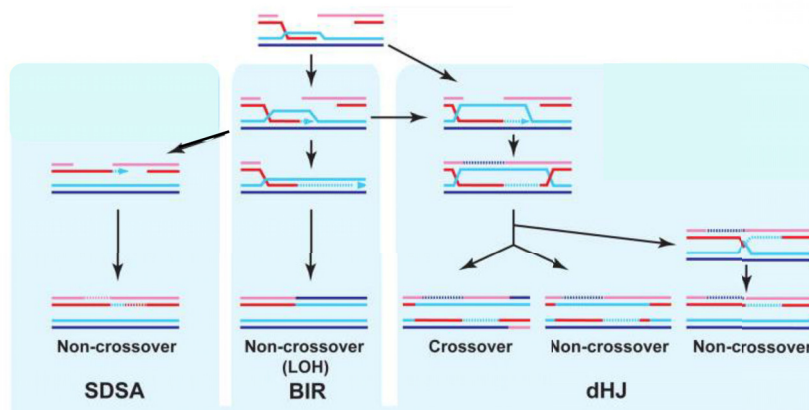


Figure 16: Different HR subpathways leading to D-loop resolution are represented above. The name of the subpathway and the potential rearrangements (crossovers) are represented (Heyer, Ehmsen et al. 2010).

HR process is restricted to S and G2 phases of cell cycle. This is tightly regulated in multiple ways. First, BRCA2 and RAD51 are only expressed in S and G2 phases, making HR impossible in G1 (Chen, Nievera et al. 2008). Second, CDK2 which is active at the G1/S transition and S phase, catalyzes the phosphorylation of CtIP that is required for its binding to MRN complex and subsequent activation of MRN nuclease activity. Third, G0 and G1 phases have not replicated DNA thereby lacking sister chromatid that provides a template for HR.

Thus, NHEJ is mainly associated with G1 phase while HR is the major DNA repair pathway associated with S and G2 phase.

4.2 CELL CYCLE CHECKPOINTS

DNA repair is tightly regulated throughout the cell cycle. The current dogma is that the DNA damage response (DDR) affects proliferation such that the DDR can reversibly arrest cell cycle progression to allow time for DNA repair and, upon completion of DNA repair, the DDR is turned off to allow cell cycle resumption. Errors in DNA repair as well as compromised cell cycle checkpoints, may derive in genomic instability accumulation and initiation of tumor progression.

The major proteins that couple DNA damage repair and cell cycle checkpoints are ATM and ATR. As seen above, both proteins are activated following DNA damage and in turn they activate different substrates related with DNA damage signaling such as H2AX or BRCA1. Nevertheless, ATM and ATR are also well-known to mediate cell cycle arrest following DNA damage, thereby avoiding cell cycle progression unless DNA integrity is established.

The aim of this section is to briefly describe ATM/ATR roles in cell cycle checkpoints as well as the main functions of their effectors.

ATM and ATR are well-established to promote genome integrity. Consistently, their deficiency results in Ataxia Telangiectasia and Seckel Syndrome (O'Driscoll, Ruiz-Perez et al. 2003) respectively. As ATM is activated by MRN complex, and this complex binds DSBs throughout the cell cycle, ATM is active in G1, S and G2/M checkpoints. In contrast, ATR is activated by RPA-coated ssDNA in HR. Consistently, it is only active in S and G2/M checkpoints.

Besides, the cell cycle response initiated by ATM is mediated by CHK2, and the response initiated by ATR is mediated by CHK1. Briefly, the downstream pathways are discussed below.

- G1 arrest: this checkpoint is mediated only by ATM-CHK2 pathway. Activated CHK2 leads to first, CDC25A proteasomal degradation, resulting in sustained CDK2-inhibiting phosphorylation and G1 arrest; and second, p53 activation which promotes p21-dependent CDK2 and CDK4 inhibition leading to sustained G1 arrest too.
- S arrest: this checkpoint is mediated by ATM-CHK2 and ATR-CHK1 pathways. In this case, CHK2 downstream effectors are the same as in G1; CHK1 in turns also promotes p53 activation and CDC25A inhibition. However, it also activates WEE1 kinase, which phosphorylates CDK2 thereby inhibiting its activity.
- G2/M arrest: this checkpoint is also mediated by ATM-CHK2 and ATR-CHK1 pathways. In this case, as occurred before, CHK2 and CHK1 promote p53-mediated p21 activation, which in G2 phase leads to CDK1-cyclinB complex inhibition. Besides, they promote CDC25C inhibition, avoiding CDK1-activating dephosphorylation which is an essential step for M entrance. In addition, as in S phase, CHK1 may activate WEE1 kinase, in this case phosphorylating and inhibiting CDK1, thereby impeding M entrance.

Finally, it is interesting to remark that DSB repair during mitosis is inactivated by mitotic kinases. In fact, active DSB repair during mitosis affects chromosome segregation, which often results in apoptosis, aneuploidy, or other chromosome aberrations. On the other hand, DSB repair inactivation drives to higher sensitivity to genotoxic agents in M phase, thereby sensitizing cells to IR among others (Terasawa, Shinohara et al. 2014).

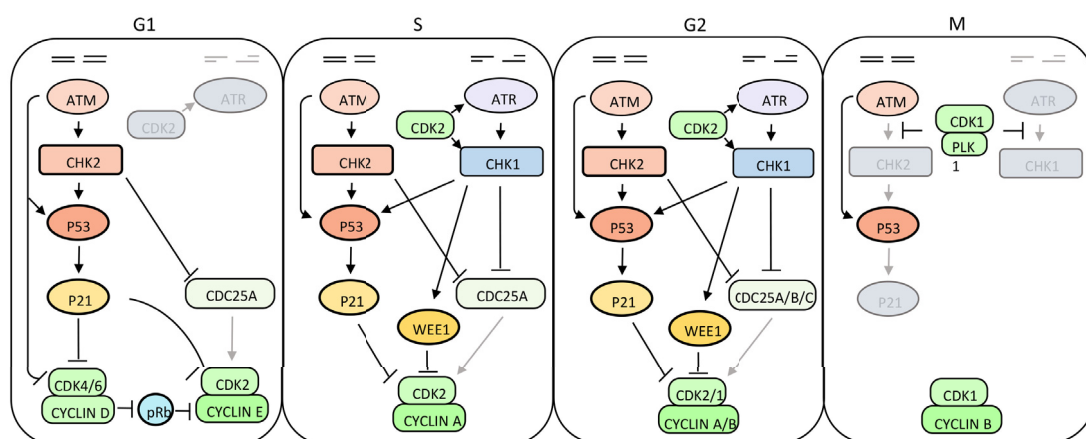


Figure 17: DNA damage signaling after DSBs in the various stages of the cell cycle. Interplay between the cell cycle machinery and the DDR results in distinct signaling in response to DSBs (Shaltiel, Krenning et al. 2015).

5 CELL SURVIVAL: mTOR PATHWAY

5.1 GENERAL VIEW

TOR (Target Of Rapamycin) is a highly conserved serine/threonine kinase that plays a significant role in controlling cell growth and metabolism. Rapamycin is an antifungal compound that was isolated from a soil sample of Rapa Nui islands in the 1970s (Vezina, Kudelski et al. 1975). In 1991, a genetic screen for rapamycin-resistant mutations in budding yeast *Saccharomyces cerevisiae* led to the discovery of both TOR1 and TOR2 genes (Heitman, Movva et al. 1991), the yeast homologues of mammalian mTOR. Subsequent biochemical studies in mammalian cells further led to the identification of a 289 kDa protein, which was termed mTOR (mammalian target of rapamycin) (Brown, Albers et al. 1994). mTOR is an atypical serine/threonine kinase, belonging to the PIKK (phosphoinositide 3-kinase related protein kinase) super-family, which comprises large proteins that enable organisms to cope with metabolic, environmental and genetic stresses.

5.1.1 mTOR BINDING PROTEINS

mTOR is the catalytic subunit of two distinct complexes called mTOR complex 1 and 2 (mTORC1 and mTORC2).

Regulatory-Associated Protein of mTOR (RAPTOR) and Rapamycin-Insensitive Companion of mTOR (RICTOR) define mTORC1 and mTORC2, respectively. Both proteins interact with DEPTOR (DEP domain-containing mTOR interacting protein) and MLST8 (Mammalian Lethal with Sec13 protein 8). However, they differently function as scaffolds for assembling other proteins: PRAs40 (40 kDa Pro-rich Akt substrate) in the case of mTORC1; PROTOR (Protein Observed with RICTOR) and mSIN1 (mammalian Stress-activated map kinase-Interacting protein 1) in the case of mTORC2 (Zoncu, Efeyan et al. 2011).

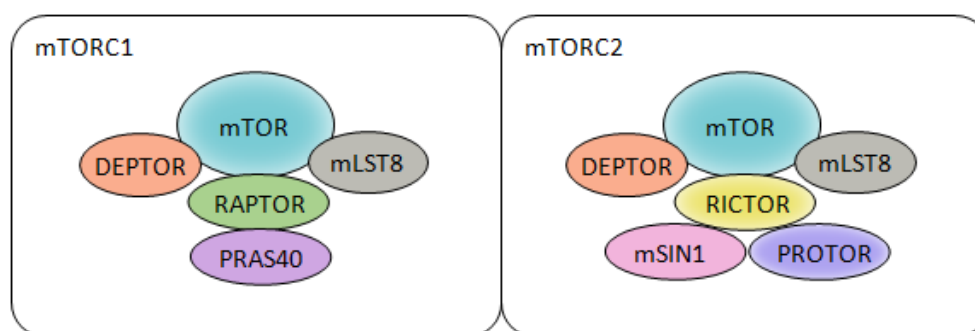


Figure 18: Organization of mTORC1 and mTORC2 complexes. Both complexes contain mTOR, mSIN1 and DEPTOR. RAPTOR and PRAS40 are unique to mTORC1, while mSIN1 and PROTOR are specific to mTORC2 (Zoncu, Efeyan et al. 2011).

5.2 mTOR UPSTREAM SIGNALING PATHWAYS

5.2.1 UPSTREAM TSC:

5.2.1.1 GROWTH FACTOR SIGNALING THROUGH TYROSINE KINASE RECEPTORS (TKR)

Tyrosine Kinase Receptors are well-established to mediate growth factors signaling. The most common TKR involved in mTOR signaling are enumerated below:

- HER (Human Epidermal growth factor Receptor): this family consists of 4 structurally related receptors: HER1 (EGFR), HER2, HER3, and HER4. They are activated by ligand-induced dimerization, leading to the activation of the intrinsic tyrosine kinase domain and subsequent phosphorylation on specific tyrosine residues, promoting the activation of different downstream signaling cascades, including RAS-RAF-MEK-ERK and PI3K-AKT (Holbro, Civenni et al. 2003).
- PDGFR (Platelet-Derived Growth Factor Receptor): The two PDGF receptors, PDGFR α and PDGFR β , respectively are structurally similar. Ligand binding causes dimerization of the receptors. The dimerization is a key event in activation since it brings the intracellular parts of the receptors close to each other promoting autophosphorylation (Heldin 2013).

Once the TKR has been phosphorylated, adaptor molecules are needed in order to activate the downstream pathways. Hence, GRB2 binding to the activated RTK and subsequent recruitment of the nucleotide exchange molecule SOS1 is needed for RAS activation. On the other hand, PI3K owns two activating mechanisms. First, PI3K is active when its regulatory subunit p85 is recruited to the RTK thereby promoting the activation of the p110 catalytic subunit. Second, RAS activation can directly activate p110.

- **RAS-RAF-MEK-ERK pathway**

MAPK (RAS–Mitogen Activated Protein Kinase) signalling pathway is initiated by RTK-mediated activation of RAS. Downstream RAS, the RAS-RAF-MEK-ERK cascade is initiated. Once activated, ERK (Extracellular signal-Regulated Kinase) modulates different pathways. Thus, while in the nucleus ERK stimulates multiple transcription factors, resulting in the control of key cellular functions, in the cytoplasm it phosphorylates TSC2 thereby inhibiting it (Ma, Chen et al. 2005) and promoting mTORC1 activation.

- **PI3K pathway**

Active Class I PI3K (PI3KCI) is able to phosphorylate phosphatidylinositol (PI) to generate phosphatidylinositol (3,4,5)-phosphate (PIP3). PIP3 then binds to PH domain of AKT, thereby promoting its translocation to the plasma membrane. In this location, AKT is phosphorylated by PI3K-Dependent Kinase 1 and 2 (PDK1 and PDK2) at Thr308 and Ser473 respectively leading to AKT activation. More recently, RICTOR complex has been identified as PDK2, hence being responsible for Ser473 phosphorylation of AKT (Sarbasov, Guertin et al. 2005).

This process is counteracted by PTEN. This tumor suppressor antagonizes the activity of PI3K by dephosphorylating PIP3. However, its activity will be deeper analyzed in the next section. Once active, AKT can potentially phosphorylate over 9000 proteins (Lawlor and Alessi 2001), although several lines of evidence point to three conserved downstream effectors:

- The forkhead family of transcription factors (FOXO) is directly phosphorylated and inactivated by AKT (Brunet, Bonni et al. 1999), consequently promoting cell proliferation.
- CHK1 also phosphorylated by AKT, promoting the signaling towards proteasome degradation. This pathway is further analyzed in “PTEN” section.
- mTOR pathway activation through AKT signaling has been recently described. This process is mediated by AKT-direct phosphorylation of TSC, thereby promoting its inhibition.

5.2.1.2 ENERGY AND STRESS SIGNALING THROUGH AMPK PATHWAY

The AMP-activated protein kinase (AMPK) is a heterotrimer composed of a catalytic (AMPK α) subunit and two regulatory (AMPK β and AMPK γ) subunits. AMPK is a sensor of cellular bioenergetics, specifically in response to energy stress. During energy depletion, AMPK is activated by a decreased ATP/AMP ratio through LKB1 kinase. Specifically, active AMPK can directly phosphorylate and inhibit RAPTOR (Gwinn, Shackelford et al. 2008). Besides, AMPK can phosphorylate and activate Tuberous sclerosis complex 1 and 2 (TSC1/TSC2 complex), undirectly leading to mTORC1 inhibition (Inoki, Zhu et al. 2003). Thereby, active AMPK leads to mTORC1 inhibition (through direct and undirect mechanisms) and autophagy activation.

Apart from ATP/AMP ratio, other inductors of AMPK have been described. Thus, an increase in the cytosolic free Ca²⁺ concentration activates AMPK via Ca²⁺/calmodulin-dependent kinase kinase β (CaMKK β). In addition, metabolic stress via TAK1 and genotoxic stress via p53 lead also lead to AMPK activation, mTORC1 inhibition and autophagy induction (Corcelle, Puustinen et al. 2009).

5.2.2 FROM TSC TO mTOR

The signals starting from RAS, PI3K and AMPK, they all converge in TSC. TSC1 and TSC2 form a heterodimer which acts as a GTPase Activating Protein (GAP) for RHEB, since GDP-loaded RHEB is unable to activate mTORC1 (Gao, Zhang et al. 2002). Thus, both PI3K and RAS pathway phosphorylate TSC1/2 hence inhibiting it. Consequently, its GTPase activity is not promoted so GTP-loaded RHEB may induce mTOR activation.

In contrast, in the case of AMPK-mediated phosphorylation of TSC1/2 complex, the phosphorylation leads to its activation facilitating GDP-loaded RHEB and avoiding mTOR activation.

5.2.3 DOWNSTREAM mTOR

mTOR activation modulates different substrates, driving to different cellular effects related with cell growth and proliferation:

- Translation initiation, through two different pathways:
 - Activation by phosphorylation of ribosomal p70 S6 kinase 1 (p70S6K1): this kinase phosphorylates ribosomal protein S6 (RPS6), increasing the affinity of ribosomes for TOP-dependent mRNA thereby promoting their translation (Price, Grove et al. 1992).
 - mTOR inhibitory phosphorylation of 4EBP1, which activates eIF4E transcription factor allowing cap-dependent translation (Fingar, Salama et al. 2002).
- Autophagy inhibition, since mTORC1 is responsible for ULK phosphorylation. This will be further explained in the “Autophagy” section.
- Activation of hypoxia inducible factor 1 α (HIF1 α) which is a positive regulator of many glycolytic genes (Hudson, Liu et al. 2002).
- Activation of the transcription factor Sterol Regulatory Element Binding Protein 1c (SREBP1c), which enhances the accumulation of lipids (Yecies, Zhang et al. 2011).

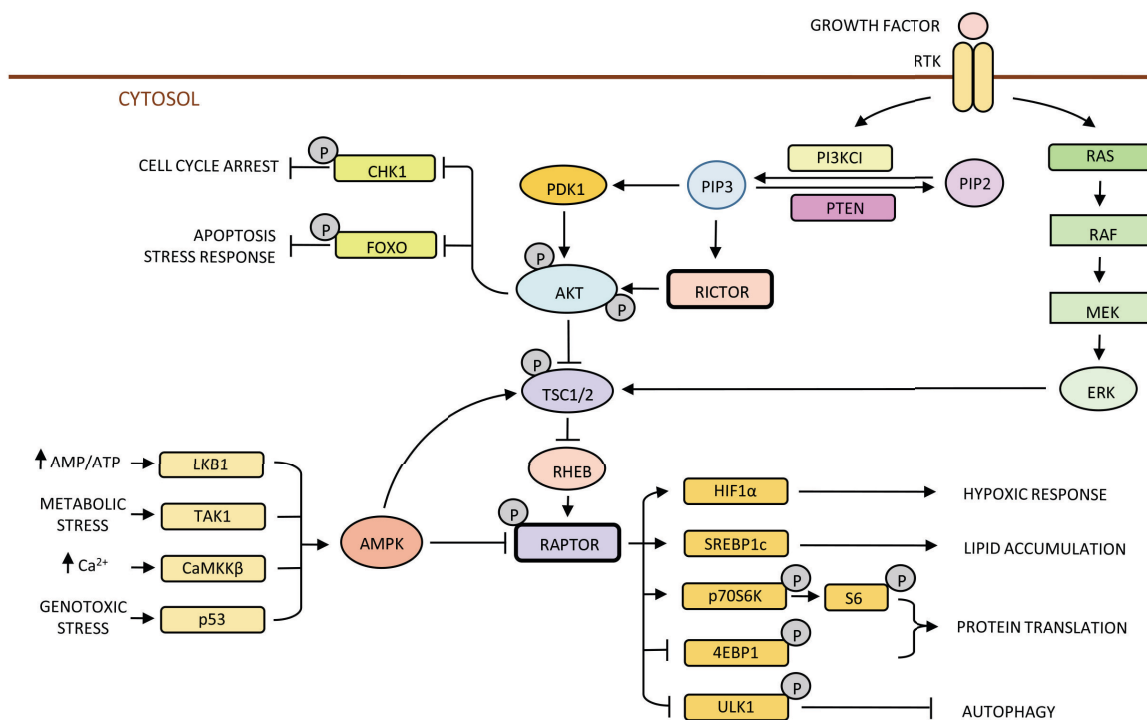


Figure 19: The mTOR signaling pathway. Signals starting from RTK and AMPK are summarized. Both pathways converge in RAPTOR, thereby modulating key processes such as hypoxic response, lipid accumulation, protein translation or autophagy. (Shackelford and Shaw 2009, Zoncu, Efeyan et al. 2011). Adapted.

5.3 mTOR PATHWAY AND GBM

As described in the “GBM” section, mTOR pathway is frequently mutated in GBM, being *EGFR*, *PDGFR* and *PTEN* the most common mutated genes in this pathway. Altogether, these mutations lead to overactivated AKT which leads to apoptosis inhibition and mTOR overactivation, thereby increasing protein translation and hypoxic response, as well as downregulation of autophagy.

Indeed, elevated AKT phosphorylation has been observed in up to 85% of glioblastoma cell lines and patient samples (Wang, Wang et al. 2004). Unfortunately, AKT inhibitors showed limited benefit in the clinics. In addition, several publications propose targeting autophagy in order to overcome this brain tumor (Lefranc and Kiss 2006, Salazar, Carracedo et al. 2009, Fan and Weiss 2011).

Thus, mTOR pathway overactivation must be taken into account in order to design new approaches to target this tumor or, at least, improve the survival of GBM patients.

6 CELL SURVIVAL: PTEN

Although PTEN can be considered as a part of mTOR pathway, a specific section is focused on PTEN due to its importance on this project.

6.1 GENERAL VIEW

PTEN (Phosphatase and TENsin homolog) is a protein encoded by a gene located in 10q23 chromosome region. The relationship between this chromosome region and tumor development was early described in the bibliography. In 1979 it was defined as a fragile chromosome region (Sutherland 1979) and some years later it was related with GBM development (Bello, de Campos et al. 1994).

However, PTEN was not described until 1997. Mapping of homozygous deletions on human chromosome 10q23 led to the isolation of a candidate tumor suppressor gene, PTEN, mutated at considerable frequency in human cancers (Li, Yen et al. 1997), including GBM as explained in the corresponding section above.

Before long, Cowden syndrome (CS), a rare genetic disorder which involves high predisposition to tumor development and Bannayan-Riley-Ruvalcava syndrome (BRRS), were associated with PTEN mutation (Arch, Goodman et al. 1997, Liaw, Marsh et al. 1997). Currently, PTEN mutation is well-known to be involved in 80% of classic CS, 60% of BRRS, up to 20% of Proteus syndrome (PS), and approximately 50% of a Proteus-like syndrome (PSL). Collectively, these four syndromes are referred to as PTEN Hamartoma-Tumor Syndromes (PHTS), further reinforcing the role of PTEN on tumor development (Eng 2003).

6.2 PTEN STRUCTURE

PTEN structure consists of three major domains: a phosphatase domain (residues 15-186), a C2 domain (186-351), and a C-terminal fragment (352-403). In addition, other motifs have been described (Wang and Jiang 2008). The PIP2 binding motif spans from residues 6 to 15, and the PEST motifs from 350 to 375. Finally, a “Loop” stands for the conserved but flexible region (286-309) within the C2 domain.

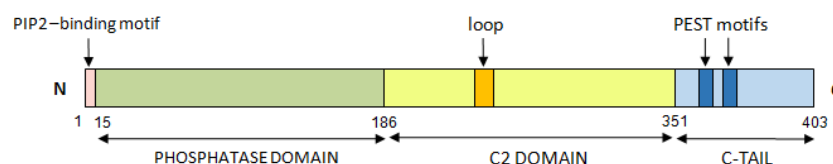


FIG 20: PTEN structure. The three major domains of PTEN, the phosphatase domain (“Phosphatase”, residues 15-186), the C2 domain (186-351), and the C-terminal fragment (“C-tail”, 352-403) are labeled. The numbers denote the amino acid positions of individual domains or motifs of human PTEN (Wang and Jiang 2008).

6.3 PTEN SUBCELLULAR LOCATION AND FUNCTIONS

6.3.1 CYTOSOL

Soon after its discovery, PTEN was assigned a serin-threonin phosphatase function (Myers, Stolarov et al. 1997). Only a few months later, this activity was described as essential for PTEN to exert its tumor suppressor activity (Furnari, Lin et al. 1997).

6.3.1.1 PTEN CYTOSOLIC FUNCTIONS

- **PTEN role as lipid-phosphatase**

Specifically, PTEN dephosphorylates the lipid second messenger Phosphatidylinositol 3,4,5-Trisphosphate (PIP3), which consequently is transformed in Phosphatidylinositol 4,5-Bisphosphate (PIP2) (Maehama and Dixon 1998). This activity counteracts the function of phosphatidylinositol-3-kinase (PI3K), negatively regulating PKB/AKT pathway (Stambolic, Suzuki et al. 1998). This pathway dictates multiple downstream signaling events, as broadly explained in the previous section.

Interestingly, AKT pathway and consequently PTEN are involved in spindle pole formation. Toyoshima's group reported in 2007 (Toyoshima, Matsumura et al. 2007) PIP3 involvement in spindle pole orientation and PTEN modulation of this process. Subsequent studies (Leonard, Hill et al. 2013) have shown PTEN-dependent pericentrin recruitment to mitotic centrosomes and PTEN localization to mitotic centrosomes, which is dependent on AKT kinase activity. Consequently, either knockdown of PTEN or inhibition of AKT increase centrosome defects.

- **PTEN role as protein-phosphatase**

Although the lipid phosphatase activity is the best-established function of PTEN, it can also target different proteins. Focal adhesion kinase (FAK) has been identified as a direct protein target of PTEN. Similarly, PTEN also reduces the tyrosine phosphorylation of p130^{cas}, a FAK downstream effector (Tamura, Gu et al. 1998).

6.3.2 NUCLEUS

Three years after PTEN identification, nuclear location for PTEN was firstly described (Lachyankar, Sultana et al. 2000). Since then, PTEN nuclear functions have been elucidated as crucial for genomic and mitotic maintenance.

Due to the importance of both PTEN and genomic and mitotic stability in this work, we will review in detail PTEN nuclear functions and PTEN nuclear import. The understanding of these processes is essential for the correct analysis of the results exposed in this thesis.

6.3.2.1 PTEN NUCLEAR FUNCTIONS

- **PTEN role in Homologous Recombination pathway**

Shen's group (Baker 2007, Shen, Balajee et al. 2007) determined that PTEN binds DNA in a sequence-specific manner, remodeling chromatin of the *RAD51* promoter so that the access of E2F1 transcription factor to *RAD51* promoter is facilitated and E2F1-mediated transcription of *RAD51* is increased. Consistently, PTEN-deficient MEFs showed increased nuclear foci containing phosphorylated histone H2AX, supporting increased DNA damage and compromised genome stability in absence of PTEN. This function is found to be phosphatase-dependent because the phosphatase deficient PTEN mutant (C124S) is unable to induce *RAD51* expression in *PTEN*-null cancer cells.

Nevertheless, different groups have not corroborated PTEN-*RAD51* relationship, neither in prostate cancer (Fraser, Zhao et al. 2012) nor lung cancer (Pappas, Zumstein et al. 2007), thereby suggesting a tumor type-dependent effect of PTEN on *RAD51* expression, and possibly that other pathways involved in this mechanism remain to be elucidated.

- **PTEN's role in centromere stability**

Shen's group (Shen, Balajee et al. 2007) also described a second nuclear PTEN function. PTEN contributes to centromere stability through its interaction with the core centromeric protein CENP-C. This group showed PTEN co-immunoprecipitated with this protein, which is required for proper kinetochore assembly and for the metaphase to anaphase transition.

In addition, this interaction was proved to be phosphatase-independent since the C terminus, but not the phosphatase domain of PTEN, was required for this interaction.

- **PTEN's role in CHK1 checkpoint**

CHK1-mediated checkpoint is tightly regulated by ATR kinase. In response to genotoxic stress, ATR targets CHK1, including serines 317 and 345. Phosphorylation of these residues results in CHK1 kinase activation and nuclear location, signaling for cell cycle arrest as it was further explained in the "Cell cycle" section.

In contrast, AKT phosphorylates CHK1 at serine 280. This phosphorylation acts as a signal for its ubiquitination and sequestration in the cytoplasm.

PTEN has been described to modulate CHK1 through its lipid-phosphatase activity. Counteracting PI3K/AKT pathway, PTEN avoids serine 280 phosphorylation and allows CHK1 to enter the nucleus in order to develop its role in cell cycle checkpoint (Puc, Keniry et al. 2005, Puc and Parsons 2005).

Although this role is lipid-phosphatase-dependent and is exerted by PTEN in the cytoplasm, it is explained in this section as PTEN is operating in order to allow the correct development of G1 checkpoint, thereby supporting a nuclear function.

• **PTEN's role in mitotic checkpoint**

Cell cycle progression is controlled by ubiquitination-mediated proteolysis of cell-cycle machinery. One of the major E3 ubiquitin ligases controlling this process is APC/C, active from mitosis to late G1 to ensure proper sister chromatids segregation in mitosis, as it was further reviewed in "Cell cycle" section.

APC/C was described as a PTEN-interacting protein by mass spectrometry (Song, Carracedo et al. 2011), promoting the association between APC and its partner CDH1 thereby enhancing the formation of APC-CDH1 complex. This complex maintains APC activity during late mitosis and G1 phase. In addition, they proved this association to be phosphatase-independent.

APC-CDH1 targets such as Aurora kinases or PLK1 display increased levels upon PTEN-loss, suggesting that PTEN-deficient tumors might exhibit "addiction" to these kinases and hence hypersensitivity to their pharmacological inhibition.

The discovery of these new PTEN functions has been crucial to understand in more details how loss of PTEN predisposes to tumorigenicity, which is an unavoidable step in order to counteract tumor development.

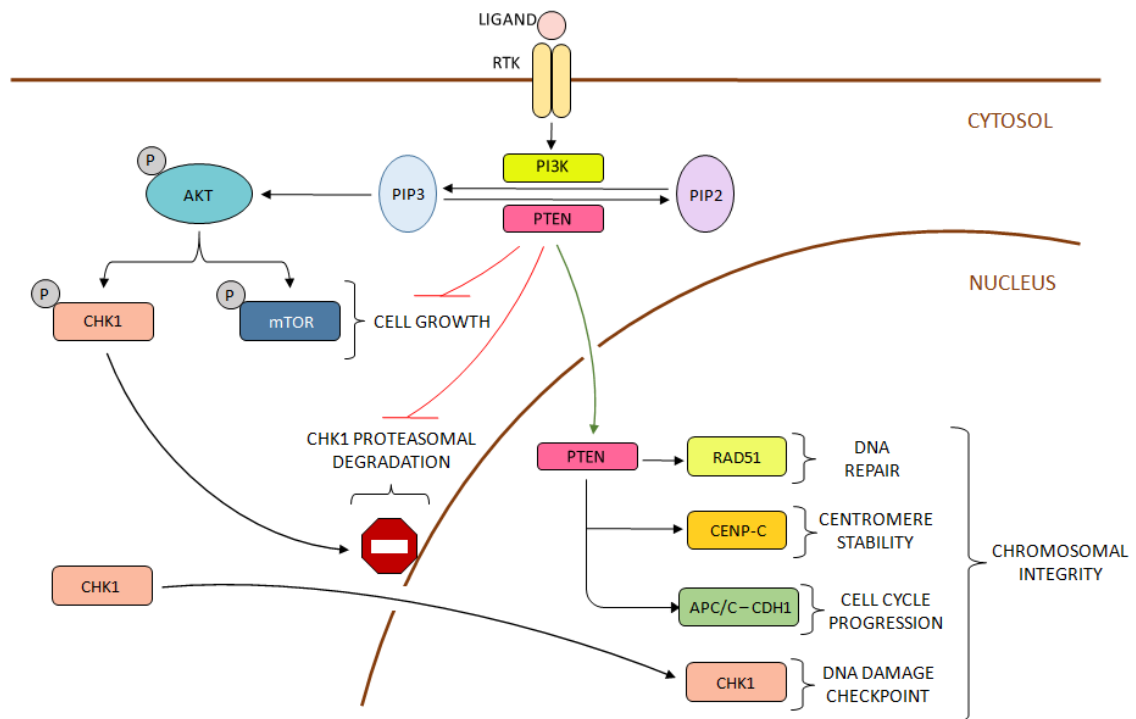


Figure 21: Proposed nuclear and cytoplasmic functions of PTEN and their regulation. In the cytosol, PTEN functions as a lipid phosphatase and antagonizes AKT activation and enhanced growth and proliferation. In contrast, when PTEN localizes in the nucleus it is involved in maintaining chromosomal integrity and develops functions phosphatase dependent and independent (Baker 2007). Adapted.

6.3.2.2 *PTEN's STRATEGIES TO ENTER THE NUCLEUS*

Since PTEN nuclear functions are well defined and essential for genome integrity, and loss of nuclear PTEN correlates with increased tumorigenicity (Gimm, Perren et al. 2000), PTEN nuclear translocation must be a finely-tuned process. Hence, different mechanisms have been described to modulate this mechanism:

- **Nuclear Location Signal-like mediated transport**

Although canonical Nuclear Location Signal (NLS) has not been found for PTEN, putative NLS (required for Major Vault Protein (MVP)–mediated nuclear translocation) are described (Chung, Ginn-Pease et al. 2005). Besides, the same group has shown that PTEN-MVP interaction is Calcium-dependent (Minaguchi, Waite et al. 2006).

- **Diffusion**

Liu and colleagues described diffusion mechanism is involved in PTEN nuclear localization since PTEN fusion proteins larger than 60 kDa (which is the limit for passive diffusion through nuclear pores) show decreased nuclear location (Liu, Wagner et al. 2005).

- **Ubiquitylation**

In 2007, Trotman and collaborators (Trotman, Wang et al. 2007) demonstrated that PTEN import is regulated by mono-ubiquitylation in Lys13 and Lys289. PTEN poly-ubiquitination, in contrast, leads to its cytoplasmic retention and degradation. This activity is modulated by NEDD4-1, which can both mono- and poly-ubiquitylate PTEN. Since mono-ubiquitylation is essential for PTEN function, NEDD4-1 effectively has both oncogenic (PTEN degradation) and tumor suppressive (PTEN shuttling) potential. In addition, NEDD4-1 requires Ndfiq1 (which is a NEDD-4-1 adaptor protein) to carry out PTEN ubiquitylation (Howitt, Lackovic et al. 2012), and this system is influenced by the presence of Rab5, which is a marker of early endosomes (Li, Low et al. 2014).

- **SUMOylation regulation of PTEN nuclear location**

In 2013, Bassi and colleagues reported that Lys254 is a SUMOylation site and SUMOylated PTEN is predominantly nuclear (Bassi, Ho et al. 2013). In addition, SUMO-PTEN is phosphorylated after IR in an ATM-dependent manner, excluding it from the nuclear fraction. Interestingly, a crosstalk between SUMOylation and ubiquitylation has been reported (Gonzalez-Santamaria, Campagna et al. 2012) although the cellular implications of this interaction are not completely understood.

6.4 PTEN AND PARP

For long, increased efficacy of PARP inhibition alone (suggesting synthetic lethality) (Mendes-Pereira, Martin et al. 2009, McEllin, Camacho et al. 2010) or combined (Minami, Takigawa et al. 2013, Gonzalez-Billalabeitia, Seitzer et al. 2014, Lin, de Gooijer et al. 2014) in PTEN mutant tumors has well been reported. Interestingly, some of these papers describe an effect in GBM (McEllin, Camacho et al. 2010, Lin, de Gooijer et al. 2014).

The relationship between PARP and PTEN had only been explained through their common involvement in DNA repair pathways. Nevertheless, a new connection between PARP and PTEN has been reported in 2015 (Li, Zhang et al. 2015). Thus, Tankyrases have been shown to PARylate PTEN, promoting its degradation and consequent tumor growth. Therefore, a new approach for the use of PARP inhibition in tumor treatment is highlighted.

7 CELL DEATH

In 1973 Schweichel and Merker (Schweichel and Merker 1973) proposed a classification of several cell death modalities, including ‘type I cell death’ associated with heterophagy, ‘type II cell death’ associated with autophagy and ‘type III cell death’, which was not associated with any type of digestion, corresponding to apoptosis, autophagic cell death and necrosis, respectively.

The very first categorizations of cell death necessarily relied on morphological traits. Currently, the scientific community has not yet adopted a systematic classification of cell death modalities based only on biochemical criteria. Nevertheless, the Nomenclature Committee on Cell Death (NCCD), on its rounds of recommendations in 2005, 2009 and 2012 (Kroemer, El-Deiry et al. 2005, Kroemer, Galluzzi et al. 2009, Galluzzi, Vitale et al. 2012), has made an effort for adopting a systematic classification of cell death based on measurable biochemical features.

In 2015 the NCCD (Galluzzi, Bravo-San Pedro et al. 2015) has sharpened some recommendations to classify cell death. Thus, a classification based on two broad, mutually exclusive categories: “accidental” and “regulated” is proposed. Accidental Cell Death (ACD) is caused by severe insults, including physical, chemical or mechanical stimuli. Although it can occur in vivo, it cannot be prevented or modulated and does not involve a specific molecular machinery. Hence, it does not constitute a direct target for therapy. In contrast, Regulated Cell Death (RCD) involves a genetically encoded molecular machinery, that can be targeted for therapy. Importantly, RCD occurs not only as a consequence of microenvironmental perturbations but also in physiological contexts such as post-embryonic development, tissue homeostasis or immune responses. These completely physiologic instances of RCD are generally referred to as ‘Programmed Cell Death’ (PCD).

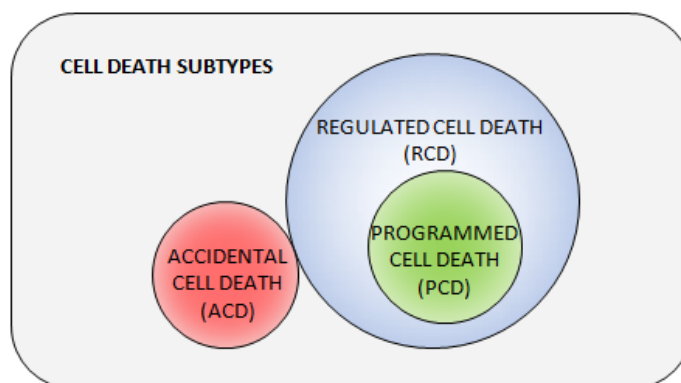


FIGURE 22: TYPES OF CELL DEATH. Cells exposed to extreme stimuli may succumb in an uncontrolled death process named “Accidental Cell Death” (ACD). Alternatively, “Regulated Cell Death” (RCD) can be initiated by a genetically encoded machinery and it can be pharmacologically or genetically targeted. The term “Programmed Cell Death” (PCD) is used to indicate RCD instances that occur as part of a physiological process (Galluzzi, Bravo-San Pedro et al. 2015).

According to NCCD, different kinds of regulated cell death have been characterized. Next, a brief description of them is provided. However apoptosis, autophagy and mitotic catastrophe are not reviewed in this subheading since further information will be provided below. Besides, for parthanatos description check the “PARP and cell death” section in the PARP chapter.

- ANOIKIS: Literally meaning 'the state of being homeless', this term of ancient Greek derivation was introduced by Frisch and Francis in 1994 to describe the apoptotic response of adherent cells due to the absence of cell-to-matrix interactions (Frisch and Francis 1994).
- ENTOSIS: Firstly described by Overholtzer et colleagues in 2007 (Overholtzer, Mailloux et al. 2007), entosis is provoked by the loss of extracellular matrix (ECM) interaction, but does not entail the activation of apoptotic executioners. Instead, it is a process that involves E-cadherin and RHO-GTPase, whereby cells become internalized into neighboring cells, forming the so-called 'cell-in-cell' structures. Once internalized, the cell may divide, escape or die, in a type of cell death that involves autophagy machinery and lysosome degradation (Florey, Kim et al. 2011).
- PYROPTOSIS was firstly reported in 2000 by Brennan and Cookson to functionally describe the peculiar death of macrophages infected by *Salmonella typhimurium* (Brennan and Cookson 2000). It is a caspase 1-caspase 3 dependent cell death subroutine which is associated with the generation of pyrogenic mediators such as IL-1 β and IL-18. It remains to be clarified whether pyroptosis truly constitutes a cell death subroutine on its own or whether it represents a particular case of caspase-dependent intrinsic apoptosis cell death.
- NETOSIS: netosis occurs in response to stimuli that provoke the release of Neutrophil Extracellular Traps (NETs), that is, microbicidal structures composed of nuclear chromatin, histones and granular antimicrobial proteins. It has been described in granulocytic cells and it is characterized by massive vacuolization of the cytoplasm, rapid chromatin decondensation and breakdown of both the nuclear and granular membranes, which is required for proper NET formation (Fuchs, Abed et al. 2007). Besides, it is downregulated following pharmacological inhibition of NADPH oxidase.
- CORNIFICATION: cells of the external layer of the epidermis (keratinocytes) continuously undergo a physiological cell death subroutine that has been dubbed cornification (Candi, Schmidt et al. 2005). Molecularly, cornification is associated with caspase 14, since its blockade alters (but not abrogates) this pathway.
- PROGRAMMED NECROSIS: for a long time, necrosis has been considered as a merely ACD mechanism and has been defined by the absence of morphological traits of apoptosis or autophagy. However, it is now clear that necrosis can occur in a regulated manner, and that necrotic cell death has a prominent role in multiple physiological and pathological settings. Indeed, when caspases are inhibited or blocked, RIP1 and its homolog RIP3 are not degraded and rather engage in physical and functional interactions that ultimately activate the execution of necrotic cell death (Galluzzi, Kepp et al. 2009).

7.1 APOPTOSIS OR TYPE I CELL DEATH

Apoptosis is essential to maintain homeostasis in multicellular organisms. Indeed, its implication in pathologies seemed clear from the beginning (Kerr, Wyllie et al. 1972, Wyllie, Kerr et al. 1980).

7.1.1 APOPTOSIS INITIATION: EXTRINSIC AND INTRINSIC BIOCHEMICAL PATHWAYS

7.1.1.1 EXTRINSIC OR DEATH RECEPTOR-TRIGGERED PATHWAY

'Extrinsic apoptosis' has been extensively used to indicate instances of apoptotic cell death that are induced by extracellular stress signals that are sensed and propagated by specific transmembrane receptors. It is initiated by the binding of lethal ligands to their Death Receptors (DR), which are members of the TNF Receptor (TNFR) superfamily, owing a cysteine-rich extracellular domain and a cytoplasmic domain named Death Domain (DD).

Currently, the best characterized lethal ligands are FAS/CD95 Ligand (FASL/CD95L), Tumor Necrosis Factor α (TNF α) and TNF-Related Apoptosis Inducing Ligand (TRAIL), which bind to their DR (FAS/CD95, TNF α Receptor 1 (TNFR1) and TRAIL receptor (TRAILR) 1–2, respectively (Trauth, Klas et al. 1989, Pan, O'Rourke et al. 1997, Ashkenazi and Dixit 1998).

The extrinsic phase of apoptosis is initiated when a cluster of three death receptors binds its homologous trimeric ligand (Chan 2007). Then, the receptors recruit cytoplasmic adapter proteins (FADD) through death domains (Chinnaiyan, O'Rourke et al. 1995) creating the Death-Inducing Signaling Complex (DISC). Although the exact composition of the DISC depends on the receptor, it always includes FADD. FADD then associates with pro-caspases via its Death Effector Domain (DED) which results in the autocatalytic activation of the initiator caspase 8 or 10 (Kischkel, Hellbardt et al. 1995, Muzio, Chinnaiyan et al. 1996).

- **Extrinsic pathway modulators: FLIP**

The death receptor-triggered pathway can be inhibited by FLIP, a protein that binds to FADD and caspase-8, rendering them ineffective (Scaffidi, Schmitz et al. 1999). Consequently, additional modulation of this pathway is reached, independently of the DISC ability to activate executioner caspases.

7.1.1.2 EXTRINSIC AND INTRINSIC PATHWAY CONNECTION: BID

Cells can be classified according to the efficacy of the extrinsic apoptotic pathway. In some cells, executioner caspases 3, 6 or 7 become effectively activated following activation of initiator caspase 8 or 10. However, other cells achieve only limited levels of executioner caspases activation following DISC formation, needing a mitochondrial amplification loop to finally trigger apoptosis (Scaffidi, Fulda et al. 1998). This loop occurs through caspase 8-mediated processing of the proapoptotic protein Bid. Truncated Bid (tBid) starts a biochemical signaling that leads to activation of the intrinsic apoptotic pathway through mitochondrial membrane permeabilization (Luo, Budihardjo et al. 1998).

7.1.1.3 INTRINSIC OR MITOCHONDRIAL PATHWAY:

The intrinsic or mitochondrial apoptotic signaling pathway is carried out by diverse non-receptor-mediated stimuli (Joza, Kroemer et al. 2002). This route, mainly mediated by the mitochondria, becomes activated as a result of the presence of different kinds of stimuli (e.g. radiation, toxins, hypoxia, free radicals) or the absence of an inhibitory signal (such as growth factors).

The canonical intrinsic apoptotic pathway is started when, following the stimuli, a mitochondrial permeability transition (MPT) pore is formed. Consequently, two processes are developed. First, Mitochondrial Outer Membrane Permeabilization (MOMP) takes place. Next, proapoptotic proteins are released from the Intermembrane Space (IMS) to the cytosol (Yang and Cortopassi 1998), inducing the mitochondrial apoptotic signaling pathway. The proteins released can be divided in two subgroups.

The first subgroup of released proteins contributes to caspase-dependent cell death, and is composed by cytochrome C, Smac (DIABLO) and HtrA2/Omi. When cytochrome C is released, it binds Apaf1 (Zou, Henzel et al. 1997). Then, Apaf1 suffers a first conformational change, exposing its nucleotide binding site. If available, dATP binds Apaf1 inducing a second conformational change thereby activating it. Subsequently, a heptameric protein complex of Apaf1 binds procaspase 9, forming the apoptosome and leading to caspase 9 activation (Zou, Li et al. 1999). Once active, caspase 9 promotes caspase 3, 6 or 7 activation and apoptosis execution. This process may be reverted by targeting caspases. However, if the apoptotic stimulus persists, a positive feedback on permeabilized mitochondria induces continued cytochrome C release. Finally, the situation derives in mitochondrial potential loss, which is established as a point-of-no-return in the apoptotic process (Saelens, Festjens et al. 2004).

In addition to cytochrome C, Smac (DIABLO) and HtrA2/Omi are also released from mitochondria. They promote caspase activation through the inhibition of IAPs (Inhibitors of Apoptosis Proteins) (Du, Fang et al. 2000, Suzuki, Imai et al. 2001).

The second group of released proteins has been related with caspase-independent rather than dependent cell death. In this modality AIF (Apoptosis Inducing Factor) and endonuclease G (endoG) translocate from the mitochondria to the nucleus where they degrade nuclear DNA in a caspase-independent way (Daugas, Susin et al. 2000, Li, Luo et al. 2001).

- **Intrinsic pathway modulators: BCL2 family**

The first member of BCL-2 family was discovered in lymphocyte B cells in 1984 (Tsujimoto, Finger et al. 1984). Since then, the family has been broadly described. Structurally, it is characterized by the presence of BCL-2 Homology (BH) conserved domains, which are the basis for BCL-2 family classification:

- The anti-apoptotic members are multidomain proteins that contain four BH domains (BH1, BH2, BH3 and BH4). This group includes BCL-2, BCL-XL, BCL-w, Mcl1 and BAG, among others. Functionally, they dimerize with a pro-apoptotic member of the family, impeding their activity.

- The pro-apoptotic members can be divided in two subgroups.
 - First, multidomain proteins, exemplified by Bax and Bak, containing three BH domains (BH1, BH2 and BH3) are involved in mitochondria permeabilization induction.
 - Second, BH only proteins, containing only a BH3 domain, can either inhibit antiapoptotic members or directly activate multidomain proapoptotic proteins (Letai, Bassik et al. 2002, Galonek and Hardwick 2006). The components of this group are BID, BIM, PUMA, BAD, NOXA, BMF and HRK.

Interestingly, different members of BCL2 family are involved in GBM malignancy. BCL2L12 is a potent inhibitor of post-mitochondrial effector caspase activation and the p53 tumor suppressor activity. Enforced expression confers marked apoptosis resistance in astrocytes, and, conversely, its RNA interference (RNAi)-mediated knockdown sensitizes glioma towards apoptosis both *in vivo* and *in vitro* (Stegh, Kim et al. 2007). In addition, GBM chemoresistance is known to be mediated by the anti-apoptotic member BCL-xL (Liwak, Jordan et al. 2013), which is regulated by the tumor suppressor programmed cell death 4 (PDCD4). Thus, a strong correlation between low expression of PDCD4 and high expression of BCL-xL has been demonstrated and associated with poor prognosis.

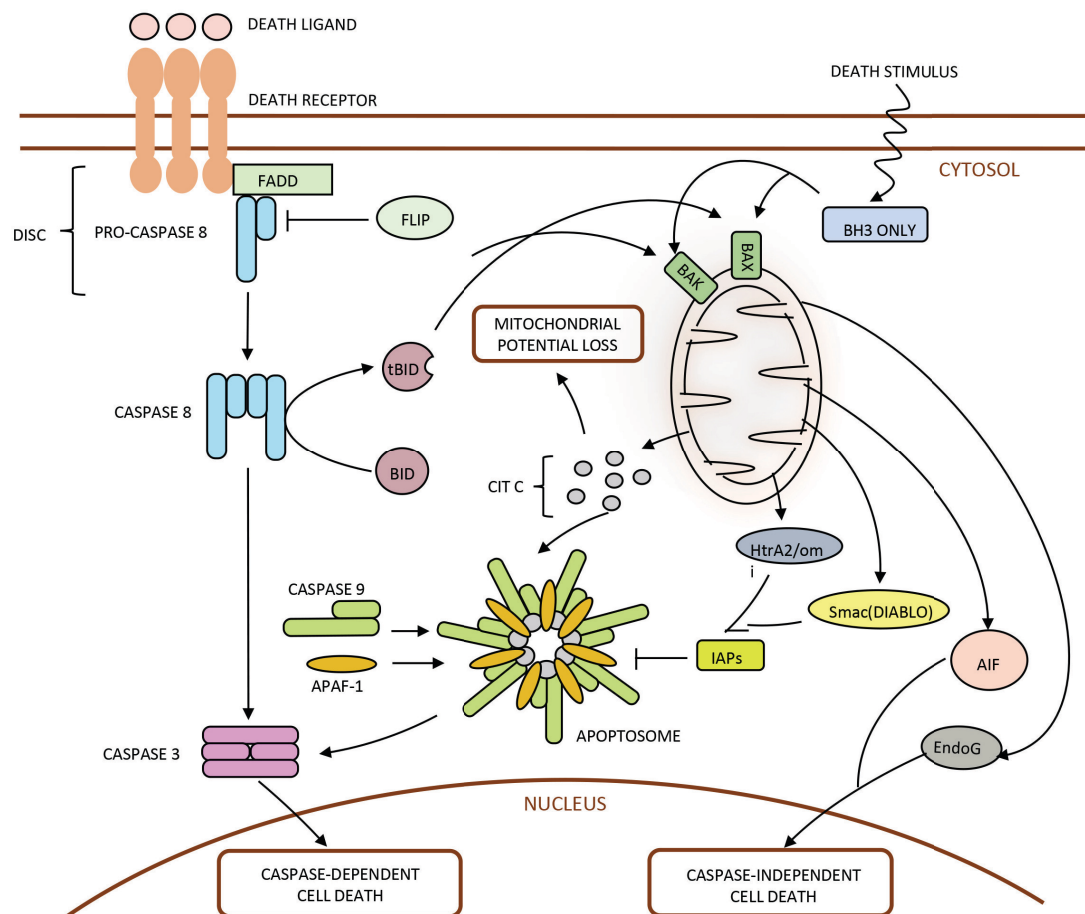


FIGURE 23: APOPTOSIS INTRINSIC AND EXTRINSIC PATHWAYS. Crosstalk between intrinsic and extrinsic apoptotic signaling pathways. The most important mediators and effectors of apoptosis, as well as their effects in cell, are represented above (Tilly 2001, Carlo-Stella, Lavazza et al. 2007). Adapted.

7.1.2 APOPTOSIS EXECUTION: CASPASES

7.1.2.1 GENERAL VIEW

Since the discovery of caspases protein family (Miura, Zhu et al. 1993, Yuan, Shaham et al. 1993), they have been considered key effectors of apoptotic cell death. They are a family of cysteine-dependent aspartate-directed proteases (c-asp-ases), containing a conserved QACXG pentapeptide G (where X is R, Q or G) surrounding the cysteine residue in the active site.

Functionally, they can be classified in three main categories: initiators (including caspases-2, -8, -9 and -10), executioners (such as caspases-3, -6 and -7) and inflammatory caspases (caspase-1, -4, -5 and 12). Initiators and executioners caspases are both involved in the apoptosis process.

7.1.2.2 STRUCTURE AND ACTIVATION

When synthesized, caspases are inactive proenzymes or zymogens composed by different subunits: first, a variable-length N-terminal prodomain; second, a large catalytic subunit (p20) containing the active site in the middle; and third, and a small catalytic subunit (p10) at the C-terminus (Cohen 1997).

Initiators caspases own large prodomains, including Death Effector Domain (DED) (Boldin, Goncharov et al. 1996) or CAspases Recruitment Domain (CARD) (Hofmann, Bucher et al. 1997). In contrast, executor caspases, which are activated through proteolysis by initiator caspases, exhibit a small N-terminal domain (Pop and Salvesen 2009).

The step from zymogen to active caspase differs between initiators and executor caspases (Pop and Salvesen 2009):

- Initiator caspases become active through dimerization. This process is facilitated by an activation platform (such as DISC or PIDDosome). When an adaptor molecule from the activation platform binds caspase prodomains DED or CARD, it serves as a signal for two molecules interaction through their p10 domain (Boatright, Renatus et al. 2003).
- In contrast, executor caspases become active through cleavage. In this case, dimerization occurred shortly after their synthesis. However, the dimer is active by cleavage of intersubunit linkers, carried out by active initiator caspases. Once active, executor caspases cleave at least 1,000 substrates in the cell, and it is the cleavage of such substrates that causes the changes associated with apoptosis (Green 2011).

Finally, independently of the activation mechanism, the mature caspase is a heterotetramer formed by two p20 and two p10 subunits.

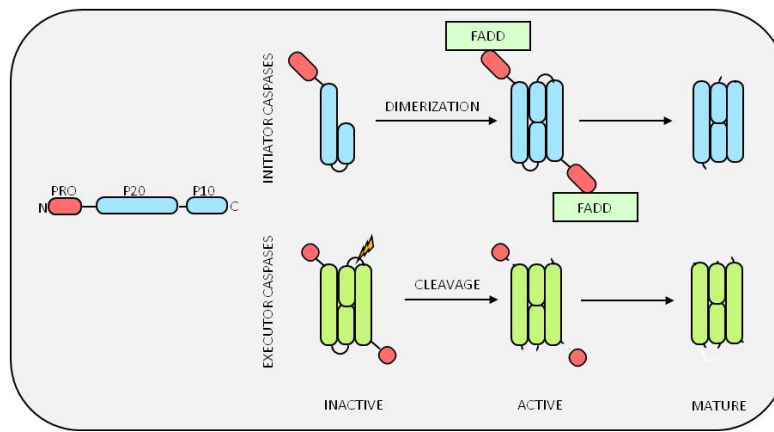


Figure 24. Caspases activation mechanisms. Through adaptor molecules, initiator caspases become recruited and dimerize. Then, by autoproteolysis, the mature form is generated. Executioner caspases, which exist as dimers, are activated by initiator caspases through proteolysis. Then, by additional proteolytic events, prodomains are removed (Pop and Salvesen 2009). Adapted.

7.1.3 APOPTOSIS CONSEQUENCES: HALLMARKS OF APOPTOSIS

Apoptotic cells are characterized by a series of traits which are enumerated below:

- Reduction in the mitochondrial trans-membrane potential (Zamzami, Marchetti et al. 1996).
- Intracellular acidification (Gottlieb, Nordberg et al. 1996).
- Production of Reactive Oxygen Species (ROS) (Hockenbery, Oltvai et al. 1993).
- Externalization of phosphatidylserine (Fadok, Voelker et al. 1992).
- Selective proteolysis of a subset of cellular proteins (Lazebnik, Kaufmann et al. 1994).
- Degradation of DNA into inter-nucleosomal fragments (Wyllie, Morris et al. 1984).
- Nuclear pyknosis and “Blebbing” (Robertson, Bird et al. 1978).

Among all these alterations, nuclear changes regarding chromatin condensation and DNA degradation are considered the hallmarks of apoptosis.

- **Chromatin condensation:** Initially, chromatin condenses around the nuclear membrane, in a process named stage I chromatin condensation, which is a caspase-independent AIF-dependent event. Later, stage II chromatin condensation, which is a caspase-dependent process, condenses chromatin into highly packed round masses (Yuste, Sanchez-Lopez et al. 2005).
- **DNA fragmentation:** Genomic DNA cleavage occurs in at least two stages during apoptosis: initial cleavage at intervals of 50 kbp, correlating with the size of chromatin loop domains, followed by a second stage of internucleosomal DNA cleavage or DNA laddering (Oberhammer, Wilson et al. 1993). While AIF (Susin, Lorenzo et al. 1999) and topoisomerase II (Li, Chen et al. 1999) have been involved in the initial cleavage step, DNA laddering has been associated with DNA fragmentation factor (Liu, Li et al. 1998), endonuclease G (Li, Luo et al. 2001, Parrish, Li et al. 2001) and DNase I (Peitsch, Polzar et al. 1993, Oliveri, Daga et al. 2001).

7.2 AUTOPHAGY OR TYPE II CELL DEATH

The term “autophagy” comes from the Greek words “phagy” meaning eat, and “auto” meaning self, and was coined by Christian de Duve at the CIB Foundation Symposium on Lysosomes in 1963 (De Duve and Wattiaux 1966). Autophagy can be defined as a primarily degradative pathway that takes place in all eukaryotic cells, conserved from yeast to mammals, which can be classified in three major intracellular pathways that share a common destiny of lysosomal degradation but are mechanistically different from one another:

- Macroautophagy, in which the cytoplasmic cargo is sequestered inside double-membrane vesicles named autophagosome. These autophagosomes are then delivered to the lysosome for degradation, thereby forming the autolysosome.
- Microautophagy, in contrast, involves the direct engulfment of cytoplasm at the lysosome surface (Kunz, Schwarz et al. 2004).
- Chaperone-Mediated Autophagy (CMA), which only occurs in mammals, translocates unfolded, soluble proteins directly across the limiting membrane of the lysosome (Cuervo and Dice 2000, Cuervo, Gomes et al. 2000).

Both micro and macro autophagy can be selective or nonselective. Nonselective autophagy is used for the turnover of bulk cytoplasm under starvation conditions, whereas selective autophagy specifically targets damaged or superfluous organelles, including mitochondria and peroxisomes, as well as invasive microbes:

| | TYPE | CARGO | PROCESS ASSOCIATED |
|-----------------------|----------------------------|--|-------------------------|
| MACROAUTOPHAGY | NON-SELECTIVE | Random | AUTOPHAGOSOME FORMATION |
| | SELECTIVE | Cytoplasm to Vacuole (Cvt pathway; <i>S.cerevisiae</i>) | |
| | | Mitochondria (mitophagy) | |
| | | Peroxisomes (pexophagy) | |
| | Lipid Droplets (lipophagy) | | |
| MICROAUTOPHAGY | NON-SELECTIVE | Random | VACUOLE INVAGINATION |
| | SELECTIVE | Mitochondria | |
| | | Peroxisomes | |
| | | Nuclear membrane | |

Table 6: The main types of autophagy. Macro and microautophagy are classified according to the selectivity and content of their cargo, as well as the process that is associated with each one of them. (Feng, He et al. 2014).

The current study is focused on macroautophagy, which will be referred hereafter as autophagy. In addition to important housekeeping functions, autophagy is a mechanism that can mediate both pro-survival and pro-cell death situations. The characteristics of the process that leads to both scenarios will be further reviewed below.

7.2.1 AUTOPHAGIC PROCESS IN MAMMALS

Early studies of autophagy from the 1950s to the 1980s were based on morphological analyses. They primarily examined the different stages of the process, the steps just before and after fusion with the lysosome. Subsequent studies led to the identification of the phagophore and the amphisome, and allowed to identify the successive levels in the autophagic process that are presented below. It is important to remark that these levels are established even though the boundaries between them are not clear cut. Each one can be in turn divided in different phases:

7.2.1.1 INITIATION

- Induction of autophagy occurs when proteins involved in the early stages of the process are activated.
- Nucleation occurs when part of the cytoplasm containing long-lived proteins or organelles is surrounded by a cisternal membrane, designated the phagophore (Seglen, Gordon et al. 1990).
- Elongation is the process by which the phagophore expands to form a double-membrane vacuole, which is then sealed or closed forming the autophagosome.
- Autophagosomes use dynein motors to move along microtubules towards the microtubule-organizing center where the next level processes take place.

7.2.1.2 MATURATION

- Fusion occurs when the autophagosomes fuse with lysosomes to form autolysosomes, in a process mediated by the proteins RAB7 (Gutierrez, Munafo et al. 2004) and Lysosome Associated Membrane Protein (LAMP) (Tanaka, Guhde et al. 2000). In addition, most of the autophagosomes receive input from the endocytic compartments before they fuse with lysosomes, thereby forming a structure, named amphisome (Gordon and Seglen 1988).
- Degradation of the inner membrane and cargo is carried out by active acid hydrolases (such as Cathepsin B and D) (Ohsawa, Isahara et al. 1998).
- Recycling of the resulting macromolecules is a final step performed by permeases. In the case of degradative autophagy, the resulting products can be re-used in the cytosol to synthesize essential cellular components needed to survive starvation conditions. This cell-protective role of autophagy implies the existence of a mechanism for the recycling of the degradation products generated by autophagy. Permeases located in the limiting membrane of the vacuole could play such a role for the mobilization of amino acids resulting from autophagy (Yang and Klionsky 2007).

Interestingly, endoplasmic reticulum (ER) has recently been determined as responsible for the origin of the membranes involved in autophagosome formation (Ge and Schekman 2014).

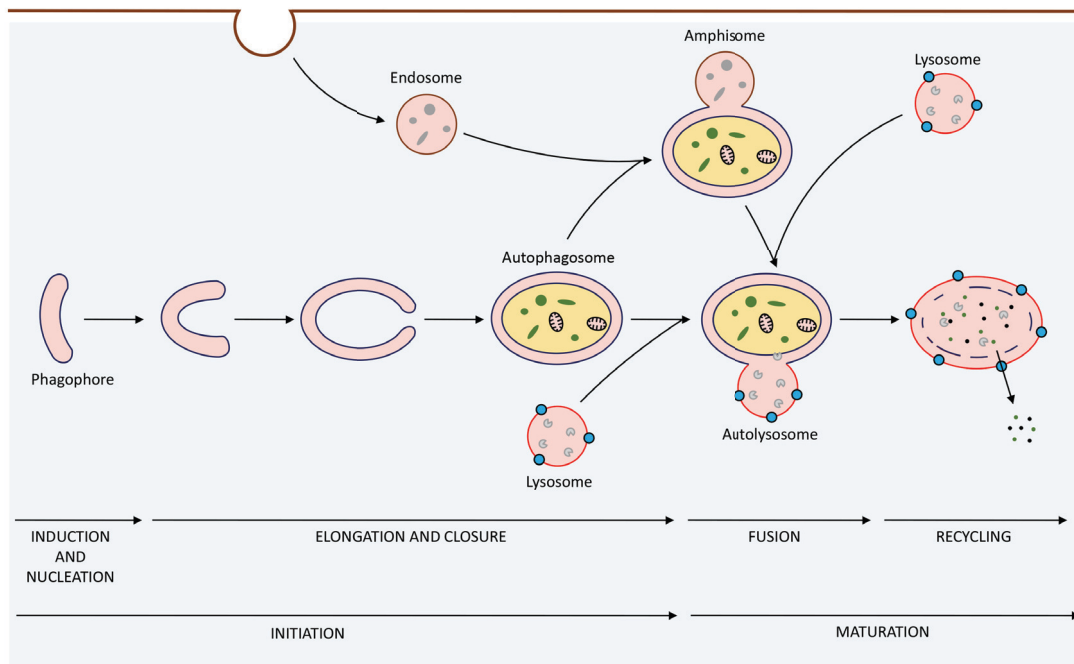


Figure 25: Steps in the autophagy process. Phagophore elongation is necessary for autophagosome formation. Before fusing with lysosome, autophagosome may, or not, bind an endosome thereby forming an intermediary structure named amphisome. Once autolysosome is formed, acid hydrolases will degrade the cargo, which is then recycled to the cytosol. (Yang and Klionsky 2010, Yang and Klionsky 2010). Adapted.

7.2.2 AUTOPHAGIC MOLECULAR PATHWAY

Insights into the molecular control of autophagy started in the late 1990s and were crucial for expanding on our understanding of the process. Pioneering work in yeast (Takeshige, Baba et al. 1992, Tsukada and Ohsumi 1993) was followed by the identification of the first Autophagy-Related-Gene (ATG) in 1997 (Matsuura, Tsukada et al. 1997). Since then, many ATG genes have been identified and the molecular pathway that is developed during autophagy activation has been well-described.

Autophagic pathway is composed of four subgroups of proteins that develop specific functions in the autophagosome formation process reviewed above. From now on, the words in brackets are related to the homologue in yeast.

7.2.2.1 ULK COMPLEX AND AUTOPHAGY INDUCTION

The ULK1 kinase complex consists of ULK1/2 (ATG1), mATG13 (ATG13), FIP200 (ATG17). Recently, a new mATG13-interacting protein, ATG101, has been uncovered (Mercer, Kaliappan et al. 2009). Under conditions that inhibit autophagy (presence of nutrients) mTOR phosphorylates and inhibits ULK1/2 and mATG13 (Hosokawa, Hara et al. 2009). Nevertheless, under conditions that induce autophagy (starvation), ULK1 and ULK2 are dephosphorylated and thereby activated. Then, ULK phosphorylates itself, and it also phosphorylates mATG13

and FIP200 (Jung, Jun et al. 2009). Autophagy is further processed once the ULK kinase complex is active.

7.2.2.2 CLASS III PI3K COMPLEX AND AUTOPHAGOSOME NUCLEATION

In mammals, the class III PI3K complex (PI3KCIII complex) plays an essential role in isolation of membrane nucleation during autophagy (Marino and Lopez-Otin 2004), while the PI3KCI is involved in the activation of AKT and mTOR (as previously reviewed in mTOR section). PI3KCIII (Vps34) is associated with Beclin1 (ATG6) and p150 (Vps15 or phosphoinositide-3-kinase, regulatory subunit 4), to form the PI3KCIII complex. The interaction of Beclin1 with PI3KCIII promotes PI3KCIII's catalytic activity, increasing the levels of phosphatidylinositol 3-phosphate (PIP) (Petiot, Ogier-Denis et al. 2000). Although it is not clear how PI3KCIII complex regulates autophagosome nucleation, PIP is proposed to be a signal for the recruitment of consecutive proteins.

The PI3KCIII complex may associate with different proteins, promoting or inhibiting autophagy activation. Thus, PI3KCIII complex promotes autophagy activation when interacting with ATG14L/Barkor (Fan, Nassiri et al. 2011) or with UVRAG. Ambra1 and Bif-1 are essential for the induction of autophagy through direct interaction with Beclin1 and UVRAG respectively (Yang and Klionsky 2010). Nevertheless, PI3KCIII complex associated with UVRAG-Rubicon negatively regulates autophagy.

7.2.2.3 TWO UBIQUITIN-LIKE PROTEINS (ATG12 AND LC3) AND AUTOPHAGOSOME ELONGATION

Studies in yeast and mammals have identified two ubiquitin-like proteins, ATG12 and microtubule-associated protein 1A/1B-Light Chain 3 (LC3) and their respective conjugation systems, which are proposed to have a role during elongation.

ATG12 is conjugated to ATG5 in a reaction that requires ATG7. The ATG12-ATG5 conjugate then interacts with ATG16L to form ATG12-ATG5-ATG16L protein complex (Mizushima, Noda et al. 1999, Kuma, Mizushima et al. 2002).

Otherwise, LC3-I (ATG8) is cleaved by cysteine protease ATG4 and then conjugated with phosphatidylethanolamine (PE) by ATG7 (Ichimura, Kirisako et al. 2000), leading to the form LC3-II, in an essential process for the formation of autophagosomes. This lipidated LC3-II then associates with newly forming autophagosome membranes. The conversion of LC3-I to LC3-II is thus well-known as a marker of autophagy-induction. However, the increase of LC3-II alone is not enough to show autophagy activation since the inhibition of LC3-II degradation in the lysosome by blocked autophagy flux can also cause its accumulation (Pyo, Nah et al. 2012).

7.2.2.4 TRANSMEMBRANE PROTEINS IN MAMMALIAN AUTOPHAGY. mATG9 AND AUTOPHAGOSOME MEMBRANA ORIGIN

Mammalian ATG9 (mATG9) is a transmembrane protein that is required for mammalian autophagy. Located in the *trans*-golgi network and late endosomes, ULK1 and PI3KCIII activity are required for mATG9 cycling (Young, Chan et al. 2006). Although its function remains

unclear, it is suggested to contribute to the delivery of membrane to the forming autophagosome (Orsi, Razi et al. 2012).

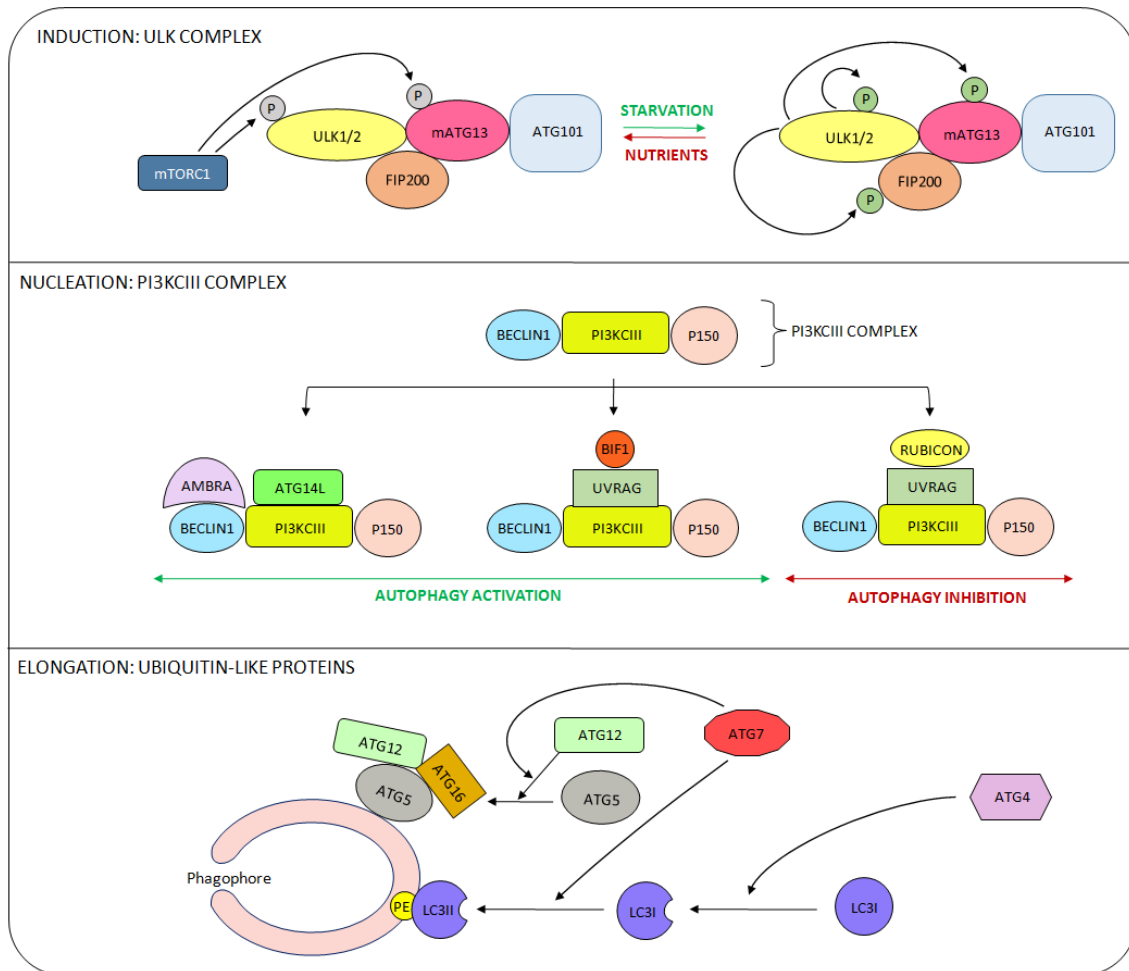


Figure 26: Induction, nucleation and elongation. Proteins involved in each one of these processes. (Yang and Klionsky 2010, Pyo, Nah et al. 2012). Adapted.

7.2.3 AUTOPHAGIC CELL DEATH

The term “autophagic cell death” has widely been used to indicate instances of cell death accompanied by increased autophagic flux. Scientists have adopted the term “autophagic cell death” and used it to imply that autophagy would actually execute the cell demise.

In response to stress and during development, eukaryotic cells often activate autophagy. Starved and stress-induced autophagy most often exerts cytoprotective functions and favors the re-establishment of homeostasis and survival of the cells by providing them with nutrients and removing damaged macromolecules and organelles. Consistently, in this case pharmacological or genetic inhibition of autophagy accelerates cell death. On the contrary, during development or in a context implying excessive stress, autophagic cells may commit suicide by undergoing so-called type II programmed or autophagic cell death. Consequently, in

this later case, inhibition of autophagy would inhibit cell death, indicating that autophagy also constitutes a lethal mechanism that mediates “autophagic cell death” (Galluzzi, Vitale et al. 2012).

Thus, autophagy is a cellular process with dual functions: while in some instances it is a pro-survival mechanism and is activated to overcome different stresses, in other cases (especially when stress is excessive) it is a major mechanism of cell death.

7.2.4 SIGNALING PATHWAYS REGULATING AUTOPHAGY

7.2.4.1 mTORC1 PATHWAY

The rapamycin-sensitive mTORC1 S/T protein kinase, broadly reviewed in previous sections, is the master energy-sensor of the cell. As a central sensor of the availability of growth factors, nutrients and energy sources, mTORC1 plays a key role in the regulation of temporal aspects of cell growth by activating protein synthesis and suppressing autophagy. Indeed, active mTORC1 is responsible for ULK phosphorylation thereby impeding autophagy activation. Contrary, under nutrient deprivation mTORC1 is inhibited promoting ULK dephosphorylation and autophagy activation (Hosokawa, Hara et al. 2009, Jung, Jun et al. 2009).

7.2.4.2 AMPK

The AMP-activated protein kinase (AMPK) is a heterotrimer composed of a catalytic (AMPK α) subunit and two regulatory (AMPK β and AMPK γ) subunits. AMPK is the master sensor of cellular bioenergetics, specifically in response to energy stress, and its activity and regulation have been previously analyzed in the “mTOR” section.

7.2.4.3 P53

The p53 tumor suppressor p53 has a dual role in autophagy. Upon genotoxic stress, active p53 first, activates AMPK leading to autophagy activation. And second, it induces mTORC1-independent autophagy through upregulation of the Damage-Regulated Autophagy Modulator (DRAM) (Crighton, Wilkinson et al. 2006). Nevertheless, p53 knockdown leads to autophagy activation, possibly due to cytosolic p53 activity. The machinery underlying these apparently contrary effects remains to be elucidated.

7.2.4.4 BCL-2 PROTEIN FAMILY

In mammals, BCL-2 family plays a dual role in autophagy regulation. While anti-apoptotic proteins such as BCL-2, BCL-X_L, BCL-X or Mcl-1 may inhibit autophagy, pro-apoptotic BH3-only proteins such as BAD can induce autophagy (Levine, Sinha et al. 2008).

The best-known process connecting apoptosis and autophagy is the binding of BCL-2 to Beclin-1, which disrupts the association of Beclin-1 with PI3KCIII thereby inhibiting autophagy (Pattingre, Tassa et al. 2005).

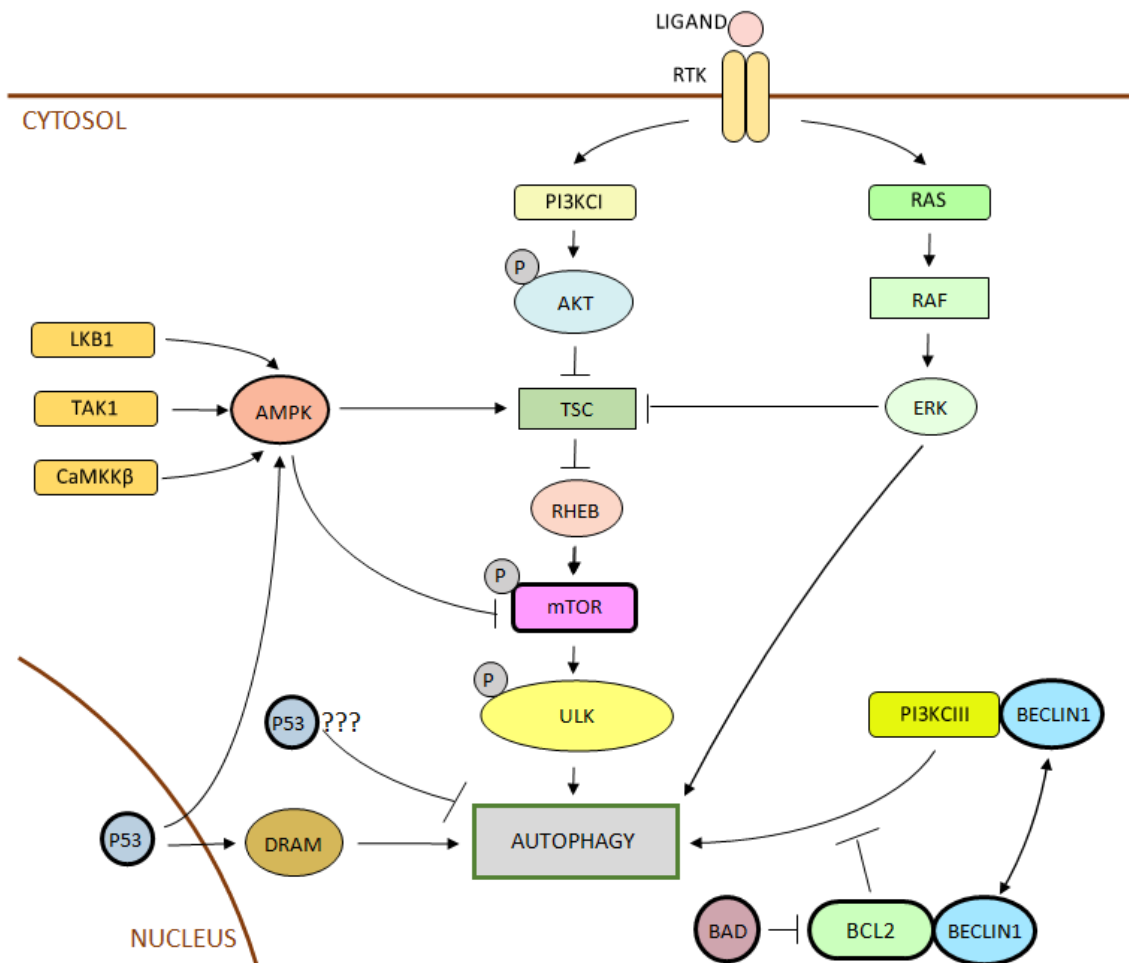


Figure 27: Signaling pathways modulating autophagy activation. AMPK, mTOR, p53 and BCL-2 family (bold outline) signaling pathways are integrated in one slide (Yang and Klionsky 2010, Yang and Klionsky 2010). Adapted.

7.2.5 LIPOPHAGY

7.2.5.1 GENERAL VIEW

Triglycerids (TG) and cholesterol are safely stored as neutral lipids in specialized cellular organelles called Lipid Droplets (LDs). Until recently, the release of LD-stored TG and cholesterol was attributed exclusively to the cytosolic hydrolytic enzymes or lipases. Nevertheless, more recently a function for macroautophagy has been assigned in the breakdown of LDs, through a pathway defined as lipophagy. Lipophagy was firstly described in hepatocytes (Singh, Kaushik et al. 2009) and it has been more recently extended to many other cell types.

The major lipid-accumulating system in the body are adipocytes. White adipocytes typically contain a single, large LD from up to 100 μ M in diameter (occupying the majority of the cytosol), which core is predominantly formed by TGs. Nevertheless, many other cell types may contain LD, in which cholesterol and TGs share the nuclear core of the droplet and where the

droplet is usually less than 1 μM in size except for extreme pathological cases, such as hepatocytes in steatosis (Suzuki, Shinohara et al. 2011). Non-adipocyte LDs are often observed juxtaposed next to the endoplasmic reticulum (ER) and exhibit directional movement across long distances through interaction of LD-associated proteins with microtubules (Welte 2009).

7.2.5.2 LIPID DROPLETS MOBILIZATION MECHANISMS

Lipid droplets consist of intracellular deposits of lipid esters (TG and cholesterol) surrounded by a monolayer of phospholipids, and separated from the hydrophilic cytosolic environment by a coat of structural proteins known as perilipins (Greenberg, Egan et al. 1991).

Besides, the surface of the LD is also coated by many proteins involved in LD metabolism. LD degradation or lipolysis is mediated, as explained above, by lipases and lipophagy. Consequently, proteins involved in both mechanisms interact with the LD. Thus, lipases are found at the surface of the LD, where they can interact with lipases activators or inhibitors in order to modulate the rate of lipolysis. In addition, lipophagy machinery is also associated to the LD surface. Thereby, LC3, ATG7 and ATG5 have also been found in located areas of the LD surface (Singh, Kaushik et al. 2009).

7.2.5.3 LIPOPHAGY PROCESS

Lipophagy starts with the recruitment of LC3 to the LD surface. There, LC3 initiates the formation of a limiting membrane through ATG7-dependent conjugation, leading to the establishment of an autophagosome. This autophagosome may be classified in three groups according to its content:

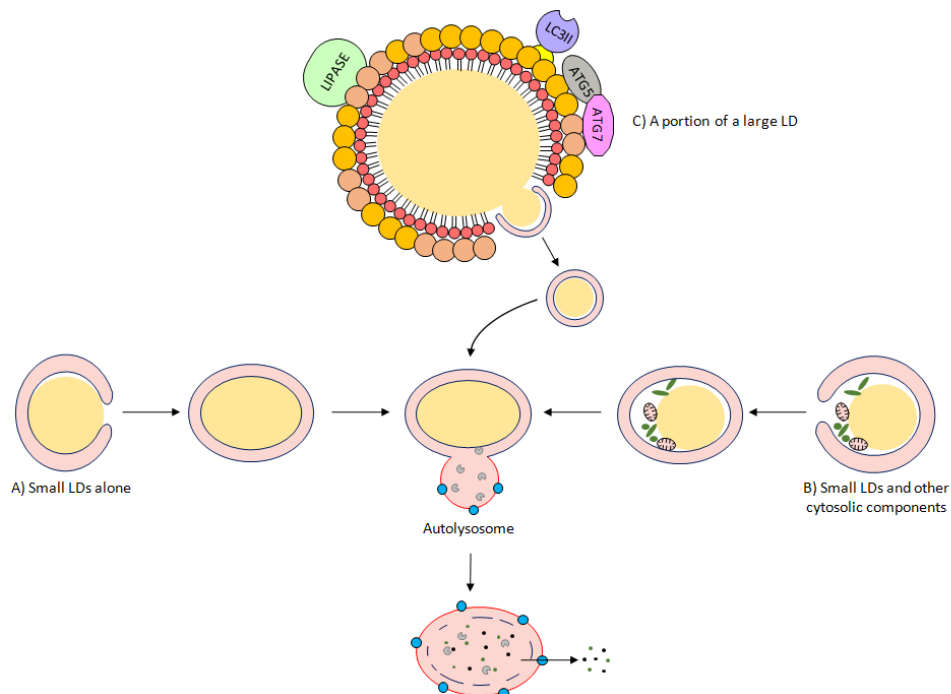


Figure 28: Different cargo in lipophagy signaling. During lipophagy, three different kind of autophagosomes are formed according to the content of their cargo (Singh and Cuervo 2012, Liu and Czaja 2013). Adapted.

- Whole small LDs alone.
- Small LDs and other cytosolic components that may also become trapped in the sealing vesicle.
- A portion of the LD, which occurs in cases of too large LDs.

7.2.5.4 PATHWAYS AND STIMULUS FOR LD FORMATION AND DEGRADATION

The pathways involved in LD formation and degradation are briefly explained as follows:

- LD are formed starting from Free Fatty Acids (FFA) that are converted to neutral lipids. Two pathways are involved in the accumulation of FFA in the cell, which may then be used for LD formation:
 - De novo synthesis of FFA is initiated with Acetyl-CoA, which is transformed in Malonil-CoA through Acetyl-CoA Carboxylase (ACC). Next, Fatty Acid Synthase (FASN) performs the condensation of Acetyl-CoA and Malonyl-CoA to produce the saturated Fatty Acid (FA) Palmitate and other saturated long chain FAs. Saturated long-chain FAs can be further modified by elongases or desaturases to form more complex FAs which are used for the synthesis of various cellular lipids (Menendez and Lupu 2007).
 - Phospholipids degradation through cytosolic Phospholipase A2 (cPLA2), which is an enzyme responsible for the hydrolysis of membrane phospholipids. Following activation, cPLA2 cleaves phospholipid to yield FFA and lysophosphatidic acid.
- Following stimulus that promote LD degradation, the pool of FFA is again increased in the cell. These FFA may have different destinations:
 - β -oxidation, which is the process by which fatty acids are broken down to produce energy. First, FA is added a CoA group by Fatty Acid CoA Synthetase (FACS). Second, Carnitine Palmitoyl Transferase 1 (CPT1) converts the newly-formed acyl-CoA to acylcarnitine, which is then transported inside the mitochondrial matrix. CPT2 then converts acylcarnitine back to acyl-CoA. Third, acyl-CoA can then enter the β -oxidation pathway, resulting in the production of one acetyl-CoA from each cycle of β -oxidation. This acetyl-CoA may then enter the Tri-Carboxylic-Acid (TCA) cycle in order to obtain Energy.
 - Phospholipid synthesis starts with lysophosphatidic acid synthesis. Acyl-CoA is added to glycerol 3-phosphate to produce first lysophosphatidic acid, and then to phosphatidic acid. This reaction is catalyzed by glycerol 3-phosphate acyltransferase. Phosphatidic acid can be then used in the synthesis of several phospholipids.

Thus, according with the cellular conditions, FFA may be synthesized and kept in LD; then, when needed, they may be degraded to obtain again FFA and used as a source of energy, or alternatively in phospholipid synthesis.

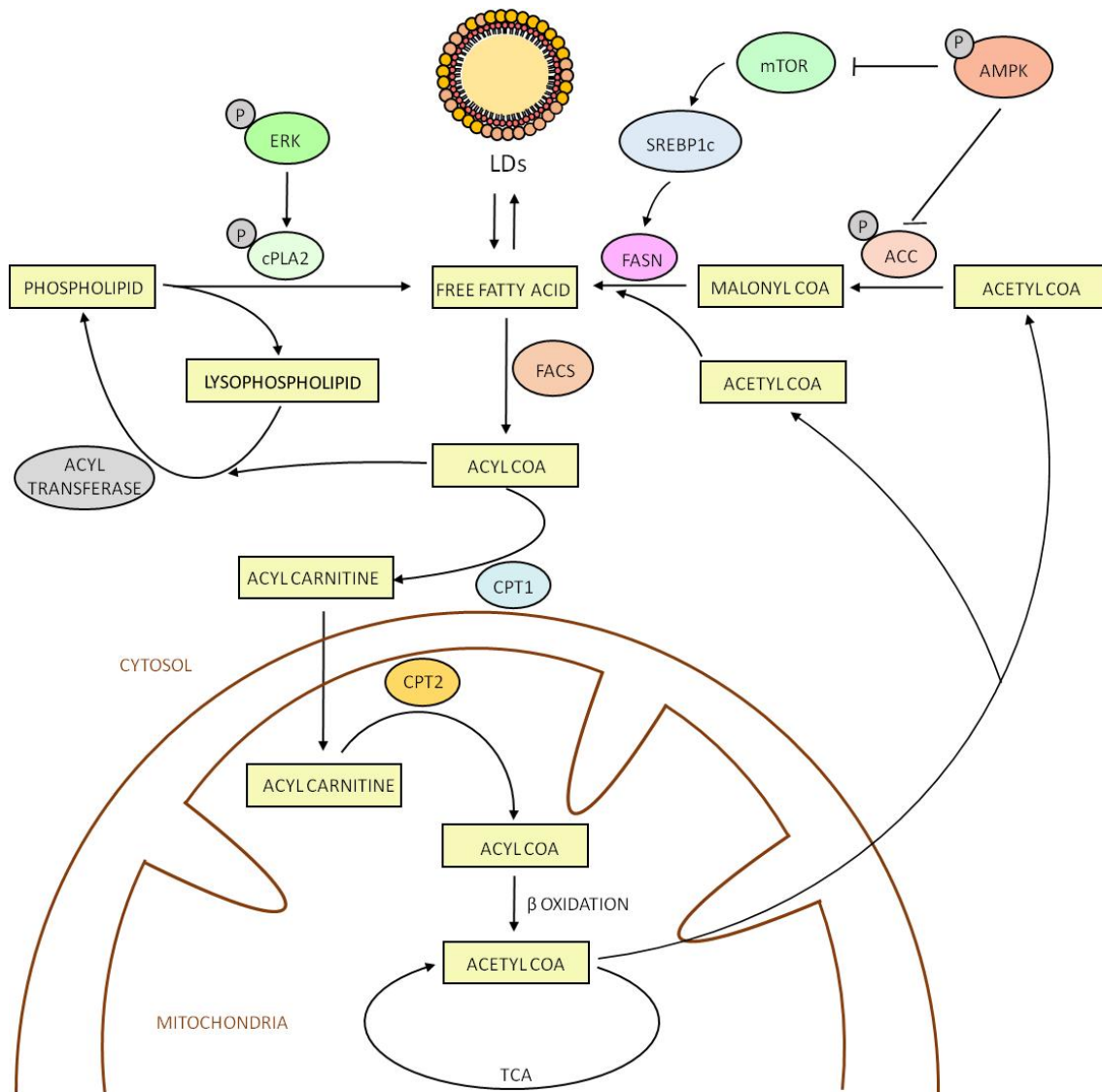


Figure 29: Signaling pathways modulating lipid droplets synthesis and degradation. FFA may be obtained through phospholipid degradation or through de novo synthesis via FASN. According to the cell status, these FFA undergo lipid droplets formation or degradation in order to obtain Energy through β -oxidation and Tri-Carboxylic Acid cycle.

7.2.5.5 LIPID DROPLETS MOBILIZATION SIGNALS

LD synthesis and degradation is a dynamic process. Both may take place at the same time; hence, the global balance between both processes is crucial for determining the cell's choice towards LD synthesis or degradation.

Although LD mobilization takes place under basal situation in the cell, three kinds of stimulus have been described to promote lipid mobilization:

- Nutrient status determines the availability of FFA in the cell (Singh, Kaushik et al. 2009, Singh and Cuervo 2012).
 - In starvation, low FFA promotes LD degradation which are used to increase FFA and β -oxidation.
 - In contrast, high FFA promotes LD synthesis allowing then the storage of the excess of FFA.
- High amount of LDs promote their own degradation. This apparently contradictory effect may be might occur as a mechanism to avoid the toxicity provoked by an excess of LD in the cell (Khalidoun, Emond-Boisjoly et al. 2014). Hence, high FFA promote LD synthesis but, too much LD synthesis will promote, at the same time, LD degradation to evade lipotoxicity.
- Oxidant stress promotes LDs degradation (Liu and Czaja 2013). In an attempt to promote DNA repair following a situation of high DNA damage, cell undergoes ATP depletion as explained in section 2.8. Low ATP levels may then act as a signal for ATP synthesis, which is promoted by LD degradation, increased FFA and β -oxidation.

As a conclusion, lipophagy is a survival pathway that is induced through different stimuli to counteract ATP depletion or cytotoxicity-related cell processes. Hence, it must be finely tuned. As a consequence, an excess or a defect in lipophagy may deregulate this route generating undesired effects that might contribute to cell death. However, further investigation is needed to better understand this mechanism.

7.3 MITOTIC CATASTROPHE

7.3.1 GENERAL VIEW

The process of microtubule disintegration was firstly described in 1984 as a microtubule catastrophe (McIntosh 1984). However, the expression “Mitotic Catastrophe” (MC) was not utilized until 1986 (Russell and Nurse 1986).

Since then, and specially during the last decade, the term “Mitotic Catastrophe” has been widely used to describe a form of cell death affecting higher eukaryotes, and several attempts have been made to precisely define MC (Vakifahmetoglu, Olsson et al. 2008).

Morphologically, gross nuclear alterations (micronucleation and multinucleation) constitute the most prominent morphological trait of MC. However, features of apoptosis and necrosis have also been observed in cells succumbing to mitotic failure (Castedo, Coquelle et al. 2006). Consequently, end-point techniques are intrinsically unsuitable for this kind of cell death, as they cannot reconstruct the sequence of events that have lead to cell death. To circumvent this issue, novel methods relying on high throughput video microscopy or time-lapse fluorescence microscopy are under development. Thus, MC would not constitute a “pure” cell death mechanism but an onco-suppressive strategy defined as follows: “a mechanism that

senses mitotic failure and responds to it by driving the cell to an irreversible fate, be it apoptosis, necrosis or senescence” (Vitale, Galluzzi et al. 2011).

7.3.2 MC INDUCERS:

A heterogeneous group of stimuli can lead to MC. Although there exist some uncharacterized pathways that can lead to MC, in general these stimuli can be divided in two groups:

- **GENOME INSTABILITY (GIN) INDUCERS OR STIMULI THAT AFFECT THE INTEGRITY OF THE GENETIC MATERIAL:** Normally, DNA damage causes lesions that are detected through the G1 and G2 checkpoint, that arrest the cell cycle allowing the DNA repair machinery to act. If DNA damage is beyond recovery, cell never enters mitosis but undergo programmed cell death. However, in some cases cells may reach mitosis without repairing DNA damage. This is accepted to happen in a context of a certain grade of apoptosis resistance (which avoids cell death even in a context of high DNA damage) (Vakifahmetoglu, Olsson et al. 2008) and, even more important, G1 and/or G2 checkpoint abrogation. If these requirements are not accomplished, cells will not undergo MC even in presence of high DNA damage.
- **CHROMOSOME INSTABILITY (CIN) INDUCERS OR STIMULI THAT AFFECT THE CORRECT SEGREGATION OF CHROMOSOMES AT ANAPHASE:** When the correct segregation of chromosomes is compromised, kinetochores generate a signal that delays anaphase until they are properly attached to the spindle microtubules. This signal is the Spindle Assembly Checkpoint or SAC. Interfering with SAC function, either by its prolonged activation or its premature inhibition, may drive often, but not always, to MC. According to it, an entire class of anticancer agents trigger mitotic MC by binding to tubulin and disrupting the mitotic spindle (Jordan and Wilson 2004).

7.3.3 MC PROGRAMMES

So far, at least three different MC programmes have been described (Galluzzi, Vitale et al. 2012):

- On the first case, which is the canonical “mitotic death”, the cell death machinery is activated when the cells have not yet exited mitosis. This means, cell death occurs while the cell is arrested in metaphase and SAC signal is active.

Nevertheless, in some cases cells can exit mitosis and undergo the next interphase through a mechanism known as “mitotic slippage” (figure 28).

- The second programme of MC defines the case in which the cell death machinery is activated once the cell has reached interphase of the next cell cycle. Interestingly, cell death can occur within hours after mitotic exit.(Suzuki, Ojima et al. 2003).

- Finally, on the third case, cells also reach the next interphase following “mitotic slippage” but cell death machinery is not activated. Instead, senescence phenomenon is initiated, which is an irreversible cell cycle arrest that also precludes the amplification of genomically unstable cells.

Although mitotic slippage seems a key event for the non-canonical MC programmes, the mechanisms that precede it are not clearly defined. For many authors, mitotic slippage occurs only after prolonged mitotic arrest. In this situation, cells would override the SAC signal and undergo mitotic exit (Vakifahmetoglu, Olsson et al. 2008). In contrast, other authors consider that SAC abrogation is a major event that precedes mitotic slippage. Consistently, different groups have reported MC following BUBR1 down-regulation (Xu, Huang et al. 2010, Ding, Hubert et al. 2013).

Reinforcing this view, down-regulation of SAC proteins, including, BUBR1, is a promising strategy to kill tumor cells. Thus, massive chromosome loss through inhibition of mitotic checkpoint members (including BUBR1) is well described to induce lethality in tumor cells (Kops, Foltz et al. 2004, Michel, Diaz-Rodriguez et al. 2004, Janssen, Kops et al. 2009). Although these authors have not assigned MC a role in this mechanism, all evidences show that targeting SAC proteins may compromise tumor viability.

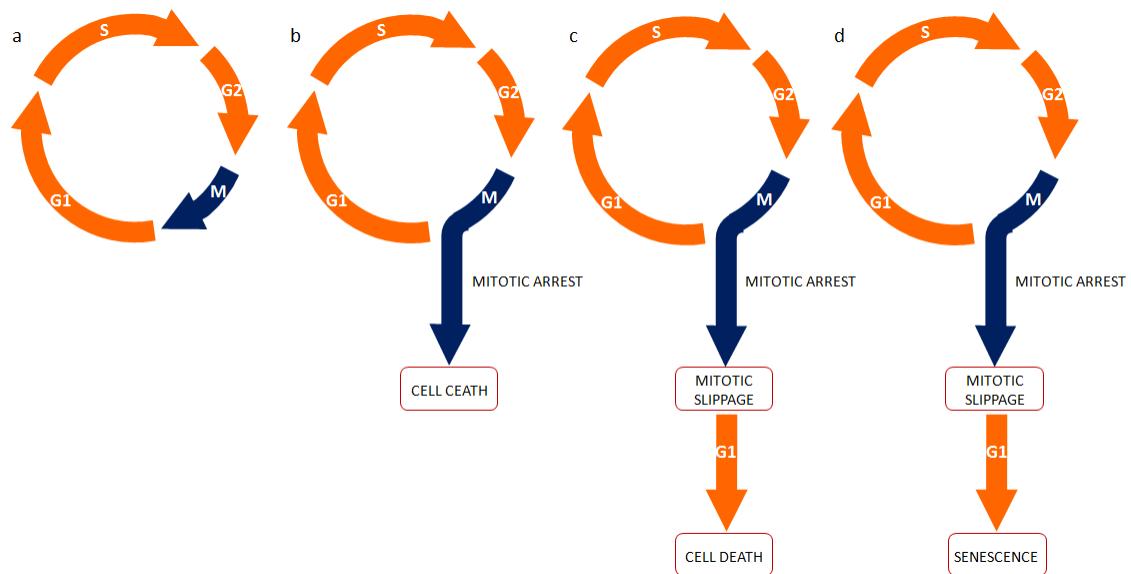


Figure 30: Mitotic catastrophe programs. A normal cell cycle is represented in (a). On the first mitotic catastrophe program (b) the cell death machinery is activated when the cells have not yet exited mitosis. On the second and third program, cells exit from M arrest through “mitotic slippage” and may undergo cell death processes (c) or senescence program (d). (Galluzzi, Vitale et al. 2012).

In addition, BUBR1 role in mitotic catastrophe may be due not only to its function on SAC, but also to its role on chromosome alignment. As demonstrated by Medema’s group (Janssen, Kops et al. 2009), BUBR1 reduction sensitized to taxol. However, the reduction of a SAC

protein not involved in chromosome alignment such as MAD2 did not generate the same effect.

One way or another, MC pathways are not fully understood, and deeper investigation is necessary to completely understand the role of SAC in general and BUBR1 in particular in this process.

7.3.4 MC EXECUTORS

The molecular pathways that regulate MC are subject to intense experimental effort. Nonetheless, although the mechanisms that precede (MC inducers) and follow MC (apoptosis, necrosis or senescence) have been well characterized, the molecular bridges between mitotic aberrations and cell death are still elusive.

In spite of this, some molecules have been proposed to be major players of MC. Most part of them are related to apoptotic cell death. Although necrotic cell death has also been described in MC, the mechanisms by which non-apoptotic cell death promote MC have not been described yet:

- CDK1-CyclinB: This complex has been reported to modulate diverse proteins involved in mitotic cell death:
 - Caspase 2: the complex CDK1–cyclinB1 is described to phosphorylate caspase-2 Ser 340 (Andersen, Johnson et al. 2009) thereby inhibiting its activity. In agreement with a “mitotic slippage” model for MC, CDK1-cyclinB1 activity must be overcome (or lost) and Ser340 must be de-phosphorylated for apoptosis to occur. As explained above, MC can also occur without apoptosis activation, so this process is restrained to apoptosis-related MC.
 - Survivin: CDK1 also phosphorylates Survivin at T34, promoting its anti-apoptotic role as well as its function in mitosis. Once CDK1-cyclinB complex is degraded, survivin stability decreases consequently stimulating apoptosis. Thus, survivin phosphorylation controls the switch between its mitotic and anti-apoptotic functions (Barrett, Osborne et al. 2009).
- p53: The new generation of tetraploid cells generated by mitotic slippage arrest their cell cycle in G1, and this arrest depends on the tumor suppressor protein p53. Consistently, the absence of TP53 is permissive for the multipolar divisions of tetraploid cells leading to the generation of an aneuploid, genomically unstable progeny (Sphyris and Harrison 2005).

To conclude, it is important to remark that cancer cells are often intrinsically more sensitive to mitotic catastrophe than their “normal” counterparts, implying the existence of a therapeutic window for inducers of MC, and suggesting that the activation of MC might constitute a highly desirable therapeutic endpoint.

OBJECTIVES

1) To analyze the effect of PARP inhibition in Glioblastoma cell viability and cell death.

- Cell lines
- GBM Stem-like Cells
- *In vivo* assays (mouse)

2) If there is an effect, examine different pathways involved in the viability decrease:

- Death pathways:
 - Apoptosis
 - Autophagy
 - Mitotic catastrophe
- Survival pathways:
 - mTOR axis
 - Lipid metabolism
- Cell cycle
- Genomic and mitotic stability
 - Homologous recombination
 - Mitosis

MATERIALS AND METHODS

8 MATERIALS

8.1 CELL CULTURE

Four GBM cell lines and two Patient-derived GBM Initiating Cells have been used in the different experiments of the present thesis.

8.1.1 CELL LINES

- **LN229** PTEN wild type, p53 and CDKN2A mutant cell line was kindly provided by Dr. Joan Seoane, Hospital Vall d'Hebron, Barcelona.
- **U87MG** p53 wild type, PTEN mutant cell line. PTEN mutation is due to Loss Of Heterocigosity (LOH) at 10q23 chromosome region. Stably transfected U87MG-DRGFP cell line was kept in culture using Ampicillin antibiotic selection.
- **U87MG-luciferase** cell line was kindly provided by Professor Yasuhiro Matsumura (National Cancer Center Hospital East, Kashiwanoha, Kashiwa City, Japan).
- **U118MG** p53, CDKN2A and PTEN mutant cell line was kindly provided by Dr. Guillermo Velasco, Universidad Complutense, Madrid.
- **SW1783** PTEN mutant grade III astrocytoma cell line was also kindly provided by Dr. Guillermo Velasco, Universidad Complutense, Madrid.

Cell lines were cultured in Dulbecco's Modified Eagle's Medium (DMEM) high glucose (4,5g/l) supplemented with L-Glutamine, 10 % inactive fetal bovine serum at 37 °C in a humidified 5% CO₂ atmosphere. To avoid bacterial contamination, Gentamicine 50mg/l was alterned with a mixture of Penicillin 100mg/l and Streptomycin 500U.

In all cases, cells were plated 24 hours before the treatments.

8.1.2 PATIENT-DERIVED GBM STEM-LIKE CELLS (GSCs)

TG1 and OB1 cells were obtained at Sainte Anne Hospital, Paris, France. The biopsies were collected by a pathologist. All patients were 18 years old or older, had signed a written agreement for participation to the Research Project after having being informed of the goals, potential interest of the research and methods, according to the declaration of Helsinki (PATRU 2010). To accomplish this thesis, both cells were cultured at Dra. Julie Gavard's laboratory at Hôpital Cochin, Paris.

Cells were maintained in DMEM/F12 plus N2, G5 and B27 (Invitrogen), providing the mixture of growth factors and mitogens necessary to avoid cell differentiation and were cultured in the absence of serum at 37 °C in a humidified 5% CO₂ atmosphere. Gentamicine 50mg/l was used to avoid bacterial contamination and Amphotericin B was used to avoid fungal contamination. In all cases, cells were kept in suspension.

8.2 REAGENTS

8.2.1 CULTURE MEDIUM

Culture medium DMEM y DMEM:F12, Fetal Bovine Serum, N2, G5 and B27 supplements, trypsin, Gentamicine and Penicillin/Streptomycin antibiotics and the antifungal Amphotericin B were obtained from Gibco, Invitrogen.

8.2.2 DRUGS AND INHIBITORS

- Different PARylation inhibitors have been utilized in this thesis. PARP inhibitors PJ34 ([N-(6-Oxo-5,6-dihydrophenanthridin-2-yl)-(N,N-dimethylamino) acetamide hydrochloride]) with $EC_{50}=20$ nM (Alexis Biochemicals, San Diego, CA) and AZD2281/olaparib (AZD2281, Ku-0059436) with $EC_{50}=5$ nM (Deltaclon) were used. Olaparib was dissolved in DMSO (Dimethyl Sulfoxide) at a concentration of 10 mM and PJ34 was dissolved in water at a concentration of 50 mM. Both were stored at -20°C . Cells were treated with 10 μM olaparib or 10 to 20 μM PJ34 during 24, 48 or 72 hours.
- Temozolomide (T2577-25MG Sigma-Aldrich, St Louis, USA) was dissolved in DMSO at a concentration of 100 mM and stored at -20°C . Cells were treated with 100 μM Temozolomide during 24, 48 or 72 hours.
- mTORC1 inhibitor Rapamycin (#553210 Calbiochem, Germany) was dissolved in ethanol at a concentration of 1 mM and was used at a final concentration of 100 nM.
- Autophagy inhibitor Chloroquine (C6628 Sigma-Aldrich, St Louis, Mo), which avoids autophagosome-lysosome fusion increasing pH in the inside of the lysosome, was dissolved in H_2O at a concentration of 10 mM and used at a final concentration of 10 and 25 μM .
- EGFR inhibitor Erlotinib (2048-1000 Biovision) was dissolved in DMSO at a concentration of 50mM and stored at -20°C . Cells were treated at a final concentration of 10 μM .

8.2.3 ANTIBODIES

Primary antibodies have been classified in the chart below according to the main cellular pathway where they are involved.

| Name | Host | Trading house | Reference | kDa |
|--------------------------------|--------|--|----------------------|-------|
| Survival Pathways | | | | |
| phospho-ERK | Mouse | Santa Cruz Biotechnology | Sc-7383 | 42-44 |
| PAN-ERK | Rabbit | Invitrogen | 61-7400 | 42-44 |
| phospho-P70S6K (Thr389) | Rabbit | Cell Signaling Technology, Beverly, MA | #9205 | 70 |
| PAN-p70S6K | Rabbit | Cell Signaling Technology, Beverly, MA | #9202 | 70 |
| ILK | Rabbit | Millipore | MABT66 clone EP1593Y | 51 |
| phospho-mTOR (S2481) | Rabbit | Cell Signaling Technology, Beverly, MA | #2971 | 289 |
| PAN-mTOR | Rabbit | Cell Signaling Technology, Beverly, MA | #2983 | 289 |
| RapTOR | Rabbit | Cell Signaling Technology, Beverly, MA | #2280 | 150 |
| RicTOR | Rabbit | Cell Signaling Technology, Beverly, MA | #2114 | 200 |
| phospho-ACC (S79) | Rabbit | Millipore | 07-303 | 280 |
| phospho-AMPK (T172) | Rabbit | Cell Signaling Technology, Beverly, MA | #2535S | 62 |
| phospho-AKT (S473) | Rabbit | Cell Signaling Technology, Beverly, MA | #4060/#9271 | 60 |
| phospho-AKT (T308) | Rabbit | Cell Signaling Technology, Beverly, MA | #2965 | 60 |
| PAN-AKT | Rabbit | Cell Signaling Technology, Beverly, MA | #4691 | 60 |
| phospho-PTEN (S380) | Rabbit | Cell Signaling Technology, Beverly, MA | #9551 | 54 |
| PAN-PTEN | Mouse | Santa Cruz Biotechnology | sc-7974 | 54 |
| phospho-GSK3B (S21/9) | Rabbit | Cell Signaling Technology, Beverly, MA | #9336 | 46 |
| phospho-S6 (S235/6) | Rabbit | Cell Signaling Technology, Beverly, MA | #2211 | 32 |
| β-catenin | Rabbit | Sigma | C2206 | 90 |

| Autophagic pathway | | | | |
|--|--------|---|-------------|-------|
| LC3B | Rabbit | MBL | PD014 | 14-16 |
| | | Cell Signaling Technology, Beverly, MA | #3868 | |
| ULK1 | Rabbit | Cell Signaling Technology, Beverly, MA | #4776 | 150 |
| DNA damage detection and repair machinery | | | | |
| PARP-1 C2-10 | Mouse | ALEXIS, LA | ALX-804-210 | 118 |
| BUBR1 | Mouse | BD Bioscience. Erembodegem, Belgium | 612503 | 130 |
| RAD51 | Rabbit | Santa Cruz Biotechnology | sc-8349 | 37 |
| BRCA1 | Rabbit | Santa Cruz Biotechnology | sc-642 | 220 |
| phospho-H2AX | Mouse | Millipore | 05-636 | 17 |
| Differentiation | | | | |
| SOX2 | Rabbit | Millipore | AB5603 | 39 |
| Loading Control | | | | |
| β-Actin | | Sigma-Aldrich | A5316 | 42 |
| α-Tubulin | Mouse | Santa Cruz Biotechnology | SC8035 | 55 |
| GAPDH | Mouse | Sigma-Aldrich | G9545 | 36 |

Table 1: List of antibodies.

8.2.4 RNA INTERFERENCE

The next double-stranded RNA duplexes were ordered to SIGMA-Aldrich in the case of Scrambled, *BUBR1*, *PTEN* and *ATG1*, or Ambion Applied Biosystems in the case of *PARP1*:

| | |
|--|-------------------------------|
| Control (Scrambled) | 5'–CCUACAUCCCGAUCGAUGAUGUU–3' |
| <i>PARP1</i> | 5'–GAAGAUGGUGGACCCGGAGdTdT–3' |
| <i>BUBR1</i> | 5'–CGGGCAUUUGAAUAUGAAAdTdT–3' |
| <i>PTEN</i> | 5'–GCUACCUUUAAAGAAUCAdTdT–3' |
| <i>ATG1</i> (sequences kindly provided by Dr. Guillermo Velasco) | 5'–CAGCAUCACUGCCGAGAGGUU–3' |
| | 5'–CCACGCAGGUGCAGAACUAUU–3' |
| | 5'–GCACAGAGACCGUGGGCAAUU–3' |
| | 5'–UCACUGACCUCCUAAUU–3' |

Table 2: List of siRNA.

8.2.5 BUFFERS

The composition of the buffers that have been used in this thesis is detailed below.

| TECHNIQUE | BUFFER | COMPOSITION | |
|---------------------|--|---|--|
| WESTERN BLOT | Lisis buffer <i>Laemli</i> : | Tris 100 mM ph 6.8, Glicerol 10%, SDS 2.5%, | |
| | Lisis buffer TR3 | Na ₂ HPO ₄ 10 mM, Glicerol 10%, SDS 20%. | |
| | PBS 10x pH 7.4 | NaCl 140 mM, KCl 2.7 mM, Na ₂ HPO ₄ 10 mM, KH ₂ PO ₄ 1.8 mM | |
| | Running Buffer 10x pH 8.8 | TRIS-HCl 0.24 M, Glycin 2 M, SDS 20% | |
| | Semidry Transference Buffer 1x | TRIS-HCl 1 M, Glycin 0.03 M, Metanol 20%, SDS 0.0035% | |
| | Wet transference Buffer 10x | Tris-HCl 0.2 M, Glycin 1.2 M | |
| | Wet Transference Buffer 1x | 100 ml Buffer 10x, 200 ml Metanol, 700 ml miliQ H ₂ O | |
| | Acrilamide-Bisacrilamide gel | | 30% Acrilamide/Bis solution 29:1 (#161-0156) |
| | | | Separating Buffer 4x (Lower Buffer): Tris 1.5 M, SDS 10%, pH 8.8 |
| | | | Stacking Buffer 4x (Upper Buffer): Tris 0.5 M, SDS 10%, pH 6.8 |
| | | | Ammonium persulfate (APS) (0486-100G Amresco) |
| | Developing liquids (1 ml A Solution, 10 µl B Solution and 1 µl H ₂ O ₂) | | N,N,N',N'-tetramethylethylenediamine (TEMED) (#161-0800 Bio-Rad) |
| | | | A Solution: 50 mg Luminol , 200 ml Tris-HCl 0.1 M pH 8.6 |
| | | B Solution: 11 mg p-Coumaric acid in 11 ml DMSO. | |
| IMMUNO-FLUORESCENCE | Fixation Solution | Paraformaldehyde 3% mas/vol, Sacarosa 2% in PBS 1x | |
| | Permeabilization Solution | Triton X100 0.5% in PBS 1x | |
| | Blocking Solution | BSA 2% in PBS 1x | |

| | | |
|----------------------------|--------------------|---|
| ELECTRON MICROSCOPY | Fixation Solution | Glutaraldehyde 2%, Formaldehyde 1% in Cacodilate buffer 0.05 M pH 7.4 |
| | Washing Solution | Cacodilate 0.1 M pH 7.4 |
| | Staining Solution | Uranyl Acetate 2% in miliQ H ₂ O |
| LIPID DROPLETS STAINING | Sudan III Solution | 100 mg Sudan III in 50 ml EtOH. (EtOH must be heated at 60°C and solution must be kept in agitation for correct dissolution and filtered with filter paper before use) |

Table 3: List of buffers and solutions.

8.2.6 PRIMERS

First, cDNA sequence was obtained using *ENSEMBL* software. Next, primers were designed using *FRODO* software.

| | | |
|---------------|---------|--------------------------------|
| <i>SOX2</i> | Forward | 5'-CAAAAATGGCCATGCAGGTT-3' |
| | Reverse | 5'-AGTTGGGATCGAACAAAAGCTATT-3' |
| <i>NESTIN</i> | Forward | 5'-TTCTCTTGTCCTCCGACACTT-3' |
| | Reverse | 5'-AACAGCGACGGAGGTCTCTA-3' |
| <i>GAPDH</i> | Forward | 5'-GTGGACCTGACCTGCCGTCT-3' |
| | Reverse | 5'-GGAGGAGTGGGTGTCGCTGT-3' |

Table 4: List of primers.

8.2.7 PLASMIDS FOR GENE RESTORATION

pSG5L-Flag-HA Plasmid, pSG5L-Myr-HA-PTEN Plasmid, GFP-PTEN Plasmid or pCDNA3-GFP Plasmid were all from Addgene (Cambridge, MA, USA).

9 METHODS

9.1 WESTERN BLOT:

9.1.1 PROTEIN EXTRACTION

Cells were plated in 6 wells at a density of 2×10^5 cells per well. After the treatments, cells were washed twice with PBS, resuspended in 100-200 μ l of TR3 Lysis Buffer or Laemli Lysis Buffer (Table 3) and lysed using a scrapper. Then cells were sonicated and, after separating 5 μ l for protein quantification, 50% β -mercaptoethanol - 50% Bromofenol blue was added in a ratio of 1:10. The lysate was then heated at 95°C during 10 minutes.

9.1.2 PROTEIN QUANTIFICATION

Protein concentration was determined using the Lowry assay.

To quantify protein concentration amount in the lysate, Dc Protein Assay Reagent A, B y S (BioRad, Hercules, CA, USA) was used. In order to perform the calibration curve, increasing amounts of Bovine Serum Albumine (BSA) (from 0 to 25 μ l) were utilized, and in order to calculate protein concentration of the samples, 5 μ l of every test sample were used. Both BSA and samples tests were incubated in *ependorf* tubes with 100 μ l A + S solution (1 ml de A + 20 μ l de S) for 5 minutes. Next, 800 μ l B solution were added and the mixture was incubated for 15 minutes. Finally, 200 μ l of every sample were placed in duplicate in 96 well-plates. Plate absorbance was read at a wavelength of 750 nm in VERSAmax plate reader (Molecular Devices).

To calculate protein concentration in test samples, data from the calibration curve were interpolated using *SoftMax Pro 4.3.1* software.

9.1.3 WESTERN BLOT:

Proteins were resolved on SDS-polyacrylamide gels at a concentration of 7.5, 10 or 12% (Table 3) according to the molecular weight of the protein and utilizing electrophoresis vertical chambers from Bio-Rad.

In addition, Amersham™ ECL™ Gel 4-12% (28-9898-06 GE Healthcare) and 8-16% (28-9898-07 GE Healthcare) gradient gels were used in electrophoresis horizontal chambers from Amersham.

In both cases, proteins were transferred onto PVDF Membrane FluoroTrans® W 3.3 (PALL, Life Sciences) using wet transference system from Bio-Rad for high and medium molecular weight proteins, or semidry transference system from Bio-Rad for low molecular weight proteins (Table 3).

The blot was then blocked with 5% milk powder in PBS 0.1% Tween-20 for 60 minutes and incubated overnight with primary antibody in 1% milk powder in PBS with 0.1% Tween-20.

The day after, the membrane was washed 3 times with PBS 0.1% Tween-20 and incubated with secondary antibody in 1% milk powder in PBS with 0.1% Tween-20. Finally, the membrane was washed again 3 times with PBS 0.1% Tween-20.

9.1.4 DEVELOPMENT

Bands were visualized using the following developing reagents:

- Amersham™ ECL™ Western Blotting Detection Reagent (RPN2106 GE Healthcare)
- Amersham™ ECL™ Prime Western Blotting Detection Reagents (RPN2232 GE Healthcare)
- “Homemade” developing liquids (Table 3)

Pictures were taken with the imaging system ChemiDoc XRS System (Bio-Rad) and medical X-ray films (AGFA).

9.2 IMMUNOFLUORESCENCE

9.2.1 SAMPLES PREPARATION

Cells were plated in 6 wells at a density of 6×10^4 cells per well, or in 12 wells at a density of $2,5 \times 10^4$ cells per well on glass cover-slips.

After the treatments cells were fixed with Paraformaldehyde Solution (Table 3) for 10 minutes at room temperature, permeabilized with PBS 1X 0,5% Triton x100 (Table 3) for 5 minutes at room temperature and blocked with 1% BSA in PBS 0.1% Tween-20 for 60 minutes.

Cells were then incubated with primary antibody in 1% BSA in PBS 0.1% Tween-20 for 60 minutes and subsequently, incubated with secondary antibody in 1% BSA in PBS 0.1% Tween-20 for 20 minutes. Nuclear counterstaining with DAPI at a concentration 1:5000 was performed after removal of excess secondary antibody.

Every step was intercalated by at least three PBS washes.

Finally, samples were mounted on coverslips using Vectashield® (H-1000 Vector Laboratories) and sealed using nail varnish.

9.2.1.1 Samples preparation for GICs neurospheres

In the case of suspension GICs, a circle was drawn using Dako Pen (Code 2002, Dako) on treated slides in order to achieve cell adherence (Microscope slide Polysine adhesion Thermo Scientific J2800AMNZ).

Next, 100 μ l cell culture were placed inside the drawn circle. Fixation was carried out after one minute of incubation.

From here, protocol was realized following the same steps. The only difference is that these steps were accomplished directly in the slide instead of the well.

9.2.2 MICROSCOPY

Immunostaining was visualized with Zeiss Fluorescence Microscopy or with Confocal Leica LCS SP5 Fluorescence Microscope. Images were taken using LAS AF software.

9.3 SHORT TRANSIENT RNA INTERFERENCE

Short transient RNA interference was carried out using two different transfection reagents: Lipofectamine[®] and Jet Prime[®].

For Lipofectamine transfection, cells were plated in 6 wells at a density of 9×10^4 cells per well in complete medium without antibiotic. 24 hours later, cells were transfected with the indicated siRNAs at 60 nM using Lipofectamine[®] 2000 (11668-019 Invitrogen[™]) in DMEM without FBSi or antibiotic supplementation according to the manufacturer's guide. Transfection reagent was replaced by complete medium without antibiotic 5 hours after transfection.

JetPRIME (Polyplus Transfection[®] Illkirch, France) transfection was carried out in the same conditions, although this reagent allowed firstly, to increase the number of plated cells and secondly, the use of complete medium during all the experiment. Transfection reagent was removed 24 hours after transfection and siRNA was optimized at a concentration of 40 nM.

In both cases, gene silencing was effective 48 hours after transfection. Thus, all treatments started after this time. In addition, gene silencing was confirmed to last 120 hours, which allowed the fulfillment of long time gene silencing experiments.

9.4 PLASMIDIC DNA TRANSIENT TRANSFECTION

Cells were plated in 6 wells at a density of 1×10^5 cells per well. 24 hours later, transfection was performed with 0,5 μ g plasmid DNA using JetPRIME[™] (Polyplus transfection, Illkirch, France) according to the manufacturer's protocol. Cells were treated 48 hours after the transfection and harvested following the treatment in order to develop Cell Cycle and Western Blot analysis.

9.5 CELL CYCLE ASSAY

Cell cycle analysis by flow cytometry allowed to determine the rate of apoptotic cells, the cell cycle arrest in G2/M as well as polyploidy rate (superG2 population).

9.5.1 CELLS PREPARATION

Cells were plated in 6 wells at a density of 1.5×10^5 cells.

All the protocol was performed at 4°C. After the treatments, cells were trypsinized, washed with PBS, permeabilized with 100 µl PBS and 900 µl 70% ice cold ethanol during at least 15 minutes, washed again with PBS and incubated with propidium iodide 40 µg/ml and 100 µg/ml RNAase A (Ribonuclease A from bovine pancreas R6513-10MG Sigma-Aldrich, St Louis, USA) at 37°C in dark for 20 min.

In the case of GFP-transfected cells, a 30 minutes fixation step with paraformaldehyde was performed before permeabilization with 70% ice cold ethanol during 15 minutes; this time was used to minimize the loss of the GFP fluorescence. The paraformaldehyde fixation solution was set up adapting Christophori's group recommendations (Lamm, Steinlein et al. 1997):

| COMPOSITION | 10 ml FINAL VOLUMEN |
|-----------------------------|-------------------------|
| Paraformaldehyde (PFA) 0,5% | 1,25 ml 4% PFA solution |
| NaCl 10 mM | 400 µl 2.5 M solution |
| Sucrose 300 mM | 1 g |
| MgCl ₂ 3 mM | 30 µl 1 M solution |
| EGTA 1 mM | 20 µl 0,5 M solution |
| PIPES pH 6,8 10 mM | 400 µl 250 mM solution |

Table 5: paraformaldehyde fixation solution for for detecting apoptosis by flow cytometry in transiently transfected cells.

9.5.2 FLOW CITOMETRY AND DATA ANALYSIS

Cells were analyzed on a FACScan using CellQuest software (Becton Dickinson, Mountain View, CA, USA), and cell cycle was determined using FlowJo software.

9.6 PROLIFERATION AND CELL VIABILITY ASSAYS

9.6.1 SHORT TERM VIABILITY ASSAY: MTT

For MTT (3-(4, 5-Dimethylthiazol-2-yl)-2,5-diphenyl Tetrazolium Bromide) assay, cells were plated in 96 wells at a density of 8×10^3 cells. MTT assay was performed using Cell Proliferation Kit I (MTT, 1-65-007, Roche, Mh Germany) following manufacturer's instructions.

Plate absorbance was read at a wavelength of 570 nm in VERSAmax plate reader (Molecular Devices).

9.6.2 NEUROSPHERES SELF-RENEWAL ASSAY

Neurospheres self-renewal assay is not exactly considered a proliferation assay as it does not evaluate GICs proliferation. Self-renewal capability, which is a marker of stemness in GSCs, is evaluated in this experiment. Thus, this assay is developed using primary patient-derived PTEN-proficient GSCs.

GSCs were dissociated by up-and-down pipetting and plated in 48 wells. PARP inhibitor was added every 24 hours during the three first days of experiment. GSCs were dissociated every day by up and down pipetting using the 1000 µl pipete, in order to check their ability to form secondary neurospheres at the end of the experiment. Every group of 5 or more cells was considered neurosphere. The 7th day, counts were blindly performed on 10 fields of view with the 10x objective, and the mean number of neurospheres per field of view was calculated.

9.7 CELL DEATH ASSAYS

Experiments based on loss of plasmatic membrane integrity have been considered global cell death assays.

9.7.1 CELL DEATH QUANTIFICATION BY FLOW CITOMETRY

9.7.1.1 CELL PREPARATION

Cells were plated in 6 wells at a density of 1.5×10^5 cells.

All the protocol was performed at 4°C. After the treatments, cells were trypsinized, washed with PBS and incubated with propidium iodide 40 µg/ml at 37°C in dark for 20 min.

9.7.1.2 FLOW CITOMETRY AND DATA ANALYSIS

Cells were analyzed on a FACScan using CellQuest software (Becton Dickinson, Mountain View, CA, USA) and gated population was evaluated using FlowJo software.

9.8 APOPTOSIS ASSAYS

9.8.1 SUBG1 ANALYSIS BY FLOW CITOMETRY

Sub G1 population was determined through Cell Cycle assay, as described in section 9.5.

9.8.2 CASPASE 3/7 ACTIVATION

Cells were plated in 96 wells at a density of 6×10^3 cells per well. Following the treatments, The Caspase – Glo reagent[®] (Caspase-Glo 3/7 Assay G8091, Promega) was added directly to cells according to the manufacturers instructions and incubated at room temperature for 30 minutes before recording luminescence in a TECAN infinite 200 Luminometer.

Etoposide was used as apoptosis positive control although results were not included in the final data representation. Each point represents the average of 3 wells per condition to 3 independent experiments.

9.8.3 PIKNOTIC NUCLEI QUANTIFICATION

9.8.3.1 SAMPLES PREPARATION

Cells were plated in 6 wells at a density of 5×10^4 cells per well after introducing a coverslip in the bottom of the well. After the treatments, cells were firstly fixed in Paraformaldehyde for 10 minutes at room temperature (Table 3). Secondly, cells were permeabilized with triton x100 (Table 3) for 5 minutes. Thirdly, incubation with DAPI at a concentration 1:5000 was performed for 10 minutes. Every step was intercalated by at least 3 PBS washes.

Finally, samples were mounted on coverslips using Vectashield[®] (H-1000 Vector Laboratories) and sealed using nail varnish.

9.8.3.2 MICROSCOPY

The number of cells with nuclear apoptotic morphology was determined using a Zeiss Fluorescence Microscope. Counts were performed on 10 fields of view, and the mean number of pyknotic nuclei per field of view was calculated.

9.9 LIPID DROPLETS QUANTIFICATION

9.9.1 BODIPY ASSAY

9.9.1.1 SAMPLES PREPARATION

Cells were plated in 24 wells at a density of 1×10^4 cells per well after introducing a coverslip in the bottom of the well.

After the treatments, cells were firstly fixed in Paraformaldehyde for 10 minutes at room temperature (Table 3). Secondly, cells were permeabilized with triton x100 (Table 3) for 5 minutes. Next, lipid droplets were labeled with BODIPY 493/503[®] (D-3922, Molecular Probes) for 5 minutes at room temperature. Then, incubation with DAPI at a concentration 1:5000 was performed for 10 minutes. Every step was intercalated by at least 3 PBS washes.

Finally, samples were mounted on coverslips using Vectashield[®] (H-1000 Vector Laboratories) and sealed using nail varnish.

For the positive control of lipid droplets, Chloroquine 25 μM was added during 48 hours.

9.9.1.2 MICROSCOPY

The number of cells bearing lipid droplets was determined using a Zeiss Fluorescence Microscope. 10 fields of view were examined in order to obtain qualitative analysis of LDs formation.

9.9.2 SUDAN RED STAINING

9.9.2.1 SAMPLES PREPARATION

Cells were plated in 24 wells at a density of 1×10^4 cells per well after introducing a coverslip in the bottom of the well.

After the treatments, cells were firstly fixed in Paraformaldehyde for 10 minutes at room temperature (Table 3). Secondly, cells were permeabilized with triton x100 (Table 3) for 5 minutes. Next, the samples were incubated in dark with Sudan III 0.2% during 20 minutes. Then, staining with DAPI at a concentration 1:5000 was performed for 10 minutes. Every step was intercalated by at least 3 PBS washes.

Finally, samples were mounted on coverslips using Vectashield[®] (H-1000 Vector Laboratories) and sealed using nail varnish.

9.9.2.2 MICROSCOPY

The number of cells bearing lipid droplets was determined using a Confocal Leica LCS SP5 Fluorescence Microscope. Images were taken using LAS AF software.

9.10 ELECTRON MICROSCOPY

Cells were plated in p100 wells at a density of 10^6 cells.

After the treatments, cells were trypsinized, washed with PBS 1X and fixed in fixation solution (Table 3) for 5 hours. Next, cells were incubated in washing solution (Table 3) for 15 minutes. This step was repeated three times. Finally, samples were stained with uranyl acetate (Table 3). The ultrathin sections were performed with a diamond knife in an ultramicrotome (Reichert Ultracut S). The samples were analyzed in a TEM Zeiss 902 with 80 Kv of voltage acceleration (CIC-UGR).

9.11 HOMOLOGOUS RECOMBINATION ASSAY

U87MG and LN229 glioma cells were stably transfected with a pDR-GFP plasmid containing a mutated GFP gene with an 18 bp SclI site and were maintained under puromycin selection before use. Transient transfection of SclI in both cell lines creates a DSB at the relevant site in the integrated GFP gene. Homologous recombination repair (HRR) of this break restores GFP gene expression (Weinstock, Nakanishi et al. 2006).

Cells were plated in 6 wells at a density of 9×10^4 cells per well for stable transfection with DR-GFP. 24 hours later, cells were transfected with 1 μ g DR-GFP plasmid per well using JetPEI™ (Polyplus transfection, Illkirch, France), according to the manufacturer's protocol. Transfected cells were maintained under puromycin selection, and transfection was proved by PCR with the primers:

DRGFP1 5'AGGGCGGGGTTCCGGCTTCTGG 3'

DRGFP2 5'CCTTCGGGCATGGCGGACTTGA 3'

For the transient transfection with SclI, cells were plated in 6 wells at a density of 9×10^4 cells per well. 24 hours later, cells were transfected with 4 μ g SclI plasmid per well using JetPRIME™ (Polyplus transfection, Illkirch, France) according to the manufacturer's protocol. 24 hours after the transfection, cells were treated with PJ34 4 hours during 48 hours. Finally, cells were trypsinized and percentage of GFP expressing cells was measured by flow cytometry on a FACScan.

Frequency of recombination events was calculated as mean percentage of GFP positive cells transfected with SclI divided by mean percentage of GFP positive cells transfected with pEGFP. Results were represented through Kolmogorov-Smirnov adjust using CellQuest software.

9.12 GENOMIC INSTABILITY ANALYSIS: MICRONUCLEI DETECTION

9.12.1 SAMPLES PREPARATION

DAPI counterstain described for pyknotic nuclei quantification in 2.9.4.1 was also used in order to analyze micronuclei frequency.

9.12.2 MICROSCOPY

Cell counts were performed on 10 fields of view in a Zeiss microscope, and micronuclei counting was developed using Image J software. The mean number of micronuclei per field of view was calculated.

9.13 PCR:

9.13.1 RNA EXTRACTION

GSCs were plated in 6 wells at a density of 9×10^4 cells. RNA extraction was carried out using RNeasy MiniKit (Qiagen Inc., Valencia; California) according to manufacturer's instructions. RNA quantification was performed using *NanoDROP® ND-1000 Spectrophotometer*.

9.13.2 RETROTRANSCRIPTION

Complementary DNA or cDNA obtaining was performed with Maxima First Strand cDNA Synthesis Kit for RT-PCR (#k1641; Thermo Fisher Scientific), starting from 200 ng RNA and according to manufacturer's instructions.

9.13.3 PCR:

PCR was carried out with REDTaq® ReadyMix™ PCR Reaction Mix (R2523, Sigma-Aldrich), according to manufacturers protocol and using 2 µl cDNA in all cases. Primers sequence was detailed in 1.2.5.

1,5% agarose gel electrophoresis was used in order to visualize PCR products and to analyze quantitatively gene expression changes.

9.14 DNA REPAIR AND CELL CYCLE EXPRESSION MICROARRAY

Cells were plated in p60 at a density of 1×10^6 cells. The following steps were performed after the treatments:

9.14.1 RNA EXTRACTION

RNA extraction was fulfilled as explained **above**.

9.14.2 RETROTRANSCRIPTION

Retrotranscription was developed with RT2 First Strand kit (Qiagen), which includes a step for genomic RNA removal, thus allowing maximal efficiency in the process, according to manufacturer's guide.

9.14.3 EXPRESSION MICROARRAY

cDNA was tested by RT2 Profiler PCR Array - Human DNA Damage Signaling Pathway (Qiagen) according to the manufacturer's protocol. Data were analyzed by the $\Delta\Delta C_t$ method.

9.15 CELLS IRRADIATION

Cells were plated in 12 wells at a density of 2.5×10^4 cells. In order to execute cell irradiation, Perkin Elmer 1470 automatic gamma counter from Centro de Instrumentación Científica (UGR, Granada) was used. Cells were irradiated at values from 0,5 to 9 Greys.

9.16 PATIENT DATASETS AND DATA ANALYSIS

The microarray gene expression data was obtained from EMBO-EBI (<http://www.ebi.ac.uk/arrayexpress/>) and the clinical data was obtained from the database Oncomine (<https://www.oncomine.org/>) using data available on October 1st, 2010. Diagnoses were also made at the respective clinics. At the time of access, 343 glioma patient samples with both gene expression data and corresponding survival times were available on the Rembrandt database. These included 413 GBMs, 138 overexpressing *BUB1B* and 275 rest of samples.

9.17 ETHICS STATEMENT

All human subjects data was publicly available in de-identified form on the Oncomine. website (<https://www.oncomine.org/>). Therefore, its use was not classified as human subjects research, and no Institutional Review Board approval was needed.

9.18 IN VIVO BIOLUMINESCENCE ASSAY

This study was performed in strict accordance with the recommendations in the Guide for the Care and Use of Laboratory Animals of the Bioethical Committee of CIBM-UGR. The protocol was approved by the Committee on the Ethics of Animal Experiments of the CIBM-UGR. All surgery was performed under ketamine – xylazine anesthesia, and every effort was made to minimize suffering.

Thirteen-weeks-old male Balb/cnu/nu mice (Charles River Laboratories, Wilmington, MA, USA) were injected intracranially with U87MG-luc cells (1×10^5) by introducing stereotactically the needle of a Hamilton syringe. The day after injection of tumour cells, mice were treated three times per week mice with PJ34 at a dose of 10mg/kg body weight and/or erlotinib at a dose of 50 mg/kg body weight injected intraperitoneally. Sodium Chloride solution/60% DMSO was used as vehicle. In order to develop in vivo bioluminescence measurement, mice were injected intraperitoneally with D-luciferin solution dissolved in phosphate-buffered saline at a dose of 150 mg/kg body weight. After 5 minutes, the animals were anesthetized in the dark chamber using 3% isoflurane in air at 1.5 L/min and O₂ at 0.2 L/min/mouse, and animals were imaged in a chamber connected to a camera (IVIS, Xenogen, Alameda, CA). The quantification of light emission was performed in photons/second/cm²/steradian using Living Image 2.6.1 software (Xenogen). Tumour growth was monitored at 0, 2, 8, 15 and 21 days by in vivo imaging and

bioluminescence measurement. After 21 days, mice were sacrificed, and brains were dissected and placed in Petri dishes with D-luciferin solution at a dose of 20 μ g/ml. Ex vivo quantification of light emission was performed by introducing the petri dishes inside the chamber connected to IVIS as explained before. Finally, brains were stored in GreenFix solution until histological staining.

9.19 STATISTICAL ANALYSIS

Independent experiments were pooled when the coefficient of variance could be assumed identical. Statistical significance was evaluated using t-test (n=number of independent experiments). P-values below 0.05 were considered significant. (* $p < 0.05$, ** $p < 0.01$, *** $p < 0.001$).

RESULTS

1 PARP TARGETING COUNTERACTS GLIOMAGENESIS THROUGH INDUCTION OF MITOTIC CATASTROPHE AND AGGRAVATION OF DEFICIENCY IN HOMOLOGOUS RECOMBINATION IN PTEN-MUTANT GLIOMA

1.1 PARP INHIBITION IMPACTS DIFFERENTLY ON CELL VIABILITY IN PTEN WILD TYPE AND PTEN-MUTANT GLIOMA CELLS

As a first approach, we analyzed the potential of PARPi as monotherapy against GBM. PJ34 targets mainly PARPs synthesizing proteins but some off-target effects have also been reported, suggesting the effect of PJ34 on cancer cells may not be attributed exclusively to PARP inhibition (Castiel, Visochek et al. 2011, Castiel, Visochek et al. 2013). For that reason we also used the clinically relevant PARPi olaparib.

PARPi was first tested against established GBM cell lines bearing either wild type (LN229) or mutant PTEN (U87MG, SW1783, U118MG). Treatment with PJ34 resulted in loss of cell viability (figure 1A) and cell death induction (figure 1B). Due to the previously explained off-target effects of PJ34, the PARP inhibitor Olaparib was also tested, exerting similar results (figure 1C).

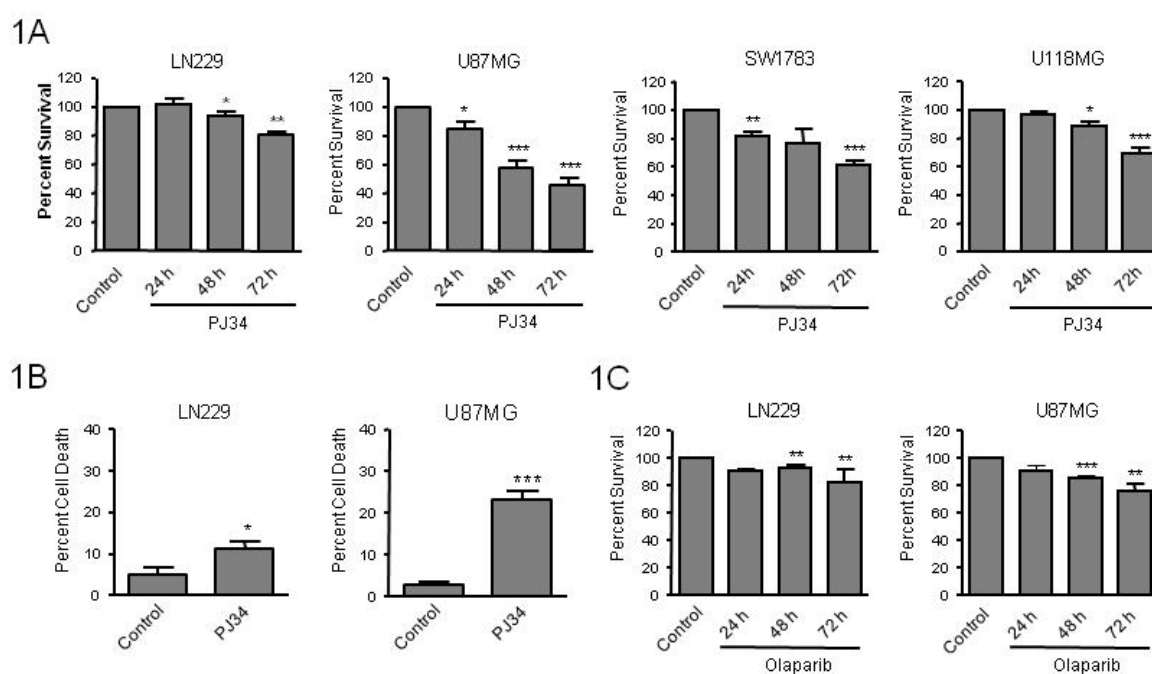


Figure 1: Effect of PARP inhibition on GBM PTEN proficient (LN229) and PTEN deficient (U87MG, SW1783, U118MG) cell lines. (A) Viability analysis by MTT assay of cells treated with 20 μ M PJ34. **(B)** Propidium iodide (PI) intake was analysed by flow cytometry 72 hours after the treatment in order to check cell death. **(C)** Viability analysis by MTT assay following 10 μ M Olaparib. Data were normalized and expressed as a percentage of the control. * $p < 0.05$, ** $p < 0.01$, *** $p < 0.001$ versus control group by t-test.

Interestingly, PTEN deficient cells including U87MG displayed an increased sensitivity to PARPi. However, U87MG cells, which have been previously described to be extremely resistant to apoptotic cell death (Sgorbissa, Tomasella et al. 2011), barely increased apoptosis following

PARPi (figure 2A,B,C) or PARP-1 knockdown (figure 2D) when compared with LN229 PTEN proficient cell line.

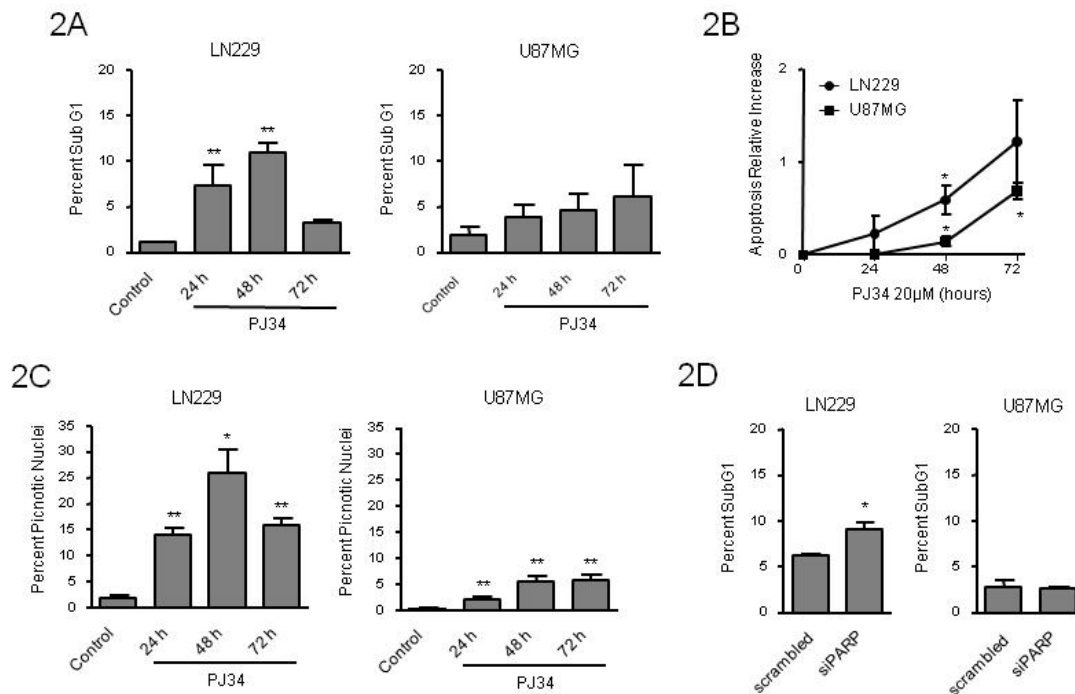


Figure 2: Apoptosis activation in absence of PARP. (A) SubG1 fraction was analysed by flow cytometry following staining with PI. **(B)** Caspase 3 activation was measured. Data were taken as Relative Luminescence Units (RLU), normalized and expressed as a fraction of the control. **(C)** Picnotic nuclei countage (ten fields of view per condition) was performed after the treatments. **(D)** SubG1 fraction was also quantified following PARP-1 knockdown. * $p < 0.05$, ** $p < 0.01$, *** $p < 0.001$ versus control group by t-test.

Intriguingly, both PTEN silencing in LN229 cells and PTEN restoration in U87MG cells displayed increased apoptotic cell death following PARPi (figure 3). This apparently contradictory result may be explained through the genetic background of each cell line: LN229 cells own functional apoptotic machinery that is activated following both PARP inhibition and PTEN absence. In contrast, U87MG cells do not present functional apoptotic machinery, although our results denote that it can be partially restored following PTEN overexpression. Nevertheless, further investigation is required in order to better understand this phenomenon.

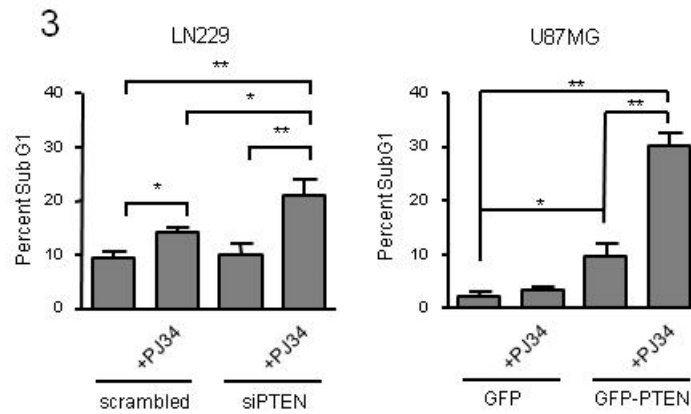


Figure 3: Apoptosis increase following PTEN silencing/PTEN restoration. PTEN knockdown in LN229 cells provoked apoptosis increase following PARPi (left panel). Curiously, PTEN restoration in U87MG generated the same effect (right panel).

Next, we tested the effect of combining PARPi and the currently therapy against GBM. The methylating agent temozolomide (TMZ) had a very mild effect on cell viability as single agent and did not increased the efficiency in cell killing of PARP inhibition (figure 4A,B,C). In addition, neither Ionizing Radiation (IR) increased PJ34 effect on cell viability (data not shown). Thus, PARP inhibition per se was sufficient to induce cell death in PTEN deficient cells more efficiently than the currently used chemotherapeutic drug TMZ.

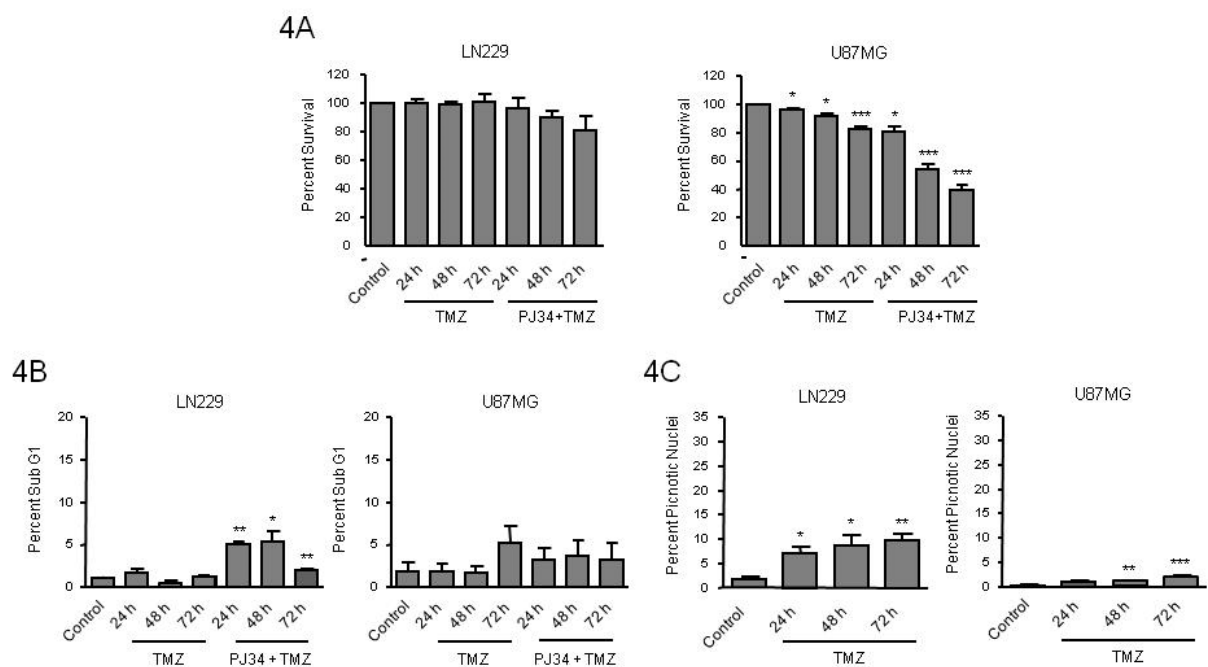


Figure 4: Temozolomide (100 μ M) effect in LN229 and U87MG is less striking than PARP inhibition (20 μ M) effect, alone or combined. (A) Viability analysis by MTT assay of glioblastoma cells. (B) Effect of Temozolomide, alone or combined with PJ34, on subG1 fraction. (C) Picnotic nuclei countage (ten fields of view per condition) was performed after Temozolomide treatment. * $p < 0.05$, ** $p < 0.01$, * $p < 0.001$ versus control group by t-test.**

Moreover, the G2/M arrest was also notably diminished in U87MG cells following PARPi respect to PTEN wild type cells (figure 5A and 5B) and U87MG cells transiently restored with PTEN partially recovered G2/M arrest (figure 5C). In addition, TMZ remarkably induced an arrest in G2/M at 72 hours. However, the combination with PARPi reached arrest levels similar to PARP inhibition alone (figure 5D).

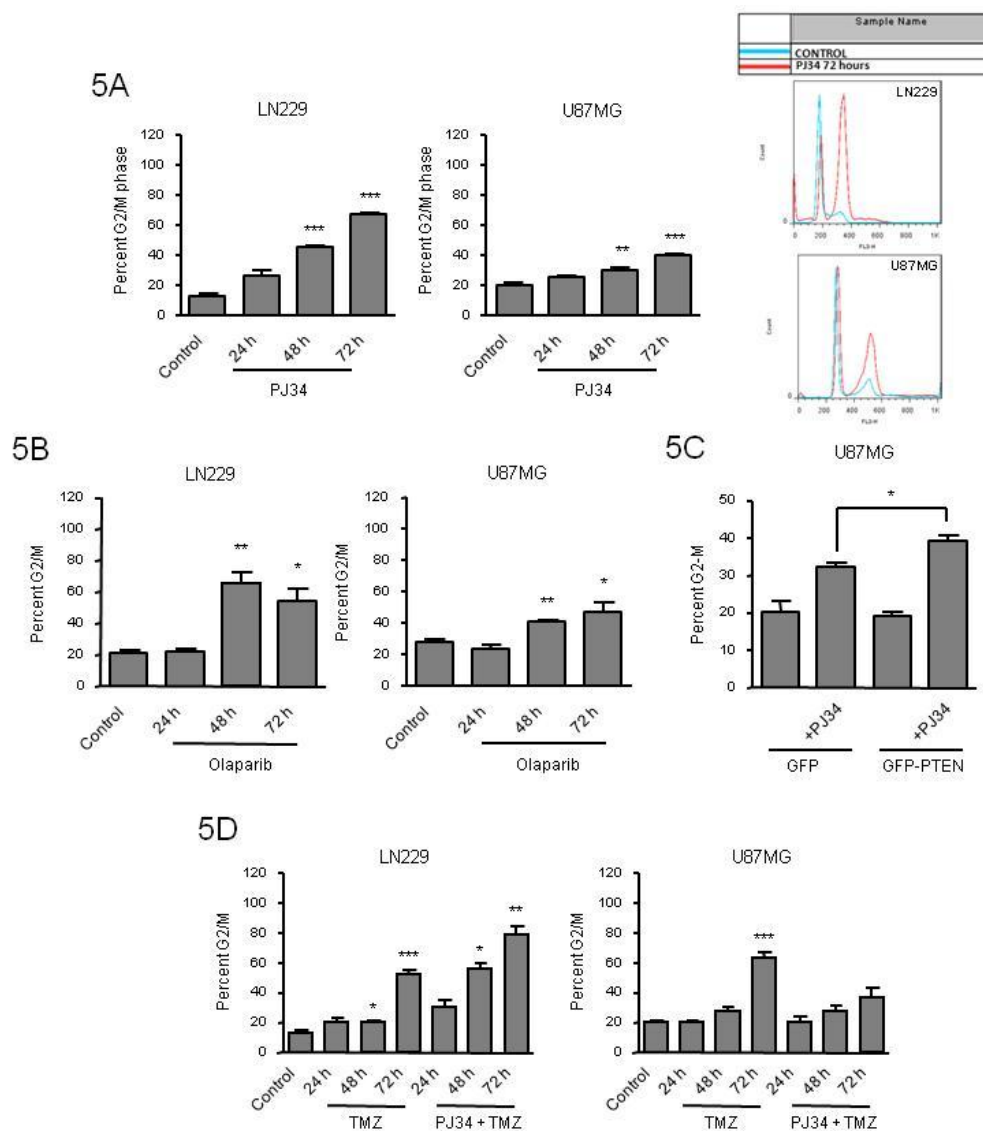


Figure 5: G2/M arrest following PARPi is increased in presence of PTEN. Combined treatment of TMZ and PARPi arrests cell cycle similarly to PARPi alone. G2/M fraction was analysed by flow cytometry following staining with PI, after (A) PJ34 treatment or (B) Olaparib treatment. (C) PTEN was overexpressed in U87MG cells and G2/M fraction was analysed 72 hours after the treatment. (D) Effect of Temozolomide, alone or combined with PJ34, on G2/M fraction. * $p < 0.05$, ** $p < 0.01$, * $p < 0.001$ versus control group by t-test.**

1.2 PARP INHIBITION INDUCED DOWN-REGULATION OF THE SPINDLE ASSEMBLY CHECKPOINT (SAC) PROTEIN BUBR1, LEADING TO MITOTIC INSTABILITY IN PTEN DEFICIENT GLIOMA CELLS

To further elucidate the mechanistic aspects regarding the effect of PARP inhibition in both PTEN proficient and PTEN mutant GBM cells we explored the induction of genomic instability. As we showed above (figure 5A), PTEN deficient cells lack G2/M arrest following PARPi treatment. The BUBR1 protein ensures accurate segregation of chromosomes through its role in the mitotic checkpoint and the establishment of proper microtubule-kinetochore attachments; and sustained high-level expression of BUBR1 preserves genomic integrity (Baker, Dawlaty et al. 2013). In figure 6A we show that PARP inhibition induced BUBR1 down-regulation in U87MG PTEN-deficient cells, suggesting that the spindle assembly checkpoint is compromised in U87MG. Further confirmation for the effect of PARP inhibition on BUBR1 levels was obtained by the use of a different PARP inhibitor, olaparib, that induced BUBR1 down-regulation in U87MG but not in LN229 cells (figure 6B). Furthermore, silencing PTEN in LN229 cells also results in BUBR1 decrease after PARP inhibition (figure 6C) while introduction of PTEN in U87MG cells delayed BUBR1 loss (figure 6D).

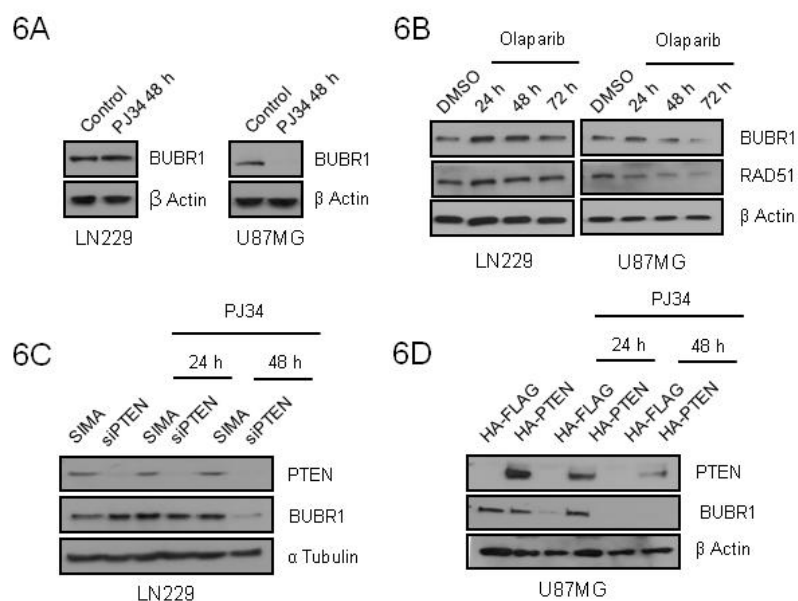


Figure 6: BUBR1 down-regulation following PARPi is delayed in presence of PTEN. BUBR1 expression was measured by Western Blot 48 hours after the treatment with (A) PJ34 or (B) olaparib. (C) BUBR1 expression was measured by Western Blot after the treatment with PJ34 following PTEN silencing in LN229 cells or (D) PTEN overexpression in U87MG cells.

In addition, in silico analysis using the database Array Express of U87MG cells transduced with wild type PTEN showed a statistically significant decrease in *BUB1B* expression in PTEN transduced cells as well as in the gene coding for the SAC-related factor (and BUBR1 associated

protein) AURKB (-2.62 and -3.31 fold decrease respectively). In order to approach the clinical relevance of these variations in BUBR1 levels as function of PTEN we used two available datasets: OncoPrint and Array Express from EMBO-EBI. *BUB1B* gene expression (the gene for BUBR1) was significantly increased in GBM patients (figure 7A; $p= 2.2E-20$, fold change 3.856, number of samples: normal brain $n=23$, glioblastoma $n=81$). Moreover, there was an inverse correlation between PTEN and *BUB1B* expression in GBM patients with low survival (figure 7B; less than 12 months; $n=15$, $p<0.001$, pearson -0.7592) further supporting that targeting BUBR1 (as PARPi does) could be used as rational therapy in PTEN deficient GBM. Interestingly, increased expression of *BUB1B* correlated with decreased patient survival (figure 7C).

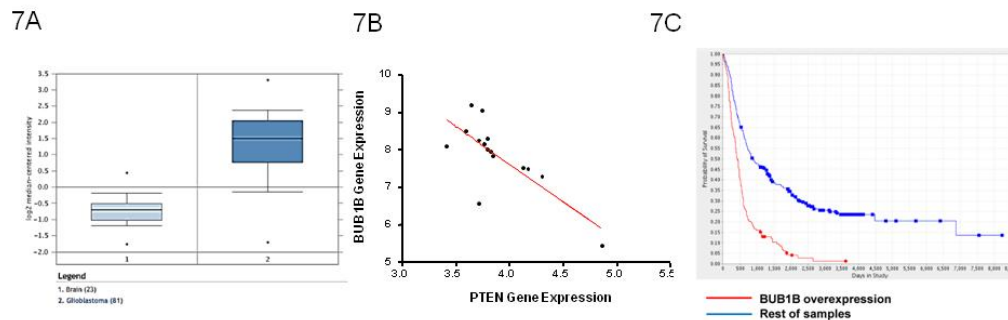


Figure 7: PTEN and BUBR1 analysis in patients database. (A) *BUB1B* gene expression in GBM and normal brain samples, obtained with the OncoPrint database. $p= 2.2E-20$, fold change 3.856, number of samples: normal brain $n=23$, glioblastoma $n=81$. **(B)** *BUB1B* gene expression correlates negatively with PTEN expression in GBM low survival patients (less than 12 months); $n=15$, $p<0.001$, pearson -0.7592. **(C)** *BUB1B* overexpression correlates with decreased patient survival. Data obtained from REMBRANDT database. $n=413$; 138 overexpressing *BUB1B* and 275 rest of samples.

Another hallmark of genomic instability is micronuclei formation. Following PARP inhibition, U87MG cells, but not LN229 cells displayed a time-dependent accumulation of micronuclei (figure 8A). Polyploids are the result of cytokinesis failure after G2/M arrest, however PTEN-deficient cells, unable to activate the G2/M checkpoint, progress to continue cell cycle and complete aberrant mitosis. As shown in figure 5A, PARP inhibition-induced arrest in G2/M in PTEN-mutant cells was almost suppressed, implying that cells will progress in cell cycle, accumulating genomic instability, and eventually MC but not polyploids (figure 8B,C). Interestingly, and consistent with increased G2/M arrest following PARPi after PTEN restoration (figure 5C), PTEN overexpression in U87MG also increased polyploidy (figure 8D). However, the slight increment observed after long-time PJ34 treatment, suggest a possible interference of the genetic background of each cell line.

Taken together, these results led us to suggest that PARP inhibition compromised mitotic checkpoint through down-regulation of BUBR1, preventing from mitotic arrest, and that this situation is exacerbated in a PTEN deficient context.

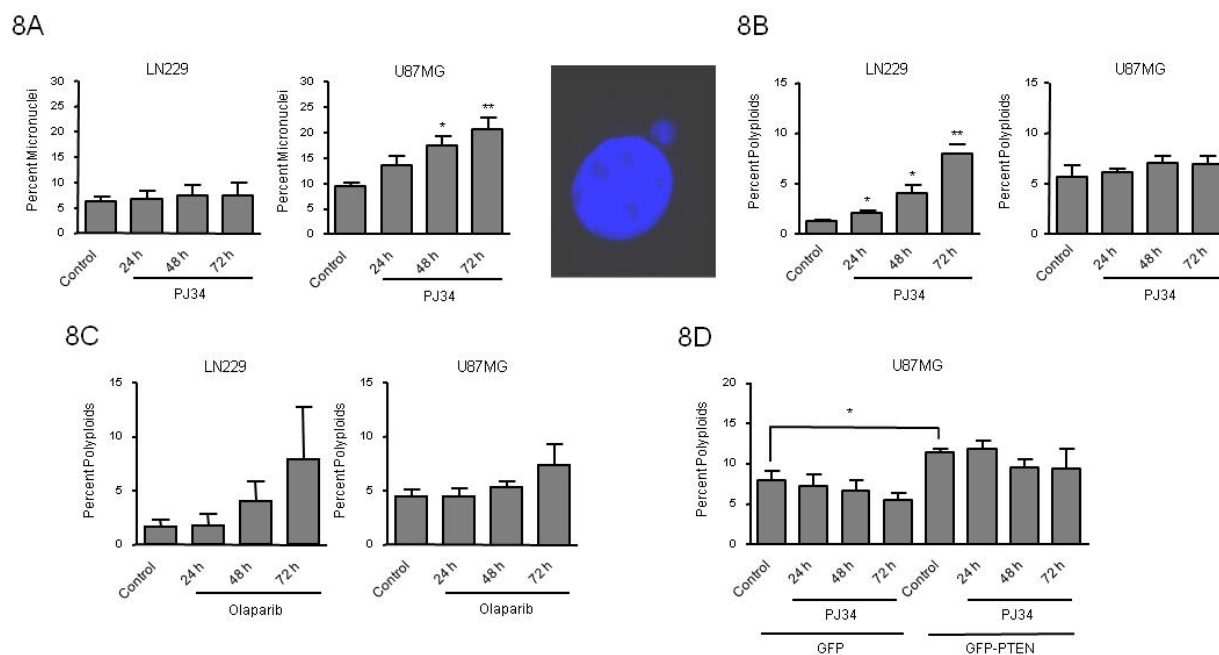


Figure 8: Genomic instability in PTEN mutant cells after PARPi inversely correlates with polyploidy. (A) Micronuclei formation after PJ34 was quantified by DAPI staining. Super G2 fraction, indicating polyplod cells, was analysed by flow cytometry after staining with PI following **(B)** PJ34 or **(C)** Olaparib treatment. **(D)** Increased basal polyplodity after PTEN restoration. * $p < 0.05$, ** $p < 0.01$ versus control group by t-test.

To further understand the impact of PARP inhibition in PTEN mutant cells we performed an expression array focalized in genes involved in cell cycle regulation and DNA repair. In table 1 we have represented genes whose expression was significantly modified after PARP inhibition in U87MG cells. Up-regulated mRNAs included p53-dependent genes such as BBC3/PUMA (a pro-apoptotic BCL2 and BH3-only pro-apoptotic subclass) and CDK1A/p21 (pro-apoptotic and CDK2 inhibitor). Up-regulation was also noted in genes involved in DNA damage, G2/M cell cycle checkpoint, and in genes implicated in DNA repair pathways such as XPA or XPC (Nucleotide Excision Repair). A number of down-regulated genes were involved in homologous recombination repair. That is the case for BARD1 and BRIP1, factors associated with BRCA1 who are needed for its activation. Moreover, RAD51 is an essential component of HR repair and its down-regulation could be detrimental for the cell to cope with DNA damage leading to cell death. Chk1, involved in cell cycle arrest after activation of ATM and ATR in response to DNA damage, is also down-regulated as well as the protein phosphatases CDC25A (which is a Chk1 substrate) and CDC25C, involved respectively in G1/S checkpoint and mitosis entry. Gene expression for exonuclease Exo1, that plays a role in mismatch repair, and the endonuclease FEN1, that removes 5' overhanging flaps in DNA repair and processes the 5' ends of Okazaki fragments in lagging strand DNA synthesis, is repressed after PARP inhibition. Mutations or deficiency in the Fanconi anemia complementation (FANC) group members is characterized by cytogenetic instability, hypersensitivity to DNA crosslinking agents, increased chromosomal breakage, and defective DNA repair. FANCG gene expression was also down-regulated after

PARP inhibition. Phosphorylation of H2AX is involved in the initial early steps of DNA damage response, in the recognition of double strand breaks. Down-regulation of γ H2AX is reflecting a strong defective signalling in the initial sensing of DNA lesions. Globally, this perturbation in DNA damage response factors after PARP inhibition suggests a discomposed scenario in the ability of these PTEN-deficient cells to cope with PARP inhibitor-induced DNA lesions that might be therapeutically exploited.

| Genes Over-Expressed | | | Genes Under-Expressed | | |
|----------------------|-----------------|----------|-----------------------|-----------------|----------|
| Gene Symbol | Fold Regulation | P-VALUE | Gene Symbol | Fold Regulation | P-VALUE |
| BBC3 | 2.8101 | 0.013791 | BARD1 | -3.613 | 0.043765 |
| CDKN1A | 3.8509 | 0.000049 | BLM | -2.6515 | 0.040151 |
| XPA | 3.3737 | 0.000464 | BRIP1 | -5.1323 | 0.007620 |
| XPC | 2.6833 | 0.001180 | CDC25A | -3.8447 | 0.004158 |
| | | | CDC25C | -4.9758 | 0.003132 |
| | | | CHEK1 | -2.2562 | 0.044566 |
| | | | EXO1 | -4.2833 | 0.004202 |
| | | | FANCG | -2.1567 | 0.031524 |
| | | | FEN1 | -2.7212 | 0.030799 |
| | | | H2AFX | -5.4313 | 0.000279 |
| | | | RAD51 | -4.5306 | 0.001705 |

Table 1: Array expression of DNA repair protein in U87MG glioblastoma cells. Genes over and under-expressed following 24 hours PJ34 (20 μ M) treatment. Data are represented as mean \pm SEM of 3 independent experiments. P-value was calculated through t-test.

1.3 IMPAIRED HOMOLOGOUS RECOMBINATION (HR) AFTER PARPi IN PTEN DEFICIENT GLIOMA CELLS

In view of the above results we tested HR efficiency in U87MG and LN229 cell lines containing an integrated copy of the DR-GFP reporter as previously described (Weinstock, Nakanishi et al. 2006). This reporter allows to determine the rate of HR repair of a Scel endonuclease-generated DSB in the chromosome by the restoration of an intact green fluorescent protein (GFP) gene. GFP levels were quantified by Kolmogorov-Smirnov adjust, and revealed that LN229 cells expressed higher levels of GFP after transfection, indicating that PTEN mutant cells are compromised in Homologous Recombination, as has been previously reported (McEllin, Camacho et al. 2010). Moreover, PARP inhibition further disabled HR, mainly in PTEN mutant cells where we found this repair pathway profoundly down-regulated after the PARPi treatment (figure 9A).

To confirm the previous results of PARPi inducing increased HR deficiency specifically in PTEN mutant cells, we performed an assay to quantify RAD51 foci, which is also used to assess HR

efficiency. First we observed that RAD51 accumulation in U87MG cells did not correlate with the level of DNA damage and, also, it did not change in parallel to γ H2AX levels. On the contrary, RAD51 levels in LN229 raised in parallel with γ H2AX levels and these foci were resolved following 24 hours after irradiation (figure 9B). These results suggested that PTEN wild type cells, but not PTEN mutant cells, were able to couple HR activation with DNA damage levels. In addition, γ H2AX basal levels are much lower in U87MG cells (figure 9C), further confirming the perturbed status of the HR signaling that makes them unable to properly signal and resolve DNA damage. Consistently, assessing only γ H2AX positive cells, which bear DNA damage, we observed IR treatment-induced accumulation of RAD51 foci was much less efficient in PTEN mutant cells (figure 9D) and co-treatment with PJ34 further depressed RAD51 foci formation in these cells, supporting the above results obtained with DR-GFP transfection assay.

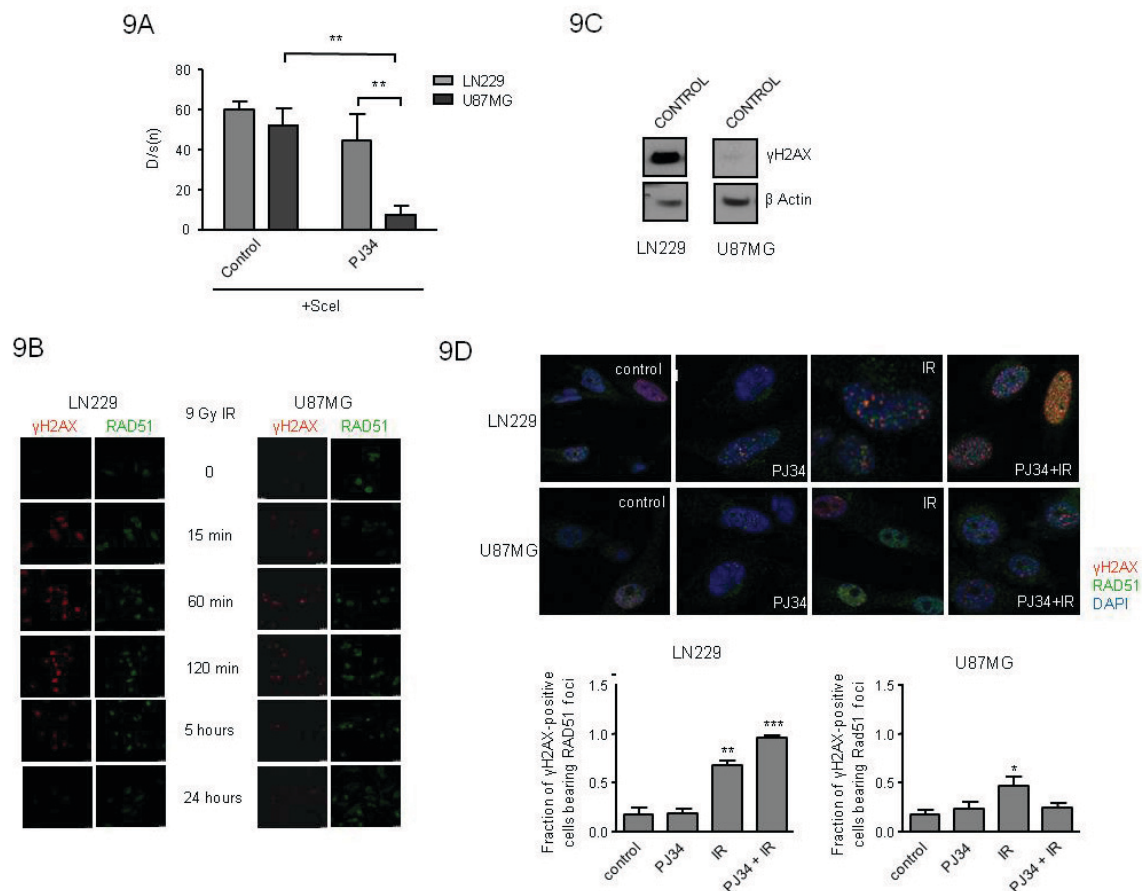


Figure 9: Homologous recombination down-regulation following PARPi. (A) Stably transfected with DR-GFP plasmid LN229 and U87MG glioblastoma cell lines were transiently transfected with Scel plasmid. Two days later, they were treated with PARP inhibitor PJ34 (10 μ M) for 48 hours. GFP expression was analysed by flow cytometry and the results were processed by Kolmogorov-Smirnov test. **(B)** Immunofluorescence analysis of γ H2AX and RAD51 foci after 9 Gy irradiation. Bar = 25 μ m. **(C)** Western blot analysis of γ H2AX basal expression levels **(D)** Distribution of Rad51 and γ H2AX foci; nuclear staining was performed with DAPI. Cells were treated with PJ34 (20 μ M) during 48 hours and subsequently irradiated at 2Gy during 4 hours. Fraction of positive γ H2AX population bearing RAD51 foci was quantified. * p < 0.05, ** p < 0.01, *** p < 0.001 versus control group by t-test.

Next, we analyzed the expression of RAD51. The levels of RAD51 were rapidly down-regulated in U87MG, but not in LN229 where they only decreased 48 hours following PARP inhibition (figure 10A). PARP-1 silencing, however, affected similarly to RAD51 levels irrespective of the PTEN-status (figure 10B). Levels of BRCA1 protein were also reduced in PTEN deficient cells (figure 10A). Similar results were obtained using the PARPi Olaparib (figure 6B). To further confirm the association between RAD51 decrease, PARPi treatment and PTEN status, we silenced PTEN in LN229 and we found a decrease in RAD51 levels (figure 10C); on the other hand, restoring PTEN in U87MG cells led to a delay in RAD51 down-regulation after the treatment (figure 10D). As we described above, the expression of the SAC regulatory factor BUBR1 was reduced after PARPi treatment in PTEN mutant cells (figure 6A,B). To better understand the association between BUBR1 down-regulation and impaired HR we knocked-down BUBR1 in PTEN proficient cells and we observed a recovery in RAD51 following PARP inhibition (figure 10E). This apparently contradictory result might be explained because PARP inhibition, in siBUBR1 cells, is acting in a BUBR1 deficient scenario since the beginning, contrary to the situation on U87MG cells. This RAD51 recovery might reflect a compensatory mechanism initiated by the cell to avoid massive DNA damage in the absence of an efficient mitotic checkpoint.

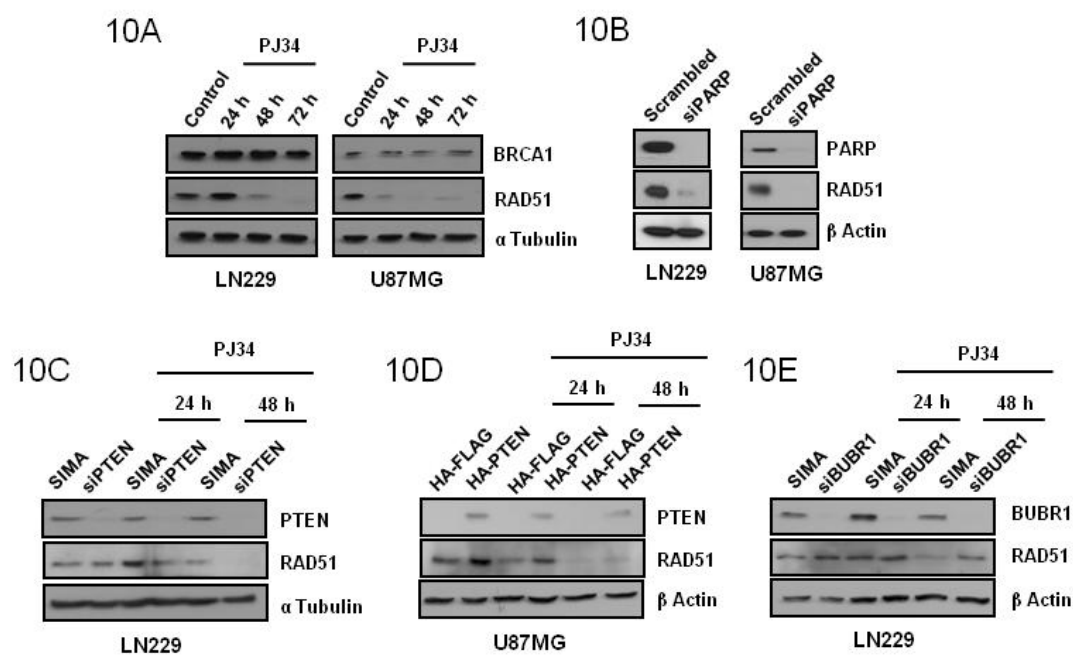


Figure 10: RAD51 down-regulation following PARPi is delayed in presence of PTEN. (A) BRCA1 and RAD51 expression was analysed by western blot 24, 48 and 72 hours after 20 μ M PJ34 treatment or (B) following PARP knockdown. (C) RAD51 expression was measured by Western Blot after the treatment with PJ34 following PTEN silencing in LN229 cells or (D) PTEN overexpression in U87MG cells. (E) RAD51 expression was measured by Western Blot after the treatment with PJ34 following BUBR1 silencing in LN229 cells.

1.4

PARP BLOCKADE POTENTIATED IN VITRO AND IN VIVO EFFECT OF EGFR INHIBITION ON PTEN MUTANT GLIOMA CELLS

In spite U87MG glioma cells are not mutant for EGFR, they constitutively activate MAP kinase pathway in virtue of mutations affecting Focal Adhesion Kinases and GRP3 (Park, Kim et al. 2002, Clark, Homer et al. 2010). PARP inhibition did not prevent ERK1/2 activation making this treatment only partially effective in suppressing this proliferative pathway. We reasoned that avoiding signalling arising from EGFR might deregulate the activation of MAP kinase pathway and potentiate the effect of PARP inhibition. While treatment with EGFR inhibitor erlotinib alone prevented ERK1/2 activation in LN229 cells, U87MG cells were refractory to the effect of erlotinib (figure 11A). Interestingly, co-treatment with PJ34 and erlotinib resulted in a complete suppression of ERK1/2 activation (figure 11B). Nonetheless, combination of both drugs did not further decrease PARPi-induced cytotoxicity (Figure 11C).

The full abrogation of ERK1/2 activation prompted us to test the *in vivo* efficacy of this combination. To this end, we performed an orthotopic assay inoculating U87MG cells that expressed luciferase allowing *in vivo* visualisation of the evolution of tumor mass. While the effect of PJ34 or erlotinib were limited separately (35 and 50% respectively), the combination of both treatments reduced tumor growth to more than 90% after 14 days (figure 11D). Mice were sacrificed after 21 days due excessive tumor growth in vehicle treated mice; at this time PJ34 continued to be effective as anti-tumor agent indicating that the combined inhibition of a pro-survival pathway (using erlotinib) together with the inactivation of HR and the induction of genomic instability by PARP inhibition has a synergic *in vivo* anti-tumor effect.

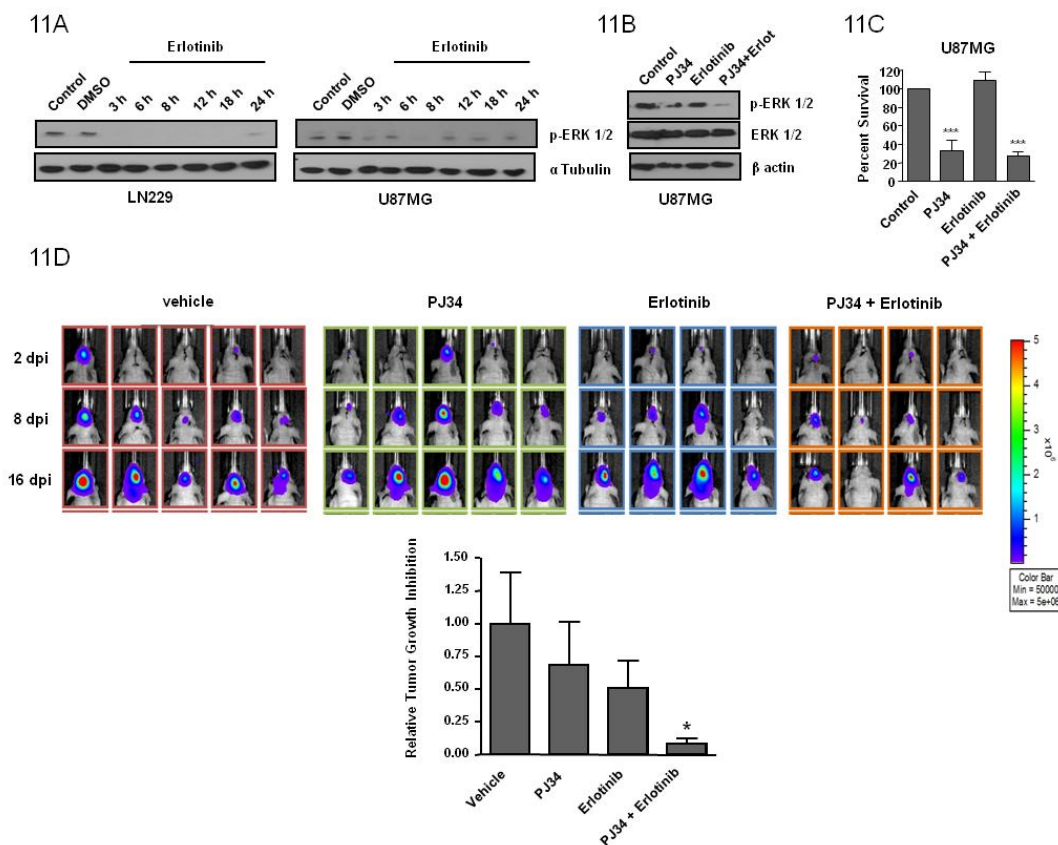


Figure 11: In vitro effect of EGFR inhibitor erlotinib and decreased tumor growth in vivo after combined treatment with PARPi and erlotinib. (A) Time course analysis of phospho-ERK-1/2 expression levels after treatment with erlotinib. U87MG cells were treated with erlotinib alone or combined with PJ34 during 72 hours. (B) phospho-ERK-1/2 expression was measured by Western Blot and (C) MTT reduction was analysed. (D) Mice were inoculated with U87MG-luciferase human cell line. Localization and intensity of luciferase expression were monitored by in vivo bioluminescence imaging (dpi, days post cells injection). Representation of tumor growth inhibition on the 16th day. A statistically significant reduction is observed in the combined treatment of PJ34 and erlotinib. *** $p < 0.001$ versus control group by t-test. * $p < 0.05$ versus control group by t-test. Data are represented as mean \pm SEM of 3 independent experiments.

2 mTOR PATHWAY DOWN-REGULATION AND LIPOPHAGY IN ABSENCE OF PARP

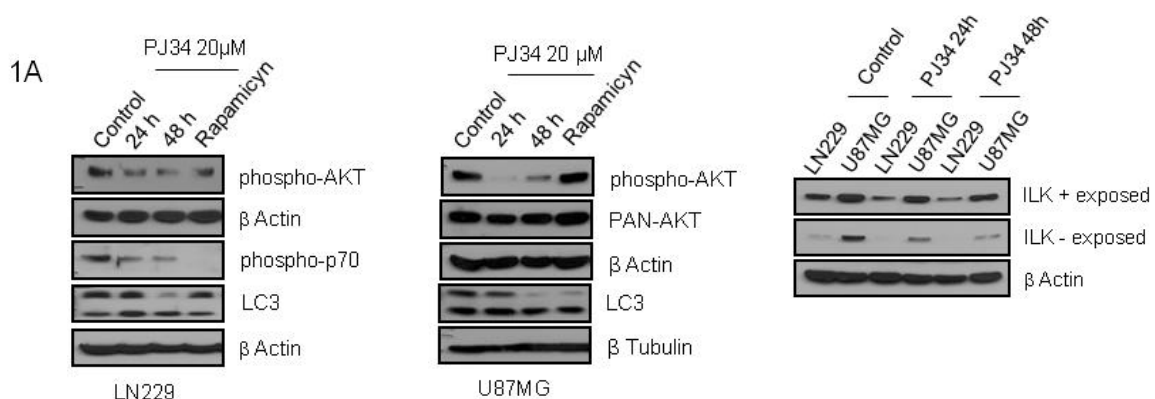
2.1 mTOR PATHWAY DOWNREGULATION AND AUTOPHAGY ACTIVATION FOLLOWING PARP INHIBITION

As pointed in chapter 1, although neither U87MG nor LN229 are mutant for or exhibit amplification of EGFR, they constitutively activate survival pathways. Besides, this activation is enhanced in U87MG cells, which are mutants for PTEN consequently lacking a brake for EGFR signalling.

In addition, the effect of PARP inhibition on the loss of cell viability has been settled in chapter 1. Although a mechanistic explanation related with genomic and mitotic instability, as well as an interesting effect of combining PARPi and erlotinib has been proved, we also decided to examine the status of survival pathways downstream of EGFR, specifically mTOR pathway, following PARPi in monotherapy.

Moreover, a connection between mTOR pathway and autophagy is well established. Hence, the inhibition of the survival mTOR axis entails the activation of autophagy process, that may promote cell survival or cell death in function of the intensity and duration of the stimulus (Wang, Yu et al. 2011). In addition, autophagy has been revealed as a potential target against GBM (Lefranc and Kiss 2006). Consistently, the study of both mTOR pathway and autophagy becomes crucial in order to understand PARP role in GBM biology.

Firstly, we assessed the status of different mTOR axis members 24 or 48 hours after PARPi. Interestingly, a strong decrease on the activity of mTOR activators such as phosphorylated AKT or ILK, as well as a reduction on mTOR substrates such as phosphorylated p70S6K, was observed. Consistently, autophagy was activated after PARPi, measured by the translocation of the form I to the form II of LC3 (figure 1A). Next, we confirmed that PARP-1 knockdown exerted the same effect as PARP inhibition (figure 1B) thereby evidencing that PARP-1, the main member of PARP family, is responsible for mTOR down-regulation, and discarding any off-target effect of PJ34 in this result. However, PARP-1 knockdown was unable to downregulate AKT activation suggesting that other mechanistic interactions may be also acting to modulate the activation of this protein.



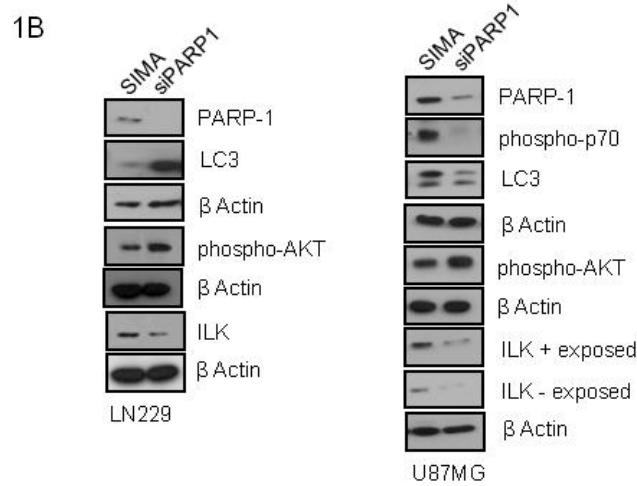


Figure 1: PARP inhibition induces mTOR down-regulation and autophagy activation. mTOR cascade and autophagy activation were analysed by western blot (A) after treatment with 20 μ M PJ34 or (B) following PARP-1 silencing.

Subsequently, we wondered if PARPi exerted the same effect in mTOR pathway when examined in the short time and at lower doses. Thus, we performed a dose-response/time-course for both PJ34 (figure 2A) and Olaparib (figure 2B). Interestingly, low doses of PARP inhibitor were sufficient to activate autophagy as early as two hours after the treatment; pAKT levels, which is an upstream modulator of mTORc1, were mostly unchanged, suggesting that autophagy at this time was independent of mTOR inactivation.

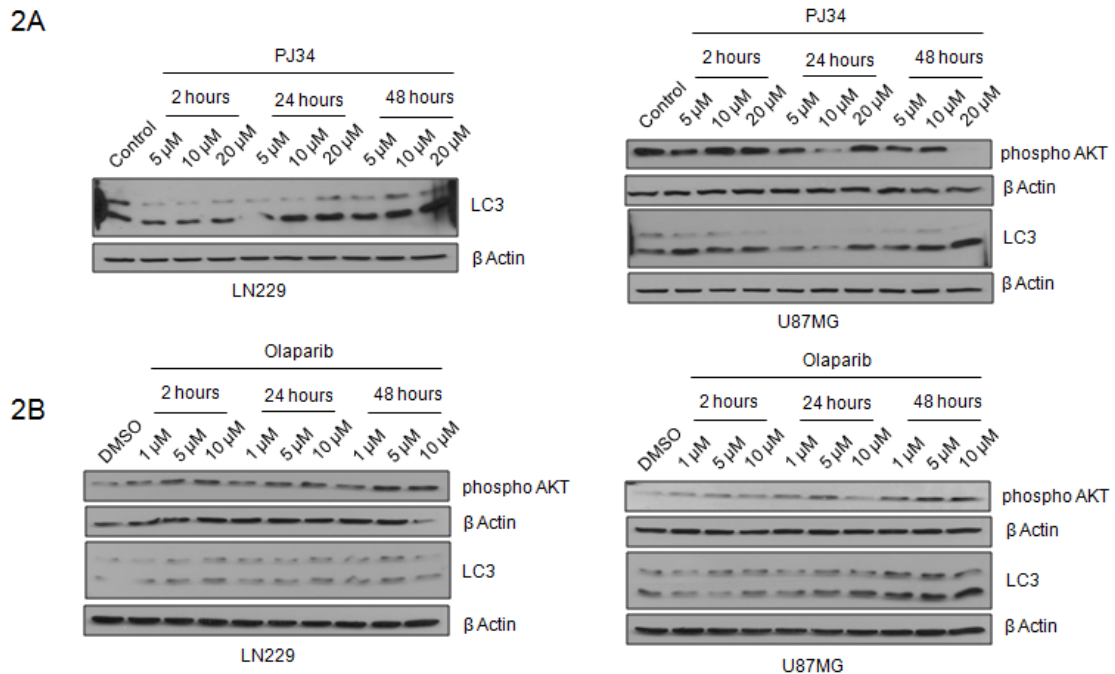


Figure 2: mTOR down-regulation and autophagy activation after shorter times and at lower doses of PARPi. mTOR cascade and autophagy activation were also checked by western blot after 2, 24 or 48 hours treatment with (A) 5, 10 or 20 μ M PJ34 or (B) 1, 5 or 10 μ M of Olaparib.

To further corroborate that autophagy was active after PARPi, we performed Transmission Electron Microscopy (TEM) in order to better visualize this phenomenon. As observed in figure 3, we could also verify basal autophagy activation (especially in U87MG cells) which was further increased following PARPi.

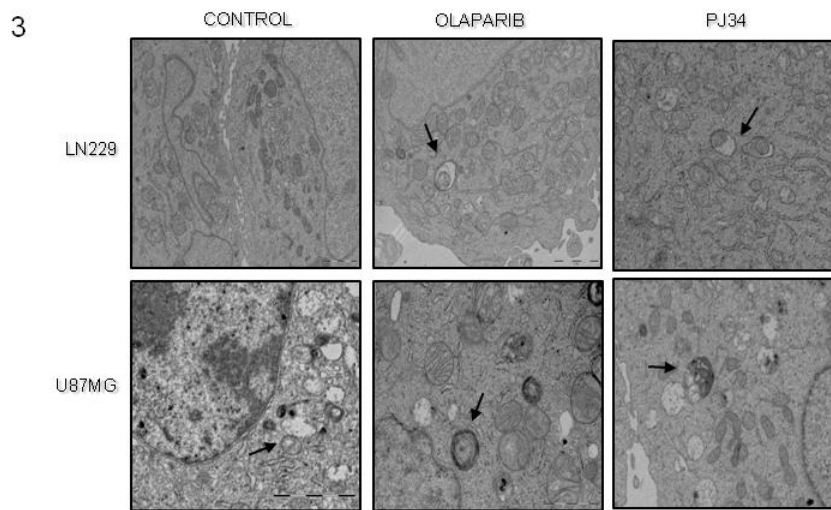


Figure 3: TEM analysis of PARPi-induced autophagy. The figure shows representative images of autophagosome formation after 48 hours of PARP inhibition with either 10 μ M Olaparib or 20 μ M PJ34. Arrows indicate the double-membrane structure of autophagosomes.

2.2 LIPID DROPLETS FORMATION AFTER PARP INHIBITION

The “lipid phenotype” is well known to be adopted by tumor cells. In fact, many proteins related to lipid metabolism, such as Fatty Acid Synthase (FASN) are overexpressed in cancer cells (Menendez and Lupu 2007). Hence, tumor cells increase the pool of fatty acids and this phenomenon correlates with tumor progression.

According to this, we aimed to assess the status of lipid synthesis in our cells. Cytosolic Phospholipase A2 (cPLA2) is well established to contribute to phospholipids (PL) metabolism. When active, this protein is phosphorylated, thereby promoting phospholipids degradation towards lysophosphatidic acid and Free Fatty Acids (FFA). Thus, it induces an increase in the FFA levels through PL-degradative pathway. Interestingly, cPLA2 is known to be activated by MAPK pathway (Waterman, Molski et al. 1996) which, as explained in chapter 1 (figure 11), is modulated by PARP inhibition.

For this reason, we studied if FFA synthesis was altered after PARPi, by testing the status of PL-degradative pathway through phospho-cPLA2 levels (figure 4). Interestingly, we observed an increase in the activation cPLA2 only 2 hours after PARPi, which was followed by a down-regulation after 24 or 48 hours. This results show PARPi activates FFA formation in the short term (2 hours), although long term (24-48 hours) treatment with PARPi results in FFA synthesis down-regulation. We hypothesized that this effect might be due to a feed-back loop that promotes the inhibition of FFA synthesis after an excess on their synthesis activation.

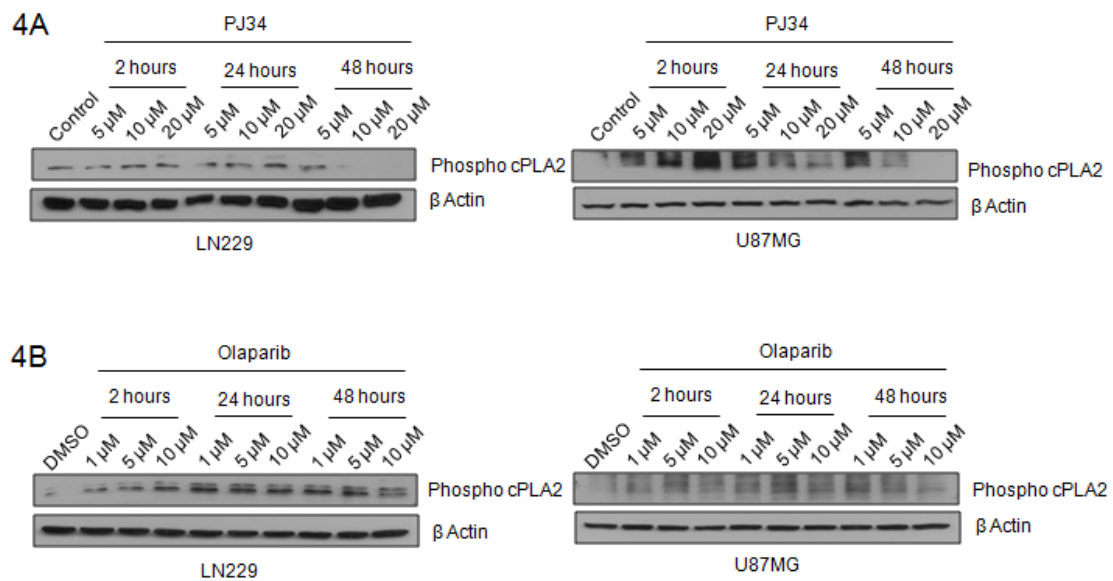
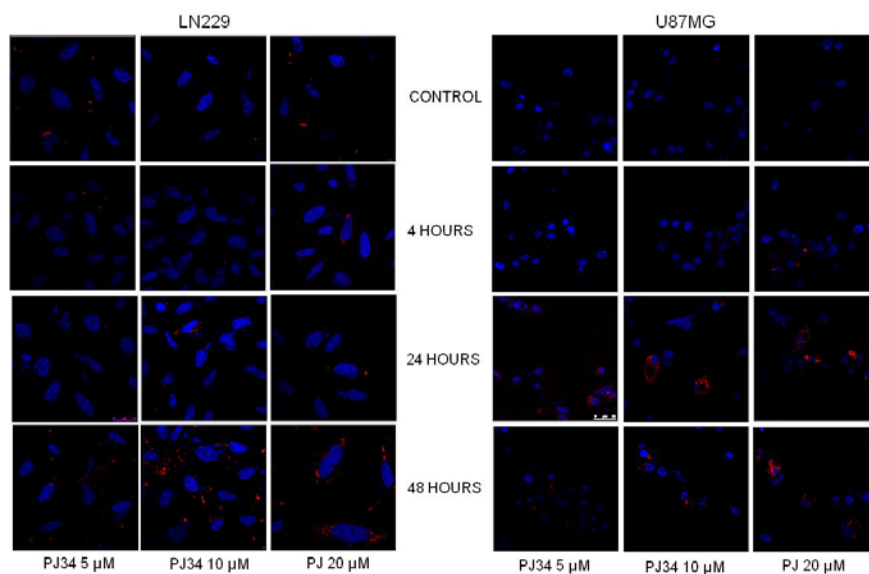


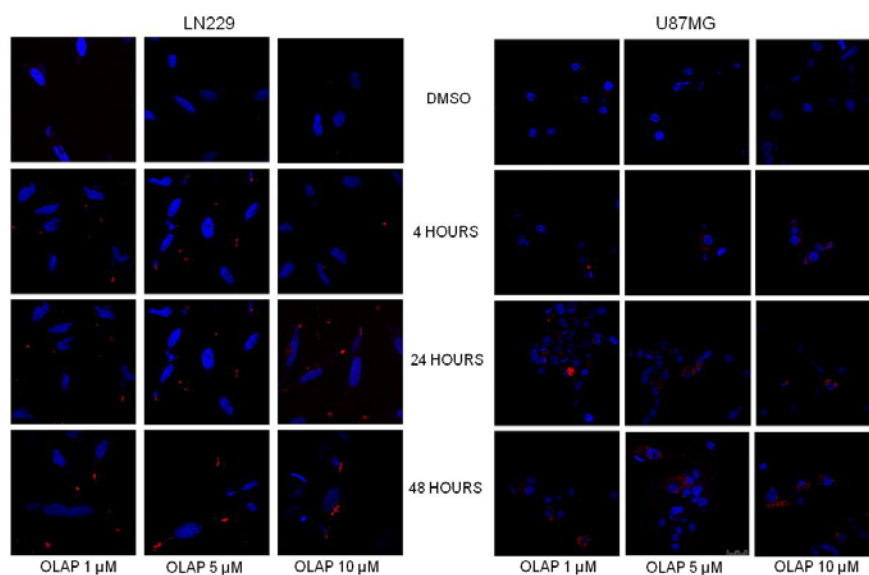
Figure 4: FFA synthesis is altered after PARPi. cPLA2 status (indicating FFAs synthesis) was tested 2, 24 and 48 hours after PARPi with **(A)** 5, 10 or 20 μ M PJ34 or **(B)** 1, 5 or 10 μ M of Olaparib.

Lipid droplets (LDs) are intracellular deposits of lipid esters (TGs and cholesterol) surrounded by a monolayer of phospholipids, and separated from the hydrophilic cytosolic environment by a coat of structural proteins. They play an essential role in energy storage. Besides, LDs supply FFA, which undergo β -oxidation in the mitochondria to support ATP production. In addition to their metabolic role, they are also involved in cellular lipid homeostasis, temporal protein storage, and protein degradation (Thiele and Spandl 2008). Due to the importance of LDs in cell metabolism, we wondered whether FFA were increased following PARPi and might be accumulated in LDs. To this end, we stained LN229 and U87MG cells with the lipid marker Sudan Red after PJ34 treatment (figure 5A) or Olaparib treatment (figure 5B). Additional staining with the fluorescent dye Bodipy[®]493/503 corroborated LDs accumulation, as a switch from a diffuse to a punctated pattern (indicating lipid vesicles) was observed (figure 5C).

5A



5B



5C

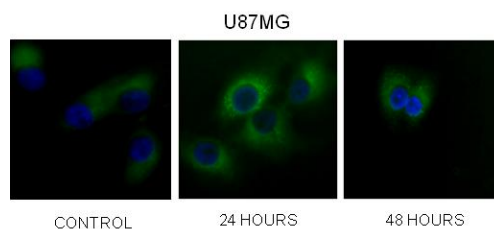


Figure 5: Lipid droplets formation after PARPi. Sudan Red staining (red) shows time and dose-dependent lipid vesicles formation after PARPi. The figure exhibits representative images of LDs formation after 2, 24 or 48 hours of PARP inhibition with either (A) PJ34 or (B) Olaparib. Figure C represents Bodipy staining after 48 hours of 20 μM PJ34, further confirming LDs accumulation in U87MG cells after the treatment. In all cases, nuclei are stained with DAPI (blue).

Interestingly, we observed a clear accumulation of lipid droplets after PARPi, which was time and dose-dependent, confirming that PARPi in the short time induces FFA synthesis and these fatty acids accumulate in lipid droplets.

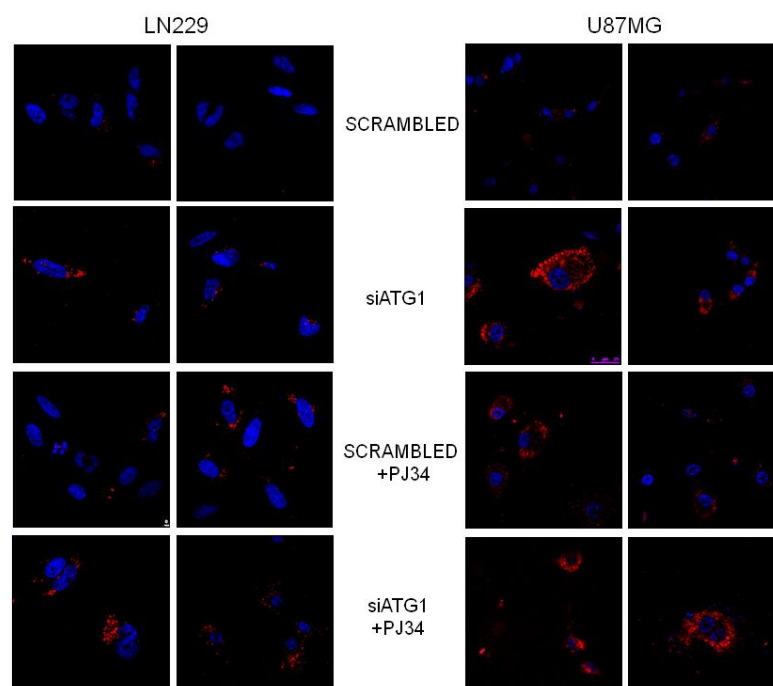
2.3 AUTOPHAGY INDUCED BY PARP INHIBITION REGULATES LIPID METABOLISM

The above results allowed us to verify that PARPi was downregulating mTOR pathway, inducing autophagy activation and promoting FFAs synthesis and LDs accumulation.

Although LDs degradation pathway, or lipolysis, is mainly developed by cytosolic lipases, the regulation of size and number of these organelles cannot be attributed solely to the lipases. In 2009, Cuervo's group demonstrated the involvement of autophagy in LDs lipolysis in hepatocytes (Singh, Kaushik et al. 2009). This fact prompted us to test if PARPi-induced autophagy was a mechanism activated to promote LDs degradation.

To this aim, we blocked the autophagic pathway by genetically silencing ATG1 gene (figure 6A). Interestingly, we verified that autophagy was targeting LDs synthesis since ATG1 depletion increased LDs accumulation, even in absence of PARPi, as measured by Sudan Red staining. These results suggest on the one hand, that GBM cell lines tend to accumulate LDs even in a basal situation, so that autophagy (in this case lipophagy) is a mechanism that must always be active to counteract LDs increase and avoid lipotoxicity. On the other hand, that treatments that induce LDs formation, such as PARPi, also activate lipophagy so that excessive LDs accumulation is prevented. Further confirmation of lipophagy signaling was obtained through Bodipy analysis of LDs following chemical inhibition of autophagy with chloroquine (figure 6B).

6A



6B

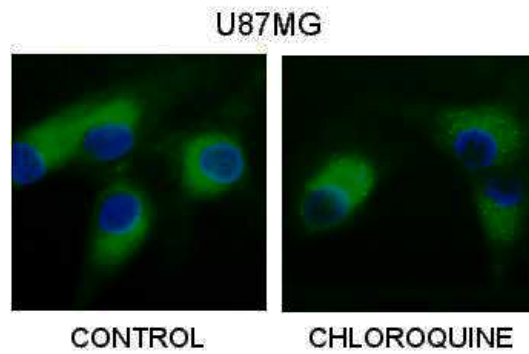


Figure 6. Autophagy blockade induces LDs accumulation. (A) Sudan Red staining (red) shows increased lipid vesicles formation in absence of PARP (48 hours treatment with 10 μ M PJ34), which is dramatically augmented when autophagy is genetically silenced. The figure shows representative images of LDs formation. (B) Further confirmation of this process is represented by Bodipy staining after chemically blocking autophagy with chloroquine. In both cases, nuclei are stained with DAPI (blue).

Furthermore, we found that basal LDs accumulation after ATG1 knockdown (in absence of PARPi) was increased in U87MG respect to LN229 cells. Interestingly, this cell line exhibited higher levels of basal autophagy (figure 1A, figure 3). Taken together, these results indicate that a cell that tends to accumulate LDs, also induces lipophagy in order to counteract the negative effects of this accumulation. Moreover, that PARPi-induced LDs are neutralized by activation of the lipophagic process.

Next, we wanted to elucidate if LDs accumulation in absence of autophagy may modulate fatty acid synthesis. Thus, we tested if PARPi effect on phospho-cPLA2 levels was altered when autophagy is genetically inhibited. Unexpectedly, we observed that cPLA2 down-regulation was accelerated after silencing ATG, suggesting that the increase on LDs formation in absence of autophagy may act as a negative loop to impede FFA accumulation and subsequent LDs increase (figure 7).

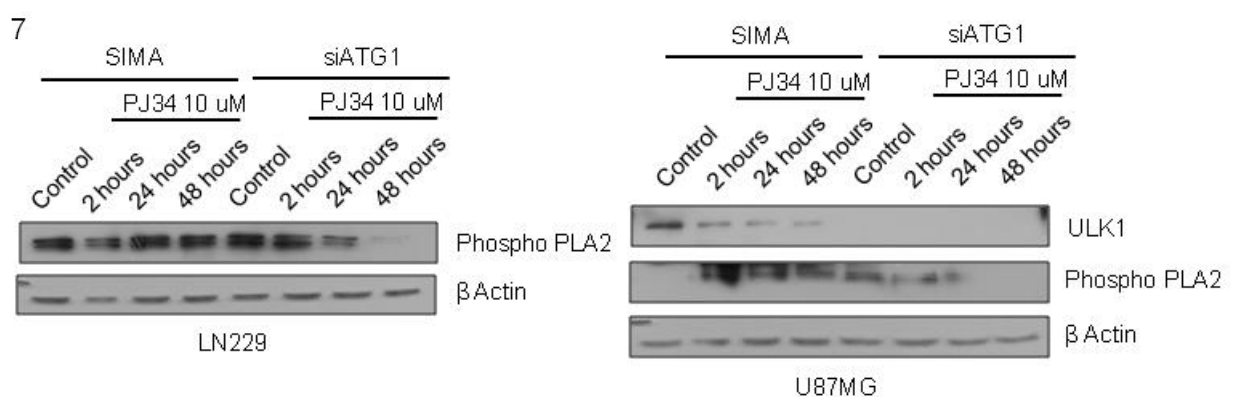


Figure 7: phospho-cPLA2 down-regulation following PARPi is accelerated in absence of autophagy. When autophagy is genetically silenced, the down-regulation of phospho-cPLA2 levels after PARPi is intensified, specially following 48 hours PARPi.

Altogether, these results show GBM is a model with high addiction for autophagy, pro-survival pathways such as mTOR axis, as well as a tendency towards lipogenic metabolism, which is targeted through lipophagic processes. Importantly, PARPs play a crucial role in these mechanisms as their inhibition acts as a brake for pro-survival strategies in GBM.

2.4 GBM CELLS POTENTIATE THEIR OWN ADDICTION TO SURVIVAL PATHWAYS WHEN EXPOSED TO PARPi

To further understand GBM dependence for survival pathways, we wondered if GBM cells might secrete pro-survival factors to potentiate their own growth, and if PARPi effect may be mediated by the secretion of stress factors that would counteract survival pathways activation.

To check this hypothesis, we analyzed the impact of the factors secreted by GBM cells on PARPi effect. Thus, we tested the effect of conditioned medium (CM) which had previously been in contact with cells with or without PARPi during 48 hours, on new-plated GBM cells (figure 8).

No remarkable differences were observed in the status of mTOR pathway (measured through p70S6K phosphorylation) and autophagy (analyzed through LC3I to LC3II translocation) following CM treatment alone, suggesting that in a basal state, pro-survival factors secreted by the own cells were not relevant as to promote survival pathways addiction but other intracellular signalling was responsible for this situation. However, a strong decrease on autophagy activation was observed in the conditioned medium – treated cells in presence of PJ34, suggesting that after PARPi treatment, GBM cells do not promote stress factors secretion.

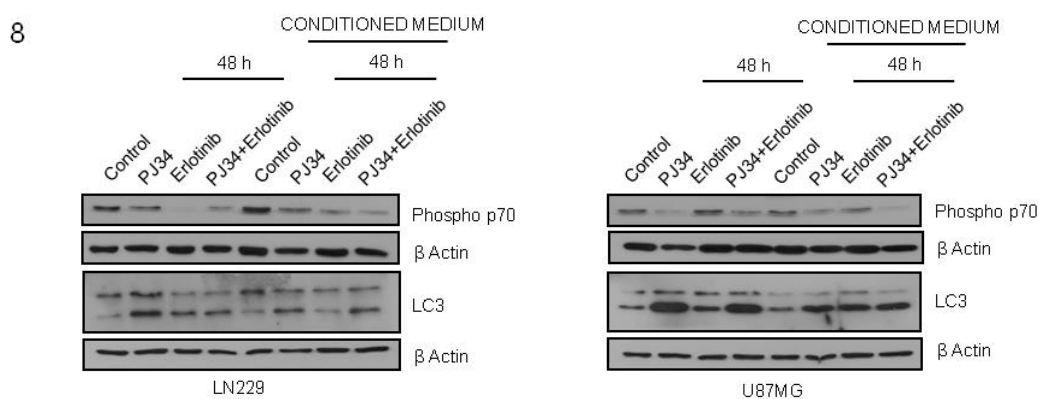


Figure 8: PARPi effect on autophagy and survival axis is influenced by conditioned medium. Slight delay on mTOR downregulation and strong decrease in autophagy activation following incubation with PARPi – treated CM. Cells were treated with medium alone – bearing 48 hours 10 μ M PJ34, or conditioned medium from cells treated during 48 hours with 10 μ M PJ34.

Furthermore, the effect of PARPi was also tested in combination with erlotinib. Blockade of growth factors receptor EGFR did not completely revert the effect of the PARPi-treated CM, indicating that PARPi-induced autocrine factors may bind to receptors different to EGFR, or in case EGFR is mediating this signalling, erlotinib is not enough to abrogate it. In addition, it is important to remark that changes in autophagy activation did not completely correlate with mTOR levels, as the autophagy delay induced by CM was not reflected as a strong recovery of phospho-p70S6K levels, suggesting that mTOR-independent autophagy was taking part in this case.

Thus, strategies targeting PARP in GBM should take into account that PARPi induces mTOR pathway downregulation, autophagy activation and LDs synthesis which is targeted by lipophagy. Besides, autophagy may in part be activated through mTOR-independent mechanisms and cells may counteract this effect through their own secretion of pro-survival factors to the extracellular medium.

To conclude, these results show a pleyade of important effects of PARPi in GBM survival and lipogenic pathways. The understanding of the mechanisms that lead to the activation of these routes, as well as the comprehension of the interrelations among all of them, is a crucial step to get insights into GBM biology and design new and more strategies to improve the clinical output of this tumor.

3 PARP TARGETING COUNTERACTS GLIOMA STEM-LIKE CELLS PHENOTYPE THROUGH THE PROMOTION OF VIABILITY DECREASE, mTOR AXIS DOWN-REGULATION AND CELL DIFFERENTIATION.

3.1 PARPi PROMOTES GSCs VIABILITY DECREASE

The presence and involvement of Glioma Stem-like Cells (GSCs), also named Glioma Initiating Cells (GICs) in the initiation and propagation of GBM is broadly accepted, and the comprehension of their biology is a key factor to understand tumor relapse and failure of treatments. Currently, any anti-tumor approach against GBM must necessarily target, one way or another, GSCs population.

Consequently, to fully recognize the effect of PARPi against GBM we aimed to evaluate its effect on GSCs. For this purpose, we used primary patient-derived PTEN-proficient glioma cells TG1 and OB1 (Patru, Romao et al. 2010).

Due to the difficulty to extinguish GSCs, we decided to extend the times of treatment with PARPi to one week so we could check a reliable effect that might be masked in shorter times. Besides, as GSCs bear surface ABC transporters able to efflux cytotoxic agents (Dean, Fojo et al. 2005), we tested the effect of PARPi both without or without re-addition of PARPi during the first three days of the experiment.

Firstly, we observed that PARPi treatment resulted in loss of cell viability in both TG1 and OB1 cells, either with PJ34 or Olaparib. Although we found a significant viability decrease without re-addition (figure 1A), the effect was notably potentiated after re-addition (figure 1B).

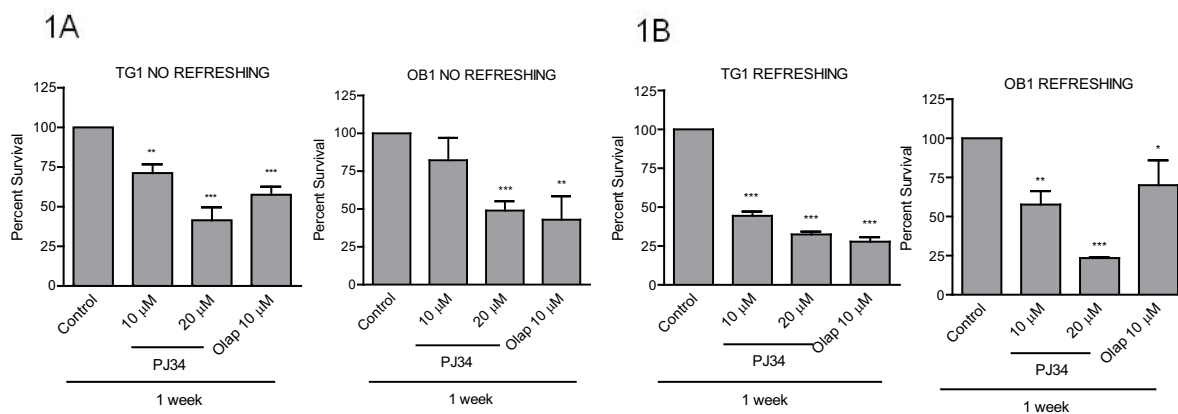


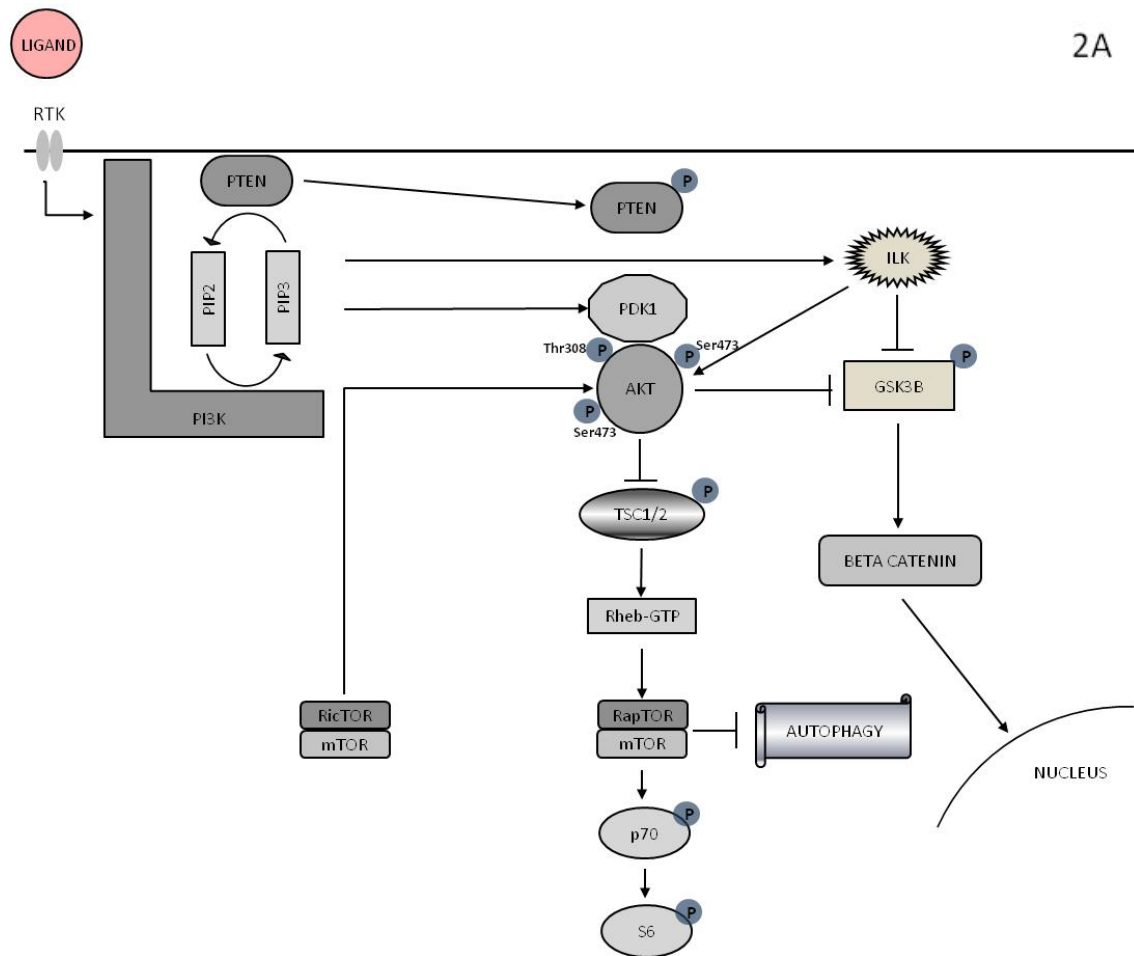
Figure 1: PARP inhibition compromises GSCs viability. Viability analysis by MTT assay of GSCs treated with 10 and 20 μM PJ34, or 10 μM Olaparib during one week, **(A)** without re-addition of the treatment or **(B)** re-adding it during the three first days of the experiment. Data were normalized and expressed as a percentage of the control. * $p < 0.05$, ** $p < 0.01$, *** $p < 0.001$ versus control group by t-test.

3.2 PARPi DOWNREGULATES mTOR AXIS AND PROMOTES AUTOPHAGY ACTIVATION IN GSCs.

Due to the specific effect of PARP inhibition on the loss of cell viability, we decided to find a mechanistic explanation connecting PARP inactivation and the downstream effects on cell survival.

As mTOR pathway activation inhibits autophagy (Yang and Klionsky 2010) and this process has been described to favour tumor adaptation to changing micro-environment conditions (Pavlides, Vera et al.), autophagy has emerged as a potential target to overcome GBM. Hence, to have a global overview of the status of these pathways in GBM, we decided aimed to examine mTOR pathway and autophagy status in GSCs following PARPi.

PARPi with either PJ34 or Olaparib resulted in mTOR pathway down-regulation (figure 2). Upstream mTORC1 we observed loss of PTEN phosphorylation, which leads to its activation and consequently constitutes a brake for mTOR signaling. In addition, down-regulation of phospho-AKT levels for both Ser473 and Thr308, which leads to its inhibition, was detected accompanied by loss of phospho-GSK3 β , which is a downstream effector of AKT, and inhibition of β -catenin downstream GSK3 β . We also examined mTOR status by determining the phosphorylation of the ribosomal protein S6, and autophagy activation through the endogenous LC3 translocation.



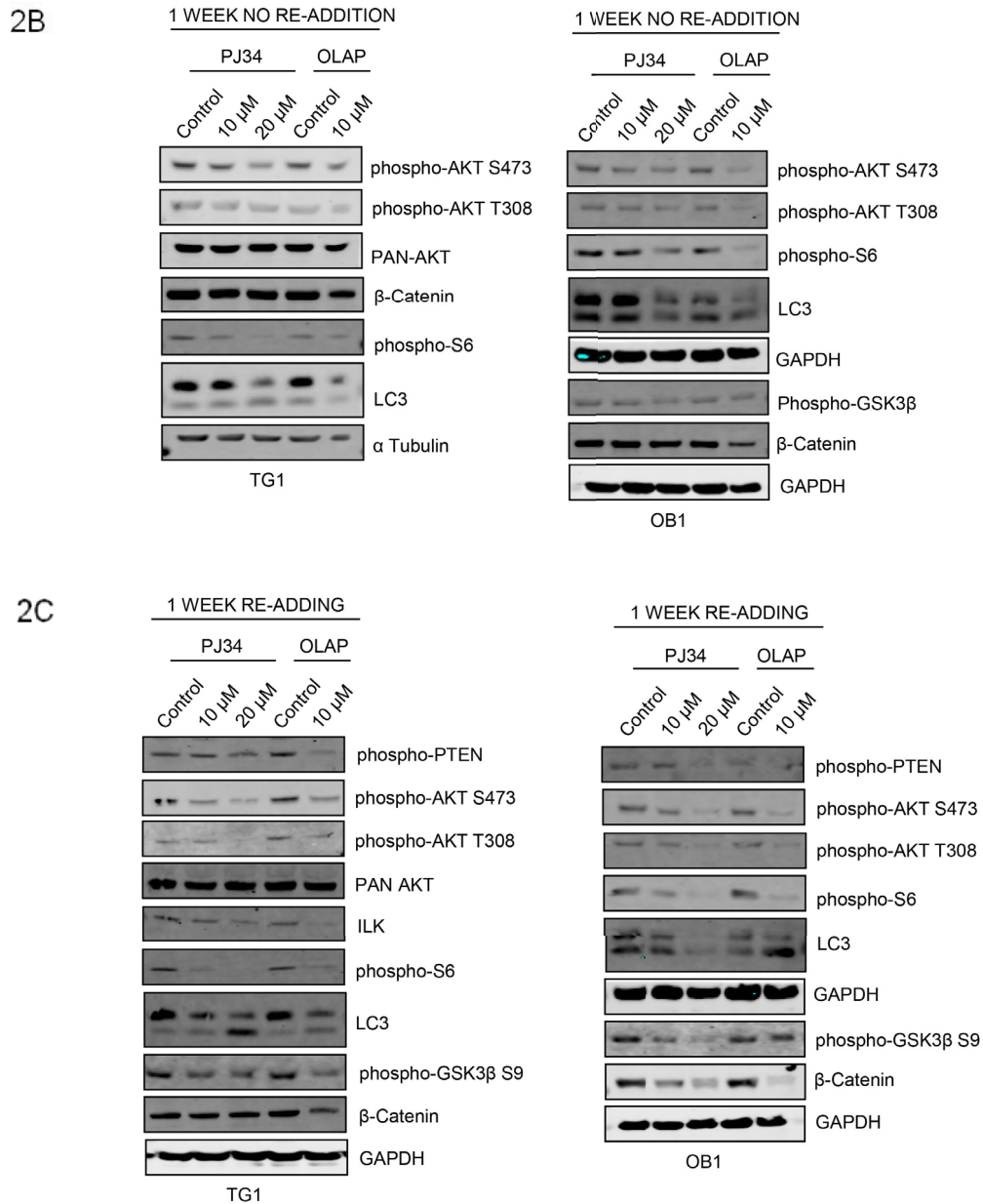


Figure 2: PARP inhibition induces mTOR down-regulation and autophagy activation. mTOR cascade and autophagy activation were analysed by western blot following the treatment with 10 and 20 μ M PJ34, or 10 μ M Olaparib during one week. For a better understanding of the results, a diagram indicating the pathway has been represented (A). Results are shown without re-addition of the treatment or (B) re-adding it during the three first days of the experiment (C).

Interestingly, a firm effect on mTOR down-regulation and autophagy activation was observed without re-addition (figure 2B), and this effect was potentiated by the re-addition of the treatment (figure 2C).

3.3 PARPi ABROGATES GSCs PHENOTYPE, SUGGESTING THE INDUCTION OF CELL DIFFERENTIATION

Hitherto, we have demonstrated loss of cell viability and survival pathways down-regulation in GSCs following PARPi. However, to fully target GSCs phenotype it is highly relevant to promote loss of stemness and/or cell differentiation towards normal tumor cells, since these steps are well described to be one of the main strategies to overcome GBM and avoid tumor recurrence.

To study this process, we decided to check both functional and molecular markers so that these approaches may provide us with a global vision of the process. To have a functional approach about stem phenotype following PARP inhibition, we evaluated self-renewal capability, which is a marker of stemness in primary cells, through neurospheres formation assay following PARPi. Again, one week treatment with or without re-addition of the inhibitor was performed, which allowed us to corroborate a strong reduction in the number of neurospheres at the end of the experiment as consequence of PARPi (figure 3A,B,C).

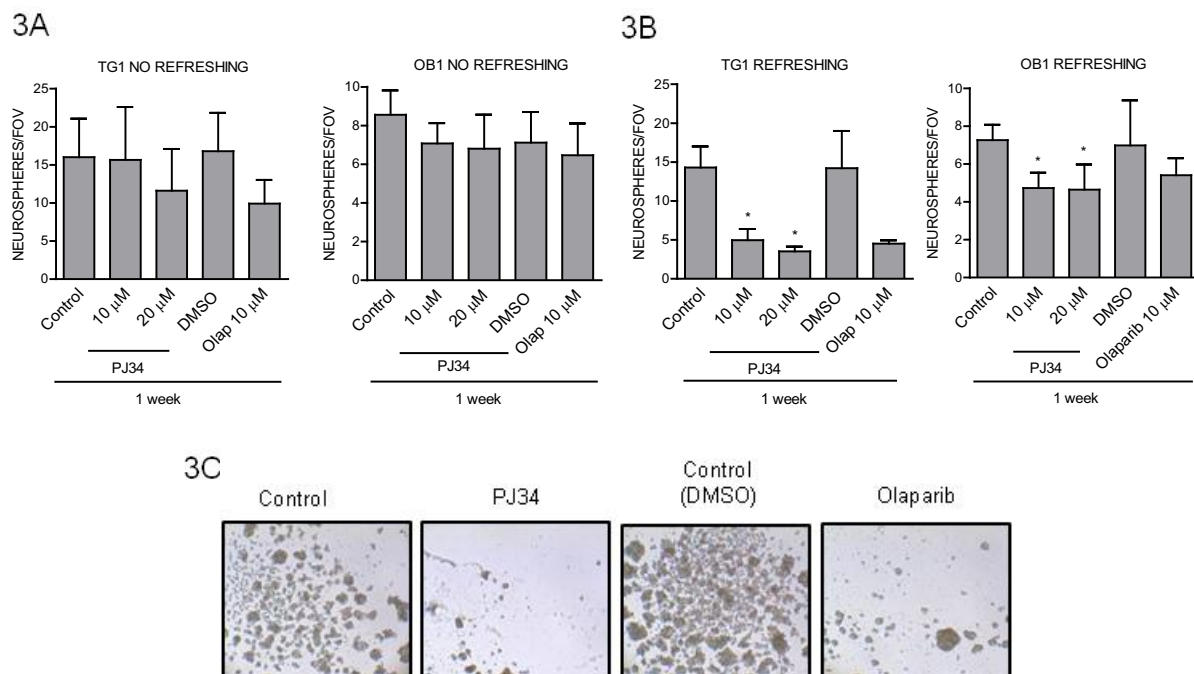


Figure 3: Neurosphere formation ability is compromised following PARPi: Neurosphere Formation Assay (NFA) of GSCs treated with PJ34 or Olaparib, **(A)** without re-adding or **(B)** re-adding the treatment during the three first days of the experiment. After one week, neurosphere countage (10 fields of view (FOV) per condition) was performed. **(C)** Images of TG1 neurospheres after treatment re-addition. * $p < 0.05$ versus control group by t-test.

Similar results have been reported by Rich and colleagues showing that PARPi preferentially targeted GSCs (Venere, Hamerlik et al. 2014). Our data support that PARPi targets primary glioma cells in part by perturbing self renewal/GSCs phenotype.

Next, we analyzed the status of molecular stem markers such as SOX2 or Nestin following PARP inhibition. In the case of SOX2, although no gene expression changes were observed following PARPi (figure 4A), a solid decrease was observed at the protein level, measured by western blot (figure 4B) and immunofluorescence (figure 4C). However, no important changes in Nestin expression were observed after the treatments (figure 4C).

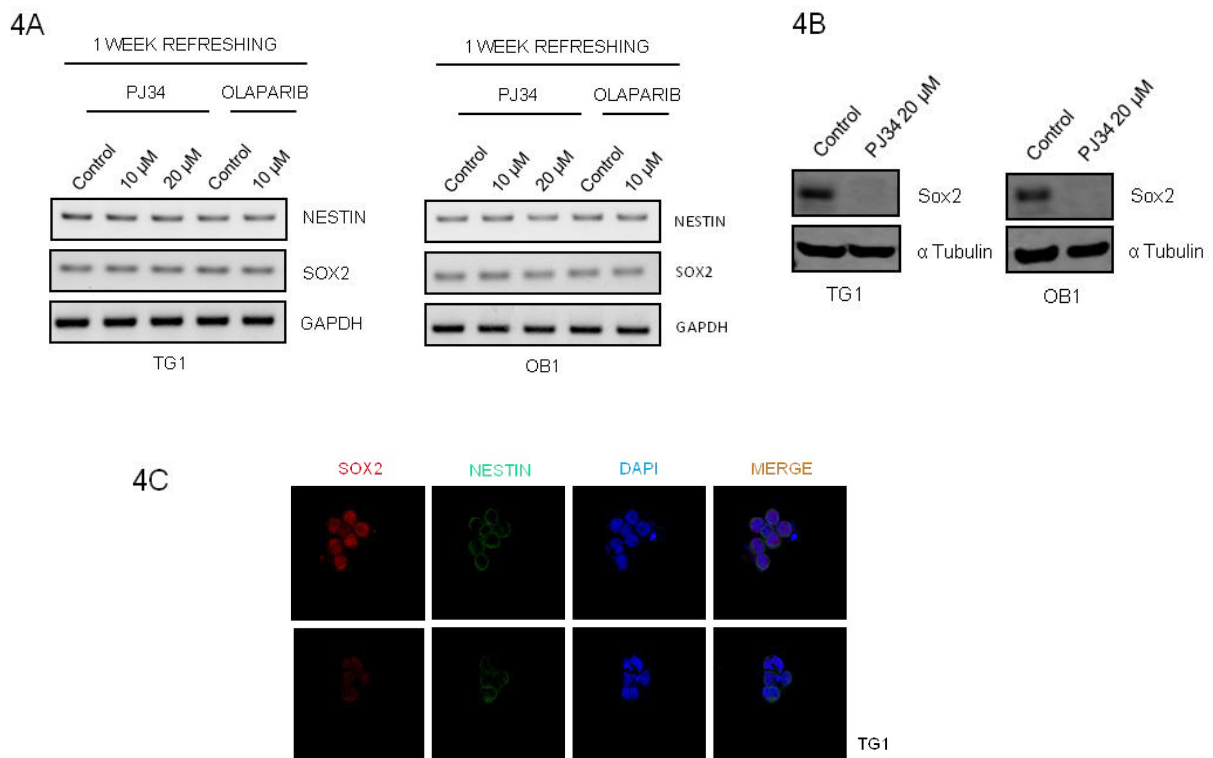


Figure 4: Loss of stem markers after PARPi: The expression of stemness markers was analyzed following PARPi. **(A)** Nestin and Sox2 RNA levels showed no changes after the treatment with PJ34 or Olaparib. However, Sox2 protein levels were potently diminished when examined by **(B)** western blot or **(C)** immunofluorescence. No effect was observed in Nestin protein levels.

Thus, a clear effect of PARPi is observed in GSCs viability and loss of stemness, which is an unavoidable requirement for globally targeting GBM thereby preventing tumor recurrence. However, the specific mechanisms by which PARPi is involved in loss of stem phenotype remain to be elucidated.

DISCUSSION

1 GENERAL DISCUSSION

Glioblastoma multiforme (GBM) is the most common primary brain tumour in adults and one of the most aggressive cancers. Although the current understanding of the mechanisms which underlie brain tumorigenesis is limited, glioblastoma lethality and resistance to therapy can be partially explained by their ability to promote cell survival almost in any situation and under any circumstance. The mechanisms by which these processes occur have been deeply analyzed in the introduction of this thesis. However, for a better comprehension of the main aspects of the discussion, the mechanisms underlying glioblastoma aggressiveness are summarized as follows (Krakstad and Chekenya 2010, Nobusawa, Lachuer et al. 2010).

- High tolerance to DNA damage through abrogation of DNA damage response, and subsequent tendency to develop genomic instability.
- Deregulated mitotic checkpoint, thereby promoting mitotic instability.
- Increased cell death resistance, which is accomplished through apoptosis inhibition.
- Constitutively active pro-survival pathways. In particular mTOR axis is upregulated, which involves exacerbated protein and lipid synthesis.
- Presence of Glioma Stem-like Cells (GSCs), which are responsible for the initiation and recurrence of the tumor, and treatment failure.

In spite these processes are well-defined, the understanding of the whole scenario that leads to GBM development still remains elusive. Hence, this fact severely limits preventative and therapeutic options for glioblastoma patients. The current standard treatment for GBM involves surgical resection followed by adjuvant radiotherapy (RT) with ionising radiation, with or without concomitant chemotherapy. Disappointingly, this regimen only affords GBM patients a median survival benefit of 14.6 months- a 12 month improvement over resection alone. It is important to note that radio- and chemotherapies are, at the molecular level, based on inducing enough DNA damage in the tumour cell to result in lethality (Wilson, Karajannis et al. 2014). The results shown in this study reflect that PARP inhibition results in a profound remodeling on different aspects of glioma biology. This panel of alterations will be discussed separately for each chapter of results previously shown.

2 PARP TARGETING COUNTERACTS GLIOMAGENESIS THROUGH INDUCTION OF MITOTIC CATASTROPHE AND AGGRAVATION OF DEFICIENCY IN HOMOLOGOUS RECOMBINATION IN PTEN-MUTANT GLIOMA

In this chapter, we examined the effect of PARP inhibition on the mechanisms that lead to the accumulation of genomic and mitotic instability in glioma cells. When we checked the effect of PARPi in PTEN proficient and PTEN deficient cells, we observed a preferential accumulation of genomic instability in PTEN-deficient glioma cells. Thus, we observed downregulation of mitotic checkpoint, compromised homologous recombination repair and decreased G2 arrest in absence of PTEN. Genomic instability increase was measured through micronuclei analysis, as hallmark of Mitotic Catastrophe (MC).

The protein kinase BUBR1 plays a key role in the maintenance of chromosomal stability (Ricke and van Deursen 2013) owing to its involvement in the formation of proper chromosome-spindle attachments. Briefly, BUBR1 down-regulation activates Aurora B kinase and the kinetochore protein CENP-A, resulting in the loss of kinetochore-microtubule attachments (Lampson and Kapoor 2005). Besides, it avoids sister chromatids separation in anaphase when chromosome-spindle attachments are uncorrect, since it is involved on the Mitotic Checkpoint (Spindle Assembly Checkpoint or SAC) (Burton and Solomon 2007). When interactions between kinetochores and microtubules are unstable in metaphase, BUBR1, acting together with MAD2 and BUB3, join CDC20 avoiding APC activation and preventing sister chromatids separation in anaphase. Remarkably, gene expression of *BUB1B* (the gene coding for BUBR1) is very significantly up-regulated in GBM patients and its expression was inversely correlated with PTEN in short-survival patients. In line with this finding recently it has been described that *BUB1B* is differentially required for GSCs expansion in glioblastoma tumours and genetically transformed cells that have added requirement for *BUB1B* to suppress lethal consequences of altered kinetochore (Ding, Hubert et al. 2013). In our study, we describe that PARPi induces BUBR1 down-regulation in absence of PTEN, as BUBR1 levels decreased in PTEN mutant cell line. This result was reinforced as BUBR1 reduction was delayed after PTEN restoration in PTEN mutant cells, and it was accelerated after PTEN knockdown in PTEN proficient cells. Hence, we describe that PTEN is involved in the mechanism by which PARP inhibition modulates BUBR1 levels, thereby compromising both SAC and microtubule-kinetochore attachments.

In the current study we have also found that homologous recombination repair deficiency in PTEN mutant glioma cells is further disabled after PARP inhibition due in part to RAD51 down-regulation. A previous study has shown that PARPi down-regulates RAD51 and BRCA1 leading to HR deficiency at times where an elevated loss of cell viability was observed (Hegan, Lu et al. 2010). In our study, PARP inhibition leads to a profound amplification of HR deficiency in PTEN mutant cells already at 24 hours (figure 3C and Table 1 results chapter 1), where no cytotoxic effect is still appreciated (figure 1A results chapter 1). Moreover, the expression pattern of key components of the DNA damage response (see Table 1 results chapter 1) is strongly affected after blunting PARP activity (PARP-1 or other PARP family members with poly ADP-ribosylation

activity), including perturbation of the HR machinery and other DNA repair pathways as well as factors involved in genomic instability, beyond affecting RAD51. PTEN restoration in U87MG slowed RAD51 decrease, whereas PTEN silencing in LN229 augmented RAD51 down-regulation after PARP inhibition. It has previously been shown that PTEN plays a role in HR repair as it contributes to remodeling the chromatin of *RAD51* promoter so that the access of E2F1 transcription factor is facilitated (Shen, Balajee et al. 2007). Here, we firstly show that the absence of PTEN and the inhibition of PARP exert an accumulative effect on the down-regulation of RAD51 levels and the disabling of HR function, which should be taken into account in a possible clinical setting using PARP inhibitors.

In consonance with above, G2 arrest after PARPi decreased in absence of PTEN. A possible explanation for this effect could be the role of PTEN in CHK1 nuclear location (Puc, Keniry et al. 2005, Puc and Parsons 2005): in absence of PTEN, as it is the case for U87MG cells, CHK1 is retained in the cytoplasm and marked for proteasomal degradation, avoiding a proper signaling of cell cycle checkpoints.. Since DNA damage response involves an orchestrated actuation of DNA repair pathways and cell cycle checkpoints, we may hypothesize that in U87MG PTEN-deficient cells, following PARPi, DNA repair through HR pathway is compromised (as confirmed by HR assay and RAD51 and YH2AX expression) and moreover, G2 arrest is also affected due to low levels of CHK1. Interestingly, the arrest is partially restored following PTEN reintroduction, as a consequence of the restoration of DNA repair machinery and cell cycle checkpoints in presence of PTEN.

The benefit of combining PARP inhibitors with currently used chemotherapy has been largely reported including the potentiating effect of PJ34 (Tang, Svilar et al. 2011, Tentori, Ricci-Vitiani et al. 2014). Here we also show compelling evidences that cell death pathway by which PARP inhibition impacts on cell viability of PTEN-deficient cells is Mitotic Catastrophe (MC). MC is a mechanism activated following genomic instability. It senses mitotic failure and responds to it by driving the cell to an irreversible fate, be it apoptosis, necrosis or senescence (Vitale, Galluzzi et al. 2011, Galluzzi, Vitale et al. 2012). The stimuli and perturbations that are described to trigger MC can be divided in two groups. The first group of inducers interfere with the faithful segregation of chromosomes in mitosis. The second group directly affects the integrity of the genetic material, for example DNA-damaging agents or compromised DNA-repair pathways. Thus, in our case, aberrant mitotic spindle organization and DNA segregation due to BUBR1 down-regulation constitute a “first-group inducer” of MC while impaired HR repair due to compromised RAD51 is “second trigger” of MC (figure 1 discussion). However, in spite of the increasingly detailed description of the mechanisms that precede and follow MC, the molecular bridges between mitotic aberrations and cell death are still largely elusive.

In an attempt to increase the *in vivo* cell killing effect of PARP inhibition on glioma cells we ideated (given the up-regulation of pro-survival signalling pathways in PTEN-deficient glioma cells) the co-treatment with an inhibitor of EGFR to disable pro-survival signals. Although no *in vitro* potentiation by erlotinib of PARP-induced cytotoxic effect was observed, this combination was very effective in the suppression of ERK1/2 activation and, more interestingly, *in vivo* co-treatment was synergic in slowing-down tumour growth. This enhanced *in vivo* potentiation

using co-treatment of anti-neoplastic agents with PARP inhibitors has been already described for different preclinical models and has been related to the increased vascular function after inhibition of PARP resulting in amelioration of drug availability in the tumour milieu (Ali, Telfer et al. 2009). Moreover, besides this general property of PARP inhibitors, the use of these compounds takes advantage of the elevated propensity to display genomic instability (which is related with aggressiveness trait) of PTEN deficient glioma cells. The ultimate mechanism underlying the synergistic effect of PARP1 and EGFR remains to be elucidated, but one possibility is that in specific settings inhibition of PARP with PJ34 activates pro-survival pathways as has been shown for p38/MAPK during osteoclast differentiation (Robaszekiewicz, Valko et al. 2014). In addition to shutting-down EGFR signalling, other combinatorial treatments could be envisaged based on the rational knowledge of glioma cells molecular alterations. Another broad field to explore is the use of PARP inhibitors to act as radio-potentiators against GBM and overcome tumour resistance to standard radiation therapy. In summary PARP inhibitors represent an exciting new class of antineoplastic drugs and there may well have much wider clinical indications not just restricted to BRCA1/2 mutant tumours but to others where PARP inhibitor treatment enhances HR deficiency and mitotic alterations, driving the cell towards a status of genomic instability.

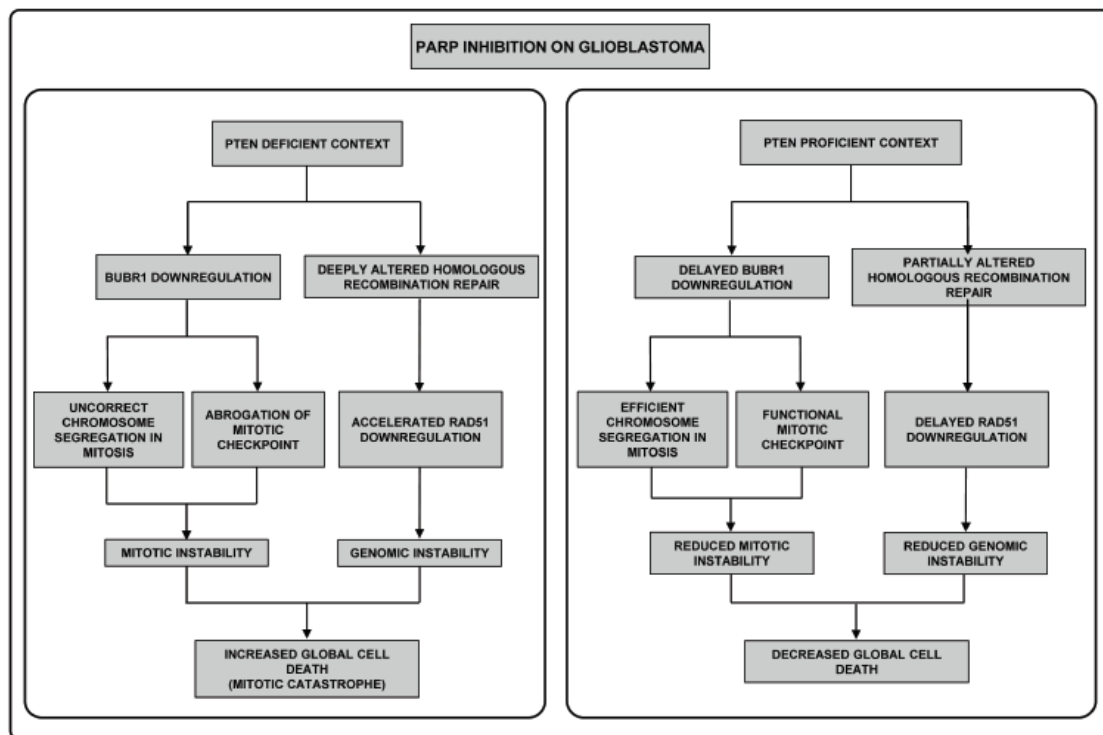


Figure 1: Different effect of PARPi in GBM according to PTEN status. In the absence of PTEN (**left panel**) PARPi perturbs the correct segregation of chromosomes, due to BUBR1 down-regulation; besides, PARPi compromises integrity of the genomic material, as consequence of the alteration of HR repair. Both situations have been well-described to induce MC. In contrast, in a PTEN-proficient context (**right panel**) BUBR1 down-regulation is retarded allowing correct chromosome segregation in mitosis and, besides, HR repair is less affected. Thus, mitotic and genomic instability are reduced and MC-independent cell death pathways are activated.

3 PARP REGULATES mTOR ACTIVATION AND LIPID DROPLETS TURNOVER IN GLIOBLASTOMA

As constitutively active mTOR pathway is another well-known process in GBM, in this chapter we aimed to elucidate the effect of PARP inhibition on survival pathways and lipogenesis activation.

The mechanisms underlying mTOR upregulation in GBM are multiple. PI3KCI is overactivated, due to Tyrosine Kinase Receptors overactivation. Different mutations are responsible for this situation. Hence, EGFR amplification or mutation (EGFRVIII) are drivers of mTOR activation. Besides, PDGFR may be also overactivated, thereby promoting PI3KCI activation. Another key factor in PI3KCI gain of function is the absence of PTEN, which is one of the most common alterations in GBM (Cancer Genome Atlas Research 2008).

This scenario promotes the constitutive activation of different survival cascades, mainly MAPK and mTOR pathway. As a result, a wide range of mTOR downstream effectors become activated. Thus, there is an exacerbated protein and lipid synthesis, accompanied by the adaptation to hypoxic environment, as well as autophagy inhibition. This cellular response will promote cell survival and proliferation, hence facilitating tumor growth. As a result, strategies focused in the abrogation of mTOR activation become crucial in order to avoid tumor survival.

The aim of our study is to elucidate the implications of PARPi on GBM cell biology. Thus, an unavoidable step in our investigation is to check the status of survival pathways such as mTOR and MAPK. Consequently, we analyzed the effect of PARPi on the expression of different proteins in mTOR axis. Interestingly, we observed a striking decrease on survival pathways, which was consistently accompanied by autophagy activation. Unexpectedly, several lines of evidence point to mTOR-independent autophagy activation in the short time, ie, the initial effects of PARPi involved induction of autophagy without affecting the pAKT/mTOR pathway (figure 2 results chapter 2).

As a result of constitutively active survival pathways, cancer cells proliferate rapidly and they exhibit increased demands for energy and macronutrients. Hence, different strategies have been developed in order to promote tumor adaptation to this context. For long it has been known that cancer cells show avid glucose uptake and use the glycolytic pathway regardless oxygen is present, through a process called Warburg effect (Warburg 1956). A second adaptation to high tumor cell demands is a high rate of protein (Clemens 2004) and DNA synthesis (Rahman, Voeller et al. 2004). Besides, it is now broadly accepted that tumors frequently exhibit an increased ability to synthesize lipids (Kuhajda, Pizer et al. 2000, Baron, Migita et al. 2004, Menendez and Lupu 2007). Increased expression of lipogenic enzymes has been reported as a common trait in tumor development, and in GBM in particular (Guo, Bell et al. 2013), driving to the so-called "lipidic phenotype". Consistently, upregulation of FASN represents a common alteration in most human malignancies, and although disturbances in signaling pathways responsible for oncogenic transformation can contribute to increased lipogenesis in tumors, FASN overactivation represents not only a secondary phenomenon but rather a selected mechanism that confers survival advantage (Menendez and Lupu 2007).

Discussion

Interestingly, one of the downstream effectors of mTOR is SREBP1c, which is a well-known partner for FASN regulation. According to this, PARPi-induced mTOR downregulation would involve *de novo* fatty acid (FA) synthesis inhibition, suggesting a link between mTOR axis inhibition and lipid synthesis modulation.

To further analyze the effect of PARPi in other proteins involved in *de novo* lipogenesis we assessed the status of AMPK and ACC, which are upstream modulators of FASN, in our cells. However, no remarkable differences were observed after PARPi treatment (data not shown).

Nevertheless, although lipogenesis has been considered as the major means of FA acquisition in cancer cells, recent reports show that lipolysis may also be used as a source for FA (Kuemmerle, Rysman et al. 2011). Next, we aimed to study if lipolytic pathway was acting as a pro-tumoral source of FA in our model, by evaluating cPLA2 levels. Recent reports propose targeting cPLA2 (which is responsible for FA increase through phospholipids degradation) as an emerging antitumor strategy (Patel, Singh et al. 2008). Remarkably, PARPi promoted an increase in cPLA2 levels in the short time, followed by a decrease 48 hours after the treatment.

Putting together these results, strong mTOR axis abrogation suggests the inhibition of FASN partner SREBP1, which still remains to be examined in our project. On the other hand, lipolytic pathway analysis indicates an early augmentation of cPLA2 levels, followed by its downregulation after 48 hours of PARPi treatment. Hence, although lipolytic pathway becomes active two hours after PARPi, both lipogenic and lipolytic axis are inhibited 48 hours after PARPi, suggesting a decrease on FA synthesis induced by long-time treatment.

Another hallmark of “lipidic phenotype” consists on the formation of Lipid Droplets (LDs), which synthesis correlates with tumor promotion (Bozza and Viola 2010). These organelles mainly consist of TAG and cholesterol. LDs biogenesis needs to be contemplated in the context of the synthesis and degradation of their major components. Hence, LDs formation is influenced by FA synthesis in the cell and active cPLA2 is well-proven to promote LDs synthesis (Guijas, Rodriguez et al. 2014). As expected, early cPLA2 upregulation in our model correlated with rapid LDs increase, indicating that FA synthesis in GBM cell lines involved their accumulation in lipid vesicles.

For a global study of LDs metabolism it is important to check not only the mechanisms leading to LDs synthesis but also the routes involved in their degradation. LDs breakdown is a crucial process that releases FA, which may be used as energy source through β -oxidation. Traditionally, mobilization of LDs has been attributed to LD-associated lipases. However, recent studies have pointed out a role for autophagy in LDs breakage (Singh, Kaushik et al. 2009). As we had observed autophagy activation and LDs formation following PARPi, we wondered if lipophagy might be connecting both processes in our model. Interestingly we corroborated lipophagy activation, since autophagy knockdown promoted LDs increase. Importantly, we also confirmed that lipophagy is a major process occurring in GBM cell lines also in the basal state, as autophagy abrogation enhanced LDs formation even in absence of PARPi. Remarkably, the increase in LDs formation after blunting autophagy correlated with the basal levels of autophagy on each cell line. Besides, as mTOR-independent autophagy

activation was reported early after PARPi, we propose that it may be activated in order to target the early-formed lipid droplets. However, the exact mechanism driving to mTOR-independent autophagy needs to be studied.

Unexpectedly, autophagy blockade by ATG1 gene silencing induced not only LDs increase but also accelerated cPLA2 downregulation after PARPi. Although this process is not fully understood, a feedback loop promoted by excessive LD increase is suggested.

Finally, this study highlights many aspects by which PARP modulates survival pathways and lipid metabolism. However, there are still many open questions that remain to be elucidated.

First of all, the mechanism by which PARPi promotes mTOR and cPLA2 downregulation following 48 hours treatment is poorly understood. We initially hypothesized that a decrease in growth factor autocrine release after PARPi could be responsible for PARPi-induced downregulation of prosurvival pathways; however, experiments using conditioned medium demonstrated, on the contrary, that PARPi treatment actually delayed autophagy induction probably through the increase of anti-autophagic secreted factors. At this stage these factors have not been identified but it may limit the antitumor activity of PARPi. Why PARPi induced autophagy while CM delayed it? Although the ultimate reason for this is not known yet, PARPi intracellular actions are obviously avoided by just using CM. In anycase, we discard that PARPi effect on mTOR axis is modulated at the autocrine or paracrine level.

ERK2 (one of the main members of MAPK cascade) phosphorylates PARP-1 thereby activating it independently of DNA damage. In addition ERK2 activity is also enhanced in presence of PARP-1 (Cohen-Armon, Visochek et al. 2007). As mTOR pathway is modulated by MAPK cascade, this may explain, at least in part, mTOR inhibition in the absence or after inhibition of PARP. In addition, for long it has been known that cPLA2 levels are regulated by MAPK pathway (Waterman, Molski et al. 1996). Thus, cPLA2 downregulation after 48 hours of PARPi treatment might be mediated by ERK2 inhibition in absence of PARP. However, the mechanism that leads to cPLA2 activation two hours after the treatment remains elusive.

Secondly, the mechanisms underlying PARPi-induced lipophagy still remain to be elucidated. On the one hand, in absence of PARP, DNA damage is increased. As a result, DNA repair mechanisms are activated thereby promoting ATP consumption. Lipophagy may be a pathway activated to utilize FA as a source of energy through β -oxidation, so that ATP depletion may be neutralized. On the other hand, PARPi induces LDs accumulation even after short time of treatment. To prevent LDs-induced toxicity, cells may promote lipophagy in order to counteract lipotoxicity (Khalidoun, Emond-Boisjoly et al. 2014). This explanation is reinforced by two observations. First, lipophagy occurs even in the absence of PARP inhibition, so a hypothesis based strictly on the presence of DNA damage would not make sense in this case. Second, ATP depletion by DNA damage would need several rounds of replication to induce lipophagy, further supporting lipotoxicity-induced lipophagy.

One way or another, PARPi is well proven to induce mTOR axis downregulation, LDs synthesis and LDs degradation by lipophagy. The increase of both LDs formation and degradation may

seem an apparent contradictory effect of PARPi. However, we propose that LDs formation is a dynamic mechanism and, in our case, the balance towards one process or another changes over time. We have not been able to observe LDs decrease 48 hours after PARPi although autophagy has been active almost from the beginning of the treatment. We propose that it is a time-dependent process and longer analysis of LDs turnover would possibly reveal a decrease on LDs amount (figure 2 discussion).

Nevertheless, the consequences of this process on cell viability have not been examined yet. Although this investigation points out to a prosurvival role of autophagy on this process, suggesting that combining PARPi and autophagy inhibitors may be clinically relevant, deeper investigation is needed before confirming this hypothesis.

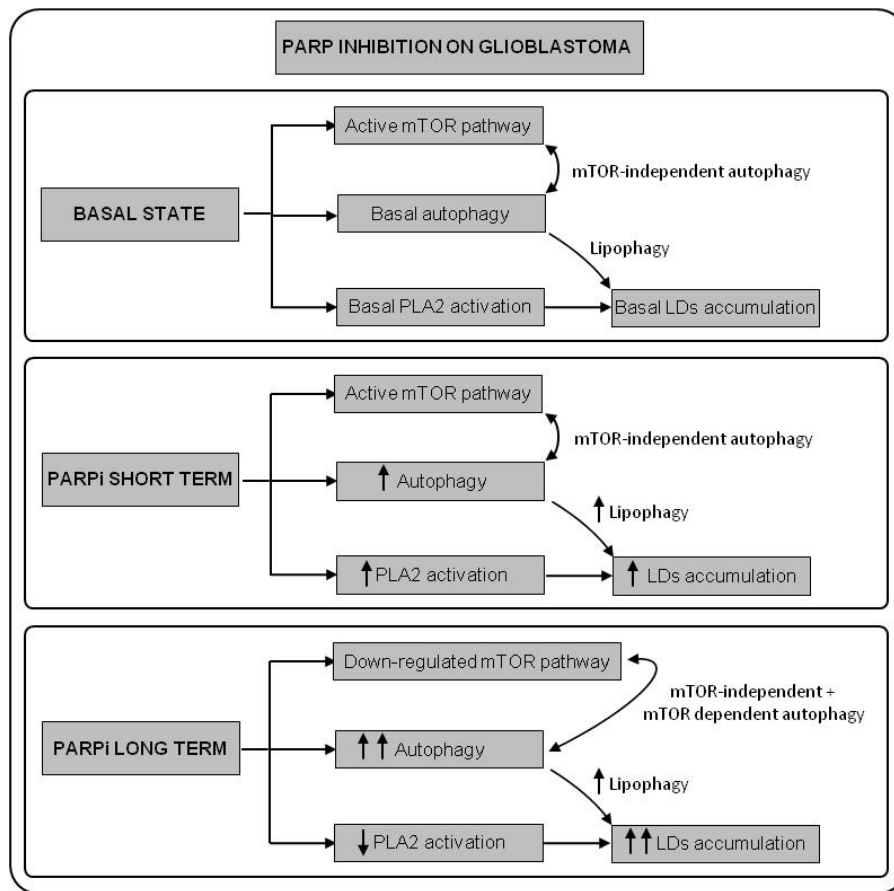


Figure 2: mTOR pathway down-regulation and lipophagy following PARPi. Glioblastoma cells present constitutively active AKT-mTOR axis concomitant with autophagy, implying that at least in part this process is mediated by mTOR-independent pathways. Moreover, there exists basal LDs formation (**upper pannel**). Only two hours following PARPi, we observe on the one hand, that autophagy is increased in spite AKT axis is not abrogated, further supporting mTOR-independent regulation. And on the other hand, PLA2 activation levels are enhanced, correlating with increased LDs formation (**central pannel**). One or two days after PARPi, mTOR is downregulated and autophagy is potently increased, indicating that possibly mTOR –dependent and independent autophagy is occurring at the same time. In all cases, we suggest that autophagy regulates LDs as genetically abrogating ATG1 increased LDs formation, implying that lipophagy is the subtype of the global autophagy observed. The increased levels in LDs formation 48 hours after PARPi, despite lipophagy activation and PLA2 down-regulation, possibly indicates that at this time lipophagy process has not been enough to target the previously formed LDs pool (**lower pannel**).

4 PARP TARGETING COUNTERACTS GLIOMA STEM-LIKE CELLS PHENOTYPE THROUGH THE PROMOTION OF VIABILITY DECREASE, mTOR AXIS DOWN-REGULATION AND CELL DIFFERENTIATION.

Another characteristic of GBM is the presence of Glioma Initiating Cells, also named Glioma Stem-like Cells (GSCs). This population has both self-renewal and differentiation ability, as well as cancer initiation capability upon orthotopic implantation. Although the population of GSCs does not represent more than 1% of the whole tumor mass, it is highly resistant to traditional chemo and radiotherapy, becoming responsible of tumor initiation and recurrence after the treatment (Vescovi, Galli et al. 2006).

According to this data, we aimed to understand PARP effect on GSCs, as targeting this population is crucial for a clinical approach. For this issue, we addressed the main aspects of our investigation in GBM cell lines to GSCs and we examined PARPi effect on GSCs differentiation. Interestingly, we found that PARP is involved in GSCs proliferation and stemness maintenance.

Due to the well-proven presence of membrane transporters that allow the efflux of cytotoxic drugs (Dean, Fojo et al. 2005), we decided to check the effect of the treatment in the long time, one week, instead of 48 or 72 hours as we had tested in the cell lines assays. This decision was made as we observed that 72 hours treatment exerted a mild effect, which was consistent with GSCs aggressiveness and membrane transporters presence. Besides, we also decided to examine the effect of repetitively adding the treatment to these cells; as efflux ability was likely to compromise the effect of a single treatment. Thus, we tested the effect of PARPi during one week, when the treatment was added one day, or re-added during the first three days of the experiment.

Jeopardizing cell viability in GSCs is the first step in order to eliminate this compartment. As expected, we observed a relevant viability decrease, measured by loss of proliferation by MTT assay, following PARPi treatment (figure 1 results chapter 3). This result is reinforced as different inhibitors and different doses were tested, thereby minimizing a possible off-target effect. Interestingly, the effect was accelerated when PARP inhibitor was re-added during the first three days of the experiment indicating that, due to the specific characteristics of GSCs biology, a continued treatment is necessary in order to clinically target GSCs.

A deep analysis of mTOR pathway expression was able to reveal that PARPi effect on cell viability was, at least in part, mediated by the downregulation of survival pathways. As previously observed in GBM cell lines, we confirmed a significative downregulation of the whole mTOR axis and as well as an important activation of autophagy after PARPi, which was further accelerated when the treatment was re-added. Interestingly, mTOR cascade in GSCs is involved not only in survival mechanisms, but also in the maintenance of the stem phenotype (Bleau, Hambardzumyan et al. 2009, Galan-Moya, Le Guelte et al. 2011). Thus, this result may be connected not only with the survival decrease but also with a possible loss of stemness.

As GSCs differentiation towards normal glioma cells is a key action to promote their susceptibility to traditional antitumoral treatment, checking stem cell phenotype alterations following PARPi is a key step to confirm the effectiveness of this treatment. Both functional and molecular approaches confirmed that inhibiting PARP promotes the loss of stem phenotype, as neurosphere formation was abolished after PARP inhibition and a clear loss of the stemness marker SOX2 was confirmed at the protein level (figure 4 results chapter 3).

In spite neurosphere formation, which analyzes self-renewal capability, is a clear marker of stemness, the results we obtained showed a reduction on the number of neurospheres not only by the loss of the capability to form this structures, but also by a decrease in the global number of cells in the well, which would be related not only with the loss of stemness but with the loss of cell viability. Thus, examining this result alone is not enough to ensure loss of stemness following PARPi. However, the combination of neurosphere formation decrease with a clear reduction on SOX2 levels and mTOR axis down-regulation provides enough data to confirm that stemness phenotype is compromised following PARPi.

PARP is well-proven to interact with and PARylate SOX2 (Gao, Kwon et al. 2009, Lai, Chang et al. 2012). Nevertheless, Lai's group proposes that PARP-1 autoPARylation negatively regulates SOX2 expression in Embrionic Stem Cells. As these results are not consistent with PARPi-driven loss of SOX2 expression in GSCs, further investigation is needed to determine this effect.

Moreover, it is important to remark that although loss of stemness is clearly related with the acquisition of differentiation markers, a specific study of differentiation markers such as β III Tubulin or GFAP would be required to further confirm this result.

To summarize, in spite additional research is necessary to understand the mechanisms that lead to the loss of GSCs phenotype, our results suggest that PARP inhibition may also target the most aggressive compartment in this lethal brain tumor (figure 3 discussion).

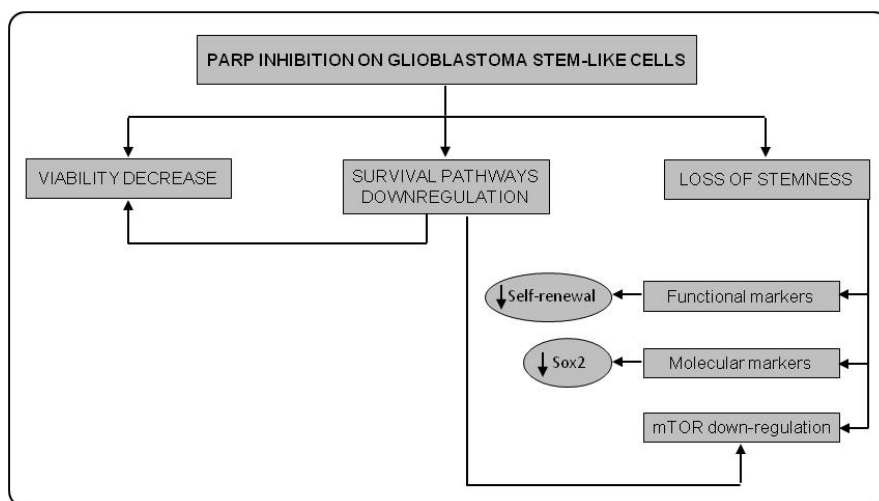


Figure 3: PARP targeting counteracts GSCs phenotype. The effect exerted by PARPi in GSCs phenotype is mediated by cell viability decrease, survival pathways downregulation and loss of stemness confirmed by both functional and molecular markers. The downregulation of survival pathways mTOR may also be connected with the loss of stemness as well as the viability decrease.

5 REMARKABLE POINTS

For long, basic and clinical investigation support PARP inhibition effect in tumor treatment. As explained in the introduction of this study, its antitumoral effect has been well-proven in monotherapy and in combination with chemo and radiotherapy.

This research highlights new mechanisms by which PARP inhibition targets glioblastoma, impacting on different aspects of tumor biology. Thus, many of the mechanisms that confer tumor aggressiveness are weakened in absence of PARP activity. As explained above, PARP inhibition takes advantage of PTEN-deficient tumors bearing genomic and mitotic instability, increasing these mechanisms and promoting loss of viability even in a model highly resistant to cell death. In addition, an important part of the aggressiveness of this brain tumor is exerted by survival pathways overactivation, which is also counteracted following PARP inhibition. Moreover, the poor prognosis of GBM patients is mainly mediated by GSCs survival following surgical resection and chemo and radiotherapy. Importantly, PARP inhibition also targeted this population, emerging as an important tool to diminish tumor recurrence.

Altogether, these results show that, although PARP inhibition is not enough to abolish GBM, it may emerge as a promising strategy that, used in combined therapy, may contribute to improve the life expectancy of GBM patients. Thus, using PARPi following surgical resection and chemo and radiotherapy, may help to minimize the risk of tumor recurrence. Furthermore, it would be interesting to clinically test the combined effect of PARPi and molecular therapies towards tumor-specific genetic alterations, addressing mTOR, RTK (as it is the case of erlotinib), apoptosis or angiogenic pathway. The current clinical presence of PARP inhibitors facilitates this process, as in these cases clinical trials do not need to test drug toxicity.

Nevertheless, we should not forget that the main step to overcome a disease, in this case GBM, is the fully comprehension of the mechanisms that lead to its emergence, maintenance and recurrence. In our case, we have advanced in the understanding of the mechanisms by which PARPs are involved in GBM biology. However, more specific investigation needs to be executed to deeply analyze PARP role in GBM. In this line, inhibitors for each one of PARP family members need to be developed. Besides, although many advances have been performed in the recent years, specific, off-target free, PARP inhibitors are required to improve the quality of PARP-related investigation.

One way or another, PARP is pointed as a mediator in GBM aggressiveness. In view of our results, we hope to have contributed, at least in part, to the understanding of the basic role of PARP in the biology of this lethal disease, and to the opening of a potential therapeutic opportunity that may help to overcome this tumor.

CONCLUSIONES

- La inhibición de PARP afecta de manera diferente a las líneas celulares de glioblastoma multiforme, en función del estatus de PTEN.
 - La parada en G2 inducida por la inhibición de PARP aumenta en presencia de PTEN.
 - La disminución de la expresión de RAD51 inducida por la inhibición de PARP aumenta en ausencia de PTEN, comprometiendo los mecanismos de reparación por recombinación homóloga.
 - La disminución de la expresión de BUBR1 inducida por la inhibición de PARP aumenta en ausencia de PTEN, afectando a las uniones cinetocoro-microtúbulo así como al punto de control de ciclo celular en mitosis.
 - La pérdida de viabilidad inducida por la inhibición de PARP en las líneas celulares mutadas para PTEN está mediada por un aumento en la inestabilidad genómica y mitótica como consecuencia de la ausencia de RAD51 y BUBR1. El mecanismo que proponemos mediante el cual ocurre esta pérdida de viabilidad es la catástrofe mitótica.

- La combinación de la inhibición de PARP con la inhibición de EGFR (erlotinib) provoca una disminución de la ruta de supervivencia de las MAPK in vitro, y disminuye el desarrollo tumoral en un modelo murino ortotópico de GBM.

- La inhibición de PARP produce la inhibición de rutas de supervivencia.
 - Existe una inhibición en la ruta de mTOR y una activación de procesos de autofagia como consecuencia de la inhibición de PARP.
 - La inhibición de PARP induce la síntesis de ácidos grasos, a través de la ruta de degradación de fosfolípidos. Como consecuencia, estos ácidos grasos libres se van a acumular en vesículas lipídicas.
 - La autofagia es un mecanismo activado con el objeto de degradar las vesículas lipídicas existentes en la célula tanto en situaciones basales como después del tratamiento con inhibidor de PARP.

- La inhibición de PARP afecta a las células iniciadoras del glioblastoma.
 - Se produce una pérdida de viabilidad como consecuencia de la inhibición de PARP.
 - La activación de la ruta de mTOR también disminuye tras inhibir PARP.
 - Los marcadores de pluripotencia, tanto funcionales como moleculares, disminuyen su expresión en ausencia de actividad de PARP.

BIBLIOGRAPHY

- (2008). "Comprehensive genomic characterization defines human glioblastoma genes and core pathways." Nature **455**(7216): 1061-1068.
- Adelfalk, C., M. Kontou, M. Hirsch-Kauffmann and M. Schweiger (2003). "Physical and functional interaction of the Werner syndrome protein with poly-ADP ribosyl transferase." FEBS Lett **554**(1-2): 55-58.
- Aguilar-Quesada, R., J. A. Munoz-Gamez, D. Martin-Oliva, A. Peralta-Leal, R. Quiles-Perez, J. M. Rodriguez-Vargas, M. Ruiz de Almodovar, C. Conde, A. Ruiz-Extremera and F. J. Oliver (2007). "Modulation of transcription by PARP-1: consequences in carcinogenesis and inflammation." Curr Med Chem **14**(11): 1179-1187.
- Aguilar-Quesada, R., J. A. Munoz-Gamez, D. Martin-Oliva, A. Peralta, M. T. Valenzuela, R. Matinez-Romero, R. Quiles-Perez, J. Menissier-de Murcia, G. de Murcia, M. Ruiz de Almodovar and F. J. Oliver (2007). "Interaction between ATM and PARP-1 in response to DNA damage and sensitization of ATM deficient cells through PARP inhibition." BMC Mol Biol **8**: 29.
- Ahel, I., D. Ahel, T. Matsusaka, A. J. Clark, J. Pines, S. J. Boulton and S. C. West (2008). "Poly(ADP-ribose)-binding zinc finger motifs in DNA repair/checkpoint proteins." Nature **451**(7174): 81-85.
- Ahmed, N., V. S. Salsman, Y. Kew, D. Shaffer, S. Powell, Y. J. Zhang, R. G. Grossman, H. E. Heslop and S. Gottschalk (2010). "HER2-specific T cells target primary glioblastoma stem cells and induce regression of autologous experimental tumors." Clin Cancer Res **16**(2): 474-485.
- Ali, M., B. A. Telfer, C. McCrudden, M. O'Rourke, H. D. Thomas, M. Kamjoo, S. Kyle, T. Robson, C. Shaw, D. G. Hirst, N. J. Curtin and K. J. Williams (2009). "Vasoactivity of AG014699, a clinically active small molecule inhibitor of poly(ADP-ribose) polymerase: a contributory factor to chemopotential in vivo?" Clin Cancer Res **15**(19): 6106-6112.
- Altman, J. (1966). "Proliferation and migration of undifferentiated precursor cells in the rat during postnatal gliogenesis." Exp Neurol **16**(3): 263-278.
- Altman, J. and G. D. Das (1965). "Autoradiographic and histological evidence of postnatal hippocampal neurogenesis in rats." J Comp Neurol **124**(3): 319-335.
- Ambrose, H. E., V. Papadopoulou, R. W. Beswick and S. D. Wagner (2007). "Poly-(ADP-ribose) polymerase-1 (Parp-1) binds in a sequence-specific manner at the Bcl-6 locus and contributes to the regulation of Bcl-6 transcription." Oncogene **26**(42): 6244-6252.
- Amiri, K. I., H. C. Ha, M. E. Smulson and A. Richmond (2006). "Differential regulation of CXC ligand 1 transcription in melanoma cell lines by poly(ADP-ribose) polymerase-1." Oncogene **25**(59): 7714-7722.
- Andersen, J. L., C. E. Johnson, C. D. Freil, A. B. Parrish, J. L. Day, M. R. Buchakjian, L. K. Nutt, J. W. Thompson, M. A. Moseley and S. Kornbluth (2009). "Restraint of apoptosis during mitosis through interdomain phosphorylation of caspase-2." EMBO J **28**(20): 3216-3227.

Bibliography

- Andrabi, S. A., N. S. Kim, S. W. Yu, H. Wang, D. W. Koh, M. Sasaki, J. A. Klaus, T. Otsuka, Z. Zhang, R. C. Koehler, P. D. Hurn, G. G. Poirier, V. L. Dawson and T. M. Dawson (2006). "Poly(ADP-ribose) (PAR) polymer is a death signal." Proc Natl Acad Sci U S A **103**(48): 18308-18313.
- Anido, J., A. Saez-Borderias, A. Gonzalez-Junca, L. Rodon, G. Folch, M. A. Carmona, R. M. Prieto-Sanchez, I. Barba, E. Martinez-Saez, L. Prudkin, I. Cuartas, C. Raventos, F. Martinez-Ricarte, M. A. Poca, D. Garcia-Dorado, M. M. Lahn, J. M. Yingling, J. Rodon, J. Sahuquillo, J. Baselga and J. Seoane (2010). "TGF-beta Receptor Inhibitors Target the CD44(high)/Id1(high) Glioma-Initiating Cell Population in Human Glioblastoma." Cancer Cell **18**(6): 655-668.
- Aravind, L. (2001). "The WWE domain: a common interaction module in protein ubiquitination and ADP ribosylation." Trends Biochem Sci **26**(5): 273-275.
- Arch, E. M., B. K. Goodman, R. A. Van Wesep, D. Liaw, K. Clarke, R. Parsons, V. A. McKusick and M. T. Geraghty (1997). "Deletion of PTEN in a patient with Bannayan-Riley-Ruvalcaba syndrome suggests allelism with Cowden disease." Am J Med Genet **71**(4): 489-493.
- Aredia, F. and A. I. Scovassi (2014). "Poly(ADP-ribose): a signaling molecule in different paradigms of cell death." Biochem Pharmacol **92**(1): 157-163.
- Ashkenazi, A. and V. M. Dixit (1998). "Death receptors: signaling and modulation." Science **281**(5381): 1305-1308.
- Audebert, M., B. Salles and P. Calsou (2004). "Involvement of poly(ADP-ribose) polymerase-1 and XRCC1/DNA ligase III in an alternative route for DNA double-strand breaks rejoining." J Biol Chem **279**(53): 55117-55126.
- Augustin, A., C. Spenlehauer, H. Dumond, J. Menissier-De Murcia, M. Piel, A. C. Schmit, F. Apiou, J. L. Vonesch, M. Kock, M. Bornens and G. De Murcia (2003). "PARP-3 localizes preferentially to the daughter centriole and interferes with the G1/S cell cycle progression." J Cell Sci **116**(Pt 8): 1551-1562.
- Bai, P., S. M. Houten, A. Huber, V. Schreiber, M. Watanabe, B. Kiss, G. de Murcia, J. Auwerx and J. Menissier-de Murcia (2007). "Poly(ADP-ribose) polymerase-2 [corrected] controls adipocyte differentiation and adipose tissue function through the regulation of the activity of the retinoid X receptor/peroxisome proliferator-activated receptor-gamma [corrected] heterodimer." J Biol Chem **282**(52): 37738-37746.
- Baker, D. J., M. M. Dawlaty, T. Wijshake, K. B. Jeganathan, L. Malureanu, J. H. van Ree, R. Crespo-Diaz, S. Reyes, L. Seaburg, V. Shapiro, A. Behfar, A. Terzic, B. van de Sluis and J. M. van Deursen (2013). "Increased expression of BubR1 protects against aneuploidy and cancer and extends healthy lifespan." Nat Cell Biol **15**(1): 96-102.
- Baker, D. J., K. B. Jeganathan, J. D. Cameron, M. Thompson, S. Juneja, A. Kopecka, R. Kumar, R. B. Jenkins, P. C. de Groen, P. Roche and J. M. van Deursen (2004). "BubR1 insufficiency causes early onset of aging-associated phenotypes and infertility in mice." Nat Genet **36**(7): 744-749.
- Baker, S. J. (2007). "PTEN enters the nuclear age." Cell **128**(1): 25-28.

- Banasik, M., H. Komura, M. Shimoyama and K. Ueda (1992). "Specific inhibitors of poly(ADP-ribose) synthetase and mono(ADP-ribosyl)transferase." J Biol Chem **267**(3): 1569-1575.
- Bar, E. E., A. Chaudhry, A. Lin, X. Fan, K. Schreck, W. Matsui, S. Piccirillo, A. L. Vescovi, F. DiMeco, A. Olivi and C. G. Eberhart (2007). "Cyclopamine-mediated hedgehog pathway inhibition depletes stem-like cancer cells in glioblastoma." Stem Cells **25**(10): 2524-2533.
- Baron, A., T. Migita, D. Tang and M. Loda (2004). "Fatty acid synthase: a metabolic oncogene in prostate cancer?" J Cell Biochem **91**(1): 47-53.
- Barr, A. R. and F. Gergely (2007). "Aurora-A: the maker and breaker of spindle poles." J Cell Sci **120**(Pt 17): 2987-2996.
- Barrett, R. M., T. P. Osborne and S. P. Wheatley (2009). "Phosphorylation of survivin at threonine 34 inhibits its mitotic function and enhances its cytoprotective activity." Cell Cycle **8**(2): 278-283.
- Bassi, C., J. Ho, T. Srikumar, R. J. Dowling, C. Gorrini, S. J. Miller, T. W. Mak, B. G. Neel, B. Raught and V. Stambolic (2013). "Nuclear PTEN controls DNA repair and sensitivity to genotoxic stress." Science **341**(6144): 395-399.
- Baud, V. and M. Karin (2001). "Signal transduction by tumor necrosis factor and its relatives." Trends Cell Biol **11**(9): 372-377.
- Bauer, P. I., G. Farkas, L. Buday, G. Mikala, G. Meszaros, E. Kun and A. Farago (1992). "Inhibition of DNA binding by the phosphorylation of poly ADP-ribose polymerase protein catalysed by protein kinase C." Biochem Biophys Res Commun **187**(2): 730-736.
- Bedikian, A. Y., N. E. Papadopoulos, K. B. Kim, W. J. Hwu, J. Homsy, M. R. Glass, S. Cain, P. Rudewicz, L. Vernillet and P. Hwu (2009). "A phase IB trial of intravenous INO-1001 plus oral temozolomide in subjects with unresectable stage-III or IV melanoma." Cancer Invest **27**(7): 756-763.
- Bello, M. J., J. M. de Campos, M. E. Kusak, J. Vaquero, J. L. Sarasa, A. Pestana and J. A. Rey (1994). "Molecular analysis of genomic abnormalities in human gliomas." Cancer Genet Cytogenet **73**(2): 122-129.
- Bello, M. J., J. M. de Campos, J. Vaquero, M. E. Kusak, J. L. Sarasa, A. Pestana and J. A. Rey (1994). "Molecular and cytogenetic analysis of chromosome 9 deletions in 75 malignant gliomas." Genes Chromosomes Cancer **9**(1): 33-41.
- Berger, N. A. (1985). "Poly(ADP-ribose) in the cellular response to DNA damage." Radiat Res **101**(1): 4-15.
- Berger, N. A., J. L. Sims, D. M. Catino and S. J. Berger (1983). "Poly(ADP-ribose) polymerase mediates the suicide response to massive DNA damage: studies in normal and DNA-repair defective cells." Princess Takamatsu Symp **13**: 219-226.
- Bernet, D., R. M. Pinto, M. J. Costas, J. Canales and J. C. Cameselle (1994). "Rat liver mitochondrial ADP-ribose pyrophosphatase in the matrix space with low Km for free ADP-ribose." Biochem J **299** (Pt 3): 679-682.

Bibliography

- Berti, M., A. Ray Chaudhuri, S. Thangavel, S. Gomathinayagam, S. Kenig, M. Vujanovic, F. Odreman, T. Glatter, S. Graziano, R. Mendoza-Maldonado, F. Marino, B. Lucic, V. Biasin, M. Gstaiger, R. Aebersold, J. M. Sidorova, R. J. Monnat, Jr., M. Lopes and A. Vindigni (2013). "Human RECQ1 promotes restart of replication forks reversed by DNA topoisomerase I inhibition." Nat Struct Mol Biol **20**(3): 347-354.
- Bieche, I., G. de Murcia and R. Lidereau (1996). "Poly(ADP-ribose) polymerase gene expression status and genomic instability in human breast cancer." Clin Cancer Res **2**(7): 1163-1167.
- Bleau, A. M., D. Hambarzumyan, T. Ozawa, E. I. Fomchenko, J. T. Huse, C. W. Brennan and E. C. Holland (2009). "PTEN/PI3K/Akt pathway regulates the side population phenotype and ABCG2 activity in glioma tumor stem-like cells." Cell Stem Cell **4**(3): 226-235.
- Boatright, K. M., M. Renatus, F. L. Scott, S. Sperandio, H. Shin, I. M. Pedersen, J. E. Ricci, W. A. Edris, D. P. Sutherlin, D. R. Green and G. S. Salvesen (2003). "A unified model for apical caspase activation." Mol Cell **11**(2): 529-541.
- Bobola, M. S., S. H. Tseng, A. Blank, M. S. Berger and J. R. Silber (1996). "Role of O6-methylguanine-DNA methyltransferase in resistance of human brain tumor cell lines to the clinically relevant methylating agents temozolomide and streptozotocin." Clin Cancer Res **2**(4): 735-741.
- Boehler, C. and F. Dantzer (2011). "PARP-3, a DNA-dependent PARP with emerging roles in double-strand break repair and mitotic progression." Cell Cycle **10**(7): 1023-1024.
- Boehler, C., L. R. Gauthier, O. Mortusewicz, D. S. Biard, J. M. Saliou, A. Bresson, S. Sanglier-Cianferani, S. Smith, V. Schreiber, F. Boussin and F. Dantzer (2011). "Poly(ADP-ribose) polymerase 3 (PARP3), a newcomer in cellular response to DNA damage and mitotic progression." Proc Natl Acad Sci U S A **108**(7): 2783-2788.
- Bolanos-Garcia, V. M. and T. L. Blundell (2011). "BUB1 and BUBR1: multifaceted kinases of the cell cycle." Trends Biochem Sci **36**(3): 141-150.
- Boldin, M. P., T. M. Goncharov, Y. V. Goltsev and D. Wallach (1996). "Involvement of MACH, a novel MORT1/FADD-interacting protease, in Fas/APO-1- and TNF receptor-induced cell death." Cell **85**(6): 803-815.
- Bork, P., K. Hofmann, P. Bucher, A. F. Neuwald, S. F. Altschul and E. V. Koonin (1997). "A superfamily of conserved domains in DNA damage-responsive cell cycle checkpoint proteins." FASEB J **11**(1): 68-76.
- Borovski, T., J. J. Verhoeff, R. ten Cate, K. Cameron, N. A. de Vries, O. van Tellingen, D. J. Richel, W. R. van Furth, J. P. Medema and M. R. Sprick (2009). "Tumor microvasculature supports proliferation and expansion of glioma-propagating cells." Int J Cancer **125**(5): 1222-1230.
- Boulikas, T. (1992). "Poly(ADP-ribose) synthesis and degradation in mammalian nuclei." Anal Biochem **203**(2): 252-258.
- Bozza, P. T. and J. P. Viola (2010). "Lipid droplets in inflammation and cancer." Prostaglandins Leukot Essent Fatty Acids **82**(4-6): 243-250.

- Brennan, M. A. and B. T. Cookson (2000). "Salmonella induces macrophage death by caspase-1-dependent necrosis." Mol Microbiol **38**(1): 31-40.
- Brochu, G., C. Duchaine, L. Thibeault, J. Lagueux, G. M. Shah and G. G. Poirier (1994). "Mode of action of poly(ADP-ribose) glycohydrolase." Biochim Biophys Acta **1219**(2): 342-350.
- Brown, E. J., M. W. Albers, T. B. Shin, K. Ichikawa, C. T. Keith, W. S. Lane and S. L. Schreiber (1994). "A mammalian protein targeted by G1-arresting rapamycin-receptor complex." Nature **369**(6483): 756-758.
- Brunet, A., A. Bonni, M. J. Zigmund, M. Z. Lin, P. Juo, L. S. Hu, M. J. Anderson, K. C. Arden, J. Blenis and M. E. Greenberg (1999). "Akt promotes cell survival by phosphorylating and inhibiting a Forkhead transcription factor." Cell **96**(6): 857-868.
- Bryant, H. E., E. Petermann, N. Schultz, A. S. Jemth, O. Loseva, N. Issaeva, F. Johansson, S. Fernandez, P. McGlynn and T. Helleday (2009). "PARP is activated at stalled forks to mediate Mre11-dependent replication restart and recombination." EMBO J **28**(17): 2601-2615.
- Bryant, H. E., N. Schultz, H. D. Thomas, K. M. Parker, D. Flower, E. Lopez, S. Kyle, M. Meuth, N. J. Curtin and T. Helleday (2005). "Specific killing of BRCA2-deficient tumours with inhibitors of poly(ADP-ribose) polymerase." Nature **434**(7035): 913-917.
- Burger, P. C. (1995). "Revising the World Health Organization (WHO) Blue Book--'Histological typing of tumours of the central nervous system'." J Neurooncol **24**(1): 3-7.
- Burkle, A. and L. Virag (2013). "Poly(ADP-ribose): PARadigms and PARadoxes." Mol Aspects Med **34**(6): 1046-1065.
- Burton, J. L. and M. J. Solomon (2007). "Mad3p, a pseudosubstrate inhibitor of APCCdc20 in the spindle assembly checkpoint." Genes Dev **21**(6): 655-667.
- Calabrese, C., H. Poppleton, M. Kocak, T. L. Hogg, C. Fuller, B. Hamner, E. Y. Oh, M. W. Gaber, D. Finklestein, M. Allen, A. Frank, I. T. Bayazitov, S. S. Zakharenko, A. Gajjar, A. Davidoff and R. J. Gilbertson (2007). "A perivascular niche for brain tumor stem cells." Cancer Cell **11**(1): 69-82.
- Cancer Genome Atlas Research, N. (2008). "Comprehensive genomic characterization defines human glioblastoma genes and core pathways." Nature **455**(7216): 1061-1068.
- Candi, E., R. Schmidt and G. Melino (2005). "The cornified envelope: a model of cell death in the skin." Nat Rev Mol Cell Biol **6**(4): 328-340.
- Carlo-Stella, C., C. Lavazza, A. Locatelli, L. Vigano, A. M. Gianni and L. Gianni (2007). "Targeting TRAIL agonistic receptors for cancer therapy." Clin Cancer Res **13**(8): 2313-2317.
- Carmena, M., M. Wheelock, H. Funabiki and W. C. Earnshaw (2012). "The chromosomal passenger complex (CPC): from easy rider to the godfather of mitosis." Nat Rev Mol Cell Biol **13**(12): 789-803.
- Carreira, A., J. Hilario, I. Amitani, R. J. Baskin, M. K. Shivji, A. R. Venkitaraman and S. C. Kowalczykowski (2009). "The BRC repeats of BRCA2 modulate the DNA-binding selectivity of RAD51." Cell **136**(6): 1032-1043.

Bibliography

- Castedo, M., A. Coquelle, S. Vivet, I. Vitale, A. Kauffmann, P. Dessen, M. O. Pequignot, N. Casares, A. Valent, S. Mouhamad, E. Schmitt, N. Modjtahedi, W. Vainchenker, L. Zitvogel, V. Lazar, C. Garrido and G. Kroemer (2006). "Apoptosis regulation in tetraploid cancer cells." EMBO J **25**(11): 2584-2595.
- Castiel, A., L. Visochek, L. Mittelman, F. Dantzer, S. Izraeli and M. Cohen-Armon (2011). "A phenanthrene derived PARP inhibitor is an extra-centrosomes de-clustering agent exclusively eradicating human cancer cells." BMC Cancer **11**: 412.
- Castiel, A., L. Visochek, L. Mittelman, Y. Zilberstein, F. Dantzer, S. Izraeli and M. Cohen-Armon (2013). "Cell death associated with abnormal mitosis observed by confocal imaging in live cancer cells." J Vis Exp(78): e50568.
- Clark, M. J., N. Homer, B. D. O'Connor, Z. Chen, A. Eskin, H. Lee, B. Merriman and S. F. Nelson (2010). "U87MG decoded: the genomic sequence of a cytogenetically aberrant human cancer cell line." PLoS Genet **6**(1): e1000832.
- Clemens, M. J. (2004). "Targets and mechanisms for the regulation of translation in malignant transformation." Oncogene **23**(18): 3180-3188.
- Cohen-Armon, M. (2007). "PARP-1 activation in the ERK signaling pathway." Trends Pharmacol Sci **28**(11): 556-560.
- Cohen-Armon, M., L. Visochek, D. Rozensal, A. Kalal, I. Geistrikh, R. Klein, S. Bendetz-Nezer, Z. Yao and R. Seger (2007). "DNA-independent PARP-1 activation by phosphorylated ERK2 increases Elk1 activity: a link to histone acetylation." Mol Cell **25**(2): 297-308.
- Cohen, G. M. (1997). "Caspases: the executioners of apoptosis." Biochem J **326 (Pt 1)**: 1-16.
- Conde, C., M. Mark, F. J. Oliver, A. Huber, G. de Murcia and J. Menissier-de Murcia (2001). "Loss of poly(ADP-ribose) polymerase-1 causes increased tumour latency in p53-deficient mice." Embo J **20**(13): 3535-3543.
- Corcelle, E. A., P. Puustinen and M. Jaattela (2009). "Apoptosis and autophagy: Targeting autophagy signalling in cancer cells -'trick or treats'?" FEBS J **276**(21): 6084-6096.
- Cregan, S. P., A. Fortin, J. G. MacLaurin, S. M. Callaghan, F. Cecconi, S. W. Yu, T. M. Dawson, V. L. Dawson, D. S. Park, G. Kroemer and R. S. Slack (2002). "Apoptosis-inducing factor is involved in the regulation of caspase-independent neuronal cell death." J Cell Biol **158**(3): 507-517.
- Crighton, D., S. Wilkinson, J. O'Prey, N. Syed, P. Smith, P. R. Harrison, M. Gasco, O. Garrone, T. Crook and K. M. Ryan (2006). "DRAM, a p53-induced modulator of autophagy, is critical for apoptosis." Cell **126**(1): 121-134.
- Cuervo, A. M. and J. F. Dice (2000). "Age-related decline in chaperone-mediated autophagy." J Biol Chem **275**(40): 31505-31513.
- Cuervo, A. M., A. V. Gomes, J. A. Barnes and J. F. Dice (2000). "Selective degradation of annexins by chaperone-mediated autophagy." J Biol Chem **275**(43): 33329-33335.

- Chambon, P., J. D. Weill and P. Mandel (1963). "Nicotinamide mononucleotide activation of new DNA-dependent polyadenylic acid synthesizing nuclear enzyme." Biochem Biophys Res Commun **11**: 39-43.
- Chan, F. K. (2007). "Three is better than one: pre-ligand receptor assembly in the regulation of TNF receptor signaling." Cytokine **37**(2): 101-107.
- Chang, P., M. Coughlin and T. J. Mitchison (2009). "Interaction between Poly(ADP-ribose) and NuMA contributes to mitotic spindle pole assembly." Mol Biol Cell **20**(21): 4575-4585.
- Chang, W., J. N. Dynek and S. Smith (2005). "NuMA is a major acceptor of poly(ADP-ribosyl)ation by tankyrase 1 in mitosis." Biochem J **391**(Pt 2): 177-184.
- Charron, M. J. and S. Bonner-Weir (1999). "Implicating PARP and NAD⁺ depletion in type I diabetes." Nat Med **5**(3): 269-270.
- Chen, G. and D. V. Goeddel (2002). "TNF-R1 signaling: a beautiful pathway." Science **296**(5573): 1634-1635.
- Chen, L., C. J. Nievera, A. Y. Lee and X. Wu (2008). "Cell cycle-dependent complex formation of BRCA1.CtIP.MRN is important for DNA double-strand break repair." J Biol Chem **283**(12): 7713-7720.
- Chen, X., C. Wang, L. Teng, Y. Liu, G. Yang, L. Wang, H. Liu, Z. Liu, D. Zhang, Y. Zhang, H. Guan, X. Li, C. Fu, B. Zhao, F. Yin and S. Zhao (2014). "Calcitriol enhances 5-aminolevulinic acid-induced fluorescence and the effect of photodynamic therapy in human glioma." Acta Oncol **53**(3): 405-413.
- Chevanne, M., M. Zampieri, R. Caldini, A. Rizzo, F. Ciccarone, A. Catizone, C. D'Angelo, T. Guastafierro, A. Biroccio, A. Reale, G. Zupi and P. Caiafa (2010). "Inhibition of PARP activity by PJ-34 leads to growth impairment and cell death associated with aberrant mitotic pattern and nucleolar actin accumulation in M14 melanoma cell line." J Cell Physiol **222**(2): 401-410.
- Chiang, Y. J., S. J. Hsiao, D. Yver, S. W. Cushman, L. Tessarollo, S. Smith and R. J. Hodes (2008). "Tankyrase 1 and tankyrase 2 are essential but redundant for mouse embryonic development." PLoS One **3**(7): e2639.
- Chiang, Y. J., M. L. Nguyen, S. Gurunathan, P. Kaminker, L. Tessarollo, J. Campisi and R. J. Hodes (2006). "Generation and characterization of telomere length maintenance in tankyrase 2-deficient mice." Mol Cell Biol **26**(6): 2037-2043.
- Chinnaiyan, A. M., K. O'Rourke, M. Tewari and V. M. Dixit (1995). "FADD, a novel death domain-containing protein, interacts with the death domain of Fas and initiates apoptosis." Cell **81**(4): 505-512.
- Cho, D. Y., S. Z. Lin, W. K. Yang, H. C. Lee, D. M. Hsu, H. L. Lin, C. C. Chen, C. L. Liu, W. Y. Lee and L. H. Ho (2013). "Targeting cancer stem cells for treatment of glioblastoma multiforme." Cell Transplant **22**(4): 731-739.

Bibliography

- Chung, J. H., M. E. Ginn-Pease and C. Eng (2005). "Phosphatase and tensin homologue deleted on chromosome 10 (PTEN) has nuclear localization signal-like sequences for nuclear import mediated by major vault protein." Cancer Res **65**(10): 4108-4116.
- Chung, R., J. Whaley, N. Kley, K. Anderson, D. Louis, A. Menon, C. Hettlich, R. Freiman, E. T. Hedley-Whyte, R. Martuza and et al. (1991). "TP53 gene mutations and 17p deletions in human astrocytomas." Genes Chromosomes Cancer **3**(5): 323-331.
- d'Adda di Fagagna, F., M. P. Hande, W. M. Tong, P. M. Lansdorp, Z. Q. Wang and S. P. Jackson (1999). "Functions of poly(ADP-ribose) polymerase in controlling telomere length and chromosomal stability." Nat Genet **23**(1): 76-80.
- Dantzer, F., H. P. Nasheuer, J. L. Vonesch, G. de Murcia and J. Menissier-de Murcia (1998). "Functional association of poly(ADP-ribose) polymerase with DNA polymerase alpha-primase complex: a link between DNA strand break detection and DNA replication." Nucleic Acids Res **26**(8): 1891-1898.
- Dantzer, F. and R. Santoro (2013). "The expanding role of PARPs in the establishment and maintenance of heterochromatin." FEBS J **280**(15): 3508-3518.
- Daugas, E., D. Nochy, L. Ravagnan, M. Loeffler, S. A. Susin, N. Zamzami and G. Kroemer (2000). "Apoptosis-inducing factor (AIF): a ubiquitous mitochondrial oxidoreductase involved in apoptosis." FEBS Lett **476**(3): 118-123.
- Daugas, E., S. A. Susin, N. Zamzami, K. F. Ferri, T. Irinopoulou, N. Larochette, M. C. Prevost, B. Leber, D. Andrews, J. Penninger and G. Kroemer (2000). "Mitochondrio-nuclear translocation of AIF in apoptosis and necrosis." FASEB J **14**(5): 729-739.
- Davenport, J., L. D. Harris and R. Goorha (2006). "Spindle checkpoint function requires Mad2-dependent Cdc20 binding to the Mad3 homology domain of BubR1." Exp Cell Res **312**(10): 1831-1842.
- Davidovic, L., M. Vodenicharov, E. B. Affar and G. G. Poirier (2001). "Importance of poly(ADP-ribose) glycohydrolase in the control of poly(ADP-ribose) metabolism." Exp Cell Res **268**(1): 7-13.
- De Duve, C. and R. Wattiaux (1966). "Functions of lysosomes." Annu Rev Physiol **28**: 435-492.
- De Lorenzo, S. B., A. G. Patel, R. M. Hurley and S. H. Kaufmann (2013). "The Elephant and the Blind Men: Making Sense of PARP Inhibitors in Homologous Recombination Deficient Tumor Cells." Front Oncol **3**: 228.
- de Murcia, G., V. Schreiber, M. Molinete, B. Saulier, O. Poch, M. Masson, C. Niedergang and J. Menissier de Murcia (1994). "Structure and function of poly(ADP-ribose) polymerase." Mol Cell Biochem **138**(1-2): 15-24.
- de Murcia, J. M., C. Niedergang, C. Trucco, M. Ricoul, B. Dutrillaux, M. Mark, F. J. Oliver, M. Masson, A. Dierich, M. LeMeur, C. Walztinger, P. Chambon and G. de Murcia (1997). "Requirement of poly(ADP-ribose) polymerase in recovery from DNA damage in mice and in cells." Proc Natl Acad Sci U S A **94**(14): 7303-7307.

- Dean, M., T. Fojo and S. Bates (2005). "Tumour stem cells and drug resistance." Nat Rev Cancer **5**(4): 275-284.
- Dent, R. A., G. J. Lindeman, M. Clemons, H. Wildiers, A. Chan, N. J. McCarthy, C. F. Singer, E. S. Lowe, C. L. Watkins and J. Carmichael (2013). "Phase I trial of the oral PARP inhibitor olaparib in combination with paclitaxel for first- or second-line treatment of patients with metastatic triple-negative breast cancer." Breast Cancer Res **15**(5): R88.
- Desmarais, Y., L. Menard, J. Lagueux and G. G. Poirier (1991). "Enzymological properties of poly(ADP-ribose)polymerase: characterization of automodification sites and NADase activity." Biochim Biophys Acta **1078**(2): 179-186.
- Dick, J. E. (2003). "Breast cancer stem cells revealed." Proc Natl Acad Sci U S A **100**(7): 3547-3549.
- Diefenbach, J. and A. Burkle (2005). "Introduction to poly(ADP-ribose) metabolism." Cell Mol Life Sci **62**(7-8): 721-730.
- Ding, Y., C. G. Hubert, J. Herman, P. Corrin, C. M. Toledo, K. Skutt-Kakaria, J. Vazquez, R. Basom, B. Zhang, J. K. Risler, S. M. Pollard, D. H. Nam, J. J. Delrow, J. Zhu, J. Lee, J. DeLuca, J. M. Olson and P. J. Paddison (2013). "Cancer-Specific requirement for BUB1B/BUBR1 in human brain tumor isolates and genetically transformed cells." Cancer Discov **3**(2): 198-211.
- Ditchfield, C., V. L. Johnson, A. Tighe, R. Ellston, C. Haworth, T. Johnson, A. Mortlock, N. Keen and S. S. Taylor (2003). "Aurora B couples chromosome alignment with anaphase by targeting BubR1, Mad2, and Cenp-E to kinetochores." J Cell Biol **161**(2): 267-280.
- Donehower, L. A., L. A. Godley, C. M. Aldaz, R. Pyle, Y. P. Shi, D. Pinkel, J. Gray, A. Bradley, D. Medina and H. E. Varmus (1996). "The role of p53 loss in genomic instability and tumor progression in a murine mammary cancer model." Prog Clin Biol Res **395**: 1-11.
- Drake, C. G., P. M. Pfalzner and E. A. Linell (1963). "Intracavitary Irradiation of Malignant Brain Tumours." J Neurosurg **20**: 428-434.
- Du, C., M. Fang, Y. Li, L. Li and X. Wang (2000). "Smac, a mitochondrial protein that promotes cytochrome c-dependent caspase activation by eliminating IAP inhibition." Cell **102**(1): 33-42.
- Dutertre, S., M. Cazales, M. Quaranta, C. Froment, V. Trabut, C. Dozier, G. Mirey, J. P. Bouche, N. Theis-Febvre, E. Schmitt, B. Monsarrat, C. Prigent and B. Ducommun (2004). "Phosphorylation of CDC25B by Aurora-A at the centrosome contributes to the G2-M transition." J Cell Sci **117**(Pt 12): 2523-2531.
- Earle, E., A. Saxena, A. MacDonald, D. F. Hudson, L. G. Shaffer, R. Saffery, M. R. Cancilla, S. M. Cutts, E. Howman and K. H. Choo (2000). "Poly(ADP-ribose) polymerase at active centromeres and neocentromeres at metaphase." Hum Mol Genet **9**(2): 187-194.
- Elowe, S., S. Hummer, A. Uldschmid, X. Li and E. A. Nigg (2007). "Tension-sensitive Plk1 phosphorylation on BubR1 regulates the stability of kinetochore microtubule interactions." Genes Dev **21**(17): 2205-2219.

Bibliography

- Eng, C. (2003). "PTEN: one gene, many syndromes." Hum Mutat **22**(3): 183-198.
- Espejel, S., P. Klatt, J. Menissier-de Murcia, J. Martin-Caballero, J. M. Flores, G. Taccioli, G. de Murcia and M. A. Blasco (2004). "Impact of telomerase ablation on organismal viability, aging, and tumorigenesis in mice lacking the DNA repair proteins PARP-1, Ku86, or DNA-PKcs." J Cell Biol **167**(4): 627-638.
- Essig, M., T. B. Nguyen, M. S. Shiroishi, M. Saake, J. M. Provenzale, D. S. Enterline, N. Anzalone, A. Dorfler, A. Rovira, M. Wintermark and M. Law (2013). "Perfusion MRI: the five most frequently asked clinical questions." AJR Am J Roentgenol **201**(3): W495-510.
- Fadok, V. A., D. R. Voelker, P. A. Campbell, J. J. Cohen, D. L. Bratton and P. M. Henson (1992). "Exposure of phosphatidylserine on the surface of apoptotic lymphocytes triggers specific recognition and removal by macrophages." J Immunol **148**(7): 2207-2216.
- Fan, Q. W. and W. A. Weiss (2011). "Autophagy and Akt promote survival in glioma." Autophagy **7**(5): 536-538.
- Fan, W., A. Nassiri and Q. Zhong (2011). "Autophagosome targeting and membrane curvature sensing by Barkor/Atg14(L)." Proc Natl Acad Sci U S A **108**(19): 7769-7774.
- Fang, Y., T. Liu, X. Wang, Y. M. Yang, H. Deng, J. Kunicki, F. Traganos, Z. Darzynkiewicz, L. Lu and W. Dai (2006). "BubR1 is involved in regulation of DNA damage responses." Oncogene **25**(25): 3598-3605.
- Feng, Y., D. He, Z. Yao and D. J. Klionsky (2014). "The machinery of macroautophagy." Cell Res **24**(1): 24-41.
- Fingar, D. C., S. Salama, C. Tsou, E. Harlow and J. Blenis (2002). "Mammalian cell size is controlled by mTOR and its downstream targets S6K1 and 4EBP1/eIF4E." Genes Dev **16**(12): 1472-1487.
- Florey, O., S. E. Kim, C. P. Sandoval, C. M. Haynes and M. Overholtzer (2011). "Autophagy machinery mediates macroendocytic processing and entotic cell death by targeting single membranes." Nat Cell Biol **13**(11): 1335-1343.
- Fraser, M., H. Zhao, K. R. Luoto, C. Lundin, C. Coackley, N. Chan, A. M. Joshua, T. A. Bismar, A. Evans, T. Helleday and R. G. Bristow (2012). "PTEN deletion in prostate cancer cells does not associate with loss of RAD51 function: implications for radiotherapy and chemotherapy." Clin Cancer Res **18**(4): 1015-1027.
- Frisch, S. M. and H. Francis (1994). "Disruption of epithelial cell-matrix interactions induces apoptosis." J Cell Biol **124**(4): 619-626.
- Frouin, I., G. Maga, M. Denegri, F. Riva, M. Savio, S. Spadari, E. Prospero and A. I. Scovassi (2003). "Human proliferating cell nuclear antigen, poly(ADP-ribose) polymerase-1, and p21waf1/cip1. A dynamic exchange of partners." J Biol Chem **278**(41): 39265-39268.
- Fuchs, T. A., U. Abed, C. Goosmann, R. Hurwitz, I. Schulze, V. Wahn, Y. Weinrauch, V. Brinkmann and A. Zychlinsky (2007). "Novel cell death program leads to neutrophil extracellular traps." J Cell Biol **176**(2): 231-241.

- Furnari, F. B., H. Lin, H. S. Huang and W. K. Cavenee (1997). "Growth suppression of glioma cells by PTEN requires a functional phosphatase catalytic domain." Proc Natl Acad Sci U S A **94**(23): 12479-12484.
- Gagne, J. P., M. Isabelle, K. S. Lo, S. Bourassa, M. J. Hendzel, V. L. Dawson, T. M. Dawson and G. G. Poirier (2008). "Proteome-wide identification of poly(ADP-ribose) binding proteins and poly(ADP-ribose)-associated protein complexes." Nucleic Acids Res **36**(22): 6959-6976.
- Galan-Moya, E. M., A. Le Guelte, E. Lima Fernandes, C. Thirant, J. Dwyer, N. Bidere, P. O. Couraud, M. G. Scott, M. P. Junier, H. Chneiweiss and J. Gavard (2011). "Secreted factors from brain endothelial cells maintain glioblastoma stem-like cell expansion through the mTOR pathway." EMBO Rep **12**(5): 470-476.
- Galonek, H. L. and J. M. Hardwick (2006). "Upgrading the BCL-2 network." Nat Cell Biol **8**(12): 1317-1319.
- Galli, R., E. Binda, U. Orfanelli, B. Cipelletti, A. Gritti, S. De Vitis, R. Fiocco, C. Foroni, F. Dimeco and A. Vescovi (2004). "Isolation and characterization of tumorigenic, stem-like neural precursors from human glioblastoma." Cancer Res **64**(19): 7011-7021.
- Galluzzi, L., J. M. Bravo-San Pedro, I. Vitale, S. A. Aaronson, J. M. Abrams, D. Adam, E. S. Alnemri, L. Altucci, D. Andrews, M. Annicchiarico-Petruzzelli, E. H. Baehrecke, N. G. Bazan, M. J. Bertrand, K. Bianchi, M. V. Blagosklonny, K. Blomgren, C. Borner, D. E. Bredesen, C. Brenner, M. Campanella, E. Candi, F. Cecconi, F. K. Chan, N. S. Chandel, E. H. Cheng, J. E. Chipuk, J. A. Cidlowski, A. Ciechanover, T. M. Dawson, V. L. Dawson, V. De Laurenzi, R. De Maria, K. M. Debatin, N. Di Daniele, V. M. Dixit, B. D. Dynlacht, W. S. El-Deiry, G. M. Fimia, R. A. Flavell, S. Fulda, C. Garrido, M. L. Gougeon, D. R. Green, H. Gronemeyer, G. Hajnoczky, J. M. Hardwick, M. O. Hengartner, H. Ichijo, B. Joseph, P. J. Jost, T. Kaufmann, O. Kepp, D. J. Klionsky, R. A. Knight, S. Kumar, J. J. Lemasters, B. Levine, A. Linkermann, S. A. Lipton, R. A. Lockshin, C. Lopez-Otin, E. Lugli, F. Madeo, W. Malorni, J. C. Marine, S. J. Martin, J. C. Martinou, J. P. Medema, P. Meier, S. Melino, N. Mizushima, U. Moll, C. Munoz-Pinedo, G. Nunez, A. Oberst, T. Panaretakis, J. M. Penninger, M. E. Peter, M. Piacentini, P. Pinton, J. H. Prehn, H. Puthalakath, G. A. Rabinovich, K. S. Ravichandran, R. Rizzuto, C. M. Rodrigues, D. C. Rubinsztein, T. Rudel, Y. Shi, H. U. Simon, B. R. Stockwell, G. Szabadkai, S. W. Tait, H. L. Tang, N. Tavernarakis, Y. Tsujimoto, T. Vanden Berghe, P. Vandenabeele, A. Villunger, E. F. Wagner, H. Walczak, E. White, W. G. Wood, J. Yuan, Z. Zakeri, B. Zhivotovsky, G. Melino and G. Kroemer (2015). "Essential versus accessory aspects of cell death: recommendations of the NCCD 2015." Cell Death Differ **22**(1): 58-73.
- Galluzzi, L., O. Kepp and G. Kroemer (2009). "RIP kinases initiate programmed necrosis." J Mol Cell Biol **1**(1): 8-10.
- Galluzzi, L., I. Vitale, J. M. Abrams, E. S. Alnemri, E. H. Baehrecke, M. V. Blagosklonny, T. M. Dawson, V. L. Dawson, W. S. El-Deiry, S. Fulda, E. Gottlieb, D. R. Green, M. O. Hengartner, O. Kepp, R. A. Knight, S. Kumar, S. A. Lipton, X. Lu, F. Madeo, W. Malorni, P. Mehlen, G. Nunez, M. E. Peter, M. Piacentini, D. C. Rubinsztein, Y. Shi, H. U. Simon, P. Vandenabeele, E. White, J. Yuan, B. Zhivotovsky, G. Melino and G. Kroemer (2012). "Molecular definitions of cell death subroutines: recommendations of the Nomenclature Committee on Cell Death 2012." Cell Death Differ **19**(1): 107-120.

Bibliography

- Gangemi, R. M., F. Griffero, D. Marubbi, M. Perera, M. C. Capra, P. Malatesta, G. L. Ravetti, G. L. Zona, A. Daga and G. Corte (2009). "SOX2 silencing in glioblastoma tumor-initiating cells causes stop of proliferation and loss of tumorigenicity." Stem Cells **27**(1): 40-48.
- Gao, F., S. W. Kwon, Y. Zhao and Y. Jin (2009). "PARP1 poly(ADP-ribosyl)ates Sox2 to control Sox2 protein levels and FGF4 expression during embryonic stem cell differentiation." J Biol Chem **284**(33): 22263-22273.
- Gao, X., Y. Zhang, P. Arrazola, O. Hino, T. Kobayashi, R. S. Yeung, B. Ru and D. Pan (2002). "Tsc tumour suppressor proteins antagonize amino-acid-TOR signalling." Nat Cell Biol **4**(9): 699-704.
- Ge, L. and R. Schekman (2014). "The ER-Golgi intermediate compartment feeds the phagophore membrane." Autophagy **10**(1): 170-172.
- Gibson, B. A. and W. L. Kraus (2012). "New insights into the molecular and cellular functions of poly(ADP-ribose) and PARPs." Nat Rev Mol Cell Biol **13**(7): 411-424.
- Gimm, O., A. Perren, L. P. Weng, D. J. Marsh, J. J. Yeh, U. Ziebold, E. Gil, R. Hinze, L. Delbridge, J. A. Lees, G. L. Mutter, B. G. Robinson, P. Komminoth, H. Dralle and C. Eng (2000). "Differential nuclear and cytoplasmic expression of PTEN in normal thyroid tissue, and benign and malignant epithelial thyroid tumors." Am J Pathol **156**(5): 1693-1700.
- Gonzalez-Billalabeitia, E., N. Seitzer, S. J. Song, M. S. Song, A. Patnaik, X. S. Liu, M. T. Epping, A. Papa, R. M. Hobbs, M. Chen, A. Lunardi, C. Ng, K. A. Webster, S. Signoretti, M. Loda, J. M. Asara, C. Nardella, J. G. Clohessy, L. C. Cantley and P. P. Pandolfi (2014). "Vulnerabilities of PTEN-TP53-deficient prostate cancers to compound PARP-PI3K inhibition." Cancer Discov **4**(8): 896-904.
- Gonzalez-Flores, A., R. Aguilar-Quesada, E. Siles, S. Pozo, M. I. Rodriguez-Lara, L. Lopez-Jimenez, M. Lopez-Rodriguez, A. Peralta-Leal, D. Villar, D. Martin-Oliva, L. Del Peso, E. Berra and F. J. Oliver (2013). "Interaction between PARP-1 and HIF-2alpha in the hypoxic response." Oncogene.
- Gonzalez-Flores, A., R. Aguilar-Quesada, E. Siles, S. Pozo, M. I. Rodriguez-Lara, L. Lopez-Jimenez, M. Lopez-Rodriguez, A. Peralta-Leal, D. Villar, D. Martin-Oliva, L. del Peso, E. Berra and F. J. Oliver (2014). "Interaction between PARP-1 and HIF-2alpha in the hypoxic response." Oncogene **33**(7): 891-898.
- Gonzalez-Santamaria, J., M. Campagna, A. Ortega-Molina, L. Marcos-Villar, C. F. de la Cruz-Herrera, D. Gonzalez, P. Gallego, F. Lopitz-Otsoa, M. Esteban, M. S. Rodriguez, M. Serrano and C. Rivas (2012). "Regulation of the tumor suppressor PTEN by SUMO." Cell Death Dis **3**: e393.
- Goodenberger, M. L. and R. B. Jenkins (2012). "Genetics of adult glioma." Cancer Genet **205**(12): 613-621.
- Gordon, P. B. and P. O. Seglen (1988). "Prelysosomal convergence of autophagic and endocytic pathways." Biochem Biophys Res Commun **151**(1): 40-47.

- Gottlieb, R. A., J. Nordberg, E. Skowronski and B. M. Babior (1996). "Apoptosis induced in Jurkat cells by several agents is preceded by intracellular acidification." Proc Natl Acad Sci U S A **93**(2): 654-658.
- Gottschalk, A. J., G. Timinszky, S. E. Kong, J. Jin, Y. Cai, S. K. Swanson, M. P. Washburn, L. Florens, A. G. Ladurner, J. W. Conaway and R. C. Conaway (2009). "Poly(ADP-ribose) directs recruitment and activation of an ATP-dependent chromatin remodeler." Proc Natl Acad Sci U S A **106**(33): 13770-13774.
- Green, D. R. (2011). "The end and after: how dying cells impact the living organism." Immunity **35**(4): 441-444.
- Greenberg, A. S., J. J. Egan, S. A. Wek, N. B. Garty, E. J. Blanchette-Mackie and C. Londos (1991). "Perilipin, a major hormonally regulated adipocyte-specific phosphoprotein associated with the periphery of lipid storage droplets." J Biol Chem **266**(17): 11341-11346.
- Guijas, C., J. P. Rodriguez, J. M. Rubio, M. A. Balboa and J. Balsinde (2014). "Phospholipase A2 regulation of lipid droplet formation." Biochim Biophys Acta **1841**(12): 1661-1671.
- Guo, D., E. H. Bell and A. Chakravarti (2013). "Lipid metabolism emerges as a promising target for malignant glioma therapy." CNS Oncol **2**(3): 289-299.
- Guo, Y., C. Kim, S. Ahmad, J. Zhang and Y. Mao (2012). "CENP-E--dependent BubR1 autophosphorylation enhances chromosome alignment and the mitotic checkpoint." J Cell Biol **198**(2): 205-217.
- Gutierrez, M. G., D. B. Munafo, W. Beron and M. I. Colombo (2004). "Rab7 is required for the normal progression of the autophagic pathway in mammalian cells." J Cell Sci **117**(Pt 13): 2687-2697.
- Gwinn, D. M., D. B. Shackelford, D. F. Egan, M. M. Mihaylova, A. Mery, D. S. Vasquez, B. E. Turk and R. J. Shaw (2008). "AMPK phosphorylation of raptor mediates a metabolic checkpoint." Mol Cell **30**(2): 214-226.
- Ha, H. C. and S. H. Snyder (1999). "Poly(ADP-ribose) polymerase is a mediator of necrotic cell death by ATP depletion." Proc Natl Acad Sci U S A **96**(24): 13978-13982.
- Hager, J. C. and G. H. Heppner (1983). "Breast cancer stem cells." Prog Clin Biol Res **132C**: 137-146.
- Haince, J. F., D. McDonald, A. Rodrigue, U. Dery, J. Y. Masson, M. J. Hendzel and G. G. Poirier (2008). "PARP1-dependent kinetics of recruitment of MRE11 and NBS1 proteins to multiple DNA damage sites." J Biol Chem **283**(2): 1197-1208.
- Hakem, R. (2008). "DNA-damage repair; the good, the bad, and the ugly." EMBO J **27**(4): 589-605.
- Hassa, P. O., S. S. Haenni, C. Buerki, N. I. Meier, W. S. Lane, H. Owen, M. Gersbach, R. Imhof and M. O. Hottiger (2005). "Acetylation of poly(ADP-ribose) polymerase-1 by p300/CREB-binding protein regulates coactivation of NF-kappaB-dependent transcription." J Biol Chem **280**(49): 40450-40464.

Bibliography

- Hassa, P. O. and M. O. Hottiger (1999). "A role of poly (ADP-ribose) polymerase in NF-kappaB transcriptional activation." Biol Chem **380**(7-8): 953-959.
- Hassa, P. O. and M. O. Hottiger (2008). "The diverse biological roles of mammalian PARPs, a small but powerful family of poly-ADP-ribose polymerases." Front Biosci **13**: 3046-3082.
- Hegan, D. C., Y. Lu, G. C. Stachelek, M. E. Crosby, R. S. Bindra and P. M. Glazer (2010). "Inhibition of poly(ADP-ribose) polymerase down-regulates BRCA1 and RAD51 in a pathway mediated by E2F4 and p130." Proc Natl Acad Sci U S A **107**(5): 2201-2206.
- Hegedus, C., P. Lakatos, G. Olah, B. I. Toth, S. Gergely, E. Szabo, T. Biro, C. Szabo and L. Virag (2008). "Protein kinase C protects from DNA damage-induced necrotic cell death by inhibiting poly(ADP-ribose) polymerase-1." FEBS Lett **582**(12): 1672-1678.
- Hegi, M. E., L. Liu, J. G. Herman, R. Stupp, W. Wick, M. Weller, M. P. Mehta and M. R. Gilbert (2008). "Correlation of O6-methylguanine methyltransferase (MGMT) promoter methylation with clinical outcomes in glioblastoma and clinical strategies to modulate MGMT activity." J Clin Oncol **26**(25): 4189-4199.
- Heitman, J., N. R. Movva and M. N. Hall (1991). "Targets for cell cycle arrest by the immunosuppressant rapamycin in yeast." Science **253**(5022): 905-909.
- Heldin, C. H. (2013). "Targeting the PDGF signaling pathway in tumor treatment." Cell Commun Signal **11**: 97.
- Hemberger, M., T. Nozaki, E. Winterhager, H. Yamamoto, H. Nakagama, N. Kamada, H. Suzuki, T. Ohta, M. Ohki, M. Masutani and J. C. Cross (2003). "Parp1-deficiency induces differentiation of ES cells into trophoblast derivatives." Dev Biol **257**(2): 371-381.
- Hemmati, H. D., I. Nakano, J. A. Lazareff, M. Masterman-Smith, D. H. Geschwind, M. Bronner-Fraser and H. I. Kornblum (2003). "Cancerous stem cells can arise from pediatric brain tumors." Proc Natl Acad Sci U S A **100**(25): 15178-15183.
- Herzog, H., B. U. Zabel, R. Schneider, B. Auer, M. Hirsch-Kauffmann and M. Schweiger (1989). "Human nuclear NAD+ ADP-ribosyltransferase: localization of the gene on chromosome 1q41-q42 and expression of an active human enzyme in Escherichia coli." Proc Natl Acad Sci U S A **86**(10): 3514-3518.
- Heyer, W. D., K. T. Ehmsen and J. Liu (2010). "Regulation of homologous recombination in eukaryotes." Annu Rev Genet **44**: 113-139.
- Hirvonen, H. E., R. Salonen, M. M. Sandberg, E. Vuorio, I. Vastrik, E. Kotilainen and H. Kalimo (1994). "Differential expression of myc, max and RB1 genes in human gliomas and glioma cell lines." Br J Cancer **69**(1): 16-25.
- Hockenbery, D. M., Z. N. Oltvai, X. M. Yin, C. L. Millman and S. J. Korsmeyer (1993). "Bcl-2 functions in an antioxidant pathway to prevent apoptosis." Cell **75**(2): 241-251.
- Hofmann, K., P. Bucher and J. Tschoopp (1997). "The CARD domain: a new apoptotic signalling motif." Trends Biochem Sci **22**(5): 155-156.
- Holbro, T., G. Civenni and N. E. Hynes (2003). "The ErbB receptors and their role in cancer progression." Exp Cell Res **284**(1): 99-110.

- Hosokawa, N., T. Hara, T. Kaizuka, C. Kishi, A. Takamura, Y. Miura, S. Iemura, T. Natsume, K. Takehana, N. Yamada, J. L. Guan, N. Oshiro and N. Mizushima (2009). "Nutrient-dependent mTORC1 association with the ULK1-Atg13-FIP200 complex required for autophagy." Mol Biol Cell **20**(7): 1981-1991.
- Hottiger, M. O., P. O. Hassa, B. Luscher, H. Schuler and F. Koch-Nolte (2010). "Toward a unified nomenclature for mammalian ADP-ribosyltransferases." Trends Biochem Sci **35**(4): 208-219.
- Hovinga, K. E., F. Shimizu, R. Wang, G. Panagiotakos, M. Van Der Heijden, H. Moayedpardazi, A. S. Correia, D. Soulet, T. Major, J. Menon and V. Tabar (2010). "Inhibition of notch signaling in glioblastoma targets cancer stem cells via an endothelial cell intermediate." Stem Cells **28**(6): 1019-1029.
- Howitt, J., J. Lackovic, L. H. Low, A. Naguib, A. Macintyre, C. P. Goh, J. K. Callaway, V. Hammond, T. Thomas, M. Dixon, U. Putz, J. Silke, P. Bartlett, B. Yang, S. Kumar, L. C. Trotman and S. S. Tan (2012). "Ndfip1 regulates nuclear Pten import in vivo to promote neuronal survival following cerebral ischemia." J Cell Biol **196**(1): 29-36.
- Hoyt, M. A., L. Totis and B. T. Roberts (1991). "S. cerevisiae genes required for cell cycle arrest in response to loss of microtubule function." Cell **66**(3): 507-517.
- Hu, B., Z. Wu, P. Hergert, C. A. Henke, P. B. Bitterman and S. H. Phan (2013). "Regulation of myofibroblast differentiation by poly(ADP-ribose) polymerase 1." Am J Pathol **182**(1): 71-83.
- Hu, L., X. Liu, Y. Chervona, F. Yang, M. S. Tang, Z. Darzynkiewicz and W. Dai (2011). "Chromium induces chromosomal instability, which is partly due to deregulation of BubR1 and Emi1, two APC/C inhibitors." Cell Cycle **10**(14): 2373-2379.
- Huang, H., J. Hittle, F. Zappacosta, R. S. Annan, A. Hershko and T. J. Yen (2008). "Phosphorylation sites in BubR1 that regulate kinetochore attachment, tension, and mitotic exit." J Cell Biol **183**(4): 667-680.
- Hudson, C. C., M. Liu, G. G. Chiang, D. M. Otterness, D. C. Loomis, F. Kaper, A. J. Giaccia and R. T. Abraham (2002). "Regulation of hypoxia-inducible factor 1alpha expression and function by the mammalian target of rapamycin." Mol Cell Biol **22**(20): 7004-7014.
- Huertas, P. (2010). "DNA resection in eukaryotes: deciding how to fix the break." Nat Struct Mol Biol **17**(1): 11-16.
- Hwang, L. H., L. F. Lau, D. L. Smith, C. A. Mistrot, K. G. Hardwick, E. S. Hwang, A. Amon and A. W. Murray (1998). "Budding yeast Cdc20: a target of the spindle checkpoint." Science **279**(5353): 1041-1044.
- Ichimura, Y., T. Kirisako, T. Takao, Y. Satomi, Y. Shimonishi, N. Ishihara, N. Mizushima, I. Tanida, E. Kominami, M. Ohsumi, T. Noda and Y. Ohsumi (2000). "A ubiquitin-like system mediates protein lipidation." Nature **408**(6811): 488-492.
- Ignatova, T. N., V. G. Kukekov, E. D. Laywell, O. N. Suslov, F. D. Vrionis and D. A. Steindler (2002). "Human cortical glial tumors contain neural stem-like cells expressing astroglial and neuronal markers in vitro." Glia **39**(3): 193-206.

Bibliography

- Ikushima, H., T. Todo, Y. Ino, M. Takahashi, K. Miyazawa and K. Miyazono (2009). "Autocrine TGF-beta signaling maintains tumorigenicity of glioma-initiating cells through Sry-related HMG-box factors." Cell Stem Cell **5**(5): 504-514.
- Inoki, K., T. Zhu and K. L. Guan (2003). "TSC2 mediates cellular energy response to control cell growth and survival." Cell **115**(5): 577-590.
- Jagtap, P. and C. Szabo (2005). "Poly(ADP-ribose) polymerase and the therapeutic effects of its inhibitors." Nat Rev Drug Discov **4**(5): 421-440.
- Jankevicius, G., M. Hassler, B. Golia, V. Rybin, M. Zacharias, G. Timinszky and A. G. Ladurner (2013). "A family of macrodomain proteins reverses cellular mono-ADP-ribosylation." Nat Struct Mol Biol **20**(4): 508-514.
- Janssen, A., G. J. Kops and R. H. Medema (2009). "Elevating the frequency of chromosome mis-segregation as a strategy to kill tumor cells." Proc Natl Acad Sci U S A **106**(45): 19108-19113.
- Jensen, R. B., A. Ozes, T. Kim, A. Estep and S. C. Kowalczykowski (2013). "BRCA2 is epistatic to the RAD51 paralogs in response to DNA damage." DNA Repair (Amst) **12**(4): 306-311.
- Ji, Y. and A. V. Tulin (2010). "The roles of PARP1 in gene control and cell differentiation." Curr Opin Genet Dev **20**(5): 512-518.
- Jiang, H., C. Gomez-Manzano, H. Aoki, M. M. Alonso, S. Kondo, F. McCormick, J. Xu, Y. Kondo, B. N. Bekele, H. Colman, F. F. Lang and J. Fueyo (2007). "Examination of the therapeutic potential of Delta-24-RGD in brain tumor stem cells: role of autophagic cell death." J Natl Cancer Inst **99**(18): 1410-1414.
- Jordan, M. A. and L. Wilson (2004). "Microtubules as a target for anticancer drugs." Nat Rev Cancer **4**(4): 253-265.
- Joza, N., G. Kroemer and J. M. Penninger (2002). "Genetic analysis of the mammalian cell death machinery." Trends Genet **18**(3): 142-149.
- Jung, C. H., C. B. Jun, S. H. Ro, Y. M. Kim, N. M. Otto, J. Cao, M. Kundu and D. H. Kim (2009). "ULK-Atg13-FIP200 complexes mediate mTOR signaling to the autophagy machinery." Mol Biol Cell **20**(7): 1992-2003.
- Kameshita, I., Z. Matsuda, T. Taniguchi and Y. Shizuta (1984). "Poly (ADP-Ribose) synthetase. Separation and identification of three proteolytic fragments as the substrate-binding domain, the DNA-binding domain, and the automodification domain." J Biol Chem **259**(8): 4770-4776.
- Kaminker, P. G., S. H. Kim, R. D. Taylor, Y. Zebardjian, W. D. Funk, G. B. Morin, P. Yaswen and J. Campisi (2001). "TANK2, a new TRF1-associated poly(ADP-ribose) polymerase, causes rapid induction of cell death upon overexpression." J Biol Chem **276**(38): 35891-35899.
- Kanai, M., K. Hanashiro, S. H. Kim, S. Hanai, A. H. Boulares, M. Miwa and K. Fukasawa (2007). "Inhibition of Crm1-p53 interaction and nuclear export of p53 by poly(ADP-ribosylation)." Nat Cell Biol **9**(10): 1175-1183.

- Kaufmann, S. H., S. Desnoyers, Y. Ottaviano, N. E. Davidson and G. G. Poirier (1993). "Specific proteolytic cleavage of poly(ADP-ribose) polymerase: an early marker of chemotherapy-induced apoptosis." Cancer Res **53**(17): 3976-3985.
- Kerr, J. F., A. H. Wyllie and A. R. Currie (1972). "Apoptosis: a basic biological phenomenon with wide-ranging implications in tissue kinetics." Br J Cancer **26**(4): 239-257.
- Khaldoun, S. A., M. A. Emond-Boisjoly, D. Chateau, V. Carriere, M. Lacasa, M. Rousset, S. Demignot and E. Morel (2014). "Autophagosomes contribute to intracellular lipid distribution in enterocytes." Mol Biol Cell **25**(1): 118-132.
- Khan, O. A., M. Gore, P. Lorigan, J. Stone, A. Greystoke, W. Burke, J. Carmichael, A. J. Watson, G. McGown, M. Thorncroft, G. P. Margison, R. Califano, J. Larkin, S. Wellman and M. R. Middleton (2011). "A phase I study of the safety and tolerability of olaparib (AZD2281, KU0059436) and dacarbazine in patients with advanced solid tumours." Br J Cancer **104**(5): 750-755.
- Khanna, K. K., M. F. Lavin, S. P. Jackson and T. D. Mulhern (2001). "ATM, a central controller of cellular responses to DNA damage." Cell Death Differ **8**(11): 1052-1065.
- Kim, M. K., C. Dudognon and S. Smith (2012). "Tankyrase 1 regulates centrosome function by controlling CPAP stability." EMBO Rep **13**(8): 724-732.
- Kim, M. Y., S. Mauro, N. Gevry, J. T. Lis and W. L. Kraus (2004). "NAD⁺-dependent modulation of chromatin structure and transcription by nucleosome binding properties of PARP-1." Cell **119**(6): 803-814.
- Kim, M. Y., T. Zhang and W. L. Kraus (2005). "Poly(ADP-ribosyl)ation by PARP-1: 'PAR-laying' NAD⁺ into a nuclear signal." Genes Dev **19**(17): 1951-1967.
- Kim, S. H., J. S. Henkel, D. R. Beers, I. S. Sengun, E. P. Simpson, J. C. Goodman, J. I. Engelhardt, L. Siklos and S. H. Appel (2003). "PARP expression is increased in astrocytes but decreased in motor neurons in the spinal cord of sporadic ALS patients." J Neuropathol Exp Neurol **62**(1): 88-103.
- Kim, Y. J. and D. M. Wilson, 3rd (2012). "Overview of base excision repair biochemistry." Curr Mol Pharmacol **5**(1): 3-13.
- King, R. W., J. M. Peters, S. Tugendreich, M. Rolfe, P. Hieter and M. W. Kirschner (1995). "A 20S complex containing CDC27 and CDC16 catalyzes the mitosis-specific conjugation of ubiquitin to cyclin B." Cell **81**(2): 279-288.
- Kischkel, F. C., S. Hellbardt, I. Behrmann, M. Germer, M. Pawlita, P. H. Kramer and M. E. Peter (1995). "Cytotoxicity-dependent APO-1 (Fas/CD95)-associated proteins form a death-inducing signaling complex (DISC) with the receptor." EMBO J **14**(22): 5579-5588.
- Kops, G. J., D. R. Foltz and D. W. Cleveland (2004). "Lethality to human cancer cells through massive chromosome loss by inhibition of the mitotic checkpoint." Proc Natl Acad Sci U S A **101**(23): 8699-8704.
- Krakstad, C. and M. Chekenya (2010). "Survival signalling and apoptosis resistance in glioblastomas: opportunities for targeted therapeutics." Mol Cancer **9**: 135.

Bibliography

- Kraus, W. L. and J. T. Lis (2003). "PARP goes transcription." Cell **113**(6): 677-683.
- Krishnakumar, R., M. J. Gamble, K. M. Frizzell, J. G. Berrocal, M. Kininis and W. L. Kraus (2008). "Reciprocal binding of PARP-1 and histone H1 at promoters specifies transcriptional outcomes." Science **319**(5864): 819-821.
- Kroemer, G., W. S. El-Deiry, P. Golstein, M. E. Peter, D. Vaux, P. Vandenabeele, B. Zhivotovsky, M. V. Blagosklonny, W. Malorni, R. A. Knight, M. Piacentini, S. Nagata, G. Melino and D. Nomenclature Committee on Cell (2005). "Classification of cell death: recommendations of the Nomenclature Committee on Cell Death." Cell Death Differ **12 Suppl 2**: 1463-1467.
- Kroemer, G., L. Galluzzi, P. Vandenabeele, J. Abrams, E. S. Alnemri, E. H. Baehrecke, M. V. Blagosklonny, W. S. El-Deiry, P. Golstein, D. R. Green, M. Hengartner, R. A. Knight, S. Kumar, S. A. Lipton, W. Malorni, G. Nunez, M. E. Peter, J. Tschopp, J. Yuan, M. Piacentini, B. Zhivotovsky, G. Melino and D. Nomenclature Committee on Cell (2009). "Classification of cell death: recommendations of the Nomenclature Committee on Cell Death 2009." Cell Death Differ **16**(1): 3-11.
- Kuemmerle, N. B., E. Rysman, P. S. Lombardo, A. J. Flanagan, B. C. Lipe, W. A. Wells, J. R. Pettus, H. M. Froehlich, V. A. Memoli, P. M. Morganelli, J. V. Swinnen, L. A. Timmerman, L. Chaychi, C. J. Fricano, B. L. Eisenberg, W. B. Coleman and W. B. Kinlaw (2011). "Lipoprotein lipase links dietary fat to solid tumor cell proliferation." Mol Cancer Ther **10**(3): 427-436.
- Kuhajda, F. P., E. S. Pizer, J. N. Li, N. S. Mani, G. L. Frehywot and C. A. Townsend (2000). "Synthesis and antitumor activity of an inhibitor of fatty acid synthase." Proc Natl Acad Sci U S A **97**(7): 3450-3454.
- Kulukian, A., J. S. Han and D. W. Cleveland (2009). "Unattached kinetochores catalyze production of an anaphase inhibitor that requires a Mad2 template to prime Cdc20 for BubR1 binding." Dev Cell **16**(1): 105-117.
- Kuma, A., N. Mizushima, N. Ishihara and Y. Ohsumi (2002). "Formation of the approximately 350-kDa Apg12-Apg5-Apg16 multimeric complex, mediated by Apg16 oligomerization, is essential for autophagy in yeast." J Biol Chem **277**(21): 18619-18625.
- Kummar, S., A. Chen, J. Ji, Y. Zhang, J. M. Reid, M. Ames, L. Jia, M. Weil, G. Speranza, A. J. Murgo, R. Kinders, L. Wang, R. E. Parchment, J. Carter, H. Stotler, L. Rubinstein, M. Hollingshead, G. Melillo, Y. Pommier, W. Bonner, J. E. Tomaszewski and J. H. Doroshow (2011). "Phase I study of PARP inhibitor ABT-888 in combination with topotecan in adults with refractory solid tumors and lymphomas." Cancer Res **71**(17): 5626-5634.
- Kunz, J. B., H. Schwarz and A. Mayer (2004). "Determination of four sequential stages during microautophagy in vitro." J Biol Chem **279**(11): 9987-9996.
- Lachyankar, M. B., N. Sultana, C. M. Schonhoff, P. Mitra, W. Poluha, S. Lambert, P. J. Quesenberry, N. S. Litofsky, L. D. Recht, R. Nabi, S. J. Miller, S. Ohta, B. G. Neel and A. H. Ross (2000). "A role for nuclear PTEN in neuronal differentiation." J Neurosci **20**(4): 1404-1413.

- Lai, Y. S., C. W. Chang, K. M. Pawlik, D. Zhou, M. B. Renfrow and T. M. Townes (2012). "SRY (sex determining region Y)-box2 (Sox2)/poly ADP-ribose polymerase 1 (Parp1) complexes regulate pluripotency." Proc Natl Acad Sci U S A **109**(10): 3772-3777.
- Lamm, G. M., P. Steinlein, M. Cotten and G. Christofori (1997). "A rapid, quantitative and inexpensive method for detecting apoptosis by flow cytometry in transiently transfected cells." Nucleic Acids Res **25**(23): 4855-4857.
- Lampson, M. A. and T. M. Kapoor (2005). "The human mitotic checkpoint protein BubR1 regulates chromosome-spindle attachments." Nat Cell Biol **7**(1): 93-98.
- Landy, H. J., T. T. Lee, P. Potter, L. Feun and A. Markoe (2000). "Early MRI findings in high grade glioma." J Neurooncol **47**(1): 65-72.
- Langelier, M. F., J. L. Planck, S. Roy and J. M. Pascal (2012). "Structural basis for DNA damage-dependent poly(ADP-ribosylation) by human PARP-1." Science **336**(6082): 728-732.
- Langelier, M. F., A. A. Riccio and J. M. Pascal (2014). "PARP-2 and PARP-3 are selectively activated by 5' phosphorylated DNA breaks through an allosteric regulatory mechanism shared with PARP-1." Nucleic Acids Res **42**(12): 7762-7775.
- Langelier, M. F., K. M. Servent, E. E. Rogers and J. M. Pascal (2008). "A third zinc-binding domain of human poly(ADP-ribose) polymerase-1 coordinates DNA-dependent enzyme activation." J Biol Chem **283**(7): 4105-4114.
- Lara-Gonzalez, P., M. I. Scott, M. Diez, O. Sen and S. S. Taylor (2011). "BubR1 blocks substrate recruitment to the APC/C in a KEN-box-dependent manner." J Cell Sci **124**(Pt 24): 4332-4345.
- Lawlor, M. A. and D. R. Alessi (2001). "PKB/Akt: a key mediator of cell proliferation, survival and insulin responses?" J Cell Sci **114**(Pt 16): 2903-2910.
- Lazebnik, Y. A., S. H. Kaufmann, S. Desnoyers, G. G. Poirier and W. C. Earnshaw (1994). "Cleavage of poly(ADP-ribose) polymerase by a proteinase with properties like ICE." Nature **371**(6495): 346-347.
- Lefranc, F. and R. Kiss (2006). "Autophagy, the Trojan horse to combat glioblastomas." Neurosurg Focus **20**(4): E7.
- Leibel, S. A. and G. E. Sheline (1987). "Radiation therapy for neoplasms of the brain." J Neurosurg **66**(1): 1-22.
- Leibeling, D., P. Laspe and S. Emmert (2006). "Nucleotide excision repair and cancer." J Mol Histol **37**(5-7): 225-238.
- Leonard, M. K., N. T. Hill, P. A. Bubulya and M. P. Kadakia (2013). "The PTEN-Akt pathway impacts the integrity and composition of mitotic centrosomes." Cell Cycle **12**(9): 1406-1415.
- Letai, A., M. C. Bassik, L. D. Walensky, M. D. Sorcinelli, S. Weiler and S. J. Korsmeyer (2002). "Distinct BH3 domains either sensitize or activate mitochondrial apoptosis, serving as prototype cancer therapeutics." Cancer Cell **2**(3): 183-192.

Bibliography

- Levaot, N., O. Voytyuk, I. Dimitriou, F. Sircoulomb, A. Chandrakumar, M. Deckert, P. M. Krzyzanowski, A. Scotter, S. Gu, S. Janmohamed, F. Cong, P. D. Simoncic, Y. Ueki, J. La Rose and R. Rottapel (2011). "Loss of Tankyrase-mediated destruction of 3BP2 is the underlying pathogenic mechanism of cherubism." *Cell* **147**(6): 1324-1339.
- Levine, B., S. Sinha and G. Kroemer (2008). "Bcl-2 family members: dual regulators of apoptosis and autophagy." *Autophagy* **4**(5): 600-606.
- Li, J., C. Yen, D. Liaw, K. Podsypanina, S. Bose, S. I. Wang, J. Puc, C. Miliareis, L. Rodgers, R. McCombie, S. H. Bigner, B. C. Giovanella, M. Ittmann, B. Tycko, H. Hibshoosh, M. H. Wigler and R. Parsons (1997). "PTEN, a putative protein tyrosine phosphatase gene mutated in human brain, breast, and prostate cancer." *Science* **275**(5308): 1943-1947.
- Li, L., H. Wang, E. S. Yang, C. L. Arteaga and F. Xia (2008). "Erlotinib attenuates homologous recombinational repair of chromosomal breaks in human breast cancer cells." *Cancer Res* **68**(22): 9141-9146.
- Li, L. Y., X. Luo and X. Wang (2001). "Endonuclease G is an apoptotic DNase when released from mitochondria." *Nature* **412**(6842): 95-99.
- Li, M., L. Y. Lu, C. Y. Yang, S. Wang and X. Yu (2013). "The FHA and BRCT domains recognize ADP-ribosylation during DNA damage response." *Genes Dev* **27**(16): 1752-1768.
- Li, N., Y. Zhang, X. Han, K. Liang, J. Wang, L. Feng, W. Wang, Z. Songyang, C. Lin, L. Yang, Y. Yu and J. Chen (2015). "Poly-ADP ribosylation of PTEN by tankyrases promotes PTEN degradation and tumor growth." *Genes Dev* **29**(2): 157-170.
- Li, R. and A. W. Murray (1991). "Feedback control of mitosis in budding yeast." *Cell* **66**(3): 519-531.
- Li, T. K., A. Y. Chen, C. Yu, Y. Mao, H. Wang and L. F. Liu (1999). "Activation of topoisomerase II-mediated excision of chromosomal DNA loops during oxidative stress." *Genes Dev* **13**(12): 1553-1560.
- Li, Y., L. H. Low, U. Putz, C. P. Goh, S. S. Tan and J. Howitt (2014). "Rab5 and Ndfip1 are involved in Pten ubiquitination and nuclear trafficking." *Traffic* **15**(7): 749-761.
- Liaw, D., D. J. Marsh, J. Li, P. L. Dahia, S. I. Wang, Z. Zheng, S. Bose, K. M. Call, H. C. Tsou, M. Peacocke, C. Eng and R. Parsons (1997). "Germline mutations of the PTEN gene in Cowden disease, an inherited breast and thyroid cancer syndrome." *Nat Genet* **16**(1): 64-67.
- Libermann, T. A., H. R. Nusbaum, N. Razon, R. Kris, I. Lax, H. Soreq, N. Whittle, M. D. Waterfield, A. Ullrich and J. Schlessinger (1985). "Amplification, enhanced expression and possible rearrangement of EGF receptor gene in primary human brain tumours of glial origin." *Nature* **313**(5998): 144-147.
- Lin, F., M. C. de Gooijer, E. M. Roig, L. C. Buil, S. M. Christner, J. H. Beumer, T. Wurdinger, J. H. Beijnen and O. van Tellingen (2014). "ABCB1, ABCG2, and PTEN determine the response of glioblastoma to temozolomide and ABT-888 therapy." *Clin Cancer Res* **20**(10): 2703-2713.

- Lindqvist, A., V. Rodriguez-Bravo and R. H. Medema (2009). "The decision to enter mitosis: feedback and redundancy in the mitotic entry network." J Cell Biol **185**(2): 193-202.
- Lischetti, T., G. Zhang, G. G. Sedgwick, V. M. Bolanos-Garcia and J. Nilsson (2014). "The internal Cdc20 binding site in BubR1 facilitates both spindle assembly checkpoint signalling and silencing." Nat Commun **5**: 5563.
- Liu, F., S. Wagner, R. B. Campbell, J. A. Nickerson, C. A. Schiffer and A. H. Ross (2005). "PTEN enters the nucleus by diffusion." J Cell Biochem **96**(2): 221-234.
- Liu, K. and M. J. Czaja (2013). "Regulation of lipid stores and metabolism by lipophagy." Cell Death Differ **20**(1): 3-11.
- Liu, T. and J. Huang (2014). "Quality control of homologous recombination." Cell Mol Life Sci **71**(19): 3779-3797.
- Liu, X., P. Li, P. Widlak, H. Zou, X. Luo, W. T. Garrard and X. Wang (1998). "The 40-kDa subunit of DNA fragmentation factor induces DNA fragmentation and chromatin condensation during apoptosis." Proc Natl Acad Sci U S A **95**(15): 8461-8466.
- Liu, Y. and S. H. Wilson (2012). "DNA base excision repair: a mechanism of trinucleotide repeat expansion." Trends Biochem Sci **37**(4): 162-172.
- Liwak, U., L. E. Jordan, S. D. Von-Holt, P. Singh, J. E. Hanson, I. A. Lorimer, F. Roncaroli and M. Holcik (2013). "Loss of PDCD4 contributes to enhanced chemoresistance in Glioblastoma multiforme through de-repression of Bcl-xL translation." Oncotarget **4**(9): 1365-1372.
- Lombillo, V. A., C. Nislow, T. J. Yen, V. I. Gelfand and J. R. McIntosh (1995). "Antibodies to the kinesin motor domain and CENP-E inhibit microtubule depolymerization-dependent motion of chromosomes in vitro." J Cell Biol **128**(1-2): 107-115.
- London, N. and S. Biggins (2014). "Signalling dynamics in the spindle checkpoint response." Nat Rev Mol Cell Biol **15**(11): 736-747.
- Lonskaya, I., V. N. Potaman, L. S. Shlyakhtenko, E. A. Oussatcheva, Y. L. Lyubchenko and V. A. Soldatenkov (2005). "Regulation of poly(ADP-ribose) polymerase-1 by DNA structure-specific binding." J Biol Chem **280**(17): 17076-17083.
- Loseva, O., A. S. Jemth, H. E. Bryant, H. Schuler, L. Lehtio, T. Karlberg and T. Helleday (2010). "PARP-3 is a mono-ADP-ribosylase that activates PARP-1 in the absence of DNA." J Biol Chem **285**(11): 8054-8060.
- Louis, D. N., H. Ohgaki, O. D. Wiestler, W. K. Cavenee, P. C. Burger, A. Jouvett, B. W. Scheithauer and P. Kleihues (2007). "The 2007 WHO classification of tumours of the central nervous system." Acta Neuropathol **114**(2): 97-109.
- Love, S., R. Barber and G. K. Wilcock (1999). "Increased poly(ADP-ribosylation) of nuclear proteins in Alzheimer's disease." Brain **122** (Pt 2): 247-253.
- Love, S., R. Barber and G. K. Wilcock (1999). "Neuronal accumulation of poly(ADP-ribose) after brain ischaemia." Neuropathol Appl Neurobiol **25**(2): 98-103.

Bibliography

- Love, S., R. Barber and G. K. Wilcock (2000). "Neuronal death in brain infarcts in man." Neuropathol Appl Neurobiol **26**(1): 55-66.
- Luo, X., I. Budihardjo, H. Zou, C. Slaughter and X. Wang (1998). "Bid, a Bcl2 interacting protein, mediates cytochrome c release from mitochondria in response to activation of cell surface death receptors." Cell **94**(4): 481-490.
- Ma, L., Z. Chen, H. Erdjument-Bromage, P. Tempst and P. P. Pandolfi (2005). "Phosphorylation and functional inactivation of TSC2 by Erk implications for tuberous sclerosis and cancer pathogenesis." Cell **121**(2): 179-193.
- Maehama, T. and J. E. Dixon (1998). "The tumor suppressor, PTEN/MMAC1, dephosphorylates the lipid second messenger, phosphatidylinositol 3,4,5-trisphosphate." J Biol Chem **273**(22): 13375-13378.
- Malumbres, M. and M. Barbacid (2005). "Mammalian cyclin-dependent kinases." Trends Biochem Sci **30**(11): 630-641.
- Mao, Y., A. Abrieu and D. W. Cleveland (2003). "Activating and silencing the mitotic checkpoint through CENP-E-dependent activation/inactivation of BubR1." Cell **114**(1): 87-98.
- Mao, Y., A. Desai and D. W. Cleveland (2005). "Microtubule capture by CENP-E silences BubR1-dependent mitotic checkpoint signaling." J Cell Biol **170**(6): 873-880.
- Marino, G. and C. Lopez-Otin (2004). "Autophagy: molecular mechanisms, physiological functions and relevance in human pathology." Cell Mol Life Sci **61**(12): 1439-1454.
- Martin-Oliva, D., R. Aguilar-Quesada, F. O'Valle, J. A. Munoz-Gamez, R. Martinez-Romero, R. Garcia Del Moral, J. M. Ruiz de Almodovar, R. Villuendas, M. A. Piris and F. J. Oliver (2006). "Inhibition of poly(ADP-ribose) polymerase modulates tumor-related gene expression, including hypoxia-inducible factor-1 activation, during skin carcinogenesis." Cancer Res **66**(11): 5744-5756.
- Martin, L. M., B. Marples, M. Coffey, M. Lawler, T. H. Lynch, D. Hollywood and L. Marignol (2010). "DNA mismatch repair and the DNA damage response to ionizing radiation: making sense of apparently conflicting data." Cancer Treat Rev **36**(7): 518-527.
- Massague, J. (2008). "TGFbeta in Cancer." Cell **134**(2): 215-230.
- Masson, J. Y., M. C. Tarsounas, A. Z. Stasiak, A. Stasiak, R. Shah, M. J. McIlwraith, F. E. Benson and S. C. West (2001). "Identification and purification of two distinct complexes containing the five RAD51 paralogs." Genes Dev **15**(24): 3296-3307.
- Masson, M., C. Niedergang, V. Schreiber, S. Muller, J. Menissier-de Murcia and G. de Murcia (1998). "XRCC1 is specifically associated with poly(ADP-ribose) polymerase and negatively regulates its activity following DNA damage." Mol Cell Biol **18**(6): 3563-3571.
- Matsumoto, T., D. J. Baker, L. V. d'Uscio, G. Mozammel, Z. S. Katusic and J. M. van Deursen (2007). "Aging-associated vascular phenotype in mutant mice with low levels of BubR1." Stroke **38**(3): 1050-1056.

- Matsuura, A., M. Tsukada, Y. Wada and Y. Ohsumi (1997). "Apg1p, a novel protein kinase required for the autophagic process in *Saccharomyces cerevisiae*." Gene **192**(2): 245-250.
- Mattox, D. E. and D. D. Von Hoff (1980). "Culture of human head and neck cancer stem cells using soft agar." Arch Otolaryngol **106**(11): 672-674.
- McEllin, B., C. V. Camacho, B. Mukherjee, B. Hahm, N. Tomimatsu, R. M. Bachoo and S. Burma (2010). "PTEN loss compromises homologous recombination repair in astrocytes: implications for glioblastoma therapy with temozolomide or poly(ADP-ribose) polymerase inhibitors." Cancer Res **70**(13): 5457-5464.
- McIntosh, J. R. (1984). "Cell biology. Microtubule catastrophe." Nature **312**(5991): 196-197.
- Mendes-Pereira, A. M., S. A. Martin, R. Brough, A. McCarthy, J. R. Taylor, J. S. Kim, T. Waldman, C. J. Lord and A. Ashworth (2009). "Synthetic lethal targeting of PTEN mutant cells with PARP inhibitors." EMBO Mol Med **1**(6-7): 315-322.
- Menendez, J. A. and R. Lupu (2007). "Fatty acid synthase and the lipogenic phenotype in cancer pathogenesis." Nat Rev Cancer **7**(10): 763-777.
- Menissier-de Murcia, J., M. Molinete, G. Gradwohl, F. Simonin and G. de Murcia (1989). "Zinc-binding domain of poly(ADP-ribose)polymerase participates in the recognition of single strand breaks on DNA." J Mol Biol **210**(1): 229-233.
- Mercer, C. A., A. Kaliappan and P. B. Dennis (2009). "A novel, human Atg13 binding protein, Atg101, interacts with ULK1 and is essential for macroautophagy." Autophagy **5**(5): 649-662.
- Mercer, W. E., M. T. Shields, M. Amin, G. J. Sauve, E. Appella, J. W. Romano and S. J. Ullrich (1990). "Negative growth regulation in a glioblastoma tumor cell line that conditionally expresses human wild-type p53." Proc Natl Acad Sci U S A **87**(16): 6166-6170.
- Meyer-Ficca, M. L., R. G. Meyer, D. L. Coyle, E. L. Jacobson and M. K. Jacobson (2004). "Human poly(ADP-ribose) glycohydrolase is expressed in alternative splice variants yielding isoforms that localize to different cell compartments." Exp Cell Res **297**(2): 521-532.
- Meyer-Ficca, M. L., R. G. Meyer, E. L. Jacobson and M. K. Jacobson (2005). "Poly(ADP-ribose) polymerases: managing genome stability." Int J Biochem Cell Biol **37**(5): 920-926.
- Michel, L., E. Diaz-Rodriguez, G. Narayan, E. Hernando, V. V. Murty and R. Benezra (2004). "Complete loss of the tumor suppressor MAD2 causes premature cyclin B degradation and mitotic failure in human somatic cells." Proc Natl Acad Sci U S A **101**(13): 4459-4464.
- Minaguchi, T., K. A. Waite and C. Eng (2006). "Nuclear localization of PTEN is regulated by Ca(2+) through a tyrosil phosphorylation-independent conformational modification in major vault protein." Cancer Res **66**(24): 11677-11682.
- Minami, D., N. Takigawa, H. Takeda, M. Takata, N. Ochi, E. Ichihara, A. Hisamoto, K. Hotta, M. Tanimoto and K. Kiura (2013). "Synergistic effect of olaparib with combination of cisplatin on PTEN-deficient lung cancer cells." Mol Cancer Res **11**(2): 140-148.

Bibliography

- Ming, G. L. and H. Song (2005). "Adult neurogenesis in the mammalian central nervous system." Annu Rev Neurosci **28**: 223-250.
- Miura, M., H. Zhu, R. Rotello, E. A. Hartwig and J. Yuan (1993). "Induction of apoptosis in fibroblasts by IL-1 beta-converting enzyme, a mammalian homolog of the C. elegans cell death gene ced-3." Cell **75**(4): 653-660.
- Miwa, M. and T. Sugimura (1971). "Splitting of the ribose-ribose linkage of poly(adenosine diphosphate-ribose) by a calf thymus extract." J Biol Chem **246**(20): 6362-6364.
- Mizushima, N., T. Noda and Y. Ohsumi (1999). "Apg16p is required for the function of the Apg12p-Apg5p conjugate in the yeast autophagy pathway." EMBO J **18**(14): 3888-3896.
- Mladenov, E. and G. Iliakis (2011). "Induction and repair of DNA double strand breaks: the increasing spectrum of non-homologous end joining pathways." Mutat Res **711**(1-2): 61-72.
- Munoz-Gamez, J. A., J. M. Rodriguez-Vargas, R. Quiles-Perez, R. Aguilar-Quesada, D. Martin-Oliva, G. de Murcia, J. Menissier de Murcia, A. Almendros, M. Ruiz de Almodovar and F. J. Oliver (2009). "PARP-1 is involved in autophagy induced by DNA damage." Autophagy **5**(1): 61-74.
- Musacchio, A. and E. D. Salmon (2007). "The spindle-assembly checkpoint in space and time." Nat Rev Mol Cell Biol **8**(5): 379-393.
- Muzio, M., A. M. Chinnaiyan, F. C. Kischkel, K. O'Rourke, A. Shevchenko, J. Ni, C. Scaffidi, J. D. Bretz, M. Zhang, R. Gentz, M. Mann, P. H. Krammer, M. E. Peter and V. M. Dixit (1996). "FLICE, a novel FADD-homologous ICE/CED-3-like protease, is recruited to the CD95 (Fas/APO-1) death-inducing signaling complex." Cell **85**(6): 817-827.
- Myers, M. P., J. P. Stolarov, C. Eng, J. Li, S. I. Wang, M. H. Wigler, R. Parsons and N. K. Tonks (1997). "P-TEN, the tumor suppressor from human chromosome 10q23, is a dual-specificity phosphatase." Proc Natl Acad Sci U S A **94**(17): 9052-9057.
- Nakajima, H., Y. Ishikawa, M. Furuya, T. Sano, Y. Ohno, J. Horiguchi and T. Oyama (2014). "Protein expression, gene amplification, and mutational analysis of EGFR in triple-negative breast cancer." Breast Cancer **21**(1): 66-74.
- Nakayama, K. I. and K. Nakayama (2005). "Regulation of the cell cycle by SCF-type ubiquitin ligases." Semin Cell Dev Biol **16**(3): 323-333.
- Negri, C., A. I. Scovassi, A. Cerino, M. Negroni, R. M. Borzi, R. Meliconi, A. Facchini, C. M. Montecucco and G. C. Astaldi Ricotti (1990). "Autoantibodies to poly(ADP-ribose)polymerase in autoimmune diseases." Autoimmunity **6**(3): 203-209.
- Nister, M., T. A. Libermann, C. Betsholtz, M. Pettersson, L. Claesson-Welsh, C. H. Heldin, J. Schlessinger and B. Westermark (1988). "Expression of messenger RNAs for platelet-derived growth factor and transforming growth factor-alpha and their receptors in human malignant glioma cell lines." Cancer Res **48**(14): 3910-3918.

- Nobusawa, S., J. Lachuer, A. Wierinckx, Y. H. Kim, J. Huang, C. Legras, P. Kleihues and H. Ohgaki (2010). "Intratumoral patterns of genomic imbalance in glioblastomas." Brain Pathol **20**(5): 936-944.
- Norbury, C. and P. Nurse (1992). "Animal cell cycles and their control." Annu Rev Biochem **61**: 441-470.
- Nowsheen, S., J. A. Bonner, A. F. Lobuglio, H. Trummell, A. C. Whitley, M. C. Dobelbower and E. S. Yang (2011). "Cetuximab augments cytotoxicity with poly (adp-ribose) polymerase inhibition in head and neck cancer." PLoS One **6**(8): e24148.
- Nowsheen, S., T. Cooper, J. A. Stanley and E. S. Yang (2012). "Synthetic lethal interactions between EGFR and PARP inhibition in human triple negative breast cancer cells." PLoS One **7**(10): e46614.
- O'Driscoll, M., V. L. Ruiz-Perez, C. G. Woods, P. A. Jeggo and J. A. Goodship (2003). "A splicing mutation affecting expression of ataxia-telangiectasia and Rad3-related protein (ATR) results in Seckel syndrome." Nat Genet **33**(4): 497-501.
- O'Farrell, P. H. (2001). "Triggering the all-or-nothing switch into mitosis." Trends Cell Biol **11**(12): 512-519.
- Oberhammer, F., J. W. Wilson, C. Dive, I. D. Morris, J. A. Hickman, A. E. Wakeling, P. R. Walker and M. Sikorska (1993). "Apoptotic death in epithelial cells: cleavage of DNA to 300 and/or 50 kb fragments prior to or in the absence of internucleosomal fragmentation." EMBO J **12**(9): 3679-3684.
- Ogata, N., K. Ueda and O. Hayaishi (1980). "ADP-ribosylation of histone H2B. Identification of glutamic acid residue 2 as the modification site." J Biol Chem **255**(16): 7610-7615.
- Ogata, N., K. Ueda, H. Kagamiyama and O. Hayaishi (1980). "ADP-ribosylation of histone H1. Identification of glutamic acid residues 2, 14, and the COOH-terminal lysine residue as modification sites." J Biol Chem **255**(16): 7616-7620.
- Ohgaki, H. and P. Kleihues (2011). "Genetic profile of astrocytic and oligodendroglial gliomas." Brain Tumor Pathol **28**(3): 177-183.
- Ohgaki, H. and P. Kleihues (2013). "The definition of primary and secondary glioblastoma." Clin Cancer Res **19**(4): 764-772.
- Ohsawa, Y., K. Isahara, S. Kanamori, M. Shibata, S. Kametaka, T. Gotow, T. Watanabe, E. Kominami and Y. Uchiyama (1998). "An ultrastructural and immunohistochemical study of PC12 cells during apoptosis induced by serum deprivation with special reference to autophagy and lysosomal cathepsins." Arch Histol Cytol **61**(5): 395-403.
- Oka, J., K. Ueda, O. Hayaishi, H. Komura and K. Nakanishi (1984). "ADP-ribosyl protein lyase. Purification, properties, and identification of the product." J Biol Chem **259**(2): 986-995.
- Oka, S., J. Kato and J. Moss (2006). "Identification and characterization of a mammalian 39-kDa poly(ADP-ribose) glycohydrolase." J Biol Chem **281**(2): 705-713.
- Okano, S., L. Lan, K. W. Caldecott, T. Mori and A. Yasui (2003). "Spatial and temporal cellular responses to single-strand breaks in human cells." Mol Cell Biol **23**(11): 3974-3981.

Bibliography

- Okano, S., L. Lan, A. E. Tomkinson and A. Yasui (2005). "Translocation of XRCC1 and DNA ligase III α from centrosomes to chromosomes in response to DNA damage in mitotic human cells." Nucleic Acids Res **33**(1): 422-429.
- Okolie, E. E. and S. Shall (1979). "The significance of antibodies to poly(adenosine diphosphate-ribose) in systemic lupus erythematosus." Clin Exp Immunol **36**(1): 151-164.
- Olabisi, O. A., N. Soto-Nieves, E. Nieves, T. T. Yang, X. Yang, R. Y. Yu, H. Y. Suk, F. Macian and C. W. Chow (2008). "Regulation of transcription factor NFAT by ADP-ribosylation." Mol Cell Biol **28**(9): 2860-2871.
- Oliver, F. J., G. de la Rubia, V. Rolli, M. C. Ruiz-Ruiz, G. de Murcia and J. M. Murcia (1998). "Importance of poly(ADP-ribose) polymerase and its cleavage in apoptosis. Lesson from an uncleavable mutant." J Biol Chem **273**(50): 33533-33539.
- Oliver, F. J., J. Menissier-de Murcia, C. Nacci, P. Decker, R. Andriantsitohaina, S. Muller, G. de la Rubia, J. C. Stoclet and G. de Murcia (1999). "Resistance to endotoxic shock as a consequence of defective NF-kappaB activation in poly (ADP-ribose) polymerase-1 deficient mice." EMBO J **18**(16): 4446-4454.
- Oliveri, M., A. Daga, C. Cantoni, C. Lunardi, R. Millo and A. Puccetti (2001). "DNase I mediates internucleosomal DNA degradation in human cells undergoing drug-induced apoptosis." Eur J Immunol **31**(3): 743-751.
- Orsi, A., M. Razi, H. C. Dooley, D. Robinson, A. E. Weston, L. M. Collinson and S. A. Tooze (2012). "Dynamic and transient interactions of Atg9 with autophagosomes, but not membrane integration, are required for autophagy." Mol Biol Cell **23**(10): 1860-1873.
- Overholtzer, M., A. A. Mailleux, G. Mouneimne, G. Normand, S. J. Schnitt, R. W. King, E. S. Cibas and J. S. Brugge (2007). "A nonapoptotic cell death process, entosis, that occurs by cell-in-cell invasion." Cell **131**(5): 966-979.
- Pan, G., K. O'Rourke, A. M. Chinnaiyan, R. Gentz, R. Ebner, J. Ni and V. M. Dixit (1997). "The receptor for the cytotoxic ligand TRAIL." Science **276**(5309): 111-113.
- Panzeter, P. L., C. A. Realini and F. R. Althaus (1992). "Noncovalent interactions of poly(adenosine diphosphate ribose) with histones." Biochemistry **31**(5): 1379-1385.
- Pappas, G., L. A. Zumstein, A. Munshi, M. Hobbs and R. E. Meyn (2007). "Adenoviral-mediated PTEN expression radiosensitizes non-small cell lung cancer cells by suppressing DNA repair capacity." Cancer Gene Ther **14**(6): 543-549.
- Park, M. J., M. S. Kim, I. C. Park, H. S. Kang, H. Yoo, S. H. Park, C. H. Rhee, S. I. Hong and S. H. Lee (2002). "PTEN suppresses hyaluronic acid-induced matrix metalloproteinase-9 expression in U87MG glioblastoma cells through focal adhesion kinase dephosphorylation." Cancer Res **62**(21): 6318-6322.
- Parrish, J., L. Li, K. Klotz, D. Ledwich, X. Wang and D. Xue (2001). "Mitochondrial endonuclease G is important for apoptosis in *C. elegans*." Nature **412**(6842): 90-94.
- Parsons, D. W., S. Jones, X. Zhang, J. C. Lin, R. J. Leary, P. Angenendt, P. Mankoo, H. Carter, I. M. Siu, G. L. Gallia, A. Olivi, R. McLendon, B. A. Rasheed, S. Keir, T. Nikolskaya, Y.

- Nikolsky, D. A. Busam, H. Tekleab, L. A. Diaz, Jr., J. Hartigan, D. R. Smith, R. L. Strausberg, S. K. Marie, S. M. Shinjo, H. Yan, G. J. Riggins, D. D. Bigner, R. Karchin, N. Papadopoulos, G. Parmigiani, B. Vogelstein, V. E. Velculescu and K. W. Kinzler (2008). "An integrated genomic analysis of human glioblastoma multiforme." Science **321**(5897): 1807-1812.
- Patel, M. I., J. Singh, M. Niknami, C. Kurek, M. Yao, S. Lu, F. Maclean, N. J. King, M. H. Gelb, K. F. Scott, P. J. Russell, J. Boulas and Q. Dong (2008). "Cytosolic phospholipase A2-alpha: a potential therapeutic target for prostate cancer." Clin Cancer Res **14**(24): 8070-8079.
- Patru, C., L. Romao, P. Varlet, L. Coulombel, E. Raponi, J. Cadusseau, F. Renault-Mihara, C. Thirant, N. Leonard, A. Berhneim, M. Mihalescu-Maingot, J. Haiech, I. Bieche, V. Moura-Neto, C. Daumas-Duport, M. P. Junier and H. Chneiweiss (2010). "CD133, CD15/SSEA-1, CD34 or side populations do not resume tumor-initiating properties of long-term cultured cancer stem cells from human malignant glio-neuronal tumors." BMC Cancer **10**: 66.
- Pattingre, S., A. Tassa, X. Qu, R. Garuti, X. H. Liang, N. Mizushima, M. Packer, M. D. Schneider and B. Levine (2005). "Bcl-2 antiapoptotic proteins inhibit Beclin 1-dependent autophagy." Cell **122**(6): 927-939.
- Pavlidis, S., I. Vera, R. Gandara, S. Sneddon, R. G. Pestell, I. Mercier, U. E. Martinez-Outschoorn, D. Whitaker-Menezes, A. Howell, F. Sotgia and M. P. Lisanti "Warburg meets autophagy: cancer-associated fibroblasts accelerate tumor growth and metastasis via oxidative stress, mitophagy, and aerobic glycolysis." Antioxid Redox Signal **16**(11): 1264-1284.
- Peitsch, M. C., B. Polzar, H. Stephan, T. Crompton, H. R. MacDonald, H. G. Mannherz and J. Tschopp (1993). "Characterization of the endogenous deoxyribonuclease involved in nuclear DNA degradation during apoptosis (programmed cell death)." EMBO J **12**(1): 371-377.
- Penuelas, S., J. Anido, R. M. Prieto-Sanchez, G. Folch, I. Barba, I. Cuartas, D. Garcia-Dorado, M. A. Poca, J. Sahuquillo, J. Baselga and J. Seoane (2009). "TGF-beta increases glioma-initiating cell self-renewal through the induction of LIF in human glioblastoma." Cancer Cell **15**(4): 315-327.
- Peralta-Leal, A., J. M. Rodriguez-Vargas, R. Aguilar-Quesada, M. I. Rodriguez, J. L. Linares, M. R. de Almodovar and F. J. Oliver (2009). "PARP inhibitors: new partners in the therapy of cancer and inflammatory diseases." Free Radic Biol Med **47**(1): 13-26.
- Petermann, E., C. Keil and S. L. Oei (2005). "Importance of poly(ADP-ribose) polymerases in the regulation of DNA-dependent processes." Cell Mol Life Sci **62**(7-8): 731-738.
- Petiot, A., E. Ogier-Denis, E. F. Blommaert, A. J. Meijer and P. Codogno (2000). "Distinct classes of phosphatidylinositol 3'-kinases are involved in signaling pathways that control macroautophagy in HT-29 cells." J Biol Chem **275**(2): 992-998.
- Phillips, H. S., S. Kharbanda, R. Chen, W. F. Forrest, R. H. Soriano, T. D. Wu, A. Misra, J. M. Nigro, H. Colman, L. Soroceanu, P. M. Williams, Z. Modrusan, B. G. Feuerstein and K. Aldape (2006). "Molecular subclasses of high-grade glioma predict prognosis, delineate a pattern of disease progression, and resemble stages in neurogenesis." Cancer Cell **9**(3): 157-173.

Bibliography

- Piccirillo, S. G., B. A. Reynolds, N. Zanetti, G. Lamorte, E. Binda, G. Broggi, H. Brem, A. Olivi, F. Dimeco and A. L. Vescovi (2006). "Bone morphogenetic proteins inhibit the tumorigenic potential of human brain tumour-initiating cells." Nature **444**(7120): 761-765.
- Pillai, J. B., H. M. Russell, J. Raman, V. Jeevanandam and M. P. Gupta (2005). "Increased expression of poly(ADP-ribose) polymerase-1 contributes to caspase-independent myocyte cell death during heart failure." Am J Physiol Heart Circ Physiol **288**(2): H486-496.
- Pleschke, J. M., H. E. Kleczkowska, M. Strohm and F. R. Althaus (2000). "Poly(ADP-ribose) binds to specific domains in DNA damage checkpoint proteins." J Biol Chem **275**(52): 40974-40980.
- Plummer, R., C. Jones, M. Middleton, R. Wilson, J. Evans, A. Olsen, N. Curtin, A. Boddy, P. McHugh, D. Newell, A. Harris, P. Johnson, H. Steinfeldt, R. Dewji, D. Wang, L. Robson and H. Calvert (2008). "Phase I study of the poly(ADP-ribose) polymerase inhibitor, AG014699, in combination with temozolomide in patients with advanced solid tumors." Clin Cancer Res **14**(23): 7917-7923.
- Poirier, G. G., G. de Murcia, J. Jongstra-Bilen, C. Niedergang and P. Mandel (1982). "Poly(ADP-ribosyl)ation of polynucleosomes causes relaxation of chromatin structure." Proc Natl Acad Sci U S A **79**(11): 3423-3427.
- Polo, S. E. and S. P. Jackson (2011). "Dynamics of DNA damage response proteins at DNA breaks: a focus on protein modifications." Genes Dev **25**(5): 409-433.
- Pop, C. and G. S. Salvesen (2009). "Human caspases: activation, specificity, and regulation." J Biol Chem **284**(33): 21777-21781.
- Price, D. J., J. R. Grove, V. Calvo, J. Avruch and B. E. Bierer (1992). "Rapamycin-induced inhibition of the 70-kilodalton S6 protein kinase." Science **257**(5072): 973-977.
- Puc, J., M. Keniry, H. S. Li, T. K. Pandita, A. D. Choudhury, L. Memeo, M. Mansukhani, V. V. Murty, Z. Gaciong, S. E. Meek, H. Piwnica-Worms, H. Hibshoosh and R. Parsons (2005). "Lack of PTEN sequesters CHK1 and initiates genetic instability." Cancer Cell **7**(2): 193-204.
- Puc, J. and R. Parsons (2005). "PTEN loss inhibits CHK1 to cause double stranded-DNA breaks in cells." Cell Cycle **4**(7): 927-929.
- Purnell, M. R. and W. J. Whish (1980). "Novel inhibitors of poly(ADP-ribose) synthetase." Biochem J **185**(3): 775-777.
- Pyo, J. O., J. Nah and Y. K. Jung (2012). "Molecules and their functions in autophagy." Exp Mol Med **44**(2): 73-80.
- Quenet, D., V. Gasser, L. Fouillen, F. Cammas, S. Sanglier-Cianferani, R. Losson and F. Dantzer (2008). "The histone subcode: poly(ADP-ribose) polymerase-1 (Parp-1) and Parp-2 control cell differentiation by regulating the transcriptional intermediary factor TIF1beta and the heterochromatin protein HP1alpha." FASEB J **22**(11): 3853-3865.

- Rahman, L., D. Voeller, M. Rahman, S. Lipkowitz, C. Allegra, J. C. Barrett, F. J. Kaye and M. Zajac-Kaye (2004). "Thymidylate synthase as an oncogene: a novel role for an essential DNA synthesis enzyme." Cancer Cell **5**(4): 341-351.
- Reed, S. I. (2003). "Ratchets and clocks: the cell cycle, ubiquitylation and protein turnover." Nat Rev Mol Cell Biol **4**(11): 855-864.
- Reya, T., S. J. Morrison, M. F. Clarke and I. L. Weissman (2001). "Stem cells, cancer, and cancer stem cells." Nature **414**(6859): 105-111.
- Reynolds, B. A. and S. Weiss (1992). "Generation of neurons and astrocytes from isolated cells of the adult mammalian central nervous system." Science **255**(5052): 1707-1710.
- Ricke, R. M. and J. M. van Deursen (2013). "Aneuploidy in health, disease, and aging." J Cell Biol **201**(1): 11-21.
- Rieder, C. L. (2011). "Mitosis in vertebrates: the G2/M and M/A transitions and their associated checkpoints." Chromosome Res **19**(3): 291-306.
- Riffell, J. L., C. J. Lord and A. Ashworth (2012). "Tankyrase-targeted therapeutics: expanding opportunities in the PARP family." Nat Rev Drug Discov **11**(12): 923-936.
- Robaszekiewicz, A., Z. Valko, K. Kovacs, C. Hegedus, E. Bakondi, P. Bai and L. Virag (2014). "The role of p38 signaling and poly(ADP-ribose)ation-induced metabolic collapse in the osteogenic differentiation-coupled cell death pathway." Free Radic Biol Med **76**: 69-79.
- Robertson, A. M., C. C. Bird, A. W. Waddell and A. R. Currie (1978). "Morphological aspects of glucocorticoid-induced cell death in human lymphoblastoid cells." J Pathol **126**(3): 181-187.
- Rodriguez-Vargas, J. M., M. J. Ruiz-Magana, C. Ruiz-Ruiz, J. Majuelos-Melguizo, A. Peralta-Leal, M. I. Rodriguez, J. A. Munoz-Gamez, M. R. de Almodovar, E. Siles, A. L. Rivas, M. Jaattela and F. J. Oliver (2012). "ROS-induced DNA damage and PARP-1 are required for optimal induction of starvation-induced autophagy." Cell Res **22**(7): 1181-1198.
- Rodriguez, M. I., A. Gonzalez-Flores, F. Dantzer, J. Collard, A. G. de Herreros and F. J. Oliver (2011). "Poly(ADP-ribose)-dependent regulation of Snail1 protein stability." Oncogene **30**(42): 4365-4372.
- Rodriguez, M. I., A. Peralta-Leal, F. O'Valle, J. M. Rodriguez-Vargas, A. Gonzalez-Flores, J. Majuelos-Melguizo, L. Lopez, S. Serrano, A. G. de Herreros, J. C. Rodriguez-Manzaneque, R. Fernandez, R. G. Del Moral, J. M. de Almodovar and F. J. Oliver (2013). "PARP-1 regulates metastatic melanoma through modulation of vimentin-induced malignant transformation." PLoS Genet **9**(6): e1003531.
- Rouleau, M., A. Patel, M. J. Hendzel, S. H. Kaufmann and G. G. Poirier (2010). "PARP inhibition: PARP1 and beyond." Nat Rev Cancer **10**(4): 293-301.
- Ruf, A., J. Mennissier de Murcia, G. de Murcia and G. E. Schulz (1996). "Structure of the catalytic fragment of poly(AD-ribose) polymerase from chicken." Proc Natl Acad Sci U S A **93**(15): 7481-7485.

Bibliography

- Russell, P. and P. Nurse (1986). "Schizosaccharomyces pombe and Saccharomyces cerevisiae: a look at yeasts divided." Cell **45**(6): 781-782.
- Saelens, X., N. Festjens, L. Vande Walle, M. van Gorp, G. van Loo and P. Vandenabeele (2004). "Toxic proteins released from mitochondria in cell death." Oncogene **23**(16): 2861-2874.
- Sala, A., G. La Rocca, G. Burgio, E. Kotova, D. Di Gesu, M. Collesano, A. M. Ingrassia, A. V. Tulin and D. F. Corona (2008). "The nucleosome-remodeling ATPase ISWI is regulated by poly-ADP-ribosylation." PLoS Biol **6**(10): e252.
- Salazar, M., A. Carracedo, I. J. Salanueva, S. Hernandez-Tiedra, M. Lorente, A. Egia, P. Vazquez, C. Blazquez, S. Torres, S. Garcia, J. Nowak, G. M. Fimia, M. Piacentini, F. Cecconi, P. P. Pandolfi, L. Gonzalez-Feria, J. L. Iovanna, M. Guzman, P. Boya and G. Velasco (2009). "Cannabinoid action induces autophagy-mediated cell death through stimulation of ER stress in human glioma cells." J Clin Invest **119**(5): 1359-1372.
- Sanai, N., A. Alvarez-Buylla and M. S. Berger (2005). "Neural stem cells and the origin of gliomas." N Engl J Med **353**(8): 811-822.
- Sanson, M., F. J. Hosking, S. Shete, D. Zelenika, S. E. Dobbins, Y. Ma, V. Enciso-Mora, A. Idbaih, J. Y. Delattre, K. Hoang-Xuan, Y. Marie, B. Boisselier, C. Carpentier, X. W. Wang, A. L. Di Stefano, M. Labussiere, K. Gousias, J. Schramm, A. Boland, D. Lechner, I. Gut, G. Armstrong, Y. Liu, R. Yu, C. Lau, M. C. Di Bernardo, L. B. Robertson, K. Muir, S. Hepworth, A. Swerdlow, M. J. Schoemaker, H. E. Wichmann, M. Muller, S. Schreiber, A. Franke, S. Moebus, L. Eisele, A. Forsti, K. Hemminki, M. Lathrop, M. Bondy, R. S. Houlston and M. Simon (2011). "Chromosome 7p11.2 (EGFR) variation influences glioma risk." Hum Mol Genet **20**(14): 2897-2904.
- Santaguida, S. and A. Musacchio (2009). "The life and miracles of kinetochores." EMBO J **28**(17): 2511-2531.
- Sarbassov, D. D., D. A. Guertin, S. M. Ali and D. M. Sabatini (2005). "Phosphorylation and regulation of Akt/PKB by the rictor-mTOR complex." Science **307**(5712): 1098-1101.
- Sartori, A. A., C. Lukas, J. Coates, M. Mistrik, S. Fu, J. Bartek, R. Baer, J. Lukas and S. P. Jackson (2007). "Human CtIP promotes DNA end resection." Nature **450**(7169): 509-514.
- Sauermann, G. and J. Wesierska-Gadek (1986). "Poly(ADP-ribose) effectively competes with DNA for histone H4 binding." Biochem Biophys Res Commun **139**(2): 523-529.
- Saxena, A., R. Saffery, L. H. Wong, P. Kalitsis and K. H. Choo (2002). "Centromere proteins Cenpa, Cenpb, and Bub3 interact with poly(ADP-ribose) polymerase-1 protein and are poly(ADP-ribosyl)ated." J Biol Chem **277**(30): 26921-26926.
- Saxena, A., L. H. Wong, P. Kalitsis, E. Earle, L. G. Shaffer and K. H. Choo (2002). "Poly(ADP-ribose) polymerase 2 localizes to mammalian active centromeres and interacts with PARP-1, Cenpa, Cenpb and Bub3, but not Cenpc." Hum Mol Genet **11**(19): 2319-2329.
- Scaffidi, C., S. Fulda, A. Srinivasan, C. Friesen, F. Li, K. J. Tomaselli, K. M. Debatin, P. H. Kramer and M. E. Peter (1998). "Two CD95 (APO-1/Fas) signaling pathways." EMBO J **17**(6): 1675-1687.

- Scaffidi, C., I. Schmitz, P. H. Krammer and M. E. Peter (1999). "The role of c-FLIP in modulation of CD95-induced apoptosis." J Biol Chem **274**(3): 1541-1548.
- Schreiber, V., F. Dantzer, J. C. Ame and G. de Murcia (2006). "Poly(ADP-ribose): novel functions for an old molecule." Nat Rev Mol Cell Biol **7**(7): 517-528.
- Schreiber, V., M. Molinete, H. Boeuf, G. de Murcia and J. Menissier-de Murcia (1992). "The human poly(ADP-ribose) polymerase nuclear localization signal is a bipartite element functionally separate from DNA binding and catalytic activity." EMBO J **11**(9): 3263-3269.
- Schweichel, J. U. and H. J. Merker (1973). "The morphology of various types of cell death in prenatal tissues." Teratology **7**(3): 253-266.
- Seglen, P. O., P. B. Gordon and I. Holen (1990). "Non-selective autophagy." Semin Cell Biol **1**(6): 441-448.
- Sgorbissa, A., A. Tomasella, H. Potu, I. Manini and C. Brancolini (2011). "Type I IFNs signaling and apoptosis resistance in glioblastoma cells." Apoptosis **16**(12): 1229-1244.
- Shackelford, D. B. and R. J. Shaw (2009). "The LKB1-AMPK pathway: metabolism and growth control in tumour suppression." Nat Rev Cancer **9**(8): 563-575.
- Shaltiel, I. A., L. Krenning, W. Bruinsma and R. H. Medema (2015). "The same, only different - DNA damage checkpoints and their reversal throughout the cell cycle." J Cell Sci **128**(4): 607-620.
- Shen, W. H., A. S. Balajee, J. Wang, H. Wu, C. Eng, P. P. Pandolfi and Y. Yin (2007). "Essential role for nuclear PTEN in maintaining chromosomal integrity." Cell **128**(1): 157-170.
- Sherry, M. M., A. Reeves, J. K. Wu and B. H. Cochran (2009). "STAT3 is required for proliferation and maintenance of multipotency in glioblastoma stem cells." Stem Cells **27**(10): 2383-2392.
- Shete, S., F. J. Hosking, L. B. Robertson, S. E. Dobbins, M. Sanson, B. Malmer, M. Simon, Y. Marie, B. Boisselier, J. Y. Delattre, K. Hoang-Xuan, S. El Hallani, A. Idbah, D. Zelenika, U. Andersson, R. Henriksson, A. T. Bergenheim, M. Feychting, S. Lonn, A. Ahlbom, J. Schramm, M. Linnebank, K. Hemminki, R. Kumar, S. J. Hepworth, A. Price, G. Armstrong, Y. Liu, X. Gu, R. Yu, C. Lau, M. Schoemaker, K. Muir, A. Swerdlow, M. Lathrop, M. Bondy and R. S. Houlston (2009). "Genome-wide association study identifies five susceptibility loci for glioma." Nat Genet **41**(8): 899-904.
- Simbulan-Rosenthal, C. M., B. R. Haddad, D. S. Rosenthal, Z. Weaver, A. Coleman, R. Luo, H. M. Young, Z. Q. Wang, T. Ried and M. E. Smulson (1999). "Chromosomal aberrations in PARP(-/-) mice: genome stabilization in immortalized cells by reintroduction of poly(ADP-ribose) polymerase cDNA." Proc Natl Acad Sci U S A **96**(23): 13191-13196.
- Simbulan-Rosenthal, C. M., D. S. Rosenthal, H. Hilz, R. Hickey, L. Malkas, N. Applegren, Y. Wu, G. Bers and M. E. Smulson (1996). "The expression of poly(ADP-ribose) polymerase during differentiation-linked DNA replication reveals that it is a component of the multiprotein DNA replication complex." Biochemistry **35**(36): 11622-11633.

Bibliography

- Singh, R. and A. M. Cuervo (2012). "Lipophagy: connecting autophagy and lipid metabolism." Int J Cell Biol **2012**: 282041.
- Singh, R., S. Kaushik, Y. Wang, Y. Xiang, I. Novak, M. Komatsu, K. Tanaka, A. M. Cuervo and M. J. Czaja (2009). "Autophagy regulates lipid metabolism." Nature **458**(7242): 1131-1135.
- Singh, S. K., I. D. Clarke, M. Terasaki, V. E. Bonn, C. Hawkins, J. Squire and P. B. Dirks (2003). "Identification of a cancer stem cell in human brain tumors." Cancer Res **63**(18): 5821-5828.
- Smith, S., I. Gariat, A. Schmitt and T. de Lange (1998). "Tankyrase, a poly(ADP-ribose) polymerase at human telomeres." Science **282**(5393): 1484-1487.
- Soltanian, S. and M. M. Matin (2011). "Cancer stem cells and cancer therapy." Tumour Biol **32**(3): 425-440.
- Song, M. S., A. Carracedo, L. Salmena, S. J. Song, A. Egia, M. Malumbres and P. P. Pandolfi (2011). "Nuclear PTEN regulates the APC-CDH1 tumor-suppressive complex in a phosphatase-independent manner." Cell **144**(2): 187-199.
- Soos, J., J. I. Engelhardt, L. Siklos, L. Havas and K. Majtenyi (2004). "The expression of PARP, NF-kappa B and parvalbumin is increased in Parkinson disease." Neuroreport **15**(11): 1715-1718.
- Soriano, F. G., A. C. Nogueira, E. G. Caldini, M. H. Lins, A. C. Teixeira, S. B. Cappi, P. A. Lotufo, M. M. Bernik, Z. Zsengeller, M. Chen and C. Szabo (2006). "Potential role of poly(adenosine 5'-diphosphate-ribose) polymerase activation in the pathogenesis of myocardial contractile dysfunction associated with human septic shock." Crit Care Med **34**(4): 1073-1079.
- Sphyris, N. and D. J. Harrison (2005). "p53 deficiency exacerbates pleiotropic mitotic defects, changes in nuclearity and polyploidy in transdifferentiating pancreatic acinar cells." Oncogene **24**(13): 2184-2194.
- Stambolic, V., A. Suzuki, J. L. de la Pompa, G. M. Brothers, C. Mirtsos, T. Sasaki, J. Ruland, J. M. Penninger, D. P. Siderovski and T. W. Mak (1998). "Negative regulation of PKB/Akt-dependent cell survival by the tumor suppressor PTEN." Cell **95**(1): 29-39.
- Stechishin, O. D., H. A. Luchman, Y. Ruan, M. D. Blough, S. A. Nguyen, J. J. Kelly, J. G. Cairncross and S. Weiss (2013). "On-target JAK2/STAT3 inhibition slows disease progression in orthotopic xenografts of human glioblastoma brain tumor stem cells." Neuro Oncol **15**(2): 198-207.
- Stegh, A. H., H. Kim, R. M. Bachoo, K. L. Forloney, J. Zhang, H. Schulze, K. Park, G. J. Hannon, J. Yuan, D. N. Louis, R. A. DePinho and L. Chin (2007). "Bcl2L12 inhibits post-mitochondrial apoptosis signaling in glioblastoma." Genes Dev **21**(1): 98-111.
- Stracker, T. H. and J. H. Petrini (2011). "The MRE11 complex: starting from the ends." Nat Rev Mol Cell Biol **12**(2): 90-103.

- Strom, C. E., F. Johansson, M. Uhlen, C. A. Szigartyo, K. Erixon and T. Helleday (2011). "Poly (ADP-ribose) polymerase (PARP) is not involved in base excision repair but PARP inhibition traps a single-strand intermediate." Nucleic Acids Res **39**(8): 3166-3175.
- Stummer, W., U. Pichlmeier, T. Meinel, O. D. Wiestler, F. Zanella and H. J. Reulen (2006). "Fluorescence-guided surgery with 5-aminolevulinic acid for resection of malignant glioma: a randomised controlled multicentre phase III trial." Lancet Oncol **7**(5): 392-401.
- Stupp, R., W. P. Mason, M. J. van den Bent, M. Weller, B. Fisher, M. J. Taphoorn, K. Belanger, A. A. Brandes, C. Marosi, U. Bogdahn, J. Curschmann, R. C. Janzer, S. K. Ludwin, T. Gorlia, A. Allgeier, D. Lacombe, J. G. Cairncross, E. Eisenhauer and R. O. Mirimanoff (2005). "Radiotherapy plus concomitant and adjuvant temozolomide for glioblastoma." N Engl J Med **352**(10): 987-996.
- Stupp, R. and E. Newlands (2001). "New approaches for temozolomide therapy: use in newly diagnosed glioma." Semin Oncol **28**(4 Suppl 13): 19-23.
- Su, T. T. (2006). "Cellular responses to DNA damage: one signal, multiple choices." Annu Rev Genet **40**: 187-208.
- Sudakin, V., G. K. Chan and T. J. Yen (2001). "Checkpoint inhibition of the APC/C in HeLa cells is mediated by a complex of BUBR1, BUB3, CDC20, and MAD2." J Cell Biol **154**(5): 925-936.
- Suijkerbuijk, S. J., M. H. van Osch, F. L. Bos, S. Hanks, N. Rahman and G. J. Kops (2010). "Molecular causes for BUBR1 dysfunction in the human cancer predisposition syndrome mosaic variegated aneuploidy." Cancer Res **70**(12): 4891-4900.
- Suijkerbuijk, S. J., M. Vleugel, A. Teixeira and G. J. Kops (2012). "Integration of kinase and phosphatase activities by BUBR1 ensures formation of stable kinetochore-microtubule attachments." Dev Cell **23**(4): 745-755.
- Susin, S. A., H. K. Lorenzo, N. Zamzami, I. Marzo, B. E. Snow, G. M. Brothers, J. Mangion, E. Jacotot, P. Costantini, M. Loeffler, N. Larochette, D. R. Goodlett, R. Aebersold, D. P. Siderovski, J. M. Penninger and G. Kroemer (1999). "Molecular characterization of mitochondrial apoptosis-inducing factor." Nature **397**(6718): 441-446.
- Sutherland, G. R. (1979). "Heritable fragile sites on human chromosomes I. Factors affecting expression in lymphocyte culture." Am J Hum Genet **31**(2): 125-135.
- Suwaki, N., K. Klare and M. Tarsounas (2011). "RAD51 paralogs: roles in DNA damage signalling, recombinational repair and tumorigenesis." Semin Cell Dev Biol **22**(8): 898-905.
- Suzuki, H., Y. Tanaka, D. T. Buonamassa, B. Farina and E. Leone (1987). "Inhibition of ADP-ribosylation of histone H1 by analogs of diadenosine 5',5'''-p1,p4-tetraphosphate." Mol Cell Biochem **74**(1): 17-20.
- Suzuki, K., M. Ojima, S. Kodama and M. Watanabe (2003). "Radiation-induced DNA damage and delayed induced genomic instability." Oncogene **22**(45): 6988-6993.
- Suzuki, M., Y. Shinohara, Y. Ohsaki and T. Fujimoto (2011). "Lipid droplets: size matters." J Electron Microsc (Tokyo) **60 Suppl 1**: S101-116.

Bibliography

- Suzuki, Y., Y. Imai, H. Nakayama, K. Takahashi, K. Takio and R. Takahashi (2001). "A serine protease, HtrA2, is released from the mitochondria and interacts with XIAP, inducing cell death." Mol Cell **8**(3): 613-621.
- Takeshige, K., M. Baba, S. Tsuboi, T. Noda and Y. Ohsumi (1992). "Autophagy in yeast demonstrated with proteinase-deficient mutants and conditions for its induction." J Cell Biol **119**(2): 301-311.
- Tamura, M., J. Gu, K. Matsumoto, S. Aota, R. Parsons and K. M. Yamada (1998). "Inhibition of cell migration, spreading, and focal adhesions by tumor suppressor PTEN." Science **280**(5369): 1614-1617.
- Tanaka, Y., G. Guhde, A. Suter, E. L. Eskelinen, D. Hartmann, R. Lullmann-Rauch, P. M. Janssen, J. Blanz, K. von Figura and P. Saftig (2000). "Accumulation of autophagic vacuoles and cardiomyopathy in LAMP-2-deficient mice." Nature **406**(6798): 902-906.
- Tang, J. B., D. Svilar, R. N. Trivedi, X. H. Wang, E. M. Goellner, B. Moore, R. L. Hamilton, L. A. Banze, A. R. Brown and R. W. Sobol (2011). "N-methylpurine DNA glycosylase and DNA polymerase beta modulate BER inhibitor potentiation of glioma cells to temozolomide." Neuro Oncol **13**(5): 471-486.
- Tentori, L., L. Ricci-Vitiani, A. Muzi, F. Ciccarone, F. Pelacchi, R. Calabrese, D. Runci, R. Pallini, P. Caiafa and G. Graziani (2014). "Pharmacological inhibition of poly(ADP-ribose) polymerase-1 modulates resistance of human glioblastoma stem cells to temozolomide." BMC Cancer **14**: 151.
- Terasawa, M., A. Shinohara and M. Shinohara (2014). "Double-strand break repair-adox: Restoration of suppressed double-strand break repair during mitosis induces genomic instability." Cancer Sci **105**(12): 1519-1525.
- Thiele, C. and J. Spandl (2008). "Cell biology of lipid droplets." Curr Opin Cell Biol **20**(4): 378-385.
- Tilly, J. L. (2001). "Commuting the death sentence: how oocytes strive to survive." Nat Rev Mol Cell Biol **2**(11): 838-848.
- Timinszky, G., S. Till, P. O. Hassa, M. Hothorn, G. Kustatscher, B. Nijmeijer, J. Colombelli, M. Altmeyer, E. H. Stelzer, K. Scheffzek, M. O. Hottiger and A. G. Ladurner (2009). "A macrodomain-containing histone rearranges chromatin upon sensing PARP1 activation." Nat Struct Mol Biol **16**(9): 923-929.
- Toyoshima, F., S. Matsumura, H. Morimoto, M. Mitsushima and E. Nishida (2007). "PtdIns(3,4,5)P3 regulates spindle orientation in adherent cells." Dev Cell **13**(6): 796-811.
- Trauth, B. C., C. Klas, A. M. Peters, S. Matzku, P. Moller, W. Falk, K. M. Debatin and P. H. Krammer (1989). "Monoclonal antibody-mediated tumor regression by induction of apoptosis." Science **245**(4915): 301-305.
- Trotman, L. C., X. Wang, A. Alimonti, Z. Chen, J. Teruya-Feldstein, H. Yang, N. P. Pavletich, B. S. Carver, C. Cordon-Cardo, H. Erdjument-Bromage, P. Tempst, S. G. Chi, H. J. Kim, T. Misteli, X. Jiang and P. P. Pandolfi (2007). "Ubiquitination regulates PTEN nuclear import and tumor suppression." Cell **128**(1): 141-156.

- Tsujimoto, Y., L. R. Finger, J. Yunis, P. C. Nowell and C. M. Croce (1984). "Cloning of the chromosome breakpoint of neoplastic B cells with the t(14;18) chromosome translocation." Science **226**(4678): 1097-1099.
- Tsukada, M. and Y. Ohsumi (1993). "Isolation and characterization of autophagy-defective mutants of *Saccharomyces cerevisiae*." FEBS Lett **333**(1-2): 169-174.
- Tulin, A. and A. Spradling (2003). "Chromatin loosening by poly(ADP)-ribose polymerase (PARP) at *Drosophila* puff loci." Science **299**(5606): 560-562.
- Uchida, K., S. Hanai, K. Ishikawa, Y. Ozawa, M. Uchida, T. Sugimura and M. Miwa (1993). "Cloning of cDNA encoding *Drosophila* poly(ADP-ribose) polymerase: leucine zipper in the auto-modification domain." Proc Natl Acad Sci U S A **90**(8): 3481-3485.
- Vakifahmetoglu, H., M. Olsson and B. Zhivotovsky (2008). "Death through a tragedy: mitotic catastrophe." Cell Death Differ **15**(7): 1153-1162.
- Van Meir, E. G., C. G. Hadjipanayis, A. D. Norden, H. K. Shu, P. Y. Wen and J. J. Olson (2010). "Exciting new advances in neuro-oncology: the avenue to a cure for malignant glioma." CA Cancer J Clin **60**(3): 166-193.
- Vaziri, H., M. D. West, R. C. Allsopp, T. S. Davison, Y. S. Wu, C. H. Arrowsmith, G. G. Poirier and S. Benchimol (1997). "ATM-dependent telomere loss in aging human diploid fibroblasts and DNA damage lead to the post-translational activation of p53 protein involving poly(ADP-ribose) polymerase." EMBO J **16**(19): 6018-6033.
- Vecchio, D., A. Daga, E. Carra, D. Marubbi, G. Baio, C. E. Neumaier, S. Vagge, R. Corvo, M. Pia Brisigotti, J. Louis Ravetti, A. Zunino, A. Poggi, S. Mascelli, A. Raso and G. Frosina (2014). "Predictability, efficacy and safety of radiosensitization of glioblastoma-initiating cells by the ATM inhibitor KU-60019." Int J Cancer **135**(2): 479-491.
- Venere, M., P. Hamerlik, Q. Wu, R. D. Rasmussen, L. A. Song, A. Vasanji, N. Tenley, W. A. Flavahan, A. B. Hjelmeland, J. Bartek and J. N. Rich (2014). "Therapeutic targeting of constitutive PARP activation compromises stem cell phenotype and survival of glioblastoma-initiating cells." Cell Death Differ **21**(2): 258-269.
- Verhaak, R. G., K. A. Hoadley, E. Purdom, V. Wang, Y. Qi, M. D. Wilkerson, C. R. Miller, L. Ding, T. Golub, J. P. Mesirov, G. Alexe, M. Lawrence, M. O'Kelly, P. Tamayo, B. A. Weir, S. Gabriel, W. Winckler, S. Gupta, L. Jakkula, H. S. Feiler, J. G. Hodgson, C. D. James, J. N. Sarkaria, C. Brennan, A. Kahn, P. T. Spellman, R. K. Wilson, T. P. Speed, J. W. Gray, M. Meyerson, G. Getz, C. M. Perou and D. N. Hayes (2010). "Integrated genomic analysis identifies clinically relevant subtypes of glioblastoma characterized by abnormalities in PDGFRA, IDH1, EGFR, and NF1." Cancer Cell **17**(1): 98-110.
- Vescovi, A. L., R. Galli and B. A. Reynolds (2006). "Brain tumour stem cells." Nat Rev Cancer **6**(6): 425-436.
- Veto, S., P. Acs, J. Bauer, H. Lassmann, Z. Berente, G. Setalo, Jr., G. Borgulya, B. Sumegi, S. Komoly, F. Gallyas, Jr. and Z. Illes (2010). "Inhibiting poly(ADP-ribose) polymerase: a potential therapy against oligodendrocyte death." Brain **133**(Pt 3): 822-834.

Bibliography

- Vezina, C., A. Kudelski and S. N. Sehgal (1975). "Rapamycin (AY-22,989), a new antifungal antibiotic. I. Taxonomy of the producing streptomycete and isolation of the active principle." J Antibiot (Tokyo) **28**(10): 721-726.
- Virag, L., A. Robaszekiewicz, J. M. Rodriguez-Vargas and F. J. Oliver (2013). "Poly(ADP-ribose) signaling in cell death." Mol Aspects Med **34**(6): 1153-1167.
- Virag, L. and C. Szabo (2002). "The therapeutic potential of poly(ADP-ribose) polymerase inhibitors." Pharmacol Rev **54**(3): 375-429.
- Vitale, I., L. Galluzzi, M. Castedo and G. Kroemer (2011). "Mitotic catastrophe: a mechanism for avoiding genomic instability." Nat Rev Mol Cell Biol **12**(6): 385-392.
- von Kobbe, C., J. A. Harrigan, V. Schreiber, P. Stiegler, J. Piotrowski, L. Dawut and V. A. Bohr (2004). "Poly(ADP-ribose) polymerase 1 regulates both the exonuclease and helicase activities of the Werner syndrome protein." Nucleic Acids Res **32**(13): 4003-4014.
- Wang, H., H. Wang, W. Zhang, H. J. Huang, W. S. Liao and G. N. Fuller (2004). "Analysis of the activation status of Akt, NFkappaB, and Stat3 in human diffuse gliomas." Lab Invest **84**(8): 941-951.
- Wang, M., W. Wu, W. Wu, B. Rosidi, L. Zhang, H. Wang and G. Iliakis (2006). "PARP-1 and Ku compete for repair of DNA double strand breaks by distinct NHEJ pathways." Nucleic Acids Res **34**(21): 6170-6182.
- Wang, S. Y., Q. J. Yu, R. D. Zhang and B. Liu (2011). "Core signaling pathways of survival/death in autophagy-related cancer networks." Int J Biochem Cell Biol **43**(9): 1263-1266.
- Wang, X. and X. Jiang (2008). "PTEN: a default gate-keeping tumor suppressor with a versatile tail." Cell Res **18**(8): 807-816.
- Wang, Y., V. L. Dawson and T. M. Dawson (2009). "Poly(ADP-ribose) signals to mitochondrial AIF: a key event in parthanatos." Exp Neurol **218**(2): 193-202.
- Wang, Y., N. S. Kim, J. F. Haince, H. C. Kang, K. K. David, S. A. Andrabi, G. G. Poirier, V. L. Dawson and T. M. Dawson (2011). "Poly(ADP-ribose) (PAR) binding to apoptosis-inducing factor is critical for PAR polymerase-1-dependent cell death (parthanatos)." Sci Signal **4**(167): ra20.
- Warburg, O. (1956). "On the origin of cancer cells." Science **123**(3191): 309-314.
- Watanabe, K., O. Tachibana, K. Sata, Y. Yonekawa, P. Kleihues and H. Ohgaki (1996). "Overexpression of the EGF receptor and p53 mutations are mutually exclusive in the evolution of primary and secondary glioblastomas." Brain Pathol **6**(3): 217-223; discussion 223-214.
- Watanabe, N., H. Arai, Y. Nishihara, M. Taniguchi, N. Watanabe, T. Hunter and H. Osada (2004). "M-phase kinases induce phospho-dependent ubiquitination of somatic Wee1 by SCFbeta-TrCP." Proc Natl Acad Sci U S A **101**(13): 4419-4424.
- Waterman, W. H., T. F. Molski, C. K. Huang, J. L. Adams and R. I. Sha'afi (1996). "Tumour necrosis factor-alpha-induced phosphorylation and activation of cytosolic phospholipase

- A2 are abrogated by an inhibitor of the p38 mitogen-activated protein kinase cascade in human neutrophils." Biochem J **319** (Pt 1): 17-20.
- Weinstock, D. M., K. Nakanishi, H. R. Helgadottir and M. Jasin (2006). "Assaying double-strand break repair pathway choice in mammalian cells using a targeted endonuclease or the RAG recombinase." Methods Enzymol **409**: 524-540.
- Welte, M. A. (2009). "Fat on the move: intracellular motion of lipid droplets." Biochem Soc Trans **37**(Pt 5): 991-996.
- Wesierska-Gadek, J., G. Schmid and C. Cerni (1996). "ADP-ribosylation of wild-type p53 in vitro: binding of p53 protein to specific p53 consensus sequence prevents its modification." Biochem Biophys Res Commun **224**(1): 96-102.
- Wiestler, B., D. Capper, T. Holland-Letz, A. Korshunov, A. von Deimling, S. M. Pfister, M. Platten, M. Weller and W. Wick (2013). "ATRX loss refines the classification of anaplastic gliomas and identifies a subgroup of IDH mutant astrocytic tumors with better prognosis." Acta Neuropathol **126**(3): 443-451.
- Wilson, T. A., M. A. Karajannis and D. H. Harter (2014). "Glioblastoma multiforme: State of the art and future therapeutics." Surg Neurol Int **5**: 64.
- Wong, A. J., S. H. Bigner, D. D. Bigner, K. W. Kinzler, S. R. Hamilton and B. Vogelstein (1987). "Increased expression of the epidermal growth factor receptor gene in malignant gliomas is invariably associated with gene amplification." Proc Natl Acad Sci U S A **84**(19): 6899-6903.
- Wong, O. K. and G. Fang (2007). "Cdk1 phosphorylation of BubR1 controls spindle checkpoint arrest and Plk1-mediated formation of the 3F3/2 epitope." J Cell Biol **179**(4): 611-617.
- Wrensch, M., R. B. Jenkins, J. S. Chang, R. F. Yeh, Y. Xiao, P. A. Decker, K. V. Ballman, M. Berger, J. C. Buckner, S. Chang, C. Giannini, C. Halder, T. M. Kollmeyer, M. L. Kosel, D. H. LaChance, L. McCoy, B. P. O'Neill, J. Patoka, A. R. Pico, M. Prados, C. Quesenberry, T. Rice, A. L. Rynearson, I. Smirnov, T. Tihan, J. Wiemels, P. Yang and J. K. Wiencke (2009). "Variants in the CDKN2B and RTEL1 regions are associated with high-grade glioma susceptibility." Nat Genet **41**(8): 905-908.
- Wyllie, A. H., J. F. Kerr and A. R. Currie (1980). "Cell death: the significance of apoptosis." Int Rev Cytol **68**: 251-306.
- Wyllie, A. H., R. G. Morris, A. L. Smith and D. Dunlop (1984). "Chromatin cleavage in apoptosis: association with condensed chromatin morphology and dependence on macromolecular synthesis." J Pathol **142**(1): 67-77.
- Xu, H. Z., Y. Huang, Y. L. Wu, Y. Zhao, W. L. Xiao, Q. S. Lin, H. D. Sun, W. Dai and G. Q. Chen (2010). "Pharicin A, a novel natural ent-kaurene diterpenoid, induces mitotic arrest and mitotic catastrophe of cancer cells by interfering with BubR1 function." Cell Cycle **9**(14): 2897-2907.
- Xu, Y., S. Huang, Z. G. Liu and J. Han (2006). "Poly(ADP-ribose) polymerase-1 signaling to mitochondria in necrotic cell death requires RIP1/TRAF2-mediated JNK1 activation." J Biol Chem **281**(13): 8788-8795.

Bibliography

- Yamamoto, A., V. Guacci and D. Koshland (1996). "Pds1p, an inhibitor of anaphase in budding yeast, plays a critical role in the APC and checkpoint pathway(s)." J Cell Biol **133**(1): 99-110.
- Yang, J. C. and G. A. Cortopassi (1998). "Induction of the mitochondrial permeability transition causes release of the apoptogenic factor cytochrome c." Free Radic Biol Med **24**(4): 624-631.
- Yang, Z. and D. J. Klionsky (2007). "Permeases recycle amino acids resulting from autophagy." Autophagy **3**(2): 149-150.
- Yang, Z. and D. J. Klionsky (2010). "Eaten alive: a history of macroautophagy." Nat Cell Biol **12**(9): 814-822.
- Yang, Z. and D. J. Klionsky (2010). "Mammalian autophagy: core molecular machinery and signaling regulation." Curr Opin Cell Biol **22**(2): 124-131.
- Yao, X., A. Abrieu, Y. Zheng, K. F. Sullivan and D. W. Cleveland (2000). "CENP-E forms a link between attachment of spindle microtubules to kinetochores and the mitotic checkpoint." Nat Cell Biol **2**(8): 484-491.
- Yecies, J. L., H. H. Zhang, S. Menon, S. Liu, D. Yecies, A. I. Lipovsky, C. Gorgun, D. J. Kwiatkowski, G. S. Hotamisligil, C. H. Lee and B. D. Manning (2011). "Akt stimulates hepatic SREBP1c and lipogenesis through parallel mTORC1-dependent and independent pathways." Cell Metab **14**(1): 21-32.
- Yi, C. and C. He (2013). "DNA repair by reversal of DNA damage." Cold Spring Harb Perspect Biol **5**(1): a012575.
- Ying, S., F. C. Hamdy and T. Helleday (2012). "Mre11-dependent degradation of stalled DNA replication forks is prevented by BRCA2 and PARP1." Cancer Res **72**(11): 2814-2821.
- Young, A. R., E. Y. Chan, X. W. Hu, R. Kochl, S. G. Crawshaw, S. High, D. W. Hailey, J. Lippincott-Schwartz and S. A. Tooze (2006). "Starvation and ULK1-dependent cycling of mammalian Atg9 between the TGN and endosomes." J Cell Sci **119**(Pt 18): 3888-3900.
- Yu, S. W., S. A. Andrabi, H. Wang, N. S. Kim, G. G. Poirier, T. M. Dawson and V. L. Dawson (2006). "Apoptosis-inducing factor mediates poly(ADP-ribose) (PAR) polymer-induced cell death." Proc Natl Acad Sci U S A **103**(48): 18314-18319.
- Yu, S. W., H. Wang, M. F. Poitras, C. Coombs, W. J. Bowers, H. J. Federoff, G. G. Poirier, T. M. Dawson and V. L. Dawson (2002). "Mediation of poly(ADP-ribose) polymerase-1-dependent cell death by apoptosis-inducing factor." Science **297**(5579): 259-263.
- Yuan, J., S. Shaham, S. Ledoux, H. M. Ellis and H. R. Horvitz (1993). "The C. elegans cell death gene ced-3 encodes a protein similar to mammalian interleukin-1 beta-converting enzyme." Cell **75**(4): 641-652.
- Yuste, V. J., I. Sanchez-Lopez, C. Sole, R. S. Moubarak, J. R. Bayascas, X. Dolcet, M. Encinas, S. A. Susin and J. X. Comella (2005). "The contribution of apoptosis-inducing factor, caspase-activated DNase, and inhibitor of caspase-activated DNase to the nuclear phenotype and DNA degradation during apoptosis." J Biol Chem **280**(42): 35670-35683.

- Zamzami, N., P. Marchetti, M. Castedo, T. Hirsch, S. A. Susin, B. Mousse and G. Kroemer (1996). "Inhibitors of permeability transition interfere with the disruption of the mitochondrial transmembrane potential during apoptosis." FEBS Lett **384**(1): 53-57.
- Zhang, Y., J. Wang, M. Ding and Y. Yu (2013). "Site-specific characterization of the Asp- and Glu-ADP-ribosylated proteome." Nat Methods **10**(10): 981-984.
- Zhou, J., S. Ng, Q. Huang, Y. T. Wu, Z. Li, S. Q. Yao and H. M. Shen (2013). "AMPK mediates a pro-survival autophagy downstream of PARP-1 activation in response to DNA alkylating agents." FEBS Lett **587**(2): 170-177.
- Zoncu, R., A. Efeyan and D. M. Sabatini (2011). "mTOR: from growth signal integration to cancer, diabetes and ageing." Nat Rev Mol Cell Biol **12**(1): 21-35.
- Zou, H., W. J. Henzel, X. Liu, A. Lutschg and X. Wang (1997). "Apaf-1, a human protein homologous to *C. elegans* CED-4, participates in cytochrome c-dependent activation of caspase-3." Cell **90**(3): 405-413.
- Zou, H., Y. Li, X. Liu and X. Wang (1999). "An APAF-1-cytochrome c multimeric complex is a functional apoptosome that activates procaspase-9." J Biol Chem **274**(17): 11549-11556.

APPENDIX

PARP targeting counteracts gliomagenesis through induction of mitotic catastrophe and aggravation of deficiency in homologous recombination in PTEN-mutant glioma

Jara Majuelos-Melguizo¹, María Isabel Rodríguez¹, Laura López-Jiménez¹, Jose M. Rodríguez-Vargas¹, Juan M. Martí Martín-Consuegra¹, Santiago Serrano-Sáenz¹, Julie Gavard³, J. Mariano Ruiz de Almodóvar² and F. Javier Oliver¹

¹ Instituto de Parasitología y Biomedicina López Neyra, CSIC, Granada, Spain

² IBIMER, Centro de Investigación Biomédica, Universidad de Granada, Spain

³ CNRS, UMR8104, Paris, France

Correspondence to: F. Javier Oliver, email: joliver@ipb.csic.es

Keywords: BUBR1, Mitotic catastrophe, Glioblastoma, Homologous recombination, PARP1, PTEN, genomic instability, EGFR

Received: August 18, 2014

Accepted: December 10, 2014

Published: December 11, 2014

This is an open-access article distributed under the terms of the Creative Commons Attribution License, which permits unrestricted use, distribution, and reproduction in any medium, provided the original author and source are credited.

ABSTRACT

Glioblastoma multiforme (GBM) is the most common primary brain tumour in adults and one of the most aggressive cancers. PARP-1 is a nuclear protein involved in multiple facets of DNA repair and transcriptional regulation. In this study we dissected the action of PARP inhibition in different GBM cell lines with either functional or mutated PTEN that confers resistance to diverse therapies. In PTEN mutant cells, PARP inhibition induced a severe genomic instability, exacerbated homologous recombination repair (HR) deficiency and down-regulated the Spindle Assembly Checkpoint (SAC) factor BUBR1, leading to mitotic catastrophe (MC). EGFR gene amplification also represents a signature of genetic abnormality in GBM. To more effectively target GBM cells, co-treatment with a PARP inhibitor and an EGFR blocker, erlotinib, resulted in a strong suppression of ERK1/2 activation and *in vivo* the combined effect elicited a robust reduction in tumour development. In conclusion, PARP inhibition targets PTEN-deficient GBM cells through accentuation of SAC repression and aggravation of HR deficiency, leading to the induction of genomic instability and eventually deriving to mitotic catastrophe (MC); the inhibition of PARP and co-treatment with an inhibitor of pro-survival pathways strongly retarded *in vivo* gliomagenesis.

INTRODUCTION

Glioblastoma multiforme (GBM) are lethal brain tumours, highly resistant to therapy. An important improvement in therapeutic response came from the use of the alkylating agent temozolomide (TMZ) in combination with ionizing radiation (IR). Amongst the huge number of genetic alterations that populate the GBM genomic landscape, five genetic changes dominate: loss of tumour suppressor and aging biomarker (Ink4a), acute renal failure (Arf), cellular tumour antigen p53, or phosphatase and tensin homolog on chromosome 10 (PTEN); and amplification of Epidermal Growth Factor Receptor (EGFR).

Loss of PTEN is a very prominent event during gliomagenesis, occurring in about 36% of GBMs [1-3]. PTEN is a lipid phosphatase with a canonical role in turning-off the phosphatidylinositol 3-kinase (PI3K)-Akt-1 signalling pathway; hence, loss of PTEN has oncogenic consequences during gliomagenesis [4]. In addition, it is becoming increasingly clear that PTEN has novel nuclear functions, including transcriptional regulation of the RAD51 gene, whose product is essential for homologous recombination (HR) repair of DNA breaks [5].

The nuclear protein PARP-1, known to function as a DNA damage sensor and to play a role in various DNA repair pathways, has recently been implicated in a broad variety of cellular functions, including transcriptional

regulation [6, 7]. PARP inhibitors exhibit antitumour activity in part due to their ability to induce synthetic lethality in cells deficient for homologous recombination repair [8-12] and also in triple negative breast cancer cells [13, 14]. Up to date, the studies on GBM and PARP inhibitors have focused on the use of these small molecules as radio or chemo-potentiators [15-17]. In this study, we report that primary glioma stem-like cells are targeted in their ability to form neurospheres by PARP inhibitors; moreover, mutant PTEN GBM cells are also sensitive to PARP inhibitors by increasing genomic instability leading to impaired G2/M arrest and MC. Additionally, PARP inhibition strongly intensified HR deficiency in PTEN mutant cells, that had already compromised HR [18-20] and repressed the Spindle Assembly Checkpoint protein BUBR1. Moreover, the combination of PARP inhibition with an upstream blocker of pro-survival signalling pathways arising from the EGFR, the EGFR inhibitor erlotinib, induced a dramatic reduction in tumour growth in an orthotopic mouse model. Thus, taking advantage of PARP inhibitor-induced cell death in PTEN-mutant glioma cells prone to genomic instability, and disabling survival pathways through EGFR and PARP inhibition, could be therapeutically exploited in the treatment of this malignant tumour.

RESULTS

PJ34 and olaparib interfere with neurospheres formation in primary glioma cells and impacts differently on cell viability in PTEN wild type and PTEN-mutant glioma cells

As a first approach to analyze the potential of PARP inhibition (PARPi) as monotherapy against GBM we evaluated self-renewal capability, which is a marker of stemness in GSCs, using neurospheres formation assay in primary patient-derived PTEN-proficient GSCs TG1 [21] with two different PARP inhibitors: PJ34 (IC 20 nM) and olaparib (IC 5 nM). PJ34 targets mainly PARPs synthesizing proteins but some off-target effects have also been reported, suggesting the effect of PJ34 on cancer cells may not be attributed exclusively to PARP inhibition [22, 23]. For that reason we also used the clinically relevant PARPi olaparib. Following seven days of treatment, neurospheres formation decreased significantly with either PJ34 or olaparib (figure 1A). Similar results have been reported by Rich and colleagues showing that PARPi preferentially targeted GSCs [16]. Our data support that PARPi targets primary glioma cells in part by perturbing self renewal/GICs phenotype.

PTEN deficiency is one of the most common mutations in human high grade gliomas, and renders these tumours resistant to radio and chemotherapy, conferring

increased invasive properties. To further challenge PARPi as anti GBM agents we tested them against established GBM cell lines bearing either wild type or mutant PTEN. Treatment with PARPi of either PTEN wild type or mutant cell lines resulted in loss of cell viability (figure 1B, figure S1A) and cell death induction (figure 1C). Due to the previously reported off-target effects of PJ34, the PARP inhibitor olaparib was also tested, exerting similar results (figure S4A). Interestingly, PTEN deficient cells including U87MG displayed an increased sensitivity to PARPi. However, U87MG, which has been previously described to be extremely resistant to apoptotic cell death [24], hardly increased apoptosis following PARPi (figure 1D, S1B,C) or PARP-1 knockdown (figure S1D) when compared with LN229 (PTEN proficient cell line). Remarkably, PTEN silencing in LN229 cells and PTEN restoration in U87MG cells resulted in increased apoptotic cell death following PARPi (figure S2A,B). This apparently contradictory result may be explained through the genetic context of each cell line: while LN229 cells possess a functional apoptotic machinery that is activated following PARP inhibition, PTEN re-introduction in U87MG cells partially restored apoptotic ability.

Combining PARPi with the methylating agent temozolomide (TMZ) or ionising radiation (IR) did not potentiate cell killing (figure S3A,B,C and data not shown). Thus, PARP inhibition per se was sufficient to induce cell death in PTEN deficient cells more efficiently than the currently used chemotherapeutic drug TMZ or IR. Moreover, the G2/M arrest was also notably diminished in U87MG cells following PARP inhibition respect to PTEN wild type cells (figures 1E,1F and S4B) and U87MG cells transiently restored with PTEN partially recovered G2/M arrest (figure S2C). In addition, TMZ remarkably induced an arrest in G2/M at 72 hours and the combination with PARPi produced similar effect to PARP inhibition alone (figure S3D).

PARP inhibition induced down-regulation of the spindle assembly checkpoint protein BUBR1 leading to mitotic instability in PTEN deficient glioma cells

To further elucidate the mechanistic aspects regarding the effect of PARP inhibition in both PTEN proficient and PTEN mutant GBM cells we explored the induction of genomic instability. PTEN deficient cells lack G2/M arrest following PARPi treatment (figure 1E and F). The BUBR1 protein ensures accurate segregation of chromosomes through its role in the mitotic checkpoint and the establishment of proper microtubule-kinetochore attachments; and sustained high-level expression of BUBR1 preserves genomic integrity [25]. In figure 2A we show that PARP inhibition induced BUBR1 down-regulation in U87MG PTEN-deficient cells, suggesting

that the Spindle Assembly Checkpoint is compromised in U87MG. Further confirmation for the effect of PARP inhibition on BUBR1 levels was established by the use of a different PARP inhibitor, olaparib, that induced BUBR1 down-regulation in U87MG but not in LN229 cells (figure S4C). Furthermore, silencing PTEN in LN229 cells also results in BUBR1 decrease after PARP inhibition (figure 2B) while introduction of PTEN in U87MG cells delayed BUBR1 loss (figure 2B). In addition, in silico analysis using the database Array Express of U87MG cells transduced with wild type PTEN showed a statistically significant decrease in BUB1B expression (the gene for BUBR1) in PTEN transduced cells as well as in the gene coding for the SAC-related factor (and BUBR1 associated protein) AURKB (-2.62 and -3.31 fold decrease respectively). In order to approach the clinical relevance

of these variations in BUBR1 levels as function of PTEN we used two available datasets: Oncomine and Array Express from EMBO-EBI. BUB1B gene expression was significantly increased in GBM patients (Figure 2C; $p=2.2E-20$, fold change 3.856, number of samples: normal brain $n=23$, glioblastoma $n=81$). Moreover, there was an inverse correlation between PTEN and BUB1B expression in GBM patients with low survival (Figure 2D; less than 12 months; $n=15$, $p<0.001$, pearson -0.7592) further supporting that targeting BUBR1 (as PARPi does) could be used as rational therapy in PTEN deficient GBM. Interestingly, increased expression of BUB1B correlated with decreased patient survival (Figure 2E).

Another hallmark of genomic instability is micronuclei formation. Following PARP inhibition, U87MG cells, but not LN229 cells displayed a time-

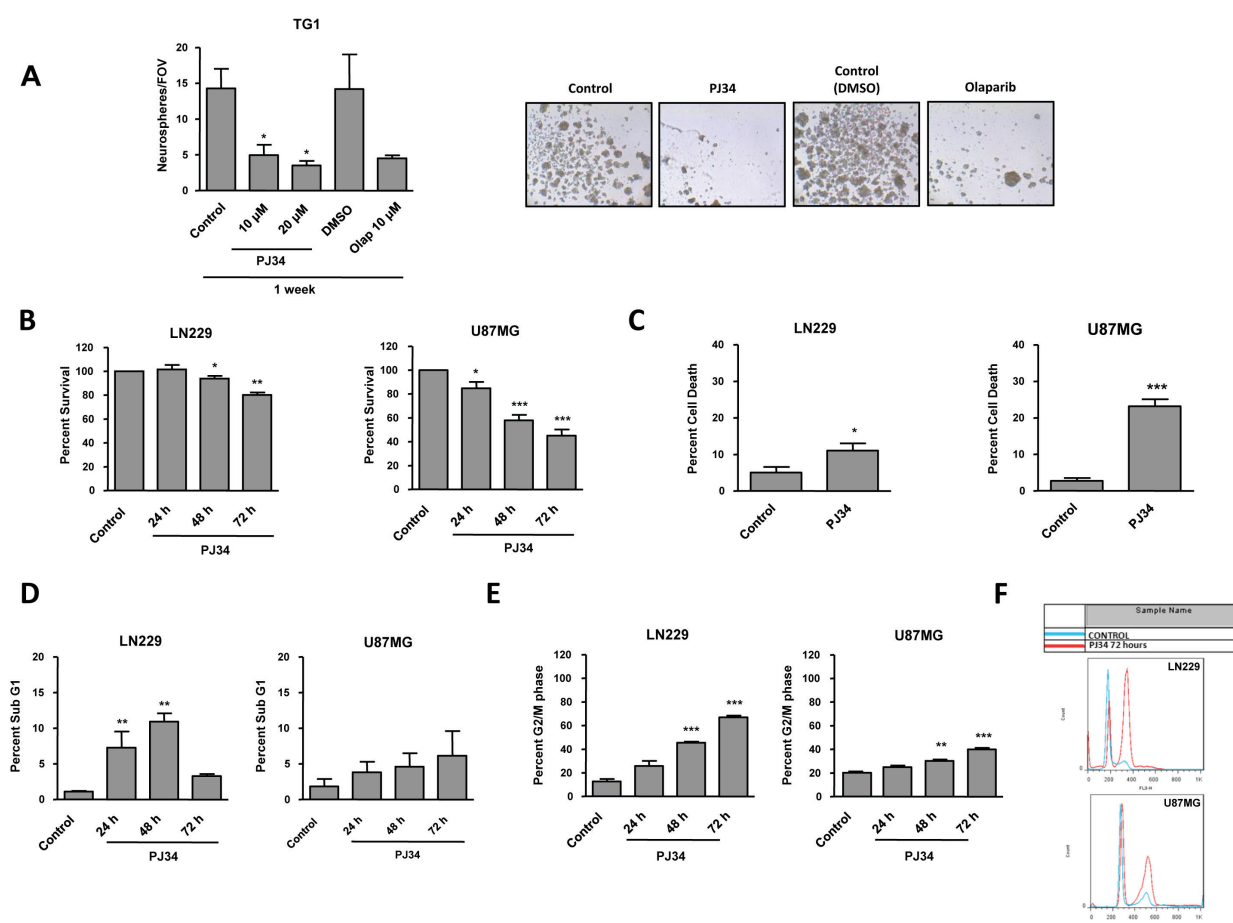


Figure 1: Cell viability in PTEN wt LN229 and PTEN mut U87MG glioblastoma cell lines after treatment with PARP inhibitor (PJ34 20 μM if not detailed). A. Neurosphere Formation Assay (NFA) of GSCs TG1 treated with PJ34 or olaparib. The drug was refreshed the three first days of the experiment. After one week, neurosphere counting (10 fields of view per condition) was performed. * $p < 0.05$ versus control group by t-test. B. Viability analysis by MTT assay of glioblastoma cells treated with PJ34 for 24, 48 and 72 hours. Data were normalized and expressed as a percentage of the control. * $p < 0.05$, ** $p < 0.01$, *** $p < 0.001$ versus control group by t-test. C. Trypan blue intake counting was in order to check cell death. D. Apoptosis activation was determined 24, 48 and 72 hours after the treatment. SubG1 fraction was analysed by flow cytometry following staining with PI. ** $p < 0.01$ versus control group by t-test. E. Cell cycle arrest was determined 24, 48 and 72 hours after the treatment. G2/M fraction was analysed by flow cytometry following staining with PI. ** $p < 0.01$, *** $p < 0.001$ versus control group by t-test. F. Cell cycle profiles referring to control and PJ34 72 hours in both cell lines are represented. Data are represented as mean \pm SEM of 3 independent experiments.

dependent accumulation of micronuclei (figure 2F).

Polyoids are the result of cytokinesis failure after G2/M arrest. However PTEN-deficient cells, unable to activate the G2/M checkpoint, progress to continue cell cycle and complete aberrant mitosis. As shown in figure 1E, PARP inhibition-induced arrest in G2/M in PTEN-mutant cells was almost suppressed, implying that cells will progress in cell cycle, accumulating genomic instability, and eventually Mitotic Catastrophe but not polyoids (figure 2G, S4D). Interestingly, and consistent with increased G2/M arrest following PARPi after PTEN restoration (figure S2C), PTEN over-expression in U87MG also increased polyoidy (figure S2D). However, the slight increase observed after long-time of PJ34 treatment suggests a possible interference of the genetic background of each cell line.

Taken together, these results led us to conclude that PARP inhibition compromised mitotic checkpoint through down-regulation of BUBR1, preventing from mitotic

arrest only in a PTEN deficient context.

To further understand the impact of PARP inhibition in PTEN mutant cells we performed an expression array focused in genes involved in cell cycle regulation and DNA repair. In table 1 we have represented genes whose expression was significantly modified after PARP inhibition in U87MG cells. Up-regulated mRNAs included p53-dependent genes such as BBC3/PUMA (a pro-apoptotic bcl2 and BH3-only pro-apoptotic subclass) and CDKN1A/p21 (pro-apoptotic and CDK2 inhibitor). Up-regulation was also noted in genes involved in DNA damage, G2/M cell cycle checkpoint, and in genes implicated in DNA repair pathways such as XPA, XPC (Nucleotide Excision Repair). A number of down-regulated genes were involved in homologous recombination repair. That is the case for BARD1 and BRIP1, factors associated with BRCA1 who are needed for its activation. Moreover, RAD51 is an essential component of HR repair and its down-regulation could be detrimental for the cell to cope

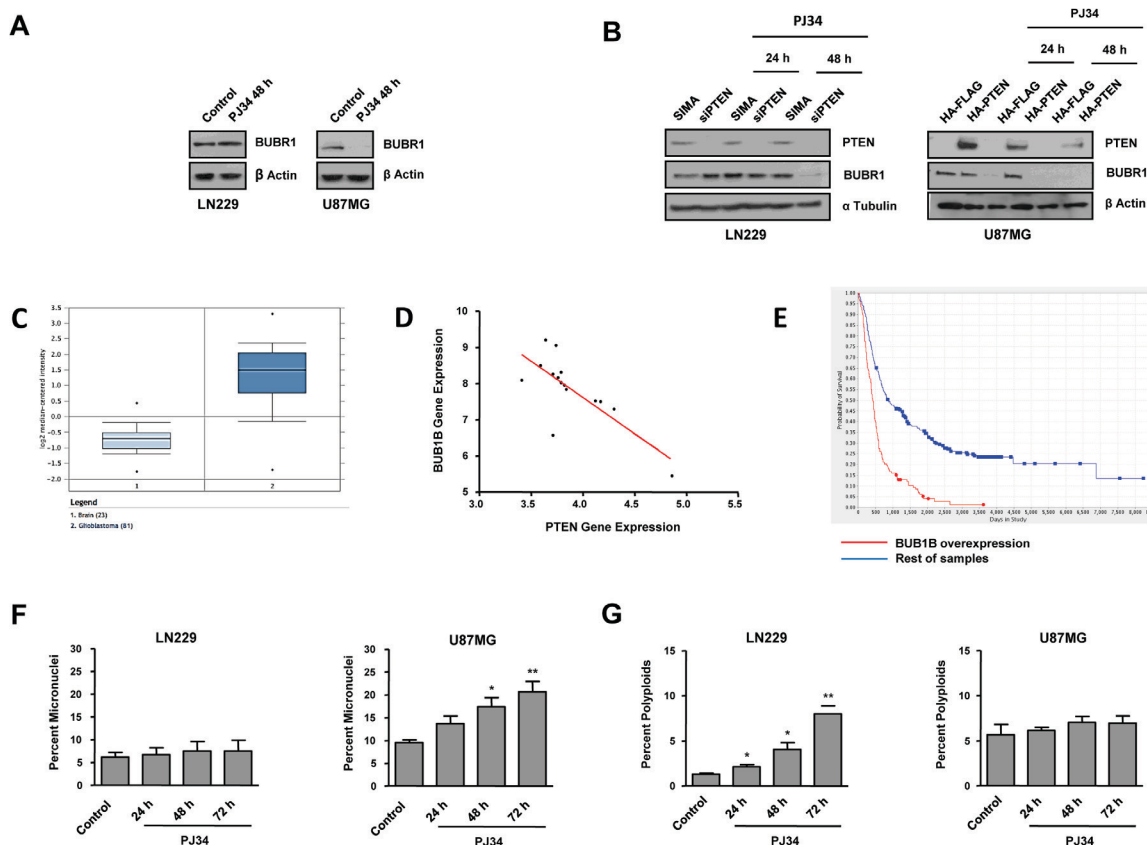


Figure 2: Mitotic instability following PARP inhibition (PJ34 20 μM). A. BUBR1 expression was measured by Western Blot 48 hours after the treatment with PJ34. B. BUBR1 expression was measured by Western Blot after the treatment with PJ34 following PTEN silencing in LN229 cells/PTEN overexpression in U87MG cells. C. BUB1B gene expression analysis obtained with the Oncomine database; $p = 2.2E-20$, fold change 3.856; number of samples: normal brain $n = 23$, glioblastoma $n = 81$. D. BUB1B gene expression correlates negatively with PTEN expression in GBM low survival patients (less than 12 months); $n = 15$, $p < 0.001$, pearson -0.7592 . E. BUB1B overexpression correlates with decreased patient survival. Data obtained from REMBRANDT database. $n = 413$; 138 overexpressing BUB1B and 275 rest of samples. F. Micronuclei formation after DAPI staining was quantified. * $p < 0.05$, ** $p < 0.01$ versus control group by t-test. G. Super G2 fraction, indicating polyoid cells, was analysed by flow cytometry after staining with PI. * $p < 0.05$, ** $p < 0.01$ versus control group by t-test. Data are represented as mean \pm SEM of 3 independent experiments.

Table 1: Expression array of DNA repair proteins in U87MG glioblastoma cells. Genes over and under-expressed following 24 hours PJ34 (20 μ M) treatment. Data are represented as mean \pm SEM of 3 independent experiments. P-value was calculated through t-test.

Genes Over-Expressed

| Gene Symbol | Fold Regulation | P-VALUE |
|-------------|-----------------|----------|
| BBC3 | 2.8101 | 0.013791 |
| CDKN1A | 3.8509 | 0.000049 |
| XPA | 3.3737 | 0.000464 |
| XPC | 2.6833 | 0.001180 |

Genes Under-Expressed

| Gene Symbol | Fold Regulation | P-VALUE |
|-------------|-----------------|----------|
| BARD1 | -3.613 | 0.043765 |
| BLM | -2.6515 | 0.040151 |
| BRIP1 | -5.1323 | 0.007620 |
| CDC25A | -3.8447 | 0.004158 |
| CDC25C | -4.9758 | 0.003132 |
| CHEK1 | -2.2562 | 0.044566 |
| EXO1 | -4.2833 | 0.004202 |
| FANCG | -2.1567 | 0.031524 |
| FEN1 | -2.7212 | 0.030799 |
| H2AFX | -5.4313 | 0.000279 |
| RAD51 | -4.5306 | 0.001705 |

with DNA damage leading to cell death. Chk1, involved in cell cycle arrest after activation of ATM and ATR in response to DNA damage, is also down-regulated as well as the protein phosphatases CDC25A (which is a Chk1 substrate) and CDC25C, involved respectively in G1/S checkpoint and mitosis entry. Gene expression for exonuclease Exo1, that plays a role in mismatch repair, and the endonuclease FEN1, that removes 5' overhanging flaps in DNA repair and processes the 5' ends of Okazaki fragments in lagging strand DNA synthesis, is repressed after PARP inhibition. Mutations or deficiency in the Fanconi anemia complementation (FANC) group members is characterized by cytogenetic instability, hypersensitivity to DNA crosslinking agents, increased chromosomal breakage, and defective DNA repair. FANCG gene expression was also down-regulated after PARP inhibition. Phosphorylation of H2AX is involved in the initial early steps of DNA damage response, in the recognition of double strand breaks. Down-regulation of γ H2AX is reflecting a strong defective signalling in the initial sensing of DNA lesions. Globally, this perturbation in DNA damage response factors after PARP inhibition

suggests a discomposed scenario in the ability of these PTEN-deficient cells to cope with PARP inhibitor-induced DNA lesions that might be therapeutically exploited.

Impaired Homologous Recombination (HR) after PARP inhibition in PTEN deficient glioma cells

In view of the above results we tested HR efficiency in U87MG and LN229 cell lines containing an integrated copy of the DR-GFP reporter as previously described [26]. This reporter allows to determine the rate of HR repair of a SclI endonuclease-generated DSB in the chromosome by the restoration of an intact green fluorescent protein (GFP) gene. GFP levels were quantified by Kolmogorov-Smirnov adjust, and revealed that LN229 cells expressed higher levels of GFP after transfection, indicating that PTEN mutant cells are compromised in Homologous Recombination, as has been previously reported [20]. Moreover, PARP inhibition further disabled HR, mainly in PTEN mutant cells where we found this repair pathway profoundly down-regulated after the PARPi treatment (figure 3A).

To confirm the previous results of PARPi inducing increased HR deficiency specifically in PTEN mutant cells, we performed an assay to quantify RAD51 foci, which is also used to assess HR efficiency. First we observed that RAD51 accumulation in U87MG cells did not correlate with the level of DNA damage and did not fluctuate in parallel to γ H2AX levels (figure S5A). On the contrary, RAD51 levels in LN229 raised in parallel with γ H2AX levels and these foci were resolved following 24 hours after irradiation. These results suggested that PTEN wild type cells, but not PTEN mutant cells, were able to couple HR activation with DNA damage levels. In addition, γ H2AX basal levels are much lower in U87MG cells, further confirming the perturbed status of the HR signalling that makes them unable to properly signal and resolve DNA damage (figure S5B).

Consistently, assessing only cell bearing γ H2AX foci, we observed that IR-induced accumulation of RAD51 foci was notably reduced in PTEN mutant cells (figure 3B) and co-treatment with PJ34 further decreased RAD51 foci formation in these cells, supporting the above results obtained with DR-GFP transfection assay. The levels of RAD51 were rapidly down-regulated in U87MG, but not in LN229 where they only decreased after 48 hours of PARP inhibition. PARP-1 silencing, however, affected similarly to RAD51 levels irrespective of the PTEN-status (figure 3C). Similar results were obtained using the PARPi olaparib (figure S4C). Levels of BRCA1 protein were also reduced in PTEN deficient cells (figure 3C). To further confirm the association between RAD51 decrease, PARPi treatment and PTEN status, we silenced PTEN in LN229 and we found a decrease in RAD51 levels (figure 3D); on the other hand, restoring PTEN in U87MG cells led

to a delay in RAD51 down-regulation after the treatment (figure 3D).

As we described above, the expression of the SAC regulatory factor BUBR1 was reduced after PARPi treatment in PTEN mutant cells (figure 2A). To better understand the association between BUBR1 down-regulation and impaired HR we knocked-down BUBR1 in PTEN proficient cells and we observed a recovery in RAD51 following PARP inhibition (figure 3E). This apparently paradoxical result might be explained because PARP inhibition, in siBUBR1 cells, is acting in a BUBR1 deficient scenario since the beginning, contrary to the situation on U87MG cells. RAD51 recovery might reflect a compensatory mechanism initiated by the cell to avoid massive DNA damage in the absence of an efficient mitotic checkpoint.

PARP blockade potentiated *in vitro* and *in vivo* effect of EGFR inhibition on PTEN mutant glioma cells

In spite U87MG glioma cells are not mutant for EGFR, they constitutively activate MAP kinase pathway in virtue of mutations affecting Focal Adhesion Kinases and GRP3 [27, 28]. PARP inhibition did not prevent ERK1/2 activation making this treatment only partially effective in suppressing this proliferative pathway. We reasoned that avoiding signalling arising from EGFR might deregulate the activation of MAP kinase pathway and potentiate the effect of PARP inhibition. While treatment with EGFR inhibitor erlotinib alone prevented ERK1/2 activation in LN229 cells, U87MG cells were refractory to the effect of erlotinib (figure 4A). Interestingly, co-treatment with PJ34 and erlotinib resulted in a complete suppression of

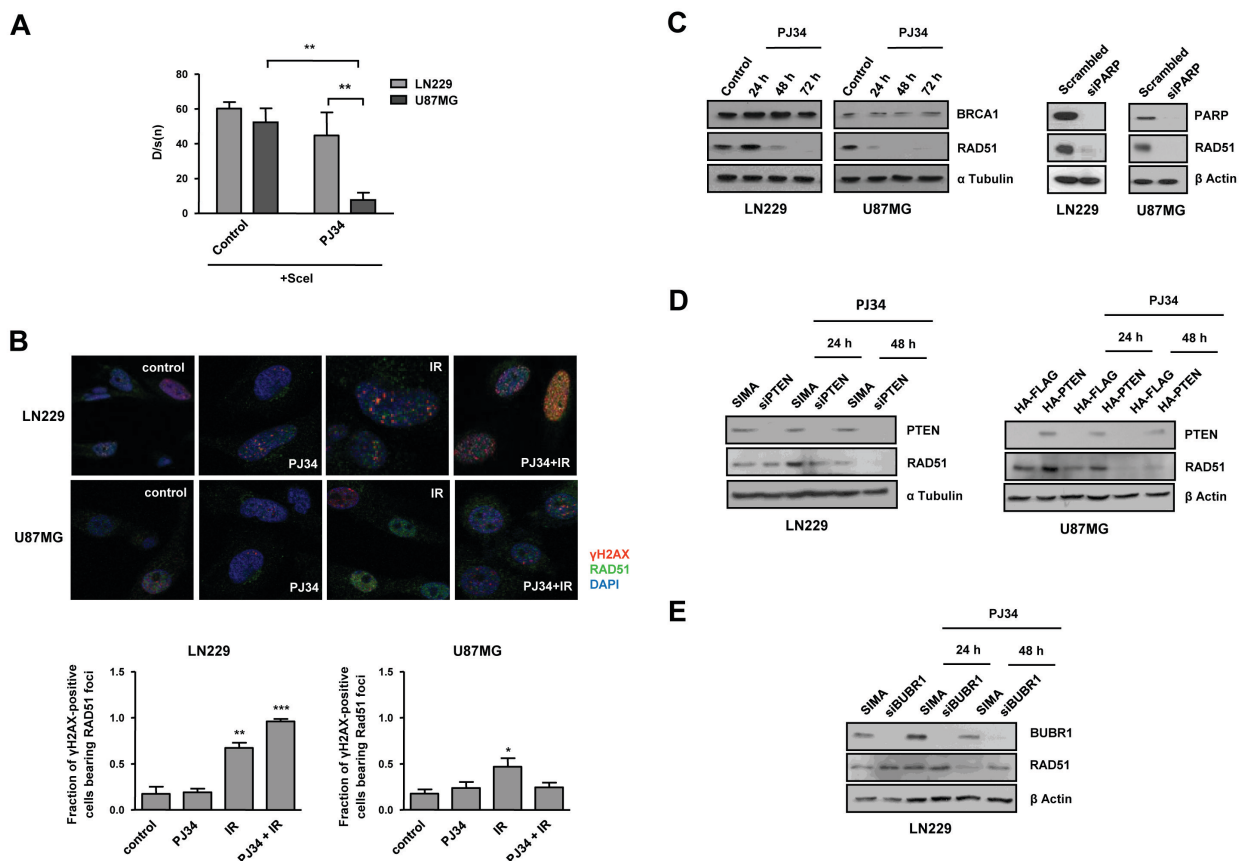


Figure 3: Homologous Recombination (HR) is compromised following PARP inhibition. A. Stably transfected with DR-GFP plasmid LN229 and U87MG glioblastoma cell lines were transiently transfected with ScelI plasmid. Two days later, they were treated with PARP inhibitor PJ34 (10 μ M) for 48 hours. GFP expression was analysed by flow cytometry and the results were processed by Kolmogorov-Smirnov test. $**p < 0.01$ by t-test. B. Distribution of Rad51 and γ H2AX foci; nuclear staining was performed with DAPI. Cells were treated with PJ34 (20 μ M) during 48 hours and subsequently irradiated at 2Gy during 4 hours. Fraction of positive γ H2AX population bearing Rad51 foci was quantified. $*p < 0.05$, $**p < 0.01$, $***p < 0.001$ versus control group by t-test. C. Homologous-Recombination (HR) proteins BRCA1 and Rad51 expression was analysed by western blot 24, 48 and 72 hours after 20 μ M PJ34 treatment and following PARP knockdown. D. RAD51 expression was measured by Western Blot after the treatment with PJ34 following PTEN silencing in LN229 cells/PTEN overexpression in U87MG cells. E. RAD51 expression was measured by Western Blot after the treatment with PJ34 following BUBR1 silencing in LN229 cells. Data are represented as mean \pm SEM of 3 independent experiments.

ERK1/2 activation (figure 4B). Nonetheless, combination of both drugs did not further decrease the PARP inhibitor-induced cytotoxicity (Figure 4C).

The full abrogation of ERK1/2 activation prompted us to test the *in vivo* efficacy of this combination. To this end, we performed an orthotopic assay inoculating U87MG cells that expressed luciferase allowing *in vivo* visualisation of the evolution of tumour mass. While the effect of PJ34 or erlotinib were limited separately (35 and 50% respectively), the combination of both treatments reduced tumour growth to more than 90% after 14 days (figure 4D). Mice were sacrificed after 21 days due excessive tumour growth in vehicle treated mice; at this time PJ34 continued to be effective as anti-tumour agent indicating that the combined inhibition of a pro-survival pathway (using erlotinib) together with the inactivation of HR and the induction of genomic instability by PARP inhibition has a synergic *in vivo* anti-tumour effect.

DISCUSSION

Our reduced understanding of the mechanisms which underlie brain tumorigenesis severely limit preventative and therapeutic options for glioblastoma patients. The current standard treatment for GBM involves surgical resection followed by adjuvant radiotherapy (RT) with ionising radiation, with or without concomitant chemotherapy. Disappointingly, this regimen only affords GBM patients a median survival benefit of 14.6 months- a 12 month improvement over resection alone. It is important to note that radio- and chemotherapies are, at the molecular level, based on inducing enough DNA damage in the tumour cell to result in lethality. The results shown in this study reflect that PARP inhibition results in a profound alteration of genomic instability in PTEN-deficient glioma cells affecting cell cycle, mitotic checkpoint and homologous recombination, leading to

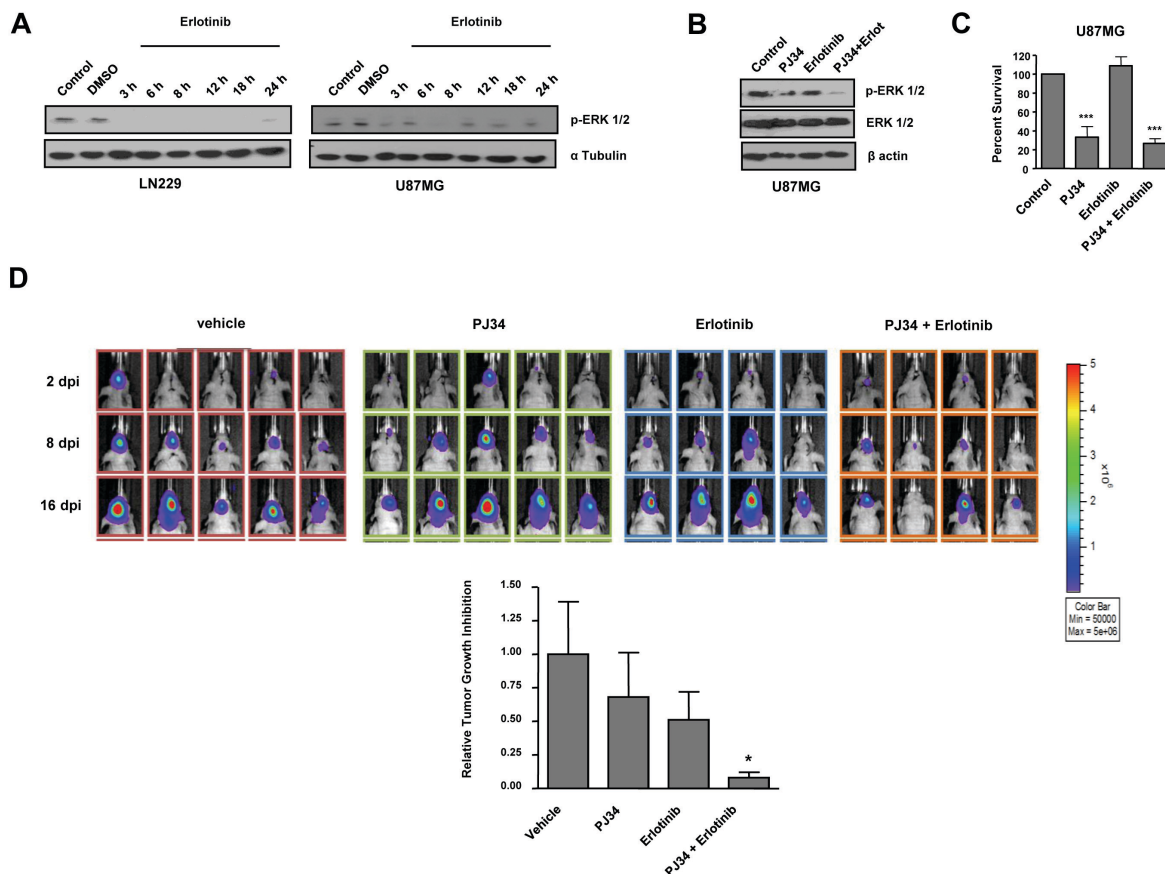


Figure 4: *In vitro* effect of EGFR inhibitor erlotinib and decreased tumours growth *in vivo* after combined treatment with PARP inhibitor and erlotinib. A. Western blot analysis of p-ERK-1/2 expression levels at different times following erlotinib treatment. B, C. U87MG cells were treated with erlotinib alone or combined with PJ34 during 72 hours. (B) p-ERK-1/2 expression was measured by Western Blot. (C) MTT reduction was analysed. $***p < 0.001$ versus control group by t-test. D. Mice were inoculated with U87MG-luciferase human cell line. Localization and intensity of luciferase expression were monitored by *in vivo* bioluminescence imaging (dpi, days post cells injection). Representation of tumours growth inhibition on the 16th day. A statistically significant reduction is observed in the combined treatment of PJ34 and erlotinib. $*p < 0.05$ versus control group by t-test. Data are represented as mean \pm SEM of 3 independent experiments.

micronuclei formation, as hallmark of MC (Figure 5). The protein kinase BUBR1 plays a key role in the maintenance of chromosomal stability [29] owing to its involvement in the formation of proper chromosome-spindle attachments. First, BUBR1 down-regulation activates Aurora B kinase and the kinetochore protein CENP-A, resulting in the loss of kinetochore-microtubule attachments [30]. Second, BUBR1 avoids sister chromatids separation in anaphase when chromosome-spindle attachments are uncorrect, since it is involved on the Mitotic Checkpoint (Spindle Assembly Checkpoint or SAC) [31]. When interactions between kinetochores and microtubules are unstable in metaphase, BUBR1, acting together with MAD2 and BUB3, join CDC20 avoiding APC activation thus preventing sister chromatids separation in anaphase. Remarkably gene expression of BUB1B (the gene coding for BUBR1) is very significantly up-regulated in GBM patients and its expression was inversely correlated with PTEN in short-survival patients. In line with this finding recently it has been described that BUB1B is differentially required for GSCs expansion in glioblastoma tumours and genetically transformed cells that have added requirement

for BUB1B to suppress lethal consequences of altered kinetochore [32].

In the current study we have found that Homologous Recombination Repair deficiency in PTEN mutant glioma cells is further disabled after PARP inhibition due in part to RAD51 down-regulation. A previous study has shown that PARPi down-regulates RAD51 and BRCA1 leading to HR deficiency at times where an elevated loss of cell viability was observed [33]. In our study, PARP inhibition leads to a profound amplification of HR deficiency in PTEN mutant cells already at 24 hours (figure 3C and Table 1), where no cytotoxic effect is still appreciated (figure 1A). Moreover, the expression pattern of key components of the DNA damage response is strongly affected after blunting PARP activity, (PARP-1 of other PARP family members with poly (ADP-ribosylation) activity), including perturbation of the HR machinery and other DNA repair pathways as well as factors involved in genomic instability, beyond affecting RAD51. PTEN restoration in U87MG slowed RAD51 decrease, whereas PTEN silencing in LN229 augmented RAD51 down-regulation after PARP inhibition. Thus, we show that PTEN is involved in

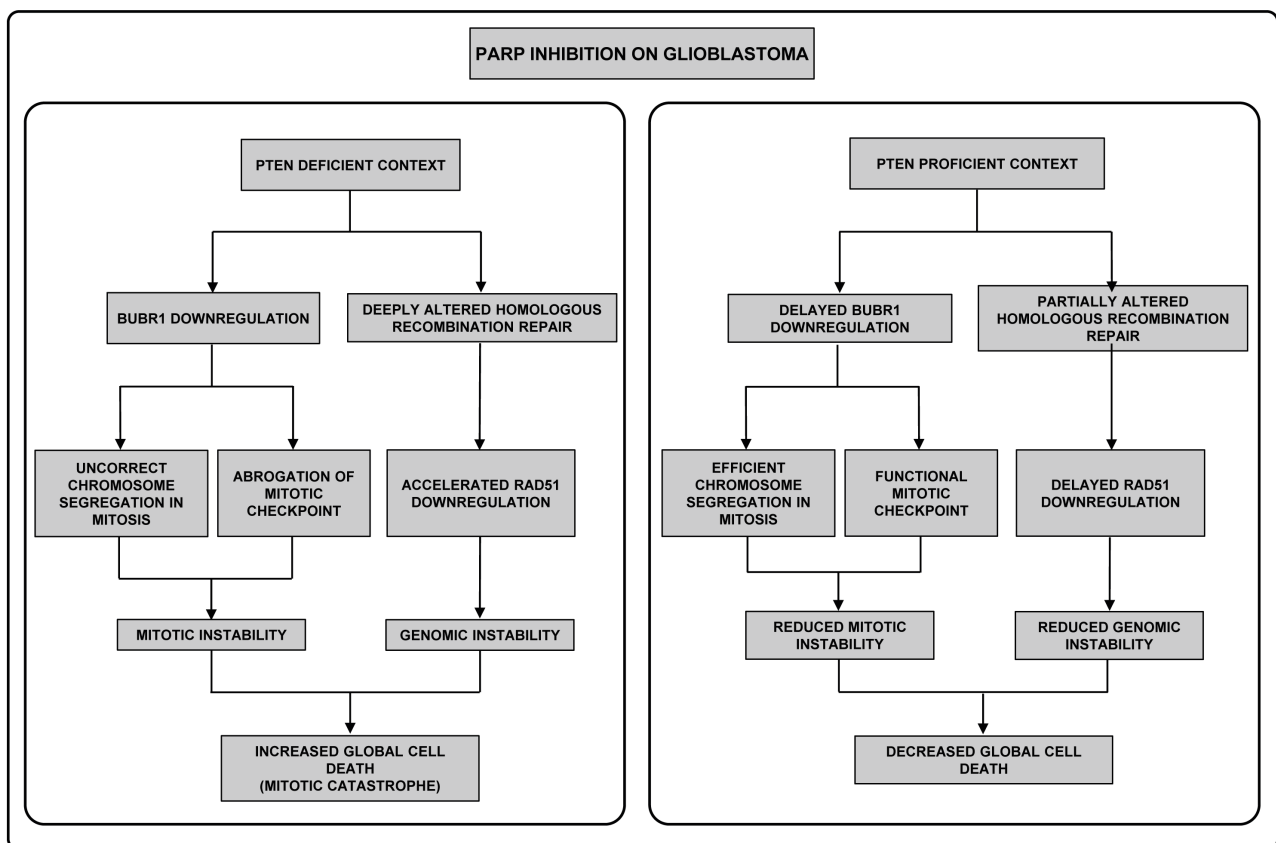


Figure 5: Different effect of PARPi in GBM according to PTEN status. First, in the absence of PTEN (left panel) PARPi perturbs the correct segregation of chromosomes, due to BUBR1 down-regulation; secondly compromised integrity of the genomic material occurs as consequence of the alteration of HR repair. Both situations have been well-described to induce Mitotic Catastrophe. In contrast, in a PTEN-proficient context (right panel) BUBR1 down-regulation is retarded allowing correct chromosome segregation in mitosis and, secondly, HR repair is less affected. Thus, mitotic and genomic instability are reduced and mitotic catastrophe-independent cell death pathways are activated.

the mechanism by which PARP inhibition is disabling Homologous Recombination machinery, which should be taken into account in a possible clinical setting.

The benefit of combining PARP inhibitors with currently used chemotherapy has been largely reported including the potentiating effect of PJ34 [34, 35]. Here we also show compelling evidences that cell death pathway by which PARP inhibition impacts on cell viability of PTEN-deficient cells is MC. MC is a mechanism activated following genomic instability. It senses mitotic failure and responds to it by driving the cell to an irreversible fate, be it apoptosis, necrosis or senescence [36, 37]. The stimuli and perturbations that are described to trigger MC can be divided in two groups. The first group of inducers interfere with the faithful segregation of chromosomes in mitosis. The second group directly affects the integrity of the genetic material, for example DNA-damaging agents or compromised DNA-repair pathways. Thus, in our case, aberrant mitotic spindle organization and DNA segregation due to BUBR1 down-regulation constitute a “first-group inducer” of MC while impaired HR repair due to compromised RAD51 is “second trigger” of MC. However, in spite of the increasingly detailed description of the mechanisms that precede and follow MC, the molecular bridges between mitotic aberrations and cell death are still largely elusive.

In an attempt to increase the *in vivo* cell killing effect of PARP inhibition on glioma cells we ideated (given the up-regulation of pro-survival signalling pathways in PTEN-deficient glioma cells) the co-treatment with an inhibitor of EGFR to disable pro-survival signals. Although no *in vitro* potentiation by erlotinib of PARP-induced cytotoxic effect was observed, this combination was very effective in the suppression of ERK1/2 activation (figure 4B) and, more interestingly, *in vivo* co-treatment was synergic in slowing-down tumour growth. This enhanced *in vivo* potentiation using co-treatment of anti-neoplastic agents with PARP inhibitors has been already described for different preclinical models and has been related to the increased vascular function after inhibition of PARP resulting in amelioration of drug availability in the tumour milieu [38]. Moreover, besides this general property of PARP inhibitors, the use of these compounds takes advantage of the elevated propensity to display genomic instability (which is related with aggressiveness trait) of PTEN deficient glioma cells. The ultimate mechanism underlying the synergistic effect of PARP1 and EGFR remains to be elucidated, but one possibility is that in specific settings inhibition of PARP with PJ34 activates pro-survival pathways as has been shown for p38/MAPK during osteoclast differentiation [39]. A different study has reported that PARP inhibitors may target different kinases in a cell-specific manner [40]. In addition to the shut-down of EGFR signalling, other combinatorial treatments could be envisaged based on the rational knowledge of glioma cells molecular alterations. Another broad field

to explore is the use of PARP inhibitors to act as radio-potentiators against GBM and overcome tumour resistance to standard radiation therapy. In summary PARP inhibitors represent an exciting new class of antineoplastic drugs and there may well have much wider clinical indications not just restricted to BRCA1/2 mutant tumours but to others where PARP inhibitor treatment enhance HR deficiency and mitotic alterations, driving the cell towards a status of genomic instability.

MATERIALS AND METHODS

Cell Culture and Treatments

U87MG and U118MG PTEN mutant and LN229 PTEN wild type (wt) glioblastoma cell lines as well as SW1783 PTEN mutant grade III astrocytoma cell line, were cultured in Dulbecco's Modified Eagle's Medium (DMEM) supplemented with 10 % inactive fetal bovine serum (FBSi, Gibco Invitrogen), at 37 °C in a humidified 5% CO₂ atmosphere.

Patient-derived Glioma Stem Cell TG1 was obtained as described previously [41] and maintained in DMEM/F12 plus N2, G5 and B27 (Invitrogen) at 37 °C in a humidified 5% CO₂ atmosphere.

PARP inhibitors PJ34 (Alexis Biochemicals) and AZD2281/olaparib (Deltaclon) were used. Olaparib was dissolved in DMSO and PJ34 was dissolved in water. Both were stored at -20°C. Cells were treated with 10 µM olaparib or 10 to 20 µM PJ34 during 24, 48 or 72 hours.

Temozolomide (T2577-25MG Sigma-Aldrich, St Louis, USA) was dissolved in DMSO and stored at -20°C. Cells were treated with 100 µM Temozolomide during 24, 48 or 72 hours.

Viability Assays

Viability decrease was determined using MTT and Propidium Iodide. For MTT (3-(4, 5-Dimethylthiazol-2-yl)-2,5-diphenyl Tetrazolium Bromide) assay, cells were plated in 96 wells at a density of 8 x 10³ cells. MTT assay was performed using Cell Proliferation Kit I (MTT, 1-65-007, Roche, Mh Germany) following manufacturer's instructions. Global cell death assay was performed with Trypan Blue (Fluka analytical, 93595). Cells were plated in 24 wells at a density of 2 x 10⁴ cells. One week after the treatment cells were trypsinized, washed with PBS and stained with Trypan Blue. Finally, cells were placed in a Neubauer counting chamber and counted in order to check the rate of blue cells (indicating dead cells) in the population.

Neurosphere Formation Assay

GSCs were dissociated by up-and-down pipetting and plated in 48 wells. PARP inhibitor was added every 24 hours during the three first days of experiment [41]. GSCs were dissociated every day in order to check their ability to form secondary neurospheres at the end of the experiment. The 7th day, counts were blindly performed on 10 fields of view, and the mean number of neurospheres per field of view was calculated.

Cell Cycle Assay

Cell cycle was analysed by flow cytometry [42]. Cells were plated in 6 wells at a density of 1.5×10^5 cells. After the treatments, cells were trypsinized, washed with PBS, permeabilized with 70% ice cold ethanol, washed again with PBS and incubated with propidium iodide and 100 $\mu\text{g/ml}$ RNAase A (Ribonuclease A from bovine pancreas R6513-10MG Sigma-Aldrich, St Louis, USA) for 20 min. When GFP population was examined, cell fixation before permeabilization was required, as previously described by Lamm et al [42]. Cells were analysed on a FACScan using CellQuest software, and cell cycle was determined using FlowJo software. In the case of PTEN overexpression, GFP population was gated in order to analyze cell cycle in a 100% transfected population.

Apoptosis Assays

Apoptosis was determined by different methods. a) Cell Cycle Assay: Sub G1 population was determined through Cell Cycle assay, as described above. b) Pyknotic nuclei: Cells were plated in 6 wells at a density of 5×10^4 cells per well. 72 hours after the treatments cells were fixed in Paraformaldehyde (4%, wt/vol in PBS1x with 2% Sucrose) for 10 minutes at room temperature and incubated with DAPI for 10 minutes. The number of cells with nuclear apoptotic morphology was determined using a Zeiss Fluorescence Microscope. c) Caspase 3/7 activity: Cells were plated in 96 wells at a density of 6×10^3 cells per well. Following the treatments, The Caspase - Glo reagent (Promega) was added directly to cells and incubated at room temperature for 30 minutes before recording luminiscence in a TECAN infinite 200 Luminometer. Each point represents the average of 3 wells per condition to 3 independent experiments.

Western Blot Analysis

Cells were plated in 6 wells at a density of 2×10^5 cells per well. After PARP inhibition, cells were washed twice with PBS and resuspended in 200 μl of TR3

Lysis Buffer (3% SDS, 10% Glycerol, 10mM Na_2HPO_4 anhidro). Then cells were sonicated and 20 μl of 50% β -mercaptoethanol - 50% Bromofenol blue were added. The protein concentration was determined using the Lowry assay. Proteins were resolved on SDS-polyacrylamide gels and transferred onto PVDF Membrane (Biorad). The blot was blocked with 5% milk powder in PBS1X with 0.1% Tween-20 for 60 minutes and incubated overnight with 1% milk powder in PBS1X with 0.1% Tween-20 with the following antibodies: anti-PARP-1(C2-10 mouse, ALEXIS, LA), anti-PTEN (Santa Cruz Biotechnology sc-7974), anti-BRCA1 (Santa Cruz Biotechnology sc-642), anti-RAD51 (Santa Cruz Biotechnology (H-92) sc-8349), anti-phosphoERK (Santa Cruz Biotechnology sc-7383), anti-ERK (Invitrogen. Carlsbad, CA 61-7400), anti-phospho H2AX (Millipore 05-636) and anti-BUBR1 (BD Bioscience. Erembodegem, Belgium). α -Tubulin (Sigma, St Louis MO) and β -Actin (Sigma, St Louis MO) were used as loading control. Bands were visualized with ECL, ECL-PLUS and ECL PRIME (Amersham Biosciences) and the pictures were taken with the imaging system ChemiDoc XRS System (BIO-RAD) and medical X-ray films (AGFA).

RNA interference

Cells were plated in 6 wells at a density of 9×10^4 cells per well. 24 hours later, cells were transfected with the indicated siRNAs at 50 nM using Lipofectamine 2000 transfection agent (Invitrogen) according to the manufacturer's guide. Double-stranded RNA duplexes corresponding to a non-targeted control (5'-CCUACAUCCCGAUCGAUGAUGUU-3'), PTEN (5'-GCUACCUGUUAAGAAUCA-3') and BUBR1 (5'-CGGGCAUUUGAAUAUGAAA-3') were ordered to SIGMA-ALDRICH, and double-stranded RNA duplexes corresponding to human PARP-1 were from Ambion Applied Biosystems. 48 hours after transfection, cells were treated with PARP inhibitors as indicated above.

PTEN restoration

Cells were plated in 6 wells at a density of 1×10^5 cells per well. 24 hours later, transfection was performed with 0,5 μg pSG5L Flag HA Plasmid, pSG5L Myr HA PTEN Plasmid, GFP-PTEN Plasmid or pCDNA3-GFP Plasmid (all from Addgene), using JetPRIME TM (Polyplus transfection, Illkirch, France) according to the manufacturer's protocol. Cells were treated 48 hours after the transfection and harvested following the treatment in order to develop Cell Cycle and Western Blot analysis.

Immunofluorescence

Cells were plated in 12 wells at a density of $2,5 \times 10^4$ cells per well on glass cover-slips. After the treatments cells were fixed with Paraformaldehyde Solution (4%, wt/vol in PBS1x with 2% Sucrose) for 10 minutes at room temperature and permeabilized with PBS 1X 0,5% Triton x100 for 5 minutes at room temperature. phospho-H2AX was detected by immunofluorescence, using monoclonal antibody (Millipore 05-636) at a dilution 1:250 and FITC-conjugated goat anti-mouse immunoglobulin (Sigma, St Louis Mo) at a dilution 1:400. RAD51 foci were detected using rabbit polyclonal IgG antibody (H-92 Santa Cruz) 1:100 and FITC-conjugated goat anti-rabbit 1:400. Nuclear counterstaining with DAPI was performed after removal of excess secondary antibody. Immunostaining was visualized with Confocal Leica LCS SP5 Fluorescence Microscope.

Homologous Recombination Assay

U87MG and LN229 glioma cells were stably transfected with a pDR-GFP plasmid containing a mutated GFP gene with an 18 bp SclI site and were maintained under puromycin selection before use. Transient transfection of SclI in both cell lines creates a DSB at the relevant site in the integrated GFP gene. Homologous recombination repair (HRR) of this break restores GFP gene expression [26].

Cells were plated in 6 wells at a density of 9×10^4 cells per well for stable transfection with DR-GFP. 24 hours later, cells were transfected with 1 μ g DR-GFP plasmid per well using JetPEI TM (Polyplus transfection, Illkirch, France), according to the manufacturer's protocol. Transfected cells were maintained under puromycin selection, and transfection was proved by PCR with the primers

DRGFP1 5'AGGGCGGGGTTTCGGCTTCTGG 3'
DRGFP2 5'CCTTCGGGCATGGCGGACTTGA 3'

For the transient transfection with SclI, cells were plated in 6 wells at a density of 9×10^4 cells per well. 24 hours later, cells were transfected with 4 μ g SclI plasmid per well using JetPRIME™ (Polyplus transfection, Illkirch, France) according to the manufacturer's protocol. 24 hours after the transfection, cells were treated with PJ34 hours during 48 hours. Finally, cells were trypsinized and percentage of GFP expressing cells was measured by flow cytometry on a FACScan.

Frequency of recombination events was calculated as mean percentage of GFP positive cells transfected with SclI divided by mean percentage of GFP positive cells transfected with pEGFP. Results were represented through Kolmogorov-Smirnov adjust using CellQuest software.

Additionally, homologous recombination was indirectly evaluated by the number of cells with rad51

foci to get the fraction of γ H2AX positive cells bearing Rad51 foci. At least 120 cells from three independent experiments were counted using Image J software.

Micronucleus assay

DAPI counterstain described for pyknotic nuclei quantification was also used in order to analyse micronuclei frequency after PARP inhibition. Micronuclei counting was performed using Image J software.

DNA repair microarray

Cells were plated in p60 at a density of 1×10^6 cells. RNA extraction was performed 24 hours after PJ34 treatment, with RNeasy MiniKit (Qiagen). Retrotranscription was developed with RT2 First Strand kit (Qiagen) and cDNA was tested by RT2 Profiler PCR Array - Human DNA Damage Signalling Pathway (Qiagen) according to the manufacturer's protocol. Data were analysed by the $\Delta\Delta$ Ct method.

Ethics Statement

All human subjects data was publicly available in de-identified form on the Oncomine website (<https://www.oncomine.org/>) Therefore, its use was not classified as human subjects research, and no Institutional Review Board approval was needed.

Patient Datasets and Data Analysis

The microarray gene expression data was obtained from EMBO-EBI (<http://www.ebi.ac.uk/arrayexpress/>) and the clinical data was obtained from the database Oncomine (<https://www.oncomine.org/>) using data available on October 1st, 2010. Diagnoses were also made at the respective clinics. At the time of access, 343 glioma patient samples with both gene expression data and corresponding survival times were available on the Rembrandt database. These included 413 GBMs, 138 overexpressing BUB1B and 275 rest of samples.

In vivo bioluminescence assay

This study was performed in strict accordance with the recommendations in the Guide for the Care and Use of Laboratory Animals of the Bioethical Committee of CIBM-UGR. The protocol was approved by the Committee on the Ethics of Animal Experiments of the CIBM-UGR. All surgery was performed under ketamine – xylazine anesthesia, and every effort was made to minimize suffering.

Thirteen-weeks-old male Balb/cnu/nu mice (Charles River Laboratories, Wilmington, MA, USA) were injected intracranially with U87MG-luc cells (1×10^5) by introducing stereotactically the needle of a Hamilton syringe. The day after injection of tumour cells mice were treated three times per week mice with PJ34 at a dose of 10mg/kg body weight and/or erlotinib at a dose of 50 mg/kg body weight injected intraperitoneally. Sodium Chloride solution/60% DMSO was used as vehicle. In order to develop *in vivo* bioluminescence measurement, mice were injected intraperitoneally with D-luciferin solution dissolved in phosphate-buffered saline at a dose of 150 mg/kg body weight. After 5 minutes, the animals were anesthetized in the dark chamber using 3% isoflurane in air at 1.5 L/min and O₂ at 0.2 L/min/mouse, and animals were imaged in a chamber connected to a camera (IVIS, Xenogen, Alameda, CA). The quantification of light emission was performed in photons/second/cm²/steradian using Living Image 2.6.1 software (Xenogen). Tumour growth was monitored at 0, 2, 8, 15 and 21 days by *in vivo* imaging and bioluminescence measurement. After 21 days, mice were sacrificed, and brains were dissected and placed in Petri dishes with D-luciferin solution at a dose of 20µg/ml. Ex vivo quantification of light emission was performed by introducing the petri dishes inside the chamber connected to IVIS as explained before.

Statistical Analysis

Independent experiments were pooled when the coefficient of variance could be assumed identical. Statistical significance was evaluated using t-test (n=number of independent experiments). *P*-values below 0.05 were considered significant.

ACKNOWLEDGEMENTS

We acknowledge Abelardo López-Rivas and Tania Sánchez (CABIMER, CSIC, Sevilla) for helpful discussions, and Eva M^a Galán Moya (Hôpital Cochin, INSERM-CNRS, Paris) for her advices for primary cells lines experiments set up and helpful discussions. Joan Seoane (Hospital Vall d'Hebron, Barcelona) for providing LN229 cells, Guillermo Velasco (Complutense University, Madrid) for providing U118MG and SW1783 cells and Professor Yasuhiro Matsumura (National Cancer Center Hospital East, Kashiwanoha, Kashiwa City, Japan), for his kindness in providing the cells U87MG luciferase. We also acknowledge Salvador Guerrero and Jose Luis Luque for excellent technical assistance. JMM has been funded by a predoctoral fellowship by the programme FPU, Spanish Ministry of Economy and Competitiveness. This work was supported by Junta de Andalucía, project of Excellence P10-CTS-0662, Spanish Ministry of Economy and Competitiveness SAF2009-13281-C02-01,

SAF2012-40011-C02-01 and RTICC RD12/0036/0026.

CONFLICT OF INTERESTS

The authors declare no conflict of interests.

REFERENCES

1. Furnari FB, Fenton T, Bachoo RM, Mukasa A, Stommel JM, Stegh A, Hahn WC, Ligon KL, Louis DN, Brennan C, Chin L, DePinho RA and Cavenee WK. Malignant astrocytic glioma: genetics, biology, and paths to treatment. *Genes & development*. 2007; 21(21):2683-2710.
2. Comprehensive genomic characterization defines human glioblastoma genes and core pathways. *Nature*. 2008; 455(7216):1061-1068.
3. Parsons DW, Jones S, Zhang X, Lin JC, Leary RJ, Angenendt P, Mankoo P, Carter H, Siu IM, Gallia GL, Olivi A, McLendon R, Rasheed BA, Keir S, Nikolskaya T, Nikolsky Y, et al. An integrated genomic analysis of human glioblastoma multiforme. *Science*. 2008; 321(5897):1807-1812.
4. Salmena L, Carracedo A and Pandolfi PP. Tenets of PTEN tumor suppression. *Cell*. 2008; 133(3):403-414.
5. Shen WH, Balajee AS, Wang J, Wu H, Eng C, Pandolfi PP and Yin Y. Essential role for nuclear PTEN in maintaining chromosomal integrity. *Cell*. 2007; 128(1):157-170.
6. Schreiber V, Dantzer F, Ame JC and de Murcia G. Poly(ADP-ribose): novel functions for an old molecule. *Nat Rev Mol Cell Biol*. 2006; 7(7):517-528.
7. Gibson BA and Kraus WL. New insights into the molecular and cellular functions of poly(ADP-ribose) and PARPs. *Nat Rev Mol Cell Biol*. 2012; 13(7):411-424.
8. Bryant HE, Schultz N, Thomas HD, Parker KM, Flower D, Lopez E, Kyle S, Meuth M, Curtin NJ and Helleday T. Specific killing of BRCA2-deficient tumours with inhibitors of poly(ADP-ribose) polymerase. *Nature*. 2005; 434(7035):913-917.
9. Farmer H, McCabe N, Lord CJ, Tutt AN, Johnson DA, Richardson TB, Santarosa M, Dillon KJ, Hickson I, Knights C, Martin NM, Jackson SP, Smith GC and Ashworth A. Targeting the DNA repair defect in BRCA mutant cells as a therapeutic strategy. *Nature*. 2005; 434(7035):917-921.
10. McCabe N, Turner NC, Lord CJ, Kluzek K, Bialkowska A, Swift S, Giavara S, O'Connor MJ, Tutt AN, Zdzienicka MZ, Smith GC and Ashworth A. Deficiency in the repair of DNA damage by homologous recombination and sensitivity to poly(ADP-ribose) polymerase inhibition. *Cancer Res*. 2006; 66(16):8109-8115.
11. Fong PC, Boss DS, Yap TA, Tutt A, Wu P, Mergui-Roelvink M, Mortimer P, Swaisland H, Lau A, O'Connor MJ, Ashworth A, Carmichael J, Kaye SB, Schellens JH and de Bono JS. Inhibition of poly(ADP-ribose) polymerase in tumors from BRCA mutation carriers. *N Engl J Med*. 2009;

361(2):123-134.

12. Sun CK, Zhang F, Xiang T, Chen Q, Pandita TK, Huang Y, Hu MC and Yang Q. Phosphorylation of ribosomal protein S6 confers PARP inhibitor resistance in BRCA1-deficient cancers. *Oncotarget*. 2014; 5(10):3375-3385.
13. Ha K, Fiskus W, Choi DS, Bhaskara S, Cerchietti L, Devaraj SG, Shah B, Sharma S, Chang JC, Melnick AM, Hiebert S and Bhalla KN. Histone deacetylase inhibitor treatment induces 'BRCAness' and synergistic lethality with PARP inhibitor and cisplatin against human triple negative breast cancer cells. *Oncotarget*. 2014; 5(14):5637-5650.
14. Ossovskaya V, Koo IC, Kaldjian EP, Alvares C and Sherman BM. Upregulation of Poly (ADP-Ribose) Polymerase-1 (PARP1) in Triple-Negative Breast Cancer and Other Primary Human Tumor Types. *Genes Cancer*. 2010; 1(8):812-821.
15. Murai J, Zhang Y, Morris J, Ji J, Takeda S, Doroshow JH and Pommier Y. Rationale for poly(ADP-ribose) polymerase (PARP) inhibitors in combination therapy with camptothecins or temozolomide based on PARP trapping versus catalytic inhibition. *J Pharmacol Exp Ther*. 2014; 349(3):408-416.
16. Venere M, Hamerlik P, Wu Q, Rasmussen RD, Song LA, Vasanji A, Tenley N, Flavahan WA, Hjelmeland AB, Bartek J and Rich JN. Therapeutic targeting of constitutive PARP activation compromises stem cell phenotype and survival of glioblastoma-initiating cells. *Cell Death Differ*. 2014; 21(2):258-269.
17. van Vuurden DG, Hulleman E, Meijer OL, Wedekind LE, Kool M, Witt H, Vandertop PW, Wurdinger T, Noske DP, Kaspers GJ and Cloos J. PARP inhibition sensitizes childhood high grade glioma, medulloblastoma and ependymoma to radiation. *Oncotarget*. 2011; 2(12):984-996.
18. McEllin B, Camacho CV, Mukherjee B, Hahm B, Tomimatsu N, Bachoo RM and Burma S. PTEN loss compromises homologous recombination repair in astrocytes: implications for glioblastoma therapy with temozolomide or poly(ADP-ribose) polymerase inhibitors. *Cancer research*. 70(13):5457-5464.
19. Mendes-Pereira AM, Martin SA, Brough R, McCarthy A, Taylor JR, Kim JS, Waldman T, Lord CJ and Ashworth A. Synthetic lethal targeting of PTEN mutant cells with PARP inhibitors. *EMBO Mol Med*. 2009; 1(6-7):315-322.
20. McEllin B, Camacho CV, Mukherjee B, Hahm B, Tomimatsu N, Bachoo RM and Burma S. PTEN loss compromises homologous recombination repair in astrocytes: implications for glioblastoma therapy with temozolomide or poly(ADP-ribose) polymerase inhibitors. *Cancer research*. 2010; 70(13):5457-5464.
21. Galan-Moya EM, Le Guelte A, Lima Fernandes E, Thirant C, Dwyer J, Bidere N, Couraud PO, Scott MG, Junier MP, Chneiweiss H and Gavard J. Secreted factors from brain endothelial cells maintain glioblastoma stem-like cell expansion through the mTOR pathway. *EMBO reports*. 2011; 12(5):470-476.
22. Castiel A, Visochek L, Mittelman L, Zilberstein Y, Dantzer F, Izraeli S and Cohen-Armon M. Cell death associated with abnormal mitosis observed by confocal imaging in live cancer cells. *J Vis Exp*. 2013; (78):e50568.
23. Castiel A, Visochek L, Mittelman L, Dantzer F, Izraeli S and Cohen-Armon M. A phenanthrene derived PARP inhibitor is an extra-centrosomes de-clustering agent exclusively eradicating human cancer cells. *BMC Cancer*. 2011; 11:412.
24. Sgorbissa A, Tomasella A, Potu H, Manini I and Brancolini C. Type I IFNs signaling and apoptosis resistance in glioblastoma cells. *Apoptosis : an international journal on programmed cell death*. 2011; 16(12):1229-1244.
25. Baker DJ, Dawlaty MM, Wijshake T, Jeganathan KB, Malureanu L, van Ree JH, Crespo-Diaz R, Reyes S, Seaburg L, Shapiro V, Behfar A, Terzic A, van de Sluis B and van Deursen JM. Increased expression of BubR1 protects against aneuploidy and cancer and extends healthy lifespan. *Nature cell biology*. 2013; 15(1):96-102.
26. Weinstock DM, Nakanishi K, Helgadottir HR and Jasin M. Assaying double-strand break repair pathway choice in mammalian cells using a targeted endonuclease or the RAG recombinase. *Methods Enzymol*. 2006; 409:524-540.
27. Park MJ, Kim MS, Park IC, Kang HS, Yoo H, Park SH, Rhee CH, Hong SI and Lee SH. PTEN suppresses hyaluronic acid-induced matrix metalloproteinase-9 expression in U87MG glioblastoma cells through focal adhesion kinase dephosphorylation. *Cancer research*. 2002; 62(21):6318-6322.
28. Clark MJ, Homer N, O'Connor BD, Chen Z, Eskin A, Lee H, Merriman B and Nelson SF. U87MG decoded: the genomic sequence of a cytogenetically aberrant human cancer cell line. *PLoS genetics*. 2010; 6(1):e1000832.
29. Ricke RM and van Deursen JM. Aneuploidy in health, disease, and aging. *J Cell Biol*. 2013; 201(1):11-21.
30. Lampson MA and Kapoor TM. The human mitotic checkpoint protein BubR1 regulates chromosome-spindle attachments. *Nat Cell Biol*. 2005; 7(1):93-98.
31. Musacchio A and Salmon ED. The spindle-assembly checkpoint in space and time. *Nat Rev Mol Cell Biol*. 2007; 8(5):379-393.
32. Ding Y, Hubert CG, Herman J, Corrin P, Toledo CM, Skutt-Kakaria K, Vazquez J, Basom R, Zhang B, Risler JK, Pollard SM, Nam DH, Delrow JJ, Zhu J, Lee J, DeLuca J, et al. Cancer-Specific requirement for BUB1B/BUBR1 in human brain tumor isolates and genetically transformed cells. *Cancer Discov*. 2013; 3(2):198-211.
33. Hegan DC, Lu Y, Stachelek GC, Crosby ME, Bindra RS and Glazer PM. Inhibition of poly(ADP-ribose) polymerase down-regulates BRCA1 and RAD51 in a pathway mediated by E2F4 and p130. *Proc Natl Acad Sci U S A*. 2010; 107(5):2201-2206.

34. Tentori L, Ricci-Vitiani L, Muzi A, Ciccarone F, Pelacchi F, Calabrese R, Runci D, Pallini R, Caiafa P and Graziani G. Pharmacological inhibition of poly(ADP-ribose) polymerase-1 modulates resistance of human glioblastoma stem cells to temozolomide. *BMC Cancer*. 2014; 14:151.
35. Tang JB, Svilar D, Trivedi RN, Wang XH, Goellner EM, Moore B, Hamilton RL, Banze LA, Brown AR and Sobol RW. N-methylpurine DNA glycosylase and DNA polymerase beta modulate BER inhibitor potentiation of glioma cells to temozolomide. *Neuro Oncol*. 2011; 13(5):471-486.
36. Galluzzi L, Vitale I, Abrams JM, Alnemri ES, Baehrecke EH, Blagosklonny MV, Dawson TM, Dawson VL, El-Deiry WS, Fulda S, Gottlieb E, Green DR, Hengartner MO, Kepp O, Knight RA, Kumar S, et al. Molecular definitions of cell death subroutines: recommendations of the Nomenclature Committee on Cell Death 2012. *Cell Death Differ*. 2012; 19(1):107-120.
37. Vitale I, Galluzzi L, Castedo M and Kroemer G. Mitotic catastrophe: a mechanism for avoiding genomic instability. *Nature reviews Molecular cell biology*. 2011; 12(6):385-392.
38. Ali M, Telfer BA, McCrudden C, O'Rourke M, Thomas HD, Kamjoo M, Kyle S, Robson T, Shaw C, Hirst DG, Curtin NJ and Williams KJ. Vasoactivity of AG014699, a clinically active small molecule inhibitor of poly(ADP-ribose) polymerase: a contributory factor to chemopotential *in vivo*? *Clin Cancer Res*. 2009; 15(19):6106-6112.
39. Robaszekiewicz A, Valko Z, Kovacs K, Hegedus C, Bakondi E, Bai P and Virag L. The role of p38 signaling and poly(ADP-ribose)ation-induced metabolic collapse in the osteogenic differentiation-coupled cell death pathway. *Free Radic Biol Med*. 2014; 76:69-79.
40. Antolin AA and Mestres J. Linking off-target kinase pharmacology to the differential cellular effects observed among PARP inhibitors. *Oncotarget*. 2014; 5(10):3023-3028.
41. Patru C, Romao L, Varlet P, Coulombel L, Raponi E, Cadusseau J, Renault-Mihara F, Thirant C, Leonard N, Berhneim A, Mihalescu-Maingot M, Haiech J, Bieche I, Moura-Neto V, Dumas-Duport C, Junier MP, et al. CD133, CD15/SSEA-1, CD34 or side populations do not resume tumor-initiating properties of long-term cultured cancer stem cells from human malignant glioma-neuronal tumors. *BMC Cancer*. 2010; 10:66.
42. Lamm GM, Steinlein P, Cotten M and Christofori G. A rapid, quantitative and inexpensive method for detecting apoptosis by flow cytometry in transiently transfected cells. *Nucleic Acids Res*. 1997; 25(23):4855-4857.

ROS-induced DNA damage and PARP-1 are required for optimal induction of starvation-induced autophagy

José Manuel Rodríguez-Vargas¹, María José Ruiz-Magaña², Carmen Ruiz-Ruiz², Jara Majuelos-Melguizo¹, Andreína Peralta-Leal¹, María Isabel Rodríguez¹, José Antonio Muñoz-Gómez³, Mariano Ruiz de Almodóvar², Eva Siles⁴, Abelardo López Rivas⁵, Marja Jäättelä⁶, F Javier Oliver¹

¹Instituto de Parasitología y Biomedicina López Neyra, CSIC, Avda. Conocimiento s/n, 18100 Armilla, Granada, Spain; ²IBIMER, Universidad de Granada, Granada, Spain; ³CIBERED, Hospital Universitario san Cecilio, Granada, Spain; ⁴Departamento de Ciencias Experimentales, Universidad de Jaén, Jaén, Spain; ⁵CABIMER, CSIC, Sevilla, Spain; ⁶Danish Cancer Society Institute of Cancer Biology, Strandboulevarden 49, Copenhagen DK-2100, Denmark

In response to nutrient stress, cells start an autophagy program that can lead to adaptation or death. The mechanisms underlying the signaling from starvation to the initiation of autophagy are not fully understood. In the current study we show that the absence or inactivation of PARP-1 strongly delays starvation-induced autophagy. We have found that DNA damage is an early event of starvation-induced autophagy as measured by γ -H2AX accumulation and comet assay, with PARP-1 knockout cells displaying a reduction in both parameters. During starvation, ROS-induced DNA damage activates PARP-1, leading to ATP depletion (an early event after nutrient deprivation). The absence of PARP-1 blunted AMPK activation and prevented the complete loss of mTOR activity, leading to a delay in autophagy. PARP-1 depletion favors apoptosis in starved cells, suggesting a pro-survival role of autophagy and PARP-1 activation after nutrient deprivation. *In vivo* results show that neonates of PARP-1 mutant mice subjected to acute starvation, also display deficient liver autophagy, implying a physiological role for PARP-1 in starvation-induced autophagy. Thus, the PARP signaling pathway is a key regulator of the initial steps of autophagy commitment following starvation.

Keywords: starvation; autophagy; DNA damage; PARP-1; mTOR; AMPK

Cell Research (2012) 22:1181-1198. doi:10.1038/cr.2012.70; published online 24 April 2012

Introduction

Nutrient starvation alarms eukaryotic cells to adjust metabolism to survive. An early response of the cellular metabolic adjustments involves inhibition of growth and induction of macroautophagy (referred to as autophagy) to optimize the usage of limited energy supplies. Autophagy, as a cellular process mobilizing intracellular nutrient resources, plays an important role in contributing to survival during these growth-unfavorable conditions. It is a highly conserved self-eating process in which intracellular membrane structures engulf a portion of cy-

toplasmic organelles for lysosomal degradation. Eukaryotic cells have developed a mechanism through which autophagy induction is tightly coupled to the regulation of cell growth. Disruption of autophagic pathways is associated with multiple disease states, including neurodegenerative diseases, cancer, infection, and several types of myopathy [1]. Autophagy is also a major mechanism by which starving cells reallocate nutrients from unnecessary to more essential processes [1]. During autophagy, a cytosolic form of light chain 3 (LC3; LC3-I) is cleaved and then conjugated to phosphatidylethanolamine to form the LC3-phosphatidylethanolamine conjugate (LC3-II), which is recruited to autophagosomal membranes [2]. Poly(ADP-ribose) (PAR) polymerase (PARP) enzymes catalyze the conversion of NAD⁺ to polymers of PAR [3]. Although its role in the DNA damage response has long been recognized, recent works indicate that PAR itself acts to directly induce cell death through stimulation of

Correspondence: F Javier Oliver

Tel: +34 958181655

E-mail: joliver@ipb.csic.es

Received 7 October 2011; revised 23 December 2011; accepted 9 January 2012; published online 24 April 2012

apoptosis-inducing factor (AIF) release [4, 5].

A recent study from our group has also implicated PARP-1 in autophagy induced by DNA damage and oxidative stress [6]. There are, however, important issues that remain unresolved, such as the involvement of PARP signaling in a physiologic model of autophagy as is the case for nutrient deprivation and the connection of PARP activation with the autophagic components. Among the numerous factors involved in the regulation of autophagy and growth, mTOR (target of rapamycin) is a key component that coordinately regulates the balance between growth and autophagy in response to physiological conditions and environmental stress.

In the current study we have found that starvation-induced autophagy results in reactive oxygen species (ROS) production, DNA damage (as measured by comet assay and γ -H2AX accumulation) and PARP-1 activation, leading to the inhibition of mTOR. Moreover, *parp-1*^{-/-} neonates display a deficient autophagy response following acute starvation. Altogether these results place PARP-1 activation and PAR formation as key players in the decision of the cell to engage autophagy.

Results

The absence or inhibition of PARP-1 delays starvation-induced autophagy

Starvation or nutrient deprivation is a physiological cellular stress to induce autophagy in eukaryotic cells. To study the role of PARP-1 in starvation-induced autophagy, we transiently transfected *parp-1*^{+/+} and *parp-1*^{-/-} mouse embryonic fibroblasts (MEFs) with GFP-LC3 and starved these cells with HANK buffer for 1, 2 and 4.5 h. The percentage of cells with punctate pattern of GFP-LC3 was counted by fluorescence microscopy. In the non-starved cells, GFP-LC3 was diffusely distributed in the cytosol and nucleus, but after treatment with HANK buffer there was a punctate pattern, indicative of an accumulation of autophagosomes (Figure 1A). The number of GFP-LC3 vesicles was higher in *parp-1*^{+/+} MEFs, with approximately 20 vesicles/cell in *parp-1*^{+/+} MEFs and 8-9 vesicles/cell in *parp-1*^{-/-} MEFs at 2 h of starvation (Supplementary information, Figure S1). At different times of starvation, a decreased number of cells with GFP-LC3 punctate pattern was observed in *parp-1*^{-/-} MEFs (Figure 1A). Rapamycin, an inhibitor of mTORC1, was used as a positive control for autophagy induction; *parp-1*^{-/-} cells were also less sensitive to rapamycin-induced autophagy than wild-type (WT) cells (Figure 1A). The conversion of LC3-I to LC3-II through proteolytic cleavage and lipidation is a hallmark of mammalian autophagy. We measured the LC3 conversion during starvation in *parp-1*^{+/+}

and *parp-1*^{-/-} cells, and found that it was decreased in *parp-1*^{-/-} MEFs (Figure 1B). These data indicate a pronounced delay of autophagy in the absence of PARP-1.

To further evaluate autophagy in this model, we used a chemical inhibitor of autophagy 3-Methyladenine (3-MA), an inhibitor of class III phosphatidylinositol 3-kinase [7], as well as the siRNA-based knockdown of an essential autophagy protein, Atg7. Treatment with 3-MA or siRNA of Atg7 led to a significant reduction in the number of cells with GFP-LC3 punctate pattern in *parp-1*^{+/+} MEFs after 2 h of starvation (Figure 1C and 1D). In starved *parp-1*^{-/-} MEFs, 3-MA or Atg7 siRNA treatment completely prevented autophagy (Figure 1C, 1D and Supplementary information, Figure S2). These data suggest that the translocation of GFP-LC3 observed in *parp-1*^{+/+} MEFs upon starvation is due to autophagy and reflects the functional role of autophagy during starvation. The absence of PARP-1 synergizes with 3-MA or ATG7 siRNA to suppress autophagy during starvation (Figure 1C and 1D). Lysosome fusion with autophagosomes was not affected in *parp-1*^{-/-} cells. Treatment with chloroquine to inhibit lysosome fusion resulted in a similar accumulation of LC3 vesicles in *parp-1*^{+/+} and *parp-1*^{-/-} cells (Supplementary information, Figure S3A).

To further evaluate the role of PARP-1 in starvation-induced autophagy, we tested the effect of the PARP-1 inhibitor DPQ and siRNA-based depletion of PARP-1 on the levels of autophagy in *parp-1*^{+/+} MEFs. Cells were transfected with GFP-LC3 and starved with HANK buffer for different time periods. Inhibition of PARP-1 with 40 μ M DPQ reduced the number of cells with a typical GFP-LC3 punctate pattern in starved *parp-1*^{+/+} MEFs, but had no effect in *parp-1*^{-/-} MEFs (Figure 2A). Similar results were also obtained using two other different PARP inhibitors, PJ34 and olaparib (Supplementary information, Figure S3B). PARP-1 silencing induced a reduction in the number of autophagic cells after 2 h of starvation (Figure 2B), similar to that in *parp-1*^{-/-} cells (Figure 2A). Further, PARP-1 knockdown reduced the conversion of endogenous LC3 during starvation (Figure 2C). The non-specific siRNA had no effect on the levels of autophagy. These data suggest that PARP-1 and PARP activation play an active role in the commitment to autophagy in situations of nutrient deprivation. To corroborate this finding, we reconstituted PARP-1 expression in *parp-1*^{-/-} MEFs with pBC-PARP-1 cDNA (Figure 2D and Supplementary information, Figure S4) and we co-transfected these cells with GFP-LC3. Cells transfected with the empty pBC vector were used as negative control. The reconstitution of PARP-1 in *parp-1*^{-/-} MEFs increased the number of autophagic cells upon starvation compared to *parp-1*^{-/-} MEFs transfected with the empty vector (Figure

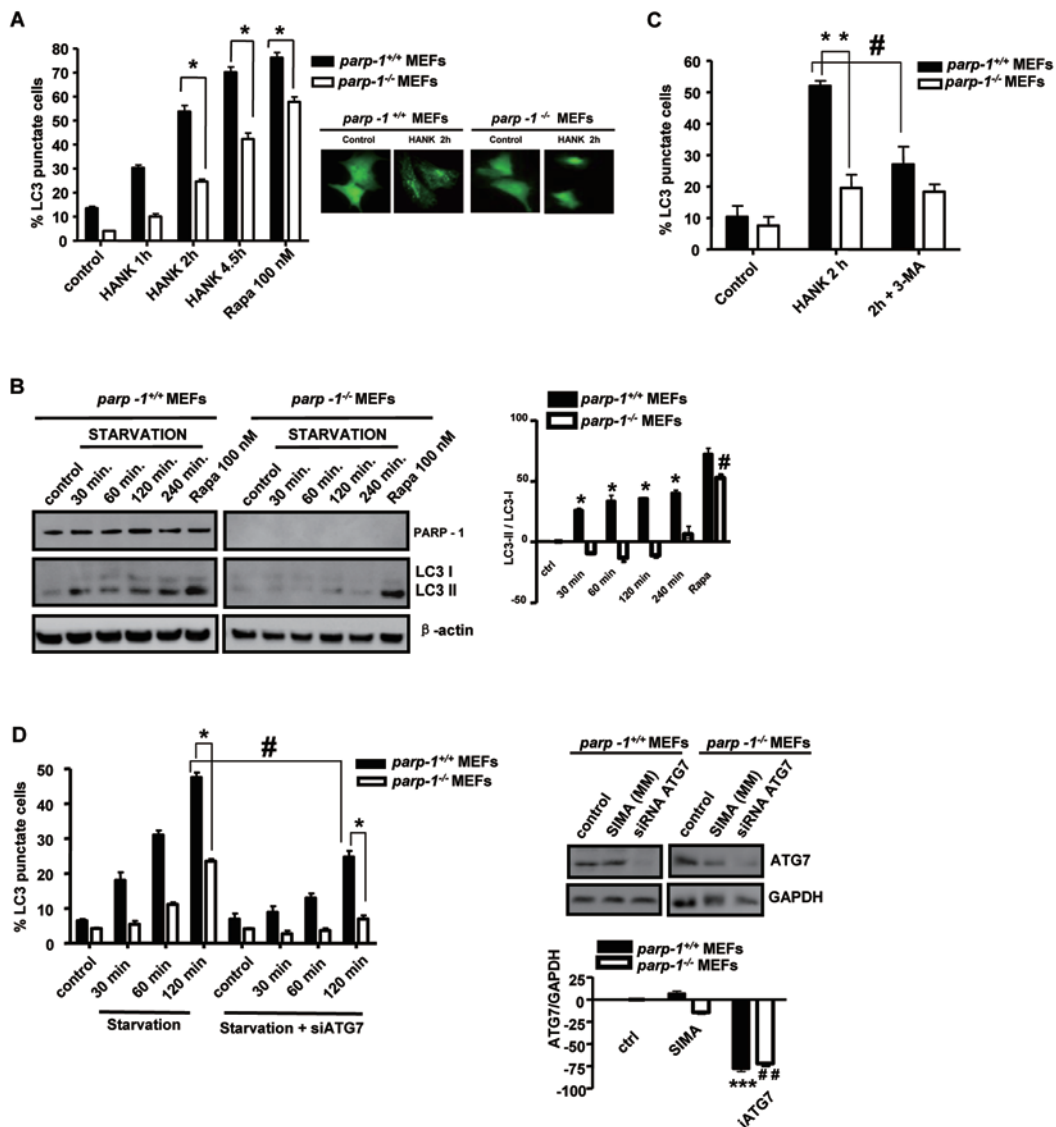


Figure 1 Starvation-induced autophagy is delayed in PARP-1 knockout cells. **(A)** *parp-1^{+/+}* and *parp-1^{-/-}* MEFs were transfected with GFP-LC3; 24 h following transfection, cells were starved with HANK buffer at 1, 2 and 4.5 h; percentages of LC3 conversion are shown. Treatment with 100 nM rapamycin for 4 h was used as positive control of autophagosome accumulation. The pictures in the right panel show representative images with the subcellular distribution of the autophagic vesicle marker LC3. **P* < 0.05 comparing between starved *parp-1^{+/+}* and *parp-1^{-/-}* MEFs. **(B)** Immunoblot analysis of endogenous LC3 conversion in control and starved cells at different times of starvation. Treatment with rapamycin was used as positive control of LC3 conversion and β -actin as loading control. Similar results were obtained in three independent experiments. **P* < 0.05 comparing between starved *parp-1^{+/+}* and *parp-1^{-/-}* MEFs. #*P* < 0.05 comparing between rapamycin-treated *parp-1^{-/-}* MEFs and non-starved control *parp-1^{-/-}* MEFs. **(C)** Effect of 2 mM 3-MA on autophagy of *parp-1^{+/+}* and *parp-1^{-/-}* MEFs during starvation. 3-MA was added 1.5 h before HANK buffer as pre-treatment and maintained during the starvation in both cell lines to slow down autophagy. ***P* < 0.01 comparing between starved *parp-1^{+/+}* and *parp-1^{-/-}* MEFs. #*P* < 0.05 comparing between starved *parp-1^{+/+}* MEFs and 3-MA-treated *parp-1^{+/+}* MEFs. **(D)** Effect of ATG7 silencing on starvation-induced autophagy. *parp-1^{+/+}* and *parp-1^{-/-}* MEFs were transfected with ATG7 siRNA (60 nM) and 48 h later they were transfected with GFP-LC3. 24 h later cells were starved with HANK buffer for 30 min, 1 h and 2 h. SIMA or non-specific siRNA was used as negative control, using the same protocol as for siRNA transfection. The right panel show the siRNA-mediated suppression of ATG7 expression in MEFs 3T3 48 h after transfection. GAPDH was used as loading control. **P* < 0.05 comparing between starved *parp-1^{+/+}* and *parp-1^{-/-}* MEFs. #*P* < 0.05 comparing between starved *parp-1^{+/+}* MEFs and ATG7-knockdown *parp-1^{+/+}* MEFs. Western blot quantification: ****P* < 0.001 comparing between ATG7-knockdown *parp-1^{+/+}* MEFs and control *parp-1^{+/+}* MEFs. ###*P* < 0.01 comparing between ATG7-knockdown *parp-1^{-/-}* MEFs and control *parp-1^{-/-}* MEFs. In **A**, **C** and **D**, at least 250 cells were counted under a Zeiss fluorescent microscope in both cell lines in three independent experiments.

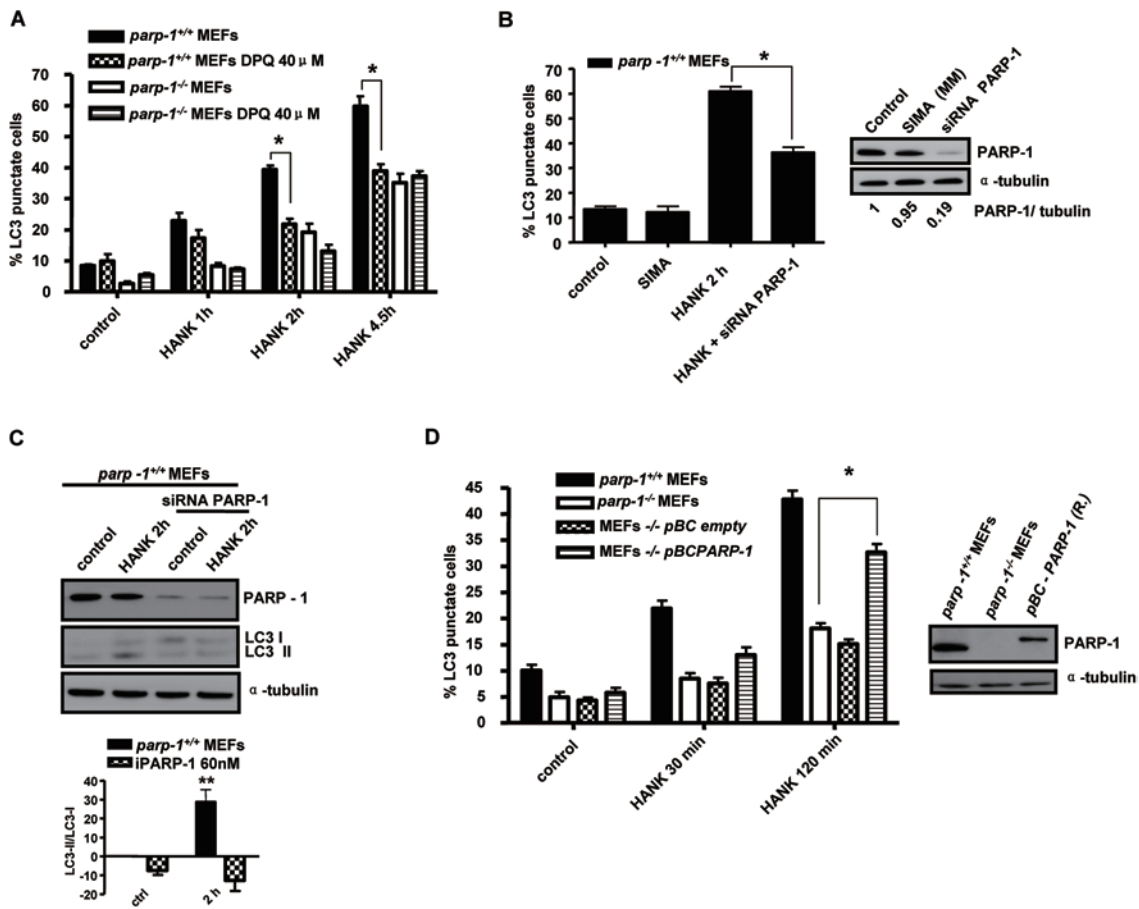


Figure 2 PARP-1 inhibition or silencing interferes with starvation-induced autophagy. **(A)** Effect of the inhibition of PARP-1 with DPQ on starvation-induced autophagy. *parp-1^{+/+}* and *parp-1^{-/-}* MEFs were transfected with GFP-LC3; 24 h later, cells were pre-treated with 40 μ M DPQ for 1.5 h. During the different starvation time periods, 40 μ M DPQ was present in HANK buffer to maintain PARP-1 inhibition. Percentages of cells with LC3 conversion are shown. **P* < 0.05 comparing between DPQ-treated starved *parp-1^{+/+}* MEFs and starved *parp-1^{+/+}* MEFs. **(B)** Effect of PARP-1 silencing on starvation-induced autophagy. *parp-1^{+/+}* MEFs were transfected with murine PARP-1 siRNA (50 nM). 48 h later cells were transfected with GFP-LC3 and 24 h later were starved for 2 h. The percentage of cells with the typical GFP-LC3 punctate pattern was compared with the percentage in non-silencing *parp-1^{+/+}* MEFs starved for the same time period. SIMA or non-specific siRNA (50 nM) was used as negative control, using the same protocol as for siRNA transfection. The right panel shows the levels of PARP-1 silencing 48 h after the transfection. α -Tubulin was used as loading control. **P* < 0.05 comparing between starved *parp-1^{+/+}* MEFs and PARP-1-knockdown starved *parp-1^{+/+}* MEFs. **(C)** Western blot analysis of the effect of PARP-1 silencing on endogenous LC3 conversion in *parp-1^{+/+}* MEFs starved for 2 h with HANK buffer. α -Tubulin was used as loading control. Similar results were obtained in three independent experiments. ***P* < 0.01 comparing between starved *parp-1^{+/+}* MEFs and PARP-1-knockdown starved *parp-1^{+/+}* MEFs. **(D)** Reconstitution of PARP-1 in *parp-1^{-/-}* MEFs and effect on starvation-induced autophagy. *parp-1^{-/-}* MEFs were transfected with pBC-PARP-1 to transiently reconstitute PARP-1 and 24 h later cells were transfected with GFP-LC3; 24 h after transfection cells were starved with HANK buffer for 30 min and 2 h. pBC empty plasmid was used as negative control. The right panel shows the expression level of PARP-1 24 h after reconstitution in *parp-1^{-/-}* MEFs and compared with the expression levels of PARP-1 in WT and knockout cells. α -Tubulin was used as loading control. **P* < 0.05 comparing between starved *parp-1^{-/-}* MEFs and PARP-1-restored *parp-1^{-/-}* MEFs. In **A**, **B** and **D**, at least 250 nuclei were counted under a Zeiss fluorescent microscope in three independent experiments.

2D and Supplementary information, Figure S4). These data suggest that PARP-1 participates in the commitment of starvation-induced autophagy and may be indirectly

involved in the formation of autophagosomes, since its inhibition or silencing leads to a delay in the autophagic response, including LC3 conversion and autophagosome

formation. Indeed, autophagy was delayed but not abrogated after PARP-1 ablation, since increasing starvation time to 8 h resulted in an equivalent autophagic rate between WT and knockout cells (data not shown).

Starvation induces ROS production, DNA damage and activation of PARP-1

PARP-1 is a nuclear enzyme activated by DNA damage; following genotoxic stress PARP-1 synthesizes a branched polymer of poly(ADP-ribose) or PAR that participates in the regulation of the nuclear homeostasis [3, 6, 8]. Many different cellular insults that cause DNA damage activate PARP-1 and induce PARP-1-dependent cell death. During starvation the production of ROS plays an important role in triggering autophagy [9, 10]. We hypothesized that ROS production during starvation could induce activation of PARP-1 and play an important role in the regulation of PARP-1-dependent autophagy.

Starvation indeed induced activation of PARP-1 in *parp-1^{+/+}* MEFs, as measured by PAR synthesis (Figure 3A). The PARP inhibitor PJ34 blocked starvation-induced PAR synthesis, and H₂O₂ was used as a positive control for activation of PARP-1 (Figure 3A and Supplementary information, Figure S5).

To demonstrate the production of ROS during starvation, we used 2',7'-dichlorofluorescein diacetate (DCFDA) as a probe to measure ROS (in particular, this probe detects H₂O₂) in *parp-1^{+/+}* and *parp-1^{-/-}* MEFs by flow cytometry [11]. PARP-1-deficient cells displayed a reduced production of ROS even at very early time points following starvation (Figure 3B). This finding is consistent with previous results showing a reduced ROS production in lymphocytes challenged with exogenous oxidative stress and treated with PARP inhibitors [12]. Assuming that ROS synthesis and their nuclear diffusion to induce DNA damage are very fast, we chose 30 min of starvation as the time point to measure DNA damage. COMET assay showed that 30 min after starvation, DNA damage was much more pronounced in *parp-1^{+/+}* MEFs (Figure 3C); the tail moment (TM) of the comets is much higher in *parp-1^{+/+}* cells, and almost full repair is achieved after 1 h, indicating that the DNA repair machinery is active (Figure 3C). By contrast, in *parp-1^{-/-}* cells the level of DNA damage is clearly reduced at 30 min, but the DNA repair machinery is not as efficient as in WT cells, resulting in a residual level of damage after 60 min of starvation (Figure 3C).

At the same time, *parp-1^{+/+}* MEFs had higher levels of phosphorylation of γ -H2AX, suggesting an increased number of DNA lesions due to the boost in ROS production (Figure 3D). γ -H2AX signal peaks at 1 h of starvation in *parp-1^{+/+}* MEFs while in PARP-1-deficient

cells γ -H2AX continues to accumulate, consistent with a less efficient repair as implicated by the COMET assay. Furthermore, indirect immunofluorescence analysis revealed that the number of *parp-1^{+/+}* cells with positive staining for γ -H2AX after 1 h of starvation was elevated compared to *parp-1^{-/-}* cells (Supplementary information, Figure S6).

To further confirm the implication of ROS in the initiation of autophagy, we used the antioxidant n-acetylcysteine (NAC). Cells exposed to this compound showed a decrease in γ -H2AX accumulation and LC3II lipidation, indicating that ROS generation is key in triggering DNA damage and subsequent autophagy (Figure 3E).

Together, these data indicate that during starvation there is an important production of ROS in *parp-1^{+/+}* MEFs and these ROS induce DNA damage and PARP-1 activation, leading to PAR synthesis and triggering the initiation of autophagy associated to nutrient deprivation. Although *parp-1^{-/-}* cells also produce ROS during starvation, this production does not lead to massive DNA damage and PARP-1 activation; consequently these cells display an impaired starvation-induced autophagy.

Lack of PARP-1 reduces ATP depletion, AMPK activation and mTOR inhibition during starvation-induced autophagy

Energy depletion, measured as an imbalance of AMP/ATP (adenosine 5'-triphosphate) ratio, is the main signal sensed by AMPK to induce autophagy. To investigate whether PARP-1 is implicated in AMPK-dependent autophagy, we measured the levels of ATP in *parp-1^{+/+}* MEFs and *parp-1^{-/-}* MEFs after different times of starvation. The levels of ATP in *parp-1^{+/+}* MEFs after 60 min of starvation decreased to less than 50% of the initial level, while in *parp-1^{-/-}* MEFs ATP levels decreased significantly more slowly (Figure 4A). Treatment with 3-MA during starvation blocked ATP depletion in *parp-1^{+/+}* cells, indicating that this energy drop was due to autophagy induced by nutrient deprivation (Figure 4A). 3-MA also prevented ATP depletion in *parp-1^{-/-}* cells, which have delayed autophagy. The depletion of ATP level corresponded with a sustained activation, through phosphorylation, of AMPK in *parp-1^{+/+}* MEFs (Figure 4B). This activation was strongly inhibited in *parp-1^{-/-}* MEFs (Figure 4B).

mTOR is a serine/threonine protein kinase that regulates cell growth, cell proliferation, cell motility, cell survival, protein synthesis, and transcription [13]. mTOR is also a sensor of the cellular energy status. For this action it is regulated by the kinase AMPK, an important activator of autophagy [14, 15]. We have thus evaluated the status of mTOR (which turns off autophagy when it

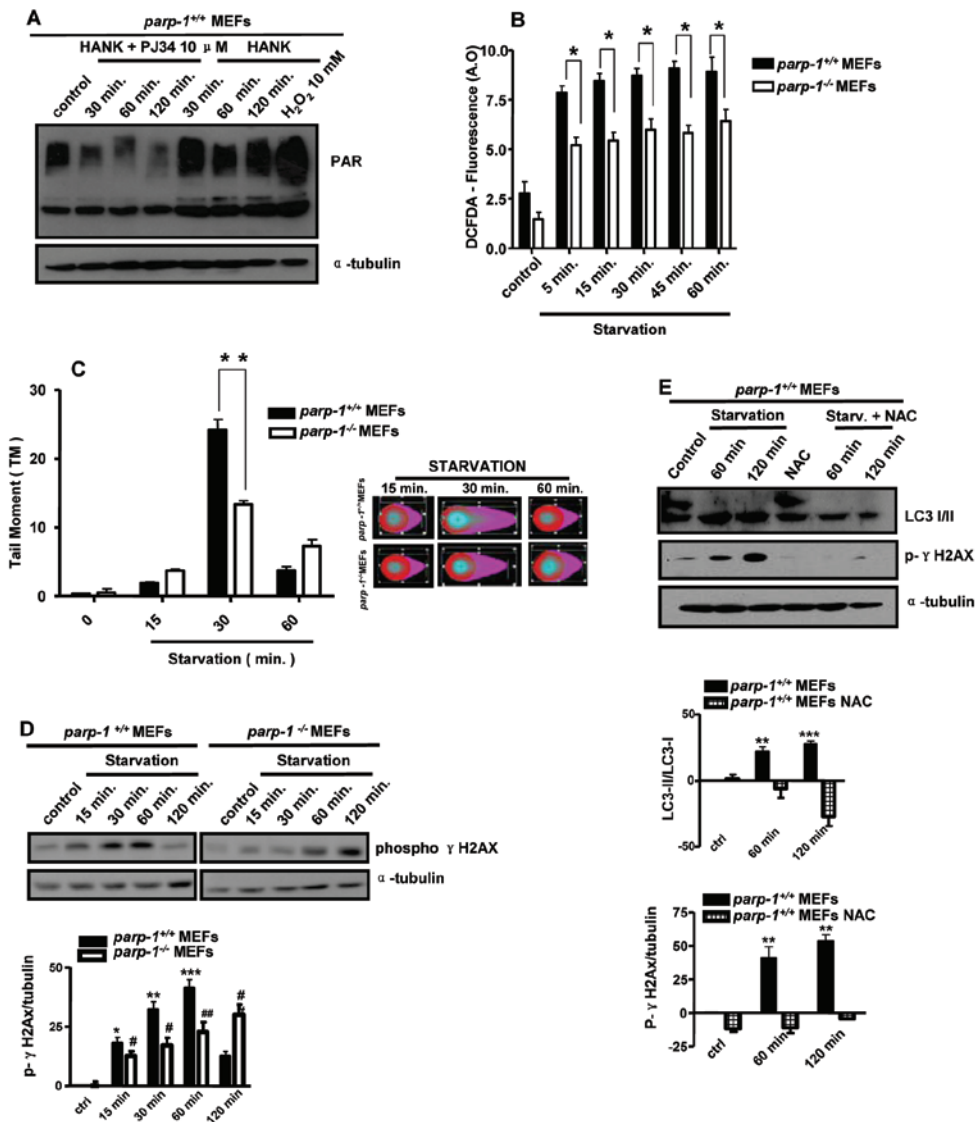
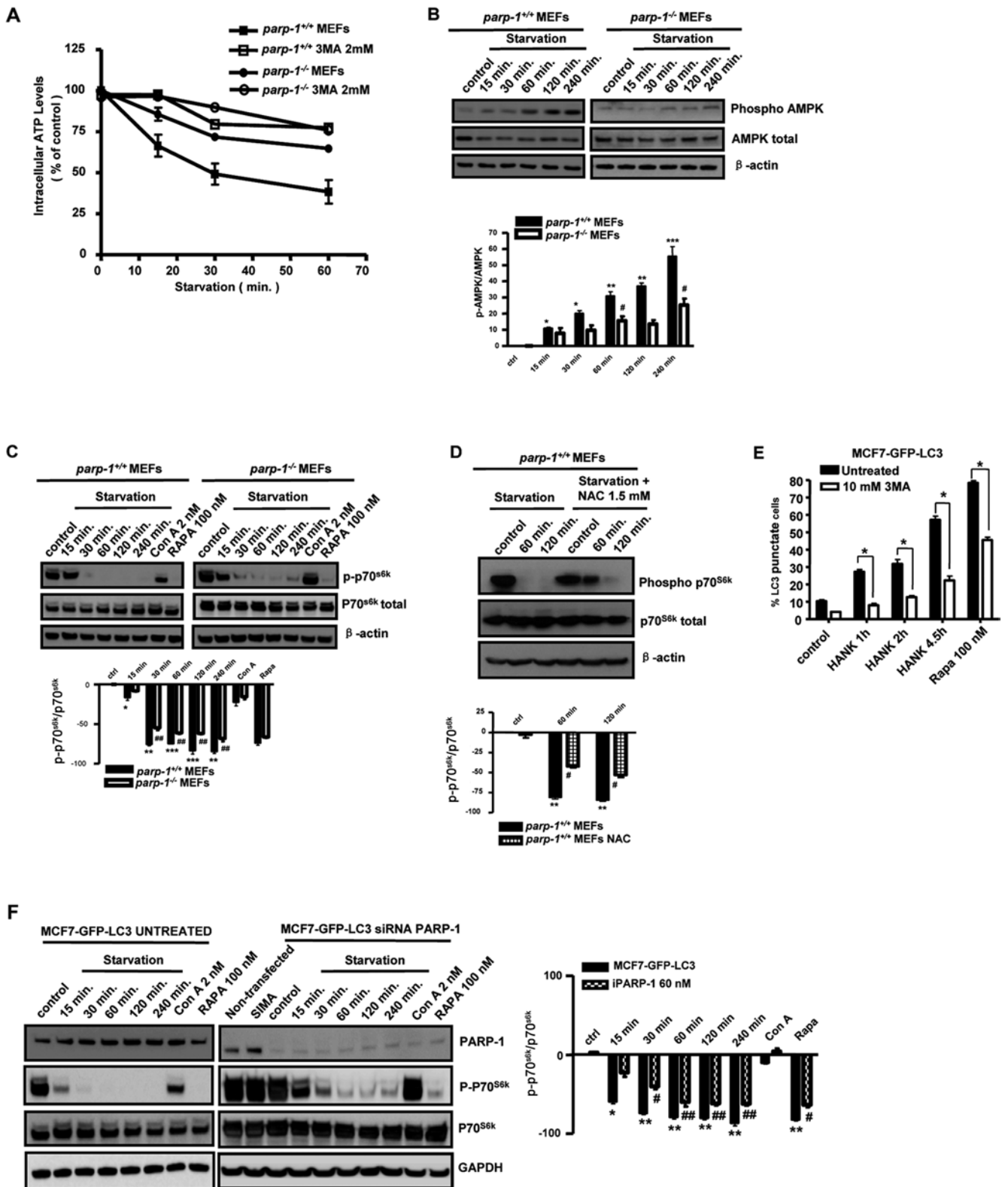


Figure 3 PAR synthesis and DNA damage during starvation-induced autophagy. **(A)** Western blot analysis of PAR formation during starvation. *parp-1^{+/+}* MEFs were starved for 30 min, 1 h and 2 h with HANK buffer. Whole cell extracts were subjected to PAGE and PAR was measured with a specific antibody. Where indicated, cells were pre-treated with PJ34, a PARP-1 inhibitor, for 1.5 h and PJ34 was maintained during the nutrient deprivation. Treatment with 10 mM H₂O₂ for 10 min was used as a positive control of PARP-1 activation and PAR synthesis. α -Tubulin was used as loading control. **(B)** ROS production during starvation. *parp-1^{+/+}* and *parp-1^{-/-}* MEFs were subjected to short times of nutrient deprivation with HANK buffer in the presence of the DCFDA probe (8 mg/ml), specific to measure ROS with a flow cytometer. Figure shows DCFDA fluorescence obtained as arbitrary units in triplicate in three independent experiments. * $P < 0.05$ comparing between starved *parp-1^{+/+}* and *parp-1^{-/-}* MEFs. **(C)** COMET assay during starvation. *parp-1^{+/+}* and *parp-1^{-/-}* MEFs were starved with HANK buffer for 15, 30 and 60 min and then were treated according to the manufacturer's instruction. Tail moment of 90 nuclei per condition in three independent experiments were analyzed by the specific software CASP (left panel). In the right panel images of the COMETs extracted from the software of each cell line for the different times of starvation are shown. ** $P < 0.01$ comparing between starved *parp-1^{+/+}* and *parp-1^{-/-}* MEFs. **(D)** Histone γ -H2AX phosphorylation during starvation. *parp-1^{+/+}* and *parp-1^{-/-}* MEFs were subjected to starvation for the indicated times. Total extract were obtained and the levels of phospho- γ -H2AX were measured by immunoblotting. Similar results were obtained in three independent experiments. α -Tubulin was used as loading control. * $P < 0.05$, ** $P < 0.01$ and *** $P < 0.001$ comparing between starved and non-starved *parp-1^{+/+}* MEFs. # $P < 0.05$, ## $P < 0.01$ comparing between starved and non-starved *parp-1^{+/+}* MEFs. **(E)** Treatment with the antioxidant NAC results in a significant delay in mTOR inactivation during starvation-induced autophagy. LC3 western blot quantification: ** $P < 0.01$, *** $P < 0.001$ comparing between starved *parp-1^{+/+}* MEFs and NAC-treated starved *parp-1^{+/+}* MEFs. Phospho- γ -H2Ax western blot quantification: ** $P < 0.01$ comparing between starved *parp-1^{+/+}* MEFs and NAC-treated starved *parp-1^{+/+}* MEFs.



is activated) by determining the phosphorylation of its substrate p70S6 kinase. Shortly after starvation (30 min) *parp-1^{+/+}* cells attained a complete inhibition of mTOR (Figure 4C), indicating that these cells were engaged in autophagy, while in *parp-1^{-/-}* cells mTOR was only partially inhibited even after 1 and 2 h of nutrient starvation; 4 h after starvation mTOR activation started to recover in the absence of PARP-1 (Figure 4C). Treatment with antioxidant NAC retarded starvation-induced mTOR inactivation (Figure 4D). These data suggest that PARP-1 may control mTOR activity during starvation and functions as a positive regulator of autophagy when cellular energy declines.

To further explore this, we analyzed the role of PARP-1 in mTOR activation regulation during starvation in a tumor cell model. In cancer cells the energy balance is critical to adapt the cell to the tumor microenvironment, which often features low nutrient and oxygen availability [16, 17]. We have performed assays with human breast cancer cell line stably transfected with GFP-LC3, MCF7-GFP-LC3. During starvation these cells showed endogenous LC3 translocation and the typical punctate pattern of GFP-LC3 under fluorescence microscope (Figure 4E).

MCF7-GFP-LC3 cells were used to determine the level of mTOR activation during starvation in the presence or absence of PARP-1 (Figure 4F). In these cells, mTOR is rapidly inhibited after starvation; 15 min after nutrient deprivation the phosphorylation levels of p70S6 kinase decreased drastically and the cells had entered into autophagy. Treatment with 3-MA retarded starvation-induced mTOR inactivation and downregulated AMPK (Supplementary information, Figure S7). In MCF7-GFP-LC3 depleted of PARP-1 using siRNA (Figure 4F), mTOR inhibition was significantly delayed. The delayed inhibition of mTOR activity in PARP-1 knockout cells and after PARP-1 silencing suggests that disabling of PARP-1 regulates autophagy by preventing complete mTOR inactivation.

To further confirm the implication of efficient DNA damage repair in the initiation of autophagy, we used HT144 melanoma cells (an ATM-deficient cell line) that are unable to properly repair γ -irradiation-induced DNA damage (data not shown). These cells displayed very high levels of DNA damage under basal conditions as shown by the elevated constitutive γ -H2AX levels (Supplementary information, Figure S8A). G361 cells

Figure 4 PARP-1 modulates AMPK activation and mTOR inhibition during starvation-induced autophagy. **(A)** Effect of nutrient starvation on ATP levels. *parp-1^{+/+}* and *parp-1^{-/-}* MEFs were starved with HANK buffer for 15, 30 and 60 min. Concentrations of ATP were normalized with total proteins in each sample and compared to the control (100%). 2 mM 3-MA was added 1.5 h before nutrient deprivation and was maintained during the experiment in order to inhibit autophagy. Error bars represent SE of the mean (SEM) of five independent experiments. **(B)** Immunoblot analysis of AMPK activation in control and starved cells at different times of starvation. The levels of phospho-AMPK in whole cell extracts were measured with a specific antibody in each cell lines after nutrient deprivation. Total AMPK was used to normalize the non-phosphorylated protein and β -actin as loading control. Similar results were obtained in three independent experiments. * $P < 0.05$, ** $P < 0.01$, *** $P < 0.001$ comparing between starved *parp-1^{+/+}* MEFs and non-starved control *parp-1^{+/+}* MEFs. # $P < 0.05$ comparing between starved *parp-1^{-/-}* MEFs and non-starved control *parp-1^{-/-}* 3T3 MEFs. **(C)** Immunoblot analysis of mTOR inhibition during starvation. The levels of phosphorylation of the mTOR substrate, p70S6 kinase, were measured by western blotting in whole cell extracts of *parp-1^{+/+}* and *parp-1^{-/-}* MEFs after different times of starvation. Treatment with concanamycin A (2 nM) for 4 h was used as control of mTOR-independent autophagy while treatment with rapamycin (100 nM) for 6 h was used as control of mTOR-dependent autophagy. Total p70S6 kinase was used to normalize the non-phosphorylated protein and β -actin as loading control. Similar results were obtained in two independent experiments. * $P < 0.05$, ** $P < 0.01$, *** $P < 0.001$ comparing between starved *parp-1^{+/+}* MEFs and non-starved control *parp-1^{+/+}* MEFs. ### $P < 0.01$ comparing between starved *parp-1^{-/-}* MEFs and non-starved control *parp-1^{-/-}* 3T3 MEFs. **(D)** Treatment with the antioxidant NAC significantly delays starvation-induced loss of mTOR activation measured as phospho-p70S6 kinase. ** $P < 0.01$ comparing between starved *parp-1^{+/+}* MEFs and non-starved control *parp-1^{+/+}* MEFs. # $P < 0.05$ comparing between NAC-treated and starved *parp-1^{+/+}* MEFs and NAC-treated and non-starved control *parp-1^{+/+}* 3T3 MEFs. **(E)** Induction of autophagy in MCF7-GFP-LC3 during starvation. Treatment with rapamycin was the positive control of autophagy. * $P < 0.05$ comparing between starved MCF7-GFP-LC3 and 3-MA-treated starved MCF7-GFP-LC3. **(F)** PARP-1 knockdown prevents autophagy-induced mTOR inhibition in a tumor cell model. Left panel: MCF7-GFP-LC3 cells were starved for different times with HANK buffer and the levels of phospho-p70S6 kinase were measured by western blotting. Concanamycin A and rapamycin were different controls of mTOR activation. p70S6 kinase and GAPDH were used to normalize protein loading. The results were obtained in 3 independent experiments. Right panel: MCF7-GFP-LC3 cells were either non-transfected, transfected with a scrambled (SIMA) siRNA or with PARP-1 siRNA (60 nM) and 48 h after transfection, cells were starved with HANK buffer; the levels of phospho-p70S6 kinase were measured by western blot. Concanamycin A and rapamycin were used as controls of mTOR activation. Total p70S6 kinase and GAPDH were used to normalize protein loading. Similar results were obtained in 3 independent experiments. * $P < 0.05$, ** $P < 0.01$ comparing between starved MCF7-GFP-LC3 and non-starved control MCF7-GFP-LC3. # $P < 0.05$, ## $P < 0.01$ comparing between PARP-1 knockdown starved MCF7-GFP-LC3 and non-starved control MCF7-GFP-LC3.

(ATM WT melanoma cells) accumulated DNA damage following starvation and inhibition of mTOR/p70S6K was achieved after 15 min. mTOR/p70S6K activity also decreased very rapidly in ATM mutant cells, but a residual activation was still detected after 30 min of starvation (Supplementary information, Figure S7A). The execution of autophagy determined as LC3 processing (Supplementary information, Figure S8B) and quantification of LC3 punctate cells (Supplementary information, Figure S8C) was delayed in ATM mutant cells, further supporting the mechanistic implication of DNA damage repair in the cell's ability to engage autophagy.

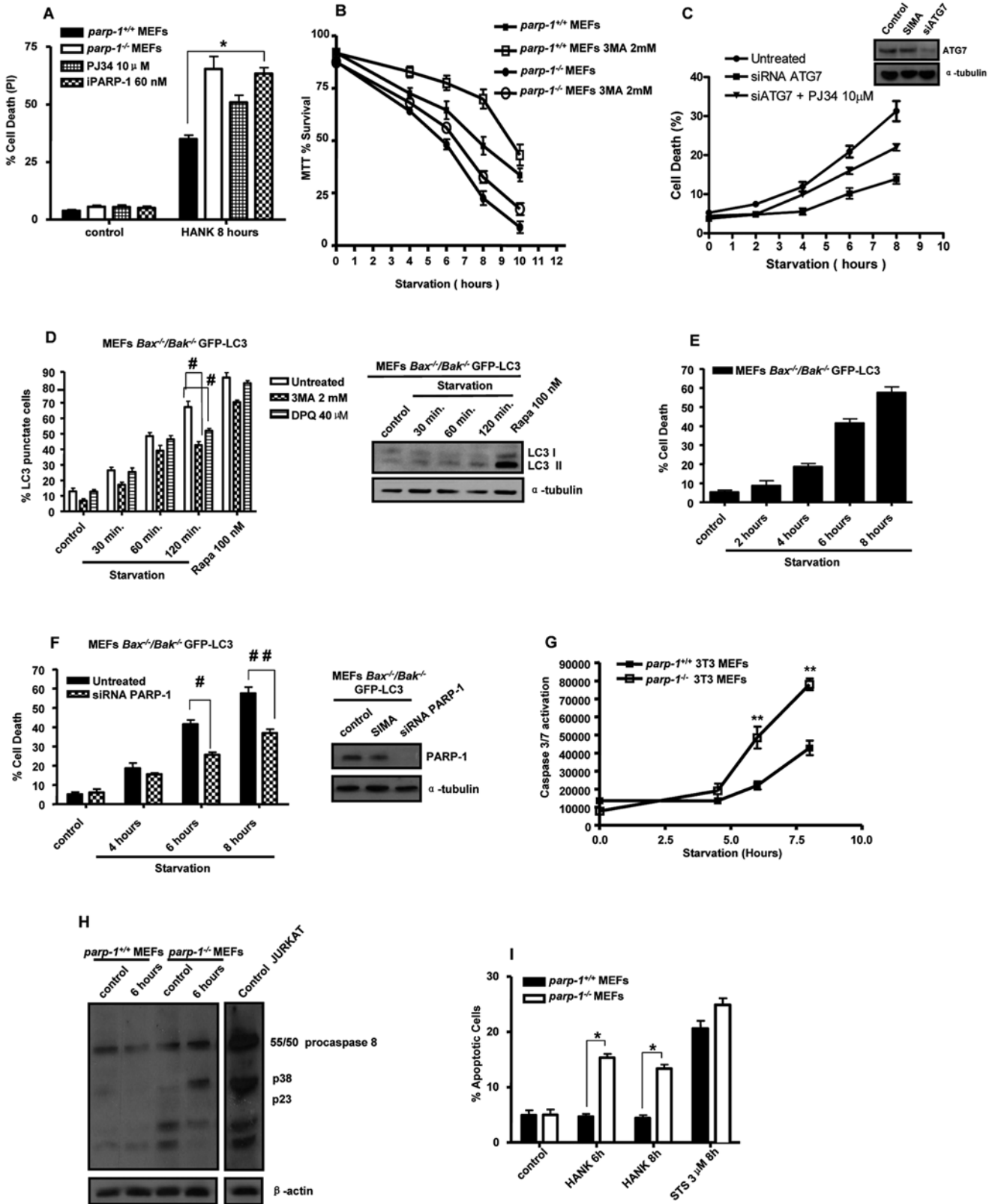
Impairment of autophagy by disabling of PARP-1 leads to increased apoptotic cell death

Autophagy is an adaptation and survival pathway under adverse conditions, but if these conditions are maintained for a long time, excessive autophagy can lead to cell death, often called autophagic cell death (ACD) [18]. ACD is morphologically defined as a type of cell death that occurs in the absence of chromatin condensation, but it is accompanied by massive autophagic vacuoles in the cytoplasm [19]. In contrast with the typical apoptotic cell death, in ACD there is no nuclear fragmentation, plasma membrane blebbing, caspase activation or engulfment by phagocytes *in vivo* [20]. Cells undergoing autophagy under adverse conditions can recover to their optimum physiological state after changing of the surrounding conditions. However, cells with inhibited autophagy or cells with disrupted mitochondrial transmembrane potential, would die even if optimal conditions are recovered [21]. To determine what is the predominant cell death process during starvation-induced autophagy upon ablation/inactivation of PARP-1, we examined both ACD and apoptotic cell death features after prolonged time of starvation. Time course analysis of total cell death following starvation showed accelerated cell death in the absence of PARP-1 as determined by propidium iodide (PI) incorporation (Figure 5A). PARP-1 inhibition with PJ34 or PARP-1 knockdown gave similar results of increased cell death after nutrient deprivation (Figure 5A). Thus, the absence of PARP-1 during starvation accelerates cell death. These results were confirmed by other methods of cell death assays such as trypan blue dye exclusion staining and MTT cell survival assay and with a different PARP-1 inhibitor DPQ (data not shown).

Autophagy has a pro-survival function after cellular stress such as nutrient withdrawal. This increased cell death following starvation after disabling of PARP-1 could be due to the decreased levels of autophagy. To determine whether autophagy has a cytoprotective role in WT cells, we inhibited autophagy with 3-MA and deter-

mined cell viability 8 h after nutrient deprivation (Figure 5B). Blocking autophagy with 3-MA protected *parp-1^{+/+}* MEFs against cell death but not PARP-1-deficient cells, suggesting that WT cells died mainly as consequence of autophagy after prolonged starvation, while the inactivation of PARP-1 may lead to non-autophagic cell death. Silencing of the autophagy gene ATG7 strongly delayed cell death in MCF-7 cells subjected to nutrient starvation while the treatment with the PARP inhibitor PJ34 still increased cell death of ATG7-silenced/autophagy-deficient cells, suggesting that autophagy-derived cell death is not involved in the accelerated cell demise caused by PARP inhibition (Figure 5C).

To analyze the type of cell death that takes place in the absence or after inhibition of PARP-1 during starvation, we used a double-knockout cell line for Bax and Bak. Bax and Bak are two essential proteins in the apoptotic process and these cells cannot undergo mitochondrial outer membrane permeabilization (MOMP) that usually occurs during apoptosis [22]. Additionally, this cell line is stably transfected with GFP-LC3. To determine the levels of autophagy, we starved these cells for different times up to 120 min (Figure 5D). Bax/Bak double-mutant cells displayed LC3 processing during starvation (Figure 5D) and the percentages of cells with the typical GFP-LC3 pattern (Figure 5D) were similar to *parp-1^{+/+}* MEFs. Moreover, co-treatment with 3-MA or the PARP inhibitor DPQ reduced the percentage of autophagic cells, as also observed for *parp-1^{+/+}* MEFs (Figures 2A and 5D). To determine to what extent the apoptotic component contributes to the increased cell death in the absence of PARP-1, we silenced PARP-1 in *Bax^{-/-}/Bak^{-/-}* GFP-LC3 MEFs by siRNA. Knockdown of PARP-1 in the context of *bax/bak* knockout decreased the levels of cell death during nutrient starvation (Figure 5E and 5F), suggesting that the gain in cell death after inactivation of PARP-1 (in the Bax/Bak WT context (Figure 5A-5C)) has an apoptotic component. To confirm this result, we have measured caspase 3/7 and caspase-8 activation by fluorimetric assay and western blot, respectively. Time course of caspase 3/7 activation was significantly increased in *parp-1^{-/-}* cells (Figure 5G); and caspase-8 processing did not take place in *parp-1^{+/+}* MEFs (Figure 5H). Moreover, by quantitation of pycnotic nuclei (data not shown) as well as double staining with annexin V and PI (Figure 5I), apoptotic cells were determined to be significantly increased in the absence of PARP-1. These data confirm that *parp-1^{-/-}* MEFs with delayed autophagy enter into apoptosis after several hours of starvation. Thus, upon prolonged starvation PARP-1 WT cells die by autophagy-dependent cell death while PARP-1 knockout cells die mainly by apoptosis.



Impaired starvation-induced autophagy in PARP-1-deficient mice

In order to analyze the *in vivo* consequences of PARP-1 ablation on autophagy, we starved pups from both *parp-1^{+/+}* and *parp-1^{-/-}* mice for 4 h. TEM (transmission electron microscopy) analysis showed that liver from fed PARP-1-proficient mice displayed characteristic abundant, well-structured mitochondria as well as lipid droplets. After starvation, autophagy-derived ultrastructural changes include concentric membrane structures engulfed in autophagosomes, ER dilation and also accumulation of lipid droplets, which were already found in non-starved liver (Figure 6A, upper panels). Concentric membrane structures reflect degradation of membranous cellular components that rearrange in membranous whorls called myelin figures. By contrast, TEM images of *parp-1^{-/-}* liver cells showed remarkable differences in ultrastructural morphology in both fed and starved pups with a well-organized ER and the absence of concentric membranes structures and lipid droplets (Figure 6A, lower panels). To further support this observation, we measured changes in LC3-I levels (no LC lipidation was

detected in this experiment) in liver samples from *parp-1^{+/+}* and *parp-1^{-/-}* pups subjected or not to starvation. Reduction in LC3-I was much more pronounced in livers from *parp-1^{+/+}* mice (Figure 6B).

The intracellular storage and utilization of lipids are critical to maintain cellular energy homeostasis. Cellular lipids are stored as triglycerides in lipid droplets in the fed liver and hydrolyzed into fatty acids for energy production, which is also one of the initial responses to starvation. A second cellular response to starvation is the induction of autophagy, which delivers intracellular proteins and organelles sequestered in double-membrane vesicles to lysosomes for degradation and use as an energy source. To further confirm the finding that *parp-1^{-/-}* liver cells did not accumulate lipid droplets in response to starvation (Figure 6A and 6B), we used the lipid fluorescence dye BODIPY® to label lipid droplets and showed that BODIPY-positive vesicles were strongly reduced in *parp-1^{-/-}* cells (Figure 6C). Thus, in the absence of PARP-1, liver from neonates has impaired autophagic response as has been reported in knockout mice for genes involved in the core complex of autophagy [23, 24].

Figure 5 Pro-survival autophagy is switched to apoptosis after PARP-1 ablation. **(A)** Effect of PARP inhibition and PARP-1 silencing on cell death during autophagy induced by nutrient deprivation. *parp-1^{+/+}* MEFs were transfected with PARP-1 siRNA (60 nM) and 48 h after transfection, cells were pre-treated with or without PJ34 (10 μ M). Cells were starved for 8 h with HANK buffer and cell death was analyzed by PI incorporation using flow cytometry in 3 independent experiments with 4 replicates per condition. * $P < 0.05$ comparing between starved PARP-1-knockdown *parp-1^{+/+}* MEFs and starved control *parp-1^{+/+}* MEFs. **(B)** Effect of autophagy inhibition with 3-MA on the survival of *parp-1^{+/+}* and *parp-1^{-/-}* MEFs during starvation. 3-MA was added 1.5 h before the HANK buffer as pre-treatment and kept during starvation in both cells lines to maintain the autophagy inhibition. Percentage of survival was obtained by MTT survival assay. Similar survival rates were obtained in three independent experiments with four replicates per condition. **(C)** Effect of ATG7 knockdown and PARP inhibition on cell death in *parp-1^{+/+}* MEFs. Percentage of survival was obtained by MTT assay. Similar survival rates were obtained in three independent experiments with four replicates per condition. While ATG7 silencing prevented cell death, PARP inhibition increased cell death even in cells with limited ability to engage autophagy. **(D)** Induction of autophagy in MEFs *Bax^{-/-}/Bak^{-/-}* GFP-LC3 during starvation. Western blot of LC3 conversion (right) and percentage of autophagic cells (left), treatment with rapamycin (100 nM) for 4 h as positive control. DPQ (40 μ M) and 3-MA (2 mM) were added 1.5 h before the HANK buffer as pre-treatment and maintained during the starvation. The experiments were repeated three times with similar results. # $P < 0.05$ comparing between starved *Bax^{-/-}/Bak^{-/-}* MEFs and 3-MA-treated starved *Bax^{-/-}/Bak^{-/-}* MEFs or DPQ-treated starved *Bax^{-/-}/Bak^{-/-}* MEFs. **(E)** Cell death in MEFs *Bax^{-/-}/Bak^{-/-}* GFP-LC3 during starvation: levels of cell death measured by PI incorporation using flow cytometry during different times of nutrient deprivation. Three independent experiments with three replicates per condition are represented. **(F)** Reduction of the percentage of cell death with PARP-1 siRNA (50 nM) during starvation. The right panel shows the silencing of PARP-1 48 h after transfection. Similar results were obtained in 4 experiments with 4 replicates per condition. # $P < 0.05$, ### $P < 0.01$ comparing between starved *Bax^{-/-}/Bak^{-/-}* MEFs and PARP-1-knockdown starved *Bax^{-/-}/Bak^{-/-}* MEFs. **(G)** Caspase 3/7 activity in 3T3 MEFs: *parp-1^{+/+}* and *parp-1^{-/-}* 3T3 MEFs cells were starved for 4.5, 6 and 8 h to induce apoptosis. The Caspase - Glo reagent was added directly to cells in 96-well plates and the final volume was 200 μ l per well. The assays were incubated at room temperature for 45 min before recording luminiscence in a TECAN infinite 200 Luminometer. Each point represents the average of three wells per condition in three independent experiments. ** $P < 0.01$ comparing between starved *parp-1^{+/+}* and *parp-1^{-/-}* 3T3 MEFs. **(H)** Activation of caspase 8 in *parp-1^{-/-}* MEFs 3T3 under nutrient deprivation. *parp-1^{+/+}* and *parp-1^{-/-}* MEFs were starved with HANK buffer for 6 h. The fragment of 38 kDa of caspase 8 processed was visualized by western blot and a Jurkat cell total lysate was used as positive control for activation of caspase 8. α -Tubulin was used as loading control. **(I)** Percentage of apoptotic cells under starvation. *parp-1^{+/+}* and *parp-1^{-/-}* MEFs were starved for 6 and 8 h and apoptosis was evaluated by double staining of annexin V and PI using flow cytometry. Results are from three independent experiments with two replicates per condition. * $P < 0.05$ comparing between starved *parp-1^{+/+}* and *parp-1^{-/-}* MEFs.

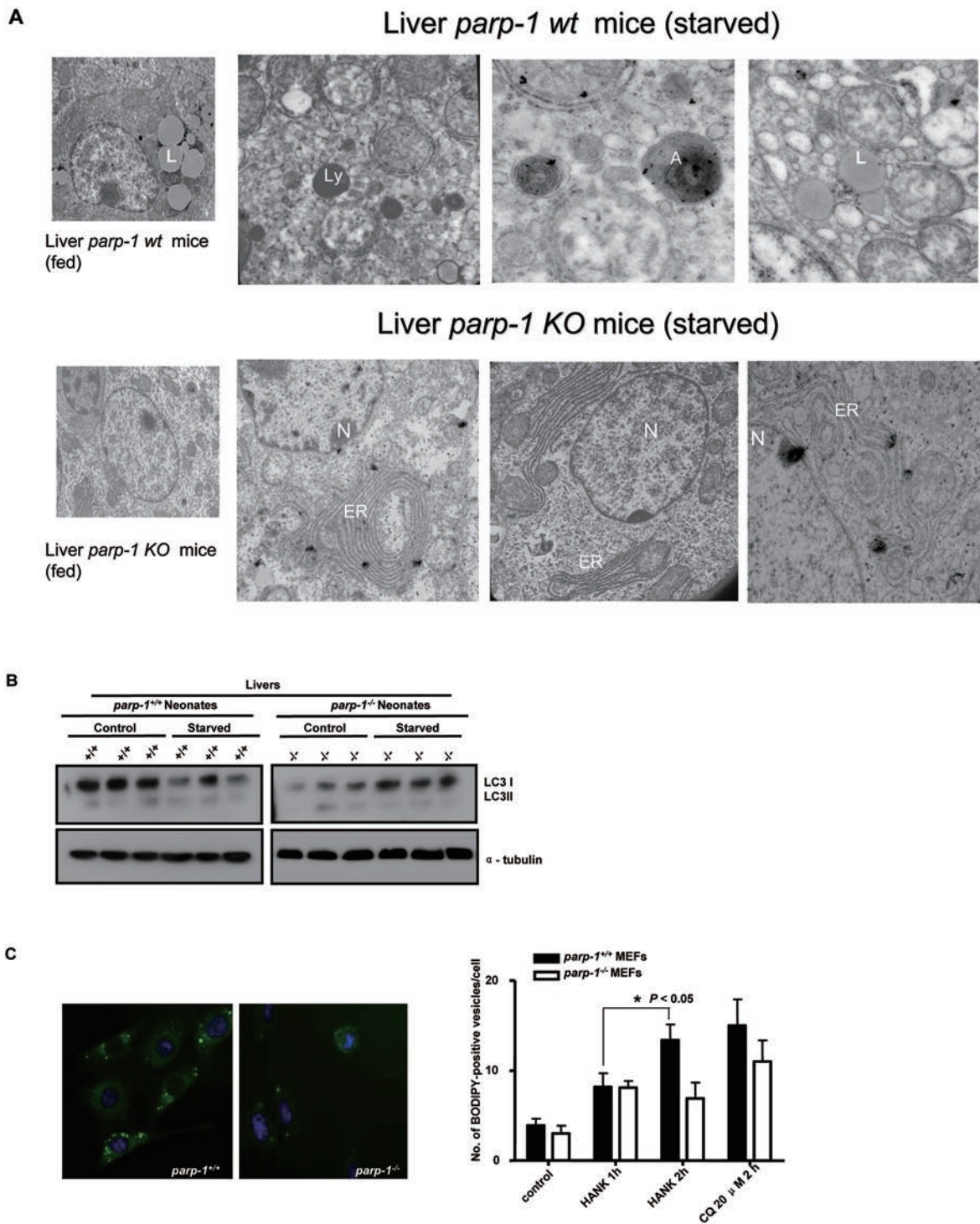


Figure 6 Deficient liver autophagy in starved PARP-1 knockout mice. 2 h after birth pups were separated from their mother and starved for 4 h according to procedures approved by the bioethics committee of the CSIC. Pups were sacrificed and livers were removed and fixed for TEM (**A**) or lysed for western blot analysis (**B**). A, Autophagosomes showing concentric membrane structures; ER, endoplasmic reticulum; L, lipid droplets; Ly, lysosomes; N, nucleus. (**B**) Immunoblot analysis of endogenous LC3 conversion in control and starved *parp-1*^{+/+} and *parp-1*^{-/-} neonatal mice. β -actin was used as loading control. Similar results were obtained in 3 independent experiments. (**C**) Lipids droplets in starved *parp-1*^{+/+} and *parp-1*^{-/-} MEFs. Cells were starved for 1 or 2 h and numbers of BODIPY-positive vesicles per cell are shown. Treatment with 20 μ M CQ for 2 h was used as positive control. * $P < 0.05$ comparing between *parp-1*^{+/+} MEFs starved for 1 h and those starved for 2 h.

Discussion

Genetic and environmental factors modulate the response of multicellular organisms to stress and the maintenance of tissue homeostasis and highly integrated response patterns are found in many organisms, but the means by which so many diverse pathways, critical for cellular, tissue and ultimately for organism survival, are coordinated, has yet to be elucidated. In this study, we show that optimal induction of autophagy induced by nutrient deprivation requires PARP-1 activation. Our results clearly show the lack of AMPK activation after disabling of PARP-1. These findings are in agreement with previous results showing an interaction between PARP-1 and AMP metabolism related to the hydrolysis of ADP-ribose [25]. In the absence of PARP-1 or after its inhibition/silencing, ATP levels are not reduced as much as in WT cells (Figure 4A); consequently AMPK remains inactive and does not signal for mTOR inactivation, leading to impaired autophagy. At present the link between PARP-1 activation and AMPK has not been established. One speculative possibility is that ROS-induced DNA damage and PARP-1 overactivation caused mitochondrial dysfunction and Ca^{2+} release, thereby activating AMPK [14]. Other possibility that may explain how PARP-1 connects with the AMPK/mTOR signaling (besides the maintenance of the energy status) is that PARP inactivation leads to unefficient ATM response that has been reported to be involved in the activation of AMPK [26, 27].

Our data suggest that the PARP-1 is an important *in vivo* regulator of autophagy and provide a link between PARP-1 function and the overall cellular response to nutrient shortage. The results demonstrate that nutrient starvation, ROS production and DNA damage lead to PARP-1 activation, which is needed for cells to engage starvation-induced autophagy.

We also show that the role of PARP-1 in starvation-induced autophagy is related to its ability to sense DNA damage and deplete energy stores after its overactivation, but we cannot exclude the possibility of perturbation in Ca^{2+} flux after PARP-1 ablation upstream of the mitochondria leading to altered ATP synthesis and AMPK activation [28]. Moreover, we have also analyzed the *in vivo* consequences of PARP-1 inactivation in starvation-induced autophagy. Starvation induces hepatic autophagy and increases the delivery of fatty acids to the liver from lipolysis of adipose tissue. Electron microscopy revealed that starvation increased the frequency of lipid droplets with increased density and asymmetrically localized multi-membrane structures. The crucial role of neonatal autophagy was clearly demonstrated by targeted inactivation of the autophagy-related genes ATG5 and ATG7

[23, 29]. Mice deficient in these genes were apparently normal at birth, except for a slightly lower body weight than control (approximately 10% in ATG5-null and 18% in ATG7-null mice), but died within 1 day after birth. One of the phenotypes of PARP-1 knockout mice was that the average litter size was smaller (about 40%) than that of *parp-1*^{+/+} mice [30]. It would be interesting to further explore whether the reduced litter size of PARP-1 knockout mice is related to the changes in autophagy.

ROS have been reported to be a hallmark of autophagy in a number of cell types and experimental settings, including nutrient starvation [9]. Although autophagy after nutrient deprivation has a pro-survival function, our findings support that PARP-1 is necessary for cells to persist in autophagy following starvation when nutrient deprivation is maintained for a long time (Figure 5B). An interesting finding in our study is that suppression of PARP activation by different means leads to impaired autophagy and eventually to increased cell death. Indeed, exposure of PARP-1-deficient cells to a longer starvation period (6 and 8 h) resulted in increased cell death (data not shown). Additionally we have defined the mechanism by which PARP-1 suppression accelerates cell death using the apoptosis-deficient cell line with double knockout for *bax* and *bak*. We found that starvation leads *bax*^{-/-}/*bak*^{-/-} cells to autophagy and cell death, suggesting that apoptosis is not the main pathway of cell demise triggered by starvation. Nonetheless, suppression of PARP-1 in this *bax*^{-/-}/*bak*^{-/-} context substantially decreased cell death, contrary to what we observed in apoptosis-proficient cells. One major observation in this study is that a physiological trigger of autophagy, such as nutrient deprivation, is able to induce DNA damage through the generation of ROS. Genotoxic stress has been reported to repress mTOR in response to oxidative stress caused by ROS through a cytoplasmic signaling node for LKB1/AMPK/TSC2 activation in response to oxidative stress [31]. The COMET assay and histone γ -H2AX accumulation confirmed the persistence of damaged DNA and the level of initial damage corresponded with the cell's ability to initiate autophagy. Treatment with antioxidant NAC prevented DNA damage and mTOR inactivation, and slowed down autophagy. Why are PARP-1-deficient cells prone to die by apoptosis following nutrient deprivation? One interesting possibility is suggested by the results in Figure 3C-3E: PARP-1 mutant cells display a defective DNA repair during starvation; thus, the cells choose to undergo apoptosis to avoid the harm of bearing unrepaired DNA; in a tumor context, where oxygen and nutrients are limited, this delayed autophagy (together with the tendency to die by apoptosis in the absence of PARP-1), might have benefits by preventing ne-

crisis, ROS and inflammatory burst from tumor growth.

The ultimate reason why PARP-1 deficiency or inactivation leads to inhibition of ROS generation is not completely understood. Interestingly, early reports have also shown that alterations in mitochondrial function during oxidant-mediated cytotoxicity, are related to PARP-1 activation rather than to direct effects of the oxidants on the mitochondria [12]. ER and mitochondrial Ca^{2+} signaling is a key mediator of cell's bioenergetic regulation and cell death. Constitutive InsP(3)R Ca^{2+} signaling is required for autophagy suppression in cells under non-starvation conditions. It has been shown that after nutrient deprivation cells become metabolically compromised due to diminished mitochondrial Ca^{2+} uptake [28]. Very recently PARP-1 and PARG (poly(ADP-ribose) glycohydrolase) have been reported to regulate Ca^{2+} influx through TRPM2 [32] and a reduction in Ca^{2+} was observed after abrogation of PARP-1. In this study by Blenn *et al.* [32], they reported that the increased Ca^{2+} flux following H_2O_2 treatment leads to caspase activation and cleavage of mitochondrial AIF, which then translocates to the nucleus to cause DNA fragmentation, chromatin condensation and cell death. Clearly, the level of ROS-derived cytotoxicity and PARP-1 activation differs in both settings: while H_2O_2 treatment produces an overwhelming burst in oxidant mediators, starvation leads to a mild ROS generation allowing the cell not to undergo direct cell death but to engage the pro-survival autophagy. In support of that, Scherz-Shouval *et al.* [9] demonstrated that ROS in starvation-induced autophagy has a pro-survival function. They showed that oxidative conditions are essential for autophagy and that the increase in ROS is both local and reversible during starvation, which is not deleterious to cells and serves to oxidize a specific target. By contrast, massive ROS production during oxidative stress will lead to ROS-derived cell death by autophagy [33]. Once starvation has initiated the commitment to autophagy, cells abrogated of PARP-1 undergo a "slow" autophagy that is eventually resolved by increased cell death, particularly (but not exclusively) apoptosis. It has been previously shown that PARP inhibition can shift the necrotic cell death to apoptosis after exposure to oxidative stress [34]. In agreement with that, our results show that the cell death observed in the absence of PARP-1 after starvation (leading to oxidative stress) is due to increased apoptosis. In this context PARP-1 is needed for cells to undergo pro-survival autophagy.

Our model is presented in Figure 7 and could be summarized as follows: after nutrient deprivation mitochondrial metabolism is rapidly shifted, leading to ROS production and ATP drop. An elevation in the AMP/ATP ratio activates the nutritional sensor kinase AMPK,

whose activation leads to mTORc1 inhibition, allowing the commitment to autophagy. In parallel, ROS production induces DNA damage and PARP-1 overactivation, contributing to the feedback loop to decrease ATP through the consumption of NAD^+ . In this scenario, the axis ROS/AMPK/mTOR and ROS/DNA damage/PARP-1 activation synergize to optimize the cell's response to nutrient deprivation by inducing pro-survival autophagy (Figure 7A). In the absence of PARP-1, ROS production, energy drop and AMPK activation are diminished and shut-off of the feedback loop responsible for massive energy depletion eventually slows down autophagy. Alternatively, the cells die through apoptosis due to suboptimal autophagy commitment (Figure 7B).

Autophagy is a potent tumor suppressive mechanism, presumably due to its essential contribution to the maintenance of genomic stability [35], the avoidance of excessive ROS generation [36] and its participation in cellular senescence [37], which constitutes a barrier against oncogenesis. Accordingly, multiple genes that are required for the induction/execution of autophagy are potent tumor suppressors, including PTEN, TSC1, TSC2, LKB1, ATG4, Beclin-1, UVRAG, and BH3-only proteins of the Bcl-2 family [38]. Here, we revealed the importance of PARP for the autophagic process in a physiologic setting following nutrient starvation. PARP-1 inhibitors are entering clinical trials for different types of cancer. Whether the ability of PARP inhibitors to favor apoptotic cell death during cellular stress, such as shortage of nutrients (which very often the case in tumor microenvironment), could also be exploited in antitumor therapy by its contribution to autophagy, remains an intriguing possibility for further investigation.

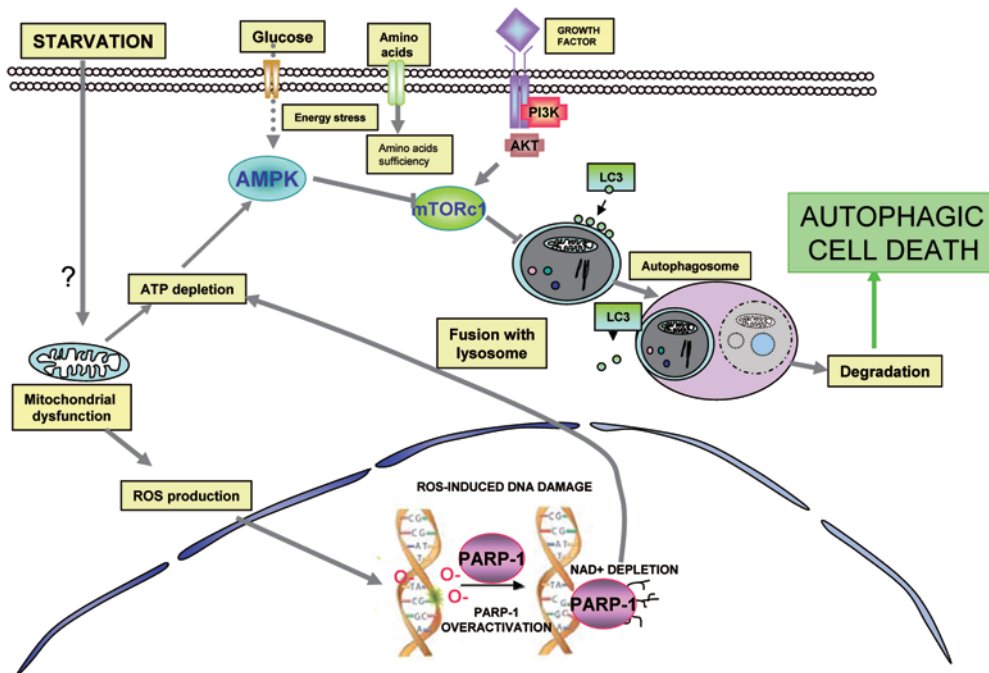
Materials and Methods

Cell culture and treatment

Immortalized MEFs 3T3, derived from both WT and PARP-1 KO mice, *Bax*^{-/-}/*Bak*^{-/-} GFP-LC3 MEFs 3T3, g361 and HT144 cell lines were cultured in Dulbecco's modified Eagle's medium supplemented with 10% inactive fetal bovine serum (FBSi, Gibco Invitrogen) at 37 °C in a humidified 5% CO_2 atmosphere. MCF7-GFP-LC3 cells were cultured in RPMI-1640 GlutaMAX (GIBCO Invitrogen) with 6% FBSi. Cells were starved with balanced HANK buffer without amino acids (NaCl 140 mM, KCl 5 mM, $\text{MgCl}_2 \cdot 6\text{H}_2\text{O}$ 1.3 mM, $\text{CaCl}_2 \cdot 2\text{H}_2\text{O}$ 2 mM, HEPES 10 mM, D-glucose 5 mM) for different time periods.

For western blot, cells were plated in six-well plates with a density of 4×10^5 cells per plate and treated with HANK buffer the next day. For the assessment of cell death, cells were plated in 24-well plates with a density of 3.5×10^4 cells per well and in six-well plates with 2.5×10^5 cells per well. To count the number of vesicles per cell, cells were plated in six-well with cell density of 4×10^4 cells per well on coverslips and starved in the next day for

A



B

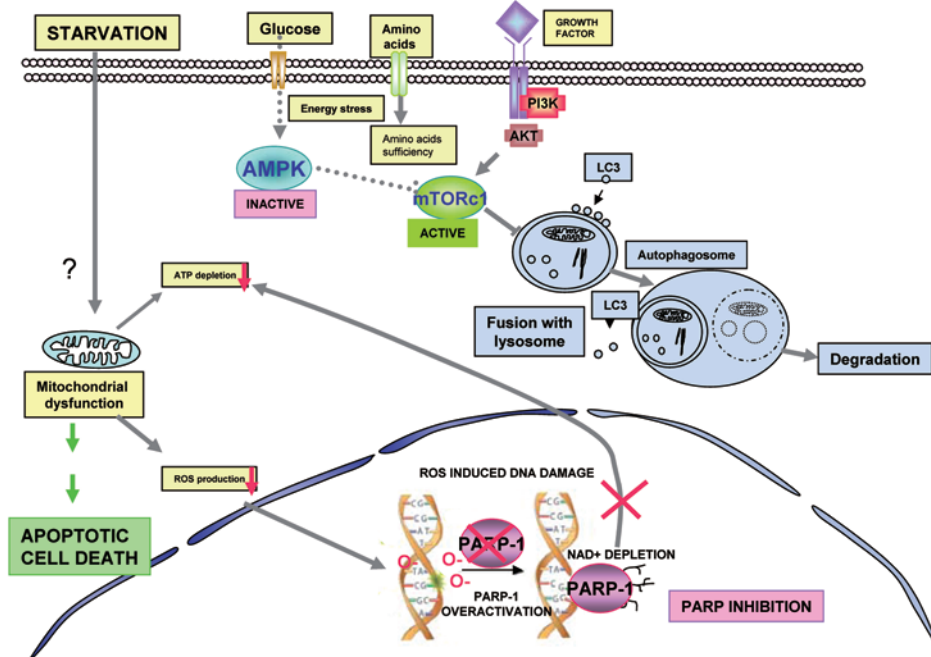


Figure 7 (A) PARP-1 is a positive modulator of starvation-induced autophagy. After nutrient starvation cells activate autophagy through the activation of AMPK/inhibition of mTOR. Upstream events involve energy depletion, ROS production and DNA damage. Under this condition, PARP-1 overactivation leads to ATP depletion, acting as a feedback loop to reactivate autophagy. This stress signal when maintained eventually leads to cell death through autophagy. **(B)** PARP inactivation delays autophagy and favors apoptosis. In the absence of PARP-1 or after PARP inactivation, ROS levels decrease and ATP drop is reduced. As a consequence, the feedback loop reactivated by PARP-1 does not take place, and apoptosis is triggered as a mode of cell death.

different time periods. Fluorescence microscopy analysis was performed with a Zeiss microscope.

The autophagy inhibitor 3-MA (M9281, Sigma-Aldrich, St Louis, MO, USA) was dissolved in culture medium and stored at -20°C (10 mM). PARP-1 inhibitor DPQ (3,4-Dihydro-5-[4-(1-piperidinyl)butoxy]-1(2H)-isoquinolinone]) and PJ34 were from Alexis Biochemicals. DPQ was dissolved in DMSO and stored at -20°C . Cells were pre-treated with 40 μM DPQ or 10 μM PJ34 for 1.5 h before starvation and maintained all the time during the experiment.

Cell viability assay

The levels of cell death in *parp-1^{+/+}* and *parp-1^{-/-}* MEFs were determined using trypan blue exclusion assay (93595, Fluka, St Louis, MO, USA) (a), MTT (b) and PI (c). (a) Trypan blue: 3T3 cells were seeded at 3.5×10^4 cells per well in 24-well plates and incubated overnight at 37°C . After starvation with HANK buffer, cells were washed and trypsinized. The cellular pellet was dissolved in 50 μl of trypan blue solution and the number of viable cells was counted under a normal microscope. (b) MTT assay (3-(4,5-Dimethylthiazol-2-yl)-2,5-diphenyl Tetrazolium Bromide) was performed using Cell Proliferation Kit I (MTT, 1-65-007, Roche, Germany) following the manufacturer's instructions. (c) PI was used as exclusion staining and a FACScalibur flow cytometer with the Cell Quest software (BD Biosciences) was used to perform analysis.

Immunofluorescence

Immunostaining for PAR was performed on cells grown on glass coverslips and fixed in ice-cold methanol-acetone (1:1) for 10 min. PAR was detected by immunofluorescence, using monoclonal antibody (Trevigen) and FITC-conjugated goat anti-mouse immunoglobulin (Sigma-Aldrich). Foci of γ -H2AX were detected with a monoclonal antibody for H2AX histone (Upstate, #05-636, clone JBW103) and FITC-conjugated goat anti-mouse antibody. Nuclear counterstaining with DAPI was performed after removal of excess secondary antibody. Immunostaining was visualized with a Zeiss fluorescence microscope.

Quantification of lipid droplets by fluorescence microscopy

parp-1^{+/+} and *parp-1^{-/-}* MEFs were seeded (4×10^4 cells per well) in six-well plates on glass coverslips. Cells were starved for 1 and 2 h and fixed with paraformaldehyde solution (4%, wt/vol in $1 \times$ PBS with 2% sucrose) for 10 min at room temperature. Lipid droplets were labeled with BODIPY® 493/503 (Invitrogen) for 5 min at room temperature and visualized under a Zeiss fluorescence microscope. Nuclear counterstaining with DAPI was performed after probing. Incubation with 20 μM of chloroquine for 2 h was used as positive control of accumulation of lipids droplets.

Western blot analysis

After the nutrient starvation with HANK buffer, cells were washed twice with PBS and resuspended in 70 μl of lysis buffer (50 mM Tris-HCl pH 8, 0.1 mM EDTA, 0.5% Triton X-100, 12.5 mM β -Mercaptoethanol) for 45 min on ice. Pellet was eliminated and the supernatant was stored at -20°C . Proteins were resolved on 10% SDS-polyacrylamide gels and transferred onto PVDF membrane (Bio-Rad). The blot was blocked with 5% milk powder in $1 \times$ PBS and 0.1% Tween-20 for 60 min, washed with PBS/

Tween, and incubated overnight with the different antibodies, anti-poly(ADP-ribose) (TREVIGEN, 20591E10, My, USA), anti-PARP-1 (C2-10 mouse, ALEXIS, LA), anti-LC3 (NanoTools, clone 5F10, Ref 03231-100/LC3-5F10), anti-Atg7 (Cell Signaling Technology, Beverly, MA, USA), anti-phospho-p70S6K (Cell Signaling Technology), anti-p70S6K (Cell Signaling Technology), anti-phospho-AMPK α (Thr172) (Cell Signaling Technology), anti-AMPK α (Cell Signaling Technology) and anti-caspase 8 (BD Pharmingen). α -Tubulin (Sigma-Aldrich), β -actin (Sigma-Aldrich) and GAPDH (Santa Cruz Biotechnology) were used as loading controls. Bands were visualized by ECL-Plus (Amersham Biosciences) and the pictures were taken with ChemiDoc XRS imaging system (Bio-Rad) or medical X-ray films (AGFA).

ATP determination

Intracellular ATP was measured using a luciferin/luciferase-based assay (ATP Bioluminescent Assay Kit, Sigma-Aldrich) following the manufacturer's guidelines. A standard curve was generated with known concentrations of ATP and used to calculate sample ATP concentrations. Protein concentration was determined using Bradford protein assay reagents (Bio-Rad). The content of ATP was normalized for protein content.

Autophagy assay

GFP-LC3-expressing cells have been used to demonstrate the induction of autophagy. The GFP-LC3 expression vector was kindly supplied by Dr T Yoshimori (National Institute for Basic Biology, Okazaki, Japan). *parp-1^{+/+}* and *parp-1^{-/-}* MEFs were transiently transfected with this vector together with jetPEITM (Polyplus transfection, Illkirch, France) according to the manufacturer's protocol. The assay was performed on cells grown on glass coverslips (4×10^4 cells per well) in six-well plates and after the different treatment with HANK buffer, cells were washed three times with sterile PBS and fixed with paraformaldehyde solution (4%, wt/vol in $1 \times$ PBS with 2% sucrose) for 10 min at room temperature. To determine LC3 localization, GFP-LC3-transfected cells were observed under a Zeiss fluorescence microscope. To determine LC3-II translocation in *parp-1^{+/+}* and *parp-1^{-/-}* MEFs, we performed western blot of LC3-I and its proteolytic derivative LC3-II (18 and 16 kDa, respectively) using a monoclonal antibody against LC3 (NanoTools, clone 5F10, Ref 03231-100/LC3-5F10).

Rapamycin (553210 Calbiochem, Germany) and Concanamycin A (C9705, Sigma-Aldrich) were used as autophagy inducers. Rapamycin was used at 100 nM for 4 h and Concanamycin A at 4 nM for 4 h.

Apoptosis assay

In addition to caspase 8 cleavage, apoptosis was determined by two different methods: (1) Pyknotic nuclei: Cells were fixed by paraformaldehyde (4%, wt/vol in $1 \times$ PBS with 2% sucrose) for 10 min at room temperature and the number of cells with nuclear apoptotic morphology was determined by DAPI staining after 6 and 8 h of starvation, using a Zeiss fluorescence microscope. Treatment with 0.5 $\mu\text{g}/\text{ml}$ cycloheximide (CHX C4859, Sigma-Aldrich) for 8 h was used as positive control of nuclear apoptotic morphology. (2) Annexin V/IP: *parp-1^{+/+}* and *parp-1^{-/-}* MEFs (5×10^5 cells per well) were cultured in 6-well plates and starved for 6 h. After starvation, cells were washed twice with PBS, trypsinized and centrifuged at 1 600 rpm for 5 min. The pellets

were re-suspended in AnnexinV/IP solution (Roche Applied, Germany) according to the manufacturer's instruction and maintained in the dark at 37 °C for 15 min. Apoptotic cells were evaluated in a FACScalibur flow cytometer with the Cell Quest software (BD Biosciences, NJ, USA). Staurosporin (6942, Sigma-Aldrich; 3 μM) for 8 h was used as a positive control of apoptosis induction.

Caspase 3/7 activity in 3T3 MEFs: *parp-1^{+/+}* and *parp-1^{-/-}* MEFs were starved for 4.5, 6 and 8 h to induce apoptosis. The Caspase-Glo reagent was added directly to cells in 96-well plates; the final volume was 200 μl per well. The cells were incubated at room temperature for 45 min before recording luminiscence in a TECAN infinite 200 Luminometer. Each point represents the average of three wells per condition in three independent experiments. The "no-cell" blank control value has been subtracted from each point. STS (2 μM for 3 h) was used as positive control of caspase activation. Data generated in apoptotic cells with STS are not shown. ***P* < 0.01 comparing between starved *parp-1^{+/+}* and *parp-1^{-/-}* MEFs.

RNA interference

Cells were transfected with the indicated siRNAs (50 nM) using Dharmafect transfection agent (Dharmacon Research, CO, USA) according to the manufacturer's guide. siRNAs corresponding to the cDNA sequences were: ATG7 no.1 from Invitrogen, human PARP-1 from Ambion Applied Biosystems and mouse PARP-1 from Santa Cruz Biotechnology.

48 h after transfection, cells were treated as described and observed under a Zeiss fluorescence microscope or the proteins were extracted.

ROS and DNA damage determination

ROS production was measured by flow cytometry in an Epics Elite ESP cytometer (Coulter) using DCFDA (35845, FLUKA; 8 mg/ml in DMSO), a specific probe to ROS. 3T3 cells were seeded at 3.5×10^5 cells per well in 6-well plates and incubated overnight at 37 °C. Cells were incubated with the probe for 30 min before the end of the deprivation and washed twice with PBS, trypsinized and the ROS production was analyzed by flow cytometry.

DNA damage was analyzed using two different methods: (1) COMET assay: DNA damage was quantified using COMET Assay kit (R&D Systems, Trevigen, MD, USA) with some modifications. 1×10^5 cells/ml were mixed with molten LM agarose at 37 °C at a ratio of 1:10 (vol/vol) and pipetted onto a COMET slide. The slides were placed for 10 min in the dark at 4 °C and were immersed in pre-chilled lysis solution. The slides were then removed from lysis buffer, washed in TBE buffer and transferred to a horizontal electrophoresis chamber. Voltage (1 V/cm) was applied for 20 min. After washed in distilled water, the slides were immersed in 70% ethanol for 5 min and allowed to air dry. Slides were stained with SYBR Green and then analyzed by fluorescence microscopy. 70-90 cells were evaluated in each sample using the COMET Assay Software Project (CASP software). DNA damage was quantified by measuring the TM calculated as percentage of DNA in the tail \times tail length. (2) phospho- γ -H2AX: To visualize foci of γ -H2AX, we performed immunofluorescence with a monoclonal antibody for H2AX histone (Upstate, #05-636, clone JBW103) and FITC-conjugated goat anti-mouse antibody. Nuclear counterstaining with DAPI was performed after removal of excess secondary antibody. Immunostaining was visualized with a Zeiss

fluorescence microscope. Western blot analysis of γ -H2AX phosphorylation was performed with the same antibody. Bands were visualized by ECL-Plus (Amersham Biosciences) and the pictures were taken with ChemiDoc XRS imaging System (Bio-Rad) or medical X-ray films (AGFA).

Electron microscopy

Animal experimental protocols were reviewed and approved by the Ethical Committee of the Spanish Council of Scientific Research (CSIC). PARP-1 WT and knockout [30] neonatal mice were used to determine the differences in autophagy induction during starvation in hepatic tissue. Neonatal mice were separated from the mother in the first 4 h after birth. Livers of WT and PARP-1 knockout mice were extracted and washed with PBS, prefixed for 30 min in a fixation solution (0.1 M cacodilate buffer pH 7.4 and osmium tetraoxyde) for 60 min at 4 °C. After this treatment, tissues were washed with MilliQ water and the samples were stained with uranyl acetate. The ultrathin sections were cut with a diamond knife in an ultramicrotome (Reichert Ultracut S). The samples were analyzed in a TEM Zeiss 902 with 80 KV of voltage acceleration (CIC-UGR).

Acknowledgments

We acknowledge Laura López for her technical assistance. JMRV is recipient of a predoctoral fellowship financed by the program JAE-Pre of CSIC and was also funded by CSIC with a Short-Term Fellowship to stay at the Danish Cancer Society Institute of Cancer Biology in Copenhagen, Denmark. This work was supported by Ministerio de Ciencia e Innovación (SAF2006-01094 and SAF2009-13281-C02-01), Fundación La Caixa (BM06-219-0) and Junta de Andalucía (P07-CTS-0239) to FJO; RTICC (RD06/0020/0068) to ALR.

References

- 1 Levine B, Kroemer G. Autophagy in the pathogenesis of disease. *Cell* 2008; **132**:27-42.
- 2 Kabeya Y, Mizushima N, Ueno T, *et al.* LC3, a mammalian homologue of yeast Apg8p, is localized in autophagosomal membranes after processing. *EMBO J* 2000; **19**:5720-5728.
- 3 Schreiber V, Dantzer F, Ame JC, de Murcia G. Poly(ADP-ribose): novel functions for an old molecule. *Nat Rev Mol Cell Biol* 2006; **7**:517-528.
- 4 David KK, Andrabi SA, Dawson TM, Dawson VL. Parthanatos, a messenger of death. *Front Biosci* 2009; **14**:1116-1128.
- 5 Wang Y, Dawson VL, Dawson TM. Poly(ADP-ribose) signals to mitochondrial AIF: a key event in parthanatos. *Exp Neurol* 2009; **218**:193-202.
- 6 Munoz-Gamez JA, Rodríguez-Vargas JM, Quiles-Perez R, *et al.* PARP-1 is involved in autophagy induced by DNA damage. *Autophagy* 2009; **5**:61-74.
- 7 Blommaert EF, Krause U, Schellens JP, Vreeling-Sindelarova H, Meijer AJ. The phosphatidylinositol 3-kinase inhibitors wortmannin and LY294002 inhibit autophagy in isolated rat hepatocytes. *Eur J Biochem* 1997; **243**:240-246.
- 8 Krishnakumar R, Kraus WL. The PARP side of the nucleus: molecular actions, physiological outcomes, and clinical tar-

- gets. *Mol Cell* 2010; **39**:8-24.
- 9 Scherz-Shouval R, Shvets E, Fass E, Shorer H, Gil L, Elazar Z. Reactive oxygen species are essential for autophagy and specifically regulate the activity of Atg4. *EMBO J* 2007; **26**:1749-1760.
 - 10 Chen Y, Azad MB, Gibson SB. Superoxide is the major reactive oxygen species regulating autophagy. *Cell Death Differ* 2009; **16**:1040-1052.
 - 11 LeBel CP, Ischiropoulos H, Bondy SC. Evaluation of the probe 2',7'-dichlorofluorescein as an indicator of reactive oxygen species formation and oxidative stress. *Chem Res Toxicol* 1992; **5**:227-231.
 - 12 Virag L, Salzman AL, Szabo C. Poly(ADP-ribose) synthetase activation mediates mitochondrial injury during oxidant-induced cell death. *J Immunol* 1998; **161**:3753-3759.
 - 13 Hay N, Sonenberg N. Upstream and downstream of mTOR. *Genes Dev* 2004; **18**:1926-1945.
 - 14 Hoyer-Hansen M, Jaattela M. AMP-activated protein kinase: a universal regulator of autophagy? *Autophagy* 2007; **3**:381-383.
 - 15 Shaw RJ, Bardeesy N, Manning BD, et al. The LKB1 tumor suppressor negatively regulates mTOR signaling. *Cancer Cell* 2004; **6**:91-99.
 - 16 Gogvadze V, Orrenius S, Zhivotovsky B. Mitochondria in cancer cells: what is so special about them? *Trends Cell Biol* 2008; **18**:165-173.
 - 17 Tomitsuka E, Kita K, Esumi H. The NADH-fumarate reductase system, a novel mitochondrial energy metabolism, is a new target for anticancer therapy in tumor microenvironments. *Ann N Y Acad Sci* 2010; **1201**:44-49.
 - 18 Kroemer G, Levine B. Autophagic cell death: the story of a misnomer. *Nat Rev Mol Cell Biol* 2008; **9**:1004-1010.
 - 19 Levine B, Yuan J. Autophagy in cell death: an innocent convict? *J Clin Invest* 2005; **115**:2679-2688.
 - 20 Baehrecke EH. Autophagy: dual roles in life and death? *Nat Rev* 2005; **6**:505-510.
 - 21 Boya P, Gonzalez-Polo RA, Casares N, et al. Inhibition of macroautophagy triggers apoptosis. *Mol Cell Biol* 2005; **25**:1025-1040.
 - 22 Caro-Maldonado A, Tait SW, Ramirez-Peinado S, et al. Glucose deprivation induces an atypical form of apoptosis mediated by caspase-8 in Bax-, Bak-deficient cells. *Cell Death Differ* 2010; **17**:1335-1344.
 - 23 Komatsu M, Waguri S, Ueno T, et al. Impairment of starvation-induced and constitutive autophagy in Atg7-deficient mice. *The J Cell Biol* 2005; **169**:425-434.
 - 24 Lee IH, Cao L, Mostoslavsky R, et al. A role for the NAD-dependent deacetylase Sirt1 in the regulation of autophagy. *Proc Natl Acad Sci USA* 2008; **105**:3374-3379.
 - 25 Formentini L, Macchiarulo A, Cipriani G, et al. Poly(ADP-ribose) catabolism triggers AMP-dependent mitochondrial energy failure. *J Biol Chem* 2009; **284**:17668-17676.
 - 26 Aguilar-Quesada R, Munoz-Gamez JA, Martin-Oliva D, et al. Interaction between ATM and PARP-1 in response to DNA damage and sensitization of ATM deficient cells through PARP inhibition. *BMC Mol Biol* 2007; **8**:29.
 - 27 Haince JF, Kozlov S, Dawson VL, et al. Ataxia telangiectasia mutated (ATM) signaling network is modulated by a novel poly(ADP-ribose)-dependent pathway in the early response to DNA-damaging agents. *J Biol Chem* 2007; **282**:16441-16453.
 - 28 Cardenas C, Miller RA, Smith I, et al. Essential regulation of cell bioenergetics by constitutive InsP3 receptor Ca²⁺ transfer to mitochondria. *Cell* 2010; **142**:270-283.
 - 29 Kuma A, Hatano M, Matsui M, et al. The role of autophagy during the early neonatal starvation period. *Nature* 2004; **432**:1032-1036.
 - 30 de Murcia JM, Niedergang C, Trucco C, et al. Requirement of poly(ADP-ribose) polymerase in recovery from DNA damage in mice and in cells. *Proc Natl Acad Sci USA* 1997; **94**:7303-7307.
 - 31 Nakada D, Saunders TL, Morrison SJ. Lkb1 regulates cell cycle and energy metabolism in haematopoietic stem cells. *Nature* 2010; **468**:653-658.
 - 32 Blenn C, Wyrsh P, Bader J, Bollhalder M, Althaus FR. Poly(ADP-ribose)glycohydrolase is an upstream regulator of Ca²⁺ fluxes in oxidative cell death. *Cell Mol Life Sci* 2011; **68**:1455-1466.
 - 33 Yu L, Alva A, Su H, et al. Regulation of an ATG7-beclin 1 program of autophagic cell death by caspase-8. *Science* 2004; **304**:1500-1502.
 - 34 Virag L, Scott GS, Cuzzocrea S, Marmer D, Salzman AL, Szabo C. Peroxynitrite-induced thymocyte apoptosis: the role of caspases and poly (ADP-ribose) synthetase (PARS) activation. *Immunology* 1998; **94**:345-355.
 - 35 Karantza-Wadsworth V, Patel S, Kravchuk O, et al. Autophagy mitigates metabolic stress and genome damage in mammary tumorigenesis. *Genes Dev* 2007; **21**:1621-1635.
 - 36 Mathew R, Karp CM, Beaudoin B, et al. Autophagy suppresses tumorigenesis through elimination of p62. *Cell* 2009; **137**:1062-1075.
 - 37 Young AR, Narita M, Ferreira M, et al. Autophagy mediates the mitotic senescence transition. *Genes Dev* 2009; **23**:798-803.
 - 38 Maiuri MC, Criollo A, Kroemer G. Crosstalk between apoptosis and autophagy within the Beclin 1 interactome. *EMBO J* 2010; **29**:515-516.

(Supplementary information is linked to the online version of the paper on the *Cell Research* website.)

PARP-1 Regulates Metastatic Melanoma through Modulation of Vimentin-induced Malignant Transformation

María Isabel Rodríguez^{1,2,3,9*}, Andreína Peralta-Leal^{1,9}, Francisco O'Valle⁴, José Manuel Rodríguez-Vargas¹, Ariannys Gonzalez-Flores¹, Jara Majuelos-Melguizo¹, Laura López¹, Santiago Serrano¹, Antonio García de Herreros⁵, Juan Carlos Rodríguez-Manzaneque⁶, Rubén Fernández⁶, Raimundo G. del Moral⁷, José Mariano de Almodóvar², F. Javier Oliver^{1*}

1 Instituto de Parasitología y Biomedicina López Neyra, CSIC, Granada, Spain, **2** IBIMER, Centro de Investigaciones Biomédicas, Universidad de Granada, Granada, Spain, **3** Departamento de Bioquímica y Biología Molecular I, Universidad de Granada, Granada, Spain, **4** Departamento de Anatomía Patológica, Universidad de Granada, Granada, Spain, **5** Institut Municipal d'Investigació Mèdica (IMIM), Universitat Pompeu Fabra, Barcelona, Spain, **6** Pfizer-University of Granada-Junta de Andalucía Centre for Genomics and Oncological Research (GENYO), Granada, Spain, **7** Unidad de Anatomía Patológica, Complejo Hospitalario y Áreas Sur y Noreste de Granada, Granada, Spain

Abstract

PARP inhibition can induce anti-neoplastic effects when used as monotherapy or in combination with chemo- or radiotherapy in various tumor settings; however, the basis for the anti-metastatic activities resulting from PARP inhibition remains unknown. PARP inhibitors may also act as modulators of tumor angiogenesis. Proteomic analysis of endothelial cells revealed that vimentin, an intermediary filament involved in angiogenesis and a specific hallmark of EndoMT (endothelial to mesenchymal transition) transformation, was down-regulated following loss of PARP-1 function in endothelial cells. VE-cadherin, an endothelial marker of vascular normalization, was up-regulated in HUVEC treated with PARP inhibitors or following PARP-1 silencing; vimentin over-expression was sufficient to drive to an EndoMT phenotype. In melanoma cells, PARP inhibition reduced pro-metastatic markers, including vasculogenic mimicry. We also demonstrated that vimentin expression was sufficient to induce increased mesenchymal/pro-metastatic phenotypic changes in melanoma cells, including ILK/GSK3- β -dependent E-cadherin down-regulation, Snail1 activation and increased cell motility and migration. In a murine model of metastatic melanoma, PARP inhibition counteracted the ability of melanoma cells to metastasize to the lung. These results suggest that inhibition of PARP interferes with key metastasis-promoting processes, leading to suppression of invasion and colonization of distal organs by aggressive metastatic cells.

Citation: Rodríguez MI, Peralta-Leal A, O'Valle F, Rodríguez-Vargas JM, Gonzalez-Flores A, et al. (2013) PARP-1 Regulates Metastatic Melanoma through Modulation of Vimentin-induced Malignant Transformation. *PLoS Genet* 9(6): e1003531. doi:10.1371/journal.pgen.1003531

Editor: Bruce E. Clurman, Fred Hutchinson Cancer Research Center, United States of America

Received: May 9, 2012; **Accepted:** April 12, 2013; **Published:** June 13, 2013

Copyright: © 2013 Rodríguez et al. This is an open-access article distributed under the terms of the Creative Commons Attribution License, which permits unrestricted use, distribution, and reproduction in any medium, provided the original author and source are credited.

Funding: This work was supported by Ministerio de Ciencia e Innovación SAF2006-01094, SAF2009-13281-C02-01, Fundación La Caixa BM06-219-0 and Junta de Andalucía P07-CTS-0239 and CTS-6602 to FJO, Ministerio de Educación y Ciencia SAF2007-64597; CICYT: SAF2009-13281-C02-02; Junta de Andalucía, P06-CTS-01385 to JMRdA and grants CEIC (P10-CTS5865) and FEDER-ISCI (P110/00883) to JCR-M. AGdH has been funded by grants from "Fundación Científica de la Asociación Española Contra el Cáncer", Ministerio de Ciencia y Tecnología SAF2010-16089, and "Fundación La Marató de TV3". JCR-M has been funded by Grants CEIC (P1 = -CTS5865) and FEDER-ISCI (P110/00883). The funders had no role in study design, data collection and analysis, decision to publish, or preparation of the manuscript.

Competing Interests: The authors have declared that no competing interests exist.

* E-mail: mirlara@ipb.csic.es (MIR); joliver@ipb.csic.es (FJO)

⁹ These authors contributed equally to this work.

Introduction

Metastatic melanoma is a fatal malignancy that is remarkably resistant to treatment; however, the mechanisms regulating the transition from the primary local tumor growth to distant metastasis remain poorly understood. Metastasis, defined as the spread of malignant tumor cells from the primary tumor mass to distant sites, involves a complex series of interconnected events.

Understanding the biochemical, molecular, and cellular processes that regulate tumor metastasis is of vital importance. The metastatic cascade is thought to be initiated by a series of genetic alterations, leading to changes in cell-cell interactions that allow the dissociation of cells from the primary tumor mass. These events are followed by local invasion and migration through proteolytically modified extracellular matrix (ECM). To establish

secondary metastatic deposits, the malignant cells evade host immune surveillance, arrest in the microvasculature, and extravasate from the circulation. Finally, tumor cells can invade the local ECM, proliferate, recruit new blood vessels by induction of angiogenesis, and then expand to form secondary metastatic foci [1].

Several key steps in metastatic progression involve tumor-associated endothelial cells (EC) [2]. Both angiogenesis and angiogenesis require disruption of endothelial integrity for tumor cell transmigration across the endothelium, EC migration and EC access for mitogenic stimulation. An essential step in angiogenesis and angiogenesis is the disruption of the adherent junctions between EC. Vascular endothelial cadherin (VE-cadherin; also known as cadherin 5) is the most important adhesive component of endothelial adherent junctions [3]; while ectopic expression of VE-

Author Summary

Metastasis is the spread of malignant tumor cells from their original site to other parts of the body and is responsible for the vast majority of solid cancer-related mortality. PARP inhibitors are emerging as promising anticancer therapeutics and are currently undergoing clinical trials. It is therefore important to elucidate the mechanisms underlying the anti-tumor actions of these drugs. In our current study, we elucidated novel anti-neoplastic properties of PARP inhibitors that are responsible for the anti-metastatic effect of these drugs in the context of malignant melanoma. These effects appear to be the result of PARP-1's ability to regulate the expression of key factors, such as vimentin and VE-cadherin, involved in vascular cell dynamics and to limit pro-malignant processes such as vasculogenic mimicry and EMT.

cadherin in malignant melanoma cells confers this tumor the capability to form vessel-like structures that contributes to the lack of efficient therapeutic strategies and increases the risk of metastatic disease [4].

Epithelial-mesenchymal transition (EMT) is a trans-differentiation characterized by decreased epithelial markers such as E-cadherin [5]. EMT is a dynamic process resulting in the acquisition of cell motility with decreased adhesive ability for body organization that includes embryonic development and wound healing. Currently, EMT is thought to be a key step in the process of cancer metastasis [6]. Molecular markers of EMT include E-cadherin down-regulation, responsible for the loss of cell-cell adhesion, up-regulation of matrix-degrading proteases and mesenchymal-related proteins such as vimentin and N-cadherin, actin cytoskeleton reorganization, and up-regulation and/or nuclear translocation of transcription factors underlying the specific gene program of EMT, such as β -catenin and members of the Snail family [6].

The nuclear protein PARP-1, known to function as a DNA damage sensor and to play a role in various DNA repair pathways, has recently been implicated in a broad variety of cellular functions, including transcriptional regulation [7]. PARP inhibitors exhibit antitumor activity in part due to their ability to induce synthetic cell lethality in cells deficient for homologous recombination repair [8,9,10,11]. PARP inhibitors also possess anti-angiogenic properties [12,13,14,15], and recently, our group reported that PARP inhibition results in the down-regulation of Snail1 by accelerating the degradation of this protein [16]. In the present study we aimed to address the potential of PARP inhibition as modulators of metastasis [16].

The results presented here indicate that PARP inhibition, through down-regulation of the intermediary filament vimentin in both endothelial and melanoma cells, led to a reversion of mesenchymal phenotype in both cell types and prevented malignant melanoma cells from developing vasculogenic mimicry. As monotherapy, PARP inhibition displayed an anti-metastatic effect in a model of murine melanoma. Moreover, we identified vimentin as an upstream modulator of EMT: forced expression of vimentin was sufficient to induce tumor cell transformation through the ILK/GSK-3 β signaling axis. The ability of PARP inhibition to modulate vimentin levels (and hence EMT), the interference with vasculogenic mimicry, and the modulation of endothelial plasticity allowed PARP inhibitors to exert a multifaceted antimetastatic effect to counteract the progression of malignant melanoma.

Results

PARP inhibition induced down-regulation of vimentin expression in endothelial cells

A number of reports from various laboratories, including ours, have identified a novel and unexpected effect of PARP inhibitors on angiogenesis, raising the possibility that PARP inhibitors may be useful as anti-angiogenic agents [13,17]. In our present study, we disrupted PARP activation in HUVECs in an attempt to elucidate the mechanism by which PARP-1 influences endothelial cell dynamics. We have previously shown that PARP inhibitors reduced angiogenesis both *in vitro* and *in vivo* ([13] and Figure S1). To further characterize this effect of PARP inhibition on endothelial cell plasticity, we performed a proteomic analysis using primary HUVEC in the presence or absence of the PARP inhibitor DPQ (Figure 1A, Figure 2 and Figure S2). The expression levels of a number of proteins were altered following PARP inhibition, as detected by 2D DIGE electrophoresis (Figure S2) and mass spectrometry analysis (Figure 1A, Figure 2). A statistically significant down-regulation of vimentin (a class III intermediary filament), tropomyosin alpha-4 chain (involved in stabilizing actin filaments), endoplasmic reticulum chaperone involved in processing and transport of secreted proteins, mitochondrial ATP synthase ATP5B, protein disulfide isomerase PDIA6, heat shock 70 kD protein-5 (glucose-regulated protein, 78 kD), heat shock protein 90 kDa alpha (cytosolic), class B member 1, and HSP90AB1 occurred following PARP inhibition. An increase in the expression of the mitochondrial heat shock protein HSPD1 was also observed after PARP inhibition.

Due to its important role in the biology of endothelial cells, we focused our study on vimentin, the main structural protein of intermediary filaments. It has been reported that vimentin can be targeted for tumor inhibition due to its specific up-regulation in tumor vasculatures [18,19]. To confirm the results of our proteomic analysis, we performed western blot in HUVEC either treated with DPQ (right) or left untreated. In Figures 1B and 1C, western blot and indirect immunofluorescence analysis indicated that vimentin expression was down-regulated in HUVEC cells treated with DPQ.

Figure 1B and 1D show that PARP inhibition affected not only vimentin levels but also Snail1 and VE-cadherin protein and mRNA levels.

Endothelial to mesenchymal transition (EndoMT) is a process by which endothelial cells disaggregate, change shape, and migrate into the surrounding tissue. The process of EndoMT is characterized by the loss of endothelial cell markers, such as vascular endothelial VE-cadherin, and the expression of mesenchymal cell markers, such as vimentin and Snail1 [20]. Endothelial cell migration was strongly inhibited by PARP inhibition (Figure 1E). These results suggest that PARP inhibition prevented the acquisition of a mesenchymal phenotype by endothelial cells.

Interplay between vimentin and PARP-1 modulates the expression and activity of proteins involved in EMT

Vimentin is a well-known marker of EMT, which is a hallmark of primary tumor progression to a metastatic phenotype. We tested the impact of vimentin down-regulation (induced by PARP inhibition or vimentin silencing) on EMT differentiation in various melanoma cell lines and in endothelial cells. One major event induced by PARP inhibition, in the process of EMT is the up-regulation of E-cadherin expression through the inactivation of the transcription factor Snail1. Snail1 and vimentin levels were both down-regulated following PARP inhibition, indicating a disruption of EMT in the absence of PARP activation (Figure 3A in G361 cells and Figure S3B in B16-F10 cells). Down-regulation of PARP

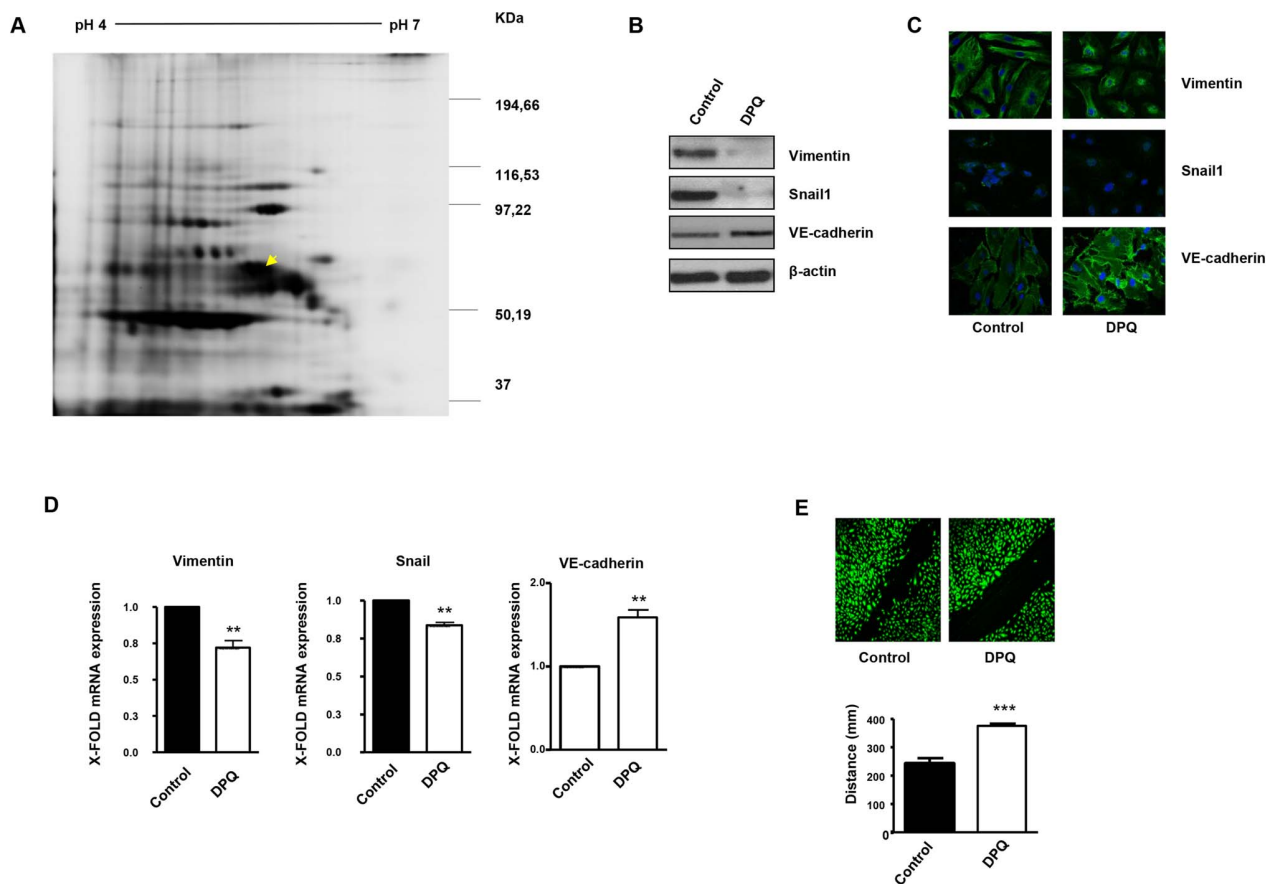


Figure 1. PARP inhibition down-regulates vimentin expression and inhibits endothelial-to-mesenchymal transition in HUVECs. Cell extracts from HUVEC either treated with vehicle or 40 μ M DPQ were subjected to 2D electrophoresis as described in Materials and Methods. Image analysis software (DeCyder) indicated that seven proteins exhibited decreased expression in HUVEC treated with DPQ compared to untreated cells. Proteins were identified using MALDI-TOF. Spots labeled with arrows indicate proteins that were identified by mass spectrometry (see Figure 2). (A) The spot with the arrow is vimentin. (B) PARP inhibition reduced the expression of both vimentin and Snail1 and up-regulated VE-cadherin in human endothelial cells (HUVEC) as determined by immunoblotting, indirect immunofluorescence (C), and mRNA levels (D). PARP inhibition decreased HUVEC cell migration (E). (** $P < 0.01$, *** $P < 0.001$ PARP inhibitor groups versus DPQ). doi:10.1371/journal.pgen.1003531.g001

activity was confirmed in G361 following H_2O_2 treatment as a positive control of PARP-1 activation and poly(ADP-ribose) (PAR) synthesis (Figure S4). Vimentin and Snail1 mRNA levels were decreased after PARP inhibition (Figure 3C and Figure S3C). In Figures 2B and Figure S3A, indirect immunofluorescence showed that vimentin expression was down-regulated in melanoma cells treated with DPQ or KU0058948 (G361 cells, Figure 3B) or PJ-34 (B16-F10 cells, Figure S3A). Using two different luciferase reporter plasmids under the control of a Snail1 responsive sequence and the E-cadherin promoter, we found that PARP inhibition affected negatively the activation of Snail1 and activated the expression of the E-cadherin promoter (Figure 3D and Figure S3D). Wound healing experiments also revealed decreased wound closing following treatment with a PARP inhibitor, PJ-34 (Figure 3E).

We have also evaluated the effect of both PARP-1 and vimentin silencing on the expression of Axl, a key determinant of cell migration and EMT promotion [21]. Following PARP-1 silencing in HUVEC or G361 cells, the EMT marker Snail1 decreased while E or VE-cadherin were upregulated (Figure 4A and 4B respectively). Interestingly, Axl expression was also down-regulated in parallel with decreased levels of vimentin. Vimentin knockdown also caused a global alteration in the expression of

EMT markers. Under these conditions, Axl levels were decreased (Figure 4A and 4B), suggesting that vimentin down-regulation was sufficient to drive tumor cells toward an epithelial state.

We next sought to determine if alterations in vimentin levels were sufficient to alter or reverse EMT progression. Vimentin is known to positively influence tumor cell migration. To test the impact of vimentin expression on cell migration and invasion we performed either silencing or over-expression in endothelial and melanoma cells. Following vimentin knockdown, wound healing closure in HUVEC cells was significantly diminished (Figure 4C) while its over-expression increased wound healing efficiency (Figure 4D). The same approach was used in B16F10 melanoma cells where over-expression of vimentin increased significantly cell migration (Figure 4E). Nonetheless, inhibition of PARP had a less impact on cell migration after vimentin over-expression, suggesting that the levels of vimentin were implicated in the effect of PARP inhibition on cell motility (Figure 4E), although a multifactorial mechanism for downstream effect of PARP inhibition could not be excluded.

To further confirm the role of vimentin in PARP-inhibitor-induced impaired cell migration we decided to analyze the effect of vimentin over-expression and PARP inhibition in a well-established model of epithelial cells, MDCK, that undergo EMT

DOWN-REGULATED PROTEINS

| Spot No. | SwissProt Access No. | Gene Symbol | Protein name | MW (Da) | pI | SCORE | Seq Cov % | Av ratio | No. prep. | Function |
|----------|----------------------|-------------|--|---------|------|-------|-----------|----------|-----------|--|
| 1 | P08670 | VIM | Vimentin | 53676 | 5.06 | 319 | 58% | -1.21 | 26 | Class-III intermediate filaments |
| 2 | P67936 | TPM4 | Tropomyosin alpha-4 chain | 28619 | 4.67 | 52 | 16% | | 40 | Stabilizes cytoskeleton and actin filaments |
| 3 | P14625 | HSP90B1 | Endoplasmic | 92696 | 4.76 | 157 | 28% | -1.32 | 37 | Adenosine triphosphate(ATP)-metabolizing molecular chaperones |
| 8 | P06576 | ATP5B | ATP synthase subunit beta, mitochondrial | 56525 | 5.26 | 251 | 63% | -1.25 | 21 | Subunit of mitochondrial ATP synthase |
| 8 | Q15084 | PDIA6 | Protein disulfide-isomerase A6 | 48490 | 4.95 | 61 | 22% | -1.25 | 7 | Catalytic activity: catalyzes the rearrangement of S-S bonds in proteins |
| 10 | P11021 | HSPA5 | 78 Kda Glucose-regulated protein | 72402 | 5.07 | 159 | 32% | | 17 | Involved in the folding and assembly of proteins in the ER |
| 11 | P08238 | HSP90AB1 | Heat shock protein hsp 90-beta | 83554 | 4.97 | 69 | 18% | -1.31 | 13 | Involved in signal transduction, protein folding and degradation and morphological evolution |

UP-REGULATED PROTEINS

| Spot No. | SwissProt Access No. | Gene Symbol | Protein name | MW (Da) | pI | SCORE | Seq Cov % | Av ratio | No. prep. | Function |
|----------|----------------------|-------------|--|---------|------|-------|-----------|----------|-----------|--|
| 4 | P10809 | HSPD1 | 60 Kda heat shock protein, mitochondrial | 61187 | 5.70 | 61 | 22% | | 7 | Implicated in mitochondrial protein import and macromolecular assembly |

Figure 2. Proteins differentially expressed and identified by mass spectrometry analysis in HUVEC. The level of expression of various proteins in HUVEC was altered following PARP inhibition as determined by 2D-DIGE, and the proteins were positively identified using mass spectrometry analysis. Of particular interest for this study was vimentin, the major structural protein of intermediary filaments (spot 1). Expression of this protein was decreased in HUVEC following PARP inhibition. The proteins were identified by MALDI-TOF. Sequence coverage (%) and number of peptides were identified with = 1% FDR (false discovery rate cut-off against decoy-concatenated randomized database). Coverage and score was determined using the MASCOT algorithm. The average ratio of protein expression between the control and cells treated with the PARP inhibitor DPQ was determined in HUVEC.
doi:10.1371/journal.pgen.1003531.g002

after hepatocyte growth factor (HGF) treatment, including fast movement and circularity (scattering) [22]. The trajectories of cell migration were determined under video-microscopy and analyzed using MetaMorph image analysis software. Global trajectories after expression of GFP-vimentin in the presence or absence of PARP inhibitor and HGF were determined. Treatment with the PARP inhibitor PJ-34 or olaparib resulted in decreased cell motility in cells transfected with empty GFP vector (Figure 4F). Vimentin expression increased cell motility (Figure 4F, right), and PARP inhibition was unable to prevent this increase, suggesting that vimentin down-regulation is needed for the effect of PARP inhibition in reversing the EMT phenotype.

To characterize more in-depth the implications of vimentin expression in the context of EMT, we expressed GFP-vimentin in both a human melanoma cell line (Figure 5A) and a human breast tumor cell line with an epithelial phenotype (MCF7) (Figure 5B and 5C); MCF7 cells were chosen due to the lack endogenous vimentin expression compared with melanoma G361 cells (Figure 5A, G361 cells and Figure 5B and 5C, MCF7 cells). GFP-vimentin over-expression alone induced a mesenchymal phenotype characterized by Snail1 up-regulation, loss of E-cadherin, increased pGSK-3 β (inactive form) and β -catenin expression (Figure 5A, 5B and 5C).

The most remarkable effect of PARP or vimentin silencing observed in our model was the down-regulation of ILK and GSK-3 β (Figure 4A and 4B). In order to get mechanistic information on the interaction between vimentin over-expression and the activation of EMT signaling pathway, we focused in the axis ILK/GSK-3 β , which plays a central role in EMT commitment, upstream of Snail1. Inhibition of GSK-3 β was achieved by LiCl treatment while its activation was driven by silencing the kinase, ILK, which is the upstream inhibitory kinase for GSK-3 β (Figure 5, central panel). Specifically, inhibition of GSK-3 β (which was confirmed by an increase in the level of inhibitory phosphorylation of GSK-3 β at Ser9) with LiCl, activated EMT and resulted in E-cadherin down-regulation, Snail1 accumulation and increased levels of β -catenin (Figure 5B); concomitantly, E-cadherin was down-regulated following GSK-3 β inhibition by LiCl (Figure 5B) or exogenous expression of vimentin (Figure 5).

GSK-3 β activation is achieved through the silencing of its upstream inhibitor integrin-linked kinase (ILK). ILK knockdown resulted in Snail1 down-regulation and increased E-cadherin expression (Figure 5C). Interestingly, exogenous vimentin expression completely prevented siILK-induced E-cadherin up-regulation and partially prevented the reduction of Snail1 expression. These results suggested that vimentin, when over-expressed, is sufficient to drive the phenotypic changes

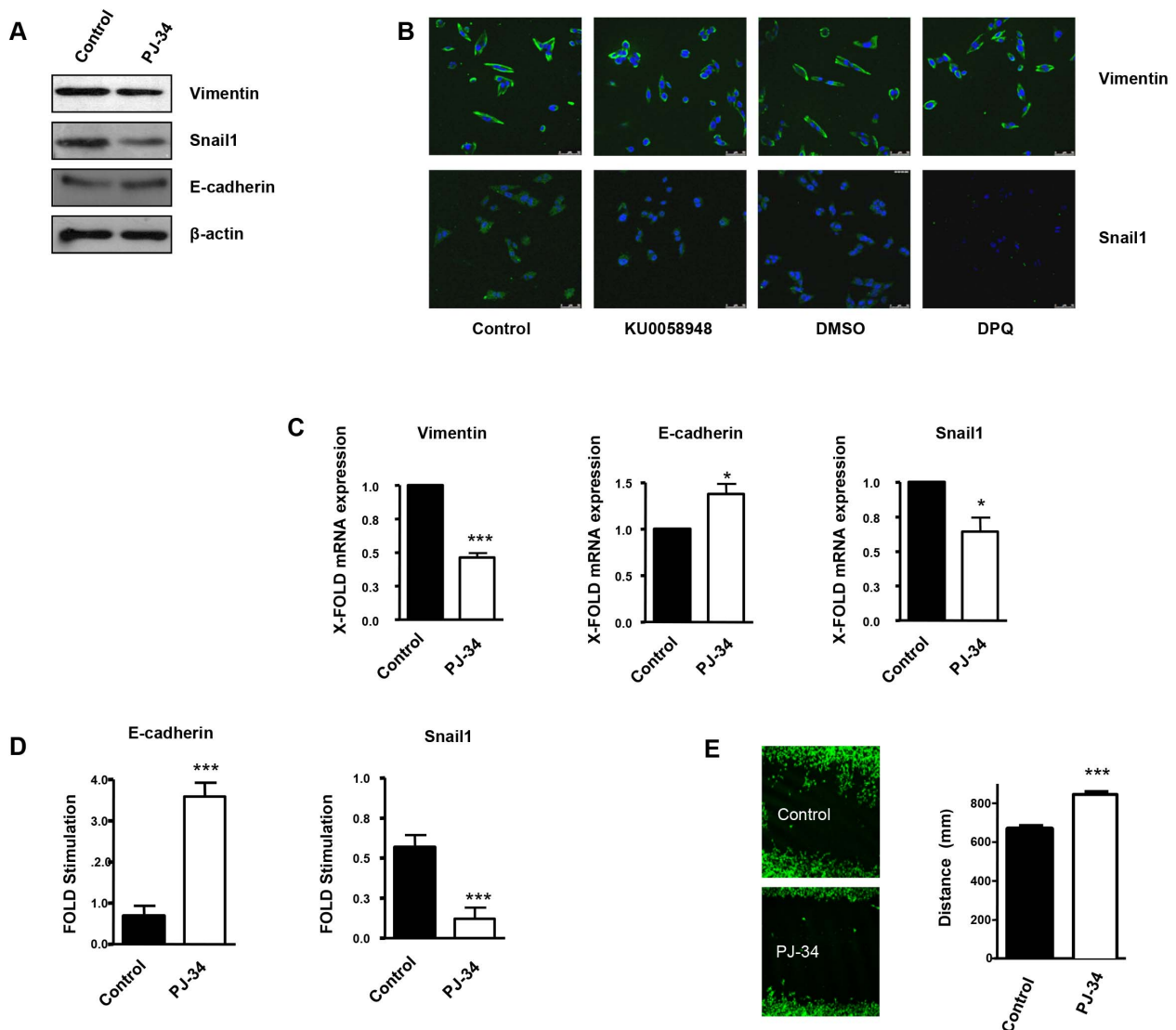


Figure 3. PARP inhibition inhibits the acquisition of an EMT phenotype in malignant melanoma cells. Human melanoma G361 cells and murine B16- F10 melanoma cells (Figure S3) were used for these experiments. Cells were treated with either DPQ (40 μ M), PJ-34 (10 μ M) or KU0058948 (100 nM) for 22 hours. IF, western blot or qPCR assays were performed to evaluate the effects of PARP inhibition on EMT markers. PARP inhibition reduced the expression of vimentin and Snail1 and up-regulated E-cadherin in human melanoma cells as determined by immunoblotting (A), indirect immunofluorescence (B), and mRNA levels (C). (* P <0.05, *** P <0.001, PARP Inhibitor groups versus the control). β -actin was used as an internal control for protein loading. (D) Snail1 and E-cadherin promoter activity are regulated by PARP inhibitors. Luciferase activity was determined after transfecting the constructions into G361 cells. Firefly Luciferase was standardized to the levels of Renilla Luciferase. Cells were cotransfected with 0.5 μ g renilla as a transfection control and 0.5 μ g of Snail1 or E-cadherin using jetPEI cationic polymer transfection reagent according to the manufacturer's instructions. Cells were compared in the presence or absence of serum (** P <0.001 control versus PJ-34). The expression of both Firefly and Renilla luciferase was analyzed 48 h after transfection. Cloning of the human Snail1 promoter (–869/+59) into pGL3 basic (Promega) was described previously (41). The E-Cadherin promoter was cloned into pGL3-basic (Promega) to generate pGL3-E-cadherin (–178/+92). (E) Inhibitory effect of PARP on B16F10 motility. Treatment with the PARP inhibitor PJ-34 (10 μ M) decreased cell migration in vitro. Migration was quantified as distance between Wound Healing limits (** P <0.001 control versus DPQ). doi:10.1371/journal.pgen.1003531.g003

associated with a mesenchymal cell status, depending on the activation of GSk-3 β , whose inhibition accentuated vimentin-induced changes, while its activation (following ILK-silencing), abolished vimentin-induced E-cadherin decrease and Snail1 accumulation (Figure 5C).

PARP inhibition suppresses vasculogenic mimicry in malignant melanoma cells

The formation of patterned networks of matrix-rich tubular structures in three-dimensional culture is a defining characteristic

of highly aggressive melanoma cells. It has been demonstrated that aggressive melanoma cells in which VE-cadherin was repressed, could not form vasculogenic-like networks [23], suggesting that tumor-associated misexpression of VE-cadherin (observed in melanoma cells) is instrumental in allowing endothelial cells to form vasculogenic networks. We measured VE-cadherin protein levels in B16-F10 cells after treatment with the PARP inhibitor PJ-34 or KU0058948. VE-cadherin expression was strongly down-regulated following PARP inhibition. We tried to confirm this

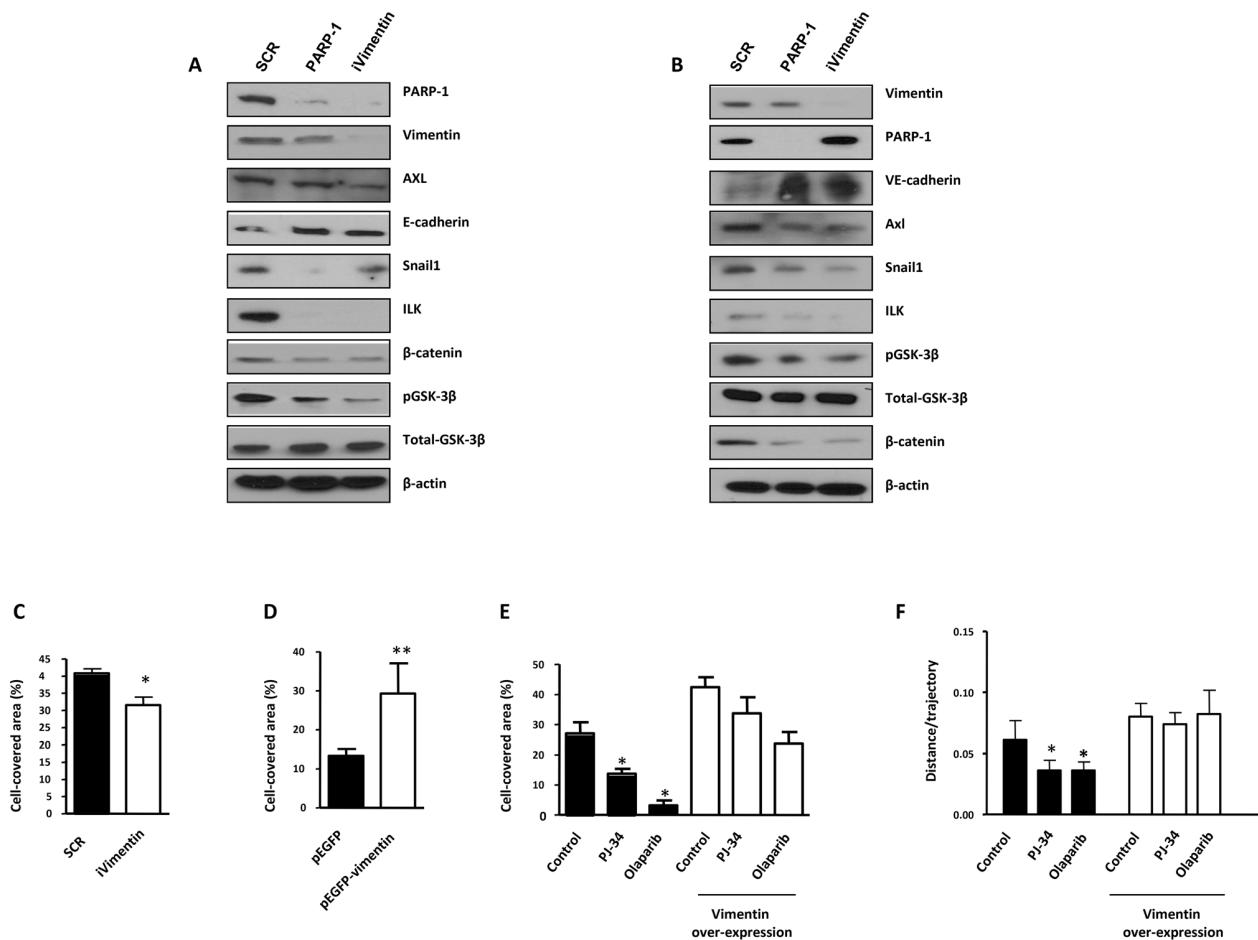


Figure 4. PARP-1 or vimentin is sufficient to reverse EMT and confer increased cell motility. (A) Melanoma (G361) and endothelial (HUVEC) (B) cells were silenced for PARP-1 or vimentin and the expression levels of Axl, E-/VE-cadherin, Snail1, ILK, β -catenin, GSK-3 β , PARP-1, and vimentin were determined by immunoblot. (C) HUVEC were silenced for vimentin and wound healing was measured. After over-expression of vimentin wound healing closure was measured in HUVEC cells (D) or B16-F10 (E). (F) Cell migration was analyzed in epithelial cell line Madin Darby canine kidney (MDCK) cells transfected with either GFP or GFP-vimentin using video-microscopy and MetaMorph Image Analysis software. While vimentin was able to increase the length of the trajectories in the absence or presence of hepatocyte growth factor (HGF), treatment with PARP inhibitor resulted in a sustained reduction in cell motility (* P <0.05 PJ-34 or olaparib versus control). doi:10.1371/journal.pgen.1003531.g004

result by indirect immunofluorescence of VE-cadherin, however the protein was barely detected, as was the case for the protein in western blot (Figure 6A). Phosphorylation of VE-cadherin has been shown to correlate with loss of function of VE-cadherin and increased vascular permeability [24], as is the case for pseudo vessels during VM. PARP inhibition was able to impact negatively on the levels of both total and phosphorylated VE-cadherin, which, indeed, had a membrane and cytoplasmic distribution (Figure 6A). The consequences for the down-regulation of both total and phosphorylated VE-cadherin by PARP inhibitors during VM are now being investigated in our laboratory.

VM was measured in vitro using B16F10 cells cultured in matrigel coated plates (Figure 6B). All markers of VM structure formation (covered area, tube length, branching points and loops) were significantly decreased after inhibition of PARP with PJ-34 (Figure 6C).

PARP inhibition protects against lung-metastasis of murine melanoma cells

We next aimed to examine the effect of PARP inhibition on melanoma tumor growth of cells subcutaneously implanted in

C57BL/6 mice. Mice were treated every two days with 15 mg/kg (i.p.) of the PARP inhibitor DPQ or vehicle. A significant difference in tumor growth was found after 14 days of tumor implantation in the DPQ-treated group compared to the control (Figure 7 and Figure S5A).

To evaluate the direct effects of the PARP inhibitor DPQ on tumor metastasis, we used a well-characterized model of experimental lung metastasis [25]. Experimental metastasis model provide several advantages for investigation. The time course for model maturity is generally rapid, the biology of metastasis is reproducible and consistent, and we control the number and type of cells that are introduced to the circulation [26]. B16-F10 cells were tail vein injected into mice, and the mice were then treated with 15 mg/kg of the PARP inhibitor DPQ or vehicle three times per week over a three-week period. Tail vein injection results primarily in pulmonary metastases. Photon emission was acquired every two days. Seven days after B16-F10 cell injection, a photon signal was already detected in the lungs (Figure 7B), and DPQ treatment significantly suppressed lung metastasis compared to the control throughout the duration of the experiment (21 days). Similar results were obtained using the clinically relevant PARP

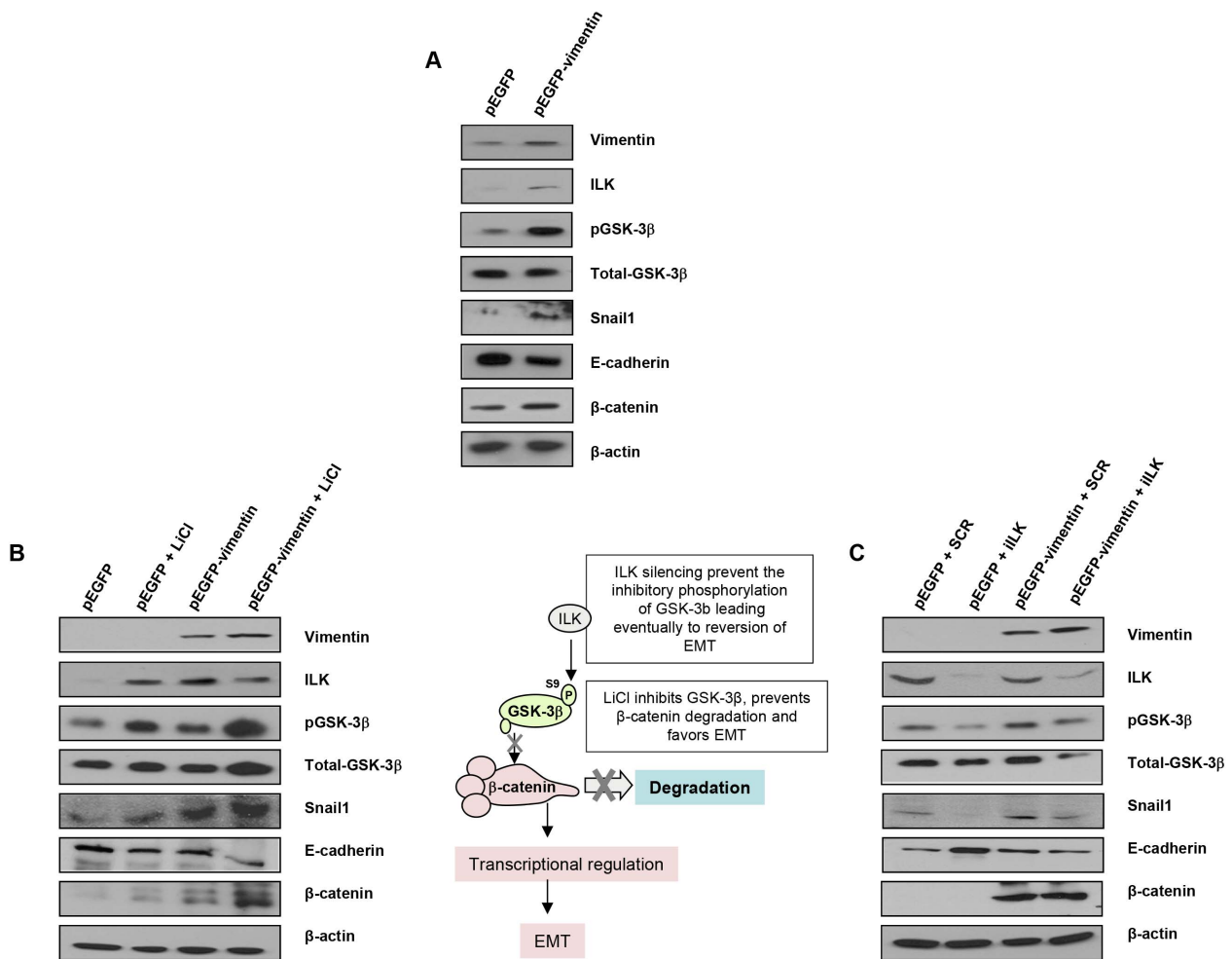


Figure 5. Interaction between vimentin over-expression and the activation of EMT signaling pathway. (A) Over-expression of vimentin in G361 cells. (B) Forced expression of vimentin drives human breast tumor epithelial cells (MCF7) to a mesenchymal phenotype through the integrin-linked-kinase/GSK-3 β axis. 5 mM LiCl was used to inhibit GSK-3 β , as detected by the accumulation of beta-catenin. (C) ILK was knocked down to analyze the significance of the interaction between vimentin and ILK in promoting the transition to a mesenchymal phenotype. doi:10.1371/journal.pgen.1003531.g005

inhibitor olaparib (Figure S6). Metastatic foci were also detected in other organs upon mice autopsy. These organs included the liver, kidney, spleen, gut, stomach and heart (Figure S5B). In all cases, the incidence of metastatic foci was reduced compared to lung metastasis. DPQ-treated mice exhibited a decreased incidence of extra-pulmonary metastasis compared to the control. Pathologic analysis of the lungs showed a decrease in size and number of metastatic foci (more than 80%) after DPQ treatment (Figure 7C) that was accompanied by a reduced number of tumor vessels in both primary subcutaneous tumors and lung metastasis (Figure 7D), suggesting that the anti-angiogenic effect of PARP inhibition may be involved in the observed reduction in metastatic progression. Apoptotic and mitotic rate were not significantly different in tumors derived from DPQ-treated or untreated mice (Figure S7). To investigate *in vivo* the effect of PARP inhibition on the expression of Snail1 and E-cadherin, we performed immunohistochemistry for these EMT markers in metastatic lung tumors (Figure 7E). We observed that Snail1 was highly expressed in the vessels of tumors derived from the untreated group. This expression exhibited both nuclear and cytoplasmic distribution as previously reported [27]. Metastatic lung tumors derived from

DPQ-treated mice displayed reduced expression of Snail1 as well as an increase in E-cadherin expression, similar to the results obtained in cultured melanoma cells. These data indicate that the *in vivo* expression of EMT markers within tumors is also reduced following treatment with PARP inhibitor. We also performed a Kaplan Meyer curve to compare the mortality of both groups of mice, and we observed a statistically significant difference in the survival rate from <4 weeks in the untreated group to >8 weeks in the DPQ-treated mice (Figure 7F). Survival of mice injected with B16-F10 cells stably expressing shRNA targeting PARP-1 (Figure 7G), was also significantly increase.

Human melanoma tissue array

To determine the correlation between PARP-1 expression and disease progression in human melanoma, we used IHC to analyze the levels of vimentin, PARP-1, Snail1, E-cadherin and MITF in nodular and metastatic melanoma frozen biopsies. Vimentin was expressed in all biopsies derived from both nodular and metastatic melanoma; however, the level of expression was elevated in nodular melanoma, which is the initial stage of the disease. PARP-1 expression was positively correlated with vimentin expression,

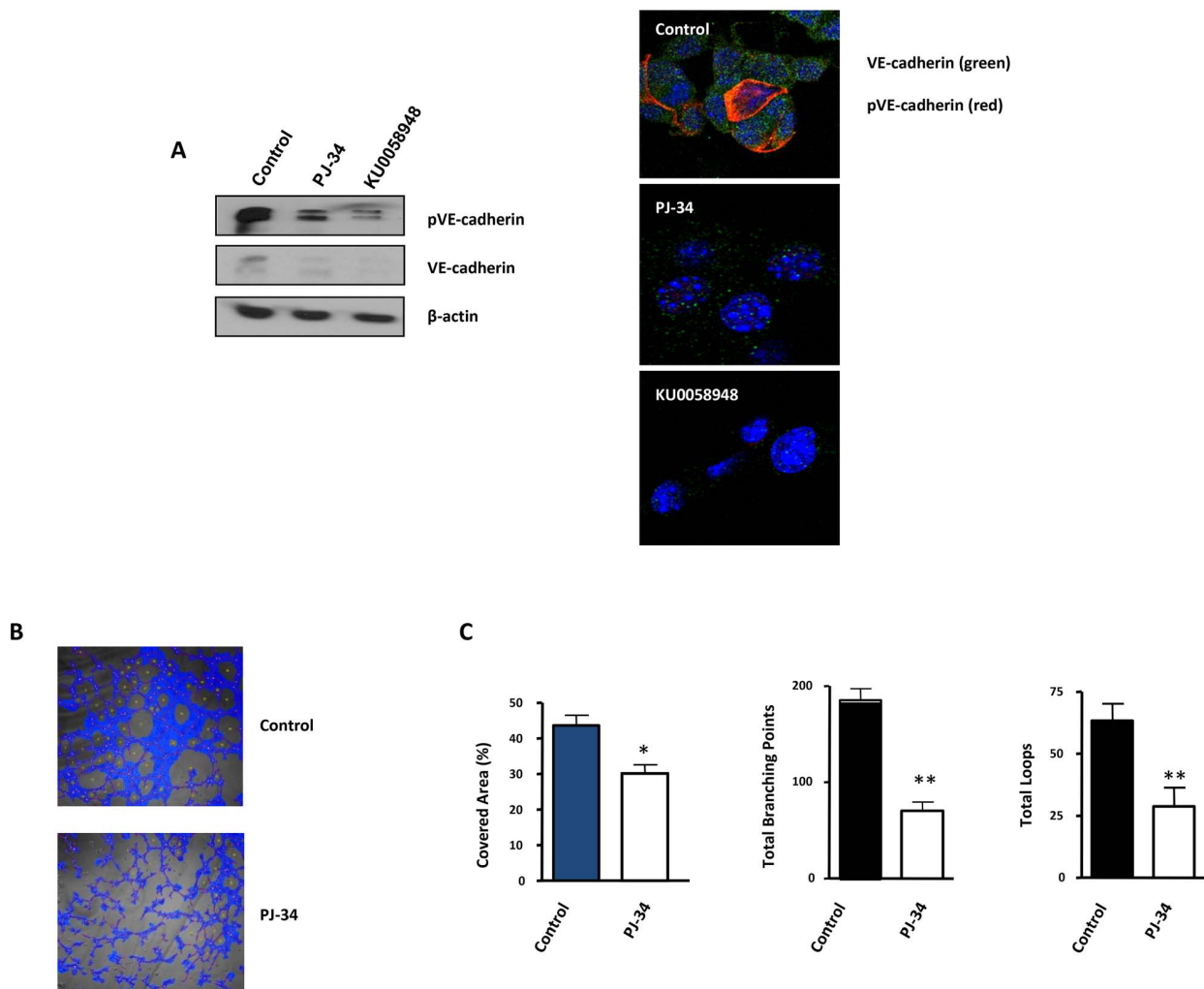


Figure 6. Vasculogenic mimicry is reduced by PARP inhibition in cells and in xenografts of malignant melanoma. (A) Western-blot and immunofluorescence of VE-cadherin and pVE-cadherin in B16-F10 cells treated with PJ-34 or KU0058948. (B, C) B16-F10 cells were cultured on polystyrene-treated culture slides and treated with the PARP inhibitor PJ-34 at 20 μ M or left untreated. Following treatment, pictures were taken and analyzed using Wimasis image analysis software. "Branching points": crossroads from at least three "branches". "Loops": Closed areas surrounded by cells. Four independent experiments were performed (* P <0.05; ** P <0.01). doi:10.1371/journal.pgen.1003531.g006

suggesting an association between the *in vivo* expression of both proteins (Figure S8, Table S1). Expression of the Snail1 and microphthalmia-associated transcription factor (MITF), which is a melanocyte marker, is also increased in metastatic melanoma. Interestingly, nodular melanoma did not express Snail1 while 40% of metastatic melanoma samples displayed Snail1 expression. Loss or reduction of E-cadherin and increased expression of EMT markers is frequently associated with the development of an invasive phenotype in cancer. Expression of E-cadherin in normal melanocytes is significantly reduced during the initial steps of melanoma progression [28]; however, elevated levels of E-cadherin are found at advanced stages of the disease [29]. E-cadherin expression was similar in both nodular and metastatic melanoma (Table S1), which is in agreement with previous publications. These findings suggest that in human melanoma, there is a complex interconnection between the expression levels of various disease markers and the expression of PARP-1, although we have detected a strong correlation between vimentin and PARP-1 expression (Figure S8).

Discussion

PARP inhibitors are a novel and important class of anticancer drugs, and there are now more than 40 clinical trials that are ongoing or in development to study the effectiveness of PARP inhibitors in the treatment of various cancers. Given the enormous interest in this target, it is important to understand the underlying mechanisms by which PARP-1 and other PARPs function in tumor cell biology. Until recently, the development of PARP-1 inhibitors has focused almost exclusively on the function of this enzyme in DNA repair. Emerging literature, however, indicates other activities of PARP-1 that may explain the *in vivo* potency of some PARP-1 inhibitors that cannot be entirely attributed to their apparent *in vitro* activity and that could provide additional targets for anti-cancer therapies. In addition to its direct role in DNA-damage recognition and repair, PARP-1 can regulate the function of several transcription factors, including p53 and NF- κ B. In the context of certain cancers, PARP-1 interacts with the transcription factors HIF1 [13] and Snail1 [16]. The mechanisms underlying

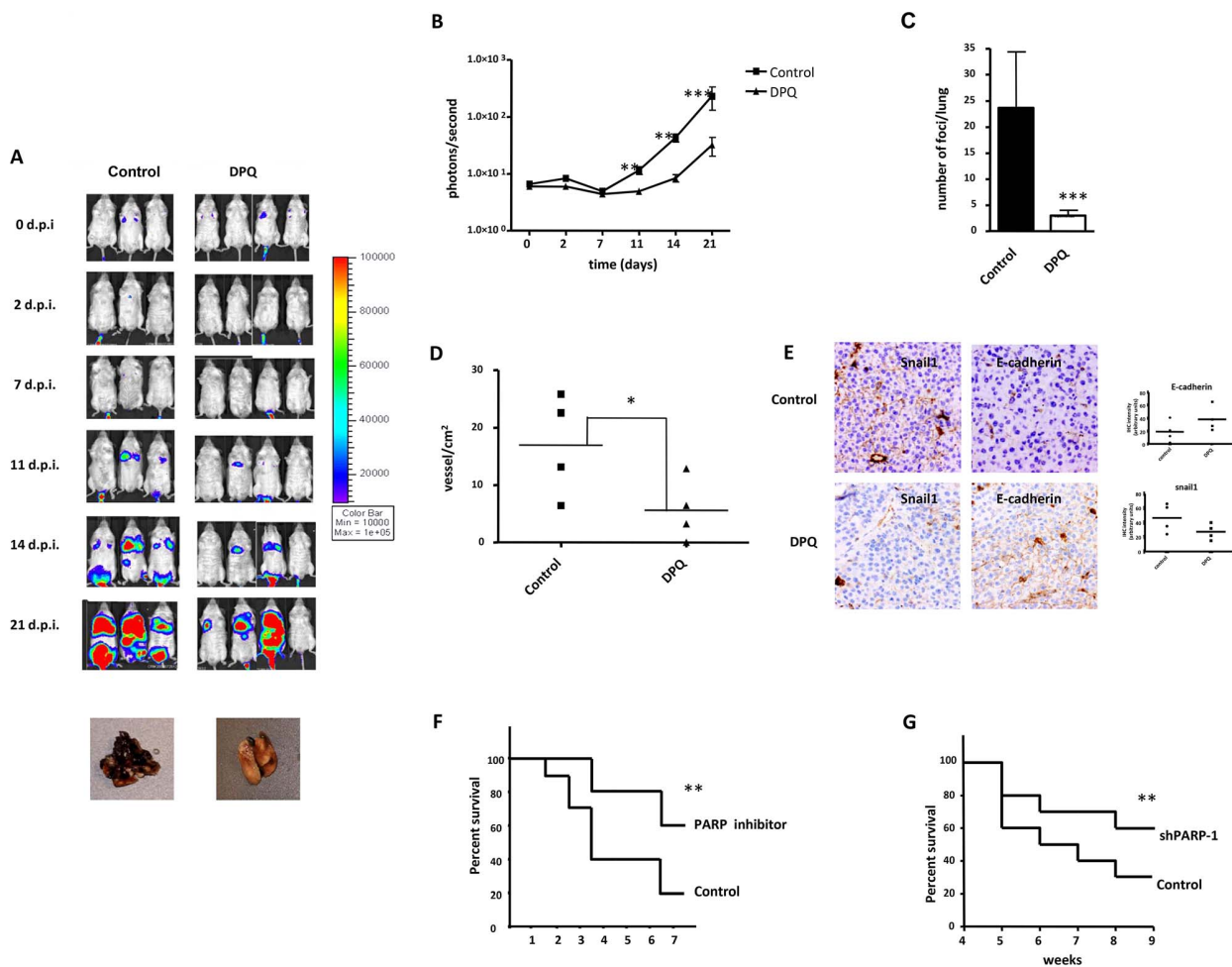


Figure 7. Decreased melanoma-induced lung metastasis following PARP inhibition. (A) Mice were inoculated with the murine melanoma cell line B16-F10-luc. Localization and the intensity of luciferase expression were monitored by *in vivo* bioluminescence imaging (dpi, days post cells injection). At the bottom of Figure A two lungs from vehicle (left) or DPQ (right) treated mice are shown. Lungs were extracted to analyze the number of melanoma foci. Quantification of luciferase activity over time shows the average light (photons) emission in photons/s (B) (** $P < 0.01$; *** $P < 0.001$ versus DPQ). (C) The number of metastatic foci/lung were counted macroscopically (*** $P < 0.001$). (D) Angiogenesis was measured using a specific endothelial cell marker (tomato lectin) and measured as blood vessels per mm² in tumor sections of lung metastasis (Columns, mean \pm SE. * $P < 0.05$, with respect to control and DPQ-treated mice. (E) Immunohistochemistry staining of Snail1 and E-Cadherin in lung metastasis and quantitation using ImageJ, colour deconvolution plugin (F and G) Kaplan-Meier survival curve shows the survival advantage of DPQ-treated mice following intravenous tail injection of melanoma cells as previously described in mice treated with DPQ (F) or injected with B16F10 stably silenced for PARP-1 (G) (** $P < 0.01$). doi:10.1371/journal.pgen.1003531.g007

the effects of PARP inhibition on vascular plasticity and metastasis remain relatively unknown. Our current study identifies PARP-1 as a pivotal modulator of the molecular and functional changes characteristic of EndoMT (involved in the loss of function of tumor-associated vessels) and of the phenotypic switch that facilitates the acquisition of pro-metastatic capacities by tumor cells. Proteomic analysis of endothelial cells that have been treated with a PARP inhibitor identifies the intermediary filament protein vimentin as a target of PARP inhibition. Intermediary filaments such as vimentin and keratins are known to play non-mechanical roles in protein trafficking and signaling (reviewed in [30]), which in turn influence cellular processes such as cell adhesion and polarization. Vimentin is abundantly expressed by mesenchymal cells and plays a critical role in wound healing, angiogenesis and cancer growth. Vimentin has also been described as a tumor-specific angiogenesis marker, and targeting endothelial vimentin in

a mouse tumor model significantly inhibited tumor growth and reduced microvessel density [31].

Vimentin is both an EMT and EndoMT marker and is also over-expressed in tumor samples compared to normal tissues. This protein also contributes to tumor phenotype and invasiveness [18,19]. Our findings indicate that PARP inhibitors reduce the metastatic potential of melanoma cells, at least in part, through their ability to down-regulate vimentin expression.

Vimentin expression has been shown to be transactivated by β -catenin/TCF and thus increasing the tumor cell invasive potential [19]. It has been shown that NF- κ B, a key protein regulating the immune and inflammatory process, also plays an important role in regulating EMT process and its inhibition in the mesenchymal cells reversed the EMT process, suggesting the importance of NF- κ B in both activation and maintenance of EMT [32]. Since vimentin is over expressed during EMT process, and NF- κ B being

one of the transcription factors binding to vimentin promoter, it would be tempting to speculate that this over-expression of vimentin is a result of activated NF- κ B in cancer cells. Also, TGF β 1 response element was found within the activated protein complex-1 region of the vimentin promoter and was involved in regulation of vimentin expression in myoblasts and myotubes [33]. Interestingly, ADP-ribosylation of Smad proteins by PARP-1 has been shown to be a key step in controlling the strength and duration of Smad-mediated transcription [34]. Regulation of vimentin levels by PARP inhibition may also involve other transcription factor such as Snail1 and HIF-1/2.

Our results also reveal that vimentin levels are not merely a hallmark of EMT. While silencing of vimentin in melanoma cells can reverse the EMT phenotype, in part by promoting down-regulation of the protein kinase Axl that is involved in cell motility, forced expression of vimentin in tumor cells lacking this protein is sufficient to trigger the switch from epithelial to mesenchymal phenotype. GSK-3 β is an upstream regulator of key factors involved in EMT such as Snail1 and β -catenin. We hypothesized that vimentin may be involved in the modulation of this upstream regulator of EMT. Indeed, vimentin expression potentiated LiCl- (a GSK-3 β inhibitor) induced EMT (Figure 5B) and counteracted the inhibitory action of ILK-silencing (leading to GSK-3 β activation) in the context of EMT (Figure 5C). Mechanical signals can inactivate GSK-3 β resulting in stabilization of β -catenin. Intermediate filaments are important in allowing individual cells, tissues and organs to cope with various types of stress, and they play a significant role in the mechanical behavior of cells [35]. It is possible that the signaling pathway that integrates PARP activation with altered vimentin expression and fluctuations in GSK-3 β activity could be related to the capability of PARP inhibitors to inactivate AKT signaling [36], which would result in GSK-3 β activation and the modulation of its downstream signaling, ultimately resulting in the reversal of EMT.

Vasculogenic mimicry, as a de novo tumor microcirculation pattern, differs from classically described endothelium-dependent angiogenesis. This is a unique process characteristic of highly aggressive melanoma cells found to express genes previously thought to be exclusively associated with endothelial cells and is characteristic of aggressive melanoma tumor cells. HIF-1 α and HIF-2 α , transcription factors that are stabilized during conditions of oxygen depletion (hypoxia), are the master regulators of VE-cadherin. HIF-mediated transcriptional regulation during hypoxia is critical as this process induces genes that are essential for tumor cell adaptation to the stress of oxygen depletion. As a result, the expression of HIF target genes is associated with increased malignancy. Although the expression of VE-cadherin is not hypoxia-regulated, HIF-2 α , but not HIF-1 α , activates the VE-cadherin promoter by binding to the HRE during normoxic conditions [37]. HIF-2 α expression is associated with developing endothelium, proper vascular development and increased tumor malignancy [38,39], raising the possibility that it may be an important protein that functions in the induction of tumor cell plasticity.

Using a mouse model of melanoma lung metastasis, we also present *in vivo* evidence indicating that targeting PARP strongly reduces metastatic dissemination of melanoma cells, at least in part through inducing a reduction in tumor microvessel density along with changes in the expression pattern of EMT markers (Snail1, vimentin and E-cadherin) within the tumor.

Snail1 is a master regulator of EMT, and the activation of this protein can mediate tumor invasiveness through the transcriptional repression of E-cadherin expression. Regulating the activity of E-cadherin repressors represents a potentially beneficial strategy

to fight cancer progression, and PARP-1 inhibitors accomplish this function by interfering with Snail1 activation.

Results from human tissue arrays of melanoma suggest a complex interaction between PARP-1 expression and melanoma progression. It is difficult to verify EMT experimentally *in vivo* due to the reversible and dynamic nature of the process. Although melanoma cells are not epithelial in nature, the EMT for this tumor is well characterized and the relevance of the cadherin switch has been previously described using several experimental approaches, demonstrating that melanoma cell lines transfected with N-cadherin are morphologically transformed from an epithelial-like shape to a fibroblast-like shape [37]. Adenoviral re-expression of E-cadherin in melanoma cells down-regulates endogenous N-cadherin and reduces the malignant potential of these cells [37].

Globally, our study shows that PARP inhibition is perturbing metastatic transformation at least at three levels (Figure 8): i) decreasing abnormal tumor angiogenesis through its ability to counteract Endo-MT; ii) preventing from acquisition of EMT and iii) limiting vasculogenic mimicry in melanoma cells.

Over the past few years, PARP has emerged as a strong and effective target for first line anticancer therapy. Due to its ability to regulate a number of cellular functions (from DNA repair to cell death and transcription), inhibition of PARP may affect multiple facets of tumor metabolism. These findings strongly indicate that several novel activities of PARP-1 may contribute to the effects of anti-cancer therapy targeting this protein by interfering with tumor physiology and the tumor microenvironment. Given these findings, it is of vital importance that we elucidate mechanisms regulating novel functions of PARP-1 and poly (ADP-ribose) in tumor biology so that PARP inhibitors can ultimately make the transition to routine clinical use.

Materials and Methods

Cell culture

Human umbilical vein endothelial cells (HUVEC) were cultured in EGM-2 Endothelial Cell Growth Medium-2 (LONZA). Cells were subjected to experimental procedures within passages 3–6. B16-F10-luc-G5 cells stably expressing plasmids pGL3 control (SV40-luc) (Promega) and pSV40/Zeo (Invitrogen). Human (G361), murine (B16-F10) malignant melanoma cells and breast cancer (MCF7) cells were cultured in DMEM containing 10% fetal bovine serum, 0.5% gentamicin (Sigma, St. Louis, MO), and 4.5% glucose. All cells were cultured at 37°C (5% CO₂). The tumor cell lines have been developed as described in detail previously [40]. Melnikova et al. [41] found that unlike human melanomas, the murine melanomas cell lines did not have activating mutations in the Braf oncogene at exon 11 or 15. All of the cell lines also expressed PTEN protein, indicating that loss of PTEN is not involved in the development of murine melanomas. This B16-F10 cell has previously been shown to be sensitive to stable depletion of PARP-1 *in vivo* melanoma growth [17]. Previous publication from our lab in G361 cells show similar results [16]. Cells were treated with the PARP inhibitors 3,4-dihydro-5-[4-(1-piperidinyl)butoxy]-1(2H)-isoquinolinone (DPQ), [N-(6-Oxo-5,6-dihydro-phenanthridin-2-yl)-N,N-dimethylacetamide] (PJ-34) (Alexis Biochemicals, San Diego, CA) (as described [42], KU0058948 (as we shown in previous publications [16] or Olaparib (KU0059436, Selleckchem) for 22 hours. For capillary-like formation assays, 25 μ L of Matrigel (BD Biosciences) were spread onto eight-chamber BD Falcon glass culture slides (BD Biosciences) or onto 96-well plates. Cells were seeded at 2.5×10^4 cells per well (high density) in eight-chamber slides and at 5×10^3

Illinois). For transfection, JetPrime was used according to the manufacturer's protocol.

24 h post-transfection, 5 μ M of LiCl (Sigma Aldrich) was added in MCF7 cells and 48 hours later, the expression of vimentin, ILK, pGSK-3 β , total-GSK-3 β , E-cadherin, Snail1 and β -catenin was measured. In other experiment, co-transfection of GFP-vimentin and ILK siRNA (Sigma Aldrich) was used according to the manufacturer's protocol. GFP and an irrelevant siRNA [44] were used as a control.

Migration/invasion assays

HUVEC and B16-F10 cells were cultured on coverslips in six-well cell culture dishes. Monolayer cultures were stained with CellTracker Green CMFDA in HUVEC cell (5-chloromethylfluorescein diacetate) (Invitrogen) according to manufacturer recommendations or with 4',6'-diamidino-2-phenylindole dihydrochloride (DAPI) (post-fixation). A wound was induced in the confluent monolayer cultures, and the cultures were then treated with the indicated inhibitor. The cells were fixed with 3.7% buffered formaldehyde and then prepared for immunofluorescence. Images were captured using a confocal microscope (LEICA TCS SP5 Argon Laser 488 nm, HeNe Laser 543 nm) when the cells were stained with CellTracker Green CMFDA Abs [522 nm] and Em [529 nm] and Zeiss Axio Imager A1 microscopy for cells stained with DAPI.

The method used to Wound Healing using a service provided by Wimasis with permits users to upload their images online at any time and form anywhere and allows their images to be analyzed and the results uploaded back to the researcher's server.

Scattering assay

Madin-Darby canine kidney (MDCK) cells (1.5×10^4) were seeded in 12-well tissue culture dish. After 24 h, cells were transfected with GFP or GFP-vimentin and 1 day after, cells were incubated with HGF (hepatocyte growth factor, Sigma Aldrich) or PBS. HGF is a mitogenic growth factor that is well known to induce the dissociation of islands of cells into individual cells, termed "cell scattering" or EMT. When inhibitors were used, cells were preincubated with PARP-1 inhibitor, PJ-34 or Olaparib for 2 h before addition of HGF. After 48 h, representative photographs were taken at $10 \times$ magnification using a Leica Spectral confocal laser microscope. The results were analyzed using the MetaMorph image analysis software.

In vitro angiogenesis assay

The effect of PARP inhibitors on the formation of tube-like structures in Matrigel (BD Biosciences) was determined according to manufacturer instructions. Briefly, 24-well plates were coated with 100 μ l of BD MatrigelTM Basement Membrane Matrix and allowed to solidify at 37°C in 5% CO₂. Cells were treated with DPQ (40 μ M) or PJ-34 (10 μ M). After 22 h of incubation at 37°C in 5% CO₂, the cells were fixed with 3.7% formaldehyde, and images were acquired using an Olympus CKX41 microscope. The formation of tube-like structures was then quantified. Each treatment was performed in triplicate, and the experiment was independently repeated at least three times.

Matrigel angiogenesis assay *in vivo*

C57BL/6 mice background (8 weeks old) were subcutaneously (s.c.) flank-injected with 600 μ l of matrigel (BD Biosciences) supplemented with VEGF (100 ng/ml) (Peprotech) and heparin (Sigma, 19 U). The negative controls contained heparin alone. Each group consisted of four animals. After seven days, mice were sacrificed and matrigel plugs were extracted. The angiogenic

response was evaluated by macroscopic analysis of the plug at autopsy and by measurement of the hemoglobin (Hb) content within the pellet of matrigel. Hb was mechanically extracted from pellets reconstituted in water and measured using the Drabkin (Sigma-Aldrich) method by spectrophotometric analysis at 540 nm. The values were expressed as optical density (OD)/100 mg of matrigel.

In vivo bioluminescence assay

This study was performed in strict accordance with the recommendations in the Guide for the Care and Use of Laboratory Animals of the Bioethical Committee of CSIC. The protocol was approved by the Committee on the Ethics of Animal Experiments of the CSIC. All surgery was performed under isoflurane anesthesia, and every effort was made to minimize suffering.

Eight-week-old male C57BL/6 albino mice (The Jackson Laboratories, Bar Harbor, MN, USA) were injected subcutaneously with B16-F10-luc-G5 cells (1×10^5) and intravenously with B16-F10-luc-G5 cells (1×10^5 or 5×10^5). Three times per week mice were injected intraperitoneally with DPQ dissolved in phosphate-buffered saline/10% DMSO at a dose of 15 mg/kg body weight or olaparib at 50 mg/kg. Mice were injected intraperitoneally with D-luciferin solution dissolved in phosphate-buffered saline at a dose of 150 mg/kg body weight. After 5 to 8 minutes, the animals were anesthetized in the dark chamber using 3% isoflurane in air at 1.5 L/min and O₂ at 0.2 L/min/mouse, and animals were imaged in a chamber connected to a camera (IVIS, Xenogen, Alameda, CA). Exposure time was 3 min in *large binning*, and the quantification of light emission was performed in photons/second using Living Image software (Xenogen). Tumor growth was monitored at 0, 2, 7, 14 and 21 days by *in vivo* imaging and bioluminescence measurement. After 21 days, mice were sacrificed, and their organs were removed and stored in buffered formalin (3.7%) until histological staining.

Indirect immunofluorescence

Immunostaining for vimentin, VE-cadherin, pVE-cadherin, Snail1 and E-Cadherin was performed on cells plated onto coverslips and grown for 22 h prior to experimental treatments. The culture medium was removed, and the cells were fixed (Paraformaldehyde 3%, Sucrose 2% in PBS) for 10 minutes at room temperature. Permeabilization was performed using 0.2% Triton X-100 in PBS. The coverslips were rinsed three times in PBS prior to incubation with primary antibody for 1 h at RT and then rinsed three times in PBS before incubation with the secondary antibody. Secondary antibodies were FITC-conjugated anti-mouse IgG or anti-rabbit (Sigma, St. Louis, MO). Antibodies were diluted in PBS containing 2% bovine serum albumin. Nuclear counterstaining with 4',6'-diamidino-2-phenylindole dihydrochloride (DAPI) was performed after removal of excess secondary antibody. Slides were prepared using Vectashield mounting medium (Vector Lab., Inc., Burlingame, CA 94010), cover slipped and stored in the dark at 4°C. Immunofluorescence images were obtained in the linear range of detection to avoid signal saturation using a fluorescent microscope (Zeiss Axio Imager A1) or confocal microscopy (Leica SP5).

Histological techniques

For conventional morphology, three buffered 4% formaldehyde-fixed, paraffin-embedded skin longitudinal tissue sections were stained with periodic acid schiff (PAS) at the end of treatment. The study was done in blinded fashion on 4- μ m sections with light microscopy. The mitosis and apoptosis cells were assessed by

examining their number in ten high power field (hpf) at 600× magnifications. The results were expressed as number of cells per mm². For evaluation of blood vessels density, tissue sections of different groups were dewaxed, hydrated, and heat-treated in 0.01 M citrate buffer for antigenic unmasking. The rest of the procedure was carried out using an automatic immunostainer (Autostainer480, Labvision, Fremont CA, USA). The incubation time with lectin Ulex europaeus biotin conjugated was 60 min, the dilution was 1:200, and the streptavidin-biotin-peroxidase method (Master Diagnostica, Granada, Spain) with diaminobezidine was used as visualization system. A millimeter scale in the eyepiece of a microscope BH2 (Olympus) with 40× objective was used to count the vessel per mm² of tissue section. The morphological and immunohistochemistry study was done in a double-blinded fashion by two pathologists.

Statistical analysis

For data shown in Figure 7 and FigureS7 we have fitted the values of the average number of tumors per mouse during carcinogenesis treatment using the Mann-Whitney u-test. Statistical analysis of other experiments used unpaired Student's t-test.

Supporting Information

Figure S1 PARP inhibitors decrease VEGF-induced tube formation in HUVECs *in vitro* and *in vivo*. Cells were collected and seeded in Matrigel-coated 48-well plates and then incubated in the absence (Control) or presence of VEGF and DPQ (40 μM) or PJ34 (20 μM). After 48 h, the morphological changes of the cells and any tubes formed were observed and recorded under a microscope. Micrographs were taken 40×. The number of tube was counted (A) (n=4), and mean is shown. Bars ± SEM (**P<0.01 *versus* control). After subcutaneous matrigel injection in the presence and absence of PARP inhibitor DPQ, a decreased in VEGF-induced *in vivo* angiogenesis was observed. The formation of vessel *in vivo* was assessed after injection of HUVEC with matrigel plug contains VEGF and heparin. The neovascularization was evaluated by measurement of HB content of matrigel plug. The histogram represents the mean (n=4) of the content, expressed as absorbance (DO)/100 mg of matrigel plug (B). (TIF)

Figure S2 2D-DIGE (Differential In-Gel Electrophoresis). HUVEC were solubilized in 2D-DIGE sample buffer (40 mM Tris, 7 M Urea, 2 M Thiourea, 1% ASB-14), sonicated and then the concentration was determined using the RC hDC Protein Assay (Bio-Rad). Fifty μg of protein was then labelled with 400 pmol of CyDye DIGE Fluor minimal dyes (GE Healthcare) and incubated on ice in the dark for at least 30 min according to manufacturer instructions Cy3 (A), Cy5 (B) for samples and Cy2 (C) for internal control consisting of equal parts of all samples). The reaction was halted by the addition of 10 mM lysine and incubated on ice for 10 min. Samples were loaded onto IPG strips (7 cm, pH 4–7) (Bio-Rad) by passive rehydration for 15 h and subjected to isoelectrofocusing using the PROTEAN IEF Cell System (Bio-Rad) according to the manufacturer's protocols. For the second dimension, strips were loaded on top of 7.5% polyacrylamide gels at 150 V for 1 h. The 2D gels were then scanned using a Typhoon Imager (GE Healthcare) at 100 μm resolution with λ_{ex}/λ_{em} of 488/520, 532/580, and 633/670 nm for Cy2, Cy3, and Cy5, respectively. Image analysis was performed using DeCyder 6.5 software (GE Healthcare) as described in the user manual. Six independent experiments were performed for each experimental setup. Briefly, the differential in-gel analysis (DIA) module was used for spot detection, spot volume quantification and volume ratio normalization of different samples in the same gel (D).

Differentially expressed spots were considered for identification based upon the fold change (>1.1) and the t-test (*P<0.05). (E) The Image analysis DeCyder Software indicated those differential spots detected in HUVEC treated with DPQ cells that were subsequently identified.

(TIF)

Figure S3 PARP inhibition reduced the expression of Vimentin and Snail1 and up-regulates E-cadherin murine melanoma cells. Cells were treated with either of the PARP inhibitors DPQ (40 μM) (not shown), PJ34 at 10 μM or KU0058948 (100 nM) during 22 hours. IF (A), western-blot (B) or qPCR (C) were performed to evaluate the impact of PARP inhibition on EMT markers. *P<0.05, ***P<0.001 PARP Inhibitor groups *versus* the control. β-actin was used as internal controls for protein loading. Luciferase activity (D) was determined after transfecting the constructions into the B16-F10 cells. *P<0.05 control *versus* DPQ. The expression of Firefly and Renilla luciferases was analyzed 48 h after transfection, according of the manufacturer's instructions.

(TIF)

Figure S4 Western-blot (A) and immunofluorescence (B) of PARP activity inhibition in G361cells treated with the PARP-1 inhibitor, DPQ.

(TIF)

Figure S5 Development of subcutaneous xenografts of melanoma is reduced by treatment with the PARP inhibitor DPQ. (A) C57BL/6 albino mice (Jackson Laboratories, Philadelphia, USA), were inoculated with B16-F10-luc cells as explained in Methods. Localization and intensity of luciferase expression was monitored by *in vivo* bioluminescence imaging. Quantitation of luciferase activity over time in photons/s, is represented in the color bar. Vehicle (n=4), DPQ (n=4). **P<0.01; ***P<0.001. (B) Ex-vivo photon emission: treatment with the PARP inhibitor DPQ reduced lung and extra-pulmonary melanoma-induced metastasis.

(PDF)

Figure S6 Treatment with the PARP inhibitor olaparib decreased metastatic spread of melanoma cells. C57BL/6 mice were inoculated with B16-F10-luc cells a treated with the PARP inhibitor olaparib (50 mg/kg) as explained in Methods. Results obtained on the 17th day are shown for quantitation. *P<0.05 olaparib *versus* control using the Mann-Whitney u-test.

(TIF)

Figure S7 Cell proliferation and apoptosis are not affected by PARP inhibition in metastasis. Mitosis and apoptosis were evaluated in histological metastasis slides using morphological criteria and evaluated in a blind observation by two different pathologists.

(TIF)

Figure S8 IHC evaluation of PARP-1 and EMT markers in human melanoma tissue array. Expression of PARP-1 and EMT markers in nodular and metastatic human melanoma. PARP-1 expression correlates with vimentin in nodular and metastatic melanoma. Snail1 and E-cadherin expression do not correlate with PARP-1 positivity.

(TIF)

Table S1 Results for all the different markers are presented. Samples were analyzed in a blind fashion by two different pathologists.

(TIF)

Table S2 Quantitation of western-blot. All western blots shown have been quantified using Quantity One software from Bio-Rad.

(PDF)

Acknowledgments

We acknowledge Victoria Longobardo from the Proteomic Service of IPBLN, CSIC and all the personnel from the animal facility of IPBLN, CSIC, in particular Clara Sangón and Francisco Ferrer. We also acknowledge Raquel Marrero from GENYO and José Luis Luque from IPBLN, CSIC.

References

- Baum B, Settleman J, Quinlan MP (2008) Transitions between epithelial and mesenchymal states in development and disease. *Semin Cell Dev Biol* 19: 294–308.
- Carmeliet P, Jain RK (2000) Angiogenesis in cancer and other diseases. *Nature* 407: 249–257.
- Vestweber D, Winderlich M, Cagna G, Nottebaum AF (2009) Cell adhesion dynamics at endothelial junctions: VE-cadherin as a major player. *Trends Cell Biol* 19: 8–15.
- Radisky DC (2005) Epithelial-mesenchymal transition. *J Cell Sci* 118: 4325–4326.
- Hugo H, Ackland ML, Blick T, Lawrence MG, Clements JA, et al. (2007) Epithelial–mesenchymal and mesenchymal–epithelial transitions in carcinoma progression. *J Cell Physiol* 213: 374–383.
- Thiery JP, Sleeman JP (2006) Complex networks orchestrate epithelial-mesenchymal transitions. *Nat Rev Mol Cell Biol* 7: 131–142.
- Schreiber V, Dantzer F, Ame JC, de Murcia G (2006) Poly(ADP-ribose): novel functions for an old molecule. *Nat Rev Mol Cell Biol* 7: 517–528.
- Bryant HE, Schultz N, Thomas HD, Parker KM, Flower D, et al. (2005) Specific killing of BRCA2-deficient tumours with inhibitors of poly(ADP-ribose) polymerase. *Nature* 434: 913–917.
- Farmer H, McCabe N, Lord CJ, Tutt AN, Johnson DA, et al. (2005) Targeting the DNA repair defect in BRCA mutant cells as a therapeutic strategy. *Nature* 434: 917–921.
- McCabe N, Turner NC, Lord CJ, Kluzek K, Bialkowska A, et al. (2006) Deficiency in the repair of DNA damage by homologous recombination and sensitivity to poly(ADP-ribose) polymerase inhibition. *Cancer Res* 66: 8109–8115.
- Fong PC, Boss DS, Yap TA, Tutt A, Wu P, et al. (2009) Inhibition of poly(ADP-ribose) polymerase in tumors from BRCA mutation carriers. *N Engl J Med* 361: 123–134.
- Quiles-Perez R, Munoz-Gamez JA, Ruiz-Extremera A, O'Valle F, Sanjuan-Nunez L, et al. (2010) Inhibition of poly adenosine diphosphate-ribose polymerase decreases hepatocellular carcinoma growth by modulation of tumor-related gene expression. *Hepatology* 51: 255–266.
- Martin-Oliva D, Aguilar-Quesada R, O'Valle F, Munoz-Gamez JA, Martinez-Romero R, et al. (2006) Inhibition of poly(ADP-ribose) polymerase modulates tumor-related gene expression, including hypoxia-inducible factor-1 activation, during skin carcinogenesis. *Cancer Res* 66: 5744–5756.
- Lacal PM, Tentori L, Muzi A, Ruffini F, Dorio AS, et al. (2009) Pharmacological inhibition of poly(ADP-ribose) polymerase activity down-regulates the expression of syndecan-4 and Id-1 in endothelial cells. *Int J Oncol* 34: 861–872.
- Pyriochou A, Olah G, Deitch EA, Szabo C, Papapetropoulos A (2008) Inhibition of angiogenesis by the poly(ADP-ribose) polymerase inhibitor PJ-34. *Int J Mol Med* 22: 113–118.
- Rodriguez MI, Gonzalez-Flores A, Dantzer F, Collard J, de Herreros AG, et al. (2011) Poly(ADP-ribose)-dependent regulation of Snail1 protein stability. *Oncogene* 30:4365–4372.
- Tentori L, Muzi A, Dorio AS, Bultrini S, Mazzon E, et al. (2008) Stable depletion of poly (ADP-ribose) polymerase-1 reduces in vivo melanoma growth and increases chemosensitivity. *Eur J Cancer* 44: 1302–1314.
- Bargagna-Mohan P, Hamza A, Kim YE, Khuan Abby Ho Y, Mor-Vaknin N, et al. (2007) The tumor inhibitor and antiangiogenic agent withaferin A targets the intermediate filament protein vimentin. *Chem Biol* 14: 623–634.
- Gilles C, Polette M, Mestdagt M, Nawrocki-Raby B, Ruggeri P, et al. (2003) Transactivation of vimentin by beta-catenin in human breast cancer cells. *Cancer Res* 63: 2658–2664.
- Kalluri R, Zeisberg M (2006) Fibroblasts in cancer. *Nat Rev Cancer* 6: 392–401.
- Vuoriluoto K, Haugen H, Kiviluoto S, Mpindi JP, Nevo J, et al. (2011) Vimentin regulates EMT induction by Slug and oncogenic H-Ras and migration by governing Axl expression in breast cancer. *Oncogene* 30: 1436–1448.
- Li Y, Bhargava MM, Joseph A, Jin L, Rosen EM, et al. (1994) Effect of hepatocyte growth factor/scatter factor and other growth factors on motility and morphology of non-tumorigenic and tumor cells. *In Vitro Cell Dev Biol Anim* 30A: 105–110.

Author Contributions

Conceived and designed the experiments: FJO MIR JCR-M FO RGdM. Performed the experiments: AP-L MIR AG-F JMR-V LL RF JM-M FO SS FJO. Analyzed the data: MIR AP-L FJO JMRdA JCR-M. Contributed reagents/materials/analysis tools: AGdH. Wrote the paper: FJO AP-L MIR.

- Hess AR, Seftor EA, Gruman LM, Kinch MS, Seftor RE, et al. (2006) VE-cadherin regulates EphA2 in aggressive melanoma cells through a novel signaling pathway: implications for vasculogenic mimicry. *Cancer Biol Ther* 5: 228–233.
- Orensigo F, Giampietro C, Ferrari A, Corada M, Galaup A, et al. (2012) Phosphorylation of VE-cadherin is modulated by haemodynamic forces and contributes to the regulation of vascular permeability in vivo. *Nat Commun* 3: 1208.
- Maeda M, Suga T, Takasuka N, Hoshi A, Sasaki T (1990) Effect of bis(bilato)-1,2-cyclohexanediamineplatinum(II) complexes on lung metastasis of B16-F10 melanoma cells in mice. *Cancer Lett* 55: 143–147.
- Khanna C, Hunter K (2005) Modeling metastasis in vivo. *Carcinogenesis* 26: 513–523.
- Pena C, Garcia JM, Larriba MJ, Barderas R, Gomez I, et al. (2009) SNAI1 expression in colon cancer related with CDH1 and VDR downregulation in normal adjacent tissue. *Oncogene* 28: 4375–4385.
- Silye R, Karayiannakis AJ, Syrigos KN, Poole S, van Noorden S, et al. (1998) E-cadherin/catenin complex in benign and malignant melanocytic lesions. *J Pathol* 186: 350–355.
- Hsu M, Andl T, Li G, Meinkoth JL, Herlyn M (2000) Cadherin repertoire determines partner-specific gap junctional communication during melanoma progression. *J Cell Sci* 113 (Pt 9): 1535–1542.
- Ivaska J, Pallari HM, Nevo J, Eriksson JE (2007) Novel functions of vimentin in cell adhesion, migration, and signaling. *Exp Cell Res* 313: 2050–2062.
- van Beijnum JR, Dings RP, van der Linden E, Zwaans BM, Ramaekers FC, et al. (2006) Gene expression of tumor angiogenesis dissected: specific targeting of colon cancer angiogenic vasculature. *Blood* 108: 2339–2348.
- Min C, Eddy SF, Sherr DH, Sonenshein GE (2008) NF-kappaB and epithelial to mesenchymal transition of cancer. *J Cell Biochem* 104: 733–744.
- Wu Y, Zhang X, Salmon M, Lin X, Zehner ZE (2007) TGFbeta1 regulation of vimentin gene expression during differentiation of the C2C12 skeletal myogenic cell line requires Smads, AP-1 and Sp1 family members. *Biochim Biophys Acta* 1773: 427–439.
- Lonn P, van der Heide LP, Dahl M, Hellman U, Heldin CH, et al. (2010) PARP-1 attenuates Smad-mediated transcription. *Mol Cell* 40: 521–532.
- Bertaud J, Qin Z, Buchler MJ (2010) Intermediate filament-deficient cells are mechanically softer at large deformation: a multi-scale simulation study. *Acta Biomater* 6: 2457–2466.
- Tapodi A, Debrecceni B, Hanto K, Bogner Z, Wittmann I, et al. (2005) Pivotal role of Akt activation in mitochondrial protection and cell survival by poly(ADP-ribose)polymerase-1 inhibition in oxidative stress. *J Biol Chem* 280: 35767–35775.
- Krengel S, Groteluschen F, Bartsch S, Tronnier M (2004) Cadherin expression pattern in melanocytic tumors more likely depends on the melanocyte environment than on tumor cell progression. *J Cutan Pathol* 31: 1–7.
- Licht AH, Muller-Holtkamp F, Flamme I, Breier G (2006) Inhibition of hypoxia-inducible factor activity in endothelial cells disrupts embryonic cardiovascular development. *Blood* 107: 584–590.
- Weis SM, Cheresch DA (2011) Tumor angiogenesis: molecular pathways and therapeutic targets. *Nat Med* 17: 1359–1370.
- Fidler IJ (1973) Selection of successive tumour lines for metastasis. *Nat New Biol* 242: 148–149.
- Melnikova VO, Bolshakov SV, Walker C, Ananthaswamy HN (2004) Genomic alterations in spontaneous and carcinogen-induced murine melanoma cell lines. *Oncogene* 23: 2347–2356.
- Chevanne M, Zampieri M, Caldini R, Rizzo A, Ciccarone F, et al. (2010) Inhibition of PARP activity by PJ-34 leads to growth impairment and cell death associated with aberrant mitotic pattern and nucleolar actin accumulation in M14 melanoma cell line. *J Cell Physiol* 222: 401–410.
- Barbera MJ, Puig I, Dominguez D, Julien-Grille S, Guaita-Esteruelas S, et al. (2004) Regulation of Snail transcription during epithelial to mesenchymal transition of tumor cells. *Oncogene* 23: 7345–7354.
- Singh SK, Hawkins C, Clarke ID, Squire JA, Bayani J, et al. (2004) Identification of human brain tumour initiating cells. *Nature* 432: 396–401.

Deciphering the Insights of Poly(ADP-Ribosylation) in Tumor Progression

María Isabel Rodríguez,¹ Jara Majuelos-Melguizo,¹ Juan Manuel Martí Martín-Consuegra,¹ Mariano Ruiz de Almodóvar,² Abelardo López-Rivas,³ and Francisco Javier Oliver¹

¹Instituto de Parasitología y Biomedicina López Neyra (IPBLN), CSIC, Granada, Spain 18016

²CIB, IBIMER, Universidad de Granada, Granada, Spain 18016

³Centro Andaluz de Biología Molecular y Medicina Regenerativa (CABIMER), Consejo Superior de Investigaciones Científicas, Sevilla, Spain 41092

Published online in Wiley Online Library (wileyonlinelibrary.com).

DOI 10.1002/med.21339



Abstract: Poly (ADP-ribose) polymerase (PARP) inhibitors are particularly efficient against tumors with defects in the homologous recombination repair pathway. Nonetheless poly(ADP-ribosylation) (PARylation) modulates prometastatic activities and adaptation of tumor to a hostile microenvironment. Modulation of metastasis-promoting traits is possible through the alteration of key transcription factors involved in the regulation of the hypoxic response, the recruitment of new vessels (or angiogenesis), and the stimulation of epithelial to mesenchymal transition (EMT). In this review, we summarized some of the findings that focalize on PARP-1's action on tumor aggressiveness, suggesting new therapeutic opportunities against an assembly of tumors not necessarily bearing DNA repair defects. Metastasis accounts for the vast majority of mortality derived from solid cancer. PARP-1 is an active player in tumor adaptation to metastasis and PARP inhibitors, recognized as promising therapeutic agents against homologous recombination deficient tumors, has novel properties responsible for the antimetastatic actions in different tumor settings. © 2015 Wiley Periodicals, Inc. *Med. Res. Rev.*, 00, No. 0, 1–20, 2015

Key words: PARP; metastasis; hypoxia; EMT; angiogenesis

1. INTRODUCTION

A. PARP Proteins. Structure and Functions

Poly(ADP-ribose) polymerases (PARPs) are a group of DNA-dependent enzymes (also named ARTD) that catalyze the synthesis and transfer of negatively charged ADP-ribose moieties from

Correspondence to: María Isabel Rodríguez and F. Javier Oliver, Instituto de Parasitología y Biomedicina López Neyra (IPBLN), CSIC Avda. Conocimiento s/n 18016 Armilla, Granada, Spain F. JAVIER OLIVER: joliver@ipb.csic.es MARÍA ISABEL RODRÍGUEZ: mirlara@ipb.csic.es

Medicinal Research Reviews, 00, No. 0, 1–20, 2015

© 2015 Wiley Periodicals, Inc.

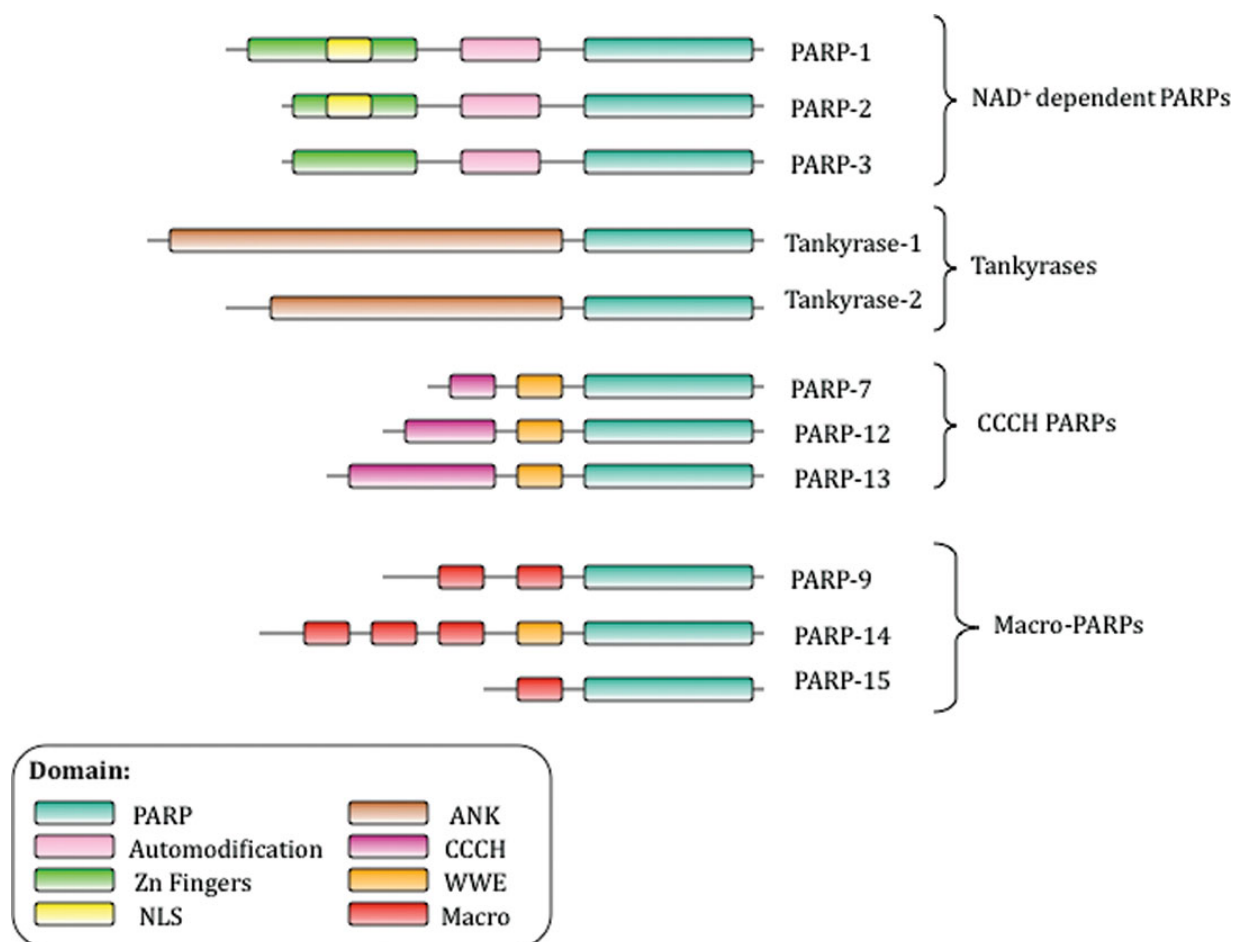


Figure 1. Representation of the structure and functions of the four subfamilies of PARP proteins. Functional domains are indicated in colored boxes. The PARP domain is responsible for the PARylation activity. The automodification domains are sequences that can be modified by ADP-ribose polymer. The Zn fingers are DNA-binding sites. NLS (Nuclear Localization Site) is the responsible for the import of the protein from the cytoplasm to the nucleus. ANK (ankyrin) are interaction modules. CCCH are RNA-binding domains. WWE domains are protein-protein interaction motifs. Macrodomains can serve as ADP-ribose or O-acetyl-ADP-ribose binding modules.

nicotinamideadeninedinucleotide (NAD⁺) to a number of target protein substrates, leading to the alteration of chromatin-associated proteins.¹ They are mainly nuclear proteins, although tankyrases can also be found in the cytoplasm.

PARP proteins constitute a family of 17 members that share a highly conserved PARP signature motif inside the catalytic domain.¹ This family is divided into four subfamilies according to their domain architectures (Fig. 1). (1) DNA-dependent PARPs (PARP-1, PARP-2, PARP-3) that are activated by DNA lesions through their DNA-binding domain. PARP-1 is the original constituent and also the most well-studied PARP member; PARP1 is a 116-kDa protein, consisting of three functional domain, a DNA-binding region, capable of binding and sensing DNA lesions; second, a middle automodification region; and third, an NAD-binding domain that functions as the catalytic domain,¹ namely N-terminal DNA-binding domain, automodification domain, and C-terminal catalytic domains (Fig. 1). The DNA-binding domain possesses three zinc fingers essential for the interaction with DNA breaks. Once the DNA-binding domain recognizes DNA lesions, it forces a conformational change of C-terminal catalytic domain to expose the activation site to NAD⁺, and activates the enzymatic activity. Besides auto-PARylation (where PARylation is poly(ADP-ribosylation)), PARP1 also induces histone PARylation at vicinity of DNA damage to induce chromatin remodeling in response to

DNA damage. (2) The group of PARPs called tankyrases contains large ankyrin domain repeats to facilitate protein–protein interactions. (3) CCCH PARPs contain first Cys-Cys-Cys-His zinc fingers that bind to RNA, and then WWE (Trp-Trp-Glu) domains that can exhibit PAR-binding activity. Finally, (4) macro-PARPs are characterized by the presence of macrodomain folds that mediate the localization of the protein to positions of poly and perhaps also mono (ADP-ribosyl)ation. Other PARP proteins do not accommodate into any of these four subgroups.²

ADP-ribosylome has recently been identified.^{3–5} From the report by Gagne et al.,⁵ only 291 proteins were experimentally identified to be PARylated after poly(ADP-ribose) antibody immunoprecipitation, while in silico they predicted a figure of 746 PAR-modified proteins. Globally, acceptor PARylated molecules are mainly proteins involved in nuclear functions, such as DNA synthesis and repair, chromatin structure modulation, transcription, and cell-cycle regulation.² More recently two different publications have analyzed the profiling of PAR-modified proteins after genotoxic stress,^{6,7} focusing, respectively, on covalently PARylated proteins or noncovalently PAR-binding proteins. Covalent PARylation affects a large number of proteins involved in RNA metabolic processes, prominently in response to oxidative and alkylation stress in comparison to UV or IR,⁶ a report by Gagne et al. showed that the consequences of PARylation go beyond early DNA damage response, impacting stress response and cell survival.⁷

It is important to remark that these different functions of PARPs are carried out through three types of regulatory mechanisms that involve PARylation: first, protein–protein interactions and protein–nucleic acid complexes. This case is represented by p53 that is PARylated and its activation is consequently modulated by PARP-1^{8,9} (see also below). Another example of PARP-1's regulatory action involving protein–protein interaction is the formation of the spindle pole, where many different proteins are attracted by PAR at some stage in mitosis.² Second, PARylation modulates protein localization and interaction scaffolds as is the case for PARP function in DNA damage sites, where different DNA damage factors are recruited in response to PARylation. For example, the histone KDM4D is PARylated and recruited to the sites of DNA damage promoting double-strand breaks repair (DSBs)¹⁰ Third, PARylation-dependent ubiquitylation is responsible for the proteolysis of different target proteins and is accomplished by several PARP proteins.² This is the case for tankyrase 2 that PARylates the adaptor protein 3BP2, acting as a signal for RNF146-mediated ubiquitylation of the protein. Mutations affecting 3BP2 PARylation sites prevent protein degradation, and activate signals that lead to cherubism disease.¹¹

There are many other examples to illustrate the complex and pleiotropic biological role of PARPs; however, describing all PARP functions would be a tremendously complex task that is out of the focus of the present review. The aim of this review is to dissect the main functions of PARP that are related with PARP's role in the development of tumors and more specifically with tumor invasion and metastasis.

B. PARP and Transcription

For long time, it has been described that PARP proteins participate in transcription processes through different molecular mechanisms that are described below.¹²

1. PARP-1 and Chromatin Modulation

In 1982, Poirier et al. described that PARP-1 PARylates chromatin proteins.¹³ Thus, the structure of chromatin changed from a condensed state to a less concentrated or “loose” state that facilitated gene transcription. More recently, PARP-1 was described as a key factor in local chromatin loosening that may assist gene transcription and chromatin remodeling in *Drosophila*

development.¹⁴ Furthermore, NAD⁺ status in the cell has been described to have a key role in PARP-mediated chromatin modulation.¹⁵ Using NAD⁺ as a substrate, PARP-1 catalyzes its own automodification and as a consequence, negatively charged polymer interacts with histones (H1, H2A, H2B). Thus, the structure of chromatin changes from the condensed to the “loose” state described above. In contrast, in the absence of NAD⁺, PARP-1 binding to nucleosomes promotes chromatin compaction into higher structure orders. Finally, PARP-1 promotes RNAPII activity through its interaction with RNAPII promoters.¹⁶ In the presence of PARP-1, which is associated with actively transcribed genes, histone H1 is depleted at these promoters. Nevertheless, a high rate of H1/PARP-1 promotes the opposite effect that is the repression of gene transcription.

Otherwise, an interaction between PARP-1 and chromatin-remodeling factors has been reported. The nucleosome remodeling ATPases, ALC1 and ISWI, have been described to interact with PARP-1. However, this interaction takes place through two different mechanisms, not fully understood: PARylated ISWI inhibits its ATPase activity, by decreasing its binding affinity for nucleosomes, generating the previously described “loose” structure of chromatin that facilitates transcription.¹⁷ Nevertheless, PARylated ALC1 stimulates its ATPase activity, promoting its recruitment to nucleosomes and the chromatin remodeling activity.¹⁸

2. Role of PARP-1 at Enhancer/Promoter Regulatory Complexes

The ability of PARP-1 to recognize particular DNA sequences has been well recognized, allowing its role as a standard enhancer factor. More recently, direct evidences of PARP-1 binding to specific DNA sequences have been reported. This is the case for the chemokine (C-X-C motif) ligand 1 (CXCL1) promoter for which Amiri et al.¹⁹ reported that while inactive PARP-1 binds to the CXCL1 promoter in a sequence-specific manner, preventing binding of NF- κ B (p65/p50) to its element, activated PARP-1 enhanced CXCL1 expression by displacing inactive PARP-1 binding to the CXCL1 promoter, favoring binding of p65 to the promoter. Ambrose et al.²⁰ identified a PARP-1 binding site and described the induction of B-cell lymphoma 6 (BCL6) transcription following PARP inhibition with 3-aminobenzamide (3-AB) and 8-hydroxy-2-methylquinazoline-4-one (NU1025). However, the exact mechanism by which PARP-1 develops its enhancer binding to gene promoters remains unclear.

3. PARP-1 and Splicing

Besides the transcriptional level, the regulation of gene expression is also finely modulated at the posttranscriptional level. The synthesis of a particular RNA transcript does not guarantee that it will generate a functional protein in the cell. Pre-mRNA has to be converted into mRNA by alternative splicing and polyadenylation, translocated from the nucleus to the cytoplasm, translated by the protein-synthesizing apparatus, and degraded by the RNA decay machinery. All these steps to process RNA are tightly controlled by RNA-binding proteins (RBPs). RBPs are associated with pre-mRNA/mRNA for the lifespan of an individual RNA. RBPs can be modified at the posttranslational level by phosphorylation, ubiquitination, and PARylation^{21,22} to get specific temporal and spatial posttranscriptional regulation of gene expression. There are two kinds of proteins that can be PARylated in order to decrease their ability to bind to RNA: hnRNPs (which join to exonic and intronic splicing silencers) and Serine-Arginine-rich splicing factor SR (which joins to exonic and intronic splicing enhancers).²³ Globally, PARylation of the RBPs (including hnRNPs, SR proteins, poly(A) polymerase, and Argonaut proteins) prevents their RNA-binding ability, with implications in RBP-dependent pathways, such as splicing, polyadenylation, maturation of miRNA, and translation (reviewed by Ji et al. 2013²⁴). More recently, PARylation has also been involved in RNA metabolic processes after genotoxic stress: the transcription and splicing factors TAF15 and THRAP3, respectively,

were modified by PARylation, known to be PAR localized to specific substructures in the nucleus.⁶

4. *PARP-1 Transcriptional Coregulator Role*

PARP-1 function as a transcriptional coregulator (either coactivator or corepressor) has been well documented for different transcription factors, such as NF- κ B, HIF, or NFAT. NF- κ B is a transcription factor implicated in the regulation of the expression of genes associated to the inflammatory and stress response. Furthermore, most of these genes have been implicated in the acquisition of malignant phenotype. PARP-1 can act both as inhibitor and activator of NF- κ B-dependent transcription.^{25,26} PARP-1 interaction with NF- κ B inhibits the binding of NF- κ B to its elements (Fig. 2A and B), and this inhibition is relieved by the auto-PARylation of PARP-1. Hypoxia inducible factors (HIFs) regulate an extensive transcription program that modulates the induction of genes involved in angiogenesis, metabolic adaptation to hypoxia, cell growth, metastasis, antiapoptosis, and others.^{27,28} However, the relationship between PARP and HIF will be further analyzed below. NFAT, the master regulator of IL-2 gene transcription, binds to and is modified by PARP-1.²⁹ p53, as transcription factor, is greatly associated with the maintenance of genome integrity, and its deficiency has been widely associated with the appearance of genome instability.³⁰ A link between PARP-1 and p53 has been well reported. In 1996, Wesierska-Gadek et al.⁹ reported PARylation of p53. Since then, subsequent publications showed an interaction of PARP-1 protein and p53 protein in vitro and in vivo.³¹ Double knockout mice for p53 and PARP-1 displayed surprisingly increased life expectancy with respect to single p53 null mice that was attributed to a diminished proinflammatory microenvironment in the absence of PARP-1.³² More recently, a key aspect of the interaction between PARP(s) and p53 has been uncovered, assigning a role to PARylation of the nuclear export protein Crm1 to the p53 nuclear retention.³³

C. *PARP-1 and Genome Instability*

PARP-1 and PARylation are involved in the maintenance of chromosome stability, when DNA is damaged by exogenous agents as well as during cell division. In accordance with the above, inhibition of PAR synthesis gives rise to enhanced incidence of DNA strand lesions, leading to gene amplification, recombination, micronuclei formation, and sister chromatid exchanges (SCEs), hallmarks of genomic instability.

1. *Genomic Instability in PARP-1^{-/-} Mice*

There is a large agreement in the fact that PARP-1^{-/-} mice develop genomic instability, in comparison to wild-type mice.³⁴⁻³⁶ The different knockout mice display elevated genomic instability, leading to the consensus that PARP-1 is a key survival factor for recovery from DNA damage, and this recovery is compromised in PARP-1^{-/-} mice. Simbulan-Rosenthal and co-workers³⁷ advanced further in this result, showing an unbalanced chromosomal gains and losses affecting regions of chromosomes 4, 5, and 14 in cells from PARP-1^{-/-} mice, which taken together are all markers of genomic instability. However, the relationship between PARP-1^{-/-} and telomere length is still discussed. d'Adda di Fagagna et al.³⁸ described that perturbation of PARP activity affects telomere length in mouse. In fact, Mouse Embryonic Fibroblasts PARP-1^{-/-} showed shortened telomere length in comparison with wild-type MEFs. Other study³⁹ described that PARP deficiency did not affect telomere length or telomere capping, although they all observed higher levels of chromosomal instability following PARP ablation.

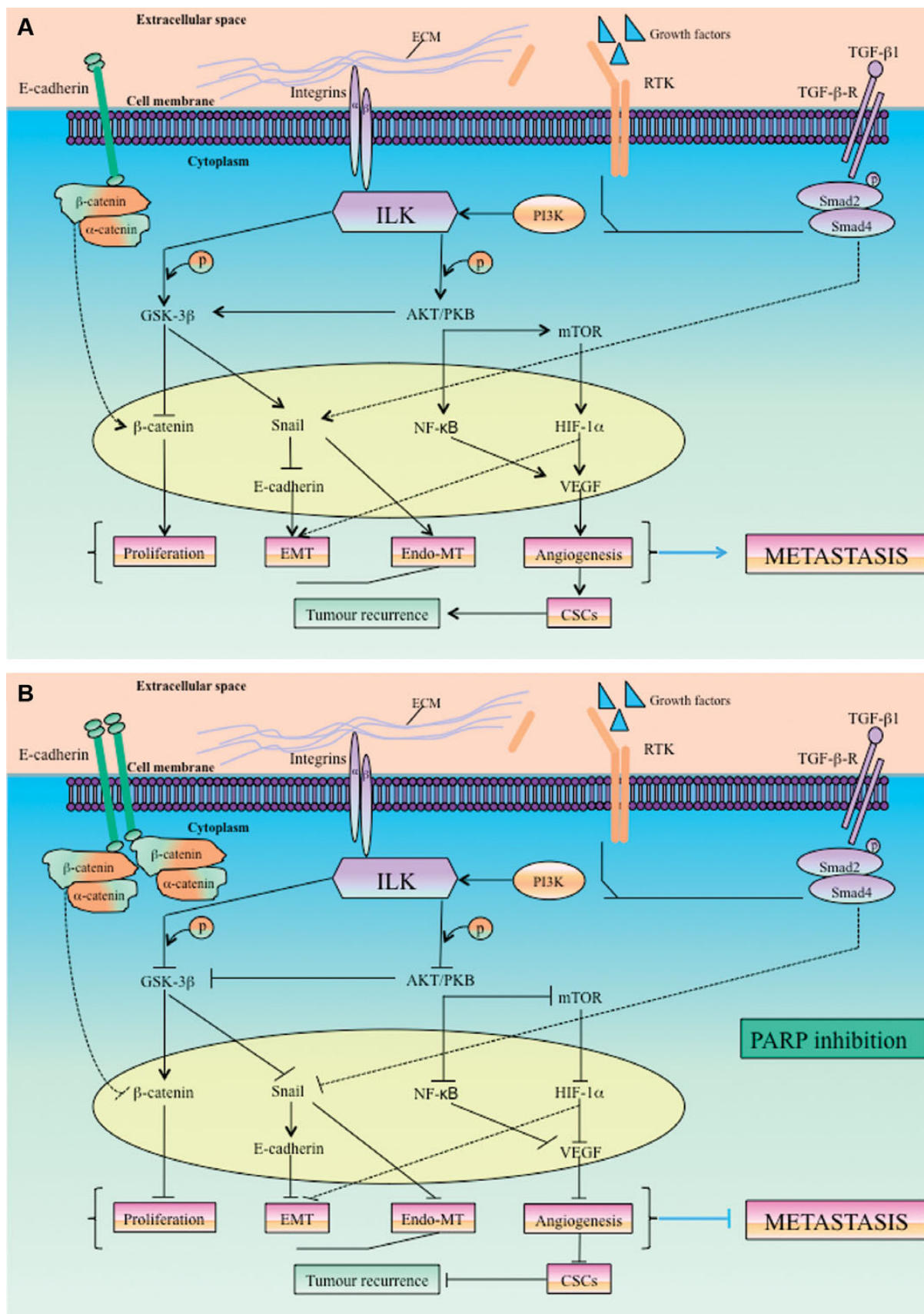


Figure 2. PARP role on tumor promoting pathways. (A) Effect of β -catenin, ILK, and TGF- β pathways on tumor proliferation, EMT, Endo-MT, and angiogenesis. (B) Tumor promotion is clearly restrained in the context of PARP inhibition. This figure is described in the text to discuss each subtopic.

2. *PARP-1 and Genomic Instability in Patients*

In addition to genomic stability defects observed in mice and cell lines following PARP ablation, Bieche et al.⁴⁰ reported genetic instability in primary breast carcinomas carrying dysregulated PARP expression. Thus, low levels of PARP gene expression were associated with loss of heterozygosity (LOH) amplification at a number of different chromosome loci.

3. *Genome Instability Consequences*

Genome integrity is necessary for the maintenance of cell and organism homeostasis. As a consequence, if PARP defects result in genome instability, it will seriously affect the organism. Genome instability is for long well documented to be a marker of tumor development.³⁸ Since PARP inhibition generates chromosomal instability, a hallmark of tumor development, it might seem contradictory with the current use of PARP inhibitors in cancer treatment.¹ However, this apparent contradiction is overcome if we take into account the following facts: first, it is possible to take advantage of it in order to kill the tumor where a large amount of genome instability, which in our case may be generated by PARP inhibition, can drive to cell death through mechanisms including mitotic catastrophe.⁴¹ Second, there are other mechanisms apart from genome instability generated by PARP inhibition that may be used to overcome tumor development as we will analyze later.

D. *PARP and Antitumoral Therapy*

Over the last two decades, antitumoral effects of PARP inhibition have been well documented. However, it should be remembered that this effect can be explained at least through two different mechanisms. Since PARP is involved in single-⁴² and double-strand DNA repair, PARP inhibitors prevent the repair of DNA damage, potentiating the effect of chemo- and radiotherapy.⁴² This chemo-potential is observed using the PARP inhibitor Rucaparib (formally called AG-014699 or PF-0136738) with temozolomide (TMZ) in phase II in patients with metastatic melanoma.⁴³ Also, the addition of Iniparib (BSI-201) to chemotherapy has demonstrated effectiveness in patients with metastatic triple-negative breast cancer.⁴⁴ Moreover, PARP inhibitors Olaparib (AZD2281) also improve progression-free survival among patients with platinum-sensitive ovarian cancer.^{45,46}

The second approach is focused on the use of PARP inhibitors as monotherapy that is explained through “synthetic lethality” operating between two genes, and defined as follows: loss of one cell function is compatible with cell life, but the simultaneous loss of both functions drives to cell death. Although the exact molecular mechanism by which synthetic lethality takes place remains unclear, PARP’s role in DNA repair is a key event to explain this phenomenon, since it mainly operates in homologous recombination BRCA2-deficient breast cancer.⁴⁷ The first attempt⁴⁷ to explain synthetic lethality focused on PARP role in base excision repair: single-strand breaks (SSBs) are usually repaired by the base excision repair pathway. PARP inhibition would drive the inhibition of this pathway, then increasing the number of unrepaired SSBs. Thus, SSBs would subsequently lead to DSBs accumulation at replication forks. Since BRCA2-deficient cells have compromised DSBs repair, the accumulation of DSBs at the replication fork would force to cell death. Nevertheless, other mechanisms have been proposed to explain synthetic lethality in BRCA-deficient tumors over the years.^{48,49}

Either way, although further research is still required to elucidate the molecular mechanism behind synthetic lethality, PARP inhibition therapy has emerged as a promising therapy to efficiently target BRCA-deficient tumors. Currently, Olaparib (phase I) therapy is proposed as a promising strategy against BRCA-deficient breast cancer. In addition, new targets have emerged in the last years in order to achieve synthetic lethality when combined with PARP inhibition.

PTEN (phosphatase and tensin homolog) mutations have been related with a wide range of human tumors. Furthermore, this protein has recently been associated with homologous recombination repair⁵⁰ through its ability to modulate Rad51 expression that makes PTEN-null tumors compromised in homologous recombination repair and consequently sensitive to PARP inhibition.^{51,52} The epidermal growth factor receptor (EGFR) is overexpressed and associated with aggressive phenotype in triple-negative breast cancer.⁵³ Recent publications have shown contextual synthetic lethality between combined targeting of EGFR and PARP.^{54,55}

Finally, PARP inhibition per se may compromise homologous recombination repair⁵⁶ through downregulation of BRCA1 and Rad51 expression. Due to the importance of this pathway on tumor development, new approaches in the use of PARP inhibitors will probably arise in the next few years, without the requirement of more aggressive therapies involving chemo- and radiotherapy. We will now focus on the role of PARP-1 in the regulation of key determinants of tumor progression and invasiveness.

2. *PARP-1 AND HYPOXIC RESPONSE*

Hypoxia is a common and critical event during tumor development. When avascular solid tumors reach a size of 1–2 mm³, adaptation to hypoxia is required for a larger mass formation and tumor promotion.⁵⁷ In consequence, uncontrolled cell growth causes low oxygen concentration in the central part of the tumor, as was described very early.⁵⁸

In hypoxic conditions, cells produce angiogenic cytokines, such as Vascular Endothelial Growth Factor, promoting tissue vascularization and tumor expansion (Fig. 2A and B). This response to hypoxia correlates with an increase in tumor cell migration, invasiveness, and metastatic capacity.⁵⁹ Moreover, the efficacy of irradiation is also reduced during hypoxia due to the reduced formation of O₂-free radicals.⁶⁰ All these adaptive effects are associated with poor prognosis.⁶¹

The response to hypoxia is mediated by a family of transcription factors called the hypoxia-inducible factors (HIFs), HIF-1 α and HIF-2 α being the best characterized members. These members are differently expressed in tissues and their target genes are similar, but not identical.⁶² This family of transcription factors is active as heterodimers, as it is composed by two constitutively expressed subunits, HIF- α and HIF- β . The HIF- α subunit is degraded during normoxia due to the hydroxylation of specific proline residues by the family of the prolyl hydroxylase domain containing proteins (PHDs) that are only active in O₂ presence. This hydroxylation allows the von Hippel-Lindau factors (pVHL) to ubiquitin the HIF- α subunit toward its degradation via proteasome.⁶³

A. *PARP-1 Interaction with HIF-1 α*

A reduction in HIF-1 α protein and mRNA expression has been described during hypoxia in skin carcinogenesis of PARP-1^{-/-} or in PARP-1^{+/+} mice after treatment with PARP inhibitor, revealing that both protein and enzymatic activity of PARP-1 are necessary for this interplay⁶⁴ (Fig. 2A and B). In the same way, HIF-1 α accumulation during hypoxia is impaired after PARP downregulation in brains of parental mice.⁶⁵

Although a number of studies proved that expression and activity of PARP-1 is necessary for HIF-1 α accumulation, exceptions have also been described. K562 (human immortalized myelogenous leukemia) and MLFs (mouse lung fibroblasts) cells treated with the hypoxic mimetic ciclopirox olamine showed HIF-1 α induction independent of PARP-1 knockdown.⁶⁶ These particular results might be due to a specific response to the hypoxic mimetic ciclopirox olamine or to specific cell model response.

Although different mechanisms could be responsible for the interaction between PARP-1 and HIF- α , the underlying explanation with experimental evidences shows that HIF- α and PARP-1 form a complex that increases during hypoxia; and PARylation of HIF optimizes HIF-dependent transcriptional activation.⁶⁶ Other mechanisms might be acting in parallel, including PARP-1 activation that induces an increase in oxidative/nitrosative status in cells during hypoxia⁶⁷ that has been associated with the augmentation of HIF-1 α stability.⁶⁸ PARP-1 downregulation decreased Reactive Oxygen Species and inducible Nitric Oxide Synthase levels during the treatment with the hypoxic mimetic desferrioxamine. Indeed, this reduction in oxidative and nitrosative stress inhibited HIF-1 α accumulation as well as its transcriptional activity.⁶⁵

Therapeutically, this functional interaction between PARP and HIF signaling has been shown to have specific consequences: under acute hypoxia, the PARP inhibitor ABT-888 radiosensitized prostate cancer and lung cancer cells to a level similar to normoxic radiosensitivity showing that PARP inhibitors can sensitize hypoxic cancer cells and increase the therapeutic ratio of radiotherapy.⁶⁹

B. PARP-1 Interaction with HIF-2 α

The effect of PARP-1 on the hypoxic response is a consequence of an interaction not only with HIF-1 α , but also with HIF-2 α , which has a similar but not identical expression and activity.⁶² As reported for HIF-1 α , PARP-1^{-/-} MEFs (as well as PARP inhibition or PARP inhibitor in HEK293T and COS cells, respectively) had impaired HIF-2 α induction during hypoxia.²⁸ Interestingly, in human renal carcinoma-derived cells RCC4 (deficient in pVHL) no differences were shown in HIF-2 α accumulation after treatment with PJ-34 ([N,(6-Oxo-5,6-dihydro-phenanthridin-2-yl)N,N-dimethylacetamide]), a PARP inhibitor, while reintroduction of pVHL restored PARP inhibitor PJ-34 capability to reduced HIF-2 α levels in hypoxia, indicating that PARP-1 is affecting HIF-2 α stability in a manner dependent on pVHL. In addition, PARP-1 binds to the HIF-2 α promoter in vivo and in vitro, regulating the levels of HIF-2 α protein at the transcriptional level. This interaction is not shown for HIF-1 α promoter.²⁸

C. PARP-1 and HIF-1 α Activity

The expression of HIF-1 α target genes, such as IGFBP3, BNIP3, and VEGF-A, after activation with hypoxia mimetic is also downregulated by PARP inhibitor DPQ (3,4-dihydro-5-[4-(1-piperidinyl)butoxy]-1(2H)-isoquinolinone).⁶⁴ HIF-1 α transcriptional activation in brains of PARP^{+/+} and PARP^{-/-} mice exposed to hypoxia showed an altered induction of the genes adrenomedullin (AM) and erythropoietin (EPO) in the absence of PARP-1, while an increased induction of the genes AM, EPO, GLUT-1, and VEGF was observed in PARP^{-/-} mice after 2 hr of reoxygenation.⁶⁵

D. PARP-1 and HIF-2 α Activity

HIF-2 α is a potential cancer target, and it is known that in hemangioblastomas (tumor of the central nervous system characterized by the absence of pVHL), HIF-2 α accumulation caused a high degree of vascularization of the tumor and helped in determining neuroblastoma aggressiveness.⁷⁰ High expression levels of HIF-1 α in non tumoral cells was changed to a predominant HIF-2 α expression during tumor development.⁷¹ We have demonstrated that in vivo experiments using PARP-1^{-/-} mice exposed to hypoxia showed a reduction in the number of red blood cells and the hemoglobin concentration.²⁸

PARP-1 can affect the hypoxic response not only by regulating the stability and accumulation of HIF-1 α and HIF-2 α , but also by modulating the activity of HIF coactivators. p300 is a central coactivator that binds HIF(s) and whose recruitment is necessary to form an active HIF α / β complex.⁶² PARP-1 and p300 form a complex that acetylates PARP-1 and enhances p300 transcriptional activity,⁷² providing another mechanistic explanation by which PARP-1 ablation reduces HIF-1 α transcriptional activity.

3. EPITHELIAL–MESENCHYMAL TRANSITION (EMT) PATHWAY

EMT is a fundamental event in morphogenesis and transforms epithelial cells into itinerant and invasive cells.⁷³ EMT in cancer is not usually a complete transition, but rather a transient and reversible process. This mesenchymal–epithelial transition (MET) process is necessary for organs configuration in the final destinations of embryonic migratory cells. Likewise, in tumors, MET is required for the founding of metastasis at distant sites.⁷³ EMT also entails the downregulation of epithelial specific *genes*, such as components of tight and gap junctions, desmosomes, cytokeratins, etc.⁷³ On the contrary, there is an induction of mesenchymal markers (e.g., N-cadherin, cadherin-11), reorganization of the cytoskeleton (e.g., switch from cytokeratins to vimentin), and the synthesis of extracellular matrix components and metalloproteases.⁷³

Cadherin mediates homotypic intercellular adhesion and interacts with intracellular proteins to establish and coordinate the morphology, polarity, and function of epithelial cells.⁷⁴ E-cadherin, a type-1 cadherin, is usually considered the prototype of all cadherins because of its early identification and its thorough characterization, both in normal and in pathological conditions.⁷⁴ E-cadherin expression is inhibited by a number of transcription factors, only a small set are known to regulate it directly. The main groups of transcription factors that bind to the E-cadherin promoter and directly repress its transcription, which will be referred to hereafter as EMT-activating transcription factors, are the Zinc finger E-box Binding homeobox and Snail (Snail1, Snail2, and Snail3) families of zinc finger proteins and the Twist family of bHLH factors (Twist1, Twist2)⁷⁵ (Fig. 2A and B). Snail1 interacts with lysyl-oxidase-like 2 and 3 (LOXL2 and LOXL3), two members of the lysyl-oxidase gene family, and prevents glycogen synthase kinase3 β (GSK3 β) induced degradation,⁷⁶ which is, however, phosphorylated by protein kinase CK1 ϵ .⁷⁷ Snail1 is also targeted for degradation in a GSK3 β -independent manner by binding to the F-box E3 ubiquitin ligase (FBXL14).⁷⁸

TGF- β is another master regulator of EMT that can promote dedifferentiation of epithelial cells to transform into malignant mesenchymal cells. Canonical Smad-dependent⁷⁹ and non-canonical Smad-independent mechanisms induce TGF- β -mediated EMT (Fig. 2A and B). Thus, Smad complexes bind to Snail1 promoter and induce Snail1 expression.

A. EMT and Cancer Stem Cells

Cancer stem like cells (CSCs) have been proposed as the driving force of tumorigenesis and the seed of metastases. Hierarchical model of cancer postulates the existence of a subgroup of cancer cells, the CSCs, that have self-renewing and differentiation capacity into all cell types of the original heterogeneous tumor, thus resembling the function of normal epithelial stem cells. Brabletz and colleagues proposed a subdivision of two types of CSCs, the stationary CSCs and the migrating CSCs (MCSC;⁸⁰), where the stationary CSCs possess all stem cell characteristics (asymmetric proliferation and drug resistance) but are unable to migrate. To propagate and metastasize, cancer cells have to activate the EMT program, therefore switching toward an MCSC phenotype.

Aggressiveness of metastatic disease is associated with an increase in EMT markers and could be explained by increased cell migration of the CSCs and increased intrinsic resistance to standard therapies (Fig. 2A and B). Mani et al. revealed that the imposed expression of Snail1 and Twist or TGF- β treatment gave rise to cells with CSC characteristic.⁸¹ Moreover, the maintenance of various somatic stem-cell populations⁸² is crucial to the activation of the Wnt/ β -catenin signaling pathway.

B. Regulation by PARP-1 of EMT

We have described above how the acquisition of CSC phenotype is related with EMT and how these CSCs with a mesenchymal phenotype are the first aspirants for suffering metastatic spread.⁸³ Preventing this route might at least limit the metastatic process (Fig. 2A and B). In our laboratory, we have shown that Snail1 is in complex with PARP-1 and is covalently modified by PARylation; the stability of this complex is blunted by PARP inhibitors PJ-34 and Ku0058948.⁸⁴ A recent publication showed that PARP-1 interacts with and PARylates Smad3 and Smad4. Smad complexes can be dissociated from DNA by PARylation that regulates Smad-mediated transcription.⁸⁵

Other key regulators of EMT have been reported to be fine-tuned by PARP-1 or PARylation. This is the case for integrin-linked kinase (ILK). ILK-dependent transactivation of Snail1 transcription required PARP-1 binding to ILK promoter.⁸⁶ Furthermore, the interaction between PARP-1 and Snail1 was also regulated through ILK by the modulation of a different pathway involving the axis ILK/GSK3 β in human melanoma cells^{84,87} (Fig. 2A and B). During the progression to metastasis, PARP inhibition with PJ-34, DPQ, KU0058948, and Olaparib has shown to counteract EMT phenotype both in melanoma cells in vitro⁸⁴ and in a mouse model of melanoma metastasis to lung in vivo.⁸⁷

Globally, these results show a new regulatory mechanism of Snail1 by PARP-1. PAR induces posttranslational modification of Snail1 and has effects on Snail1 stabilization. Furthermore, we have shown an augment in complex formation between Snail1 and PARP-1 following activation with TGF- β or DNA damage, suggesting a close functional interaction between both Snail1 and PARP-1 signaling pathways.

In conclusion, these data strengthen PARP-1 and PARP activity as key modulators of Snail1 function and EMT and imply new opportunities in the use of PARP inhibitors as a potential therapeutic target to hamper cancer cell invasion and metastasis.

4. PARP IN ANGIOGENESIS

PARP inhibitors have been used to obstruct VEGF-induced migration, proliferation, and in vitro formation of tube structures in human umbilical vein endothelial cells (HUVECs) and in tumor models.^{88,89} To study the role of PARP-1 in metastatic melanoma, Tentori et al. silenced PARP-1 in melanoma cells and they reported an important reduction in tumor-associated angiogenesis compared to the wild-type melanoma cells.⁹⁰ Similarly, radiation treatment combined with PARP-1 and PARP-2 inhibitor Veliparib (ABT-888) reduced to 50% von Willebrand factor levels in the tumor when compared to X-ray treatment alone.⁹¹

The mechanisms responsible for the effect of PARP on angiogenesis are uncertain. We have reported, using a model of skin carcinogenesis, that the treatment of mice skin with the PARP inhibitor DPQ reduced by 80% the amount of tumoral lectin positive blood vessel when compared with the untreated ones.⁶⁴ Moreover, we have shown that PARP activity modulated the expression of *genes* involved in angiogenesis, and in particular the HIF (as we referred previously) whose action was decreased both in PARP-1^{-/-} mice or inhibiting PARP during

tumor promotion. The details on the connection between HIF- α and PARP-1 have been described above.

The major conclusion arising from this diverse bibliography is the prerequisite of the PARP pathway integrity for having a correct angiogenic development, making PARP an interesting aim to reduce angiogenesis during cancer and other illnesses induced by angiogenic dysfunction. However, the antiangiogenic properties of PARP inhibitors are at this moment unclear. The activity of VEGF has been proven to be downregulated by poly(ADP-ribose), indicating that the polymer activity (but not PARP inhibition) has antiangiogenic properties.⁹² IGF-1, known as an angiogenesis promoter, downregulated PARP activity by phosphorylation contributing to augment the *gene* expression of VEGF.⁹³ This disagreement in the antiangiogenic properties of PARP inhibition can be explained by the pleiotropic effects of the PARP-1 (as protein) that can alter either positively and negatively a number of transcription factors by covalent addition of PAR or by a direct interaction with them.

In a recent work, we interrupted PARP activity in HUVECs, trying to clarify the mechanism by which PARP-1 affects endothelial cell dynamics by performing a proteomic analysis. The significant role of vimentin in the biology of endothelial cells urged us to focus our study on this protein that is the major structural protein on the intermediary filaments. It has been confirmed that due to its specific upregulation in tumoral vasculature, vimentin is a potential target against tumors.⁸⁷ Endothelial to mesenchymal transition (EndoMT) is a process by which the endothelial cells disaggregate, change its shape, and migrate to nearby tissues. This process is characterized by the reduction on endothelial cell markers, such as vascular endothelial VE-cadherin, and the upregulation of mesenchymal cell markers, such as vimentin and Snail1.⁸⁷ Mesenchymal characteristics such as cell migration are robustly reduced using PARP inhibitors, suggesting that PARP inhibition prevents the acquisition of mesenchymal phenotypes by endothelial cells.

One of the most important characteristics of highly aggressive melanoma cells is the creation of tubular structure networks when they are placed in three-dimensional culture. In this model, VE-cadherin repression prevented the formation of this vasculogenic-like network,⁹⁴ suggesting a key role of tumor-associated VE-cadherin expression in the formation of these structures.

Vimentin and keratins are well known as proteins implicated in trafficking and signaling,⁹⁵ thus modulating cellular processes such as polarization and cell adhesion. Vimentin is highly expressed in mesenchymal cells, playing a role in angiogenesis, wound healing, and tumor growth. Consistently, it has been referred as a tumor-specific angiogenesis marker. In fact, targeting vimentin significantly decreased microvessel density and tumor growth in a mouse model.⁹⁶ Vimentin is known to function in EMT and EndoMT, and it is overexpressed in tumor samples when compared to normal tissues. Vimentin expression is modulated by β -catenin/Transcription factors T-Cell Factors (TCF) that enhances the invasiveness of the tumor cell.⁹⁷ NF- κ B, a regulator of inflammatory and immune processes, has also been described to impact EMT. NF- κ B downregulation drives the reversal of EMT, involving this protein in the activation and maintenance of the process.⁹⁸ EMT process is accompanied by vimentin overexpression as well as NF- κ B binding to vimentin promoter. Therefore, it would be tempting to suggest that vimentin overexpression could be due to NF- κ B activation in tumor cells. Furthermore, TGF- β response element is located in the activated protein complex-1 region of the vimentin promoter, affecting the regulation of vimentin expression in myoblasts and myotubes.⁹⁹ Interestingly, as referred above, PARP-1-mediated PARylation of Smad proteins is involved in the control of the strength and persistence of Smad-mediated transcription.⁸⁵ Other transcription factors might also be implicated in PARP regulation of vimentin levels, such as Snail1 and HIF-1/2. Pharmacologic inhibition of PARP reverted this transition, correlating with a reduction in the number and size of metastatic melanoma foci in a mouse model.⁸⁷ Recent studies indicate an important role for PARP-1 in promoting ERK signaling. PARP-1

Table 1. Targets of PARP-1 in the Context of Hypoxia, Angiogenesis and EMT

| | Target of PARP-1 | Consequences | References |
|------------------------------|---|--|---|
| Role in hypoxia/angiogenesis | HIF-1 α | The absence or inhibition of PARP-1 reduces HIF-1 α mRNA and protein during carcinogenesis and in mice brains PARP-1 downregulation decreases nitrosative stress, leading to the inhibition of HIF-1 α accumulation and activation on mice brains | Martin-Oliva et al. ⁶⁴ Martinez-Romero et al. ⁶⁵ |
| | HIF-2 α | The absence or inhibition of PARP-1 reduces HIF-2 α accumulation in a manner dependent of pVHL In addition, PARP-1 regulates HIF-2 α transcription by binding the HIF-2 α promoter | Gonzalez-Flores et al. Oncogene ²⁸ |
| Role in EMT | p300 | PARP-1 binds p300 enhancing the HIF transcriptional activity | Hassa et al. ⁷² |
| | IGFBP3 | The inhibition of PARP-1 reduces its hypoxic-dependent induction | Martin-Oliva et al. ⁶⁴ |
| | BNIP3 | The inhibition of PARP-1 reduces its expression during hypoxia | Martin-Oliva et al. ⁶⁴ |
| | Adrenomedullin | The inhibition of PARP-1 reduces its expression | Martinez-Romero et al. ⁶⁵ |
| | EPO | The downregulation of PARP-1 reduces its expression | Martinez-Romero et al. ⁶⁵ |
| | VEGF | The inhibition of PARP-1 reduces its expression during hypoxia | Martin-Oliva et al. ⁶⁴ |
| | ILK, Snail1, E-cadherin | ILK-dependent transactivation of Snail1 transcription requires PARP-1 binding to ILK promoter in epithelial cells and results in loss of E-cadherin expression and initiation of EMT | MCPhee et al. ⁸⁶ |
| | Smad | PARYlation causes dissociation of Smad complexes from DNA PARP-1 silencing affects the initiation phase of EMT when mesenchymal markers start to appear and cells begin to elongate | Lonn et al. ⁸⁵ |
| | Snail1 | PARP-1 PARYlates Snail1 in vivo and in vitro with functional consequences in the EMT-associated phenotype in metastatic melanoma | Rodriguez et al. ⁸⁴ |
| | Snail1, E-cadherin, VE-cadherin, vimentin, AXL, ILK, GSK-3 β , β -catenin | PARP inhibition decreases abnormal tumor angiogenesis, prevents EMT acquisition, and limits VM in melanoma cells | Rodriguez et al. ⁸⁷ |

PARP-1 and PARYlation are capable to modulate different targets involved in tumor progression. PARP-1 targets and the consequences of its modulation are briefly described below.

is activated and PARylated by direct interaction with phosphoERK2 (pERK2), leading to pERK2-catalyzed phosphorylation mediated by pERK2 of target transcription factors and increased gene expression, including *genes* involved in angiogenesis.¹⁰⁰

Maniotis et al.¹⁰¹ described vasculogenic mimicry (VM) as a mechanism by which microvascular circulation is driven from tumor cells themselves without the involvement of endothelial cells. Different evidence suggest that this matrix-inserted, blood-perfused microvasculature plays a key role in tumor biology, independently of endothelial cell angiogenesis. VM is a process where tumor cells express *genes* previously described as exclusively associated with endothelial cells, among which VE-cadherin has a determining role.⁹⁴ Oxygen depletion conditions (hypoxia) stabilize HIF-1 α and HIF-2 α transcription factors. HIF-mediated regulation during hypoxia is crucial, since it transcriptionally regulates *genes* involved in tumor cell adaptation to the stress of oxygen deprivation. As a consequence, high expression of HIF target *genes* is correlated with increased malignancy.

VE-cadherin expression is not regulated by hypoxia. However, HIF-2 α , but not HIF-1 α , binds VE-cadherin hypoxia responsive elements (HRE) in normoxic conditions, activating VE-cadherin promoter.¹⁰² HIF-2 α expression is related with developing endothelium, appropriated vascular development, and augmented tumor malignancy,¹⁰³ suggesting that HIF-2 α is involved in the induction of tumor cell plasticity.

In addition, in vivo evidence of metastasis reduction following PARP inhibition was presented using a mouse model of metastatic melanoma. We showed a reduction in tumor microvessel density accompanied by changes in the expression pattern of EMT markers inside the tumor (Snail1, vimentin, and E-cadherin).⁸⁷

5. CONCLUSIONS

The significant role of the tumor microenvironment in progression of solid cancers is being increasingly recognized. The adaptations to ensure cell survival in the hostile hypoxic microenvironment and under shortening of nutrients of solid tumors allow the development of more aggressive and invasive cancer cell populations. This knowledge is also opening up new therapeutic frontiers for treating metastasis. Hypoxia, EMT, and angiogenesis are key events in tumor progression. PARP-1 has a crucial role in the development of this processes (Table I). A new generation of PARP inhibitors will come very soon and there is urgent need of selective inhibitors for research into PARP functions and its therapeutic benefits. These efforts need to be combined with development of biomarkers to assess the sensitivity and/or resistance of cancer cells to PARP inhibitors. Although the clinical results have proven that synthetic lethality is a viable anticancer strategy, additional research is required to enlarge the clinical use of PARP inhibitors through the in-depth knowledge of the modulation by PARP(s)/PARylation of cancer-related cells transformation using proteomic approaches as well as the better understanding of the pharmacology of PARP inhibitors and to improve outcomes of biological and/or clinical studies.

ACKNOWLEDGMENTS

J.M.M. has been funded by a predoctoral fellowship by the FPU program, Spanish Ministry of Economy and Competitiveness. This work was supported by Junta de Andalucía, project of Excellence P10-CTS-0662, Spanish Ministry of Economy and Competitiveness SAF2009–13281-C02–01, SAF2012–40011-C02–01, and Red Temática de Investigación Cooperativa en Cáncer (RTICC: RD06/0020/0068 and RD12/0036/0026).

REFERENCES

1. Peralta-Leal A, Rodriguez-Vargas JM, Aguilar-Quesada R, Rodriguez MI, Linares JL, de Almodovar MR, Oliver FJ. PARP inhibitors: New partners in the therapy of cancer and inflammatory diseases. *Free Radic Biol Med* 2009;47(1):13–26.
2. Gibson BA, Kraus WL. New insights into the molecular and cellular functions of poly(ADP-ribose) and PARPs. *Nat Rev Mol Cell Biol* 2012;13(7):411–424.
3. Rosenthal F, Hottiger MO. Identification of ADP-ribosylated peptides and ADP-ribose acceptor sites. *Front Biosci (Landmark Ed)* 2014;19:1041–1056.
4. Pic E, Gagne JP, Poirier GG. Mass spectrometry-based functional proteomics of poly(ADP-ribose) polymerase-1. *Expert Rev Proteomics* 2011;8(6):759–774.
5. Gagne JP, Isabelle M, Lo KS, Bourassa S, Hendzel MJ, Dawson VL, Dawson TM, Poirier GG. Proteome-wide identification of poly(ADP-ribose) binding proteins and poly(ADP-ribose)-associated protein complexes. *Nucleic Acids Res* 2008;36(22):6959–6976.
6. Jungmichel S, Rosenthal F, Altmeyer M, Lukas J, Hottiger MO, Nielsen ML. Proteome-wide identification of poly(ADP-Ribosylation) targets in different genotoxic stress responses. *Mol Cell* 2013;52(2):272–285.
7. Gagne JP, Pic E, Isabelle M, Krietsch J, Ethier C, Paquet E, Kelly I, Boutin M, Moon KM, Foster LJ, Poirier GG. Quantitative proteomics profiling of the poly(ADP-ribose)-related response to genotoxic stress. *Nucleic Acids Res* 2012;40(16):7788–7805.
8. Pleschke JM, Kleczkowska HE, Strohm M, Althaus FR. Poly(ADP-ribose) binds to specific domains in DNA damage checkpoint proteins. *J Biol Chem* 2000;275(52):40974–40980.
9. Wesierska-Gadek J, Schmid G, Cerni C. ADP-ribosylation of wild-type p53 in vitro: Binding of p53 protein to specific p53 consensus sequence prevents its modification. *Biochem Biophys Res Commun* 1996;224(1):96–102.
10. Khoury-Haddad H, Guttmann-Raviv N, Ipenberg I, Huggins D, Jeyasekharan AD, Ayoub N. PARP1-dependent recruitment of KDM4D histone demethylase to DNA damage sites promotes double-strand break repair. *Proc Natl Acad Sci USA* 2014;111(7):E728–E737.
11. Levaot N, Voytyuk O, Dimitriou I, Sircoulomb F, Chandrakumar A, Deckert M, Krzyzanowski PM, Scotter A, Gu S, Janmohamed S, Cong F, Simonic PD, Ueki Y, La Rose J, Rottapel R. Loss of tankyrase-mediated destruction of 3BP2 is the underlying pathogenic mechanism of cherubism. *Cell* 2011;147(6):1324–1339.
12. Kraus WL, Lis JT. PARP goes transcription. *Cell* 2003;113(6):677–683.
13. Poirier GG, de Murcia G, Jongstra-Bilen J, Niedergang C, Mandel P. Poly(ADP-ribosylation) of polynucleosomes causes relaxation of chromatin structure. *Proc Natl Acad Sci USA* 1982;79(11):3423–3427.
14. Tulin A, Spradling A. Chromatin loosening by poly(ADP)-ribose polymerase (PARP) at *Drosophila* puff loci. *Science* 2003;299(5606):560–562.
15. Kim MY, Mauro S, Gevry N, Lis JT, Kraus WL. NAD⁺-dependent modulation of chromatin structure and transcription by nucleosome binding properties of PARP-1. *Cell* 2004;119(6):803–814.
16. Krishnakumar R, Gamble MJ, Frizzell KM, Berrocal JG, Kininis M, Kraus WL. Reciprocal binding of PARP-1 and histone H1 at promoters specifies transcriptional outcomes. *Science* 2008;319(5864):819–821.
17. Sala A, La Rocca G, Burgio G, Kotova E, Di Gesu D, Collesano M, Ingrassia AM, Tulin AV, Corona DF. The nucleosome-remodeling ATPase ISWI is regulated by poly-ADP-ribosylation. *PLoS Biol* 2008;6(10):e252.
18. Gottschalk AJ, Timinszky G, Kong SE, Jin J, Cai Y, Swanson SK, Washburn MP, Florens L, Ladurner AG, Conaway JW, Conaway RC. Poly(ADP-ribosylation) directs recruitment and activation of an ATP-dependent chromatin remodeler. *Proc Natl Acad Sci USA* 2009;106(33):13770–13774.

19. Amiri KI, Ha HC, Smulson ME, Richmond A. Differential regulation of CXC ligand 1 transcription in melanoma cell lines by poly(ADP-ribose) polymerase-1. *Oncogene* 2006;25(59):7714–7722.
20. Ambrose HE, Papadopoulou V, Beswick RW, Wagner SD. Poly-(ADP-ribose) polymerase-1 (Parp-1) binds in a sequence-specific manner at the Bcl-6 locus and contributes to the regulation of Bcl-6 transcription. *Oncogene* 2007;26(42):6244–6252.
21. Kostka G, Schweiger A. ADP-ribosylation of proteins associated with heterogeneous nuclear RNA in rat liver nuclei. *Biochim Biophys Acta* 1982;696(2):139–144.
22. Gagne JP, Hunter JM, Labrecque B, Chabot B, Poirier GG. A proteomic approach to the identification of heterogeneous nuclear ribonucleoproteins as a new family of poly(ADP-ribose)-binding proteins. *Biochem J* 2003;371(Pt 2):331–340.
23. Ji Y, Tulin AV. The roles of PARP1 in gene control and cell differentiation. *Curr Opin Genet Dev* 2010;20(5):512–518.
24. Ji Y, Tulin AV. Post-transcriptional regulation by poly(ADP-ribosylation) of the RNA-binding proteins. *Int J Mol Sci* 2013;14(8):16168–16183.
25. Hassa PO, Hottiger MO. A role of poly (ADP-ribose) polymerase in NF-kappaB transcriptional activation. *Biol Chem* 1999;380(7–8):953–959.
26. Oliver FJ, Menissier-de Murcia J, Nacci C, Decker P, Andriantsitohaina R, Muller S, de la Rubia G, Stoclet JC, de Murcia G. Resistance to endotoxic shock as a consequence of defective NF-kappaB activation in poly (ADP-ribose) polymerase-1 deficient mice. *Embo J* 1999;18(16):4446–4454.
27. Aguilar-Quesada R, Munoz-Gamez JA, Martin-Oliva D, Peralta-Leal A, Quiles-Perez R, Rodriguez-Vargas JM, Ruiz de Almodovar M, Conde C, Ruiz-Extremera A, Oliver FJ. Modulation of transcription by PARP-1: Consequences in carcinogenesis and inflammation. *Curr Med Chem* 2007;14(11):1179–1187.
28. Gonzalez-Flores A, Aguilar-Quesada R, Siles E, Pozo S, Rodriguez-Lara MI, Lopez-Jimenez L, Lopez-Rodriguez M, Peralta-Leal A, Villar D, Martin-Oliva D, del Peso L, Berra E, Oliver FJ. Interaction between PARP-1 and HIF-2alpha in the hypoxic response. *Oncogene* 2014;33(7):891–898.
29. Olabisi OA, Soto-Nieves N, Nieves E, Yang TT, Yang X, Yu RY, Suk HY, Macian F, Chow CW. Regulation of transcription factor NFAT by ADP-ribosylation. *Mol Cell Biol* 2008;28(9):2860–2871.
30. Donehower LA, Godley LA, Aldaz CM, Pyle R, Shi YP, Pinkel D, Gray J, Bradley A, Medina D, Varmus HE. The role of p53 loss in genomic instability and tumour progression in a murine mammary cancer model. *Prog Clin Biol Res* 1996;395:1–11.
31. Vaziri H, West MD, Allsopp RC, Davison TS, Wu YS, Arrowsmith CH, Poirier GG, Benchimol S. ATM-dependent telomere loss in aging human diploid fibroblasts and DNA damage lead to the post-translational activation of p53 protein involving poly(ADP-ribose) polymerase. *EMBO J* 1997;16(19):6018–6033.
32. Conde C, Mark M, Oliver FJ, Huber A, de Murcia G, Menissier-de Murcia J. Loss of poly(ADP-ribose) polymerase-1 causes increased tumour latency in p53-deficient mice. *Embo J* 2001;20(13):3535–3543.
33. Kanai M, Hanashiro K, Kim SH, Hanai S, Boulares AH, Miwa M, Fukasawa K. Inhibition of Crm1-p53 interaction and nuclear export of p53 by poly(ADP-ribosylation). *Nat Cell Biol* 2007;9(10):1175–1183.
34. Masutani M, Nozaki T, Nishiyama E, Shimokawa T, Tachi Y, Suzuki H, Nakagama H, Wakabayashi K, Sugimura T. Function of poly(ADP-ribose) polymerase in response to DNA damage: Gene-disruption study in mice. *Mol Cell Biochem* 1999;193(1–2):149–152.
35. de Murcia JM, Niedergang C, Trucco C, Ricoul M, Dutrillaux B, Mark M, Oliver FJ, Masson M, Dierich A, LeMeur M, Walztinger C, Chambon P, de Murcia G. Requirement of poly(ADP-ribose) polymerase in recovery from DNA damage in mice and in cells. *Proc Natl Acad Sci USA* 1997;94(14):7303–7307.
36. Wang ZQ, Stingl L, Morrison C, Jantsch M, Los M, Schulze-Osthoff K, Wagner EF. PARP is important for genomic stability but dispensable in apoptosis. *Genes Dev* 1997;11(18):2347–2358.

37. Rosenthal DS, Simbulan-Rosenthal CM, Iyer S, Smith WJ, Ray R, Smulson ME. Calmodulin, poly(ADP-ribose)polymerase and p53 are targets for modulating the effects of sulfur mustard. *J Appl Toxicol* 2000;20(Suppl 1):S43–S49.
38. d’Adda di Fagagna F, Hande MP, Tong WM, Lansdorp PM, Wang ZQ, Jackson SP. Functions of poly(ADP-ribose) polymerase in controlling telomere length and chromosomal stability. *Nat Genet* 1999;23(1):76–80.
39. Espejel S, Klatt P, Menissier-de Murcia J, Martin-Caballero J, Flores JM, Taccioli G, de Murcia G, Blasco MA. Impact of telomerase ablation on organismal viability, aging, and tumorigenesis in mice lacking the DNA repair proteins PARP-1, Ku86, or DNA-PKcs. *J Cell Biol* 2004;167(4):627–638.
40. Bieche I, de Murcia G, Lidereau R. Poly(ADP-ribose) polymerase gene expression status and genomic instability in human breast cancer. *Clin Cancer Res* 1996;2(7):1163–1167.
41. Chevanne M, Zampieri M, Caldini R, Rizzo A, Ciccarone F, Catizone A, D’Angelo C, Guastafierro T, Biroccio A, Reale A, Zupi G, Caiafa P. Inhibition of PARP activity by PJ-34 leads to growth impairment and cell death associated with aberrant mitotic pattern and nucleolar actin accumulation in M14 melanoma cell line. *J Cell Physiol* 2010;222(2):401–410.
42. Dantzer F, Schreiber V, Niedergang C, Trucco C, Flatter E, De La Rubia G, Oliver J, Rolli V, Menissier-de Murcia J, de Murcia G. Involvement of poly(ADP-ribose) polymerase in base excision repair. *Biochimie* 1999;81(1–2):69–75.
43. Plummer R, Lorigan P, Steven N, Scott L, Middleton MR, Wilson RH, Mulligan E, Curtin N, Wang D, Dewji R, Abbattista A, Gallo J, Calvert H. A phase II study of the potent PARP inhibitor, Rucaparib (PF-01367338, AG014699), with temozolomide in patients with metastatic melanoma demonstrating evidence of chemopotential. *Cancer Chemother Pharmacol* 2013;71(5):1191–1199.
44. O’Shaughnessy J, Osborne C, Pippen JE, Yoffe M, Patt D, Rocha C, Koo IC, Sherman BM, Bradley C. Iniparib plus chemotherapy in metastatic triple-negative breast cancer. *N Engl J Med* 2011;364(3):205–214.
45. Ledermann J, Harter P, Gourley C, Friedlander M, Vergote I, Rustin G, Scott C, Meier W, Shapira-Frommer R, Safra T, Matei D, Macpherson E, Watkins C, Carmichael J, Matulonis U. Olaparib maintenance therapy in platinum-sensitive relapsed ovarian cancer. *N Engl J Med* 2012;366(15):1382–1392.
46. Ledermann J, Harter P, Gourley C, Friedlander M, Vergote I, Rustin G, Scott CL, Meier W, Shapira-Frommer R, Safra T, Matei D, Fielding A, Spencer S, Dougherty B, Orr M, Hodgson D, Barrett JC, Matulonis U. Olaparib maintenance therapy in patients with platinum-sensitive relapsed serous ovarian cancer: A preplanned retrospective analysis of outcomes by BRCA status in a randomised phase 2 trial. *Lancet Oncol* 2014;15(8):852–61.
47. Bryant HE, Schultz N, Thomas HD, Parker KM, Flower D, Lopez E, Kyle S, Meuth M, Curtin NJ, Helleday T. Specific killing of BRCA2-deficient tumours with inhibitors of poly(ADP-ribose) polymerase. *Nature* 2005;434(7035):913–917.
48. Strom CE, Johansson F, Uhlen M, Szgyarto CA, Erixon K, Helleday T. Poly (ADP-ribose) polymerase (PARP) is not involved in base excision repair but PARP inhibition traps a single-strand intermediate. *Nucleic Acids Res* 2011;39(8):3166–3175.
49. Ying S, Hamdy FC, Helleday T. Mre11-dependent degradation of stalled DNA replication forks is prevented by BRCA2 and PARP1. *Cancer Res* 2012;72(11):2814–2821.
50. Shen WH, Balajee AS, Wang J, Wu H, Eng C, Pandolfi PP, Yin Y. Essential role for nuclear PTEN in maintaining chromosomal integrity. *Cell* 2007;128(1):157–170.
51. Mendes-Pereira AM, Martin SA, Brough R, McCarthy A, Taylor JR, Kim JS, Waldman T, Lord CJ, Ashworth A. Synthetic lethal targeting of PTEN mutant cells with PARP inhibitors. *EMBO Mol Med* 2009;1(6–7):315–322.
52. McEllin B, Camacho CV, Mukherjee B, Hahm B, Tomimatsu N, Bachoo RM, Burma S. PTEN loss compromises homologous recombination repair in astrocytes: Implications for glioblastoma therapy with temozolomide or poly(ADP-ribose) polymerase inhibitors. *Cancer Res* 2010;70(13):5457–5464.

53. Nakajima H, Ishikawa Y, Furuya M, Sano T, Ohno Y, Horiguchi J, Oyama T. Protein expression, gene amplification, and mutational analysis of EGFR in triple-negative breast cancer. *Breast Cancer* 2014;21(1):66–74.
54. Nowsheen S, Bonner JA, Lobuglio AF, Trummell H, Whitley AC, Dobelbower MC, Yang ES. Cetuximab augments cytotoxicity with poly (ADP-ribose) polymerase inhibition in head and neck cancer. *PLoS One* 2011;6(8):e24148.
55. Nowsheen S, Cooper T, Stanley JA, Yang ES. Synthetic lethal interactions between EGFR and PARP inhibition in human triple negative breast cancer cells. *PLoS One* 2012;7(10):e46614.
56. Hegan DC, Lu Y, Stachelek GC, Crosby ME, Bindra RS, Glazer PM. Inhibition of poly(ADP-ribose) polymerase down-regulates BRCA1 and RAD51 in a pathway mediated by E2F4 and p130. *Proc Natl Acad Sci USA* 2010;107(5):2201–2206.
57. Sooriakumaran P, Kaba R. Angiogenesis and the tumour hypoxia response in prostate cancer: A review. *Int J Surg* 2005;3(1):61–67.
58. Thomlinson RH, Gray LH. The histological structure of some human lung cancers and the possible implications for radiotherapy. *Br J Cancer* 1955;9(4):539–549.
59. Rofstad EK, Danielsen T. Hypoxia-induced metastasis of human melanoma cells: Involvement of vascular endothelial growth factor-mediated angiogenesis. *Br J Cancer* 1999;80(11):1697–1707.
60. Semenza GL. Hypoxia and cancer. *Cancer Metastasis Rev* 2007;26(2):223–224.
61. Semenza GL. HIF-1 and tumour progression: Pathophysiology and therapeutics. *Trends Mol Med* 2002;8(4 Suppl):S62–7.
62. Loboda A, Jozkowicz A, Dulak J. HIF-1 and HIF-2 transcription factors—similar but not identical. *Mol Cells* 29(5):435–442.
63. Weidemann A, Johnson RS. Biology of HIF-1alpha. *Cell Death Differ* 2008;15(4):621–627.
64. Martin-Oliva D, Aguilar-Quesada R, O’Valle F, Munoz-Gamez JA, Martinez-Romero R, Garcia Del Moral R, Ruiz de Almodovar JM, Villuendas R, Piris MA, Oliver FJ. Inhibition of poly(ADP-ribose) polymerase modulates tumour-related gene expression, including hypoxia-inducible factor-1 activation, during skin carcinogenesis. *Cancer Res* 2006;66(11):5744–5756.
65. Martinez-Romero R, Canuelo A, Martinez-Lara E, Javier Oliver F, Cardenas S, Siles E. Poly(ADP-ribose) polymerase-1 modulation of in vivo response of brain hypoxia-inducible factor-1 to hypoxia/reoxygenation is mediated by nitric oxide and factor inhibiting HIF. *J Neurochem* 2009;111(1):150–159.
66. Elser M, Borsig L, Hassa PO, Erener S, Messner S, Valovka T, Keller S, Gassmann M, Hottiger MO. Poly(ADP-ribose) polymerase 1 promotes tumour cell survival by coactivating hypoxia-inducible factor-1-dependent gene expression. *Mol Cancer Res* 2008;6(2):282–290.
67. Canuelo A, Martinez-Romero R, Martinez-Lara E, Sanchez-Alcazar JA, Siles E. The hypoxic preconditioning agent deferroxamine induces poly(ADP-ribose) polymerase-1-dependent inhibition of the mitochondrial respiratory chain. *Mol Cell Biochem* 363(1–2):101–108.
68. Quintero M, Brennan PA, Thomas GJ, Moncada S. Nitric oxide is a factor in the stabilization of hypoxia-inducible factor-1alpha in cancer: Role of free radical formation. *Cancer Res* 2006;66(2):770–774.
69. Liu SK, Coackley C, Krause M, Jalali F, Chan N, Bristow RG. A novel poly(ADP-ribose) polymerase inhibitor, ABT-888, radiosensitizes malignant human cell lines under hypoxia. *Radiother Oncol* 2008;88(2):258–268.
70. Raval RR, Lau KW, Tran MG, Sowter HM, Mandriota SJ, Li JL, Pugh CW, Maxwell PH, Harris AL, Ratcliffe PJ. Contrasting properties of hypoxia-inducible factor 1 (HIF-1) and HIF-2 in von Hippel-Lindau-associated renal cell carcinoma. *Mol Cell Biol* 2005;25(13):5675–5686.
71. Holmquist-Mengelbier L, Fredlund E, Lofstedt T, Noguera R, Navarro S, Nilsson H, Pietras A, Vallon-Christersson J, Borg A, Gradin K, Poellinger L, Pahlman S. Recruitment of HIF-1alpha and HIF-2alpha to common target genes is differentially regulated in neuroblastoma: HIF-2alpha promotes an aggressive phenotype. *Cancer Cell* 2006;10(5):413–423.

72. Hassa PO, Haenni SS, Buerki C, Meier NI, Lane WS, Owen H, Gersbach M, Imhof R, Hottiger MO. Acetylation of poly(ADP-ribose) polymerase-1 by p300/CREB-binding protein regulates coactivation of NF-kappaB-dependent transcription. *J Biol Chem* 2005;280(49):40450–40464.
73. Thiery JP, Acloque H, Huang RY, Nieto MA. Epithelial-mesenchymal transitions in development and disease. *Cell* 2009;139(5):871–890.
74. Baum B, Georgiou M. Dynamics of adherens junctions in epithelial establishment, maintenance, and remodeling. *J Cell Biol* 2011;192(6):907–917.
75. Kalluri R, Weinberg RA. The basics of epithelial-mesenchymal transition. *J Clin Invest* 2009;119(6):1420–1428.
76. Peinado H, Del Carmen Iglesias-de la Cruz M, Olmeda D, Csiszar K, Fong KS, Vega S, Nieto MA, Cano A, Portillo F. A molecular role for lysyl oxidase-like 2 enzyme in snail regulation and tumour progression. *Embo J* 2005;24(19):3446–3458.
77. Xu Y, Lee SH, Kim HS, Kim NH, Piao S, Park SH, Jung YS, Yook JI, Park BJ, Ha NC. Role of CK1 in GSK3beta-mediated phosphorylation and degradation of snail. *Oncogene* 2010;29(21):3124–3133.
78. Vinas-Castells R, Beltran M, Valls G, Gomez I, Garcia JM, Montserrat-Sentis B, Baulida J, Bonilla F, de Herreros AG, Diaz VM. The hypoxia-controlled FBXL14 ubiquitin ligase targets SNAIL1 for proteasome degradation. *J Biol Chem* 2010;285(6):3794–3805.
79. de Graauw M, van Miltenburg MH, Schmidt MK, Pont C, Lalai R, Kartopawiro J, Pardali E, Le Devedec SE, Smit VT, van der Wal A, Van'tVeer LJ, Cleton-Jansen AM, ten Dijke P, van de Water B. Annexin A1 regulates TGF-beta signaling and promotes metastasis formation of basal-like breast cancer cells. *Proc Natl Acad Sci USA* 2010;107(14):6340–6345.
80. Brabletz T, Jung A, Spaderna S, Hlubek F, Kirchner T. Opinion: Migrating cancer stem cells—An integrated concept of malignant tumour progression. *Nat Rev Cancer* 2005;5(9):744–749.
81. Mani SA, Guo W, Liao MJ, Eaton EN, Ayyanan A, Zhou AY, Brooks M, Reinhard F, Zhang CC, Shipitsin M, Campbell LL, Polyak K, Brisken C, Yang J, Weinberg RA. The epithelial-mesenchymal transition generates cells with properties of stem cells. *Cell* 2008;133(4):704–715.
82. Goessling W, North TE, Loewer S, Lord AM, Lee S, Stoick-Cooper CL, Weidinger G, Puder M, Daley GQ, Moon RT, Zon LI. Genetic interaction of PGE2 and Wnt signaling regulates developmental specification of stem cells and regeneration. *Cell* 2009;136(6):1136–1147.
83. Floor S, van Staveren WC, Larsimont D, Dumont JE, Maenhaut C. Cancer cells in epithelial-to-mesenchymal transition and tumour-propagating-cancer stem cells: Distinct, overlapping or same populations. *Oncogene* 2011;30(46):4609–4621.
84. Rodriguez MI, Gonzalez-Flores A, Dantzer F, Collard J, de Herreros AG, Oliver FJ. Poly(ADP-ribose)-dependent regulation of Snail1 protein stability. *Oncogene* 2011;30(42):4365–4372.
85. Lonn P, van der Heide LP, Dahl M, Hellman U, Heldin CH, Moustakas A. PARP-1 attenuates Smad-mediated transcription. *Mol Cell* 2010;40(4):521–532.
86. McPhee TR, McDonald PC, Oloumi A, Dedhar S. Integrin-linked kinase regulates E-cadherin expression through PARP-1. *Dev Dyn* 2008;237(10):2737–2747.
87. Rodriguez MI, Peralta-Leal A, O'Valle F, Rodriguez-Vargas JM, Gonzalez-Flores A, Majuelos-Melguizo J, Lopez L, Serrano S, de Herreros AG, Rodriguez-Manzanares JC, Fernandez R, Del Moral RG, de Almodovar JM, Oliver FJ. PARP-1 regulates metastatic melanoma through modulation of vimentin-induced malignant transformation. *PLoS Genet* 2013;9(6):e1003531.
88. Rajesh M, Mukhopadhyay P, Batkai S, Godlewski G, Hasko G, Liaudet L, Pacher P. Pharmacological inhibition of poly(ADP-ribose) polymerase inhibits angiogenesis. *Biochem Biophys Res Commun* 2006;350(2):352–357.
89. Tentori L, Lacal PM, Muzi A, Dorio AS, Leonetti C, Scarsella M, Ruffini F, Xu W, Min W, Stoppacciaro A, Colarossi C, Wang ZQ, Zhang J, Graziani G. Poly(ADP-ribose) polymerase (PARP) inhibition or PARP-1 gene deletion reduces angiogenesis. *Eur J Cancer* 2007;43(14):2124–2133.
90. Tentori L, Muzi A, Dorio AS, Bultrini S, Mazzon E, Lacal PM, Shah GM, Zhang J, Navarra P, Nocentini G, Cuzzocrea S, Graziani G. Stable depletion of poly (ADP-ribose) polymerase-1 reduces in vivo melanoma growth and increases chemosensitivity. *Eur J Cancer* 2008;44(9):1302–1314.

91. Albert JM, Cao C, Kim KW, Willey CD, Geng L, Xiao D, Wang H, Sandler A, Johnson DH, Colevas AD, Low J, Rothenberg ML, Lu B. Inhibition of poly(ADP-ribose) polymerase enhances cell death and improves tumour growth delay in irradiated lung cancer models. *Clin Cancer Res* 2007;13(10):3033–3042.
92. Kumar VB, Viji RI, Kiran MS, Sudhakaran PR. Endothelial cell response to lactate: Implication of PAR modification of VEGF. *J Cell Physiol* 2007;211(2):477–485.
93. Beckert S, Farrahi F, Perveen Ghani Q, Aslam R, Scheuenstuhl H, Coerper S, Konigsrainer A, Hunt TK, Hussain MZ. IGF-I-induced VEGF expression in HUVEC involves phosphorylation and inhibition of poly(ADP-ribose)polymerase. *Biochem Biophys Res Commun* 2006;341(1):67–72.
94. Hess AR, Seftor EA, Gruman LM, Kinch MS, Seftor RE, Hendrix MJ. VE-cadherin regulates EphA2 in aggressive melanoma cells through a novel signaling pathway: Implications for vasculogenic mimicry. *Cancer Biol Ther* 2006;5(2):228–233.
95. Ivaska J, Pallari HM, Nevo J, Eriksson JE. Novel functions of vimentin in cell adhesion, migration, and signaling. *Exp Cell Res* 2007;313(10):2050–2062.
96. van Beijnum JR, Dings RP, van der Linden E, Zwaans BM, Ramaekers FC, Mayo KH, Griffioen AW. Gene expression of tumour angiogenesis dissected: Specific targeting of colon cancer angiogenic vasculature. *Blood* 2006;108(7):2339–2348.
97. Gilles C, Polette M, Mestdagt M, Nawrocki-Raby B, Ruggeri P, Birembaut P, Foidart JM. Transactivation of vimentin by beta-catenin in human breast cancer cells. *Cancer Res* 2003;63(10):2658–2664.
98. Min C, Eddy SF, Sherr DH, Sonenshein GE. NF-kappaB and epithelial to mesenchymal transition of cancer. *J Cell Biochem* 2008;104(3):733–744.
99. Wu Y, Zhang X, Salmon M, Lin X, Zehner ZE. TGFbeta1 regulation of vimentin gene expression during differentiation of the C2C12 skeletal myogenic cell line requires Smads, AP-1 and Sp1 family members. *Biochim Biophys Acta* 2007;1773(3):427–439.
100. Cohen-Armon M, Visochek L, Rozensal D, Kalal A, Geistrikh I, Klein R, Bendetz-Nezer S, Yao Z, Seger R. DNA-independent PARP-1 activation by phosphorylated ERK2 increases Elk1 activity: A link to histone acetylation. *Mol Cell* 2007;25(2):297–308.
101. Maniotis AJ, Folberg R, Hess A, Seftor EA, Gardner LM, Pe'er J, Trent JM, Meltzer PS, Hendrix MJ. Vascular channel formation by human melanoma cells in vivo and in vitro: Vasculogenic mimicry. *Am J Pathol* 1999;155(3):739–752.
102. Krenkel S, Groteluschen F, Bartsch S, Tronnier M. Cadherin expression pattern in melanocytic tumours more likely depends on the melanocyte environment than on tumour cell progression. *J Cutan Pathol* 2004;31(1):1–7.
103. Licht AH, Muller-Holtkamp F, Flamme I, Breier G. Inhibition of hypoxia-inducible factor activity in endothelial cells disrupts embryonic cardiovascular development. *Blood* 2006;107(2):584–590.

María Isabel Rodríguez, *Ph.D.*, is post-doc researcher at the IPBLN, CSIC in Granada, Spain.

Jara Majuelos-Melguizo and Juan Manuel Martí Martín-Consuegra are *Ph.D.* students at IPBLN, CSIC in Granada, Spain.

Mariano Ruiz de Almodóvar, *Ph.D.*, is Research Director at the CIB, IBIMER in Granada, Spain.

Abelardo López-Rivas, *Ph.D.*, is Research Director at the CABIMER in Seville, Spain.

Francisco Javier Oliver, *Ph.D.*, is Research Director at the IPBLN, CSIC in Granada, Spain. Head of Department of Immunology and Cell Biology.